

SYNTHESIS, EVALUATION AND APPLICATION OF THIOSUGARS AND THIOGLYCOSIDES IN MEDICINAL AND BIOORGANIC CHEMISTRY

by

DANIIL AHIADORME

(Under the Direction of David Crich)

Thioglycosides and thiosugars both have a long history in bioorganic and medicinal chemistry. As presented in Chapter 1, thioglycosides and thiosugars are well-documented and well-studied mimetics of *O*-glycosides, and, to date, a considerable number of synthetic methods have been developed to access them. Despite several known examples in which thioglycosides or thiosugars showed higher inhibitory activity than the parent *O*-glycosides, these mimetics are still widely considered to be less “active” than the parent sugars.

Chapter 2 details the design and synthesis of tetravalent glycoconstructs containing 1,5-dithialaminaribiose and -triose mimetics, and evaluation of their inhibitory activity against CR3 and Dectin-1 in comparison to the appropriate analogous *O*-glycosides. The synthesized compounds showed inhibitory activity against CR3 comparable to that of monovalent 1,5-dithio mimetics, but no clear pattern emerged regarding the number of carbohydrate units in the epitope nor the usefulness of the multivalent construct.

Chapter 3 explores the impact of S- π interactions occurring between ring sulfur atoms or glycosidic sulfur atoms and aromatic amino acid residues on binding of thiosugars and thioglycosides to lectins in an attempt to improve predictions of the value of 5-thio or thioglycosidic mimetics of parent *O*-glycosides. After an extensive PDB database search and analysis of the search output two representative examples were selected for experimental validation. Accordingly, mimetics were designed, synthesized and evaluated for

their binding affinity with target lectins, and the thermodynamic parameters of binding were determined and compared with those of parent *O*-glycosides.

Chapter 4 presents an extensive variable temperature NMR study of generation and stability of reactive intermediates formed on activation of 5-thioglycosyl donors in attempt to shed light on differences in reactivity between 5-thiosugars and the corresponding parent glycosides. The tetrahydrothiopyrilium cation was successfully generated and characterized spectroscopically, and was found to be marginally more stable than the corresponding oxocarbenium cation. However, no evidence for the generation of a thienium cation was found in VT NMR experiments with 5-thioglycosyl donors, but rather the formation of dioxalenium ions and covalent triflates was observed.

INDEX WORDS: Thioglycosides, thiosugars, glycosylation, variable temperature NMR spectroscopy, mimetics

SYNTHESIS, EVALUATION AND APPLICATION OF THIOSUGARS AND THIOLYCOSIDES IN
MEDICINAL AND BIOORGANIC CHEMISTRY

by

DANIIL AHIADORME

Diploma, M.V. Lomonosov Moscow State University, Russian Federation, 2019

A Dissertation Submitted to the Graduate Faculty of The University of Georgia in Partial
Fulfillment of the Requirements for the Degree of

DOCTOR OF PHILOSOPHY

ATHENS, GEORGIA

2024

© 2024

Daniil Ahiadorme

All Rights Reserved

SYNTHESIS, EVALUATION AND APPLICATION OF THIOSUGARS AND THIOLYCOSIDES IN
MEDICINAL AND BIOORGANIC CHEMISTRY

by

DANIIL AHIADORME

Major Professor: David Crich

Committee: Eric Ferreira
Geert-Jan Boons

Electronic Version Approved:

Ron Walcott

Dean of the Graduate School

The University of Georgia

August 2024

DEDICATION

I dedicate this work to my parents, Victoria Seth Ahiadorme and Stanislav Evgenevich Ahiadorme for their support and encouragement.

ACKNOWLEDGMENTS

First, I would like to express my sincere gratitude to my advisor, Dr. David Crich, for his guidance, support, patience and compassion, and for giving me a chance to receive a Ph.D. degree in his research group. He has always pushed me to be a better chemist and reach my potential and has greatly prepared me to overcome the obstacles to come.

I would like to thank my committee members, Dr. Eric Ferreira and Dr. Geert-Jan Boons, for their time and input.

Moreover, I want to express my gratitude to Dr. Chennaiah Ande for his contribution to the synthesis of 1,5-dithio mimetics of β -(1 \rightarrow 3)-glucans, and for his guidance and advice.

In addition, I would like to express my gratitude to our collaborators, Dr. Rafael Fernandez-Botran from the University of Louisville for running biological assays on tetravalent 1,5-dithio constructs; Dr. Rich Helm, Dr. Ryan Porell, Caylyn McNaul from GlycoMIP, a National Science Foundation Materials Innovation Platform funded through Cooperative Agreement DMR-1933525, at Virginia Tech, and Prof. Rob Woods and Dr. Sawsan Mahmoud from GlycoMIP, a National Science Foundation Materials Innovation Platform funded through Cooperative Agreement DMR-1933525, at the University of Georgia CCRC for running binding assays on thio-mimetics; and Prof. Henry Schaefer III, and Houston Givhan at the University of Georgia CCQC, for running computational studies. Moreover, I would like to thank the Crich Lab members with whom I overlapped for their collaboration and lab atmosphere: Dr. Jarvis Hill, Dr. Michael Pirrone, Dr. Timothy McMillan, Dr. Kapil Upadhyaya, Dr. Ande Chennaiah, Dr. Rahul Bagul, Dr. Jonathan Quirke, Dr. Yagya Subedi, Dr. Sameera Jayanath, Dr. Emmanuel Onobun, Dr. Philemon Ngoje, Dr. Asiri Hettikankanamalage, Dr. Vikram Sarpe, Dr. Parasuraman Rajasekaran, Dr. Samir Ghosh, Dr. Anura Wickramasinghe, Dr. Santanu Jana, Dr. Pallabita Basu, Dr. Niteshlal Kadeskar, Po-Sen Tseng, Nicolas Osorio-Morales, Thomas Beckler, Wei-Chih Lo, Iftikhar Khan, Yizhi Cui, Jonathan Lin, Michael

Spieker, and Margaret Solecki. I would like to express my particular gratitude to Dr. Jarvis Hill for his advice and, for being a great colleague and friend at difficult times, and to Dr. Michael Pirrone for teaching me how to operate and fix the issues with the Orbitrap mass-spectrometer and for ensuring that laboratory operates smoothly. In addition to that, I would like to thank the “VT NMR crew”, Dr. Michael Pirrone and Dr. Sameera Jayanath for teaching and supervising me in performing VT NMR experiments, and Dr. Chennaiah Ande and Nicolas Osorio-Morales for helping me with setting up the VT NMR experiments.

TABLE OF CONTENTS

ACKNOWLEDGMENTS	v
LIST OF TABLES	x
LIST OF FIGURES	xi
LIST OF SCHEMES.....	xv
LIST OF ABBREVIATIONS.....	xix
CHAPTER	
1 INTRODUCTION TO THIOGLYCOSIDES AND THIOSUGARS AND THEIR APPLICATION IN MEDICINAL AND BIOORGANIC CHEMISTRY	1
1.1. Introduction to glycosides and glycoside mimetics.....	1
1.2. Thioglycosides and their application in bioorganic and medicinal chemistry.....	2
1.3. Thiosugars and their application in bioorganic and medicinal chemistry	7
1.4. Reactivity of 5-thiosugars.....	13
1.5. Overall goals.....	18
2 SYNTHESIS AND EVALUATION OF TETRAVALENT CONSTRUCTS CONTAINING 1,5- DITHIO MIMETICS OF β -(1 \rightarrow 3)-GLUCANS.....	19
2.1. Introduction	20
2.2. Goals of the project and considerations.....	24
2.3. Triazole system design and synthesis of tetraazide core	25

2.4. Synthesis of 1,5-dithio mimetics of laminaribiose and triose.....	26
2.5. Tetravalent triazole constructs assembly	28
2.6. Tetraamide system design and synthesis of the key precursors.....	31
2.7. Synthesis and evaluation of tetraamide constructs	33
2.8. Summary.....	39
3 EXPLORING THE IMPACT OF S-ARENE INTERACTIONS OF THIOGLYCOSIDES AND THIOSUGARS ON BINDING TO LECTINS.....	41
3.1. Introduction	42
3.2. Goals of the project and considerations.....	46
3.3. PDB search	47
3.4. Target selection.....	50
3.5. Synthesis of thio-mimetics	52
3.6. Evaluation of binding affinity.....	56
3.7. Summary.....	61
4 VT NMR STUDIES OF GENERATION AND STABILITY OF REACTIVE INTERMEDIATES GENERATED FROM 5-THIOGLYCOSYL DONORS	62
4.1. Introduction	63
4.2. Goals of the project and considerations.....	66
4.3. VT NMR studies of simple thiocarbenium cations	67
4.4. VT NMR studies with disarmed glycosyl donors.....	76
4.5. VT NMR studies with armed glycosyl donors	97
4.6. Summary of the VT NMR experiments with glucosyl and thioglucosyl donors.....	112

4.7. Conclusions	116
5 OVERALL CONCLUSIONS.....	117
6 EXPERIMENTAL SECTION	119
6.1. General experimental	119
6.2. Experimental procedures for the synthesis of compounds described in Chapter 2.....	120
6.3. Experimental procedures for the PDB database search and synthesis of compounds described in Chapter 3.....	159
6.3. Experimental procedures for the synthesis of compounds described in Chapter 4.....	174
6.4. Experimental procedures for the VT NMR experiments described in Chapter 4	195
REFERENCES	213
APPENDIX	228
AUTOBIOGRAPHICAL STATEMENT	254

LIST OF TABLES

Table 1. Ring opening rate and comparison of mutarotation rate of 5-thioglucose and glucose	16
Table 2. Percentage Inhibition of Anti-CR3 and Anti-Dectin-1-FITC Antibody Staining of Neutrophils and Macrophages by 0.1 $\mu\text{g/mL}$ substrate	38
Table 3. Percentage stimulation of phagocytosis of raw 264 macrophages by 10 $\mu\text{g/mL}$ substrate.	39
Table 4. Binding constants measured for Jacalin bound methyl α -D-galactopyranoside at different temperatures.....	57
Table 5. Binding constants measured for Jacalin bound methyl 5-thio- α -D-galactopyranoside 187 at different temperatures	58
Table 6. Thermodynamic parameters of Jacalin bound methyl α -D-galactopyranoside.....	60
Table 7. Thermodynamic parameters of Jacalin bound methyl-5-thio- α -D-galactopyranoside 187	60
Table 8. Search output data after Privateer and PyMOL analyses	228
Table 9. Examples where glycosidic S atom near aromatic residues.....	251

LIST OF FIGURES

Figure 1.1. Structure of <i>O</i> -glycosides and their <i>C</i> -, <i>S</i> - and <i>N</i> -analogs.....	1
Figure 1.2. Structures of Telithromycin, Amrubicin, and Plazomicin.	1
Figure 1.3. Comparison of <i>O</i> -glycosides and thioglycosides.	2
Figure 1.4. Structures of naturally occurring thioglycosides.	3
Figure 1.5. Three plausible conformations of the glycosidic bond in methyl β -D-xylopyranoside and Newman projections along C ₁ -O ₁ bond.	5
Figure 1.6. Structures of biologically active thioglycosides	6
Figure 1.7. Structures of aryl thioglycosides 23-25 with micromolar inhibitory activity against LecA lectin binding to the galactosylated surface in comparison to the methyl α -D-galactopyranoside 26	7
Figure 1.8. Comparison of glycosides and 5-thiosugar glycosides.....	8
Figure 1.9. Naturally occurring thiosugars.	8
Figure 1.10. Summarized synthetic approaches towards 5-thiosugars	9
Figure 1.11. Structure and biological activity of 1,5-dithio mimetics 45 , 46 of laminaribiose and triose. .	12
Figure 1.12. Structure of potent <i>in vivo</i> inhibitor of OGT.....	13
Figure 2.1. Structure of β -(1→3)-glucans and their mimetics	20
Figure 2.2. Structures of synthetic pentasaccharides with glucitol 89 and mannitol 90 terminal modification.	21
Figure 2.3. Schematic representation of the hydrophobic α -face of a β -(1→3)-glucan in complex with Trp-221 and His-223 residues in the binding pocket of the Dectin-1–lectin domain.	22
Figure 2.4. Examples of aliphatic and aromatic multivalent scaffolds.	23
Figure 2.5. Structures and inhibitory activity of the newly synthesized tetraamides 142 , 146 , 150 , and 154 with monovalent 1,5-dithio mimetics 45 and 46 and monovalent propionyl amide 156	38
Figure 3.1. Examples of CH- π interactions.....	42

Figure 3.2. Sulfur-arene contacts between aromatic residues and sulfides.....	43
Figure 3.3. Schematic representation of the minimal internal energy determined for benzene-methanethiol complex and schematic representation of the minimal internal energy determined for benzene-dimethylsulfide complex.....	44
Figure 3.4. An equilibration observed by NMR spectroscopy between two oxathiolane conformers 163 and 164	44
Figure 3.5. X-ray crystal structures of Galectin-bound thioglycosides.....	46
Figure 3.6. Statistical analysis of the PDB database search output	49
Figure 3.7. The most common arrangements of ring oxygen or glycosidic oxygen and aromatic residue.	50
Figure 3.8. X-ray crystal structures of selected targets	51
Figure 3.9. Jacalin bound methyl α -D-galactopyranoside..	55
Figure 3.10. van't-Hoff plot for the parent methyl α -D-galactopyranoside.....	58
Figure 3.11. van't-Hoff plot for methyl 5-thio- α -D-galactopyranoside 187	59
Figure 4.1. Examples of reactive intermediates generated after activation of glycosyl donors and the key chemical shifts in ^1H and ^{13}C NMR spectra.	66
Figure 4.2. gHMQC x-decoupled spectra plotted against DEPT-135 with the key peaks	71
Figure 4.3. Stacked ^1H NMR spectra from VT experiment without phase-transfer catalyst with addition of 2.2 equiv of TfOH.....	72
Figure 4.4. Computed natural bond orders, bond lengths, ring torsional angles, and internal bond angles for thienium ion 210 and oxocarbenium ion 221 and for axial covalent 2-thianyl triflate 230 and axial tetrahydropyranyl triflate 231	75
Figure 4.5. The comparison of the key ^{13}C NMR peaks of the starting material and sulfoxides.....	77
Figure 4.6. Key data from a VT NMR experiment with glucosyl sulfoxide 237	80
Figure 4.7. Structures of reactive intermediates and stacked ^1H NMR from a VT NMR experiment with glucosyl sulfoxide 237	81
Figure 4.8. Key data from a VT NMR experiment with glucosyl sulfoxide 236	83

Figure 4.9. Structures of reactive intermediates and stacked ^1H NMR from a VT NMR experiment with glucosyl sulfoxide 236 .	84
Figure 4.10. Key data from a VT NMR experiment with thioglucosyl sulfoxide 232 .	86
Figure 4.11. Structures of reactive intermediates and stacked ^1H NMR from a VT NMR experiment with thioglucosyl sulfoxide 232 .	88
Figure 4.12. Stacked ^{19}F NMR spectra from a VT experiment with thioglycosyl sulfoxide 232 .	89
Figure 4.13. Key data from a VT NMR experiment with thioglucosyl sulfoxide 234 .	91
Figure 4.14. Structures of reactive intermediates and stacked ^1H NMR from a VT NMR experiment with glucosyl sulfoxide 234 .	92
Figure 4.15. Structures of reactive intermediates and stacked ^1H NMR from a VT NMR experiment with glucosyl trichloroacetimidate 12 .	94
Figure 4.16. Structures of reactive intermediates and stacked ^1H NMR from a VT NMR experiment with thioglucosyl trichloroacetimidate 52 .	96
Figure 4.17. The comparison of the key ^{13}C NMR peaks of the starting material and sulfoxides.	99
Figure 4.18. Structures of reactive intermediates generated during a VT NMR experiment with glycosyl sulfoxide 275 and HMQC spectrum recorded at -50°C with the key cross-peaks.	101
Figure 4.19. Stacked ^1H NMR spectra from a VT NMR experiment with glycosyl sulfoxide 275 .	102
Figure 4.20. Structures of reactive intermediates generated during a VT NMR experiment with glycosyl sulfoxide 277 and HMQC spectrum recorded at -50°C with the key cross-peaks.	103
Figure 4.21. Stacked ^1H NMR spectra from a VT NMR experiment with glycosyl sulfoxide 277 .	104
Figure 4.22. Stacked ^1H NMR spectra from a VT NMR experiment with thioglucosyl sulfoxide 269 .	106
Figure 4.23. Stacked ^1H NMR spectra from a VT NMR experiment with thioglucosyl sulfoxide 272 .	108
Figure 4.24. Stacked ^1H NMR spectra from a VT NMR experiment with thioglucosyl trichloroacetimidate 291 .	110
Figure 4.25. Stacked ^1H NMR spectra from a VT NMR experiment with 5-thioglucosyl trichloroacetimidate 294 .	111

Figure 4.26. Summarized results of VT NMR experiments with peracetylated glycosyl donors.	114
Figure 4.27. Summarized results of VT NMR experiments with permethylated glycosyl donors.	115

LIST OF SCHEMES

Scheme 1. Versatile reactivity of thioglycosides	3
Scheme 2. Glycosylation reaction with thioglycosides as glycosyl donors.	4
Scheme 3. Lewis catalyzed glycosylation with a simple thiol, and base mediated coupling of a glycosyl bromide 10 with a thiol.	4
Scheme 4. Glycosylation reaction between thiol 11 and trichloroacetimidate 12 , and S _N 2 alkylation of anomeric thiolate 17 with triflate 18	5
Scheme 5. Synthesis of 5-thioglucose by Whistler.....	10
Scheme 6. Alternative synthetic route towards 5-thioglucose reported by Hashimoto	10
Scheme 7. Synthesis of 4-thioribose via a ring opening-double displacement-ring closing sequence.	11
Scheme 8. Comparison of the glycosylation outcome with 5-thioglycosyl 33 and parent glycosyl acetate 7 donors and ethanethiol.	13
Scheme 9. Glycosylation reactions with 5-thioglycosyl trichloroacetimidate 52 and various glycosyl acceptors.	14
Scheme 10. Synthesis disaccharide 64 with β -glycosidic linkage.	15
Scheme 11. Coupling reaction used in Cleland's study and proposed ring-opening and mutarotation mechanism of 5-thioglucose	16
Scheme 12. Methanolysis of 33 and 75 and structures of unexpected byproducts reported by Hashimoto	17
Scheme 13. Hydrolysis of perbenzylated methyl glycoside 38-α	17
Scheme 14. Assembly of glycocluster 93 and comparison of its affinity towards bacterial lectin LecA with monovalent derivatives 94 and 95	23

Scheme 15. Assembly of glycocluster 98 and comparison of its affinity towards bacterial lectin LecA with monovalent derivatives 95 and 96 .	24
Scheme 16. Retrosynthesis of triazole linked glycocluster 104 .	25
Scheme 17. Synthesis of tetraazide core 102 .	25
Scheme 18. Synthesis of 5-thioglucose 33 .	27
Scheme 19. Synthesis of the key triflate electrophile 63 .	27
Scheme 20. Synthesis of 5-thiooligosaccharides 117 and 120 .	28
Scheme 21. Synthesis of alkyne linkers and trial reaction with glycosyl bromide.	29
Scheme 22. Coupling of thioacetates 61 , 124 , and 126 with alkyne linker 121 .	30
Scheme 23. The CuAAC click reaction with monosaccharides 123 and 125 and target trisaccharide 127 .	31
Scheme 24. Retrosynthesis of tetraamide glycocluster 136 .	32
Scheme 25. Synthesis of tetracarboxylic acid core 134 from tetraallylated scaffold 100b .	32
Scheme 26. Synthesis of alkyl iodide linker 136 .	32
Scheme 27. Assembly of tetraamide glycocluster 142 .	33
Scheme 28. Synthesis of 5-thioglucose containing tetraamide glycocluster 146 .	34
Scheme 29. Synthesis di- and trisaccharides containing glycoclusters.	36
Scheme 30. Synthesis of the monovalent propionyl amide comparator 156 .	37
Scheme 31. Summarized research strategy.	47
Scheme 32. Retrosynthesis of peracetylated 4-thiolactose 167 .	52
Scheme 33. Synthesis of 4-thiolactose 170 .	53
Scheme 34. Retrosynthesis of 5-thiogalactose 175 .	53
Scheme 35. Attempted synthesis of 5-thiogalactose 175 .	54
Scheme 36. Synthesis of methyl 5-thio- α -D-galactopyranoside 187 .	56
Scheme 37. Study of the of benzaldehyde O,S-acetals 188 , 189 , 190 hydrolysis, and hydrolysis of monothioacetals 191 and 192 .	64

Scheme 38. Reactive intermediates generated from 1,3-dithiane in superacid; generation of thienium salts from aliphatic sulfide; generation of benzylic thienium cation; benzylic thienium cation generated with cation pool method; and thienium cation observed by NMR spectroscopy after protonation of 1,3-dithiane 201 .	65
Scheme 39. Substrates and methods to generate thiocarbenium cation during VT NMR experiments.....	67
Scheme 40. Synthesis of thiopyran derivatives 216 and 208	68
Scheme 41. VT NMR experiments with 2,3-dihydrothiopyran 208	69
Scheme 42. Summarized results of VT NMR experiments with parent 2,3-dihydropyran, various vinyl sulfides, and acetoxy derivatives.	73
Scheme 43. Synthesis of peracetylated 5-thioglycosyl sulfoxides.....	77
Scheme 44. Synthesis of peracetylated glucosyl sulfoxides.	78
Scheme 45. Intermediates and decomposition products generated during VT NMR experiments with glucosyl sulfoxide 237	81
Scheme 46. Intermediates and decomposition products generated during VT NMR experiments with glucosyl sulfoxide 236	84
Scheme 47. Proposed decomposition mechanism of the reactive intermediates generated during the VT NMR with glycosyl sulfoxides 236 and 237	85
Scheme 48. Intermediates and decomposition products generated during VT NMR experiments with thioglucosyl sulfoxide 232	89
Scheme 49. Intermediates and decomposition products generated during VT NMR experiments with glucosyl sulfoxide 234	92
Scheme 50. Synthesis of peracetylated trichloroacetimidate 12 and 52	93
Scheme 51. Structures of reactive intermediates formed during VT NMR experiments with peracetylated trichloroacetimidate 12	94
Scheme 52. Proposed mechanism to form enonyl amide 256	95

Scheme 53. Structures of reactive intermediates formed during VT NMR experiments with peracetylated thioglucosyl trichloroacetimidate 52	97
Scheme 54. Attempted synthesis of perbenzylated 5-thioglycosyl sulfoxide 264	97
Scheme 55. Synthesis of permethylated sulfoxides 269 and 272	98
Scheme 56. Synthesis of parent permethylated glucosyl sulfoxides 275 and 277	100
Scheme 57. Structures of reactive intermediates and products formed during VT NMR experiments with permethylated glycosyl sulfoxide 275	102
Scheme 58. Structures of reactive intermediates and products formed during VT NMR experiments with permethylated glycosyl sulfoxide 277	105
Scheme 59. Structures of reactive intermediates and products formed during VT NMR experiments with permethylated glycosyl sulfoxide 269	106
Scheme 60. Structures of reactive intermediates and products formed during VT NMR experiments with permethylated glycosyl sulfoxide 272	108
Scheme 61. Synthesis of permethylated trichloroacetimidates 291 and 294	109
Scheme 62. Structures of reactive intermediates and byproducts formed during VT NMR experiments with trichloroacetimidate 291	110
Scheme 63. Structures of reactive intermediates and byproducts formed during a VT NMR experiment with trichloroacetimidate 294	112

LIST OF ABBREVIATIONS

Ac — Acetyl

AIBN — Azobisisobutyronitrile

All — Allyl

Av — Average

Aq — Aqueous

AWMS — Acid-Washed Molecular Sieves

BLI — Biolayer Interferometry

Bn — Benzyl

Boc — *t*-Butoxycarbonyl

BSSE — Basis Set Superposition Error

Bu — Butyl

t-Bu — tertiary Butyl

s-Butyl — secondary Butyl

Bz — Benzoyl

CAM — Cerium Ammonium Molybdate

Cat — Catalytic

Calcd — Calculated

CCP4 — Collaborative Computational Project Number 4

CCRC — Complex Carbohydrate Research Center

CCQC — Center for Computational and Quantum Chemistry

CoA — Coenzyme A

Conc — Concentrated

COSY — Correlated Spectroscopy

CR3 — Complement Receptor 3

CuAAC — Copper-catalyzed Azide-Alkyne Cycloadditions

DAST — Diethylaminosulfur Trifluoride

DBU — 1,8-Diazabicyclo[5.4.0]undec-7-ene

DEPT — Distortionless Enhancement by Polarization Transfer

2,3-DHP — 2,3-Dihdropyran

DIAD — Diisopropyl Azodicarboxylate

DIBAL-H — Diisobutylaluminium Hydride

DIPEA — *N,N,N*-Diisopropylethylamine

DMAP — 4-(Dimethylamino)pyridine

DMF — *N,N*-Dimethylformamide

DMP — Dess-Martin Periodinane

DMPAP — Dimethoxyphenyl Acetophenone

DMSO — Dimethyl Sulfoxide

EDTA — Ethylenediaminetetraacetic Acid

Et — Ethyl

Equiv — Equivalent

ELLA — Enzyme-Linked Lectin Assay

ESI — Electrospray Ionization

Fucp — Fucopyranose

ΔG — Gibb's Free Energy Change of a Process

Galp — Galactopyranose

GalNAc — *N*-Acetylgalactosamine

gHMQC — Gradient Enhanced Heteronuclear Multiple Quantum Coherence

GlcP — Glucopyranose

GlcNAc — *N*-Acetylglucosamine

ΔH — Enthalpy Change of a Process

HD-STZ — Single High Dose of Streptozocin

His — Histidine

HMBC — Heteronuclear Multiple Bond Correlation

HMQC — Heteronuclear Multiple Quantum Coherence

HRMS — High Resolution Mass-Spectrometry

HSQC — Heteronuclear Single Quantum Coherence

IC₅₀ — Half-maximal Inhibitory Concentration

ITC — Isothermal Calorimetry

K_d — Dissociation Constant

L-selectride — Lithium Tri-*s*-butylborohydride

LCMS — Liquid Chromatography Mass-Spectrometry

*m*CPBA — *m*-Chloroperoxybenzoic Acid

Manp — Mannopyranose

Me — Methyl

MIC — Minimal Inhibitory Concentration

MP2 — Møller–Plesset Perturbation Theory (“2” refers to the second order electron correlation effect)

Ms — Methanesulfonyl

MST — Microscale thermophoresis

MW — Microwave Irradiation

Nap — Naphthylmethyl

NBS — *N*-Bromosuccinimide

Neu5Ac — *N*-Acetylneuraminic acid

NIS — *N*-Iodosuccinimide

Ni-NTA — Nickel Nitrilotriacetate

NMR — Nuclear Magnetic Resonance

n/a — Not applied

n/r — Not reported

OGT — *N*-Acetylglucosaminyl transferase

PBS — Phosphate-Buffered Saline

PDB — Protein Data Bank

Pr — Propyl

ⁱPr — Isopropyl

Ph — Phenyl

Phe — Phenylalanine

PMB — *p*-Methoxybenzyl

ppm — Parts Per Million

PTSA — *p*-Toluenesulfonic Acid Monohydrate

Py — Pyridine

PyBOP — Benzotriazol-1-yloxytripyrrolidinophosphonium Hexafluorophosphate

quant — quantitatively

R — Gas Constant (in equations)

R_f — Retention Factor

RSCC — Real Space Correlation Coefficient

ΔS — Entropy Change of a Process

Sat — Saturated (solution)

SDT — Standard Deviation

S_N1 — Unimolecular Nucleophilic Substitution

S_N2 — Bimolecular Nucleophilic Substitution

SPR — Surface Plasmon Resonance

STD-NMR — Saturation Transfer Difference Nuclear Magnetic Resonance

Stick's reagent — Imidazole-1-sulfonyl Azide Hydrogen Chloride salt

STZ — Streptozocin

TES — Triethylsilyl

Tf — Trifluoromethanesulfonyl

TFA — Trifluoroacetic Acid

THF — Tetrahydrofuran

THP — Tetrahydropyranyl

TIPS — Triisopropylsilyl

TLC — Thin-Layer Chromatography

TMS — Trimethylsilyl

Trp — Tryptophan

Ts — *p*-Toluenesulfonyl

Tyr — Tyrosine

UV — Ultra-Violet

v/v — Volumetric ratio

VT NMR — Variable Temperature Nuclear Magnetic Resonance

Xylp — Xylopyranose

CHAPTER 1

INTRODUCTION TO THIOGLYCOSIDES AND THIOSUGARS AND THEIR APPLICATION IN MEDICINAL AND BIOORGANIC CHEMISTRY

1.1. Introduction to glycosides and glycoside mimetics

Carbohydrates and carbohydrate-containing molecules are important biologically active compounds involved in crucial processes occurring in living organisms,¹⁻⁸ such that the study of carbohydrates and their application in medicinal chemistry is an important part of organic chemistry.^{9, 10} One of the most common classes of carbohydrate-containing molecules is the *O*-glycosides (from here on referred to as glycosides) (**Figure 1.1**).

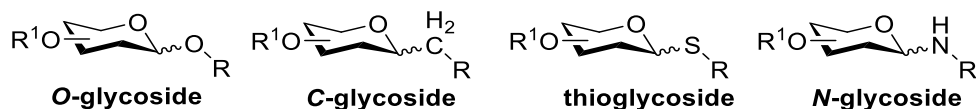


Figure 1.1. Structure of *O*-glycosides and their *C*-, *S*- and *N*-analogs.

To date great progress has been achieved in the fields of glycobiology and carbohydrate chemistry, and the structure, chemistry and reactivity of glycosides have been thoroughly studied and documented.¹¹

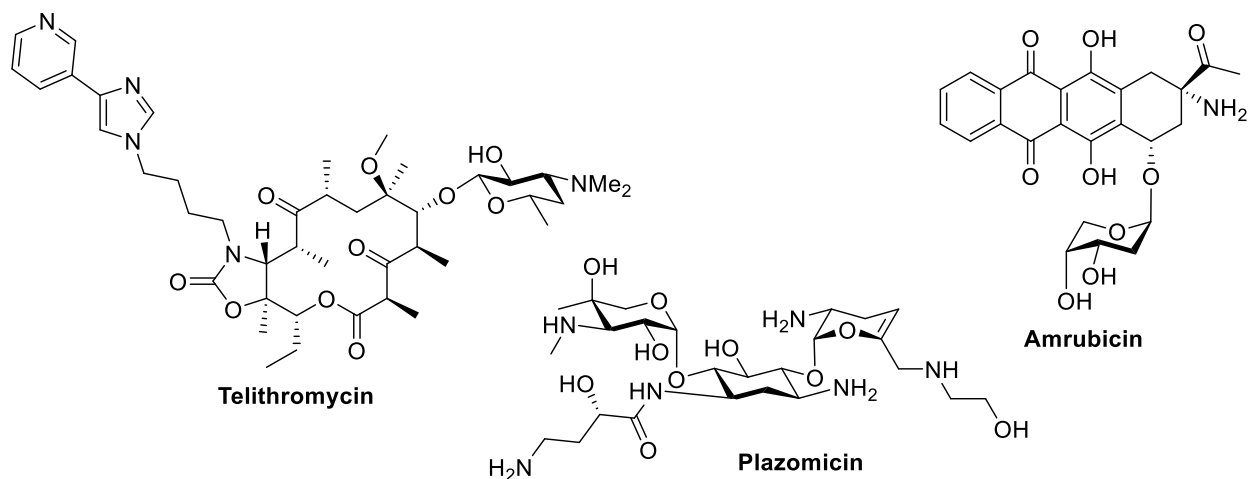


Figure 1.2. Structures of Telithromycin, Amrubicin, and Plazomicin.

In addition to that, many crystal structures of protein bound carbohydrates have been deposited in the PDB database, which provides extensive information on the structure of binding pockets, the conformation of carbohydrate ligands, and the role of the non-covalent interactions between carbohydrate ligands and protein receptors.¹² To date a considerable number of semi-synthetic glycoside-derived drugs have been approved by the FDA for use as therapeutic agents, as exemplified by Telithromycin, Luseogliflozin, and Plazomicin (**Figure 1.2**).¹³ Recently the investigation of glycoside mimetics gained much interest in carbohydrate chemistry and glycobiology as they can show unique chemical and biological properties. The glycosidic bond in such mimetics is replaced by surrogate glycosidic bonds resulting in the following derivatives: thioglycosides (*S*-glycosidic bond),¹⁴ *C*-glycosides (*C*-glycosidic bond),¹⁴ *N*-glycosides (*N*-glycosidic bond) (**Figure 1.1**).¹⁵

1.2. Thioglycosides and their application in bioorganic and medicinal chemistry

Thioglycosides, in which the glycosidic oxygen is replaced with sulfur, are perhaps the best known analogs of glycosides.¹⁴ Replacement of the glycosidic oxygen with the less electronegative¹⁶ and larger¹⁷ sulfur changes the polarity of the glycosidic bond, increases its length (1.82 Å length of C-S bond in comparison to 1.42 Å of C-O bond), and increases stability of thioglycosides toward hydrolysis (**Figure 1.3**).¹⁸

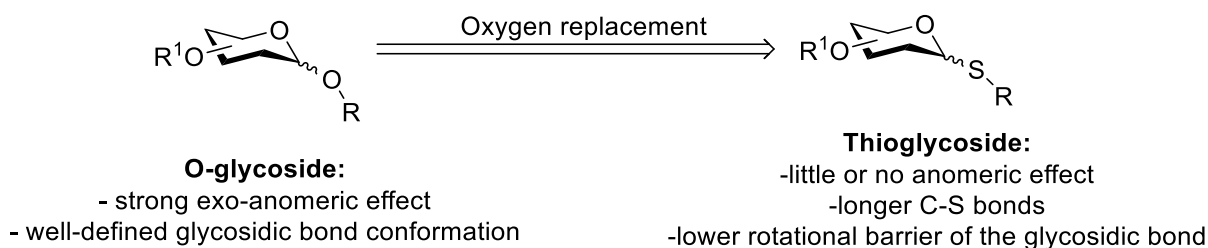


Figure 1.3. Comparison of *O*-glycosides and thioglycosides.

There are several known biologically active naturally occurring thioglycosides,¹⁴ such as the glucosinolates, which are β -glucosides of sulfated *N*-hydroxythioimides differing in the substituent R, e.g., Gluconasturtiin (**Figure 1.4**), that have been studied for their bactericidal,^{19, 20} fungicidal,²¹⁻²³ allelopathic²⁴ and other properties. Another example of a group of remarkable naturally occurring

thioglycosides are the lincomycins A-C that consist of methyl α -thiolincosaminide and differ in the substituents R' and R'' (**Figure 1.4**).¹⁴ The lincomycins A-B have found large application in clinical therapy for treatment of infections caused by Gram-positive bacteria and microplasmas.²⁵ Most known thioglycosides, however, are synthetic.

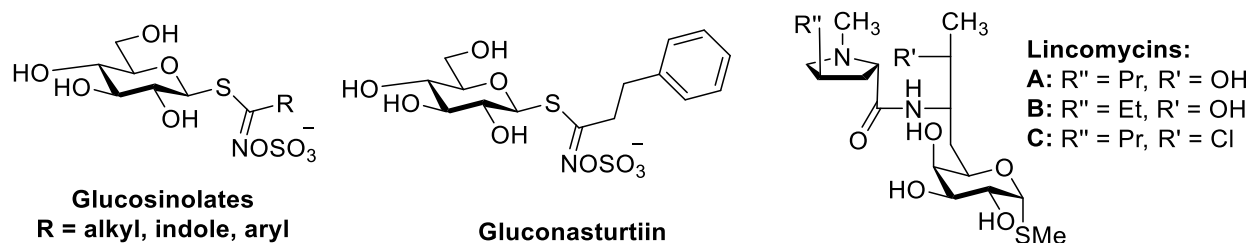
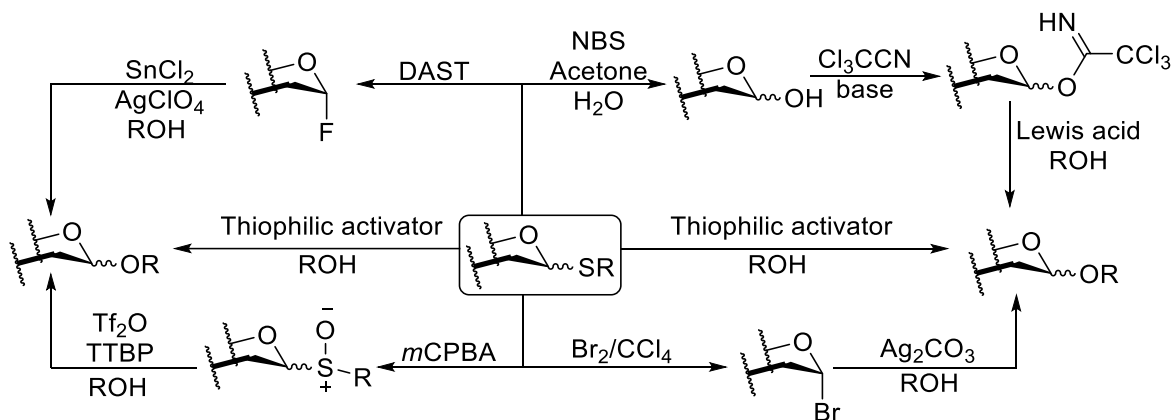
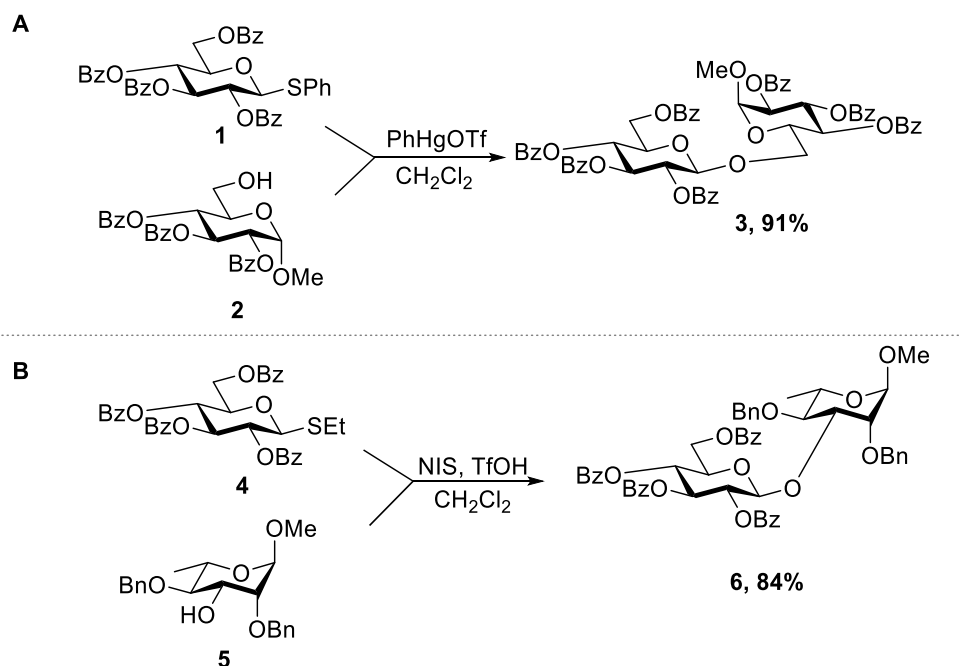


Figure 1.4. Structures of naturally occurring thioglycosides.

Thioglycosides have been extensively studied and used as glycosyl donors for the synthesis of oligosaccharides,²⁶ but the thioacetal group in such glycosides can also act as an anomeric protecting group (**Scheme 1**), showing good stability towards a wide range of reaction conditions, as well as serving as an efficient leaving group in glycosylation reactions (**Scheme 2**) upon activation with thiophilic promotor. Additionally, the presence of the sulfur atom allows a variety of reactions with soft electrophiles, e.g., halogens, and heavy metal cations (**Scheme 1**, **Scheme 2**).^{14, 27-30} The synthesis of the thioglycosides has received a great deal of attention in efforts to construct thiooligosaccharides, which can show comparable biological activity and increased resistance toward enzymatic cleavage.^{31, 32}

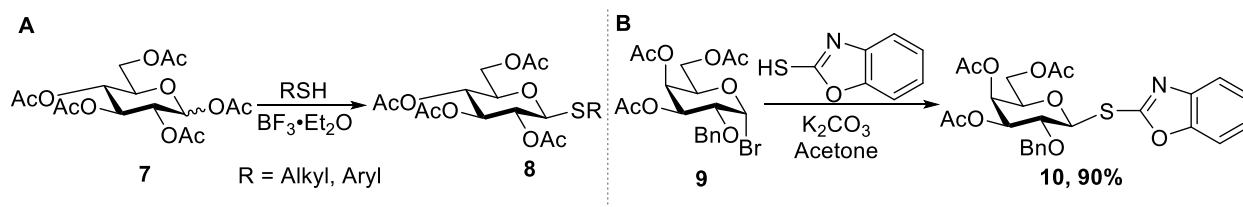


Scheme 1. Versatile reactivity of thioglycosides (figure adopted from Seeberger et al.).³⁰



Scheme 2. Glycosylation reaction with thioglycosides as glycosyl donors **A**: Soft metal salt promoted glycosylation with thioglycoside glycosyl donor **1**; **B**: Iodonium promoted glycosylation of thioglycoside glycosyl donor **4**.

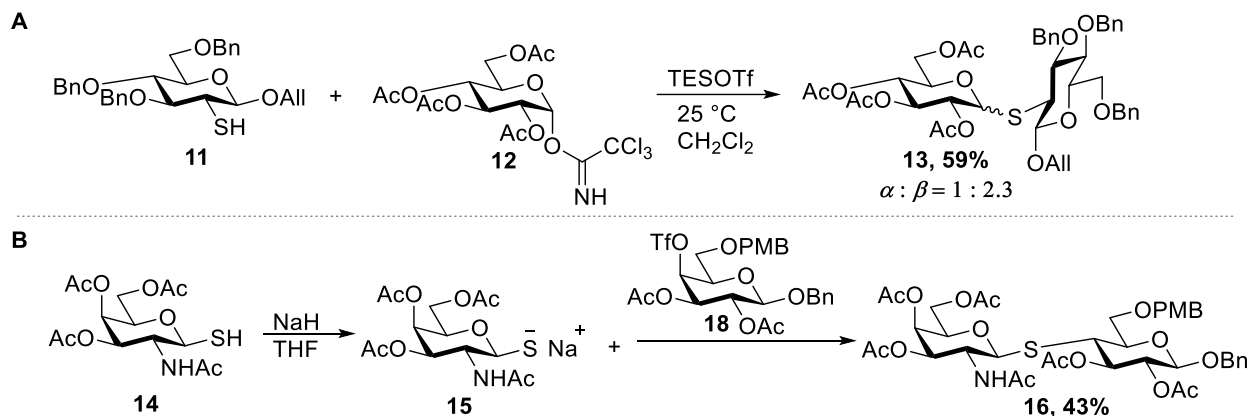
To date several synthetic methods for thioglycosides have been developed. The most common methods to synthesize simple thioglycosides are either by a Lewis acid-promoted glycosylation reaction³³ between simple alkyl(aryl) thiols and glycosyl donors with good leaving groups at C-1 (from this point onward referred to as the anomeric position) or, alternatively, by base promoted coupling of glycosyl halides with thiols (**Scheme 3**).



Scheme 3. A: Lewis acid catalyzed glycosylation with a simple thiol; **B:** Base mediated coupling of a glycosyl bromide **10** with a thiol.

More complex thiooligosaccharides can be accessed by glycosylation reactions between thiol-containing acceptors and activated glycosyl donors, such as trichloroacetimidates or glycosyl halides

(Scheme 4A).³⁴ Thioglycosides also can be accessed through S_N2 alkylation of anomeric thiolates with activated electrophiles (Scheme 4B).^{35, 36}



Scheme 4. A: Glycosylation reaction between thiol **11** and trichloroacetimidate **12**,³⁴ **B:** S_N2 alkylation of anomeric thiolate **17** with triflate **18**.³⁷

The introduction of a sulfur atom with its longer C-S bonds decreases the *exo*-anomeric effect in thioglycosides with respect to simple glycosides, where the *exo*-anomeric effect refers to the propensity of an aglycon to adopt a configuration and conformation that will result in hyperconjugation between lone pair n of the glycosidic oxygen O1 and the unoccupied antibonding molecular orbital σ^* of the C1-O5 bond (Figure 1.5).

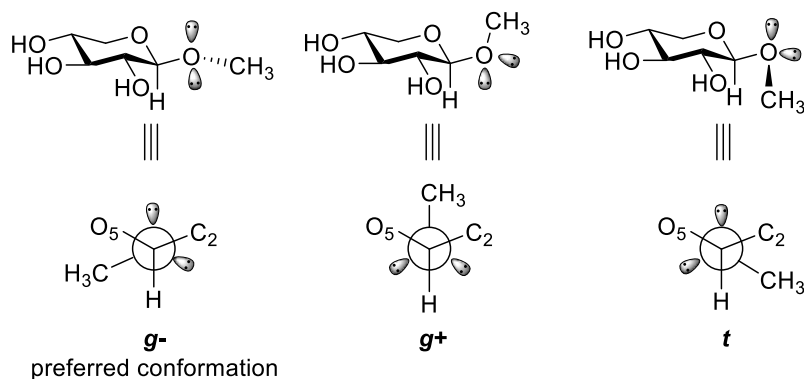


Figure 1.5. Three plausible conformations of the glycosidic bond in methyl β -D-xylopyranoside and Newman projections along C₁-O₁ bond. The symbols *g*⁺, *g*⁻, and *t* refer to the Me-O₁-C₁-O₅ torsion angle, +60°, -60° and 180° respectively (Figure adopted from Alonso et al.).³⁸

Increased bond length and less effective overlap with the 3sp³ lone pair of sulfur drastically decreases the *exo*-anomeric effect and, since the *exo*-anomeric effect is the main factor controlling the

conformation about the glycosidic bond, thioglycosides have a lower rotation barrier of glycosidic bond as compared to the parent glycosides (**Figure 1.3**).³⁹ Thus, thioglycosides must pay an increased entropic penalty on binding to a receptor that has evolved to bind the more conformationally restricted *O*-glycosides. The reduced *exo*-anomeric effect of thioglycosides and its consequences is the most common reason advanced for their frequently reduced “biological activity” over the simple glycosides.⁴⁰ However, it is not always the case that thioglycosides are less active as there are several cases where thioglycosides showed strong inhibitory activity.^{31, 41-47}

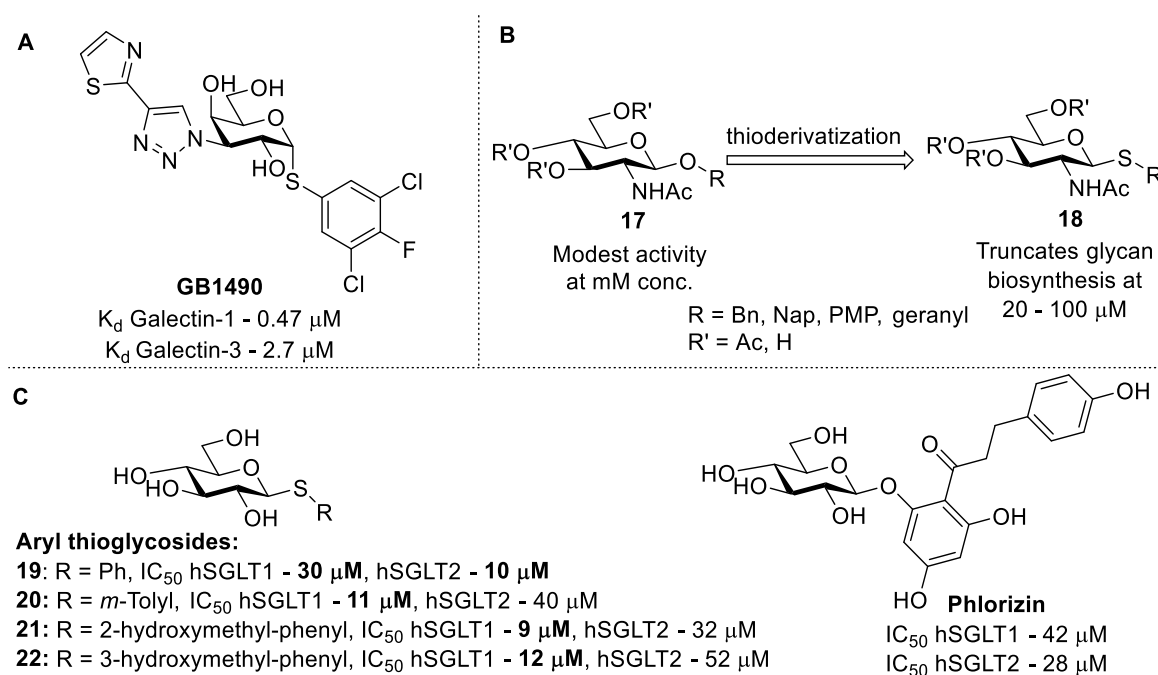


Figure 1.6. Structures of biologically active thioglycosides. **A:** Orally bioavailable thioglycoside **GB1490** with micromolar inhibitory activity against Galectin-1 and Galectin-3; **B:** Structure of thioglycosidic analogs **18** showing micromolar activity; **C:** Structures of aryl thioglycosides **19-22** with micromolar inhibitory activity against hSGLT1 and hSGLT2.

One of the most striking recent examples of this phenomena is the 2023 report by Zetterberg et al. wherein a new series of orally available thio-galactopyranosides functionalized with five-membered aryl-triazolyl substituents at C-3 were synthesized and evaluated.⁴⁸ Compound **GB1490** (**Figure 1.6A**) showed the highest micromolar inhibitory activity of Galectin-1 and Galectin-3. Another example of thioglycosides showing higher affinity than *O*-glycosides is a 2018 report by Wang et al. where it was demonstrated that thioglycosidic analog **18** of the *N*-acetylglucosamine **17** was significantly more stable toward enzymatic

hydrolysis and was able to completely stop glycan biosynthesis at μM concentrations (**Figure 1.6B**), while the *O*-glycoside **17** showed little or no inhibition in the same concentration range.⁴⁶ In addition, in recent work by Kinne,⁴³ several aryl thioglycosides **22-25** showed inhibitory activity against human sodium D-glucose cotransporters hSGLT2 or hSGLT1 and so had a potential to be used as a promising therapeutic agents to control hyperglycemia. All synthesized thioglycosides **19-22** showed improved IC_{50} against hSGLT1 (up to 5-fold increase for **21**) as compared to phlorizin, however, only thioglycoside **19** showed a high IC_{50} against hSGLT2 (**Figure 1.6C**). Finally, in a 2013 report by Roy, several aryl thioglycosides were designed, synthesized, and were evaluated for their ability to inhibit the binding of the LecA lectin to the galactosylated surface in comparison to methyl α -D-galactopyranoside. In this study thioglycosides **23-26** showed improvement in IC_{50} against the LecA lectin, up to the 23-fold increase in case of **23** in comparison to the methyl glycoside **26** (**Figure 1.7**).⁴²

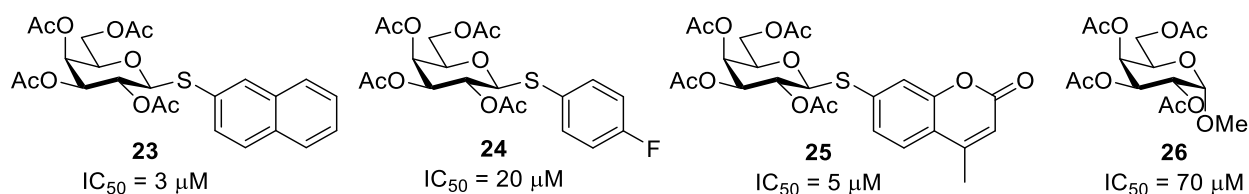


Figure 1.7. Structures of aryl thioglycosides **23-25** with micromolar inhibitory activity against LecA lectin binding to the galactosylated surface in comparison to the methyl α -D-galactopyranoside **26**.

1.3. Thiosugars and their application in bioorganic and medicinal chemistry

5-Thiosugars are another class of thio mimetics of glycosides, in which the ring oxygen, O5 for pyranosides, is replaced by sulfur. Similarly to thioglycosides, replacement of the ring oxygen with the less electronegative and larger sulfur leads to changes in the C5-S-C1 bond polarity and length, as well as in the C5-S-C1 bond angle, which results in a more puckered conformation of the 5-thiopyranose ring (**Figure 1.8**).⁴⁹ Remarkably, thiosugars tend to be more stable towards enzymatic hydrolysis than natural counterparts.^{50, 51} Moreover, thiosugars are remarkably polar compounds due to the realignment of the C-OH bonds around the ring enforced by the puckering. Additionally, thiosugars tend to have a larger

anomeric effect compared to their natural counterparts, which is mainly caused by decreased diaxial interactions in 5-thioglycopyranosyl ring upon puckering.⁵²⁻⁵⁴

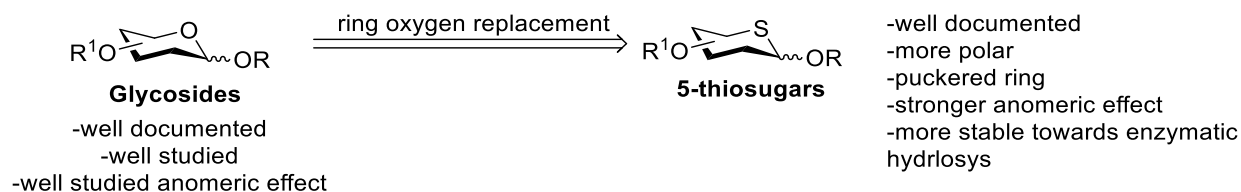


Figure 1.8. Comparison of glycosides and 5-thiosugar glycosides.

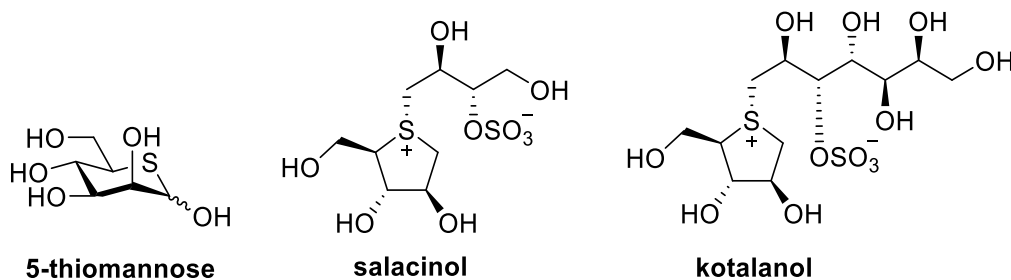


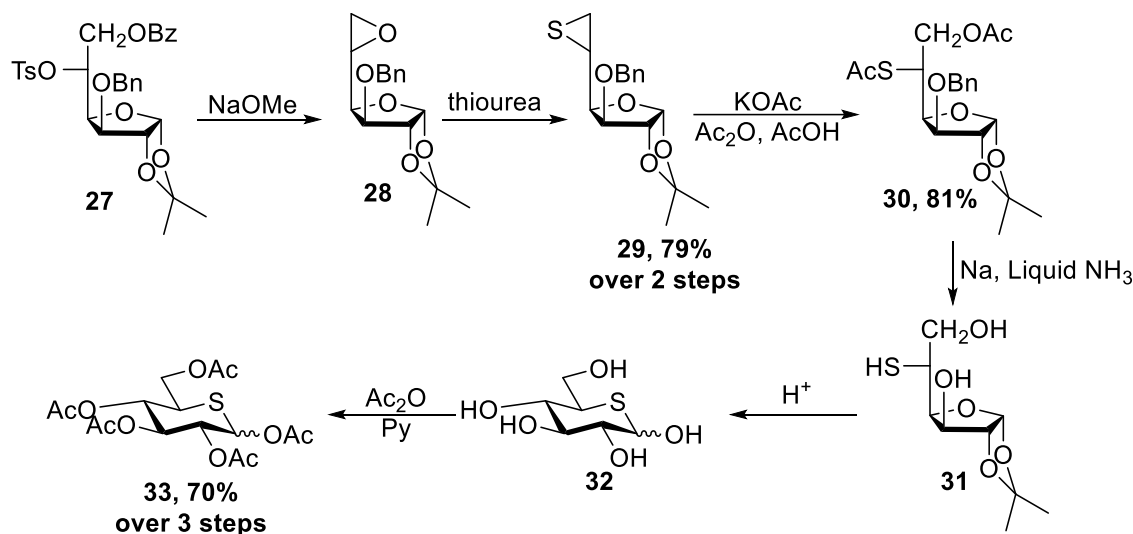
Figure 1.9. Naturally occurring thiosugars.

To date several thiosugars have been isolated from the natural sources (**Figure 1.9**), including: 5-thio-D-mannose (the first identified naturally occurring free thiosugar),⁵⁵ salacinol and kotalanol (1,4-thioanhydrosugars bearing sulfonium ion-containing heterocycles).⁵⁶ Evaluation of these thiosugars revealed a variety of biological properties, e.g., salacinol and kotalanol were found to be effective sucrose α -D-glucosylhydrolase inhibitors,^{57, 58} as well as potent inhibitors of intestinal α -glucosidases.⁵⁹

The first synthesis of 5-thio-D-xylopyranose⁶⁰ and 5-thio-D-glucose,⁶¹ reported by Whistler, raised interest in the synthesis of the general class of thiosugars.⁵⁹ Following that, to date several synthetic approaches have been reported,^{59, 62-66} and several mimetics of natural carbohydrates have been synthesized, including 4-thio-D-ribose,⁶⁷ 5-thio-L-arabinose,⁶⁸ 5-thio-D-arabinose, 5-thio-D-lyxose⁵⁴ and 5-thio-D-mannose.⁶⁹ The most common synthetic approach (**Figure 1.10**) towards 5-thiosugars is the introduction of a thiol group at C-5, which can be achieved by nucleophilic opening of the 5,6-episulfide at C6 with strong nucleophiles (e.g., acetate ion), followed by cyclization.⁶² This strategy was first used in the synthesis of 5-thioglucofuranose by Whistler (**Scheme 5**),⁷⁰ in which first, the *p*-toluenesulfonate species **27** was treated with

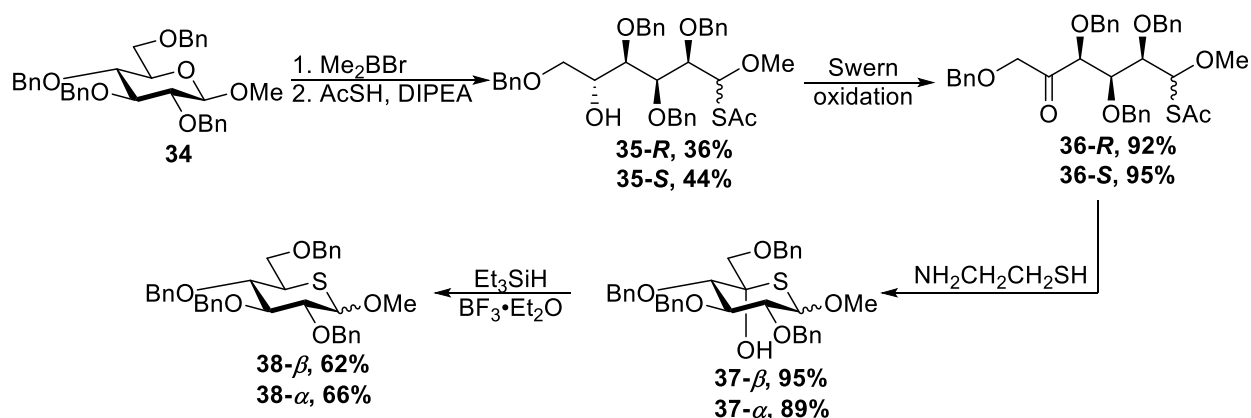
Figure 1.10. Summarized synthetic approaches towards 5-thiosugars (adopted from Al Bujuq et al.).⁶²





Scheme 5. Synthesis of 5-thioglucose by Whistler et al.⁷⁰

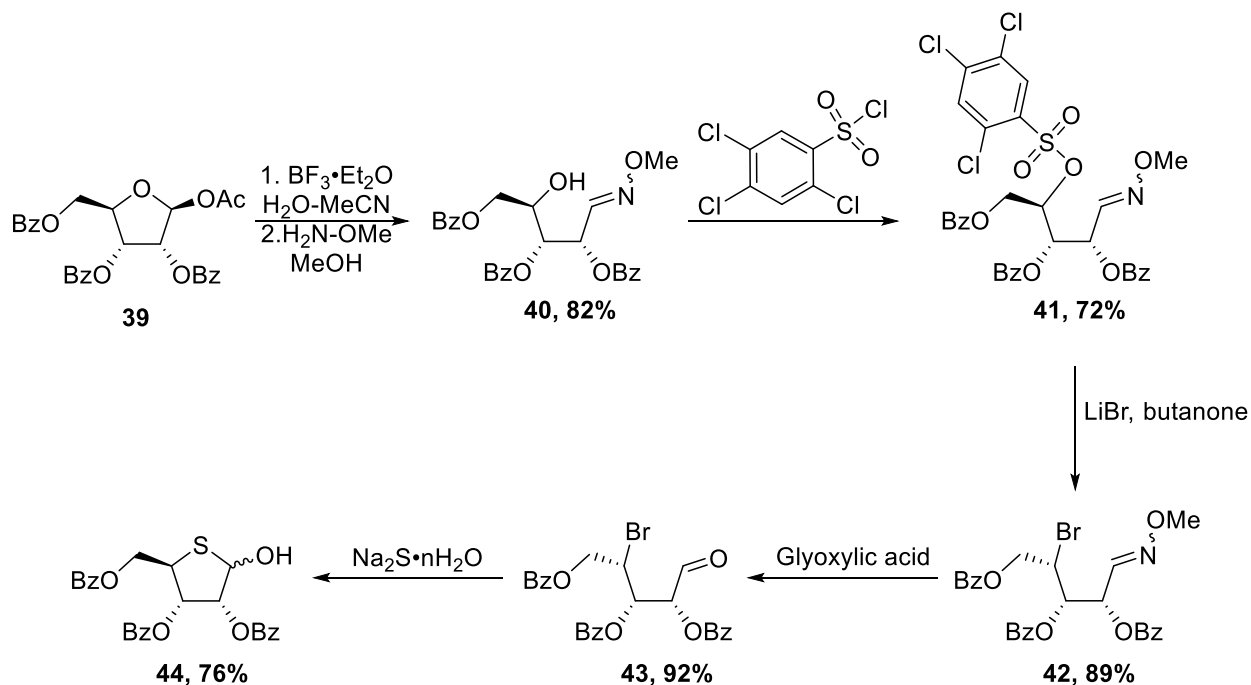
Alternatively, thiosugars can be accessed through pyranose ring opening, introduction of thiol group at either the anomeric or C-5 position, and subsequent ring closing. In 1995 Hashimoto and colleagues reported an alternative synthetic route towards 5-thioglucose (**Scheme 6**).⁷¹ This synthesis was accomplished via dimethylboron bromide and thioacetic acid induced ring opening of the methyl glycoside **34** to produce mixture of *S*-acetyl *O*-methyl monothioacetals **35-R** and **35-S**, which upon oxidation gave cyclization precursors **36-R** and **36-S**, respectively. Finally, cyclization, triggered by deprotection of the thioacetate, and subsequent deoxygenation of the tertiary alcohol **37** produced 5-thioglucose derivative **38**.



Scheme 6. Alternative synthetic route towards 5-thioglucose reported by Hashimoto.⁷¹

A 2021 report by Miller et al described the synthesis of 4-thioribose via introduction of a thiol at C-4 with double inversion of configuration (**Scheme 7**).⁷² This synthesis began with a hemiacetal, generated from **39**, and coupling with methyl hydroxylamine to produce oxime **40**. Then, sulfonylation and displacement of sulfonate produces bromide **42** with inversion of configuration at C-4. Finally, oxime hydrolysis released aldehyde **43**, and subsequent displacement of bromide with inversion and spontaneous cyclization produced 4-thioribose **44**.

Synthetic thiosugars have shown antiviral,^{73, 74} antibiotic⁷⁵ and anticancer⁷⁶ properties, however, direct comparison with the parent glycosides is not always presented in such works, as changes in 5-thiopyranose ring conformation often result in lower biological activity of 5-thiosugars in comparison to natural counterparts.^{77, 78} Nevertheless several studies have been reported demonstrating cases when thiosugars were more active than their *O*-counterparts.⁷⁹⁻⁸¹



Scheme 7. Synthesis of 4-thioribose via a ring opening-double displacement-ring closing sequence.

Recently the Crich group reported the synthesis and evaluation of 1,5-dithio mimetics of β -(1 \rightarrow 3)-glucans.⁸⁰ Dimeric, trimeric, and tetrameric 1,5-dithio analogs of laminaribiose, triose and tetraose, in

which both the endocyclic ring oxygen and the glycosidic oxygen were replaced with sulfur, were synthesized, evaluated, and compared to the parent glycosides. The biological evaluation showed the best results for the trimeric 1,5-dithio analog **46**, which displayed higher inhibition and phagocytosis in comparison to laminaritrise (**Figure 1.11**), and had activity comparable to the oligomeric glucan 300 ®. Notably, the smallest analog **45** showed higher inhibitory activity and comparable phagocytosis activity. Therefore, 1,5-dithio analogs were found to be potent mimetics of β -(1-3)-glucans, as they are relatively easier to synthesize and require shorter chain lengths than the natural β -(1-3)-glucans.⁸² Additionally, a recent report by the Vocadlo group⁷⁹ showed that the 5-thio analog **49** of *N*-acetylglucosamine was a more potent *in vivo* metabolic inhibitor of *O*-GlcNAc transferase (OGT), as compared to the parent compound **48**; moreover, the presence of the mimetic leads to a decrease of *N*-acetylglucosamine levels in tissues (**Figure 1.12**). To date several research works have been published on this general area, demonstrating that 5-thioglucose can be a competitive inhibitor of various enzymes, as well as a modulator of glucose levels.⁷⁸

83-85

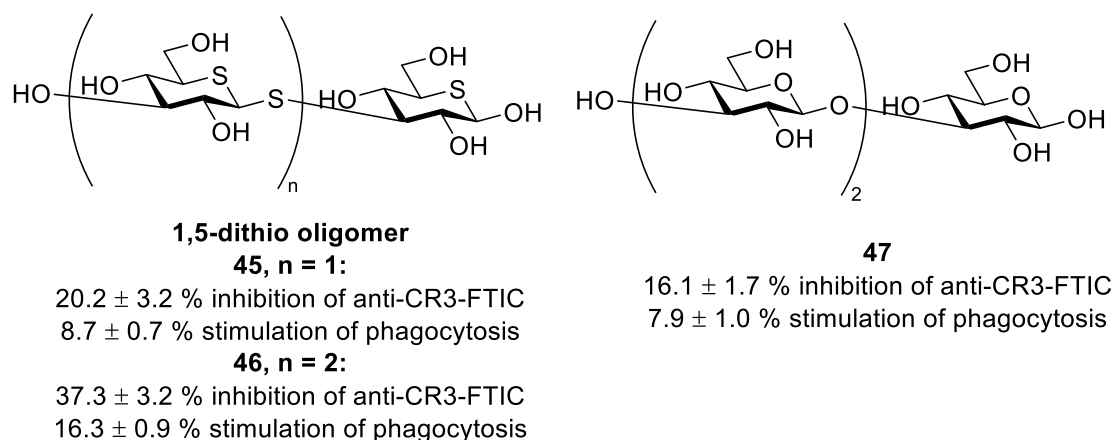


Figure 1.11. Structure and biological activity of 1,5-dithio mimetics **45**, **46** of laminaribiose and triose.

The Gleichmann group reported biological studies of high- and low-dose STZ-induced diabetes by glucose and 5-thioglucose,⁸¹ which showed that 5-thioglucose exerted better protection against HD-STZ-induced hyperglycemia in comparison to glucose.

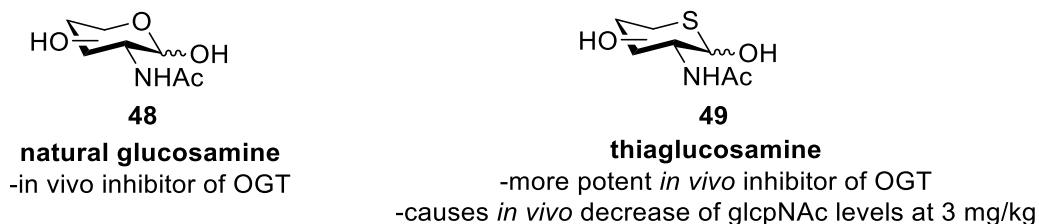
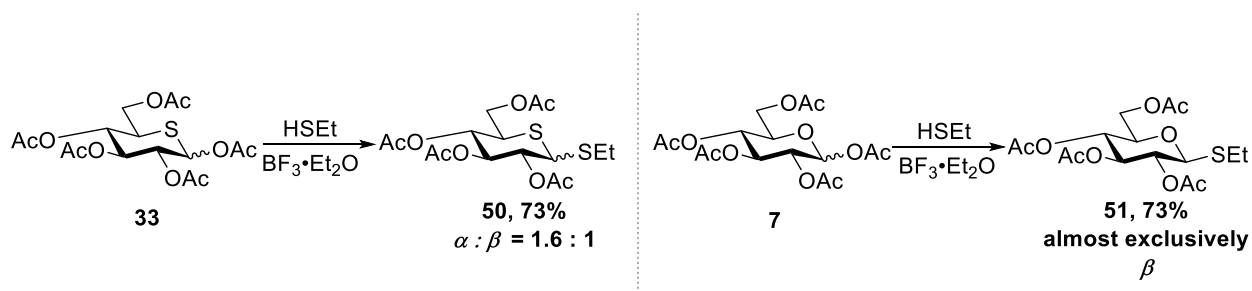


Figure 1.12. Structure of potent *in vivo* inhibitor of OGT.

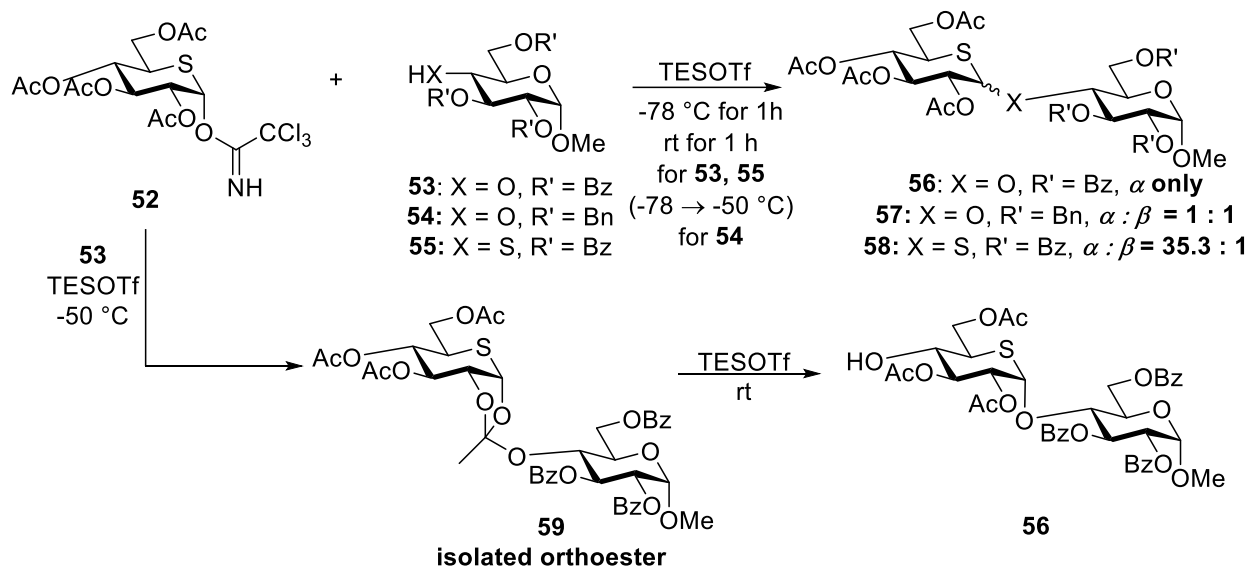
1.4. Reactivity of 5-thiosugars

Replacement of the ring oxygen with less electronegative sulfur drastically changes the electronics of the sugar ring, as well as polarity of C5-S-C1 bond, and thus impacts the behavior of the corresponding 5-thioglycosyl donors. To date several reports on the synthesis of oligosaccharides from 5-thioglycosyl donors have been published, and show that 5-thioglycosyl donors have remarkable axial selectivity in the glycosylation reactions. Pinto and coworkers in their synthesis of a sulfonium analog of castanospermine reported⁸⁶ a glycosylation reaction between peracetylated 5-thioglucose **33** and ethanethiol, which showed no selectivity (**Scheme 8**), producing mixture of thioglycosides **50** ($\alpha : \beta = 1.6 : 1$). In contrast, the same glycosylation reaction with glucose pentaacetate **7** would be expected to produce almost exclusively β -thioglycoside **51** (**Scheme 8**).⁸⁷



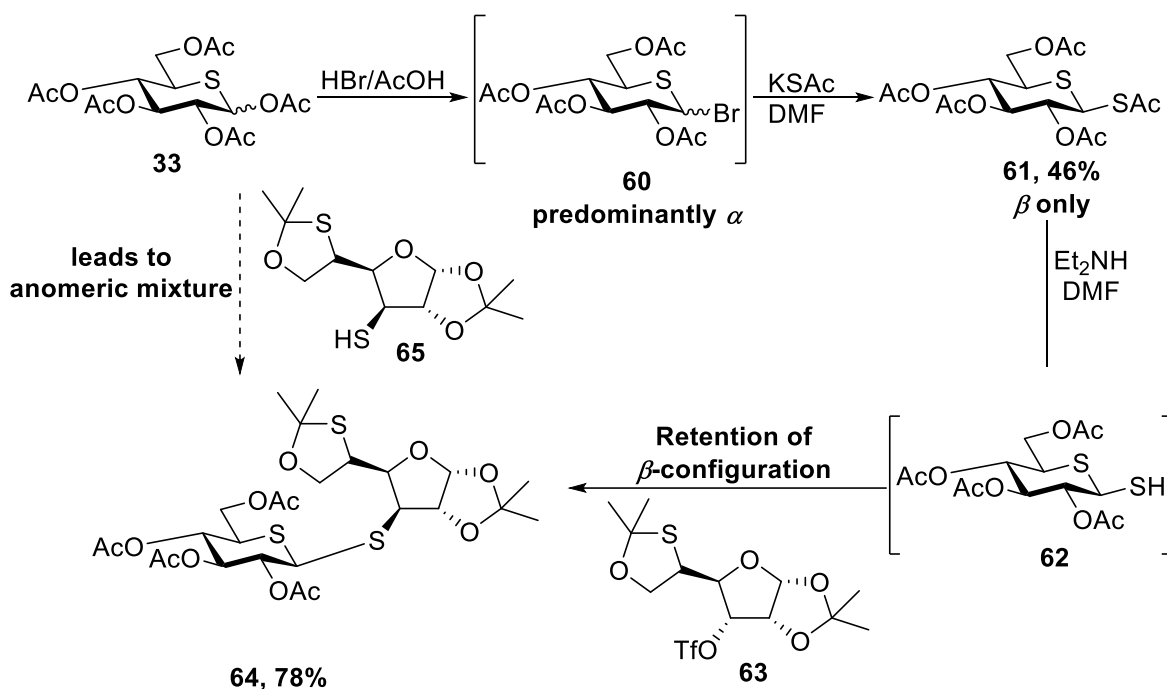
Scheme 8. Comparison of the glycosylation outcome with 5-thioglycosyl **33** and parent glycosyl acetate **7** donors and ethanethiol.

Moreover, Pinto and co-workers in their work demonstrated highly axially selective glycosylation reaction with peracetylated 5-thioglycosyl trichloroacetimidate (**Scheme 9**).



Scheme 9. Glycosylation reactions with 5-thioglycosyl trichloroacetimidate **52** and various glycosyl acceptors.

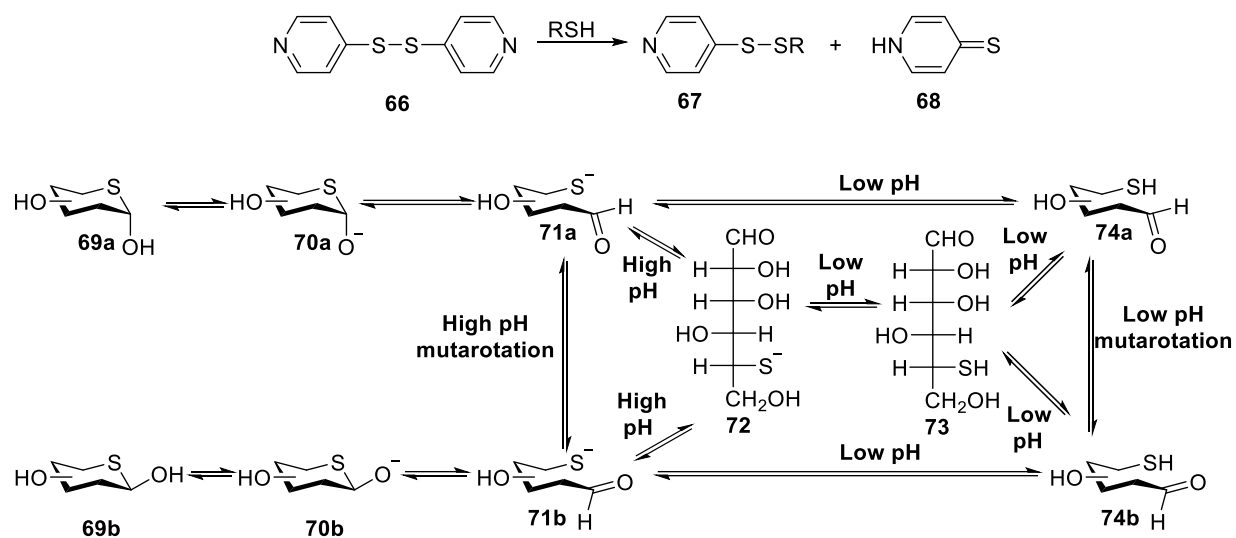
The glycosylation reaction with perbenzoylated glycosyl acceptor **53** afforded only α -linked disaccharide **56**, however, replacement of **53** with more reactive glycosyl acceptor **54** improved the β -selectivity of glycosylation reaction, producing a mixture of disaccharides **57** ($\alpha : \beta = 1 : 1$). The high axial selectivity in glycosylation reactions to form **56-58** was explained by rearrangement of the orthoesters, one of which, **59**, was successfully isolated at $-50\text{ }^\circ\text{C}$, and then subjected to the glycosylation reaction conditions at room temperature which triggered its rearrangement to the corresponding α -disaccharide **56**.⁸⁸ To circumvent the high axial selectivity of 5-thioglycosyl donors, Crich and co-workers in their synthesis of 1,5-dithio mimetics of laminaribiose, triose and tetraose, adopting the approach of Hindsgaul on synthesis of thiooligosaccharides⁸⁹ and of Hughes on synthesis of 5-thiosugar glycosides,⁹⁰ employed a 3 step sequence to ensure exclusively β -glycosylation product (**Scheme 10**).⁸⁰



Scheme 10. Synthesis disaccharide **64** with β -glycosidic linkage.

In this synthesis, bromination of pentaacetate **33** produced mixture of glycosyl bromides **60** containing predominantly α -anomer, which was subjected to S_N2 -type displacement with potassium thioacetate to afford β -thioacetate **61**. Thioacetate **61** then was subjected to glycosylation reaction with triflate **63** in presence of Et_2NH to produce disaccharide **64** with the desired β -thioglycosidic bond. On the other hand, direct glycosylation reaction of pentaacetate **33** and thiol **65** would produce mixture of anomeric disaccharides.

Cleland and co-workers reported a comprehensive study on the ring opening and closing rates for thiosugars, and their mutarotation rates.⁹¹ Simple aliphatic thiols or thiosugars were coupled (**Scheme 11**) with 4-dipyridyl disulfide **66**, which, in presence of a free thiol group (SH), can undergo disulfide exchange to form new disulfide **67** and release 4-thiopyridone **68**. The reaction was monitored spectrophotometrically, by detecting 4-thiopyridone **68** moiety generated during reaction.



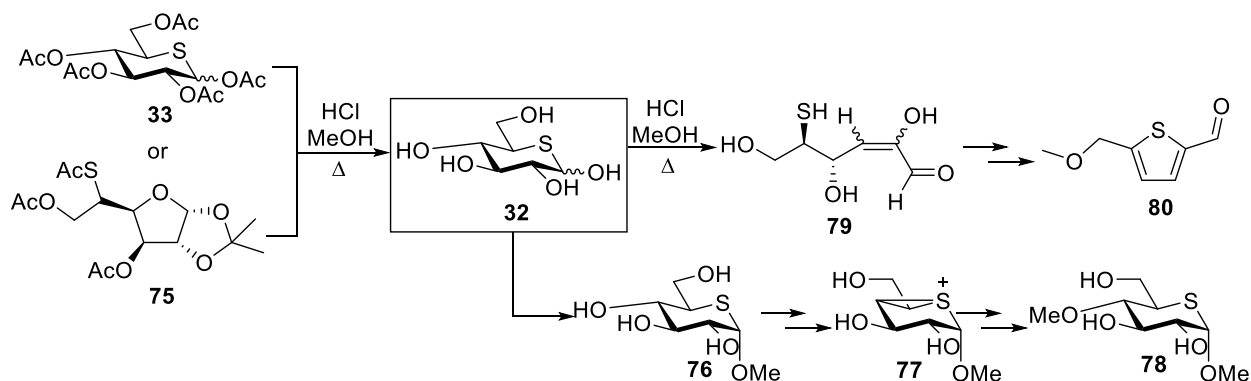
Scheme 11. Coupling reaction used in Cleland's study and proposed ring-opening and mutarotation mechanism of 5-thioglucose (adopted from Cleland et al.).⁹¹

Table 1. Ring opening rate and comparison of mutarotation rate of 5-thioglucose and glucose. k_0 — pH-independent reaction rate, k_B — base-catalyzed reaction rate.

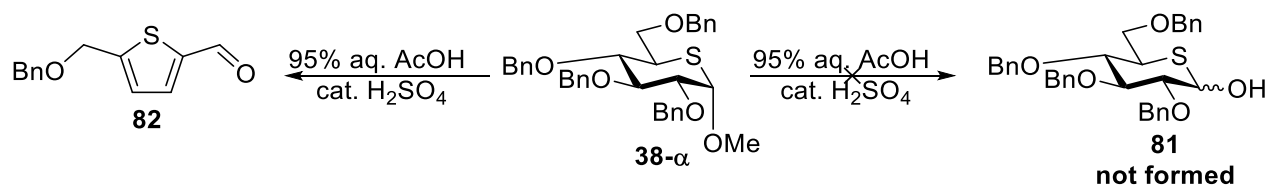
Compound	Ring-opening rate		Mutarotation rate	
	$k_0 \times 10^6 \text{ (s}^{-1}\text{)}$	$k_B \times 10^{-2} \text{ (M}^{-1} \text{s}^{-1}\text{)}$	$k_0 \times 10^6 \text{ (s}^{-1}\text{)}$	$k_B \times 10^{-2} \text{ (M}^{-1} \text{s}^{-1}\text{)}$
D-glucose	n/r	n/r	390	4.8
5-thio- α -D-glucopyranose	0.16	0.64	0.18	330

Thioglucose showed high rate constants of both pH-independent (k_0) and base-catalyzed (k_B) ring-opening reactions. In addition, 5-thioglucose showed comparable values of both pH-independent mutarotation rate constant and pH-independent ring-opening rate constant, suggesting that ring opening of the 5-thioglucose was accompanied by mutarotation. However, the base-catalyzed mutarotation rate constant was 515 times higher than base-catalyzed ring-opening rate constant, and 68 times higher than base-catalyzed ring-opening rate constant of parent D-glucose (**Table 1**). The authors rationalized their observations using a mechanism detailed for the 5-thioglucose (**Scheme 11**). In this mechanism base-catalyzed mutarotation proceeded through interconversion of **71a** and **71b** without ring opening, however at low pH charged species **71a** and **71b** were converted into **74a** and **74b**, respectively, and mutarotation proceeded through interconversion of **74a** and **74b**. When it comes to the ring opening, at high pH both **71a**

and **71b** were converted into open ring species **72**; however, at low pH species **71a** and **71b** were converted into **74a** and **74b**, respectively, and the latter was converted into open ring species **73**, which in return was converted into open ring species **72**. Later, Hashimoto et al. in their synthesis of peralkylated 5-thio-glucono-1,5-lactones reported⁹² methanolysis of pentaacetate **33** and thioacetate **75**, which produced the desired methyl glycoside **76** mixed with unexpected byproducts **78** and **80** (Scheme 12). The authors hypothesized that thiophene **80** was generated from α,β -unsaturated aldehyde species **79**, formed from **32** after dehydration at C3 position. In addition, desired methyl glycoside **76** formed episulfonium intermediate **77** via transannular participation of the ring sulfur,⁹³ nucleophilic opening of which furnished **78**. Moreover, hydrolysis of perbenzylated methyl glycoside **38- α** with 95% aq AcOH with a catalytic amount of H₂SO₄ (Scheme 13) did not produce any of the desired product **81**, and, instead, only thiophene **82** was generated. The mechanism to form thiophene **82** was assumed to be the same as that to form thiophene **80**.



Scheme 12. Methanolysis of **33** and **75** and structures of unexpected byproducts reported by Hashimoto et al.⁹²



Scheme 13. Hydrolysis of perbenzylated methyl glycoside **38- α** .

Such contrasting differences in reactivity and behavior of sugars and 5-thiosugars complicate the stereoselective synthesis of 5-thiooligosaccharides, and, perhaps, are one of the reasons why 5-thiosugar containing oligosaccharides are not very often used in medicinal and bioorganic chemistry.

1.5. Overall goals

This work seeks to rationalize the application of thioglycosides and 5-thiosugars in medicinal and bioorganic chemistry as thio-mimetics of parent *O*-glycosides. The first two projects discuss the application of both thioglycosides and 5-thiosugars in medicinal and bioorganic chemistry.

The first project, detailed in chapter 2, discusses design and synthesis of tetravalent glycoclusters containing 1,5-dithio mimetics of laminaribiose and -triose, and evaluation the of newly synthesized glycoclusters for their inhibitory activity against anti-CR3 and anti-Dectin-1 antibodies. The goal of the study was to evaluate the impact of multivalency on inhibitory activity of potent 1,5-dithio mimetics.

The second project, described in chapter 3, studies the impact of *S*- π interactions between the ring sulfur or thioglycoside bond sulfur and aromatic residues on binding affinity with lectins. The goal of the study was to create a predictive tool to predict when it is worth synthesizing 5-thio or thioglycosidic mimetics of parent *O*-glycosides.

The third project, covered in the thesis and described in chapter 4, explores the reactivity of 5-thiosugars and studies the generation and stability of reactive intermediates generated after activation of 5-thioglycosyl donors by variable temperature NMR experiments. The aim of the study is to attempt to explain the contrasting difference in reactivity and behavior between 5-thiosugars and parent *O*-counterparts.

CHAPTER 2

SYNTHESIS AND EVALUATION OF TETRAVALENT CONSTRUCTS CONTAINING 1,5-DITHIO MIMETICS OF β -(1 \rightarrow 3)-GLUCANS*

* Portions of this section and figures, included therein, and the corresponding experimental protocols, described in the Experimental Section (Chapter 6.2), are adapted with permission from D. Ahiadorme, C. Ande, R. Fernandez-Botran, and D. Crich *Carbohydr. Res.* **2023**, 525, 108781. Copyright © 2023 Elsevier.

2.1. Introduction

The β -(1 \rightarrow 3)-glucans **83** (**Figure 2.1**) are widely occurring natural immunomodulating agents found in yeasts, seaweeds and fungi,⁹⁴⁻⁹⁷ which are known to potentiate tumor-specific antibodies, modulate the effects of radiation and photodynamic therapy,⁹⁸⁻¹⁰⁰ mitigate allergic rhinitis,¹⁰¹ and regulate stress,¹⁰² in addition to other properties.¹⁰³

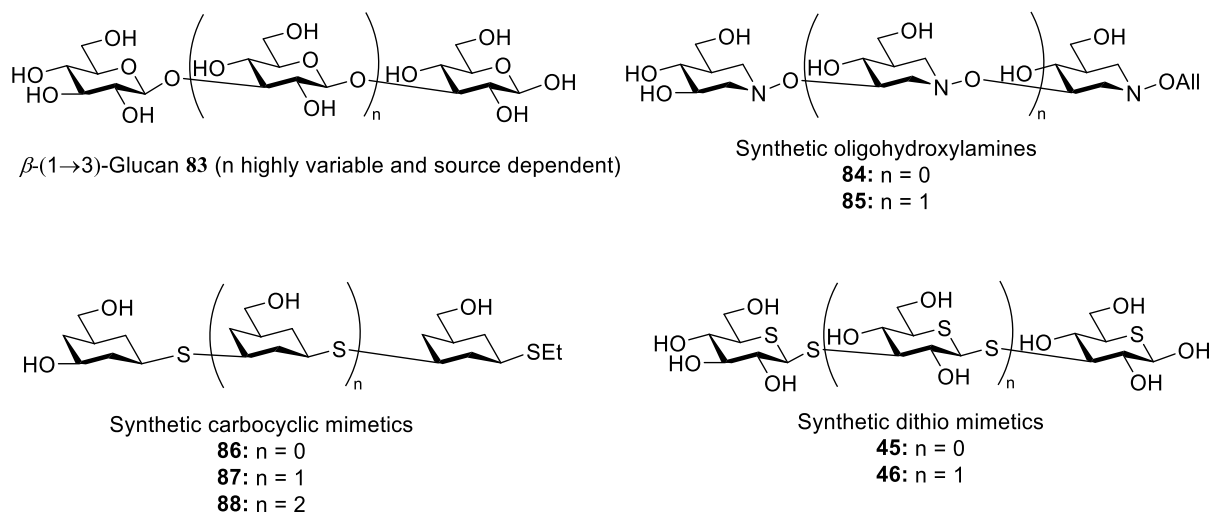


Figure 2.1. Structure of β -(1 \rightarrow 3)-glucans and their mimetics

Despite widespread availability, the isolation of pure homogenous β -(1 \rightarrow 3)-glucans is complicated, as extensive chromatographic purifications and aqueous extractions are required to isolate pure oligomeric glycans. On the other hand, to date many efforts have been devoted to the synthesis of the β -(1 \rightarrow 3)-glucan oligomers and evaluation of their immunomodulating properties.¹⁰⁴⁻¹⁰⁷ The immunostimulating properties of the β -(1 \rightarrow 3)-glucans are considered to arise from their affinity for the lectin regions of complement receptor 3 (CR3)^{102, 108, 109} and Dectin-1,¹¹⁰⁻¹¹² binding to which triggers a cascade of effects including phagocytosis, and pinocytosis. Studies⁸² of homogenous β -(1 \rightarrow 3)-glucans demonstrated that the shortest oligomer capable of detectable binding to recombinant murine Dectin-1 in a microarray format is the 10- or 11-mer. However, later it was shown^{113, 114} that hexa- or pentameric β -(1 \rightarrow 3)-glucans modified at the reducing end by the replacement of the terminal glucopyranose residue with gluco- **89** and manno-configured **90** glycitols (**Figure 2.2**) retained the ability to promote phagocytosis.

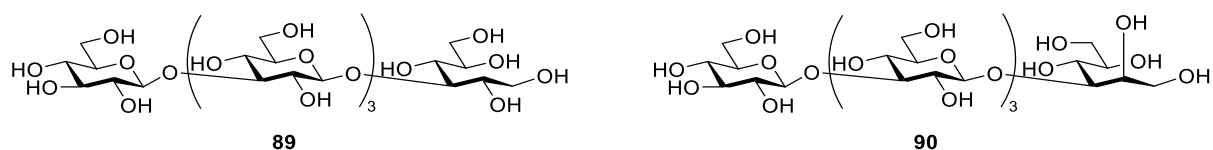


Figure 2.2. Structures of synthetic pentasaccharides with glucitol **89** and mannitol **90** terminal modification.

X-ray crystallographic studies of recombinant Dectin-1 revealed the presence of a hydrophobic pocket defined by the Trp-221 and His-223 moieties in carbohydrate binding region of lectin (**Figure 2.3**).¹¹⁵ Spectroscopic experiments have showed hydrophobic interactions between the α -face of terminal pyranose rings in natural β -(1 \rightarrow 3)-glucan and the lectin domain.¹¹⁶ In addition, recent STD NMR studies revealed that only synthetic β -(1 \rightarrow 3)-glucan hexadecamer and higher oligomers bind to the lectin domain of Dectin-1.¹¹⁷ This could be explained by an enhancement of relatively weak carbohydrate-protein¹¹⁸⁻¹²⁰ interactions by the multivalent effect arising from the repeated presence of the epitope in the form of polymeric glycans. Surface plasmon resonance (SPR) experiments revealed similar results, demonstrating binding of multiple Dectin-1 molecules to a single polymeric β -(1 \rightarrow 3)-glucan backbone with the affinity increasing in an additive fashion.¹²¹ Evidence that hydrophobic binding pockets in CR3 and Dectin-1 can accept small carbohydrate epitopes suggests that the ligand-receptor interaction may be enhanced by modification of the carbohydrate epitope. Following this idea several short synthetic β -(1 \rightarrow 3)-glucans and their 1-thio analogs were described.¹²² Pursuing a glycomimetic approach for the synthesis of improved β -(1 \rightarrow 3)-glucan analogues, the Crich group designed and evaluated hydroxylamine-based glycan analogs **84-85** (**Figure 2.1**) which showed significant affinity for CR3 and Dectin-1.¹²³ It was hypothesized that the enhanced binding of the mimetics **84-85** was caused by increased hydrophobicity of the α -face after replacement of both the C2-OH group and ring oxygen with methylene groups.

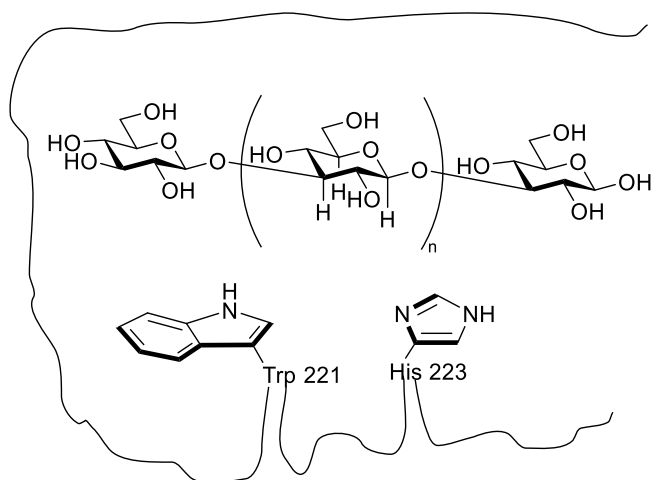


Figure 2.3. Schematic representation of the hydrophobic α -face of a β -(1 \rightarrow 3)-glucan in complex with Trp-221 and His-223 residues in the binding pocket of the Dectin-1-lectin domain.

Following that hypothesis, the Crich group reported the synthesis and evaluation of short thioether linked carbosugars **86-88**,¹²⁴ and 1,5-dithio analogs **45-46** of laminaribiose, triose, and tetraose⁸⁰ (**Figure 2.1**), all of which showed some binding affinity to the carbohydrate domains of the lectin, which was reflected in their comparable ability to stimulate phagocytosis and pinocytosis. Building on those observations, we hypothesized that incorporation of 1,5-dithio mimetics **45-46** into a multivalent core could improve overall activity as a result of multiple ligand-protein interactions occurring between the glycocluster and the lectin.

To date much effort has been made in designing multivalent cores¹²⁵ and developing glycoclusters based on those cores.^{126, 127} Small branched aliphatic or aromatic systems can be used as a multivalent scaffolds,¹²⁵ allowing assembly of a variety of multivalent constructs (**Figure 2.4**). One of the most common strategies to introduce a carbohydrate epitope to a multivalent core is the CuAAC, while the second most common strategy is the amide coupling reaction.¹²⁸⁻¹³¹ Multivalent systems containing carbohydrate units can increase binding and biological activity in comparison to the non-multivalent counterparts, as it was shown in recent reports.^{119, 131, 132}

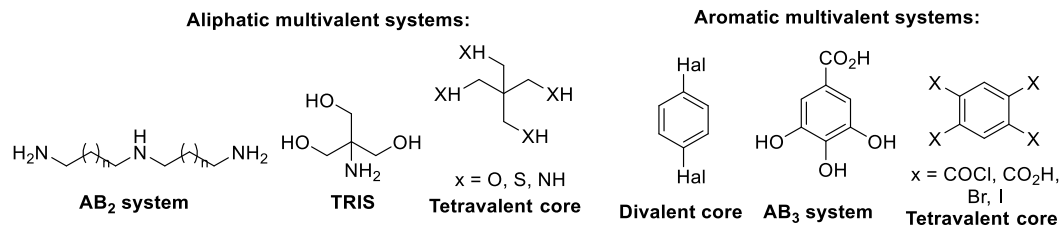
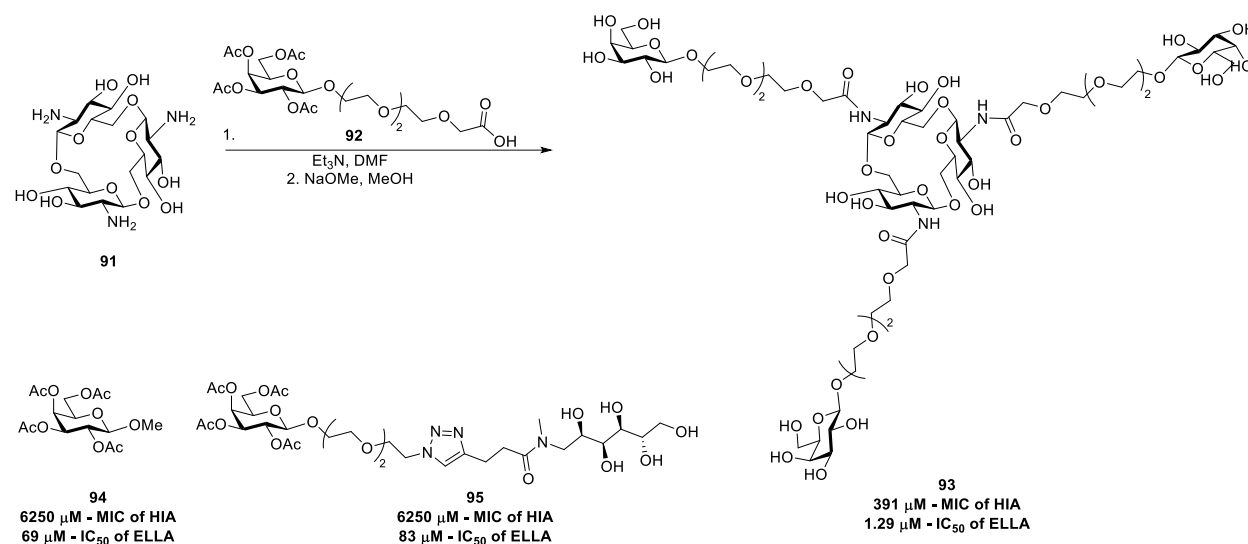


Figure 2.4. Examples of aliphatic and aromatic multivalent scaffolds.

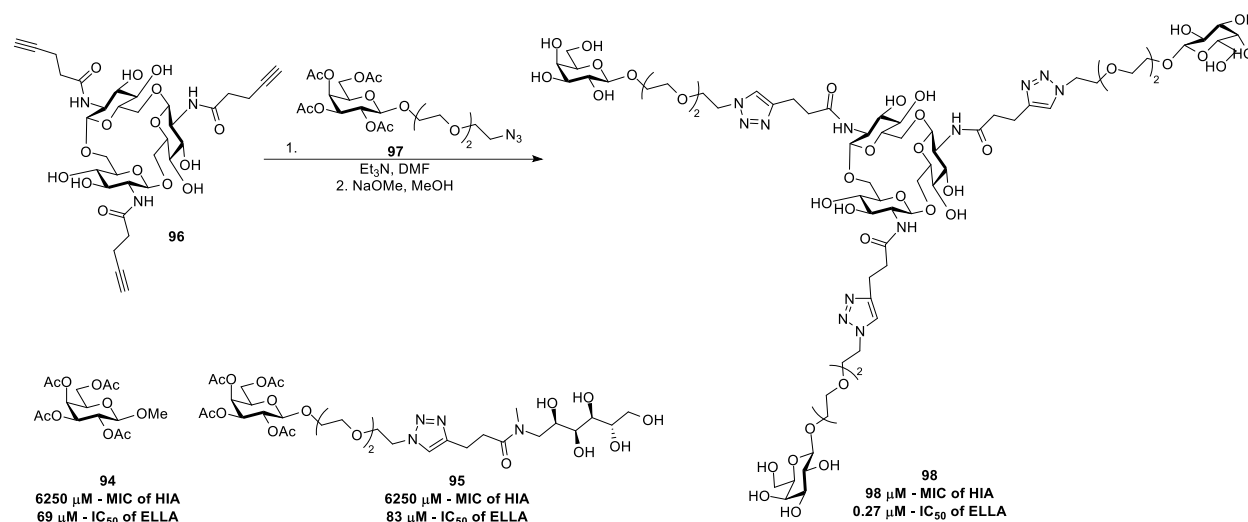
For example, Nifantiev and co-workers designed and synthesized several glycoclusters,¹³¹ including the trivalent construct **93** in which carbohydrate epitope **92** was connected to the trivalent core **91** via amide coupling reaction, and after total deprotection afforded glycocluster **93** (Scheme 14).



Scheme 14. Assembly of glycocluster **93** and comparison of its affinity towards bacterial lectin LecA with monovalent derivatives **94** and **95**.

Evaluation of the binding affinity of **93** with LecA showed a 15-fold improvement in minimal inhibitory concentration (MIC) in a hemagglutination inhibition assay, as compared to monovalent comparators **94** and **95**, as well as 53- and 64-fold increase in IC₅₀ value, measured in an enzyme-linked lectin assay (ELLA) as compared to **94** and **95** respectively. In addition, the same work described the synthesis and evaluation of triazole linked glycocluster **98**, which was assembled via CuAAC reaction between azide partner **97** and trialkyne core **96** (Scheme 15). Similarly to **93**, binding affinity of glycocluster **98** with LecA was evaluated by measuring minimal inhibitory concentration (MIC) in a hemagglutination inhibition assay and IC₅₀

values by ELLA. In both assays glycocluster **98** showed significant improvement in binding activity as compared to monovalent comparators **94** and **95**.



Scheme 15. Assembly of glycocluster **98** and comparison of its affinity towards bacterial lectin LecA with monovalent derivatives **94** and **95**.

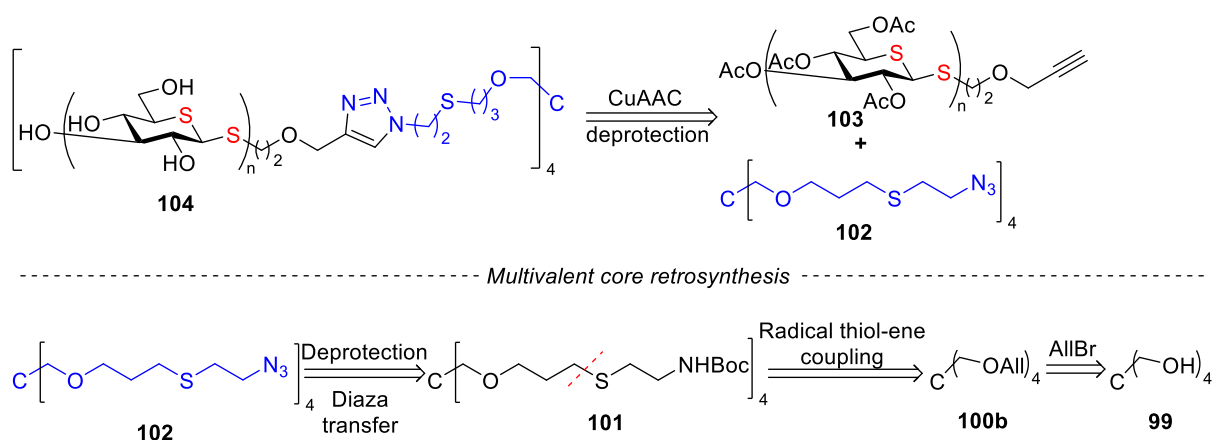
2.2. Goals of the project and considerations

The goal of the project was to synthesize 1,5-dithio mimetics of laminaribiose and laminaritriose and incorporate them into a multivalent core, and then evaluate the synthesized glycoclusters for their inhibitory activity against CR3 and Dectin-1 in comparison to the appropriate monovalent and tetravalent species.

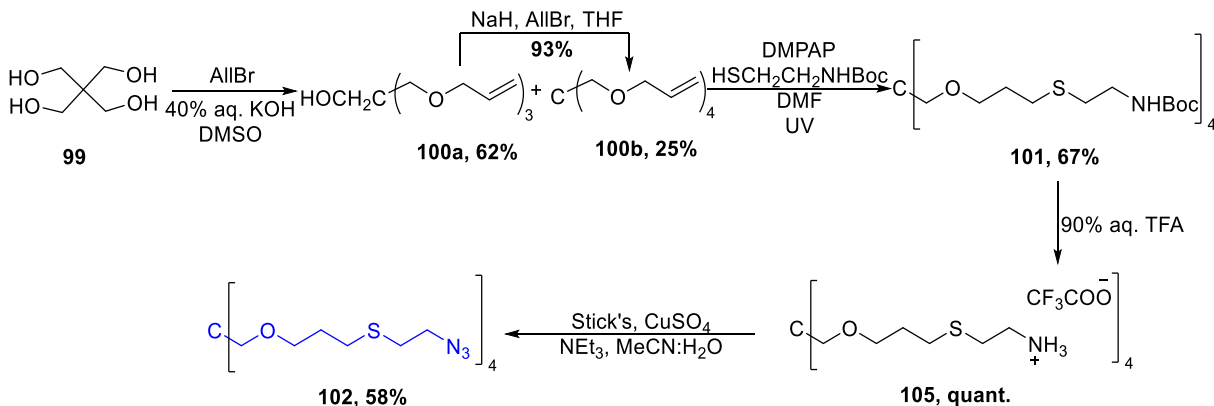
A branched tetravalent pentaerythritol-based core was selected as a scaffold for the glycoclusters. In designing the tetravalent core, we sought to distance binding sites from the bulky neopentyl system of pentaerythritol and, in addition, to provide sufficient spacing for large trisaccharide or disaccharide units. A commonly used ethylene glycol-derived linker¹¹⁵ was selected to connect the carbohydrate moiety to the tetravalent core. Finally, we sought to employ simple and reliable coupling reactions, such as CuAAC or amide coupling, to connect the linker modified carbohydrate epitopes to the tetravalent scaffold.

2.3. Triazole system design and synthesis of tetraazide core

Initially we sought to take advantage of the straightforward CuAAC click reaction to connect the linker modified carbohydrate unit to the tetravalent core. For this approach (**Scheme 16**) we envisioned that the final triazole-containing glycoclusters **104**, after total deprotection, could be accessed via CuAAC click reaction between alkyne partner **103** and tetraazide core **102**. Tetraazide core **102** could be accessed via subsequent hydrolysis and diazo-transfer reactions with tetracarbamate **101**, which in return could be accessed after radical thiol-ene coupling of tetraallylated pentaerythritol **100**, synthesized by alkylation of pentaerythritol **99** and an appropriate thiol.



Scheme 16. Retrosynthesis of triazole linked glycocluster **104**.

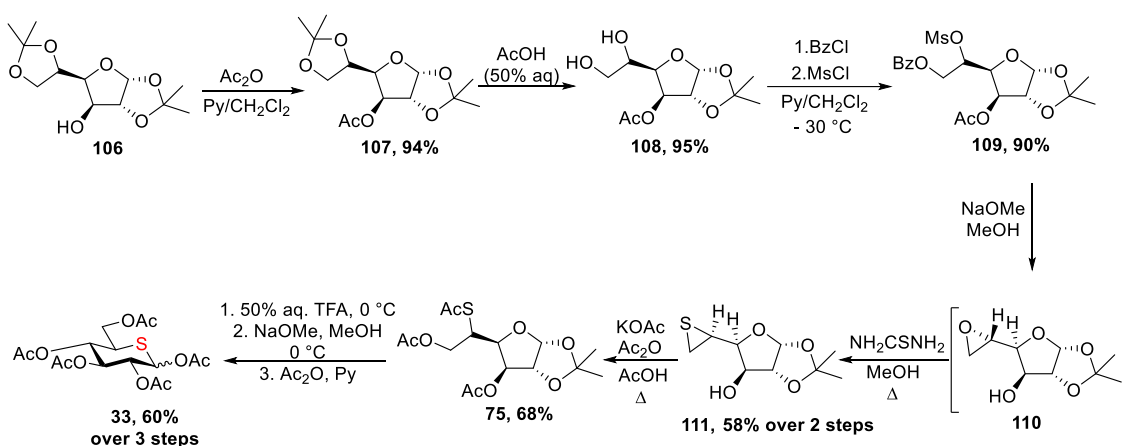


Scheme 17. Synthesis of tetraazide core **102**.

We began our synthetic efforts by preparing tetraazide core **102** (Scheme 17). Alkylation of the pentaerythritol **99** with AllBr in presence of 40% aq KOH in DMSO afforded tri- and tetra-allylated species **100a** and **100b** in 62% and 25% yield respectively. Triallylated pentaerythritol **100a** was converted to tetraallyl ether **100b** by adopting a previously reported protocol.¹²⁹ Irradiation of the DMF solution of tetraallyl ether **100b**, 2,2-dimethoxy-2-phenylacetophenone (DMPAP), and *N*-Boc-cysteamine with UV light ($\lambda = 260$ nm) allowed tetracarbamate **101** to be prepared in 67% yield. Hydrolysis of carbamate **101** with 90% aq TFA produced ammonium salt **105** quantitatively. Finally, a diazo-transfer reaction using Stick's reagent in the presence of $\text{CuSO}_4 \cdot 5\text{H}_2\text{O}$ and NEt_3 in aqueous acetonitrile afforded the tetraazide core **102** in 58% yield.

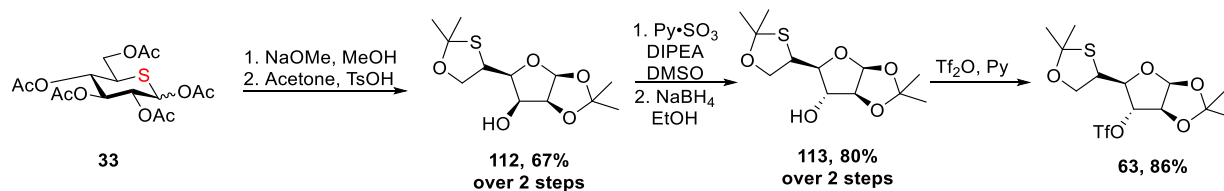
2.4. Synthesis of 1,5-dithio mimetics of laminaribiose and triose

With tetraazide core **102** in hand we commenced the synthesis of 5-thiooligosaccharides **114** and **117**. First, we sought to synthesize the key building block — peracetylated 5-thioglucose **33** (Scheme 18). Thus, adopting the protocol originally reported by Whistler⁷⁰ and previously employed by the Crich group,⁸⁰ 1,2;5,6-di-*O*-isopropylidene- α -D-glucofuranose **106** was acetylated with Ac_2O in presence of Py to produce **107** in 94% yield. Selective cleavage of 5,6-*O*-isopropylidene group with 50% aq AcOH afforded diol **108** in 95% yield, which was selectively benzoylated with BzCl and sulfonylated with MsCl to afford **109** in 90% yield. Deacylation of **109** with NaOMe in MeOH produced epoxide **110** with inversion of configuration at C-5, which then was treated with thiourea to form thiirane species **111**, with the second inversion of configuration at C-5, in 58% yield over 2 steps. Nucleophilic thiirane **111** opening with KOAc, and subsequent acetylation with Ac_2O in presence of AcOH afforded thioacetate **75** in 68% yield. Finally, deprotection of the 1,2-isopropylidene moiety with 50% aq TFA, followed by deacetylation with NaOMe in MeOH and subsequent global acetylation with Ac_2O in Py afforded 5-thioglucose pentaacetate **33** in 60% yield over 3 steps (Scheme 18).



Scheme 18. Synthesis of 5-thioglucose **33**.

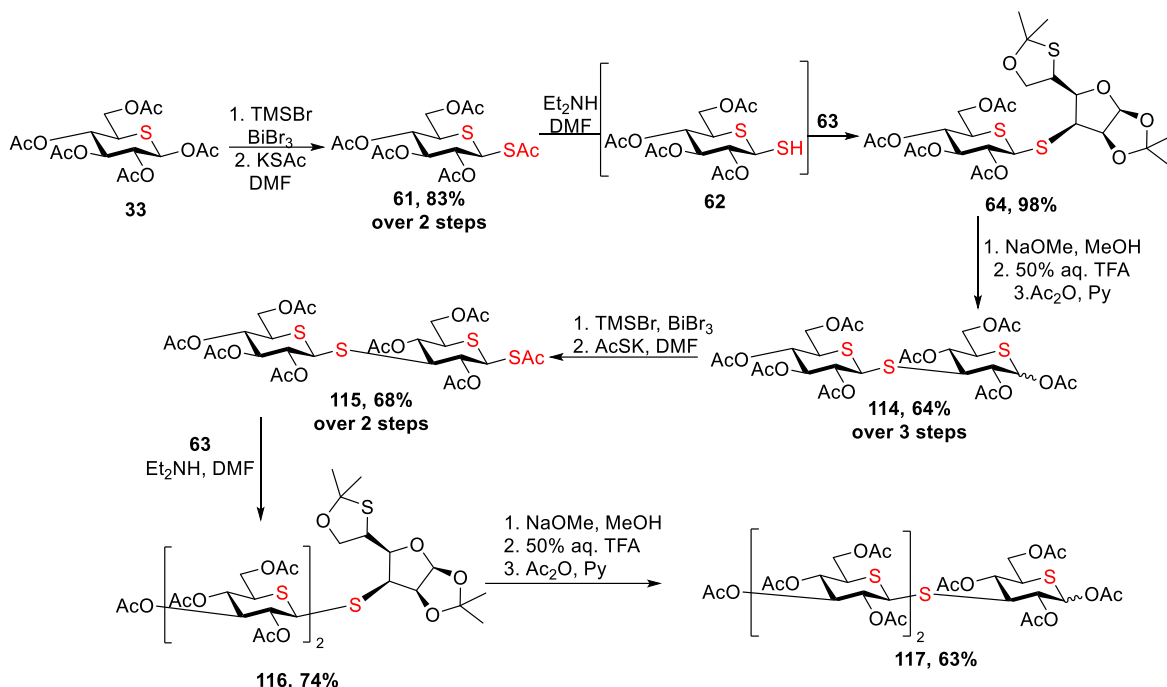
With key building block **33** synthesized, we started assembling 5-thiooligosaccharides **114** and **117** (**Scheme 20**). First, we sought to synthesize the key triflate electrophile **63** (**Scheme 19**). Thus, pentaacetate **33** was subjected to a global deprotection with NaOMe in MeOH, and subsequent condensation with acetone in presence of TsOH to afford diacetonide protected derivative **112** in 67% yield. Parikh-Doering oxidation of **112** and subsequent reduction with NaBH₄ afforded **113** in 80% yield over 2 steps. Finally, triflation of alcohol **113** with Tf₂O produced desired triflate **63** in 86% yield (**Scheme 19**).



Scheme 19. Synthesis of the key triflate electrophile **63**.

We then began the synthesis of di- and trisaccharides **114** and **117** (**Scheme 20**). First, bromination of 5-thioglucose pentaacetate **33** with TMSBr and cat. BiBr₃ afforded a glycosyl bromide, which then was subjected to S_N2-type displacement with KSac in DMF to afford thioacetate **61** with the β-configuration in 83% yield over 2 steps. Glycosylation of thioacetate **61** and triflate **63**, which proceeded through selective deprotection of the anomeric thioacetyl group with NHEt₂ to reveal anomeric thiol **62** and subsequent S_N2

displacement of triflate **63**, produced the disaccharide moiety **64**, with the β -configuration of the glycosidic linkage, in 98% yield (**Scheme 20**).



Scheme 20. Synthesis of 5-thiooligosaccharides **117** and **120**.

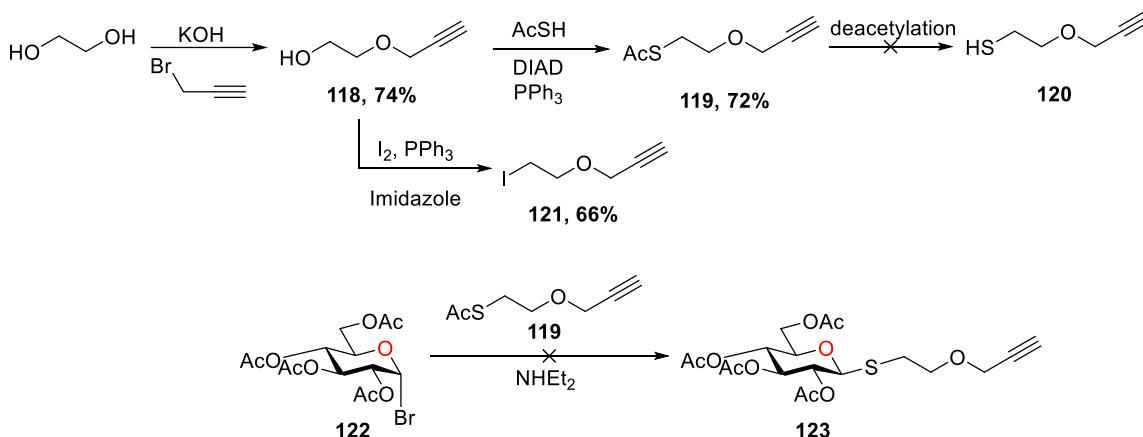
Deacetylation of **64** with NaOMe and cleavage of the isopropylidene groups with 50% aq TFA, followed by global acetylation with Ac₂O afforded peracetylated disaccharide **114** in 64% yield over 3 steps. Similarly to **33**, bromination of **114** with TMSBr and cat BiBr₃ and subsequent S_N2-type displacement with KSAc in DMF produced thioacetate **115** in 68% yield over 2 steps, which then was subjected to the glycosylation reaction conditions with triflate **63** to produce trisaccharide **116** in 74% yield. Finally, deacetylation with NaOMe and subsequent cleavage of the isopropylidene groups with 50% aq TFA, followed by global acetylation with Ac₂O afforded peracetylated trisaccharide **117** in 63% yield (**Scheme 20**).

2.5. Tetravalent triazole constructs assembly

With the key 5-thiooligosaccharides in hand, we began assembling tetravalent triazole constructs. First, we sought to introduce an alkyne moiety to the carbohydrate units, and our initial approach was to

synthesize thiol **120** and use it in a bromination/displacement sequence with **33**, **114** and **117** to introduce this aglycon with a β -thioglycosidic linkage.

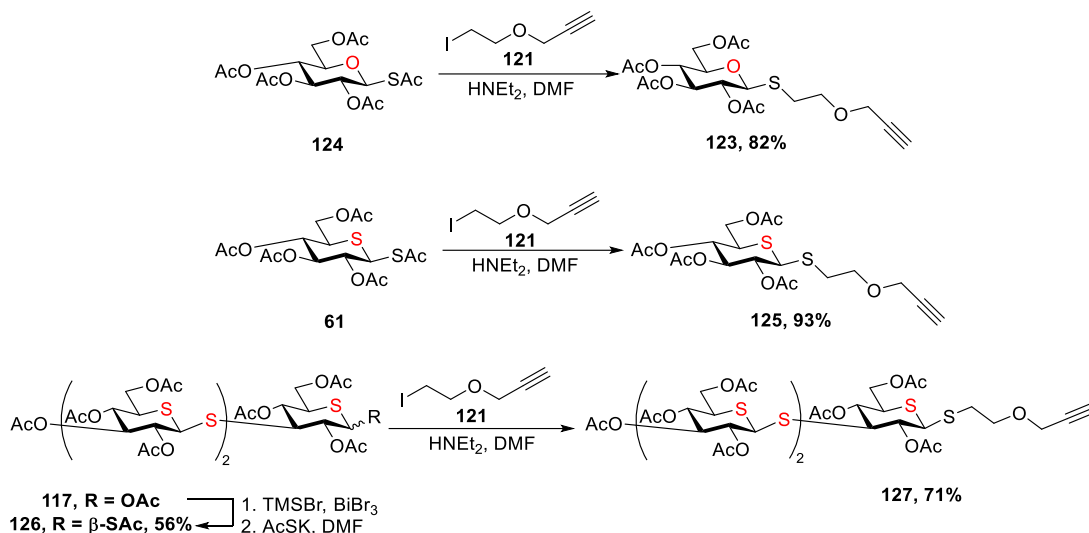
Starting with ethylene glycol, alkylation with propargyl bromide in the presence of KOH produced mono alkylated species **118** (Scheme 21). Thio-Mitsunobu reaction with AcSH successfully formed thioacetate **119** in 72% yield. However, deacetylation of **119** proved to be unreliable, as the newly formed thiol **120** was actively forming disulfide. In addition, our attempts to deprotect thioacetate **119** *in situ* and trap the resulting thiolate with glycosyl bromide **122** led to low yields of the desired product **123**, and partial deacetylation of **123**. Considering that, we changed our approach, instead targeting alkyl iodide **121** as an electrophile to be coupled with nucleophilic thiol generated from anomeric thioacetate. Thus, subjecting mono alkylated ethylene glycol species **118** to Appel iodination conditions afforded desired alkyl iodide **121** in 66% yield (Scheme 21).



Scheme 21. Synthesis of alkyne linkers and trial reaction with glycosyl bromide.

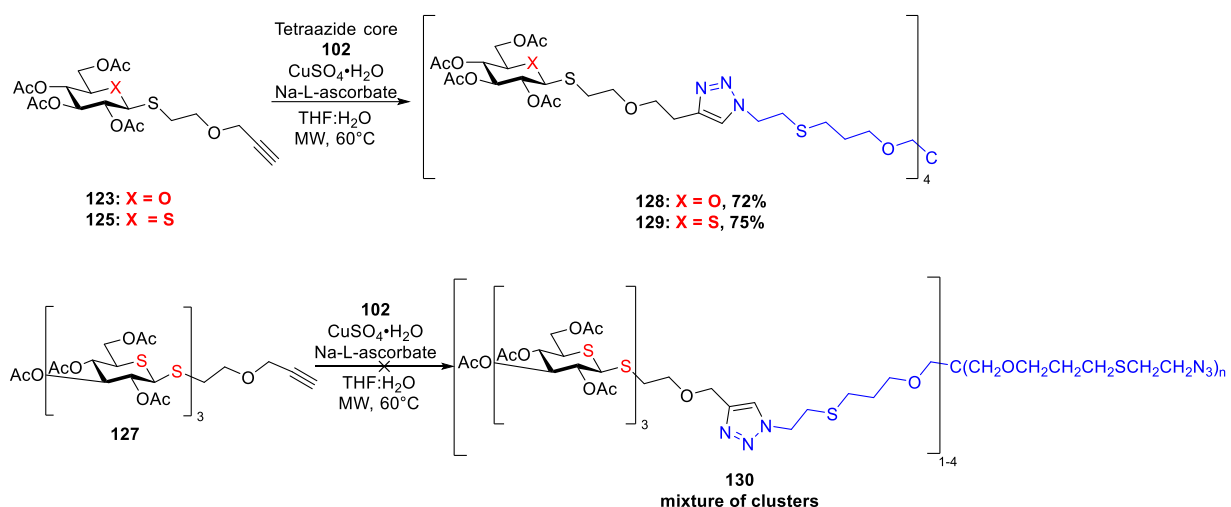
With key alkyl iodide **121** synthesized, we first performed a model coupling reaction with simple glucose thioacetate **124** (Scheme 22). Thus, treatment of a DMF solution of alkyl iodide **121** and thioacetate **124** with NHET₂ afforded thioglycoside **123** in 82% yield. We then applied this method to 5-thioglycoside **61** and trisaccharide thioacetate **126**. Thus, coupling of thioacetate **61** with alkyl iodide **121** in presence of NHET₂ afforded alkyne **125** in 93% yield. Bromination of trisaccharide **117** with TMSBr and cat BiBr₃, and

subsequent S_N2-type displacement with KSac afforded thioacetate **126** in 56% yield over 2 steps, which then was coupled with alkyl iodide to form desired alkyne **127** in 71% yield (**Scheme 22**).



Scheme 22. Coupling of thioacetates **61**, **124**, and **126** with alkyne linker **121**.

We then began assembly of the targeted triazole clusters: first, we performed the CuAAC click reaction conditions with monosaccharide compounds **123** and **125** (**Scheme 23**). Thus, microwave irradiation of alkyne partner **123** and tetraazide core **102** solution in THF-H₂O (1:1) in presence of a stoichiometric amount of CuSO₄•5H₂O and Na-L-ascorbate produced the desired triazole cluster **128** in 72% yield. Subjecting 5-thioglucose alkyne derivative **125** to the same conditions afforded triazole cluster **129** in 75% yield. However, when applied to the key trisaccharide-derived alkyne **127**, the reaction led to the formation of mixture of mono-, di-, tri-, and minor amounts of tetrameric triazole clusters **130**, and efforts to push reaction towards formation of exclusively tetramer, by changing temperature, copper catalyst, catalyst loading, and inclusion of additives, were fruitless. In addition, the NMR spectra of some of the isolated products showed broad and distorted peaks, which, according to the recently published report by Ananikov group,¹³³ led us to believe that copper salts were trapped within the molecule. Building on these observations we hypothesized that during reaction copper salts undergo competing coordination with the sulfur atoms located in C5-S-C1 and C1-S-C3 bonds between two sugar blocks, thus, retarding the click reaction and resulting in incomplete conversion, and ultimately broadening of the NMR spectra.

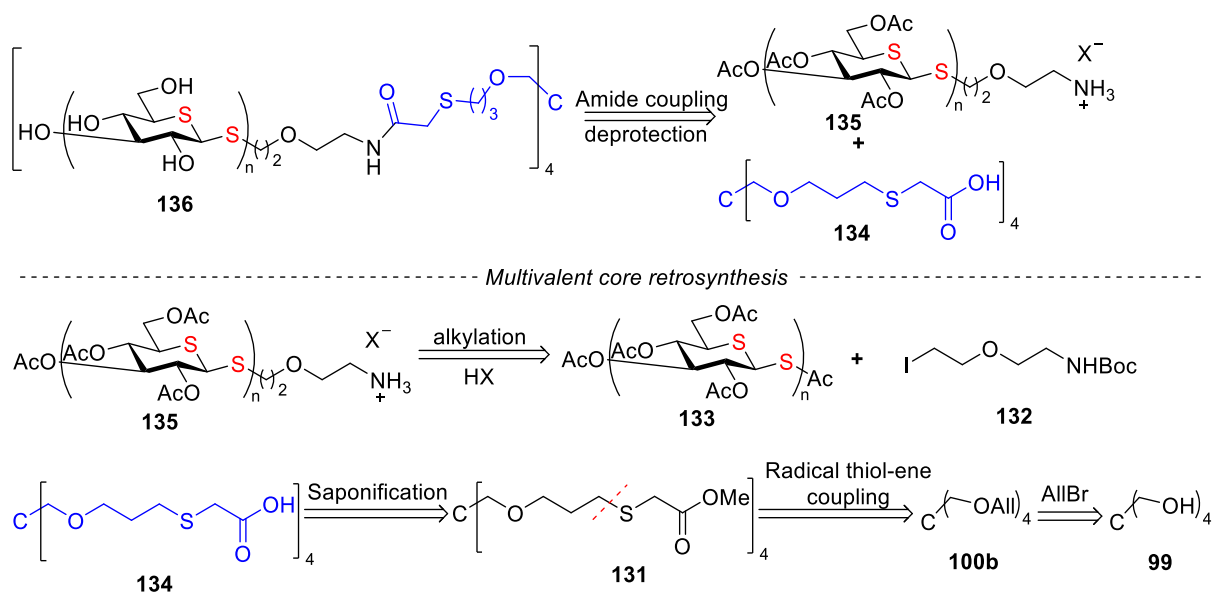


Scheme 23. The CuAAC click reaction with monosaccharides **123** and **125** and target trisaccharide **127**.

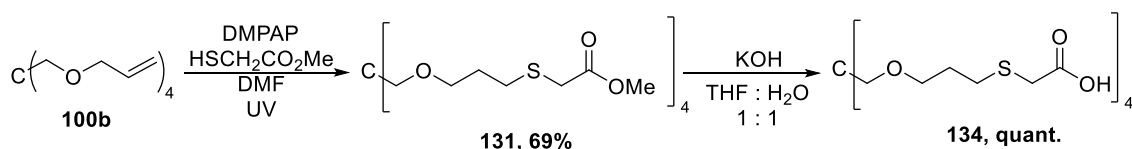
Considering those observations, we decided to change our strategy for assembly of the clusters, and, instead, used amide coupling reactions to connect the carbohydrate epitopes to the tetravalent core.

2.6. Tetraamide system design and synthesis of the key precursors

Designing an amide containing cluster, we sought to reuse the previous synthetic route to access an appropriately functionalized tetravalent core, having the same skeletal structure and similar chain length as tetraazide core **102**, and an alkyl iodide-derived linker, having the same skeletal structure and similar chain length as an alkyne **121**, and bearing an appropriate functional group. Retrosynthetically (**Scheme 24**) we envisioned that amide coupling between tetracarboxylic acid **134** and amine partner **135** could produce the desired glycoclusters **136**. We rationalized that amine partner **135** in the form of ammonium salt, which prevents acetyl group migration to nitrogen atom, could be accessed via alkylation of anomeric acetate **133** with alkyl iodide **132**, and subsequent hydrolysis of the Boc group. Tetracarboxylic acid **134** could be accessed after saponification of ester **131**, which, in return, could be accessed via radical thiol-ene coupling of an appropriate thiol and tetraallylated pentaerythritol **100b** (**Scheme 24**).



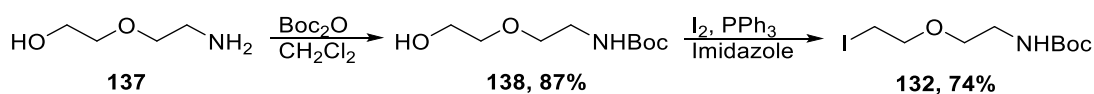
Scheme 24. Retrosynthesis of tetraamide glycocluster **136**.



Scheme 25. Synthesis of tetracarboxylic acid core **134** from tetraallylated scaffold **100b**.

Adopting the protocol used to prepare carbamate **101**, irradiation of a DMF solution of tetraallyl ether **100b**, methyl thioglycolate and DMPAP with UV light ($\lambda = 260$ nm) allowed tetraester **131** to be prepared in 69% yield. Finally, saponification of the resulting ester with excess aqueous KOH produced tetracarboxylic acid core **134** quantitatively.

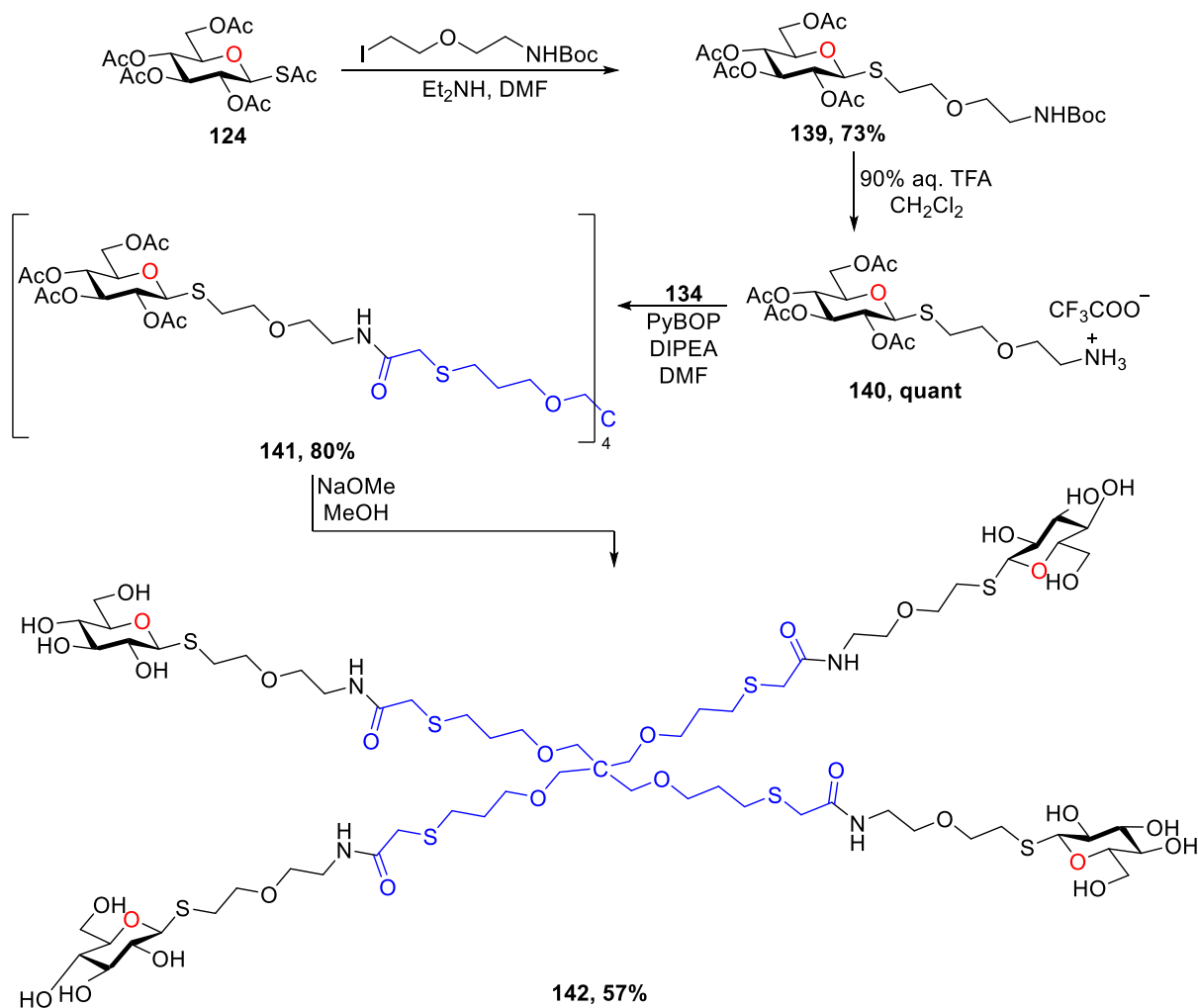
Finally, we prepared the alkyl iodide linker **132** with a terminal Boc-protected amino group. Following a previously reported protocol,¹³⁰ amino alcohol **137** was coupled with Boc_2O to produce carbamate **138** in 87% yield, and subsequent Appel iodination of **138** allowed the desired alkyl iodide **132** to be prepared in 74% yield.



Scheme 26. Synthesis of alkyl iodide linker **132**.

2.7. Synthesis and evaluation of tetraamide constructs

Having synthesized the tetravalent core **134** and an alkyl iodide linker **132**, we began assembling the tetraamide-based glycoclusters. First, we tested our synthetic route on glucose thioacetate **124** (Scheme 27).

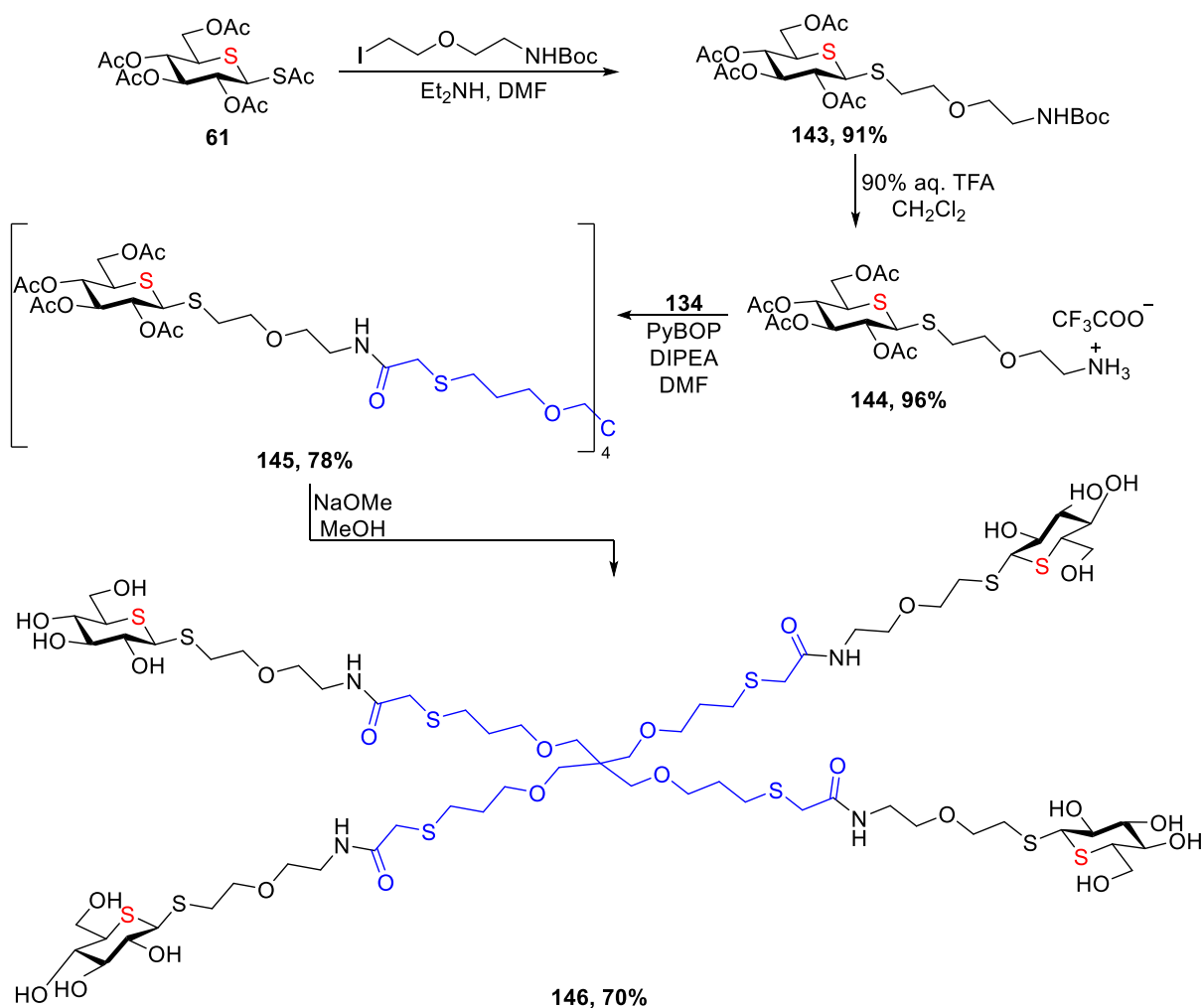


Scheme 27. Assembly of tetraamide glycocluster **142**.

Following the already established protocol, thioacetate **124** was alkylated with iodide **132** in presence of Et₂NH to produce carbamate **139** in 73% yield. Hydrolysis of the Boc group with 90% aq TFA formed compound **140** as the trifluoroacetate salt quantitatively (Scheme 27). Designing the endgame coupling reaction, we sought to employ a strong coupling reagent to ensure that all carboxylic acid groups present in the tetravalent core successfully formed amide bonds with the carbohydrate epitope. Thus, we

selected PyBOP — a potent coupling reagent used in the solid-phase peptide synthesis and for difficult amide couplings.¹³⁴ In the event, coupling of trifluoroacetate salt **140** with tetracarboxylic acid **134** in presence of excess DIPEA and PyBOP allowed peracetylated tetraamide glycocluster **141** to be formed in 80% yield. Finally, global deprotection of **141** produced the final tetraamide **142** in 58% yield (**Scheme 27**).

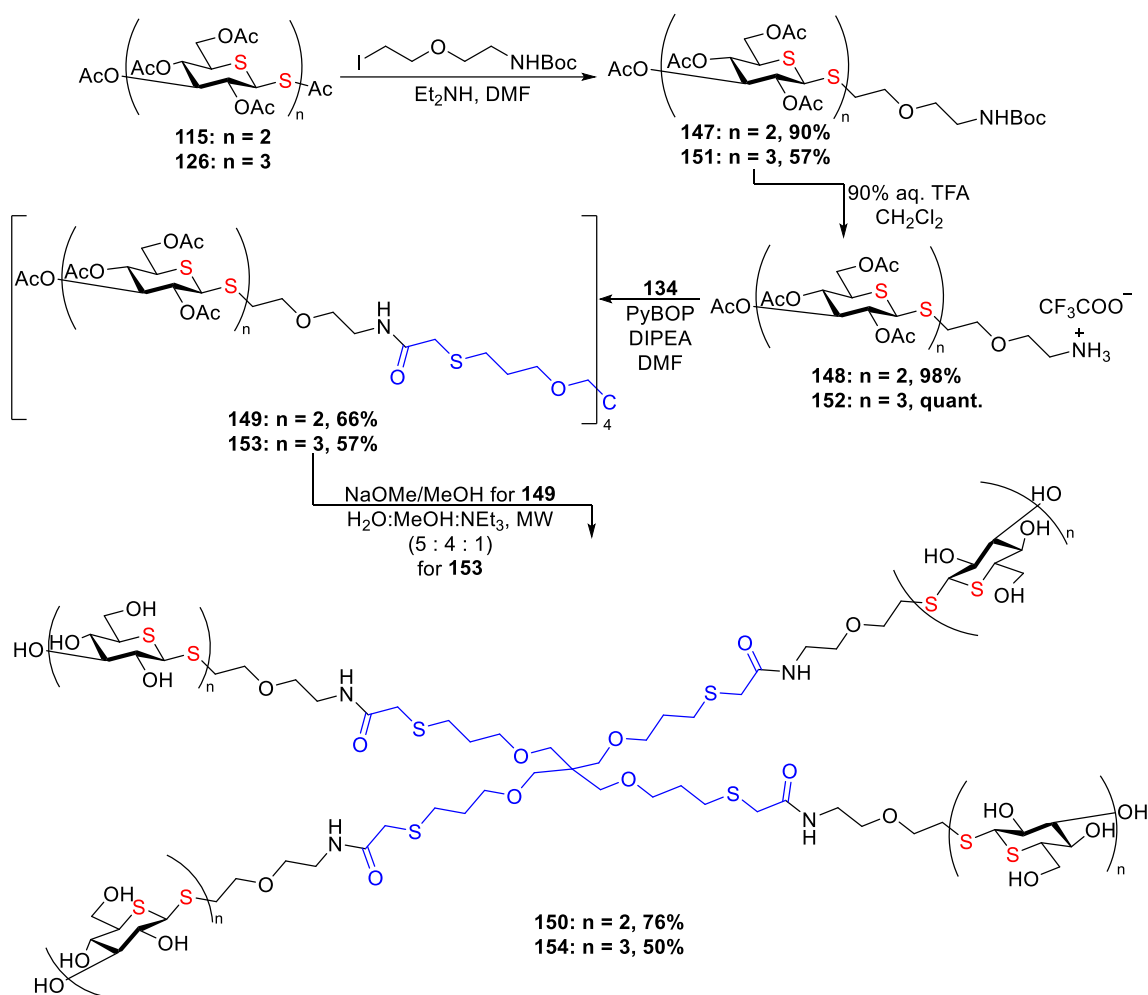
With the general synthetic route established, we applied it to the 5-thioglucose derivative **61** (**Scheme 28**). Similarly to **124**, alkylation of **61** successfully produced carbamate **143** in 91% yield, followed by Boc group cleavage with 90% aq TFA to produce trifluoroacetate salt **144** in 96% yield.



Scheme 28. Synthesis of 5-thioglucose containing tetraamide glycocluster **146**.

Coupling of the trifluoroacetate salt **144** and the tetracarboxylic acid **134** in presence of excess DIPEA and PyBOP allowed the peracetylated tetraamide glycocluster **145** to be formed in 78% yield. Finally, global deprotection produced the final tetraamide **146** (**Scheme 28**).

With tetraamide **146** successfully synthesized, we were confident that the established synthetic route can be applied to 5-thiosugars, thus we began assembly of the target glycoclusters **150** and **154** (**Scheme 29**). We started our synthetic efforts by alkylating disaccharide thioacetate **115** under optimized conditions to form carbamate **147** in 90% yield. Removal of the Boc group with 90% aq TFA allowed trifluoroacetate ammonium salt **148** to be formed in 98% yield, which was then successfully coupled with tetracarboxylic acid **134** in presence PyBOP and DIPEA, and produced the peracetylated tetraamide **149** in 66% yield.



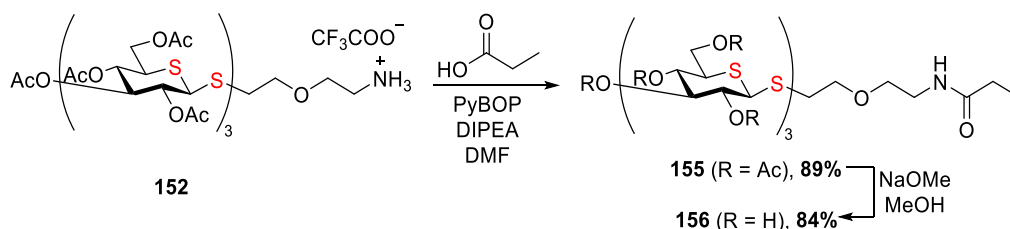
Scheme 29. Synthesis di- and trisaccharides containing glycoclusters.

Final deacetylation of **149** was performed with excess NaOMe, as our previous attempts revealed incomplete reaction when a catalytic amount of NaOMe was used. Following the modified deacetylation protocol peracetylated tetraamide **149** was converted into the final glycocluster **150** in 76% yield.

We then prepared the trisaccharide containing glycocluster **154** (Scheme 29). First, alkylation of thioacetate **126** under optimized conditions produced carbamate **151** in 57% yield. Boc group removal by treating **151** with 90% aq TFA gave the trifluoroacetate salt **152** quantitatively, which was then subsequently coupled with the tetracarboxylic acid **134** under optimized conditions to form the peracetylated tetraamide **153** in 57% yield. Unfortunately, deacetylation of **153** with either catalytic or stoichiometric amounts of NaOMe did not go to completion within a reasonable amount of time, leading to complications during

purification. To circumvent this problem, we adopted a previously reported protocol¹³⁵ and devised an alternative deacetylation procedure using NEt₃ in aq MeOH under microwave irradiation. In this way, peracetylated trisaccharide derivative **153** was successfully deprotected to produce the final tetraamide **154** in 50% yield.

Finally, yet importantly, we sought to investigate how a single branch of the multivalent core could impact inhibitory activity of the 1,5-dithio trisaccharide, thus we designed the monovalent trisaccharide derivative **156**, bearing a single propionyl amide-modified linker to mimic a single arm of the thioglucosyl amide glycocluster **154**. Subjecting the trifluoroacetate **152** and propionic acid to the optimized coupling conditions allowed the trisaccharide derivative **155** to be formed in 89% yield (**Scheme 30**). Deacetylation of **155** with NaOMe then produced propionyl amide **156** in 84% yield.



Scheme 30. Synthesis of the monovalent propionyl amide comparator **156**.

Final compounds **150**, **154**, and comparators **142**, **146**, and **156** were shipped for evaluation to our collaborator in the Department of Pathology and Laboratory Medicine at University of Louisville. First, the synthesized compounds were screened for their ability to inhibit anti-CR3 or anti-Dectin-1 fluorescein isothiocyanate (FITC)-conjugated antibody staining of human neutrophils and mouse macrophages, which is indicative of their affinity for CR3 and Dectin-1.¹³⁶

All the synthesized tetraamides **142**, **146**, **150** and **154** and propionyl amide **156** were able to inhibit anti-CR3-FITC staining of human neutrophils (**Figure 2.5**). Both monovalent **156** and tetravalent **154** trisaccharide-containing glycoconstructs showed inhibitory activity comparable to that of trimeric 1,5-dithio mimetic **46** (**Table 2**).

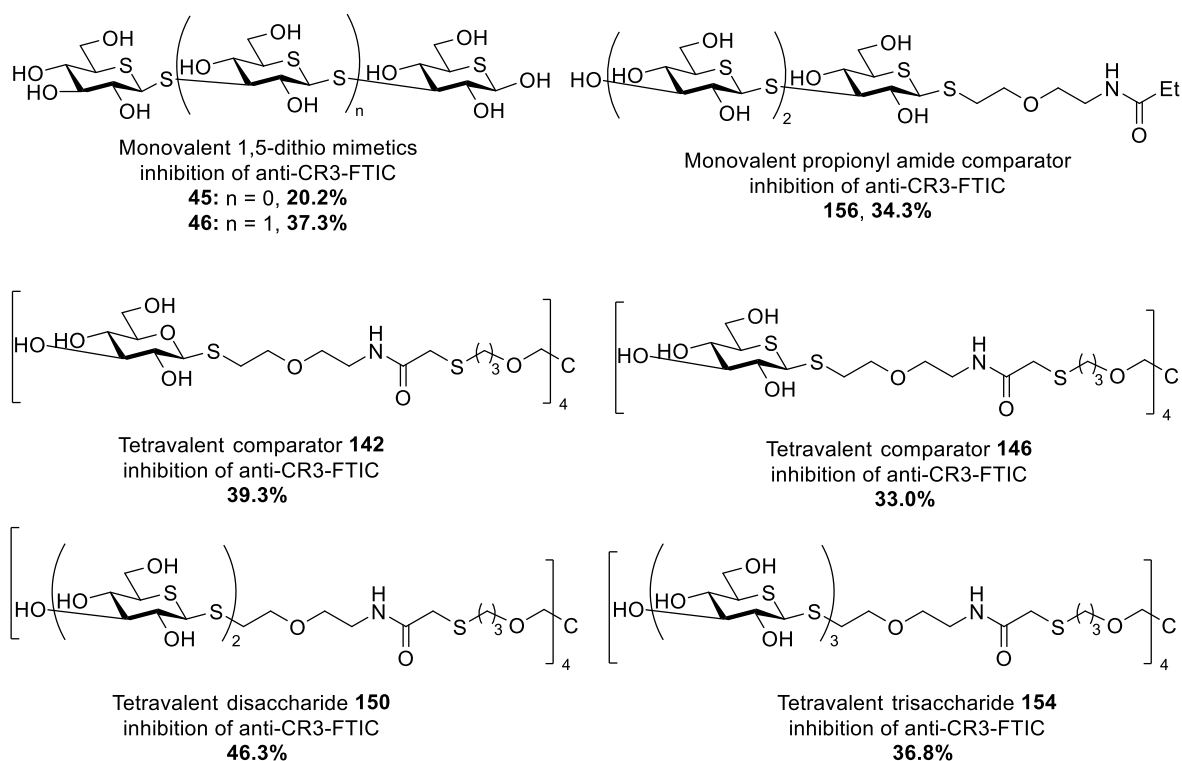


Figure 2.5. Structures and inhibitory activity of the newly synthesized tetraamides **142**, **146**, **150**, and **154** with monovalent 1,5-dithio mimetics **45** and **46** and monovalent propionyl amide **156**.

On the other hand, a two-fold increase in inhibitory activity was observed for disaccharide-containing glycocluster **150**, as compared to the dimeric 1,5-dithio mimetic **45**. In addition, monosaccharide-containing comparators **142** and **146** had inhibitory activity comparable to that of trimeric 1,5-dithio mimetic **46**.⁸⁰

Table 2. Percentage Inhibition of Anti-CR3 and Anti-Dectin-1-FITC Antibody Staining of Neutrophils and Macrophages by 0.1 µg/mL substrate.

compound	Oligomer unit no.	Type of epitope	Valency	%inhibition of anti-CR3-FITC staining of human neutrophils ^a	% inhibition of anti-Dectin-1-FITC staining of mouse macrophages ^a
45	dimer	1,5-dithioglucose	monovalent	20.2 ± 1.7	30.9 ± 3.4
46	trimer	1,5-dithioglucose	monovalent	37.3 ± 3.2	42.2 ± 3.8
156	trimer	1,5-dithioglucose	monovalent	39.3	-3.5
142	monomer	glucose	tetravalent	15.2	9.6
146	monomer	5-thioglucose	tetravalent	33.0	0.37
150	dimer	1,5-dithioglucose	tetravalent	46.3	6.1
154	trimer	1,5-dithioglucose	tetravalent	36.8	0.73

^a-Mean ± SD

This observation was suggesting that a multivalency approach significantly enhanced inhibitory activity of monosaccharides and disaccharides, suggesting poor compatibility of large, trisaccharide-containing, tetravalent constructs with the CR3 binding site. However, the same glycoclusters showed little to no inhibition of staining of mouse macrophages by fluorescent anti-Dectin-1 antibodies, which suggested that the aglycon was incompatible with the Dectin-1 binding site.

Table 3. Percentage stimulation of phagocytosis of raw 264 macrophages by 10 µg/mL substrate.

Compound	Oligomer unit no.	Type of epitope	Valency	% stimulation of phagocytosis (raw 264 macrophages, 10 µg/mL, 24 h) ^a
45	dimer	1,5-dithioglucose	monovalent	7.8 ± 1.1
46	trimer	1,5-dithioglucose	monovalent	16.6 ± 0.9
156	trimer	1,5-dithioglucose	monovalent	-5.6
142	monomer	glucose	tetravalent	-7.1
146	monomer	5-thioglucose	tetravalent	15.4
150	dimer	1,5-dithioglucose	tetravalent	0.56
154	trimer	1,5-dithioglucose	tetravalent	11.57

^a-Mean ± SD

In addition, the synthesized glycoclusters **142**, **146**, **150** and **154** and propionyl amide **156** were evaluated for their ability to stimulate phagocytosis of synthetic polymeric 2-hydroxyethyl methacrylate particles¹³⁷ by human macrophage-like RAW 264 cells (**Table 3**). Unfortunately, the data was inconsistent and so did not allow any conclusions to be drawn.

2.8. Summary

Novel tetravalent glycoclusters containing 1,5-dithio mimetics of laminaribiose and -triose and tetravalent and monovalent comparators were designed and synthesized. The synthesized glycoclusters were evaluated for their inhibitory activity against CR3 and Dectin-1 by a collaborator. The synthesized compounds showed inhibitory activity against CR3 comparable to that of monovalent 1,5-dithio mimetics, but no clear pattern emerged regarding the number of carbohydrate units in the epitope nor the usefulness of the multivalent construct. The same glycoclusters showed little to no activity in inhibition of staining of

mouse macrophages by fluorescent anti-Dectin-1 antibodies. Portions of this chapter have been published in *Carbohydrate Research* in 2023.

CHAPTER 3

EXPLORING THE IMPACT OF S-ARENE INTERACTIONS OF THIOGLYCOSIDES AND THIOSUGARS ON BINDING TO LECTINS[†]

[†] D. Ahiadorme, D. Crich. To be submitted to a peer-reviewed journal.

3.1. Introduction

Non-covalent interactions play a significant role in recognition and binding of carbohydrate epitopes to proteins.^{138, 139} One such interaction is hydrogen bonding, which occurs between hydroxyl groups of a carbohydrate ligand and polar amino acid residues of the protein, and the impact and importance of hydrogen-bond interactions in carbohydrate-protein binding is well documented.¹³⁸⁻¹⁴⁰ Another class of non-covalent interactions that can occur between carbohydrate epitopes and proteins are π -interactions. Non-covalent π -interactions are very important in carbohydrate—protein recognition and usually these interactions occur between carbohydrate C-H bonds and aromatic sidechains of amino acids (**Figure 3.1**). These CH- π interactions are well documented and studied,¹⁴¹ and the electronic nature of these interactions is explained by electron donation from the π -system into the C-H σ^* orbitals.¹⁴²⁻¹⁴⁴ Quantum mechanical calculations^{145, 146} estimate the interaction energy of such interactions to be around 3-7 kcal/mol.

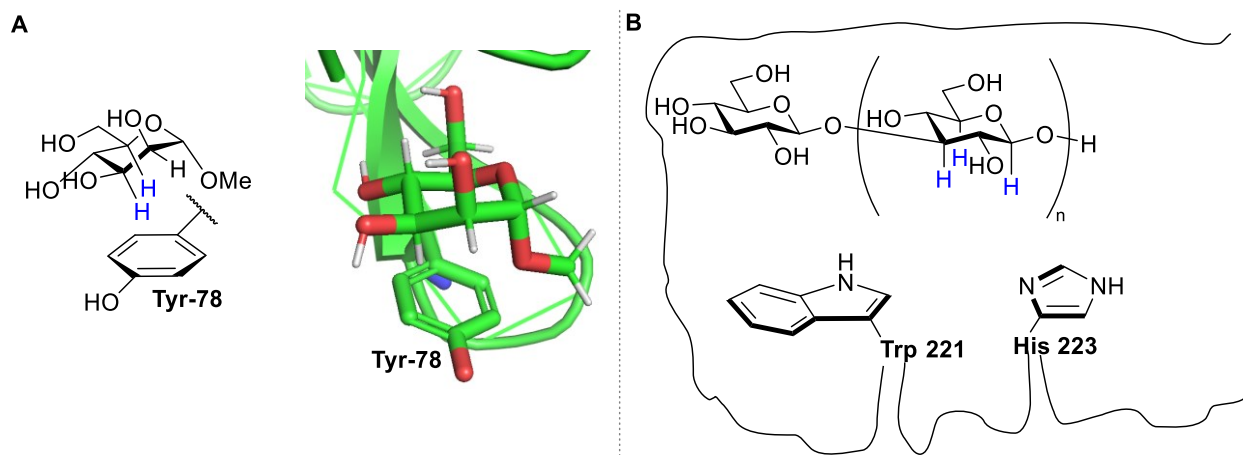


Figure 3.1. Examples of CH- π interactions (highlighted blue). **A:** CH- π interactions with Tyr-78 residue in Jacalin bound methyl α -D-mannopyranoside (PDB code: **1KUJ**); **B:** Schematic representation of CH- π interactions with Trp-221 and His-223 residues in Dectin-1 bound β -(1 \rightarrow 3)-glucan.

The ring oxygen in carbohydrate epitopes can also participate in weak non-covalent interactions with aromatic systems.¹⁴⁷ Sulfur, on the other hand, is also capable of π -interactions with aromatic systems,^{148, 149} as was shown in research works with a sulfur atom in close proximity (< 5 Å) to aromatic rings in protein¹⁵⁰ and protein-protein interfaces,¹⁵¹ which lead to the postulation of a sulfur-arene interaction (**Figure 3.2**).¹⁵²

Recently this concept has drawn significant attention¹⁵³ and has been used in drug design.¹⁴⁹ Sulfur atoms in proteins tend to approach aromatic rings along the ring edge,¹⁵⁴ and experimental data suggest that approximate stabilization energy of such interactions lies in the range of 0.3 — 0.5 kcal/mol.^{155, 156}

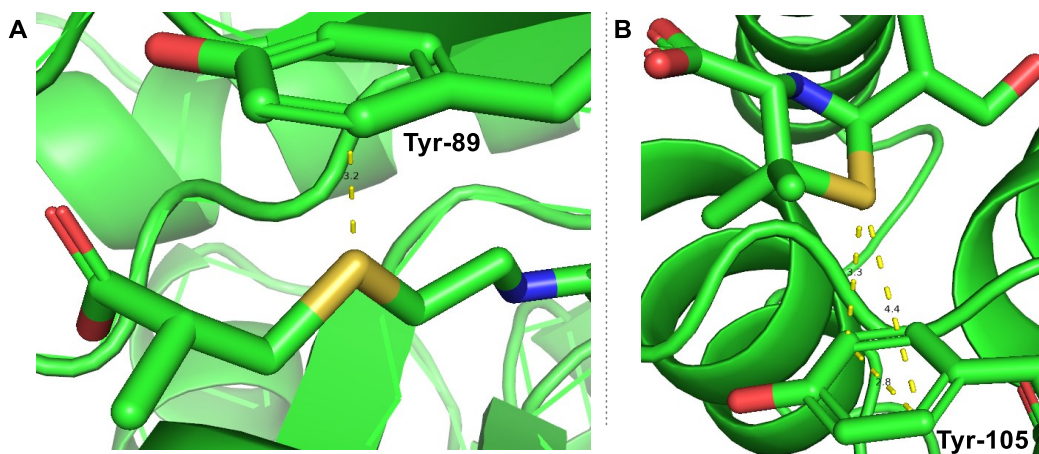


Figure 3.2. Sulfur-arene contacts between aromatic residues and sulfides. **A:** Structure of methylmalonyl-CoA mutase bound S-(*R*-2-carboxypropyl)-CoA (PDB code: **7REQ**); **B:** Structure of β -lactamase bound (hydroxymethyl)penicillanate (PDB code: **1TEM**).

Additionally, recent works by Smith and co-workers^{157, 158} correlated interaction structures with energy values, which showed that the most stable conformation was as shown in structure **157** where the sulfur atom was positioned 3.5 — 4 Å above the aromatic ring (−3.7 kcal/mol interaction energy), followed by a structure **159** where the sulfur atom was located near aromatic ring edge 2.5 Å (4.5—6 Å from ring centroid) (−1.7 kcal/mol), and followed by **158** (−1.5 kcal/mol) (**Figure 3.3A**).¹⁵² In the structure **157** a favorable electrostatic interaction between a thiol proton and an electron rich arene, together with dispersive interactions between the sulfur atom and the arene, contribute 2.6 kcal/mol of the interaction energy, with the remaining 1.1 kcal/mol accounted for by dispersive interactions between the methyl group and the arene. On the other hand, in the structure **158** repulsion between a lone pair and the electron rich arene causes an almost two-fold decrease in interaction energy. Finally, in structure **159**, wherein the thiol is oriented toward

the edge of the arene, a favorable interaction between the lone pair and arene can occur, contributing ~1.5 kcal/mol of interaction energy.

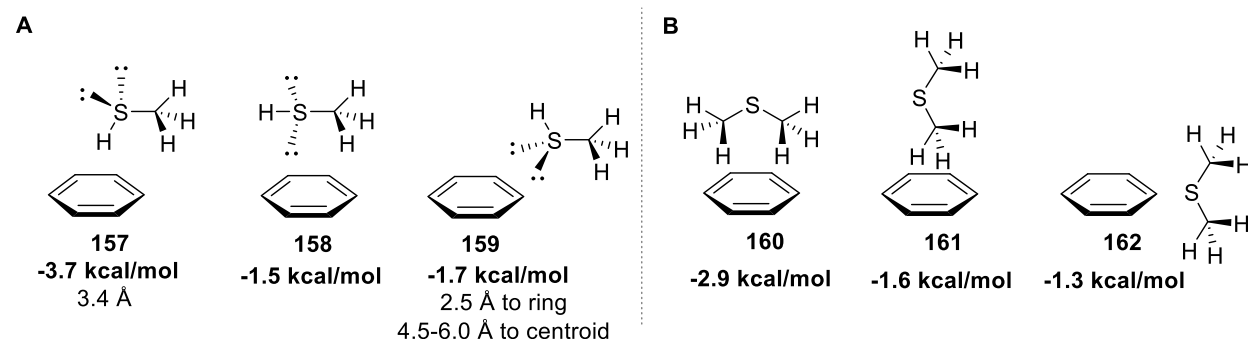


Figure 3.3. **A:** Schematic representation of the minimal internal energy determined for benzene-methanethiol complex. Reported interaction energies were calculated at the MP2/6-311+G(2d,p)//MP2/6-31G** level and corrected for BSSE; **B:** Schematic representation of the minimal internal energy determined for benzene-dimethylsulfide complex. The interaction energies for **160** and **162** were determined at the MP2/6-31G* level and at the MP2/6-31G*//B3LYP/6-31G* level for **161**.

Computational study of the benzene-dimethyl sulfide complex¹⁵⁹⁻¹⁶¹ further supports the preferred geometry of the *S*- π interactions (**Figure 3.3**). Thus, configuration **160**, in which the sulfur atom was located directly above aromatic ring, was favored by -2.9 kcal/mol, compared to the structure **161** (1.6 kcal/mol), and, finally, **162** (-1.3 kcal/mol) in which the sulfur atom is in the plane of the aromatic ring.

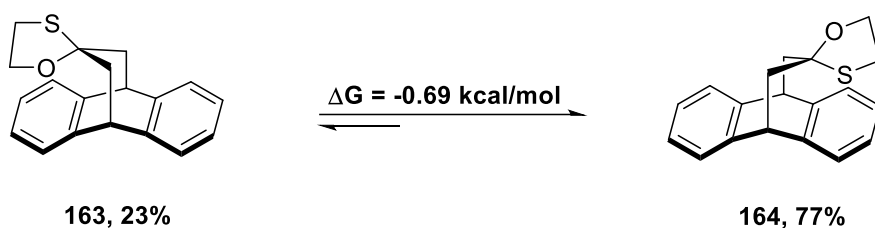


Figure 3.4. An equilibration observed by NMR spectroscopy between two oxathiolane conformers **163** and **164**.

When compared to the *O*- π interactions under the same conditions, *S*-arene interactions tend to be thermodynamically stronger,¹⁶² as it was shown in a recent report by Motherwell et al.¹⁴⁸ In that work an oxathiolane appended to a 9,10-dihydroanthracene core was equilibrated in CDCl₃ and analyzed by NMR,

which showed 77% population of the conformer **164** with the sulfur atom above aromatic ring and -0.69 kcal/mol more stable over an alternative conformation with an oxygen- π interaction (**Figure 3.4**).

Despite literature precedents, the common occurrence of divalent sulfur in clinical drugs,¹⁶³ and the widespread appreciation of CH- π interactions in carbohydrate-protein binding,^{143, 164} the possibility of sulfur- π interactions in thioglycoside and thiosugar interactions with proteins has been essentially ignored, be it either as a post-facto explanation or as a design principle. A striking exception to this rule, which clearly underlines the potential, is a recent work by Zetterberg et al.¹⁶⁵ in which a series of aryl thiogalactosides were synthesized, among which, compound **GB1107** showed nanomolar inhibitory activity against Galecin-3 ($IC_{50} = 37$ nM). X-ray crystallography analysis revealed that the glycosidic sulfur was 4.3 Å away from the center of Trp-181 aromatic ring, which led the authors to conclude that divalent glycosidic sulfur was partaking in a S- π interaction with the indole ring of Trp-181 residue (**Figure 3.5A**). Similar observations were found in the X-ray crystal structure of Galectin-1-bound compound **GB1490** ($IC_{50} = 0.47$ μ M, PDB ID: **8OJP**) where glycosidic S atom was 4.5 Å away from the center of Trp-68 aromatic ring (**Figure 3.5B**).⁴⁸

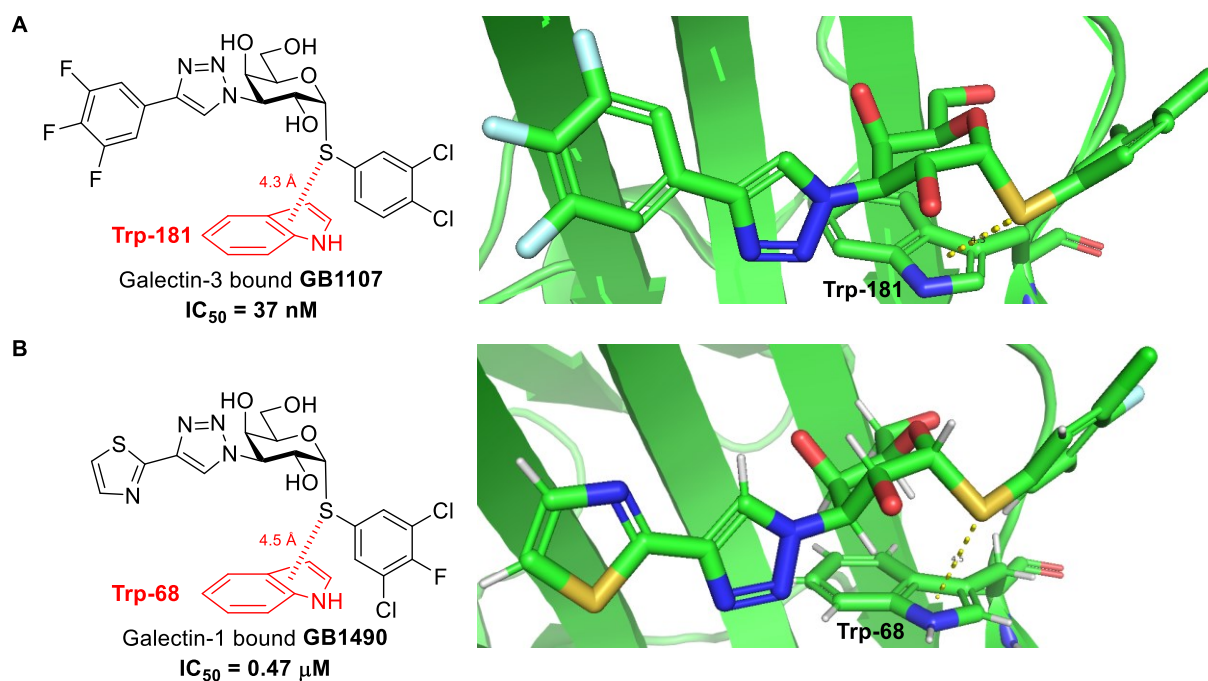


Figure 3.5. X-ray crystal structures of Galectin-bound thioglycosides. **A.** Fragment of the X-ray structure of Galectin-3 bound thiogalactoside **GB1107** (PDB code: **6EOL**) and schematic representation of $S-\pi$ interaction between glycosidic sulfur atom and Trp-181 moiety (4.3 Å); **B.** Fragment of the X-ray structure of Galectin-1 bound thiogalactoside **GB1490** (PDB code: **80JP**) and schematic representation of $S-\pi$ interaction between glycosidic sulfur atom and Trp-68 moiety (4.5 Å).

3.2. Goals of the project and considerations

The goal of the project was to explore the impact of $S-\pi$ interactions occurring between ring sulfur atoms or glycosidic sulfur atoms and aromatic amino acid residues on binding to lectins and to attempt to use the results of that analysis as a foundation for a predictive tool to help determine when it is worth synthesizing 5-thio or thioglycosidic mimetics of parent *O*-glycosides.

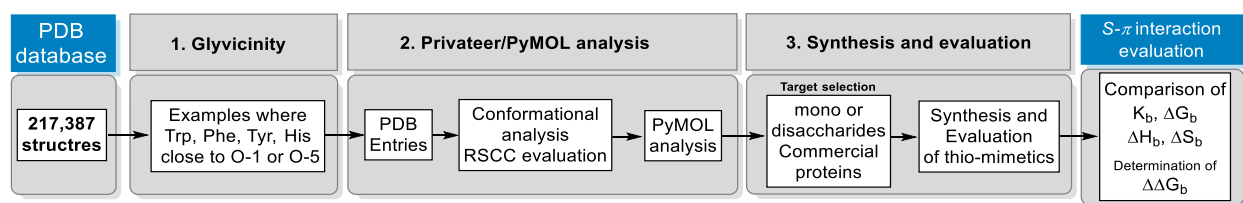
The first part of the project was a PDB database search. We sought to adopt search protocols reported by the Kiessling group for identification of $CH-\pi$ interactions,^{164, 166} and by the Crich group for determination of patterns in the manner of which glycosidases and glycosyl transferases restrict the conformation of the side chain of their substrates to enhance catalysis,¹⁶⁷⁻¹⁶⁹ and to search for examples in which either ring oxygen atom (O-5) or glycosidic oxygen atom (O-1) were in close proximity to aromatic residues. Then, after analyzing the search output, we aimed to pick suitable examples for the synthesis of

thio-mimetics. We sought to pick at least one representative target to evaluate a S- π interaction between a glycosidic sulfur atom and an aromatic residue, and one between a ring sulfur atom and an aromatic residue.

The second part of the project was synthesis and evaluation of 5-thiosugar or thioglycoside derivatives of parent glycosides. We sought to quantify the impact of the S- π interaction on binding to lectins by measuring the K_d and employing the van t' Hoff equation to determine the thermodynamic parameters of binding, and then compare them with those measured for the parent glycoside.

3.3. PDB search

We commenced the database search with Glyvicinity tool¹⁷⁰ — a statistical tool that searches the PDB database for examples in which a specific amino acid is in the vicinity of individual carbohydrate units and with subsequent focus on specific atoms within the carbohydrate molecule (**Scheme 31**). We searched through the PDB database focusing on the cases wherein amino acids with aromatic side chains, such as tryptophan (Trp), tyrosine (Tyr), phenylalanine (Phe) and histidine (His) were located within 5 Å from either a glycosidic bond oxygen (O-1), ring oxygen (O-5 for pyranoses) or thioglycoside bond sulfur (S-1) (recorded separately) atoms of the sugar moiety. To exclude possible errors in crystallographic data we limited output data to structures with resolution higher than 2 Å. The raw search output consisted of PDB IDs, the structure and composition of the carbohydrate ligand, the average distance between the selected atom in the carbohydrate unit and aromatic residue atoms, and the resolution of the X-ray crystal structure.



Scheme 31. Summarized research strategy.

The PDB database is well-known to contain many errors in the basic structure of bound carbohydrates as well as in carbohydrate conformations.¹⁷¹ Accordingly, all the connectivity and conformation of all carbohydrates identified in the GlyVicinity-directed PDB search were further analyzed

with the help of the CCP4 Privateer software (**Scheme 31**).¹⁷² Only structures identified by CCP4 Privateer as having a real space correlation coefficient (RSCC) ≥ 0.8 , where RSCC is defined as a measure of the similarity of an electron density map calculated from the structural model and the experimental data, and the correct chair conformation (e.g., 4C_1 and 1C_4 for D- and L-hexopyranoses respectively) were retained. Structures that passed Privateer analysis were further analyzed with the PyMOL software¹⁷³ to determine an approximate distance between the aromatic side chain and specific atoms of the sugar moiety and to analyze the arrangement of the glycosidic or endocyclic oxygens and the aromatic residues. In the end, out of 860 initial PDB entries located, only 234 entries successfully passed both the Privateer and PyMOL analyses. Among those entries 7 of them accounted for examples in which the glycosidic sulfur atom was in close proximity to the aromatic residues, and 1 entry accounted for example in which both the glycosidic sulfur atom and the endocyclic oxygen atom were in close proximity to the aromatic residues His and Trp, respectively (**Table 8** and **Table 9** in the Appendix). Notably, hydrolase bound carbohydrates were the most common in the search output, accounting for 46.7% of entries, followed by lectin bound carbohydrates, accounting for 22.5% of entries, and transferase bound carbohydrates, accounting for 15.9% of entries (**Figure 3.6A**). Similarly to the results reported by Kiessling for CH- π interactions,^{164, 166} the most common aromatic residue found in vicinity of either *O*-5 or *O*-1 was tryptophan (65.2% of entries), while tyrosine (29.1% of entries) was the second most common aromatic amino acid residue found in vicinity of *O*-5 or *O*-1 (**Figure 3.6B**).

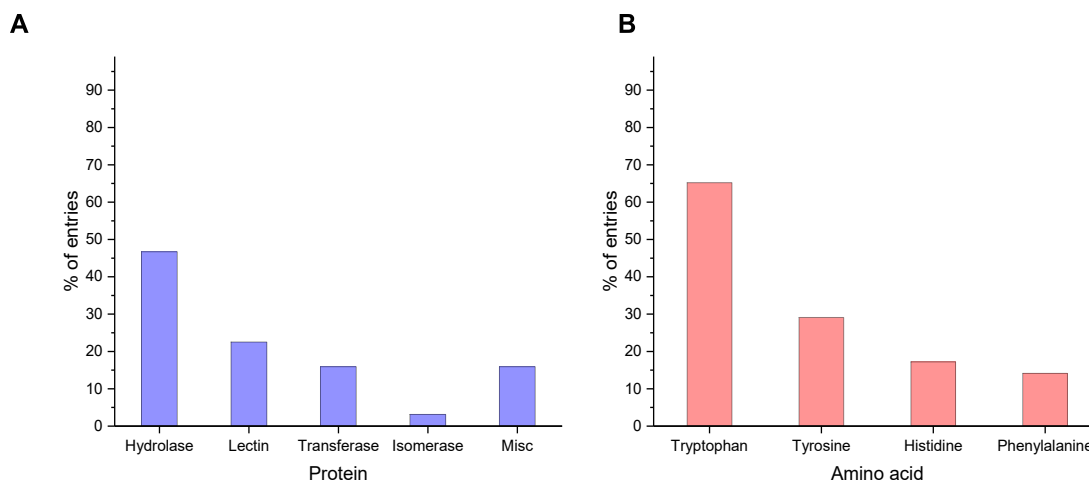


Figure 3.6. Statistical analysis of the PDB database search output. **A.** The most common types of proteins in the search output. **B.** Percentage of PDB entries with specific amino acid residue found near either *O*-5 or *O*-1.

The three most common arrangements of ring oxygens and aromatic residues were: i) stacking arrangement (the aromatic ring directly below or above the sugar ring and sugar ring oxygen) (**Figure 3.7B**); ii) ring oxygen to the edge of the aromatic ring (**Figure 3.7A**), and iii) ring oxygen to the center of the aromatic ring. The stacking arrangement between the aromatic residue and sugar ring can be attributed to the CH- π interactions between the hydrophobic face of the sugar moiety and aromatic residues,^{144, 164} and to the lesser extent to *O*- π interactions, while the other arrangements can be attributed to possible *O*- π interactions. The most common arrangement of glycosidic oxygen and aromatic residue was the stacking arrangement (**Figure 3.7C**), wherein the glycosidic oxygen was located directly below or above the aromatic residue.

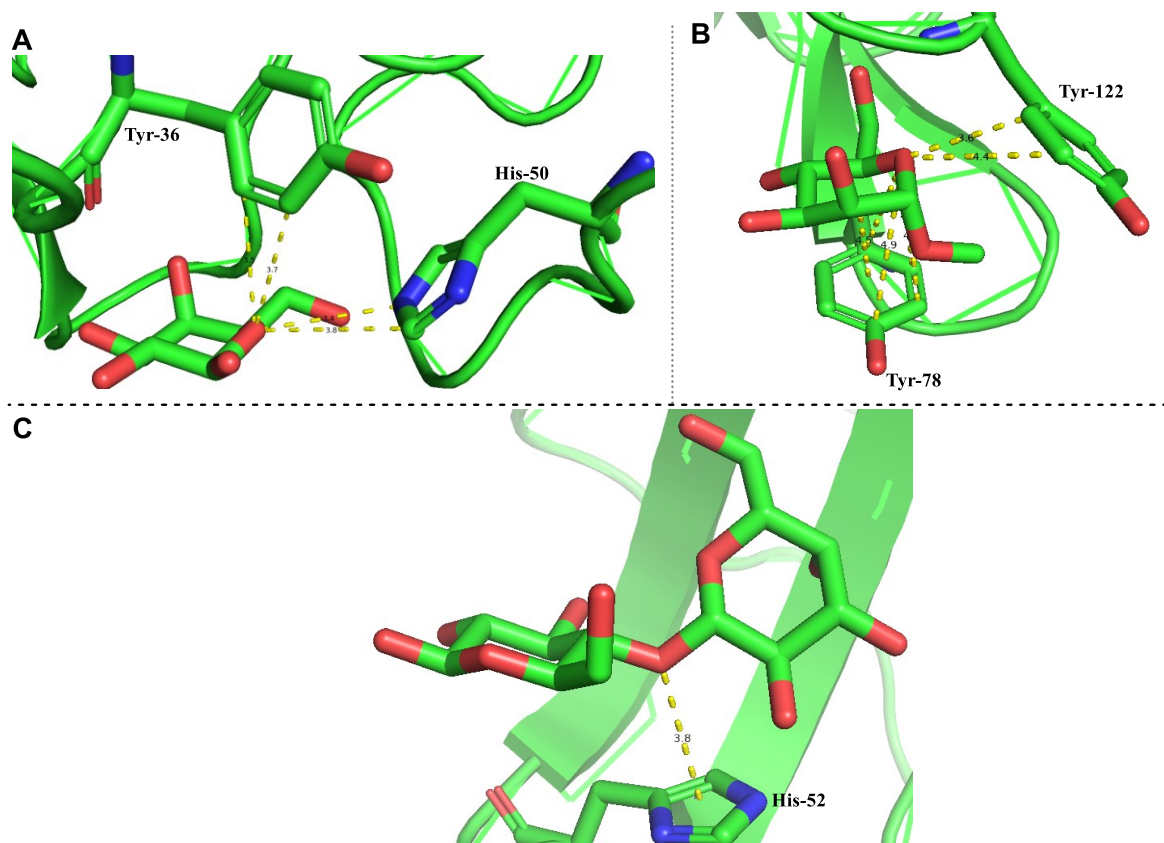


Figure 3.7. The most common arrangements of ring oxygen or glycosidic oxygen and aromatic residue. **A:** Ring oxygen to the edge of Tyr-36 and His-50 arrangement (PDB code: **1OKO**), yellow dashed lines represent distances between ring oxygen and aromatic residue: 3.5-3.7 Å between *O*-5 and Tyr-36 and 3.4-3.8 Å between *O*-5 and His-50; **B:** Stacking arrangement to the Tyr-78 and ring oxygen edge of Tyr-122 arrangement (PDB code: **1KUJ**), yellow dashed lines represent distances between ring oxygen and aromatic residue: 4.8 Å between *O*-5 and Tyr-78 and 3.6-4.4 Å between *O*-5 and Tyr-122; **C:** Stacking arrangement of glycosidic oxygen and His-52 (PDB code: **1GZW**). Yellow dashed lines represent distances between glycosidic oxygen and the center of the aromatic residue: 3.8 Å between *O*-1' and His-52.

3.4. Target selection

In selecting the targets for the synthesis of 5-thio or 1-thio analogs, we chose to focus on the lectin bound carbohydrate examples, since the impact of possible *S*- π interaction on binding affinity in those cases could be evaluated by comparing thermodynamic parameters (K_d , ΔG_d , ΔH_d), measured using well-known physical chemical methods,¹⁷⁴⁻¹⁷⁷ for the lectin bound thio-analogs and the corresponding natural comparators. In addition, we sought to pick examples of monosaccharides or disaccharides bound to commercially available proteins for the evaluation of these interactions to simplify the necessary chemical synthesis and to avoid the need for cloning and isolation of proteins.

First, we sought to investigate the influence of S - π interaction between thioglycosidic S -1 atoms and aromatic residues. Thus, we selected Galectin-1 bound lactose (PDB code: **1GZW**)¹⁷⁸ as the first target. Galectin-1 is an unspecific carbohydrate binding protein with propensity to bind β -galactosides;^{179, 180} specifically Galectin-1 shows high affinity for binding lactose-derivatives and the corresponding Galectin-1-bound lactose complexes are well documented and studied.¹⁸⁰⁻¹⁸² In the X-ray crystal structure of Galectin-1-bound lactose (PDB code: **1GZW**),¹⁷⁸ the glycosidic oxygen O -1' is located directly above the His-52 residue (**Figure 3.8A**) with a separation of 3.8 Å between O -1 and the center of the ring. To test this example, we aimed to synthesize 4-thiolactose and measure the thermodynamic parameters for its binding to the Galectin-1 and compare them with those of Galectin-1-bound lactose, and, in doing so, evaluate and quantify the impact of S - π interactions on binding affinity.

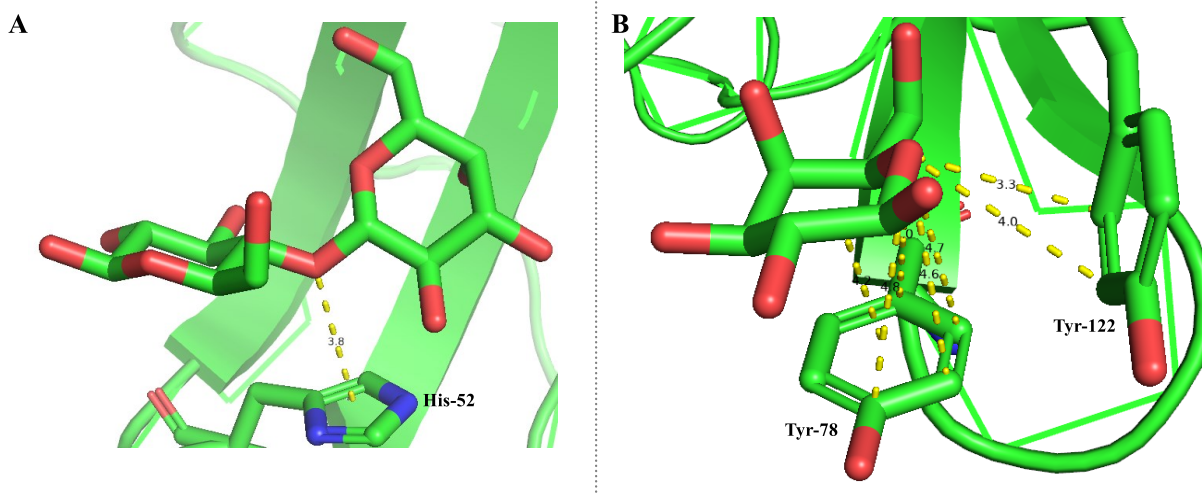


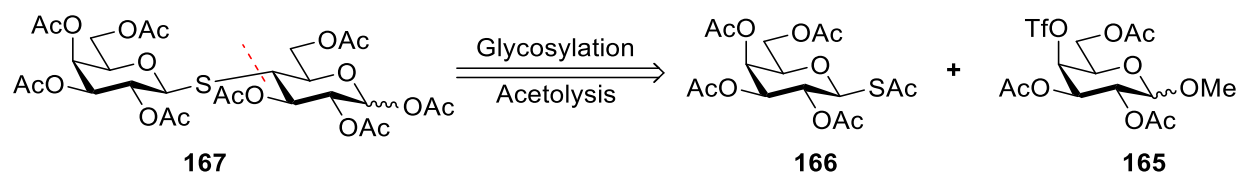
Figure 3.8. X-ray crystal structures of selected targets. **A:** Galectin-1 bound lactose (PDB code: **1GZW**). Yellow dashed lines represent distance between glycosidic oxygen and aromatic residue: 3.8 Å between O -1 and the center of His-52; **B:** Jacalin bound galactose (PDB code: **1UGW**). Yellow dashed lines represent distance between ring oxygen and aromatic residue: 4.6 Å between O -5 and the center Tyr-78, 7.3 Å between O -5 and the edge of Tyr-122.

For the second target, we sought to investigate the impact of S - π interactions between ring sulfur S -5 of thiasugars and aromatic residues on binding affinity. Initially, Jacalin-bound galactose (PDB codes: **1UGW**)^{183, 184} was picked as a suitable example. Jacalin is a major protein isolated from jackfruit seed and shows affinity for various O -glycosides,¹⁸⁵ such as methyl α -mannopyranoside,^{186, 187} and methyl α -

glucopyranoside. In the X-ray crystal structure of the Jacalin bound galactose (PDB codes: **1UGW**) the endocyclic ring oxygen *O*-5 is located above the Tyr-78 residue (**Figure 3.8B**). In addition to that, there is a *O*-5 to Tyr-122 edge residue arrangement. To test the influence of *S*- π interactions between ring sulfur (*S*-5) and aromatic residue on the binding affinity, we aimed to synthesize 5-thiogalactose and measure its thermodynamic binding parameters to Jacalin and compare them with those of Jacalin-bound galactose.

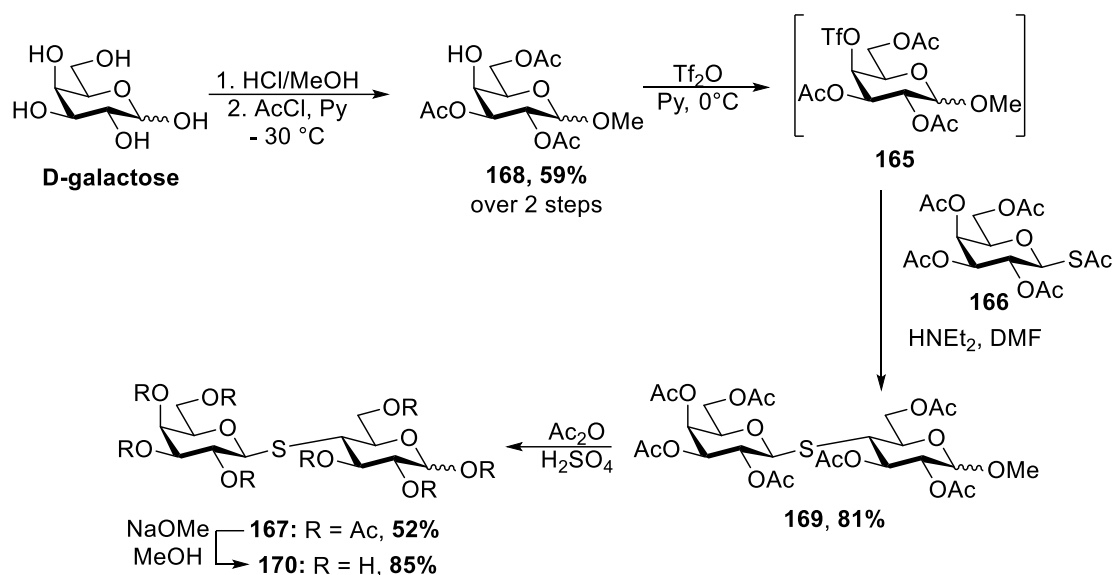
3.5. Synthesis of thio-mimetics

We began with synthesis of the thio-mimetics by preparing 4-thiolactose. Retrosynthetically we envisioned that the desired disaccharide with a β -thioglycosidic bond **167** could be assembled by a coupling reaction between anomeric thioacetate **166**, and triflate **165** (**Scheme 32**), following the same protocol used to assemble 5-thiooligosaccharides **64** and **116** (**Scheme 20**). Both **165** and **166** could be easily prepared from galactose.



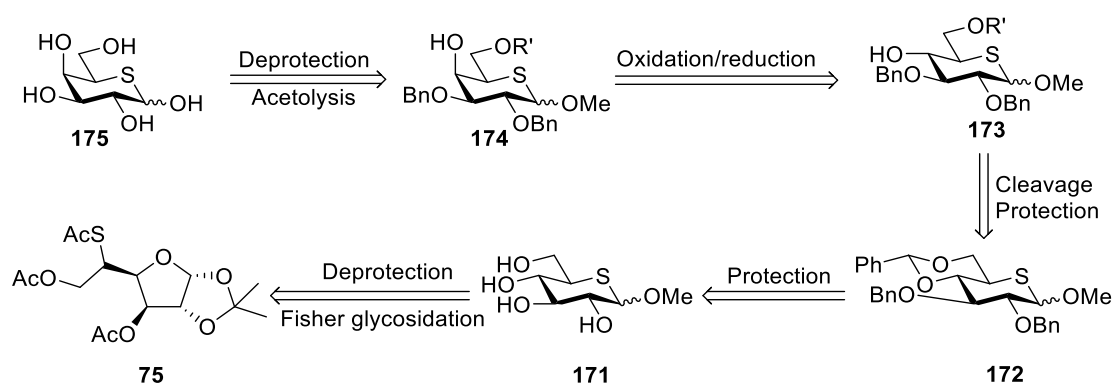
Scheme 32. Retrosynthesis of peracetylated 4-thiolactose **167**.

Thus, synthesis of 4-thiolactose began with preparation of triflate **165** (**Scheme 33**). Following a reported protocol¹⁸⁸ galactose was subjected to Fischer glycosidation conditions to give the methyl α,β -galactosides, as a temporary protecting group for the anomeric position. Selective acetylation with AcCl at -30 °C then produced the triacetate **168** in 59% yield over 2 steps. Subsequent sulfonylation of triacetate **168** with trifluoromethanesulfonic anhydride produced triflate **165**, which then was coupled with thioacetate **166**, prepared following the literature known protocol,¹⁸⁹ in presence of HNEt₂ to give disaccharide **169** in 81% yield. Acetolysis of **169** with Ac₂O in presence of cat. H₂SO₄ afforded octaacetate **167** in 52% yield, which upon global deprotection produced 4-thiolactose **170** in 85% yield.



Scheme 33. Synthesis of 4-thiolactose **170**.

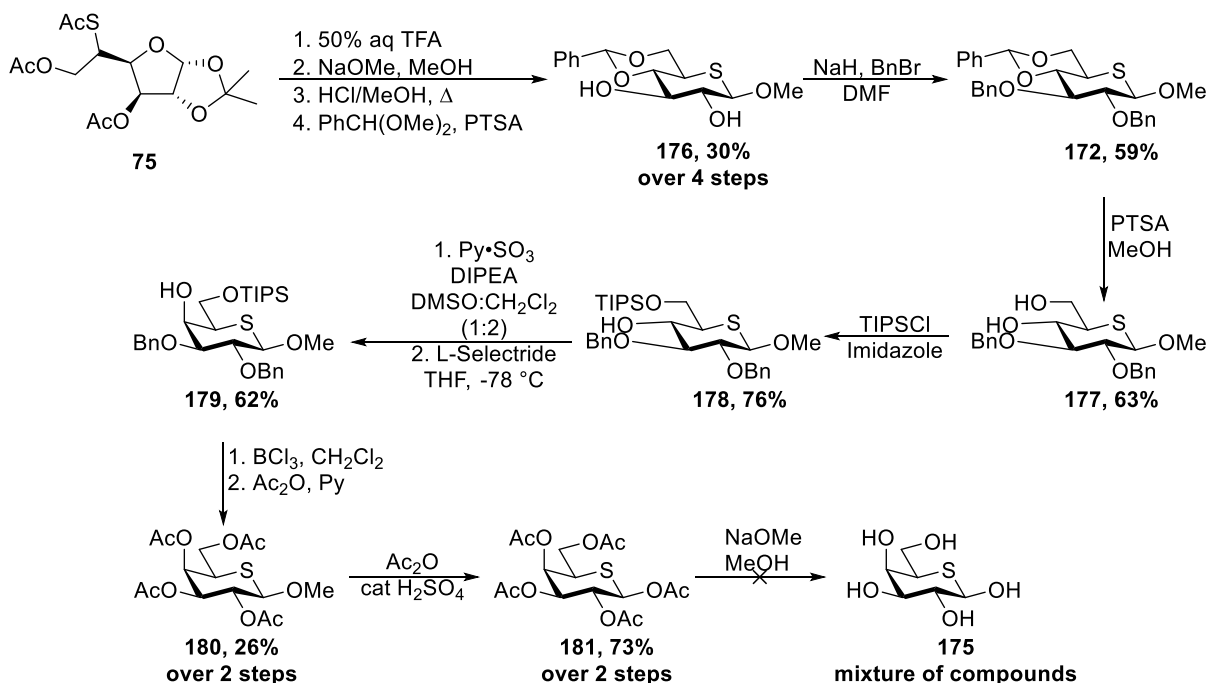
We then turned our attention to the synthesis of 5-thiogalactose. Retrosynthetically (**Scheme 34**) we envisioned that inversion of configuration of C-4 atom in **173**, via an oxidation-reduction sequence, could produce 5-thiogalactose derivative **174**. Alcohol **173** could be accessed from **172** after benzylidene deprotection and selective protection of the primary alcohol, and compound **172**, in turn, could be accessed from **171** after a sequence of protection group installations. Finally, the methyl 5-thioglucoside **171** could be synthesized from the commercially available **75** via global deprotection and Fischer glycosidation.



Scheme 34. Retrosynthesis of 5-thiogalactose **175**.

In the forward synthesis (**Scheme 35**), starting with **75**, hydrolysis of the 1,2-acetal with 50% aq TFA, followed by global deacetylation with NaOMe and Fischer glycosidation in methanolic HCl under

reflux conditions produced methyl 5-thioglucoside, which then was subsequently protected with a benzylidene protecting group to produce **176** in 30% yield over 4 steps. Benzylation of **176** with BnBr in the presence of NaH formed **172** in 59% yield, which upon cleavage of benzylidene group with methanolic PTSA produced **177** in 63% yield. The primary alcohol was then selectively protected with TIPSCl in the presence of imidazole to form **178** in 76% yield. Parikh-Doering oxidation of **178** produced ketosugar, which then was selectively reduced with L-selectride at -78 °C to produce galactose derivative **179** in 62% yield. Treatment of **179** with BCl₃ in CH₂Cl₂ lead to deprotection of both the benzyl and triisopropylsilyl ethers to briefly reveal methyl 5-thiogalactoside, which upon global acetylation produced **180** in 26% yield over 2 steps, which after subsequent acetolysis produced **181** in 73% yield. The extra acetylation steps to produce **181** were added, since purification of the prefinal compound was readily achieved on the peracetylated derivative **181**.



Scheme 35. Attempted synthesis of 5-thiogalactose **175**.

Nevertheless, the final deacetylation step produced 5-thiogalactose **175** mixed with methyl 5-thiogalactoside, and various optimization efforts were fruitless, as the sequence consistently formed methyl 5-thiogalactoside as an impurity and, in some cases, lead to caramelization of the 5-thiogalactose upon

quenching the reaction mixture with an ion-exchange resin and subsequent solvent removal. In addition, the long synthetic route towards pre-final compound **181** further complicated optimization of the global deprotection. Isolation of the pure 5-thiogalactose **175** from the reaction mixture was complicated, as 5-thiogalactose and methyl 5-thiogalactoside all had similar polarity.

Considering those observations, we decided to change our target slightly to an analogous one, thus the Jacalin-bound methyl α -D-galactoside (PDB **5JM1**)¹⁹⁰ was picked as a target. In the X-ray structure of the Jacalin-bound methyl α -D-galactopyranoside (PDB **5JM1**) the endocyclic ring oxygen *O*-5 is located above the Tyr-78 residue (**Figure 3.9**) at distance of 4.8 Å from the center of the ring. In addition, there is an *O*-5 to the edge of Tyr-122 residue arrangement with an average separation of 4.5 Å. For this target we aimed to synthesize methyl 5-thio- α -D-galactopyranoside **187** and measure its thermodynamic parameters for binding to the Jacalin in comparison to those of Jacalin-bound methyl α -D-galactopyranoside.

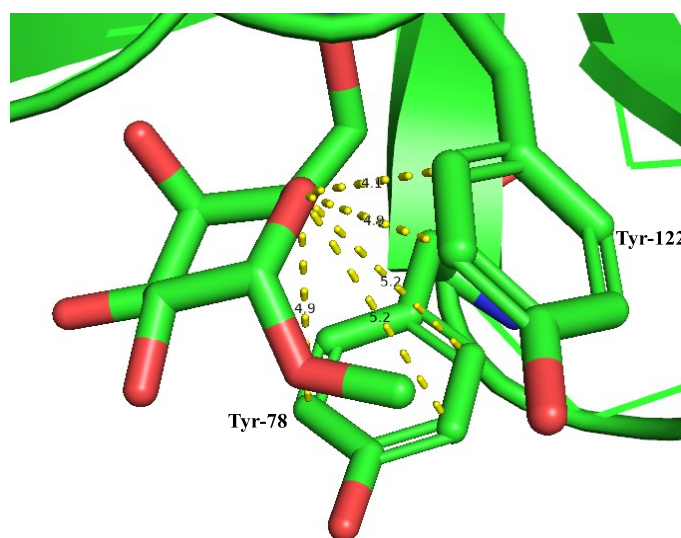
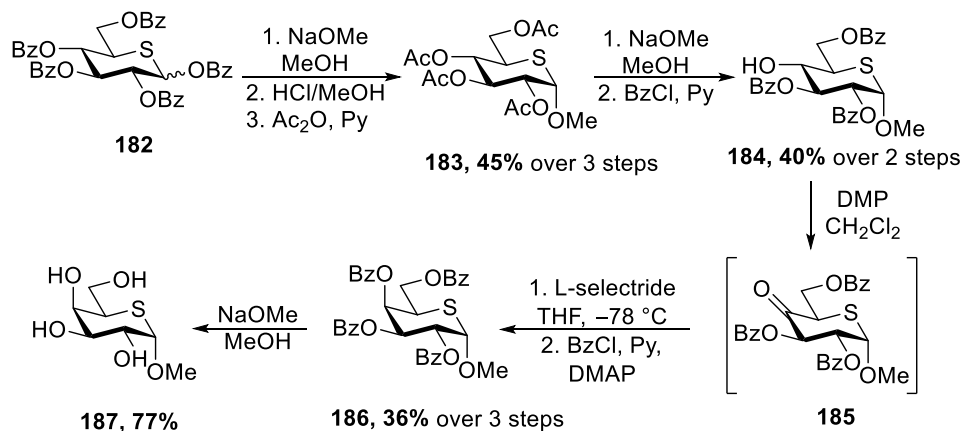


Figure 3.9. Jacalin bound methyl α -D-galactopyranoside (PDB code: **5JM1**). Yellow dashed lines represent distance between ring oxygen and aromatic residue: 4.8 Å between *O*-5 and the center of Tyr-78, 4.5 Å between *O*-5 and the edge of Tyr-122.

We then designed a synthetic route towards the target methyl 5-thiogalactoside **187**, which, similarly to the previous one (**Scheme 35**), relied on inversion of the configuration of C-4 atom of the 5-thioglucose derivative **184**. Thus, we commenced synthesis of methyl 5-thio- α -D-galactopyranoside

(Scheme 36). Starting from perbenzoylated 5-thioglucose **182**, prepared following a literature known protocol,¹⁸⁹ debenzoylation with NaOMe afforded 5-thioglucose, which then was subjected to Fischer glycosidation reaction with methanolic HCl to form the corresponding methyl glycoside, which after global acetylation with Ac₂O produced peracetylated methyl 5-thioglucoside **183** in 45% yield over 3 steps. The 3-step sequence to synthesize methyl 5-thioglucoside **183** was necessary since direct coupling between **182** and methanol in the presence of Lewis acid did not produce the desired glycoside **183**. Global deacetylation of **183** formed methyl 5-thioglucose, which then, adopting a previously reported protocol,¹⁹¹ was selectively benzoylated with BzCl to give the desired tribenzoate **184** in 40% yield over 2 steps. Oxidation of alcohol **184** with Dess-Martin periodinane produced ketosugar **185**, which slowly underwent elimination from the C-3 position to form an enone. Therefore, ketosugar **185** was quickly reduced with L-selectride to produce 5-thiogalactose derivative, which after subsequent benzoylation with BzCl in presence of DMAP and Py produced perbenzoylated galactoside **186** in 36% over 3 steps. Finally, debenzoylation of **186** with NaOMe afforded the final methyl 5-thio- α -D-galactoside **187** in 77% yield.



Scheme 36. Synthesis of methyl 5-thio- α -D-galactopyranoside **187**.

3.6. Evaluation of binding affinity

Synthesized thio-mimetics **170** and **187** and the corresponding parent comparators were shipped to the GlycoMIP facilities at Virginia Tech, and to the UGA CCRC for evaluation of the binding affinity to the selected proteins which were obtained commercially.

First, the binding affinity of methyl α -D-galactoside and methyl 5-thio- α -D-galactoside **187** for Jacalin were evaluated using MST method,^{176, 192} which is predicated on measuring changes in fluorescent caused by the movement of the fluorescent labeled receptor (protein) along the microscopic temperature gradient induced by an infrared laser. The measurements were performed at +20, +22, +24, and +26 °C temperature points in triplicate (**Table 4**, **Table 5**). Then, to determine thermodynamic parameters of binding process we built the van 't Hoff equation plot (eq 1) (**Figure 3.10**, **Figure 3.11**). Thus, we calculated logarithmic values of K_d (expressed in moles) and plotted those values against 1/T (T expressed in Kelvins) to build van 't Hoff plots for both parent methyl galactoside and methyl 5-thiogalactoside **187** (**Figure 3.10**, **Figure 3.11**).

$$\ln K_d = \frac{\Delta H_b}{RT} - \frac{\Delta S_b}{R} \quad \text{eq (1)}$$

Table 4. Binding constants measured for Jacalin bound methyl α -D-galactopyranoside at different temperatures. Highlighted the data used for van 't Hoff plot.

K_d (mM)	Av K_d	SDT K_d (mM)	$\ln(K_d(M))$	T, K	1/T (K ⁻¹)	Av $\ln(K_d)$	SDT $\ln(K_d)$
0.714	0.7297	0.02376	-7.2446276	293.15	0.003411	-7.223	0.03227
0.718			-7.239041				
0.757			-7.1861473				
0.996	0.9397	0.05012	-6.9117633	295.15	0.003388	-6.971	0.05276
0.923			-6.9878813				
0.900			-7.0131158				
0.922	0.994	0.06315	-6.9889653	297.15	0.003365	-6.915	0.06466
1.02			-6.8879527				
1.04			-6.8685346				
1.07	1.127	0.06658	-6.8400966	299.15	0.003343	-6.79	0.05856
1.2			-6.7254337				
1.11			-6.8033953				

Table 5. Binding constants measured for Jacalin bound methyl 5-thio- α -D-galactopyranoside **187** at different temperatures. Highlighted the data used for van 't Hoff plot.

K_d (mM)	$Av K_d$	SDT K_d (mM)	$Ln(K_d(M))$	T, K	1/T (K ⁻¹)	$Av Ln(K_d)$	SDT $Ln(K_d)$
2.91	2.387	0.45545	-5.839602198	293.15	0.003411223	-6.049	0.18287
2.08			-6.175387385				
2.17			-6.133028111				
2.33	2.657	0.51472	-6.061887011	295.15	0.003388108	-5.942	0.18523
2.39			-6.036461913				
3.25			-5.729100283				
3.99	4.46	1.49161	-5.523964048	297.15	0.003365304	-5.448	0.32248
3.26			-5.726028084				
6.13			-5.094560529				
5.93	5.523	0.86495	-5.127731066	299.15	0.003342805	-5.208	0.16479
6.11			-5.097828506				
4.53			-5.397033339				

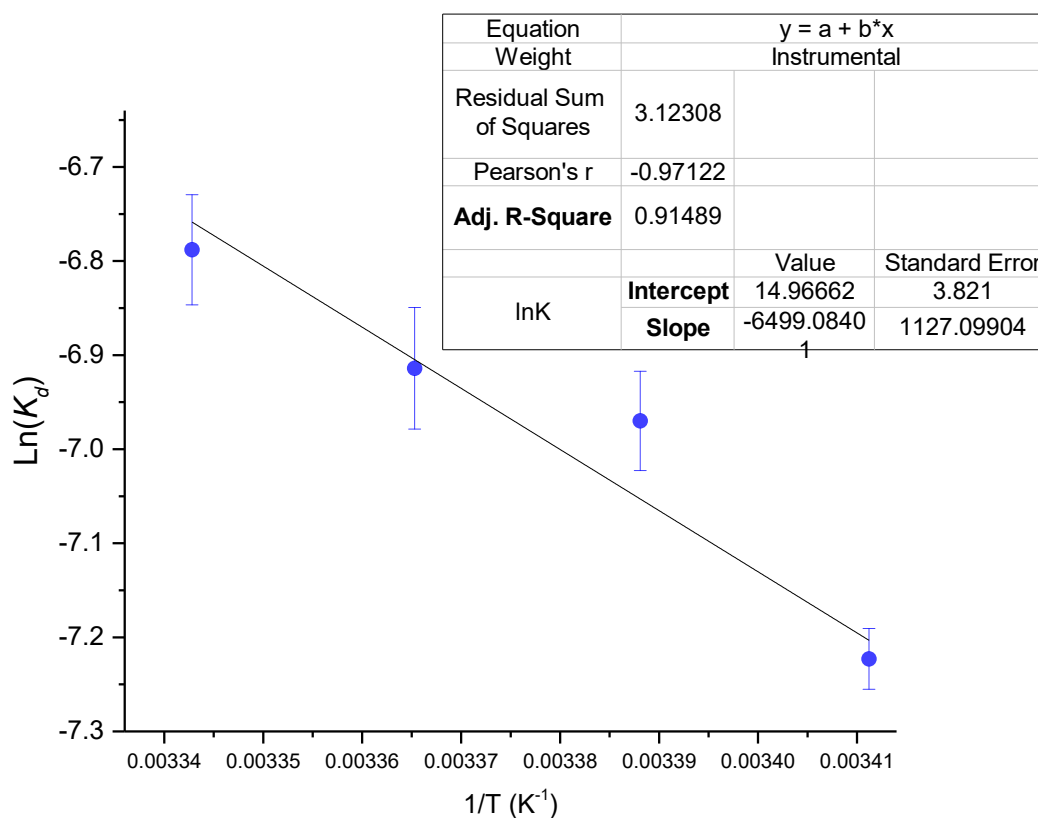


Figure 3.10. van't-Hoff plot for the parent methyl α -D-galactopyranoside

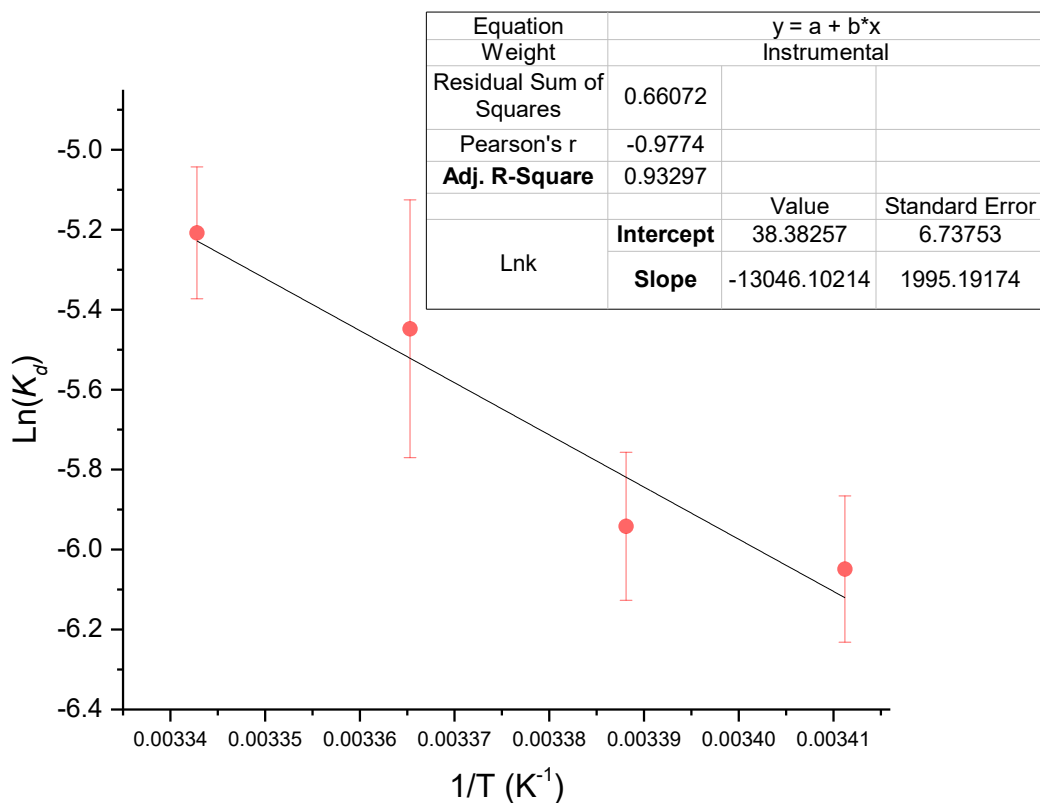


Figure 3.11. van't-Hoff plot for methyl 5-thio- α -D-galactopyranoside **187**.

After that, we performed linear regression analysis to determine the slope and intercept values for both plots, which, for the parent methyl galactoside plot were found to be -6499.084 and 14.967, respectively, and for the methyl 5-thiogalactoside -13046.102 and 38.383, respectively (**Figure 3.10**, **Figure 3.11**). Finally, using (eq 2), (eq 3), and (eq 4) we were able to determine enthalpy, entropy, and Gibbs free energy changes of the binding process (**Table 6**, **Table 7**).

$$\text{slope} = \frac{\Delta H_b}{R} \quad \text{eq (2)}$$

$$\text{intercept} = -\frac{\Delta S_b}{R} \quad \text{eq (3)}$$

$$\Delta G_b = RT \ln K_d \quad \text{eq (4)}$$

Table 6. Thermodynamic parameters of Jacalin bound methyl α -D-galactopyranoside.

T (K)	ΔG_b (kcal/mol)	SDT ΔG_b (kcal/mol)	ΔS_b (cal/mol K)	SDT ΔS_b (cal/mol K)	ΔH_b (kcal/mol)	SDT ΔH_b (kcal/mol)
293	-4.206	0.019	-31.093	7.938	-12.908	-2.239
295	-4.087	0.031				
297	-4.081	0.038				
299	-4.034	0.035				

Table 7. Thermodynamic parameters of Jacalin bound methyl 5-thio- α -D-galactopyranoside **187**.

T (K)	ΔG_b (kcal/mol)	SDT ΔG_b (kcal/mol)	$\Delta \Delta G_b^\ddagger$ (kcal/mol)	ΔS_b (cal/mol K)	SDT ΔS_b (cal/mol K)	ΔH_b (kcal/mol)	SDT ΔH_b (kcal/mol)
293	-3.522	0.10647	-0.684	-76.289	13.39	-25.93	3.966
295	-3.483	0.10858	-0.604				
297	-3.215	0.19032	-0.866				
299	-3.094	0.09791	-0.94				

Remarkably, methyl 5-thio- α -D-galactopyranoside **187** showed a two-fold increase in the enthalpy of binding in comparison to the parent methyl α -D-galactopyranoside. This could be explained by either contribution of S - π interactions between the ring sulfur atom (S -5) and Tyr-122 moieties, and possibly by the occurrence of CH- π interactions between the C5-H5 and C3-H3 bonds and the Tyr-78 moiety (**Figure 3.9**). The increased enthalpy of binding was offset by a two-fold decrease in the entropy of binding, which possibly arises from the need to deform the more puckered 5-thiopyranose ring as compared to the parent glycoside, thus, negating the impact of the two-fold enthalpy increase. Nevertheless, methyl 5-thio- α -D-galactopyranoside **187** was capable of binding to the Jacalin with micromolar binding constant, and the

[‡] ^aDifference in Gibbs free energy of binding between parent methyl galactoside and methyl 5-thiogalactopyranoside **187**.

difference in Gibbs free energy of binding ($\Delta\Delta G_b$) between parent methyl galactoside and 5-thio- α -D-galactopyranoside **187** was less than 1 kcal/mol.

Lactose and 4-thiolactose were submitted to our collaborators at GlycoMIP at the University of Georgia, CCRC for BLI assay to determine binding parameters with Galectin-1. Evaluation of binding affinity of lactose and 4-thiolactose **170** for Galectin-1 is currently ongoing, and the results of the assay will be reported as soon as possible.

3.7. Summary

An extensive PDB database search yielded 226 examples in which glycosidic or ring oxygen atoms were in close proximity to the aromatic residues, and, in addition, 7 PDB entries in which glycosidic sulfur atoms were in close proximity to the aromatic residues, and, finally, 1 PDB entry wherein both glycosidic sulfur and endocyclic ring oxygen atoms were in close proximity to the aromatic rings. Two representative examples of lectin-bound carbohydrates were selected and targeted, and the thio-mimetics of the corresponding parent glycosides were synthesized. For the case of methyl 5-thiogalactoside a positive contribution of S- π interactions between ring sulfur atom and aromatic residues towards enthalpy of binding was observed, however, a considerable entropic penalty, attributed to the ring puckering of the 5-thiogalactopyranosyl derivative, counterbalanced the enthalpic increase. At this stage the binding assay of 4-thiolactose against Galectin-1 is still ongoing, and as such no conclusion can be drawn regarding the impact of the S- π interactions between glycosidic sulfur atom and aromatic residues on binding affinity.

CHAPTER 4

VT NMR STUDIES OF GENERATION AND STABILITY OF REACTIVE INTERMEDIATES GENERATED FROM 5-THIOGLYCOSYL DONORS[§]

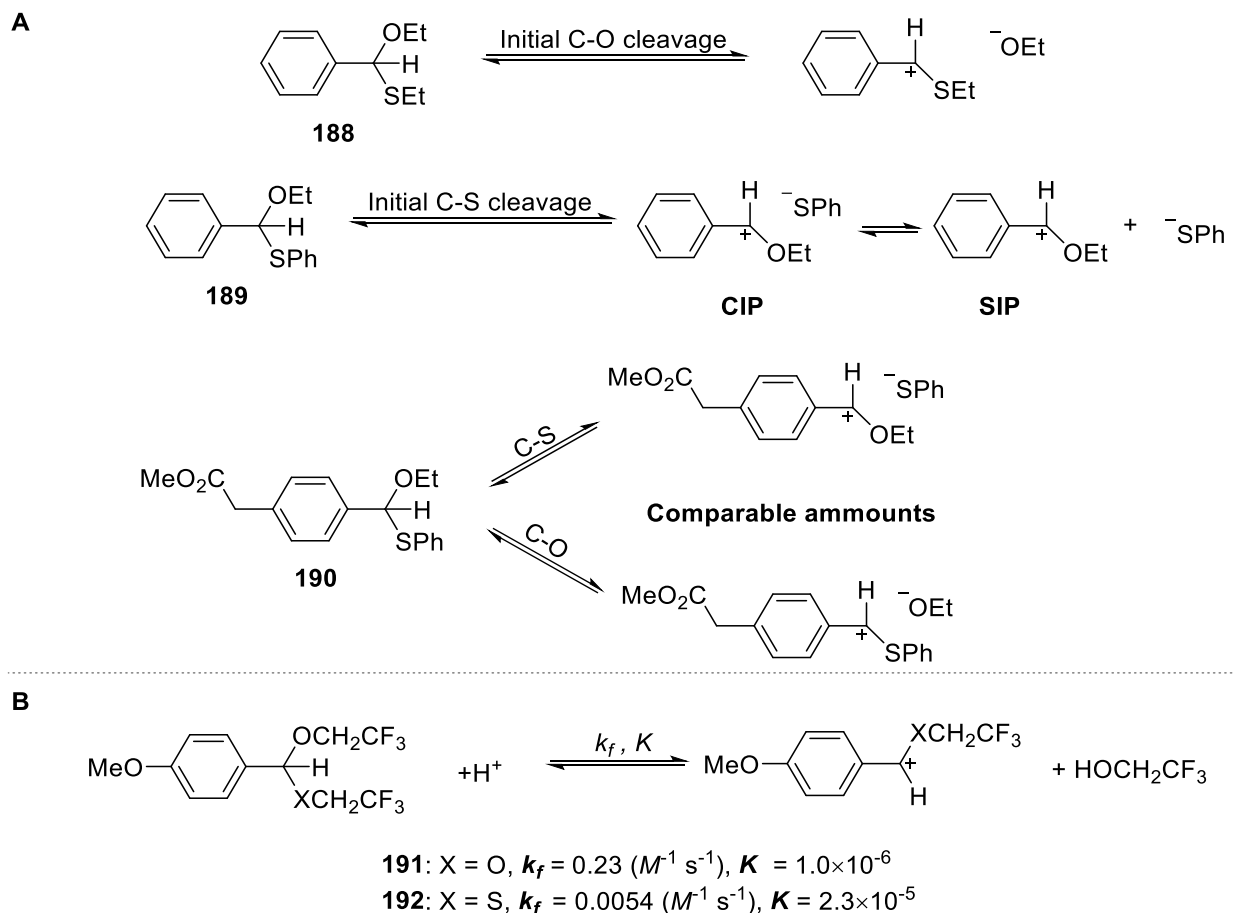
[§] D. Ahiadorme, H. Givhan, H. Schaefer III, and D. Crich to be submitted to the Journal of the American Chemical Society

4.1. Introduction

As discussed in **Chapter 1**, 5-thiosugars show differences in behavior and reactivity to the parent glycosides. One of the main challenges in the synthesis of 5-thiooligosaccharides is the high axial selectivity of 5-thioglycosyl donors, as was shown by Pinto^{86, 88} (**Scheme 8**, **Scheme 9**). Notably, 5-thioglycosyl donors carrying equatorial esters at the C-2 position suitable for the provision of equatorial glycosides by neighboring group participation are in reality axially selective under typical Lewis acidic conditions (**Scheme 8**). In the literature such contrasting behavior of 5-thioglycosyl donors, as compared the parent glycosyl donors, is often explained by the presumed stability of the intermediate thienium ions and so in terms of thermodynamic selectivity.^{37, 88, 193, 194}

Studies of aqueous acidic hydrolysis of methyl 5-thioglucopyranoside and 5-thioxylopyranoside revealed that the hydrolysis of 5-thioglycosides occurs more rapidly than that of the corresponding methyl glycosides. Moreover, hydrolysis of the thiosugars was shown to take place through fully solvent equilibrated thienium ions, whereas full equilibration of any oxocarbenium ions is not achieved in the hydrolysis of the corresponding sugars, suggestive of the greater stability of thienium ions than of their oxocarbenium ion congeners.^{53, 195-199} Beyond carbohydrates, extensive comparative studies on the hydrolysis of simple acetals and monothioacetals revealed the dependence of mechanism on substituents and conditions with the preferential formation of oxocarbenium ion intermediates in some instances and of thienium ions in others. Thus, for example, Jensen and Jencks studied the hydrolysis of benzaldehyde *O,S*-acetals and found that switching from the S*Et* group in **188** to the S*Ph* group in **189** changes the mechanism of hydrolysis, with initial C-S bond cleavage preferred over C-O bond cleavage for **189** (**Scheme 37A**),²⁰⁰ which was explained by S*Ph* being a significantly better leaving group than S*Et* and preventing initial protonation of the O atom.²⁰¹ On the other hand, for **190** comparable amounts of C-O and C-S bond cleavage were observed, which was rationalized by the increased resonance stabilization of the intermediate cations in both cases. Richard and coworkers found that simple monothioacetals **192** were cleaved more slowly than the corresponding acetals **191** under solvolytic conditions (**Scheme 37B**) even though the thienium

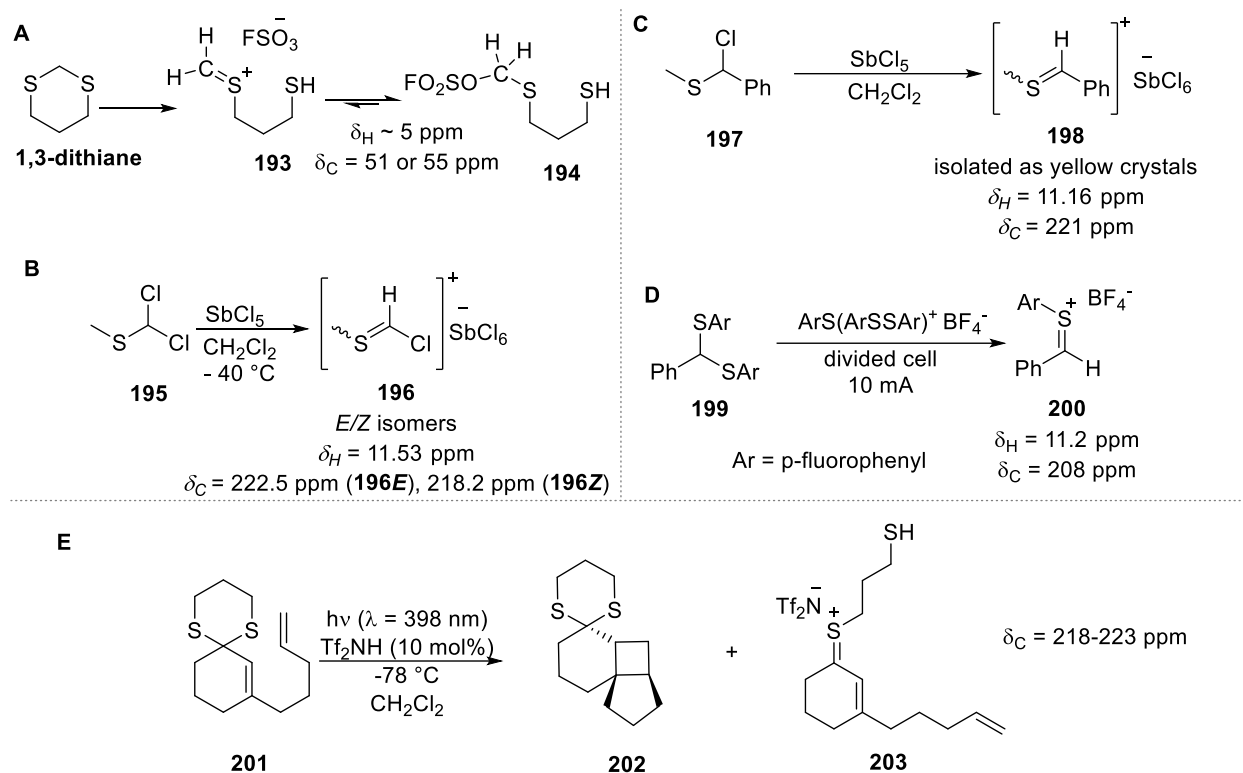
ions were judged to have longer lifetimes.²⁰² This dichotomy was rationalized in terms of a lower kinetic barrier for the formation of the less stable oxocarbenium ion owing to the smaller degree of resonance stabilization at the transition state for formation of the thienium ion.



Scheme 37. A: Study of the hydrolysis of benzaldehyde thioacetals **188**, **189**, **190** hydrolysis; **B:** Hydrolysis of monothioacetals **191** and **192**. k_f — rate constant for formation of the corresponding cation; K — equilibrium constant.

Surprisingly in view of the much-discussed stability²⁰³⁻²⁰⁵ of thienium ions, spectroscopic characterization of them in the solution phase is sparse in contrast to that of simple oxocarbenium ions in both superacid and organic media.²⁰⁶ In early work Lambert and coworkers dissolved 1,3-dithiane in fluorosulfonic acid and tentatively identified a signal at $\delta \sim 5$ ppm as belonging to the sp^2 -C bound hydrogen atom in ion **193** (Scheme 38A).²⁰⁷ The likely inconsistency of this chemical shift with structure **193** was recognized, however, leading to the alternative suggestion of an unidentified solvolysis product,²⁰⁷ which

in view of the current knowledge of oxocarbenium ions and their covalent complexes with “non-nucleophilic” counterions,^{199, 206, 208-212} can be tentatively assigned to the covalent fluorosulfonate **194**.



Scheme 38. **A**: Reactive intermediates generated from 1,3-dithiane in superacid; **B**: Generation of thienium salts from aliphatic sulfide; **C**: Generation of benzylic thienium cation; **D**: Benzylic thienium cation generated with cation pool method; **E**: Thienium cation observed by NMR spectroscopy after protonation of 1,3-dithiane **201**.

Hartke and Akgun described a thienium ion **196** (Scheme 38B) generated by treating dichloromethyl methyl sulfide **195** with SbCl_5 in $\text{CD}_3\text{NO}_2/\text{CD}_2\text{Cl}_2$,²¹³ and recorded its ^1H and ^{13}C NMR spectra, assigning signals at $\delta_{\text{C}} = 222.5$ and 218.2 ppm to the cationic carbon in forms **196E** and **196Z** respectively.²¹³ Subsequently phenyl (methylthio)methyl sulfide **198** was generated and successfully isolated as yellow crystals (Scheme 38C);²¹⁴ its ^1H and ^{13}C NMR spectra showed signals similar to those observed for **196**, most notably a downfield carbocation-type signal $\delta_{\text{C}} = 221$ ppm in the ^{13}C NMR spectrum. Much later, Yoshida and coworkers used their cation pool method to generate the benzylic thienium ion **200** at -78°C in CD_2Cl_2 and record its ^1H and ^{13}C NMR spectra, which showed peaks at $\delta_{\text{H}} = 11.2$ ppm and δ_{C}

= 208 ppm corresponding to the thienium cation (**Scheme 38D**).²¹⁵ Finally, Brenninger and Bach protonated dithiane **201** with triflimide in CD₂Cl₂ at -70 °C and observed by ¹H and ¹³C-NMR spectroscopy a substance ascribed to ion **203** with a characteristic downfield signal at δ_C = 218-223 ppm (**Scheme 38E**).²¹⁶

The reactive intermediates generated on activation of simple glycosyl donors have been extensively studied and documented.^{199, 206, 211, 217, 218} Several reactive intermediates have been generated and characterized by NMR spectroscopy (**Figure 4.1**), such as: i) glycosyl triflates,^{217, 219} ii) acyloxonium intermediates,²¹⁹ and iii) deoxyglycosyl cations generated in HF/SbF₅ superacidic media.^{212, 220, 221} However, in contrast, to date there are no reports in the literature characterizing the reactive intermediates generated on activation of 5-thioglycosyl donors.

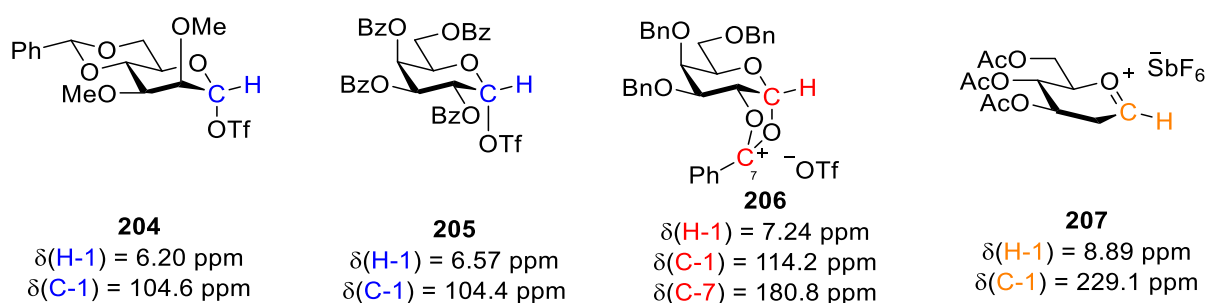


Figure 4.1. Examples of reactive intermediates generated after activation of glycosyl donors and the key chemical shifts in ¹H and ¹³C NMR spectra.

4.2. Goals of the project and considerations

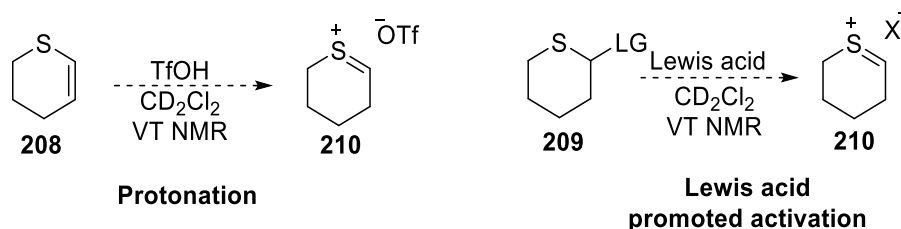
The global goal of the project was to explore, detect and characterize reactive intermediates generated after activation of various 5-thioglycosyl donors using variable temperature NMR techniques in attempt to shed light on the differences in reactivity of 5-thiosugars as compared to parent glycosides.

The first aim was to study the generation and stability of simple thiocarbenium cations and to characterize them with VT NMR spectroscopy. We sought to employ substrates that could be easily activated to form thiocarbenium cations, thus we selected various vinyl sulfides and 2,3-dihydrothiopyran as substrates that could produce thiocarbenium cations upon protonation with TfOH.

The second aim was to study reactive intermediates generated after activation of 5-thioglycosyl donors, characterize these intermediates with VT NMR spectroscopy, and compare them with those generated after activation of the parent glycosyl donors. We sought to employ both armed ester-protected and disarmed ether-protected glycosyl donors that could be easily activated by addition of a single promoter without gas evolution or precipitation.

4.3. VT NMR studies of simple thiocarbenium cations

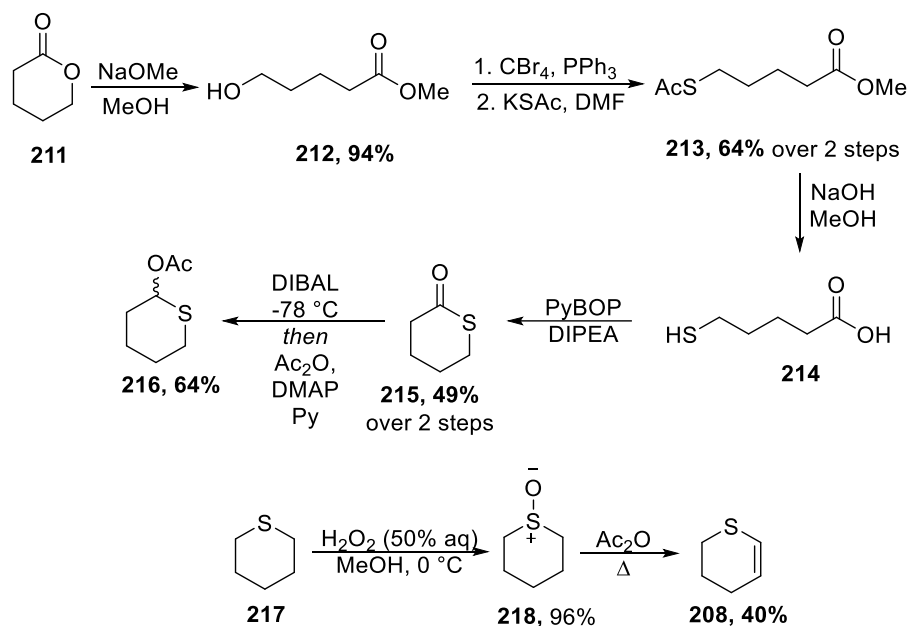
We picked tetrahydrothiopyran derivatives to study generation of simple thiocarbenium cations in the absence of multiple functional groups. Designing the experiment, we envisioned two possible avenues (**Scheme 39**) to generate a thiocarbenium cation: i) protonation of 2,3-dihydrothiopyran **208** with TfOH, and ii) Lewis acid promoted activation of thiopyran derivative **209** bearing a leaving group at the C-1 position.



Scheme 39. Substrates and methods to generate thiocarbenium cation during VT NMR experiments.

We began our synthetic efforts with the preparation of 2-acetoxythiane **216**, as a substrate that could be activated by a Lewis acid promoter, and 2,3-dihydrothiopyran **208**, which can be protonated with TfOH to potentially generate thiocarbenium cation (**Scheme 40**). Starting from commercially available δ -valerolactone, nucleophilic lactone opening with NaOMe produced methyl ester **212** in 94% yield.²²² Appel bromination of the terminal hydroxy group, followed by subsequent S_N2 displacement with KSAc in DMF allowed thioacetate **213** to be formed in 64% yield over 2 steps. Next, saponification of **213** produced 5-mercaptovaleric acid **214**, which, adopting reported protocol,²²³ then was subjected to PyBOP promoted lactonization to form thiolactone **215** in 49% yield over 2 steps. Finally, adopting Rychnovsky's protocol

for reductive acetylation of esters,^{224, 225} thiolactone was converted into 2-acetoxythiane **216** in 64% yield (Scheme 40).

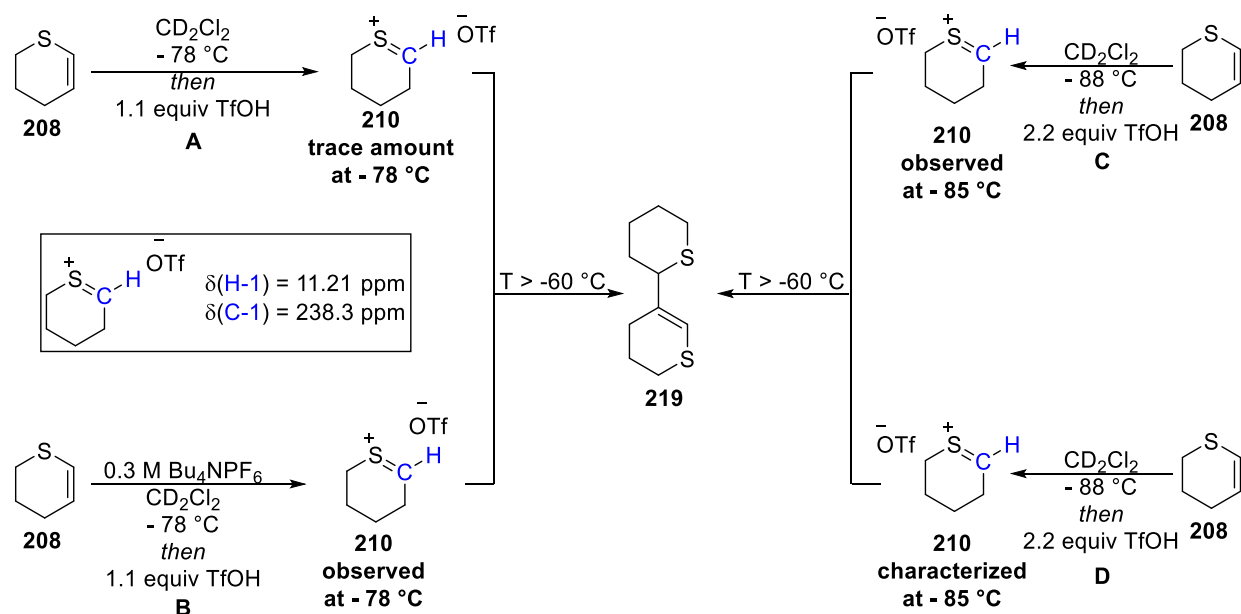


Scheme 40. Synthesis of thiopyran derivatives **216** and **208**.

Next, we synthesized 2,3-dihydrothiopyran **208**. Adopting literature protocols,^{226, 227} thiane **217** was oxidized with H_2O_2 to form sulfoxide **218** in 96% yield, which underwent Pummerer reaction in presence of Ac_2O to produce the desired 2,3-dihydrothiopyran **208** in 40% yield.

With two substrates synthesized, we commenced VT NMR experiments. We chose to use dichloromethane- d_2 as a solvent, since dichloromethane is by far the most widely used solvent for glycosylation reactions, and, in addition, has low melting point ($\sim -97^\circ\text{C}$),²²⁸ which allows low temperatures to be reached without freezing. Thus, addition of 1.1 equiv of TfOH to a 0.25 M solution of **208** in CD_2Cl_2 precooled to -78°C in the probe of the NMR spectrometer and rapid acquisition of ^1H and ^{13}C NMR spectra revealed a complex mixture that nevertheless contained what was subsequently identified as a trace amount of the desired thiocarbenium ion **210** (Scheme 41A). After termination of the VT NMR experiment, a complex mixture of self-condensation products was obtained, in which dimer **219** could be identified by

HRMS analysis and by the presence of diagnostic signals in the ^1H NMR spectrum that matched those reported in the literature.²²⁹



Scheme 41. VT NMR experiments with 2,3-dihydrothiopyran **208**. Letters under the reaction arrow denote different methods.

Taking inspiration from the Yoshida cation pool method,²³⁰ to increase the polarity of the medium we mixed **208** with freshly dried Bu_4NPF_6 (0.3 M in CD_2Cl_2) and protonated the resulting solution with 1.1 equiv of TfOH at $-78\text{ }^\circ\text{C}$. As a result, we were able to generate improved spectra of the thiocarbenium cation **210** (Scheme 41B, Figure 4.2A), which was characterized by a peak at $\delta_{\text{H}} = 11.21\text{ ppm}$ in the ^1H NMR spectrum corresponding to the proton attached directly to the thiocarbenium carbon. In the DEPT-135 spectrum a downfield resonance at $\delta_{\text{C}} = 238.3\text{ ppm}$ was observed, which showed a HMQC correlation to the peak at $\delta_{\text{H}} = 11.21\text{ ppm}$ in the ^1H NMR and was therefore assigned as the sp^2 -hybridized cationic carbon (Figure 4.2A). As TfOH is poorly soluble in CD_2Cl_2 and freezes at temperatures below $-40\text{ }^\circ\text{C}$, we reasoned that incomplete protonation of 2,3-dihydrothiopyran resulted in oligomerization. Accordingly, in the experiments without the quaternary ammonium salt we doubled the amount of TfOH added and decreased the initial temperature to $-88\text{ }^\circ\text{C}$ to compensate for the inevitable temperature spike occurring during ejection of the sample from the precooled NMR probe, rapid addition of the acid, and reinsertion of the

sample into the NMR probe. As a result, we were able to generate the thiocarbenium cation, which had the same spectral data as the one generated in the presence of the quaternary ammonium salt (**Scheme 41C**, **Figure 4.2B**). On gradual warming these signals persisted until ~ -50 °C suggestive of only moderate stability of the thiocarbenium ion under the reaction conditions (**Figure 4.3**). Attempted generation and characterization of the corresponding oxocarbenium ion **221**, previously generated electrochemically by Yoshida and coworkers in CD_2Cl_2 ,²³⁰ was unsuccessful under the same conditions and led to generation of multiple self-condensation products among which dimer **222** was identified by LCMS. In addition, we also attempted to generate the simple acyclic thiocarbenium ions **224** and **227** by the same method but were unable to observe them, presumably due to rapid self-condensation (**Scheme 42**). Finally, we performed Lewis acid promoted activation of 2-acetoxythiane **216** in an attempt to generate the same thiocarbenium cation **2** via different pathways. Notably, no cation was observed, and, instead, a mixture of decomposition products was formed, in which 2,3-dihydrothiopyran **208** was later detected by LCMS. The same results were obtained when parent 2-acetoxytetrahydropyran **229** was subjected to the same conditions.

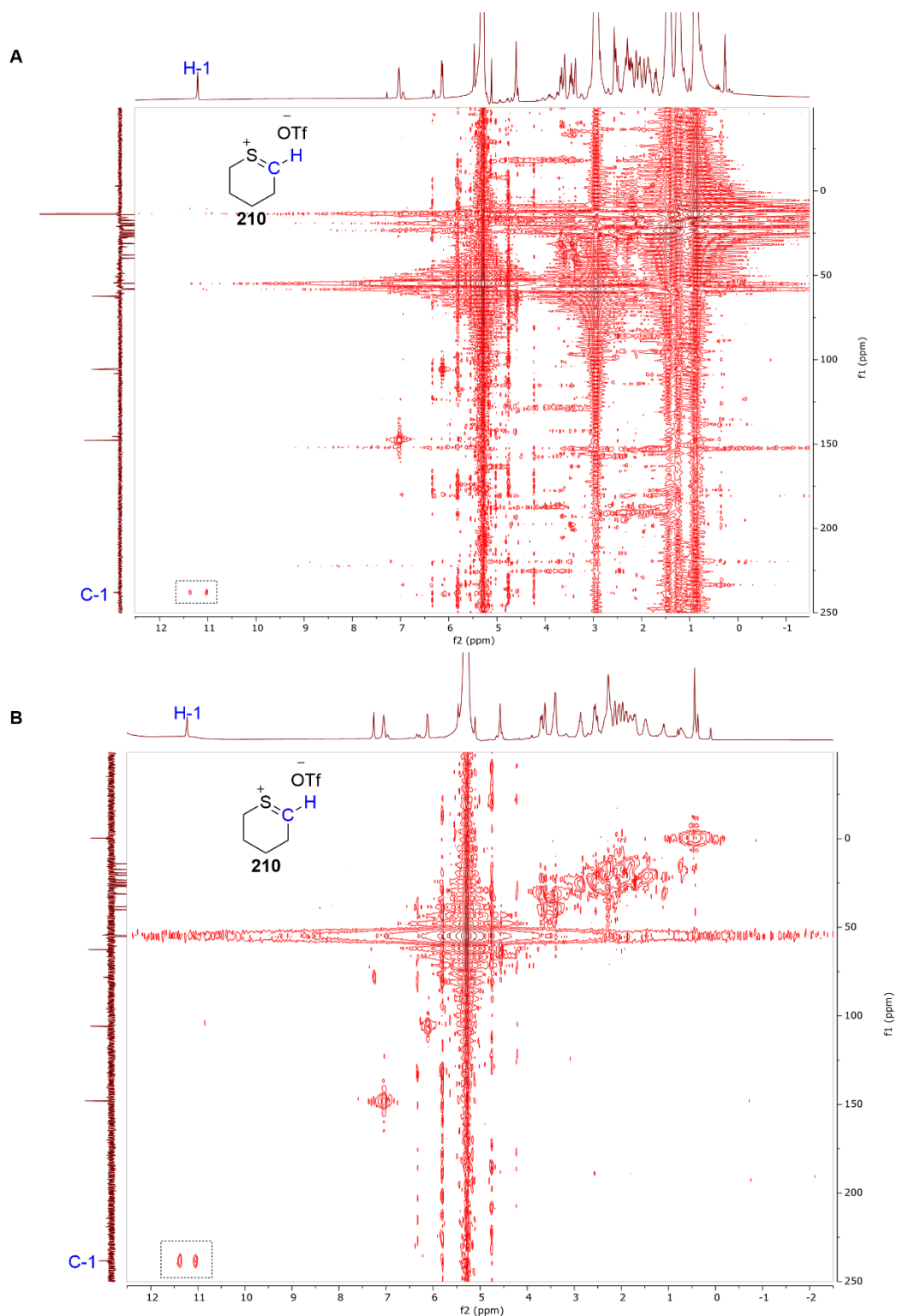


Figure 4.2. gHMQC x-decoupled spectra plotted against DEPT-135 with the key peaks; **A.** Recorded at -78 °C during VT NMR experiment with phase-transfer catalyst with addition of 1.1 equiv of TfOH; **B.** Recorded at -85 °C during VT NMR experiment without phase-transfer catalyst with addition of 2.2 equiv of TfOH.

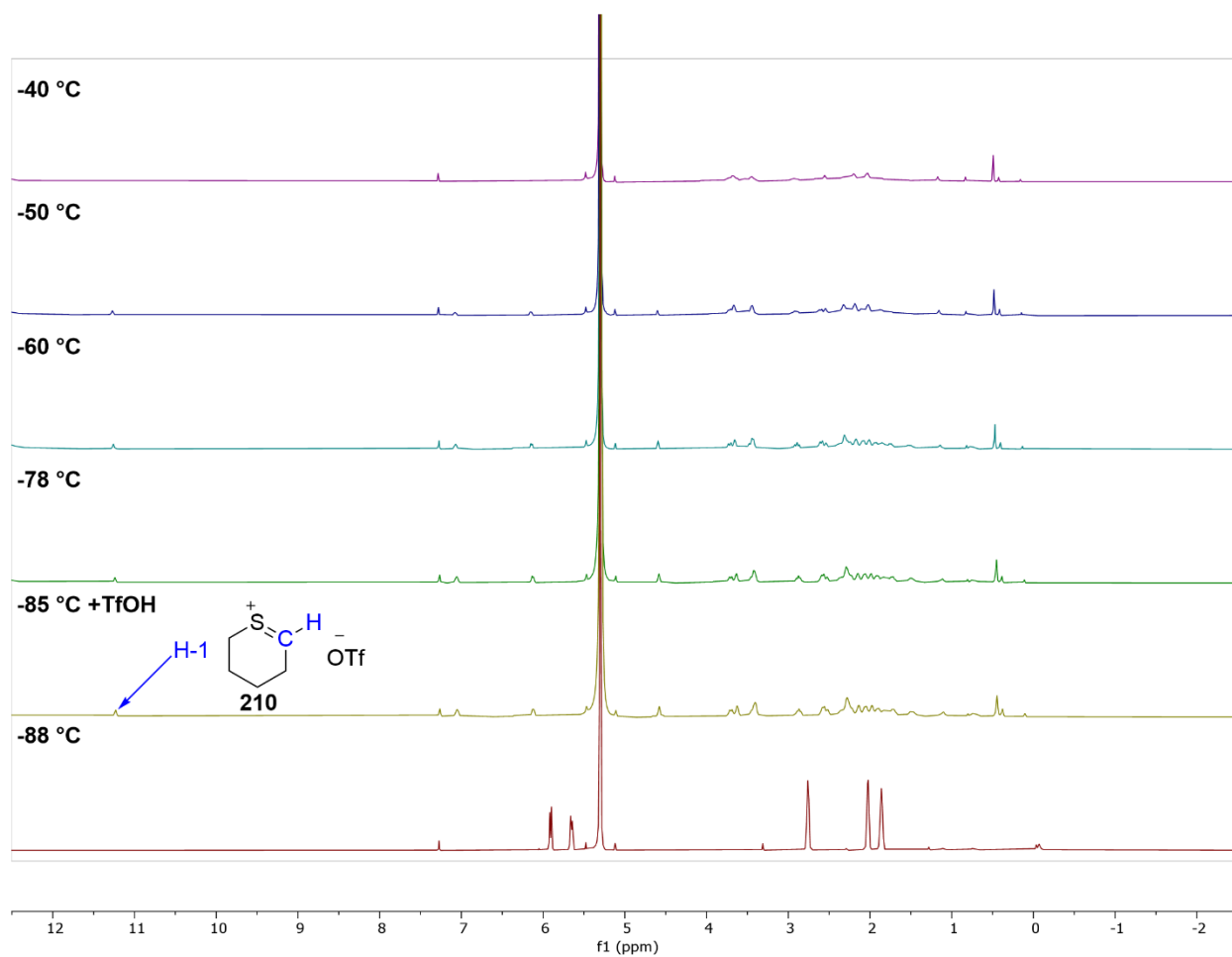
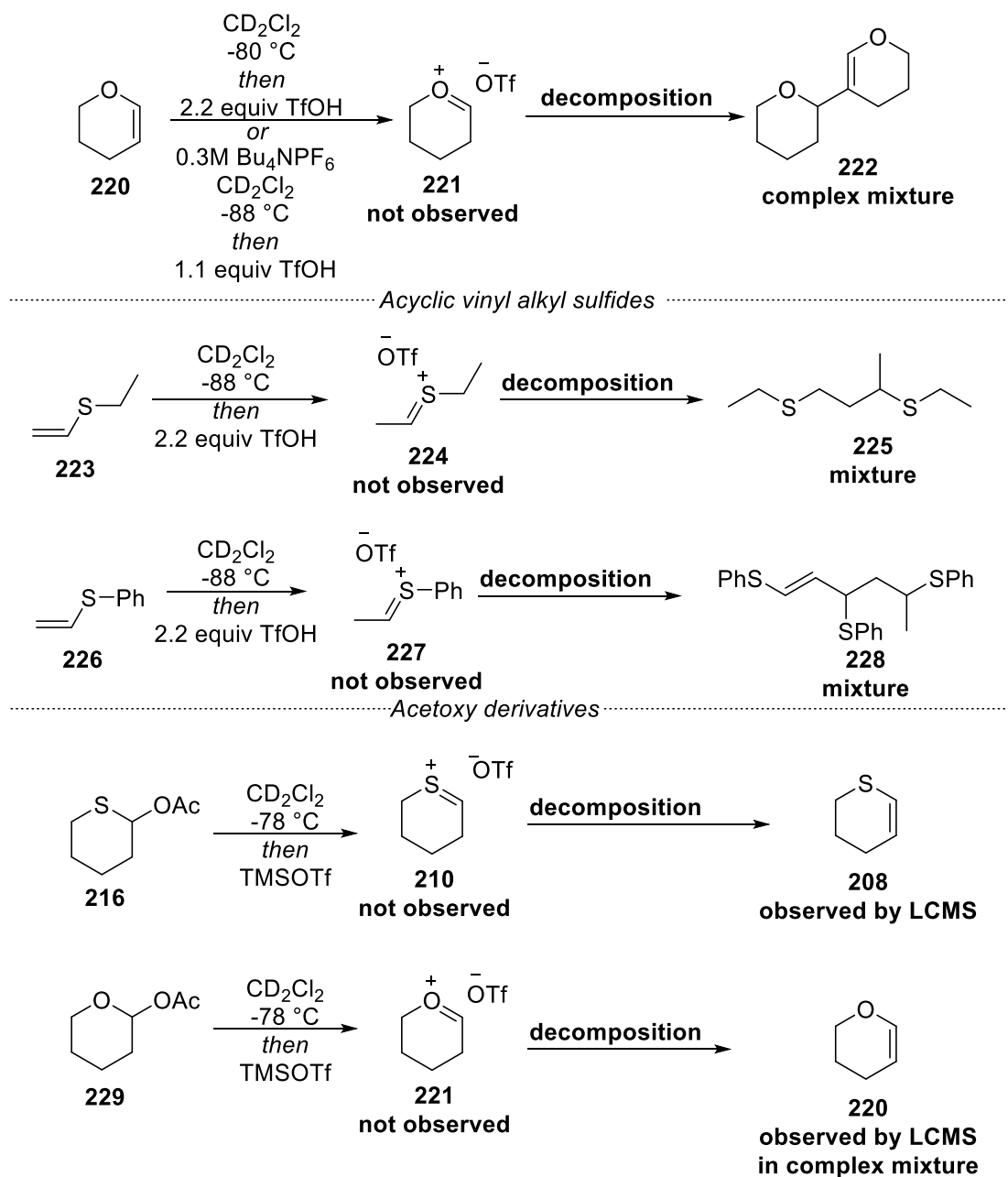


Figure 4.3. Stacked ^1H NMR spectra from VT experiment without phase-transfer catalyst with addition of 2.2 equiv of TfOH.



Scheme 42. Summarized results of VT NMR experiments with parent 2,3-dihydropyran, various vinyl sulfides, and acetoxy derivatives.

To provide further support for the structure of thiocarbenium ion **218** beyond the obvious chemical shift correlations with the data reported by Hartke and Akgun for the simple unconjugated thiocarbenium cation **196** (Scheme 38),²¹³ we turned to computation. Cognisant of the importance of counterions in glycosylation and related reactions^{211, 231} and of previous difficulties in computing oxocarbenium ion-

counterion pairs in the absence of artificial constraints to prevent spontaneous collapse to covalent adducts,^{232, 233} we turned to the method developed by Hosoya, Kosma and coworkers in which a dichloromethane solvent continuum is complemented by the inclusion of specific molecules of dichloromethane to stabilize the triflate counterion by hydrogen-bonding, that has been shown to correlate well with experiment.²³⁴⁻²³⁶ The computed structures of the two cations **210** and **221** and those of the corresponding covalent triflates **230** and **231** are presented in **Figure 4.4**. We thank Houston Givhan in the Schaefer laboratory for conducting the computations on our behalf.

The computed internal bond angles and ring torsional angles clearly indicate considerable puckering of the thiocarbenium cation as evidenced by: i) significantly decreased C5-S-C1 and S-C1-C2 bond angles (106.5° and 113.8° respectively) of **210** as compared to the C5-O-C1 and O-C1-C2 bond angles (121.4° and 126.2° respectively) in **221**, and ii) significantly increased C5-S-C1-C2 and S-C1-C2-C3 ring torsion angles (42° and -55.2° respectively) of **210** as compared to the C5-O-C1-C2 and O-C1-C2-C3 ring torsion angles (-0.2° and -8.2° respectively) in **221**, as well as C4-C5-S-C1 torsion angle (-43.4°) as compared to the C4-C5-O-C1 (-22.3°) in **221**. In addition, both cations have *ca* 1.9 bond order of S-C1 and O-C1, suggesting a high degree of π -character of both the S-C1 and O-C1 bonds (**Figure 4.4**). In addition, ring puckering is also observed in case of covalent triflate **230** as evident by: i) significantly decreased C6-S1-C2 bond angle (98.4°) of **230** as compared to the C6-O1-C2 bond angle (115.9°) in **231**, and ii) significantly increased S1-C2-C3-C4, C2-C3-C4-C5, C3-C4-C5-C6, C4-C5-C6-S1 ring torsion angles (-57.7°, 59.1°, -61.6°, and 61.6, respectively) in **230** as compared to O1-C2-C3-C4, C2-C3-C4-C5, C3-C4-C5-C6, C4-C5-C6-O1 torsion angles (-48.6°, 51.5°, -56.0°, -55.9°, and 55.9°, respectively) in **231**. A S1-C2-O-S torsion angle of 141.0° was computed for **230**, while the O1-C2-O-S torsion angle in **231** was 130.3° (**Figure 4.4**).

The computed chemical shift of δ 246 ppm in the confines of the dichloromethane-supported ion pair, for a method estimated to have an error of \pm 8 ppm, is in good agreement with the experimental value of δ 238.3 ppm and provides strong support for the structure of ion **210**. More broadly speaking, the

calculated covalent triflate – ion pair separation for both the oxygen-based system (7.27 kcal/mol) and its sulfur analog (4.79 kcal/mol) suggests that thiocarbenium ions are more stabilized than their oxocarbenium ion counterparts by as much as 2.5 kcal/mol.

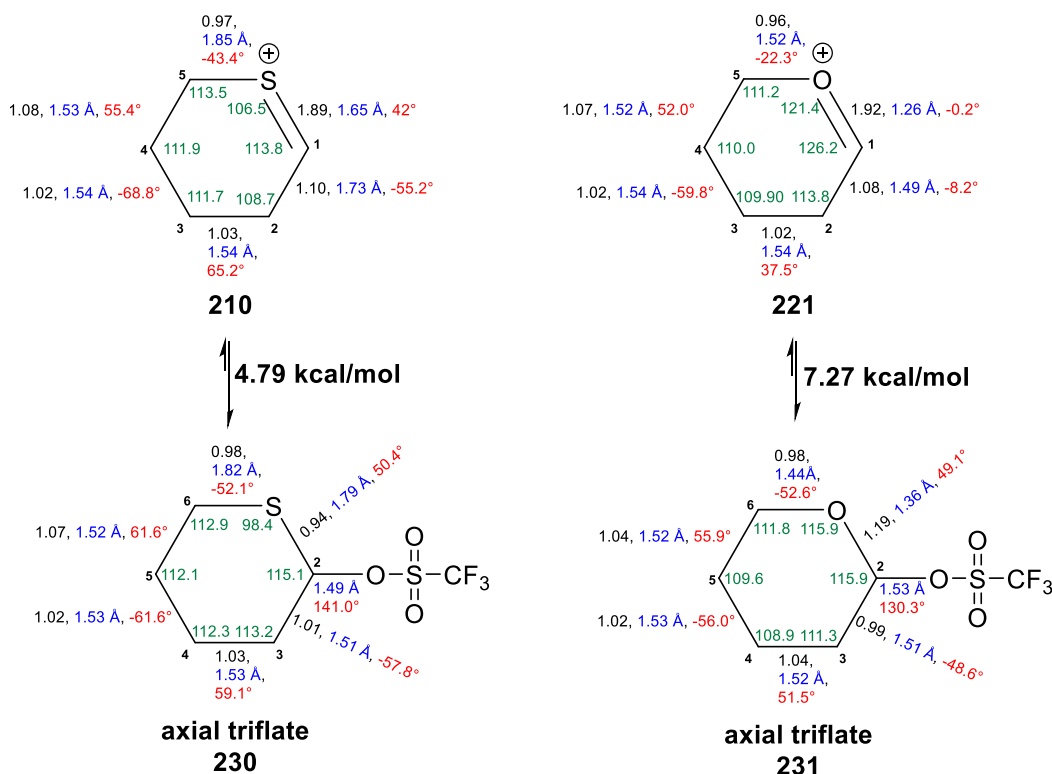


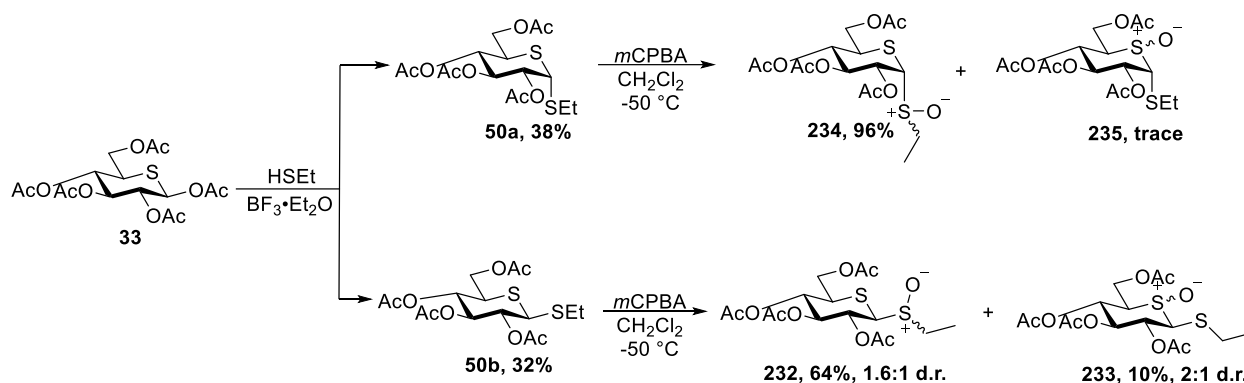
Figure 4.4. Computed natural bond orders (black), bond lengths (blue), ring torsional angles (red), and internal bond angles (green) for thienium ion **210** and oxocarbenium ion **221** and for axial covalent 2-thianyl triflate **230** and axial tetrahydropyranyl triflate **231**. MP2/cc-pvdz method was used to compute natural bond order, a CCSD(T)/cc-pvdz method was used to compute bond lengths, ring torsion angles and internal bond angles, and a MO6-2X/aug-cc-pvtz and cc-pvtz on H and Cl method was used to compute the difference of the electronic energies of the covalent triflates and the corresponding cations.

Secure in the knowledge that the simple cyclic thiocarbenium ion **210** can be generated and characterized in dichloromethane solution at -85 °C and at -78 °C in presence of a quaternary ammonium salt, we turned to the preparation of substrates for a more complete comparative VT-NMR study of the intermediates generated on activation of 5-thioglucofuranosyl and the corresponding glucofuranosyl donors with both arming ether and disarming ester protecting groups.^{237, 238}

4.4. VT NMR studies with disarmed glycosyl donors

First, we aimed to evaluate the reactive intermediates generated from disarmed ester-protected 5-thioglycosyl donors and evaluate the tendency of 5-thioglycosyl donors to generate dioxalenium species, arising from neighboring group participation of acyl group at the C-2 position. Although multiple other types of donor have been employed in VT NMR studies,^{239, 240} we initially selected the glycosyl sulfoxides for this study as they are readily prepared and characterized, are shelf-stable and are typically cleanly activated by simple addition of trifluoromethanesulfonic anhydride at -78 °C, thereby minimizing experimental complications.^{217, 241} Taking into account a study by Hashimoto²⁴² on the relative nucleophilicity of the two sulfur atoms in ethyl and phenyl 1,5-dithioglucopyranosides, ethyl thioglycosides were selected as a substrates for glycosyl sulfoxide generation because greater selectivity for oxidation of the exocyclic rather than the endocyclic sulfur was expected for the more electron rich ethylthio series than for the phenylthio series, thus allowing for a more efficient, practical synthesis of the desired substrates.

We began our synthetic efforts with preparation of 5-thioglycosyl sulfoxides **232** and **234** (Scheme 43). Following the reported protocol, and taking advantage of the unselective thioglycosylation reaction,⁸⁶ both α -thioglycoside **50a** and β -thioglycoside **50b** were synthesized from 5-thioglucose pentaacetate **33**^{70, 80} in 38% and 32% yield, respectively. Oxidation of β -thioglycoside **50b** with *m*CPBA led to generation of a mixture of sulfoxides. Taking advantage of the considerable polarity difference among the various so-formed 5-thioglycosyl sulfoxides, we were able to isolate diastereomeric 5-*S*-oxides **233** in 10% yield, as well as the desired 1-*S*-oxides **232** in 64% yield. In the parallel synthesis, *m*CPBA oxidation of the α -thioglycoside **50a** gave 1-*S*-oxide **234** as a single diastereomer in 96% yield accompanied by only a trace amount of the 5-*S*-oxide **235**.



Scheme 43. Synthesis of peracetylated 5-thioglycosyl sulfoxides.

The regioselectivity of the *m*CPBA oxidation was determined by NMR spectroscopy and comparison with literature spectral data reported for related 5-thioglycosides *S*-oxides.²⁴² Thus, in the ^1H NMR spectrum of **232**, a characteristic geminal splitting of the methylene protons of the SCH_2CH_3 group was observed, in addition to which the ^{13}C NMR spectrum revealed changes in the chemical shift of the SCH_2CH_3 methylene group carbon ($\delta_{\text{c}} = 43.3$ and 42.7 ppm) in comparison to that of the thiosugar starting material **50b** ($\delta_{\text{c}} = 24.9$ ppm), while little to no change in chemical shift of C-5 ($\delta_{\text{c}} = 43.2$ and 45.1 ppm) in comparison to the starting material **50b** ($\delta_{\text{c}} = 44.4$ ppm) was observed (**Figure 4.5**).

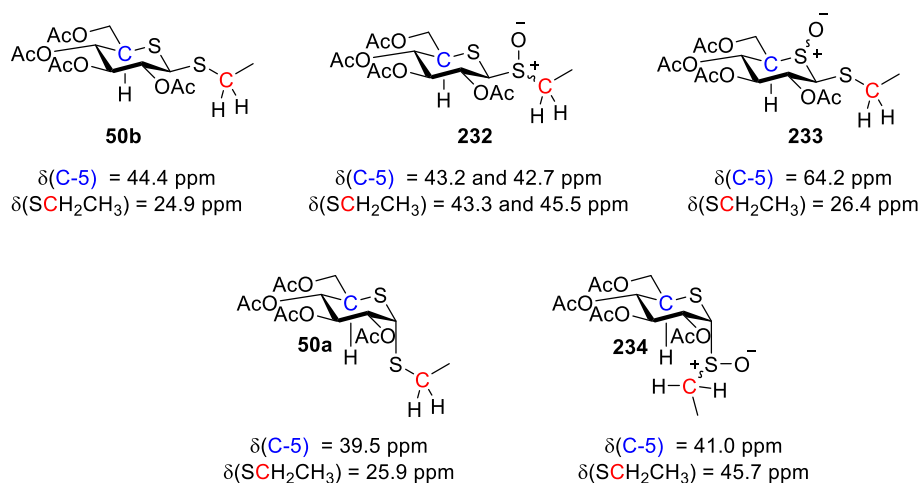
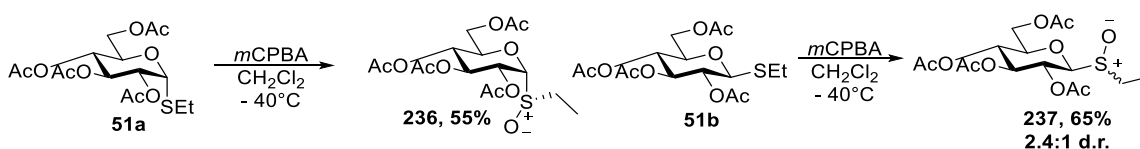


Figure 4.5. The comparison of the key ^{13}C NMR peaks of the starting material and sulfoxides.

On the other hand, no geminal splitting of the SCH_2CH_3 methylene protons was observed in the ^1H NMR spectrum of the endocyclic sulfoxide **233**. In addition, little to no change was observed in the

chemical shift of the SCH₂CH₃ methylene carbon ($\delta_c = 26.4$ ppm) of **233** compared to the starting material **50b** ($\delta_c = 24.9$ ppm) and a significant change was noted in the chemical shift of the C-5 ($\delta_c = 64.2$ ppm) with respect to the starting material **50b** ($\delta_c = 44.4$ ppm). The same analysis was conducted for α -sulfoxide **234**. In the ¹H NMR spectrum of **234**, a characteristic geminal splitting of the methylene protons of the SCH₂CH₃ group was observed, in addition to which the ¹³C NMR spectrum revealed changes in the chemical shift of the SCH₂CH₃ methylene group carbon ($\delta_c = 45.7$ ppm) in comparison to that of the thiosugar starting material **50a** ($\delta_c = 25.9$ ppm), while little to no change in chemical shift of C-5 ($\delta_c = 41.0$ ppm) in comparison to the starting material **50a** ($\delta_c = 39.5$ ppm) was observed (**Figure 4.5**).

The synthesis of the glucosyl sulfoxide comparators employed the commercially available α - and β -thioglucosides **51a** and **51b** (**Scheme 44**). Thus, *m*CPBA oxidation of the α -thioglycoside **51a** gave glucosyl sulfoxide **236** as a single diastereomer in 55% yield that was assigned the *R_S* configuration by analogy with the precedent,²⁴³ while that of β -thioglycoside **51b** afforded sulfoxides **237** as a mixture of diastereomers in 65% yield.



Scheme 44. Synthesis of peracetylated glucosyl sulfoxides.

With peracetylated glycosyl sulfoxides in hand we commenced VT NMR studies. Beginning with the parent β -glucosyl sulfoxides **237**, activation with triflic anhydride at -78 °C in deuteriodichloromethane led to the generation of mixtures comprised mainly of the “activated sulfoxide” **238**, and lesser amounts of the dioxalenium ion **239** and the α -glycosyl triflate **240** (**Figure 4.6**, **Figure 4.7**). The “activated sulfoxide” **238** was characterized by more downfield chemical shifts of the SCH₂CH₃ methylene and anomeric protons H-1 (e.g., $\delta_H = 5.18$ ppm and $\delta_H = 4.41$ ppm NMR resonances corresponding to the anomeric proton H-1 of **238** and **237**, respectively). The dioxalenium ion was characterized by two diagnostic ¹H NMR signals: i) a downfield anomeric signal at $\delta_H = 7.19$ ppm and ii) a signal at $\delta_H = 2.84$ ppm, corresponding to the

dioxalenium methyl group. Additionally, in the ^{13}C NMR spectra a downfield signal at $\delta_{\text{C}} = 191.7$ ppm, corresponding to the C-7₂₃₉, was observed, along with a signal at $\delta_{\text{C}} = 112.3$ ppm, corresponding to the anomeric carbon. The signal at $\delta_{\text{C}} = 191.7$ ppm showed a weak HMBC correlation to the anomeric proton at $\delta_{\text{H}} = 7.19$ ppm and strong one to the dioxalenium methyl group at $\delta_{\text{H}} = 2.84$ ppm, all fully consistent with the assigned structure **239** (**Figure 4.6**) and with literature data.²¹⁹ Triflate **240** was characterized by a ^1H NMR resonance at $\delta_{\text{H}} = 6.16$ ppm and by a ^{13}C NMR resonance at $\delta_{\text{C}} = 103.4$ ppm corresponding to the H-1₂₄₀ and C-1₂₄₀ atoms respectively of **240** (**Figure 4.6**), again consistent with the literature.²¹⁹ On gradual warming the activated sulfoxide **238** was converted to the dioxalenium ion **239** and the triflate **240**, with the transformation being essentially complete by ~ 20 °C. The concentration of triflate **240** reached a maximum between -20 °C and -10 °C above which it rapidly fell off, while the signals due to the dioxalenium ion **239**, were maximal between -20 °C and 0 °C (**Figure 4.7**) and persisted even at $+25$ °C. After termination of the VT NMR experiments with **237** byproducts pentaacetate **7** and enone **241** were isolated from the reaction mixture, both with spectral data in agreement with the literature.^{244, 245} Overall results of the VT NMR experiment with **237** are summarized in **Scheme 45**.

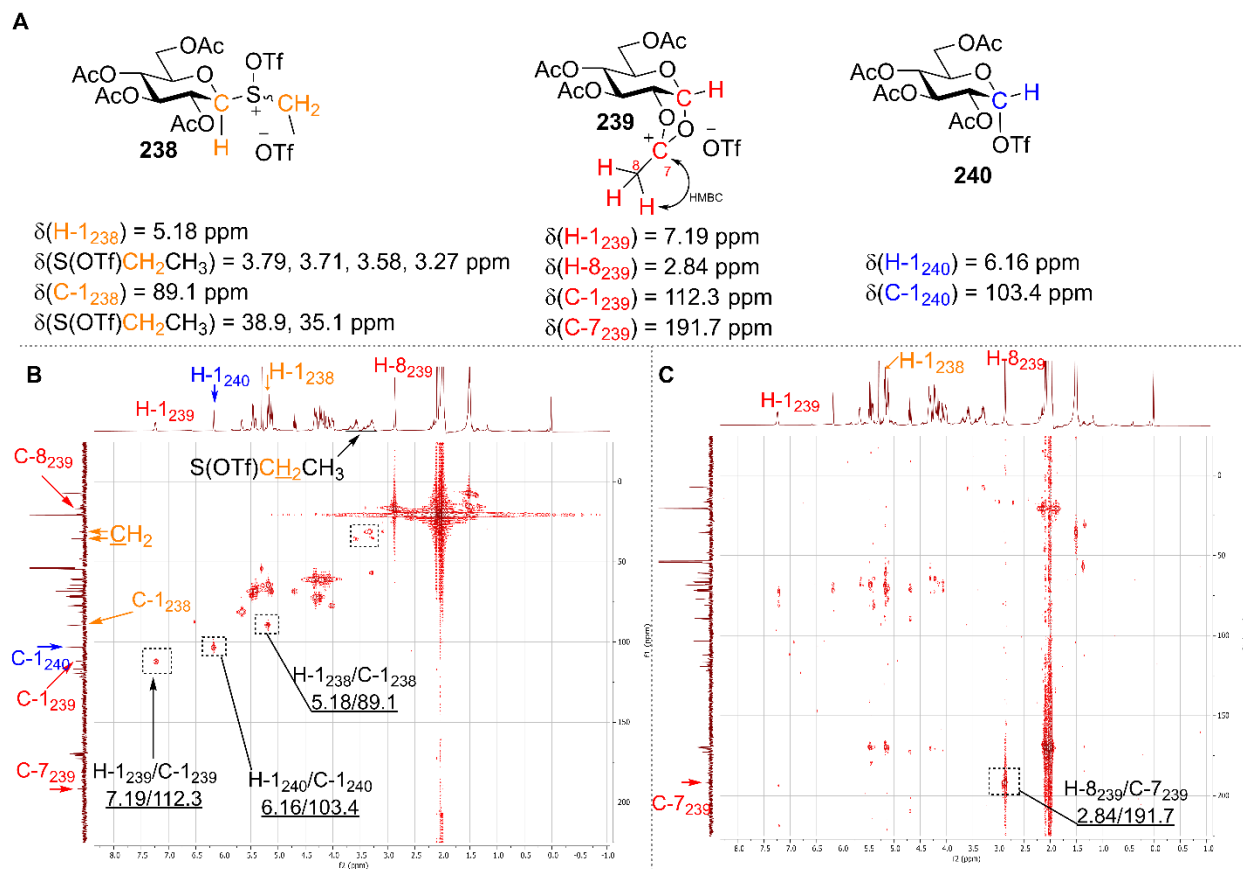


Figure 4.6. Key data from a VT NMR experiment with glucosyl sulfoxide **237**. **A:** Structures and chemical shifts of intermediates **238**, **239**, and **240**; **B:** HMQC spectrum with the key cross-peaks recorded at -30°C ; **C:** HMBC spectrum with the key cross-peak recorded at -30°C .

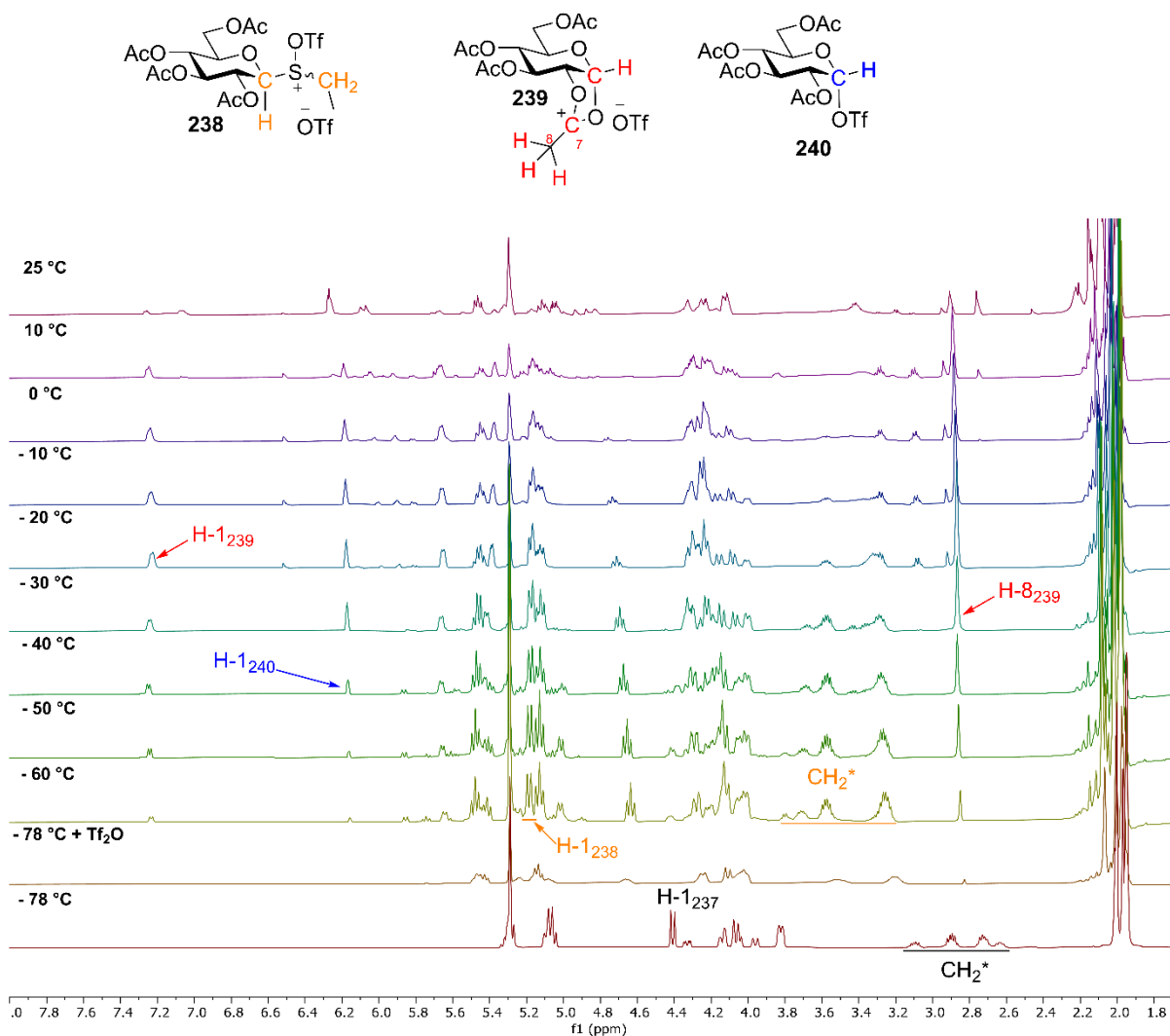
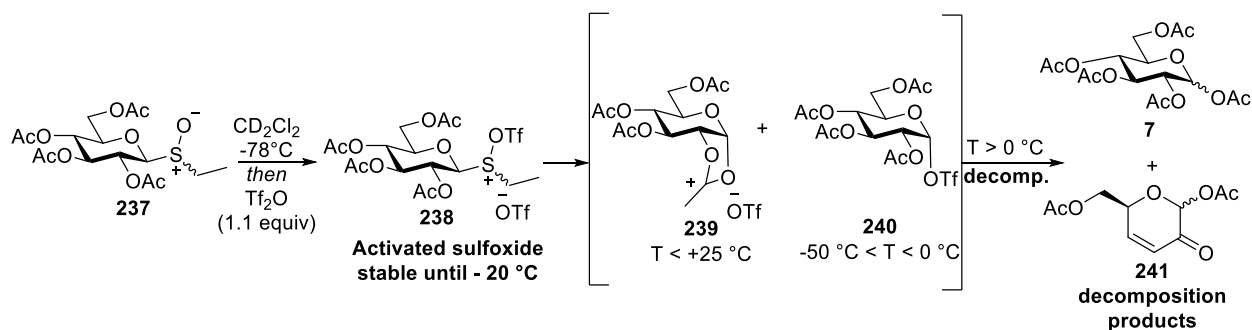


Figure 4.7. Structures of reactive intermediates and stacked ^1H NMR from a VT NMR experiment with glucosyl sulfoxide **237**.



Scheme 45. Intermediates and decomposition products generated during VT NMR experiments with glucosyl sulfoxide **237**.

We then performed the same VT NMR experiment with α -glucosyl sulfoxide **236**. Similarly to **237**, activation of glucosyl sulfoxide **236** with triflic anhydride at -78 °C in deuteriodichloromethane led to the generation of mixtures comprised of the “activated sulfoxide” **242**, and lesser amounts of the dioxalenium ion **239** and the α -glycosyl triflate **240**. Similarly to **238**, the “activated sulfoxide” **242** was characterized by more downfield chemical shifts of the SCH₂CH₃ methylene and anomeric protons H-1 (e.g., δ_{H} = 5.67 ppm and δ_{H} = 4.77 ppm NMR resonances corresponding to the anomeric proton H-1 of **242** and **236**, respectively) (**Figure 4.8**). Both observed reactive intermediates **239** and **240** had the same chemical shifts, as those observed during VT NMR experiment with β -sulfoxide **237**. Similarly to **237**, on gradual warming the activated sulfoxide **242** was converted to the dioxalenium ion **239** and the triflate **240**, with the transformation being complete by ~-20 °C (**Figure 4.9**), and, after termination of the VT NMR experiments, the same byproducts pentaacetate **7** and enone **241** were isolated from the reaction mixture. The overall results of the VT NMR experiment with glucosyl sulfoxide **237** are summarized in **Scheme 46**.

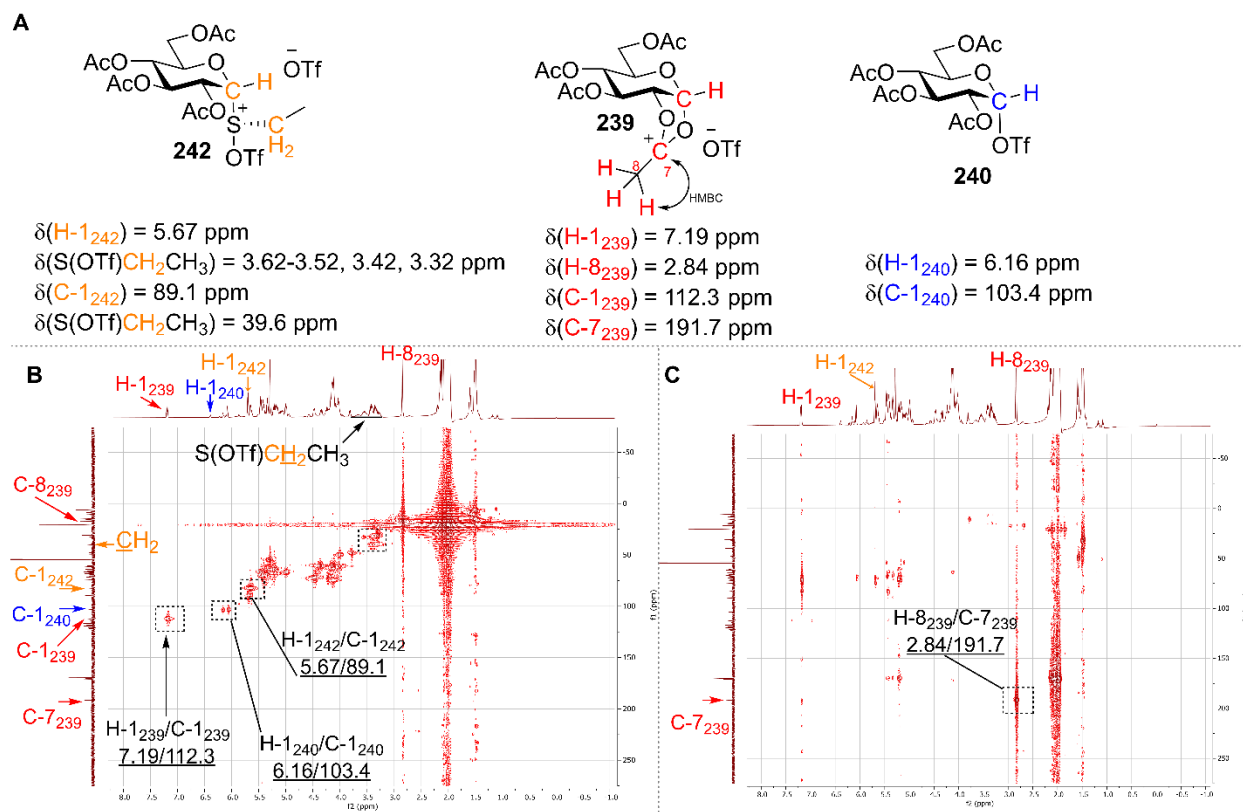


Figure 4.8. Key data from a VT NMR experiment with glucosyl sulfonide **236**. **A:** Structures and chemical shifts of intermediates **239**, **240**, and **242**; **B:** HMQC spectrum with the key cross-peaks recorded at -50°C ; **C:** HMBC spectrum with the key cross-peak recorded at -50°C .

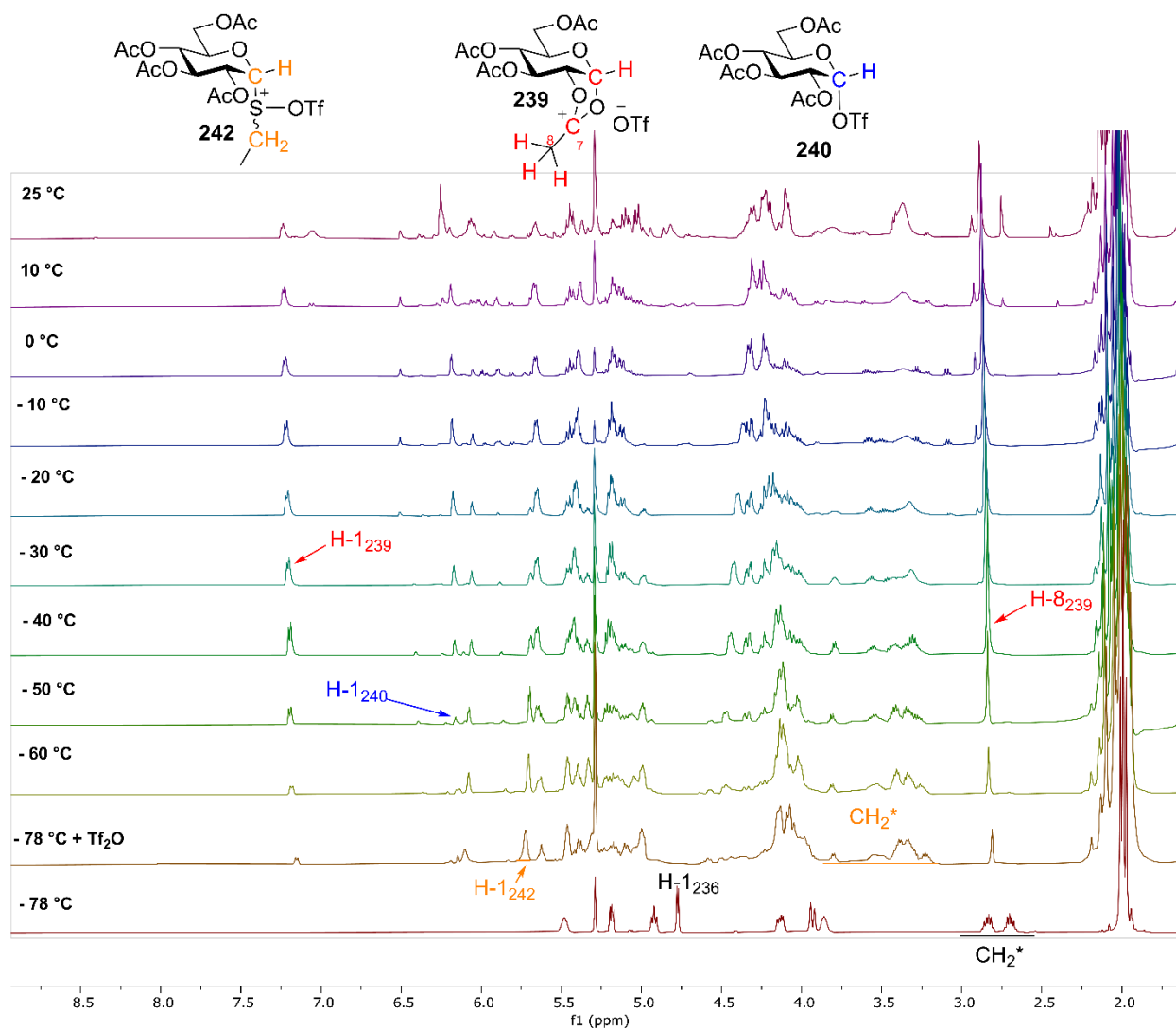
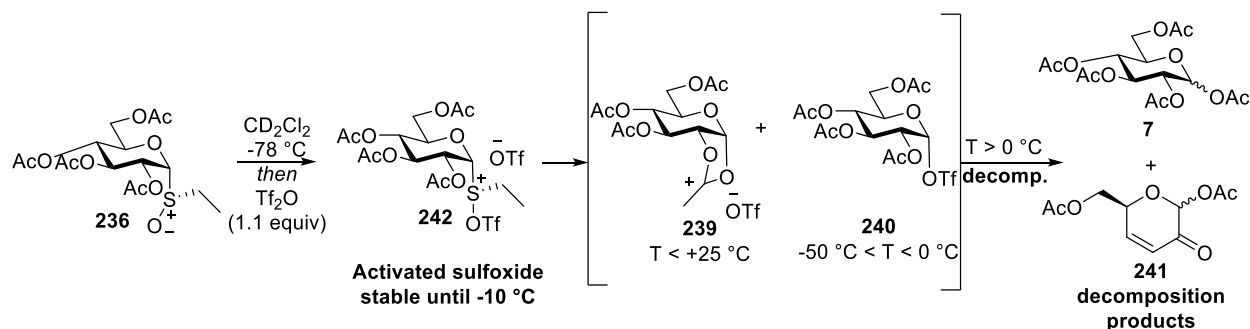
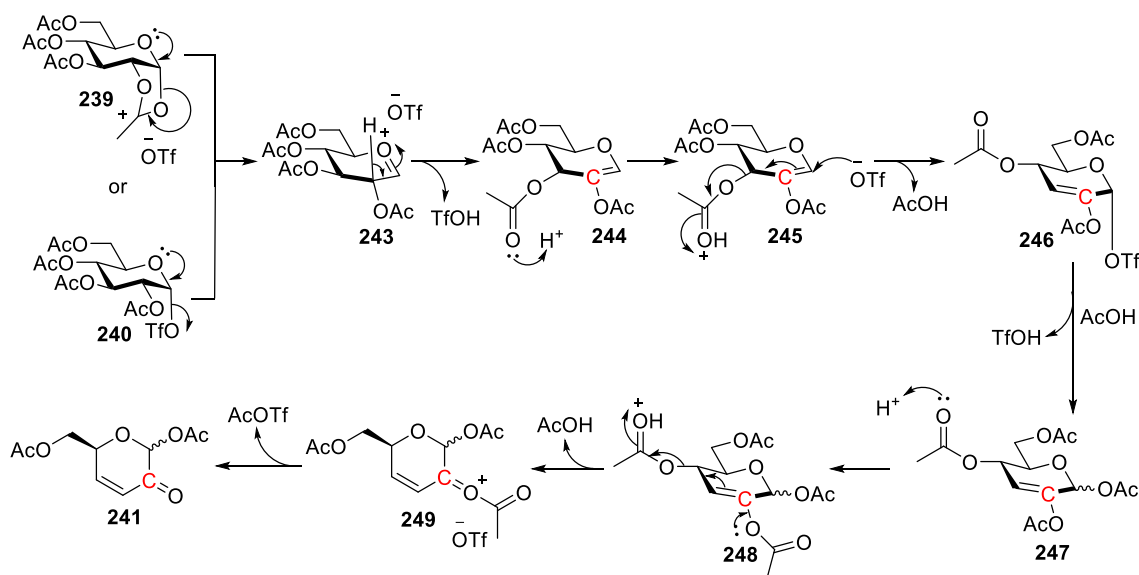


Figure 4.9. Structures of reactive intermediates and stacked ^1H NMR from a VT NMR experiment with glucosyl sulfoxide **236**.



Scheme 46. Intermediates and decomposition products generated during VT NMR experiments with glucosyl sulfoxide **236**.

The enone **241** was previously reported by Metzger²⁴⁵ who studied the thermal decomposition of α,β -glucopyranosyl pentaacetates, however, during the VT NMR experiments TfOH was unavoidably present in the reaction mixture, which led us to propose an acid-catalyzed decomposition mechanism to form the enone **241** (Scheme 47). First, the 1,2-glycal **244** is formed from either **239** or **240** at temperatures close to room temperature. The acetate group at C-3 position in the glycal **244** then undergoes protonation with TfOH to form **245**, which can undergo Ferrier rearrangement to produce triflate **246**. Triflate **246** is then recaptured by AcOH to form **247**, which, after subsequent protonation to form **248**, expels acetic acid to give the oxonium ion **249**, ultimately leading to the enone **241** (Scheme 47). The so-formed acetic acid is then captured by either dioxalenium ion **239**, triflate **240** or the 1,2-glycal **244** to give the observed pentaacetate **7**.



Scheme 47. Proposed decomposition mechanism of the reactive intermediates generated during the VT NMR with glycosyl sulfoxides **236** and **237**.

Turning to the 5-thioglycosyl sulfoxides **232** and **234**, we started by performing VT NMR experiments with β -sulfoxide **232**. Thus, activation of **232** in CD_2Cl_2 with triflic anhydride at -78°C leads to generation of “activated sulfoxide” **250**, which, similarly to the parent glucosides, was characterized by downfield shifts of the SCH_2CH_3 methylene protons and of the anomeric H-1 protons (e.g., $\delta_{\text{H}} = 4.87$ ppm and $\delta_{\text{H}} = 3.77$ ppm NMR resonances corresponding to the anomeric proton H-1 of **250** and **232**

respectively), with the connection between S(OTf)CH₂CH₃ moiety and the carbohydrate confirmed by HMQC/HMBC NMR spectroscopy (**Figure 4.10**). However, in contrast to **236** and **237**, much smaller quantities of the expected dioxalenium ion **251** and the thioglycosyl triflate **252** were formed from **250** at – 60 °C (**Figure 4.11**). Similarly to **239**, the dioxalenium ion **251** was characterized by a signal at $\delta_{\text{H}} = 2.84$ ppm, corresponding to the dioxalenium methyl group, which showed a strong HMBC correlation to the signal at $\delta_{\text{C}} = 191.7$ ppm, corresponding to the positively-charged carbon atom, and an anomeric signal at $\delta_{\text{H}} = 7.19$ ppm (**Figure 4.10**). Triflate **252** was characterized by a ¹H NMR resonance at $\delta_{\text{H}} = 6.05$ ppm and by ¹³C NMR resonance at $\delta_{\text{C}} = 87.9$ ppm corresponding to the H-1₂₅₂ and C-1₂₅₂ atoms respectively of **252** (**Figure 4.10**). Further support for covalent triflate generation was found in the ¹⁹F NMR spectrum, wherein a characteristic peak at $\delta_{\text{F}} = -75.36$ ppm was observed (**Figure 4.12**).

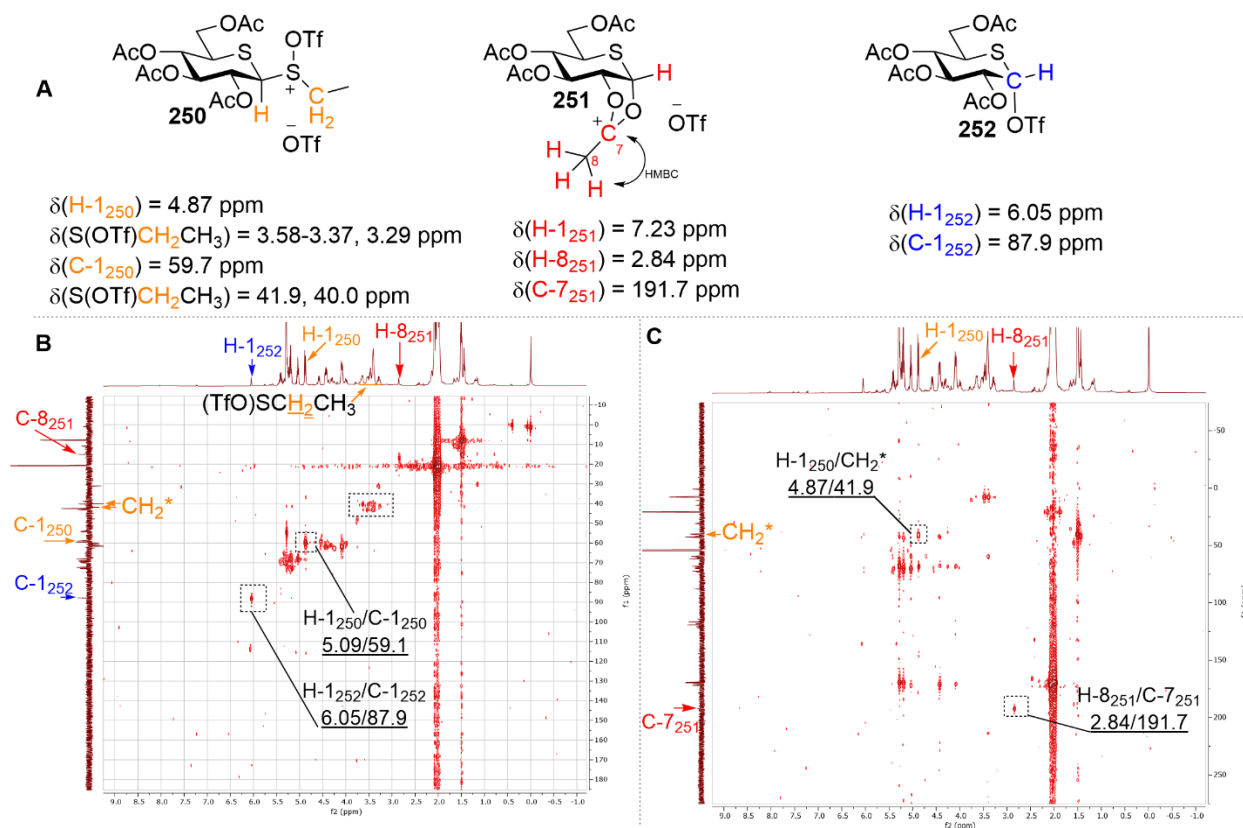


Figure 4.10. Key data from a VT NMR experiment with thioglycosyl sulfoxide **232**. **A:** Structures and chemical shifts of intermediates **250**, **251**, and **252**; **B:** HMQC spectrum plotted against DEPT-135 with the key cross-peaks recorded at -50 °C; **C:** HMBC spectrum with the key cross-peak recorded at -50 °C.

On warming, the amount of dioxalenium ion **251** present in the reaction mixture increased gradually reaching a maximum at $-40\text{ }^{\circ}\text{C}$, above which decomposition set in and was complete by $-10\text{ }^{\circ}\text{C}$ (**Figure 4.11**). Like the dioxalenium **251**, the concentration of triflate **252** present in the reaction mixture increased with temperature reaching a maximum around at $-40\text{ }^{\circ}\text{C}$ and was fully decomposed by $-10\text{ }^{\circ}\text{C}$ (**Figure 4.11**). In contrast to the relatively clean VT NMR mixture arising from the glucosyl sulfoxides **236** and **237**, by the time the NMR probe reached room temperature and the sample was retrieved from the probe, the reaction mixture was a black tar from which only the pentaacetate **33** α could be isolated. The results of the VT NMR experiment with 5-thioglucosyl sulfoxide **232** are summarized in **Scheme 48**. Notably, during the VT NMR experiment with thioglucosyl sulfoxide **232** no evidence was found at any temperature for the formation of a stable anomeric thienium cation.

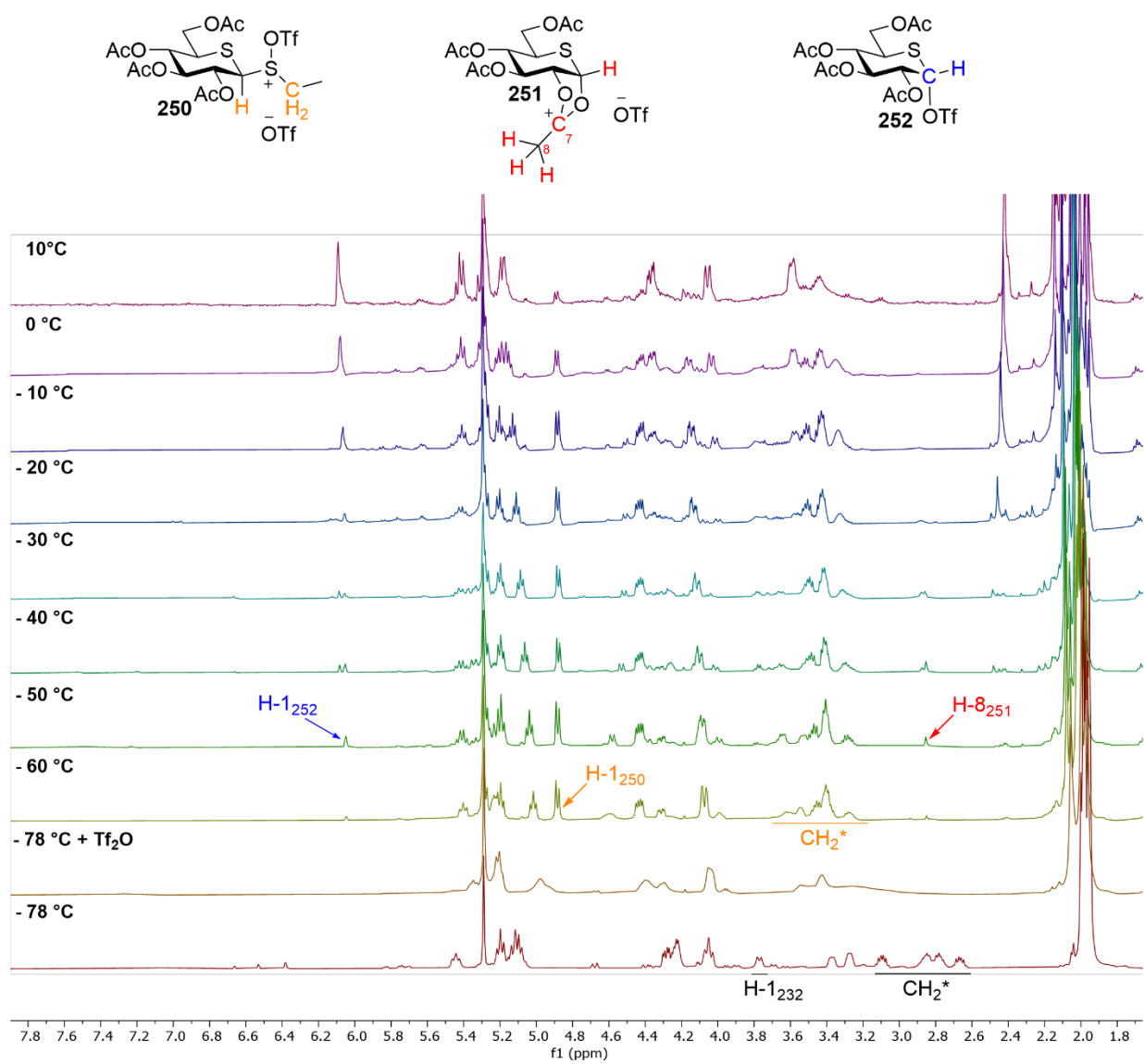


Figure 4.11. Structures of reactive intermediates and stacked ^1H NMR from a VT NMR experiment with thioglucosyl sulfoxide **232**.

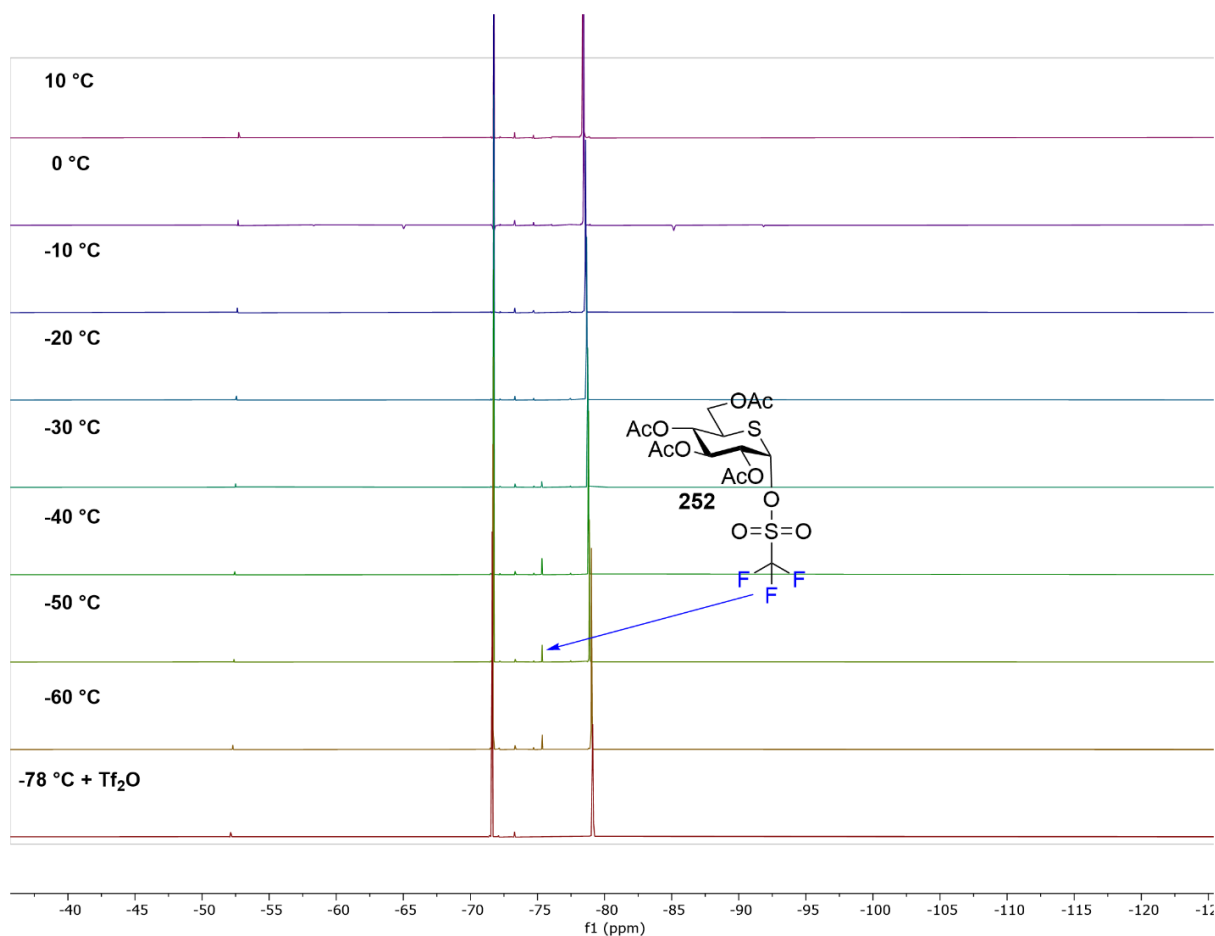
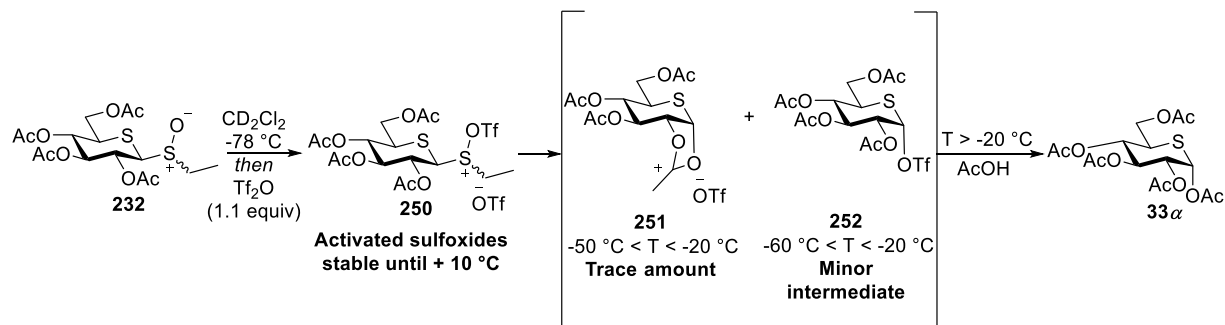


Figure 4.12. Stacked ^{19}F NMR spectra from a VT experiment with thioglycosyl sulfoxide **232**.



Scheme 48. Intermediates and decomposition products generated during VT NMR experiments with thioglycosyl sulfoxide **232**.

We then performed the same VT NMR experiment with α -sulfoxide **234**. Similarly to **232**, activation of thioglycosyl sulfoxide **234** with triflic anhydride at $-78\text{ }^{\circ}\text{C}$ in deuteriodichloromethane led to the generation of the “activated sulfoxide” **253**, which, similarly to **250**, was characterized by downfield

shifts of the SCH₂CH₃ methylene protons and of the anomeric H-1 protons (e.g., $\delta_{\text{H}} = 5.10$ ppm and $\delta_{\text{H}} = 4.10$ ppm NMR resonances corresponding to the anomeric proton H-1 of **253** and **234** respectively), with the connection between S(OTf)CH₂CH₃ moiety and the carbohydrate confirmed by HMQC/HMBC NMR spectroscopy (**Figure 4.13**). Trace amounts of the dioxalenium ion **251** and small amounts the α -glycosyl triflate **252** (**Figure 4.14**), which had the same spectral data (**Figure 4.13**) as those generated during VT NMR experiments with **232**, were formed during the experiment. Again, no evidence was found for the formation of an observable thiocarbenium ion. On gradual warming, the various reactive intermediates underwent rapid decomposition, and by -10 °C all reactive intermediates were fully decomposed, producing a tar, from which, again, only pentaacetate **33a** was isolated. The overall results of the VT NMR experiment with 5-thioglucosyl sulfoxide **234** are summarized in **Scheme 49**.

Presumably decomposition of the 5-thioglucose-derived dioxalenium ion **251** and the triflate **252** follow an analogous path to that presented for the formation of enone **241** (**Scheme 47**) from the corresponding glucosyl derivatives, but one or more of the sulfur-based intermediates is unstable and undergoes further decomposition.

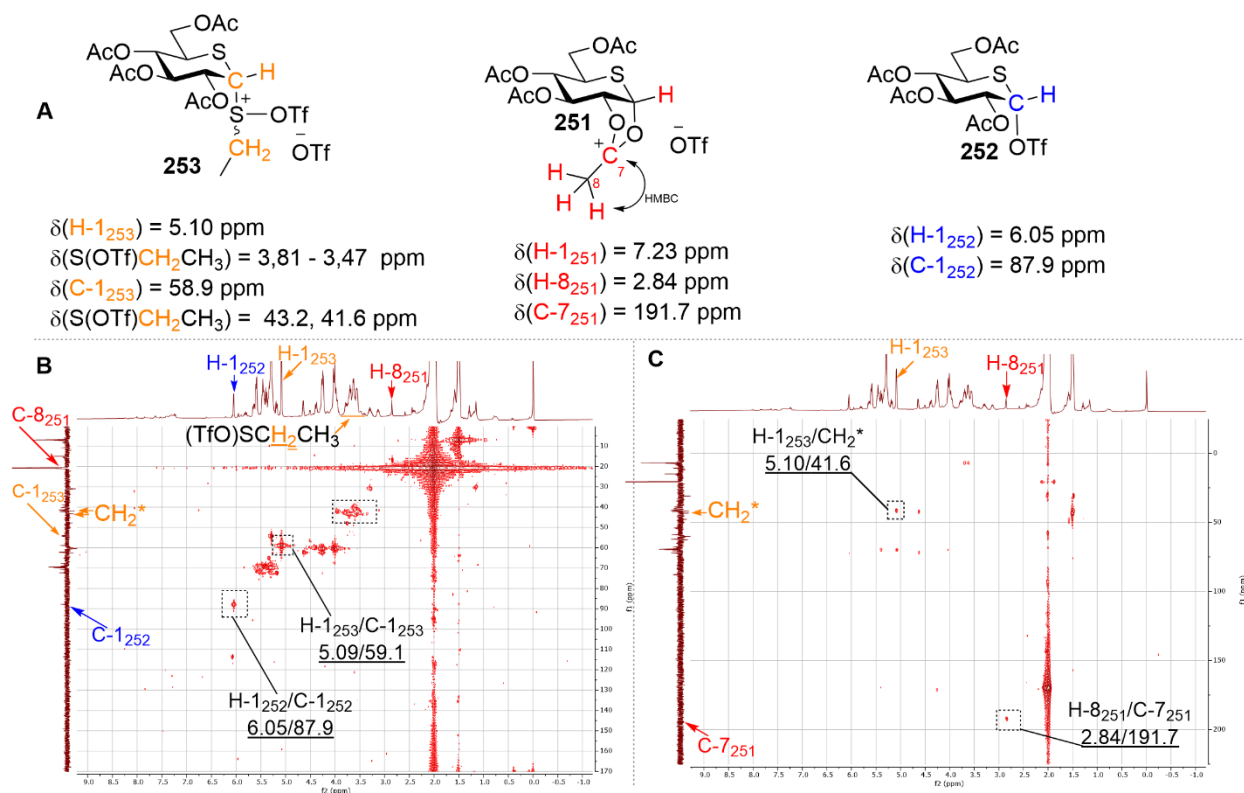


Figure 4.13. Key data from a VT NMR experiment with thioglucosyl sulfoxide **234**. **A:** Structures and chemical shifts of intermediates **253**, **251**, and **252**; **B:** HMQC spectrum plotted against DEPT-135 with the key cross-peaks recorded at -50°C ; **C:** HMBC spectrum plotted against DEPT-135 with the key cross-peaks recorded at -50°C .

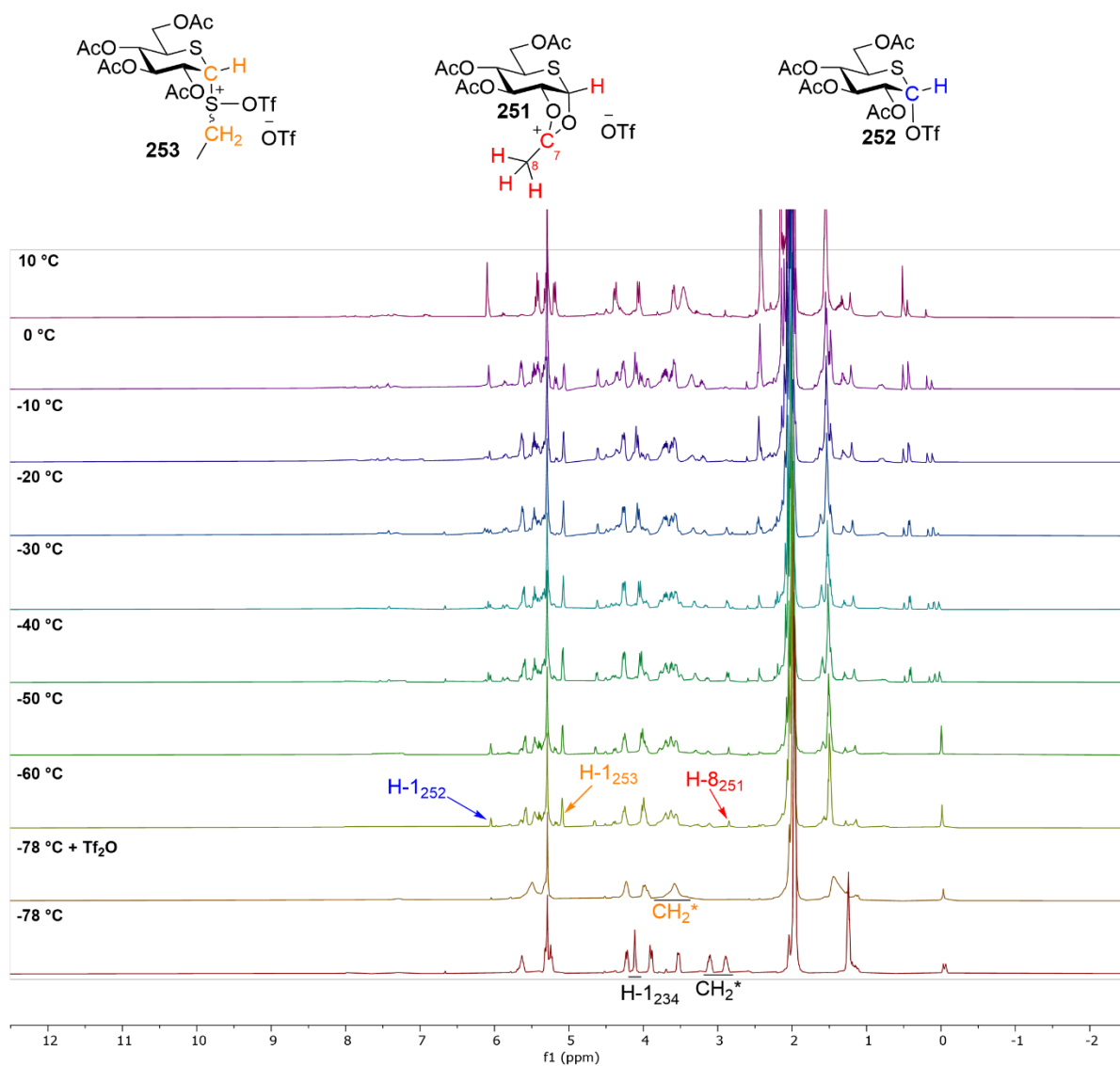
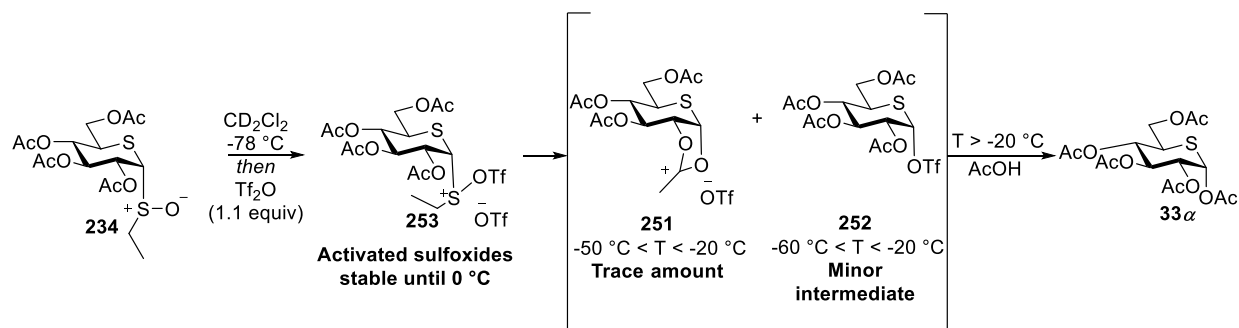


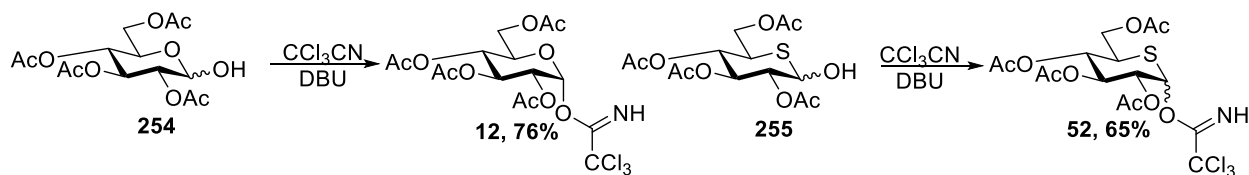
Figure 4.14. Structures of reactive intermediates and stacked ^1H NMR from a VT NMR experiment with glucosyl sulfoxide **234**.



Scheme 49. Intermediates and decomposition products generated during VT NMR experiments with glucosyl sulfoxide **234**.

The unexpected complexities observed in the activation of the various sulfoxides and particularly the apparent stability of the initial sulfoxide-triflate adducts at low temperatures resulting in their slow conversion to the anticipated dioxalenium ions and triflates prompted the synthesis and investigation of the corresponding glucosyl trichloroacetimidates as the second generation of disarmed VT NMR substrates.

To prepare the necessary trichloroacetimidates (**Scheme 50**), we started from commercially available hemiacetal **254** and 5-thioglucose hemiacetal **255**, itself prepared from 5-thioglucose pentaacetate **33** by a reported protocol.⁹² Hemiacetal **254** was coupled with trichloroacetonitrile in presence of catalytic DBU in the standard manner to give imideate **12** as a single anomer in 76% yield. In the parallel synthesis, following a reported protocol,¹⁹¹ hemiacetal **255** was coupled with trichloroacetonitrile in presence of catalytic DBU to give peracetylated imideate **52** in 65% yield.



Scheme 50. Synthesis of peracetylated trichloroacetimidate **12** and **52**.

The VT NMR experiments with **12** and **52** were performed by addition of TMSOTf at $-78\text{ }^{\circ}\text{C}$ to the trichloroacetimidate in an NMR tube followed by rapid return of the tube to the precooled probe and recording of spectra and then incremental warming with spectra recorded at each interval. Beginning with the parent glycosyl trichloroacetimidate **12**, minor amounts of both the glycosyl triflate **239** and the dioxalenium ion **240** were observed at $-78\text{ }^{\circ}\text{C}$, with the latter becoming increasingly more prominent from $-60\text{ }^{\circ}\text{C}$ and upwards, but conversion was slow at the lower temperatures and the imideate was not fully consumed until approximately $-30\text{ }^{\circ}\text{C}$, a temperature at which both the dioxalenium ion **239** and the triflate **240** no longer existed under the reaction conditions owing to conversion to glucose pentaacetate and a second decomposition product that remained stable until room temperature (**Figure 4.15**). The results of the VT NMR experiments with peracetylated glycosyl trichloroacetimidate **12** are summarized in **Scheme 51**.

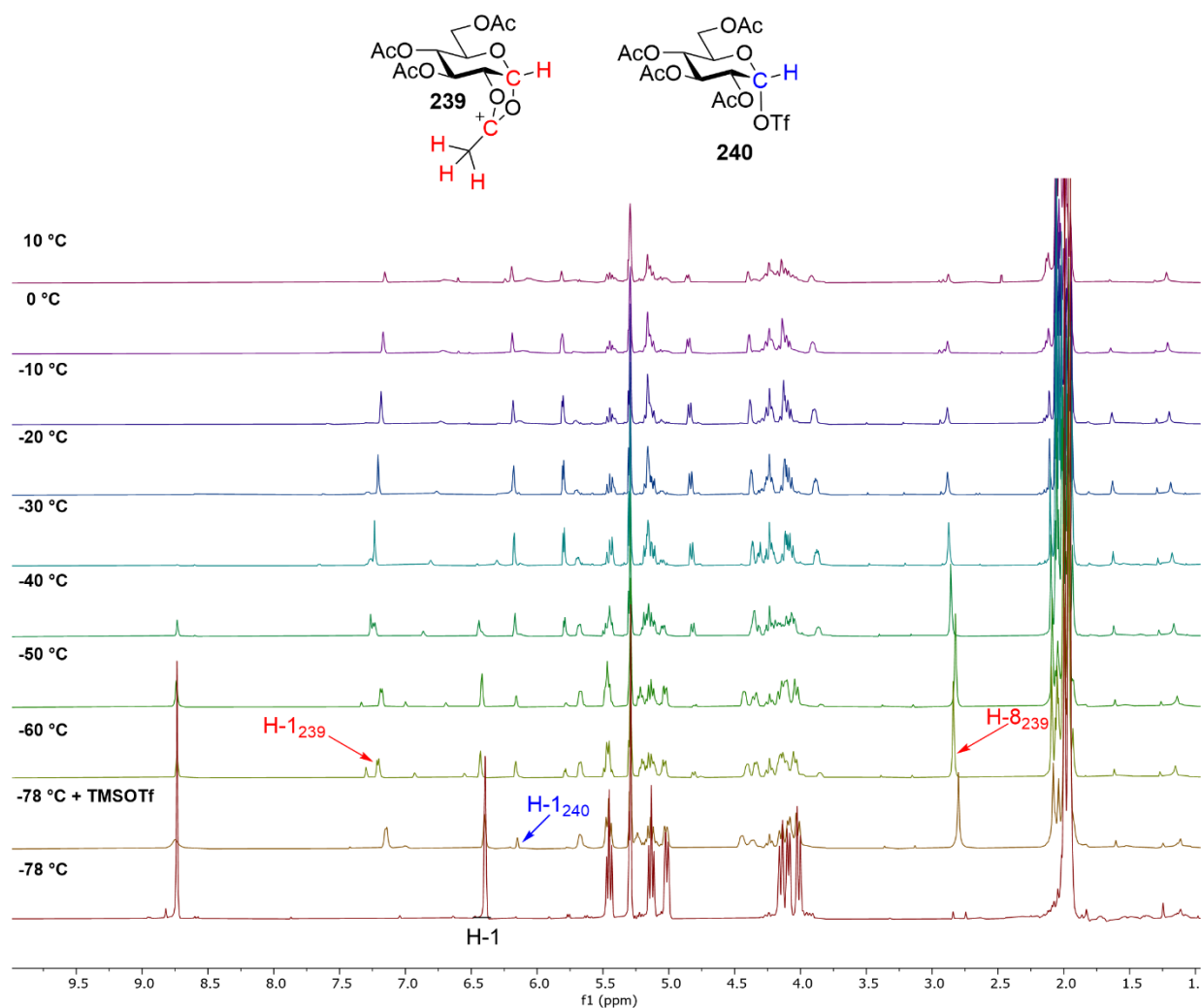
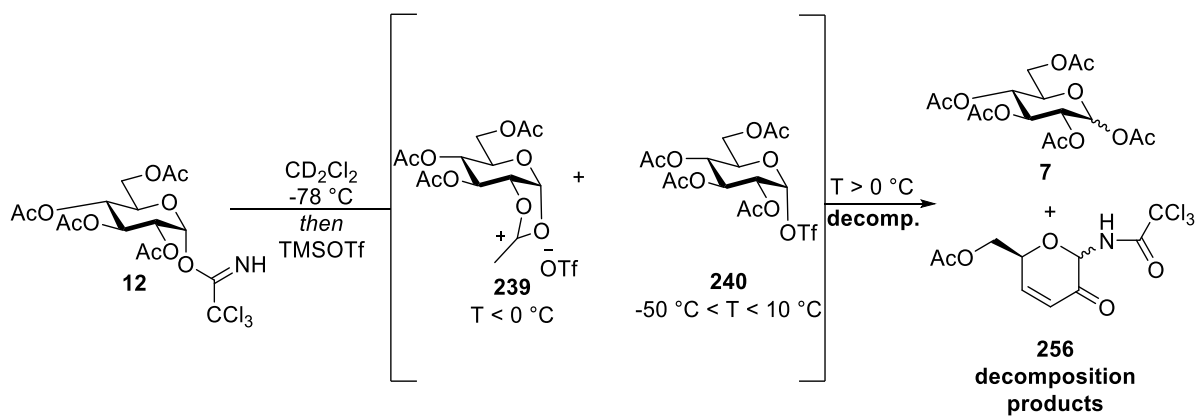
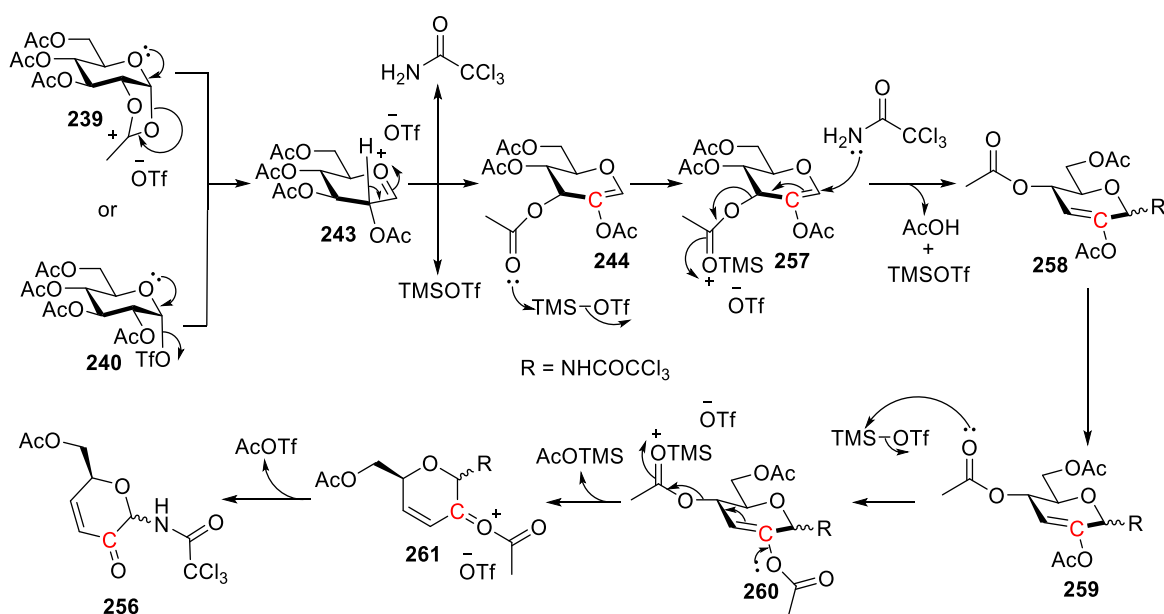


Figure 4.15. Structures of reactive intermediates and stacked ^1H NMR from a VT NMR experiment with glucosyl trichloroacetimidate **12**.



Scheme 51. Structures of reactive intermediates formed during VT NMR experiments with peracetylated trichloroacetimidate **12**.

The second isolated decomposition product was characterized following isolation as the enonyl amide derivative **256**, which presumably arises by a pathway analogous to that outlined for the formation of enonyl acetate **241** but with intervention of the trichloroacetamide derivative, formed during the activation process, as nucleophile (**Scheme 52**). Accordingly, 1,2-glycal **244**, formed upon decomposition of either **239** or **240**, can undergo activation with regenerated TMSOTf to form **257**, which then undergoes Ferrier rearrangement with trichloroacetamide to produce **258** and release AcOH. From that point the decomposition follows pathway similar to that described in **Scheme 47** to produce enonyl amide **256**.



Scheme 52. Proposed mechanism to form enonyl amide **256**.

Turning to the 5-thioglycosyl trichloroacetimidate **52**, immediately after addition of TMSOTf at $-78\text{ }^{\circ}\text{C}$, formation of dioxalenium ion **251** and considerably more covalent triflate **252** was observed. However, as with the glucosyl imidate **12**, trichloroacetimidate **52** was not fully consumed immediately on addition of TMSOTf, with complete consumption of the starting material only seen at temperatures $T > -30\text{ }^{\circ}\text{C}$ (**Figure 4.16**). Both dioxalenium ion **251** and covalent triflate **252** slowly accumulated in the reaction mixture on warming, with the dioxalenium ion reaching a maximum concentration $-60\text{ }^{\circ}\text{C} < T < -50\text{ }^{\circ}\text{C}$ and the triflate at $-50\text{ }^{\circ}\text{C}$ above which temperatures slowly set in (**Figure 4.16**). Beginning around

–40 °C a further product, identified as the thioglycal **262**, identified by the olefinic signals at $\delta_{\text{H}} = 6.07$ ppm and $\delta_{\text{C}} = 113.5$ ppm consistent with literature data⁸⁸ was observed; this product was essentially absent from the reaction mixture above –30 °C. Similarly to the sulfoxides **232** and **234**, only pentaacetate **33** was isolated from the reaction mixture after termination of the VT NMR experiment. The overall results of the VT NMR experiment with peracetylated thioglucosyl trichloroacetimidate **52** are summarized in Scheme 53.

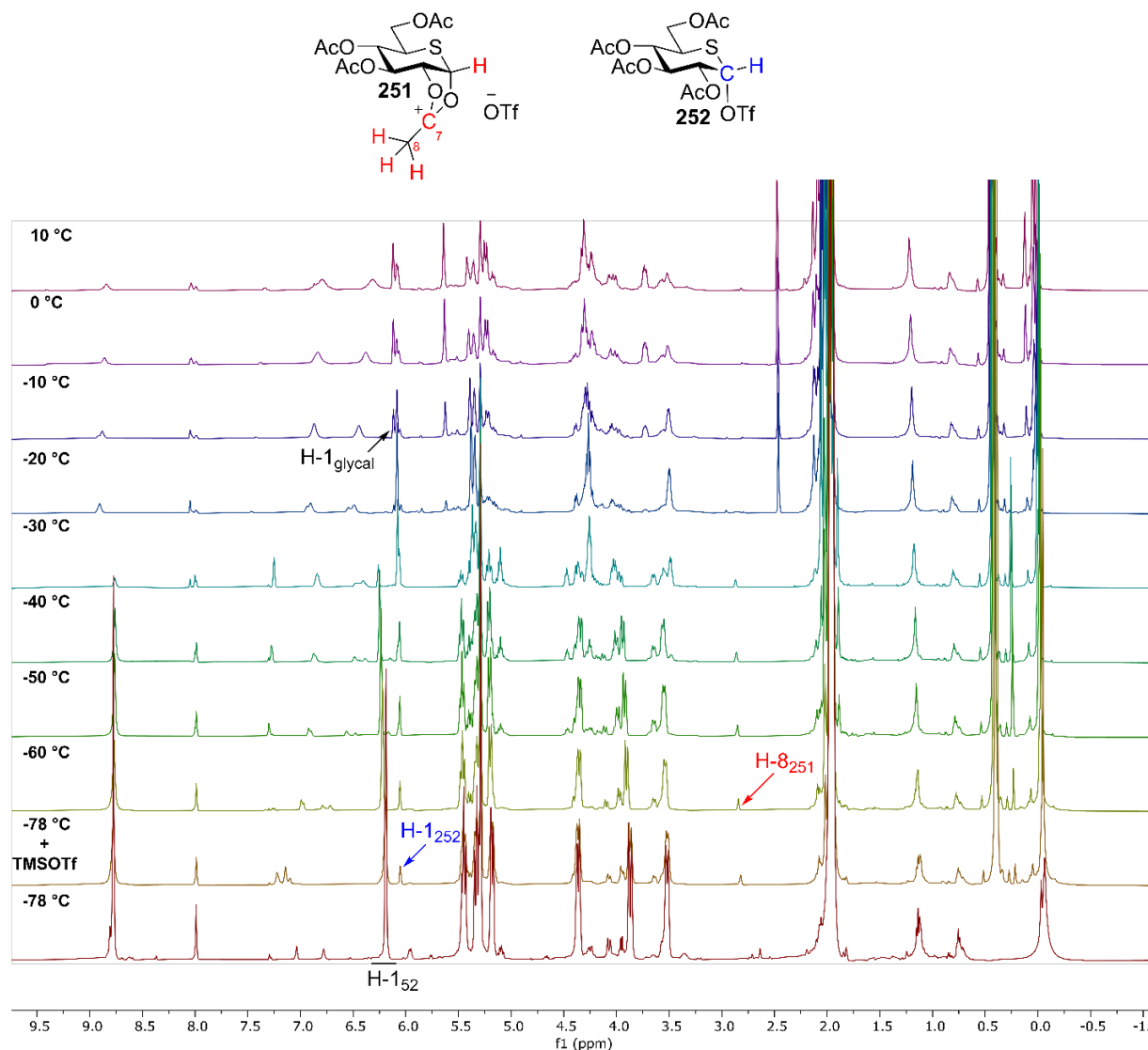
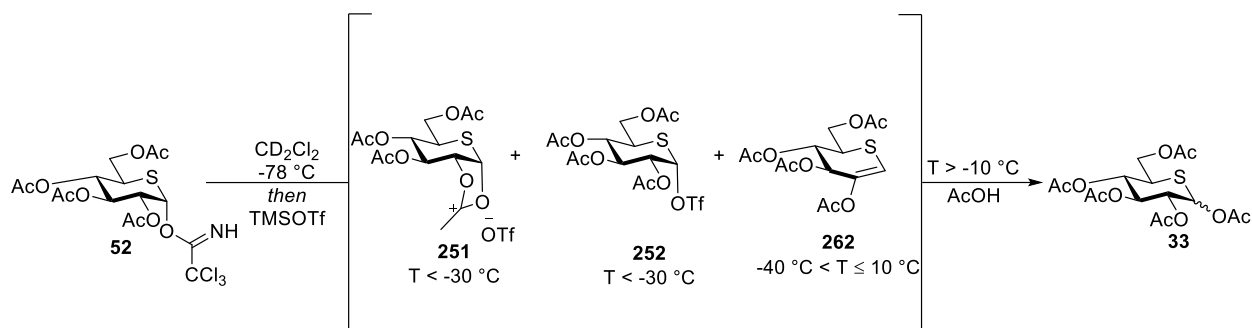


Figure 4.16. Structures of reactive intermediates and stacked ^1H NMR from a VT NMR experiment with thioglucosyl trichloroacetimidate **52**.

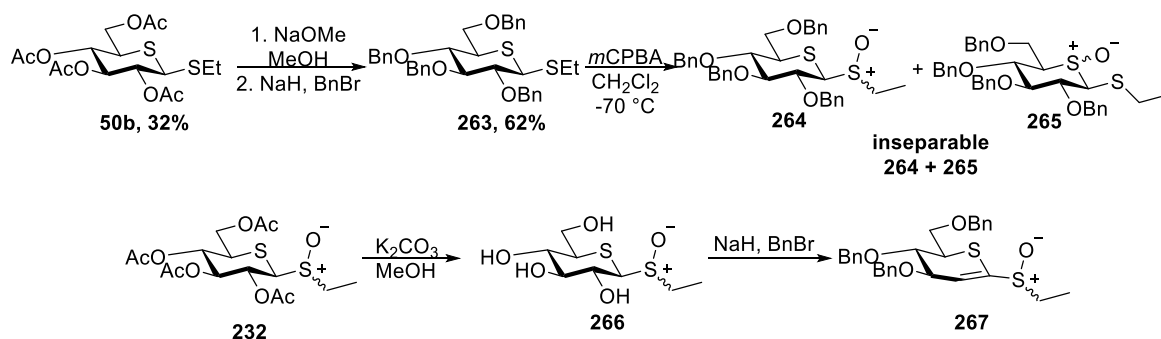


Scheme 53. Structures of reactive intermediates formed during VT NMR experiments with peracetylated thioglucosyl trichloroacetimidate **52**.

Importantly, during the VT NMR experiments with both 5-thioglycosyl sulfoxides **232** and **234** and thioglucosyl trichloroacetimidate **52** we did not detect any signals in the ^1H or ^{13}C NMR at any temperatures that could correspond to an anomeric thienium cation.

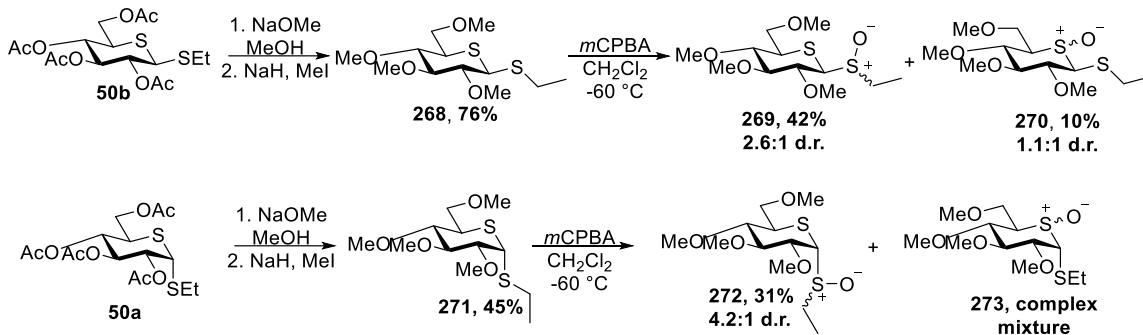
4.5. VT NMR studies with armed glycosyl donors

We then switched to armed glycosyl donors. Initially, we sought to employ benzyl protected glycosyl sulfoxides in the VT NMR studies. Accordingly, β -thioglycoside **50b** was deacetylated with methanolic NaOMe, and subsequently benzylated with BnBr in the presence of NaH to give perbenzylated thioglycoside **263** in 62% yield (Scheme 54). Oxidation of **263** with *m*CPBA afforded mixture of sulfoxides **264** and **265** respectively, which, unlike **232** and **233**, had very similar polarity and proved to be inseparable by chromatographic methods.



Scheme 54. Attempted synthesis of perbenzylated 5-thioglycosyl sulfoxide **264**.

Therefore, we tried an alternative approach towards 5-thioglycosyl sulfoxide **264**. First, adopting a reported protocol,²⁴⁶ sulfoxide **232** was deprotected to briefly reveal **266**, which then was subjected to benzylation with BnBr in the presence of NaH. Unfortunately, this did not produce the desired sulfoxide **264**, instead a mixture of partially benzylated products was formed, among which a 1,2-glycal **267**, produced through E1cB elimination, was observed. Switching to a milder base, e.g., imidazole, completely retarded the reaction. Considering that, we opted to try the more polar methyl ether as protective group for the sulfoxides to take advantage of high polarity difference between *endo*- and *exo*-sulfoxides. Thus, deacetylation of β -thioglycoside **50b** with NaOMe and subsequent methylation with MeI in presence of NaH afforded thioglycoside **268** in 76% yield. Oxidation of **268** with *m*CPBA then gave a mixture of sulfoxides, which were successfully separated to afford the desired 1-*S*-oxides **269** in 42% yield and the corresponding 5-*S*-oxides **270** in 10% yield. Parallel processing of α -thioglycoside **50a** afforded the permethylated thioglycoside **271** in 45% yield, which gave the desired 1-*S*-oxides **272** in 31% yield, and a complex mixture of 5-*S*-oxides **273** on oxidation with *m*CPBA (Scheme 55).



Scheme 55. Synthesis of permethylated sulfoxides **269** and **272**.

Similarly to **232** and **234**, the regioselectivity of the *m*CPBA oxidation was determined by comparing the chemical shifts of C-5 and SCH₂CH₃ methylene carbon of sulfoxides **269**, **270**, and **272** with the corresponding starting materials **268** and **271**, respectively. Thus, in the ¹H NMR spectrum of **269**, a characteristic geminal splitting of the methylene protons of the SCH₂CH₃ group was observed, in addition to which the ¹³C NMR spectrum revealed changes in the chemical shift of the SCH₂CH₃ methylene group carbon (δ_c = 44.8 and 45.2 ppm) in comparison to that of the thiosugar starting material **268** (δ_c = 26.1

ppm), while little to no change in chemical shift of C-5 ($\delta_c = 44.4$ and 45.6 ppm) in comparison to the starting material **268** ($\delta_c = 47.0$ ppm) was observed (**Figure 4.17**). On the other hand, similarly to **233**, no geminal splitting of the SCH₂CH₃ methylene protons was observed in the ¹H NMR spectrum of the endocyclic sulfoxide **270**. In addition, little to no change was observed in the chemical shift of the SCH₂CH₃ methylene carbon ($\delta_c = 27.3$ and 26.5 ppm) of **270** compared to the starting material **268** ($\delta_c = 26.1$ ppm) and a significant change was noted in the chemical shift of the C-5 ($\delta_c = 61.0$ ppm) with respect to the starting material **268** ($\delta_c = 47.0$ ppm) (**Figure 4.17**).

The same analysis was conducted for α -sulfoxide **272**. In the ¹H NMR spectrum of **272**, a characteristic geminal splitting of the methylene protons of the SCH₂CH₃ group was observed, in addition to which the ¹³C NMR spectrum revealed changes in the chemical shift of the SCH₂CH₃ methylene group carbon ($\delta_c = 44.5$ and 46.3 ppm) in comparison to that of the thiosugar starting material **271** ($\delta_c = 25.6$ ppm), while little to no change in chemical shift of C-5 ($\delta_c = 42.5$ ppm) in comparison to the starting material **271** ($\delta_c = 41.9$ ppm) was observed (**Figure 4.17**).

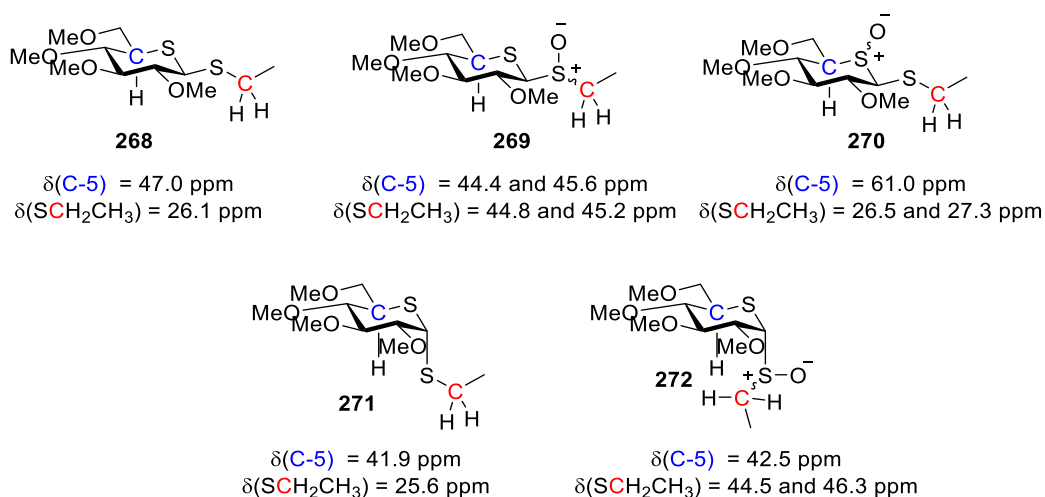
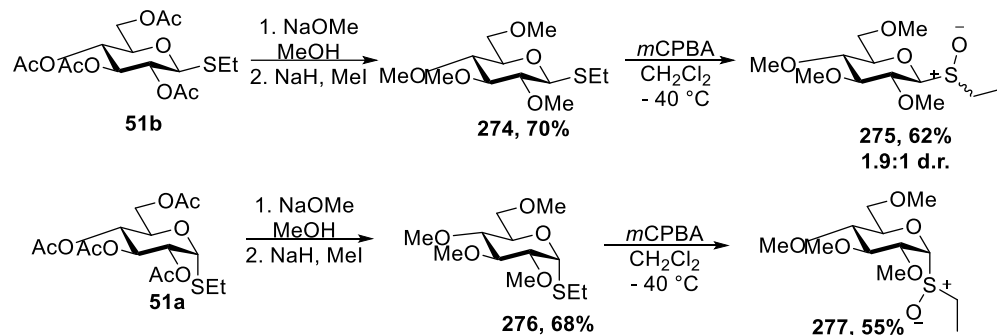


Figure 4.17. The comparison of the key ¹³C NMR peaks of the starting material and sulfoxides.

We then began synthetic efforts towards parent permethylated glucosyl sulfoxides **275** and **277** (**Scheme 55**). First, following the reported protocol,³³ β -thioglycoside **51b** was deacetylated with NaOMe and subsequently alkylated with MeI in presence of NaH to afford permethylated thioglycoside **274** in 70%

yield, *m*CPBA oxidation of which gave permethylated glucosyl sulfoxide **275** in 62% yield. The α -thioglycoside **51a** was similarly converted into permethylated thioglycoside **276** in 68% yield and then oxidized with *m*CPBA to give sulfoxide **277** as a single diastereomer in 55% yield.



Scheme 56. Synthesis of parent permethylated glucosyl sulfoxides **275** and **277**.

With permethylated glycosyl sulfoxides in hand we began VT NMR experiments. Starting with the parent β -glucosyl sulfoxides **275**, similarly to the peracetylated sulfoxide **237**, “activated sulfoxide” **278** was formed immediately on addition of $\text{ Tf}_2\text{O}$, and was characterized by downfield shifts of the SCH_2CH_3 methylene protons ($\delta_{\text{H}} = 3.87\text{--}2.83$ ppm and $\delta_{\text{H}} = 2.60$ ppm in **278** and **275** respectively), as well as corresponding downfield shifts of the anomeric proton signals. At temperatures $T > -30$ °C complete decomposition of activated sulfoxide **278** was observed (**Figure 4.19**). Formation of the covalent triflate **279**, characterized by a downfield anomeric signal at $\delta_{\text{H}} = 6.11$ ppm, and a corresponding HSQC-correlated anomeric signal at $\delta_{\text{C}} = 106.3$ ppm, was observed immediately after addition of $\text{ Tf}_2\text{O}$ (**Figure 4.18**). Triflate **279** accumulated gradually with increasing temperature reaching a maximum at -40 °C above which decomposition set in and was complete by -20 °C. At temperatures $T > -30$ °C a new species assigned as the pyrilium ion **280** was observed and accumulated rapidly with further increases in temperature (**Figure 4.19**). After termination of the experiment both **280** and pentamethyl glucose **281** were detected in the reaction mixture by LCMS, however only pentamethyl glucose **281** was isolated. The results of the VT NMR experiment with permethylated glucosyl sulfoxide **275** are summarized in **Scheme 57**. Notably, signals of methyl ethers were overlapping with pyranose ring protons and $(\text{TfO})\text{SCH}_2\text{CH}_3$ methylene group

carbon, which complicated HMBC spectra, and, thus, we were unable to clearly see the HMBC correlations between the anomeric proton and the (TfO)SCH₂CH₃ methylene group carbon.

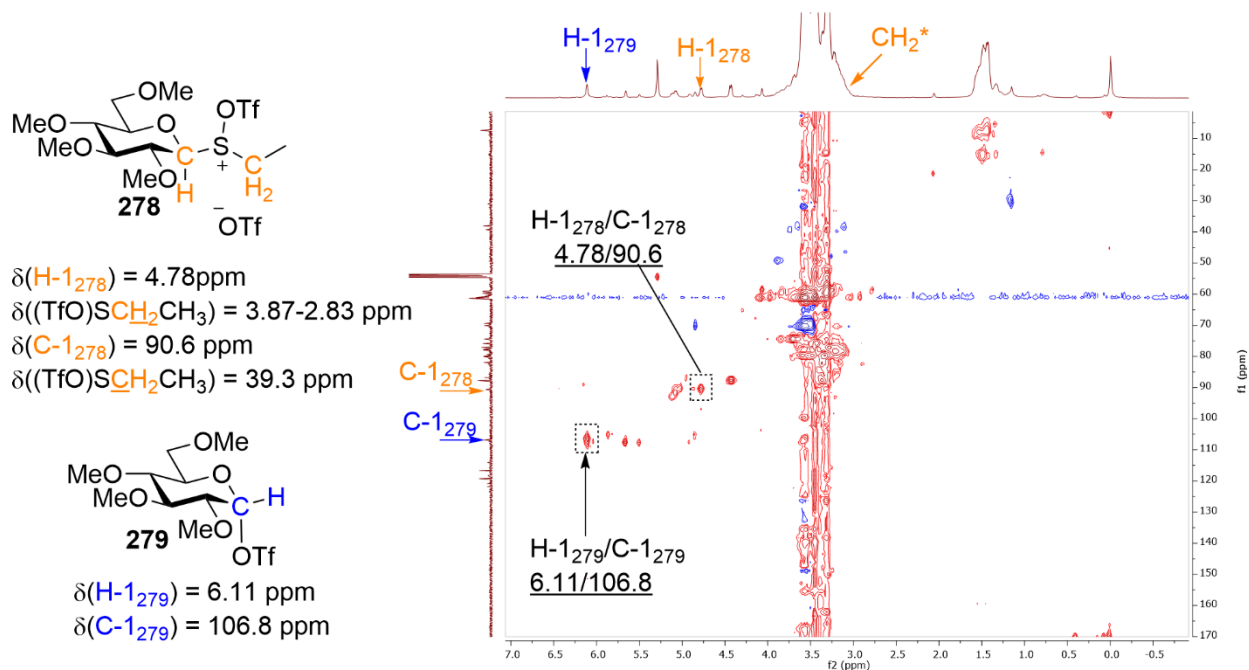


Figure 4.18. Structures of reactive intermediates generated during a VT NMR experiment with glycosyl sulfoxide **275** and HMQC spectrum recorded at -50°C with the key cross-peaks.

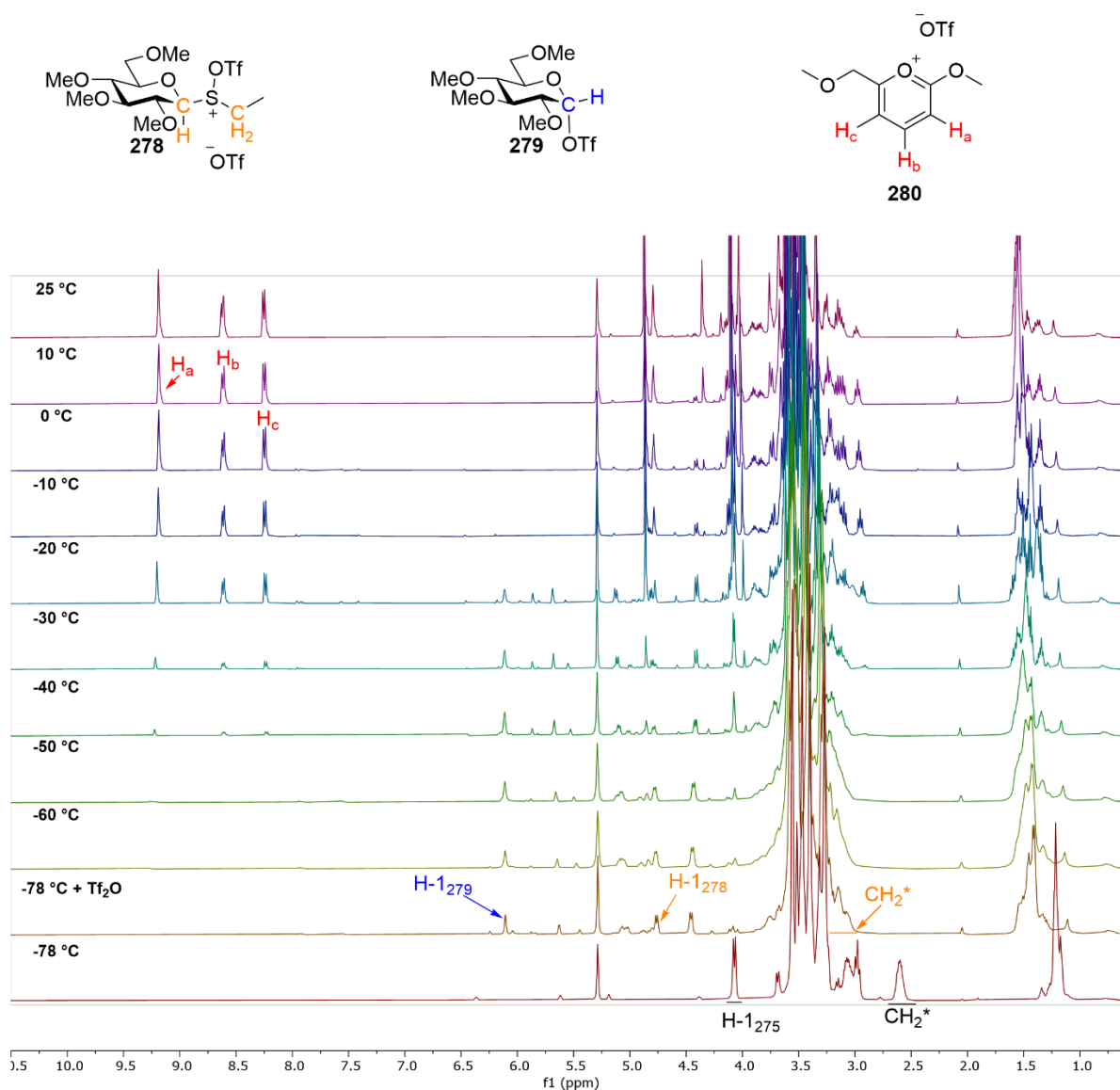
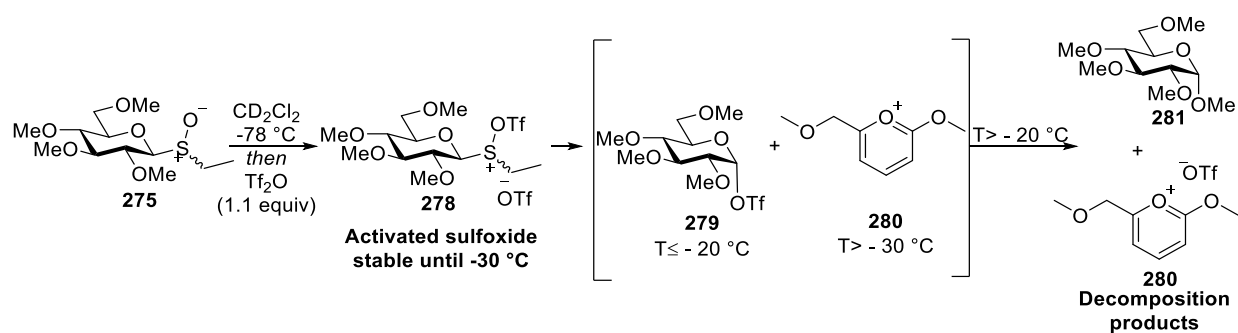


Figure 4.19. Stacked ^1H NMR spectra from a VT NMR experiment with glycosyl sulfoxide **275**.



Scheme 57. Structures of reactive intermediates and products formed during VT NMR experiments with permethylated glycosyl sulfoxide **275**.

Similar results were observed during VT NMR experiment with α -glucosyl sulfoxide **277**. Thus, immediately after addition of $\text{ Tf}_2\text{O}$ “activated sulfoxide” **282** was formed, and, similarly, was characterized by downfield shifts of the SCH_2CH_3 methylene protons ($\delta_{\text{H}} = 3.13$ ppm and $\delta_{\text{H}} = 2.78$ and 2.61 ppm in **282** and **277** respectively), as well as corresponding downfield shifts of the anomeric proton signals. However, activated glycosyl sulfoxide **282** was found to be more stable than the corresponding β -analog **278** and was observed in the reaction mixture even at $+10$ °C (**Figure 4.21**). Similarly to the VT NMR experiment with **275**, the only reactive intermediate that was observed during this experiment was glycosyl triflate **279**, which was characterized by the same signals in ^1H and ^{13}C NMR (**Figure 4.20**). The glycosyl triflate gradually accumulated with increasing temperature and reached a maximum at -40 °C above which decomposition set in and was complete by -20 °C (**Figure 4.21**). After the termination of the VT NMR experiment, the same decomposition products **280** and pentamethyl glucose **281** were detected in the reaction mixture by LCMS, and only pentamethyl glucose **281** was isolated. The results of the VT NMR experiments with permethylated glucosyl sulfoxide **277** are summarized in **Scheme 58**.

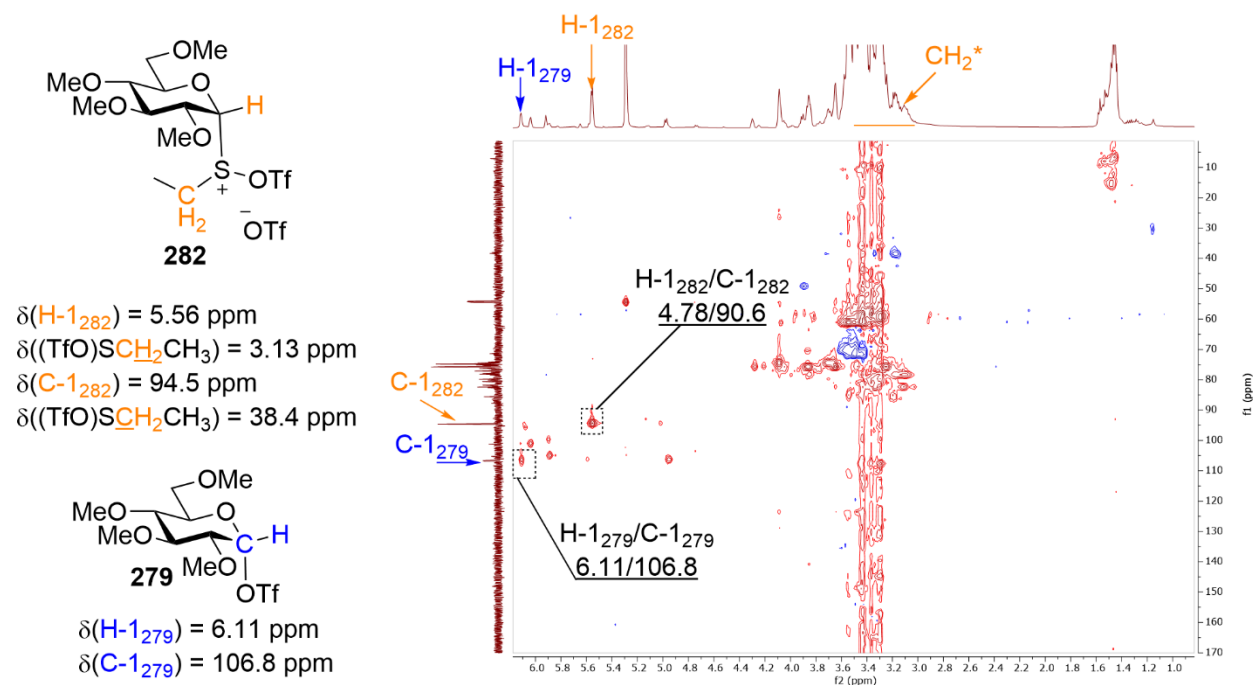


Figure 4.20. Structures of reactive intermediates generated during a VT NMR experiment with glycosyl sulfoxide **277** and HMQC spectrum recorded at -50 °C with the key cross-peaks.

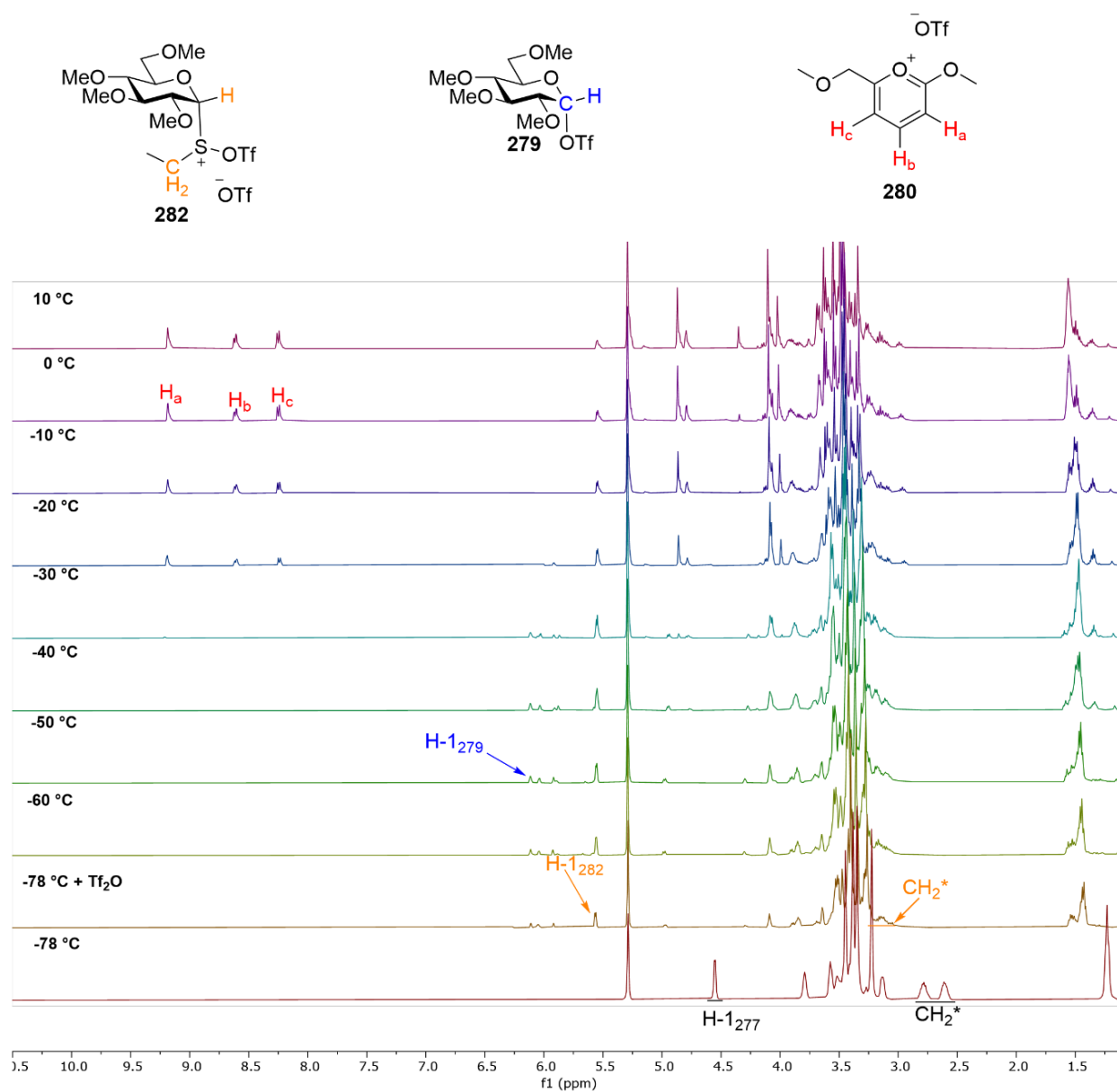
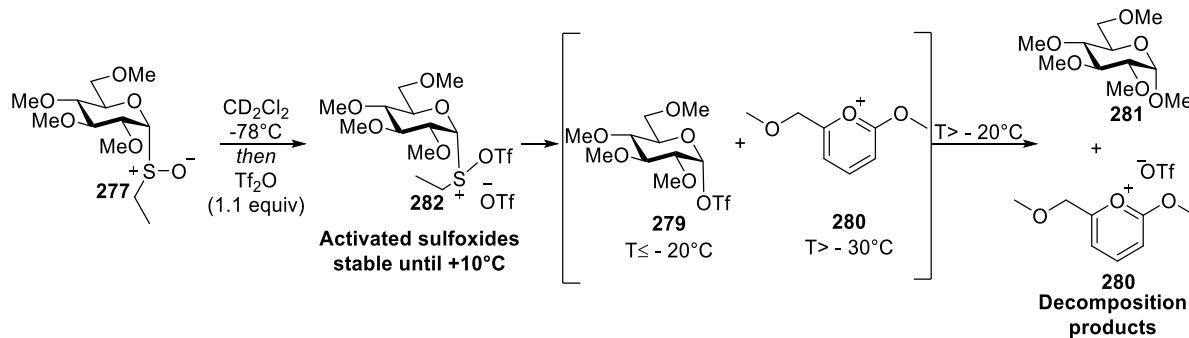


Figure 4.21. Stacked ^1H NMR spectra from a VT NMR experiment with glycosyl sulfoxide **277**.



Scheme 58. Structures of reactive intermediates and products formed during VT NMR experiments with permethylated glycosyl sulfoxide **277**.

Switching to the 5-thioglycosyl sulfoxides, we first performed VT NMR experiments with β -thioglycosyl sulfoxides **269** (Scheme 59). The “activated sulfoxide” **283** was formed immediately on addition of TiF_2O at -78°C . However, no signals corresponding to the anticipated covalent triflate **284** were observed during the reaction generation; rather the “activated sulfoxides” **283** persisted until -40°C above which decomposition set in with formation of the thioglycal **91** and of pentamethyl 5-thioglucofuranose **286**. Above $T > 0^\circ\text{C}$ glycal **285** and the residual activated sulfoxide **283** underwent further decomposition leading to the thiophene derivative **287** (Figure 4.22). After termination of the experiment both **286** and **287** were detected in the reaction mixture by LCMS, but only thiophene **287**, mixed with trace amounts of **286**, was isolated from the reaction mixture. The overall results of the VT NMR experiment with permethylated thioglycosyl sulfoxide **269** are summarized in Scheme 59.

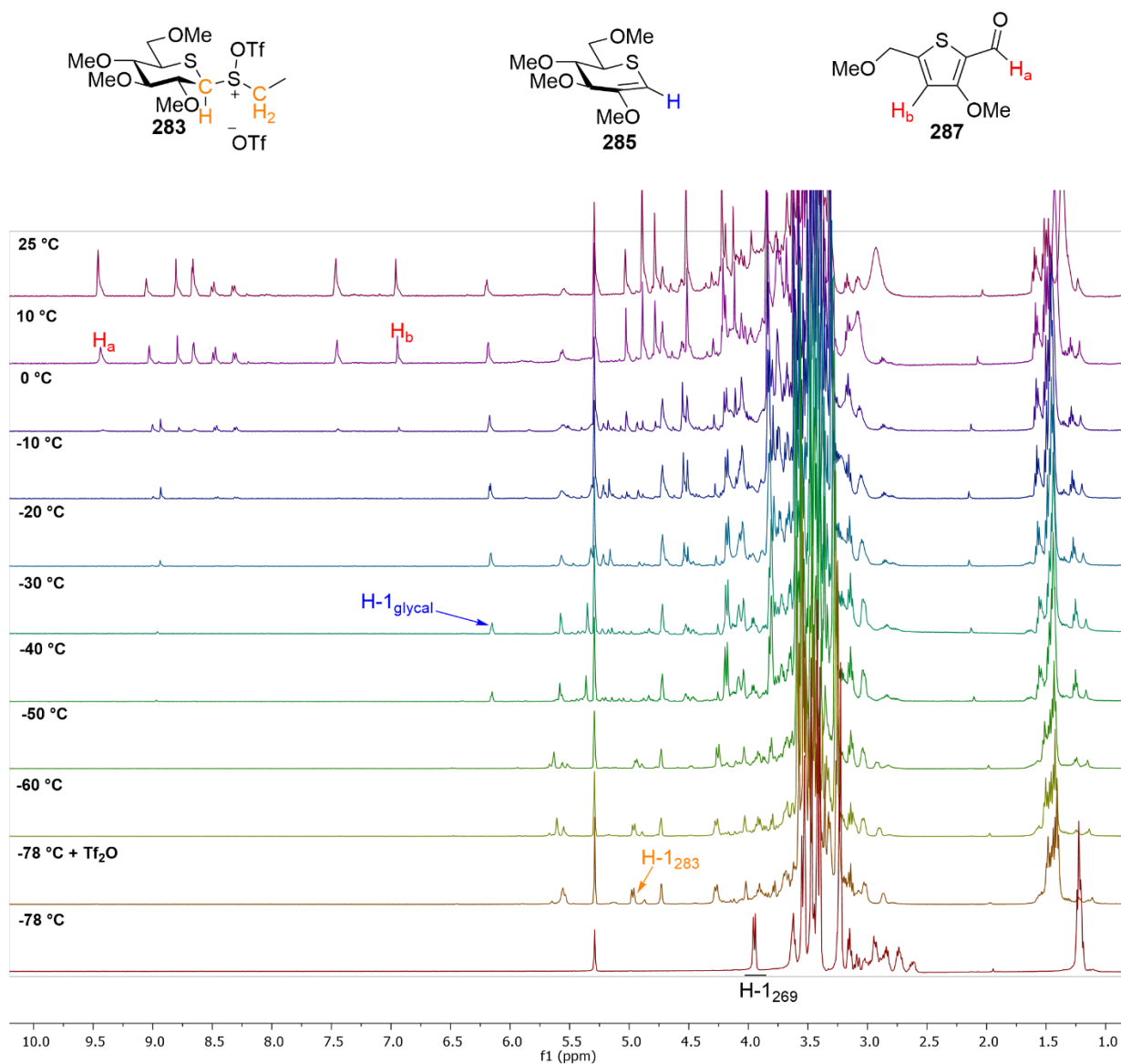
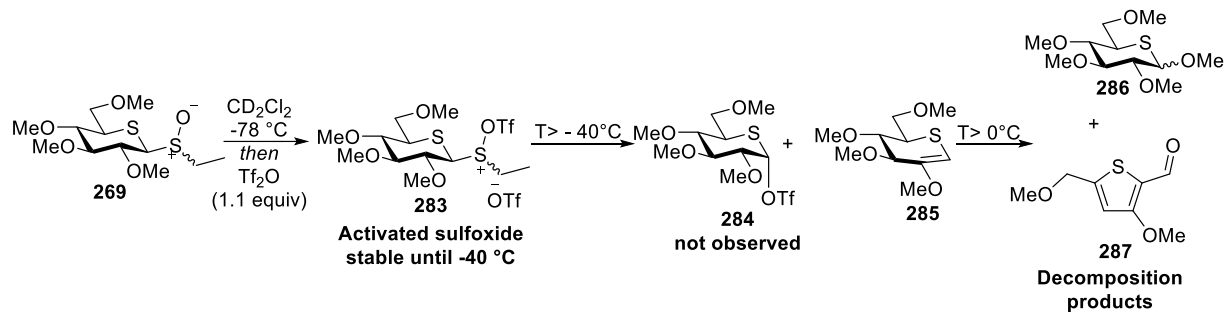


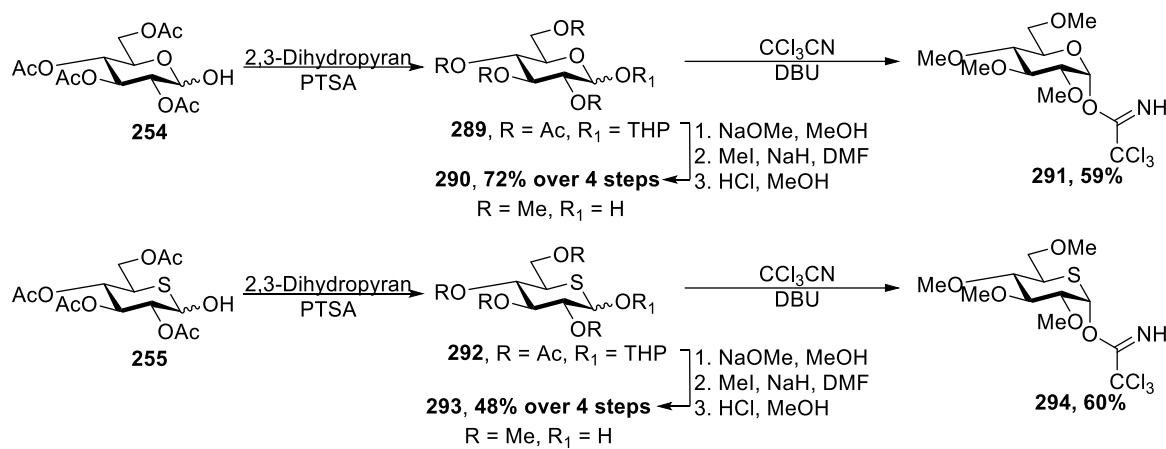
Figure 4.22. Stacked ^1H NMR spectra from a VT NMR experiment with thioglucosyl sulfoxide **269**.



Scheme 59. Structures of reactive intermediates and products formed during VT NMR experiments with permethylated glycosyl sulfoxide **269**.

We then performed VT NMR experiments with the α -anomer **272**. Accordingly, immediately after addition of Tf₂O “activated sulfoxide” **288** was formed, and, similarly to **269**, no signs of covalent triflate **284** were observed during the VT NMR experiment at any temperature. Notably, “activated sulfoxide” **288** was very stable and persisted in the reaction mixture until +25 °C (**Figure 4.23**). Similarly to **269**, after the termination of the VT NMR experiment only thiophene **287** was isolated from the reaction mixture. The overall results of the VT NMR experiment with permethylated thioglucosyl sulfoxide **272** are summarized in **Scheme 60**. Importantly, during the VT NMR experiments with both 5-thioglycosyl sulfoxides **269** and **277** we did not detect any signals in ¹H or ¹³C NMR at any temperatures that could correspond to an anomeric thienium cation.

adopted a reported protocol¹⁹¹ and devised a short synthetic scheme to access the desired permethylated glycosyl trichloroacetimidates as the second generation of armed VT NMR substrates (**Scheme 61**).



Scheme 61. Synthesis of permethylated trichloroacetimidates **291** and **294**.

Starting with the synthesis of the parent glucosyl trichloroacetimide **291**, hemiacetal **254** was coupled with 2,3-dihydropyran in presence of PTSA to give tetrahydropyranyl glycosides **289**, which after deacetylation with NaOMe, methylation with MeI in the presence of NaH and subsequent hydrolysis with methanolic HCl afforded the permethylated hemiacetal **290** in 72% yield over 4 steps. Finally, coupling of this hemiacetal with trichloroacetonitrile in presence of catalytic DBU afforded the permethylated imidate **291** in 59% yield. For the synthesis of **294**, the hemiacetal **256** was protected as the tetrahydropyranyl glycosides **292**¹⁹¹ followed by deacetylation and subsequent methylation. Hydrolysis with methanolic HCl then afforded the permethylated hemiacetal **293** in 48% yield over 4 steps. Finally, coupling of **293** with trichloroacetonitrile in presence of catalytic DBU afforded permethylated trichloroacetimide **294** in 60% yield.

With both trichloroacetimidates synthesized we began VT NMR experiments. Starting with parent glucosyl trichloroacetimide **291**, the glycosyl triflate **279** was generated immediately after addition of TMSOTf to the parent glucosyl trichloroacetimide **291** at -78 °C and by -60 °C more than 90% of the starting material **291** was converted into triflate **279** (**Figure 4.24**). Above T > -50 °C triflate **279** underwent decomposition to form the imidate **296**, which after aqueous work-up produced trichloroacetamide **295** as

the only isolated decomposition product. The results of the VT NMR experiment with permethylated glucosyl trichloroacetimidate **291** are summarized in **Scheme 62**.

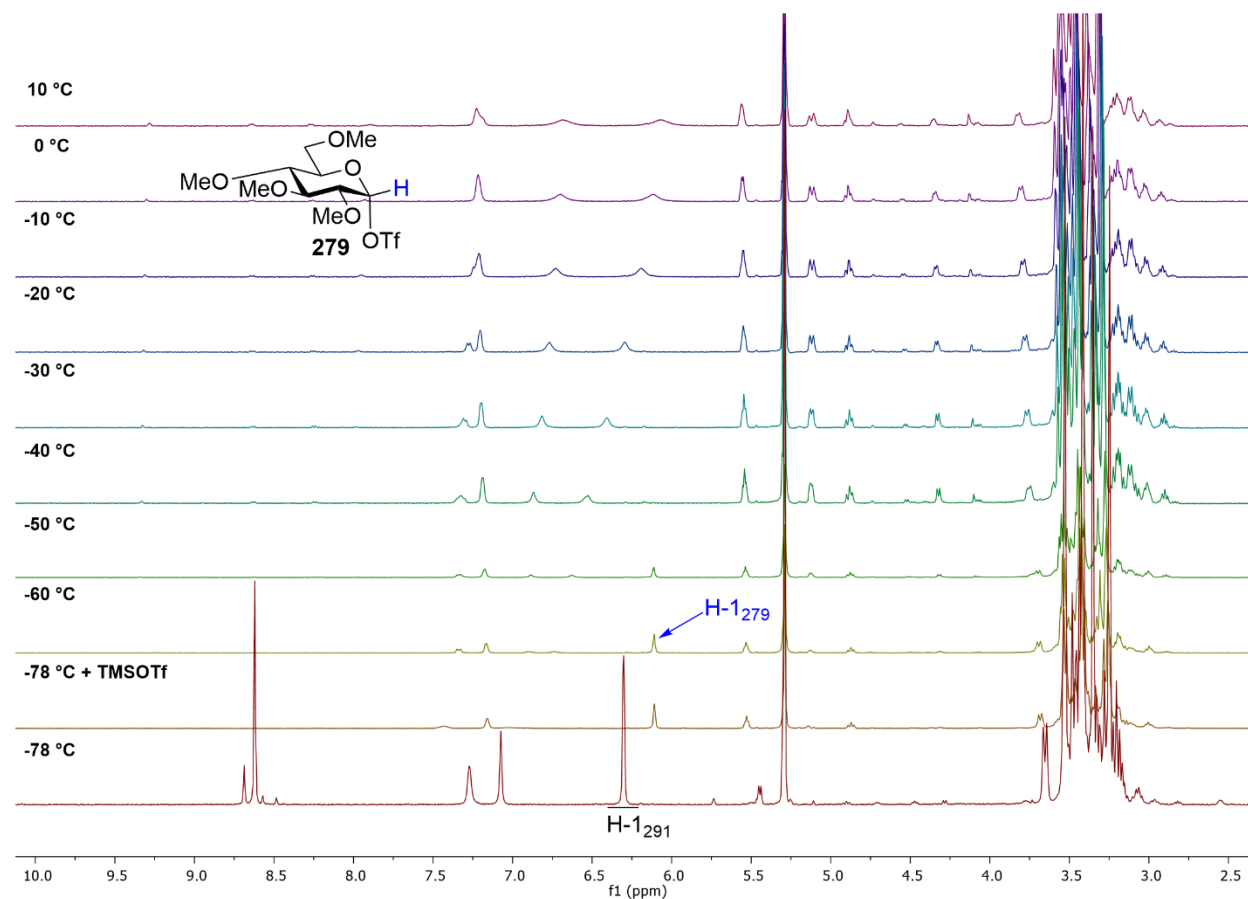
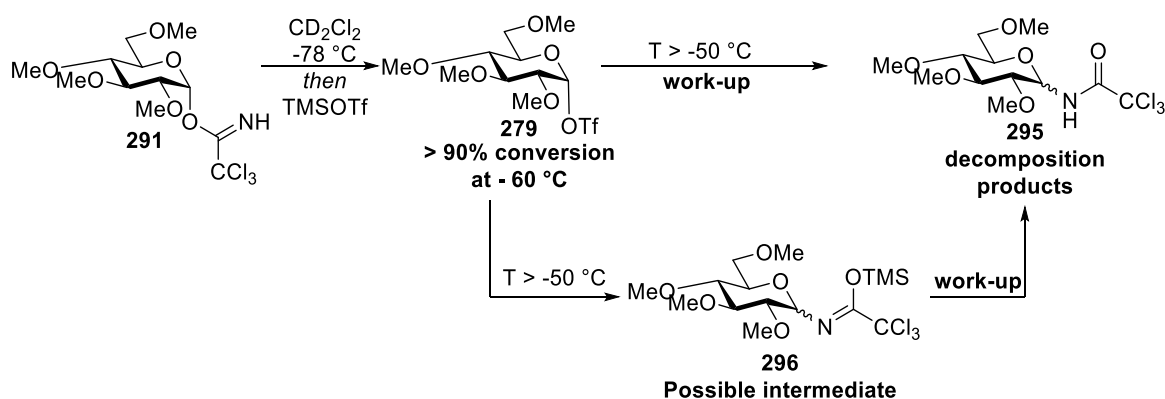


Figure 4.24. Stacked ^1H NMR spectra from a VT NMR experiment with thioglucosyl trichloroacetimidate **291**.



Scheme 62. Structures of reactive intermediates and byproducts formed during VT NMR experiments with trichloroacetimidate **291**.

We then performed VT NMR experiment with 5-thioglycosyl trichloroacetimidate **294**. No evidence was found to support the formation of a covalent 5-thioglycosyl triflate **284** on activation of 5-thioglycosyl trichloroacetimidate **294** with TMSOTf at $-78\text{ }^{\circ}\text{C}$ or on gradual warming (**Figure 4.25**). Rather slow conversion directly to the presumed imidate **297** was observed, resulting after work-up in trichloroacetamide **298**, which was the only decomposition product isolated. The overall results of the VT NMR experiment with permethylated are summarized in **Scheme 63**.

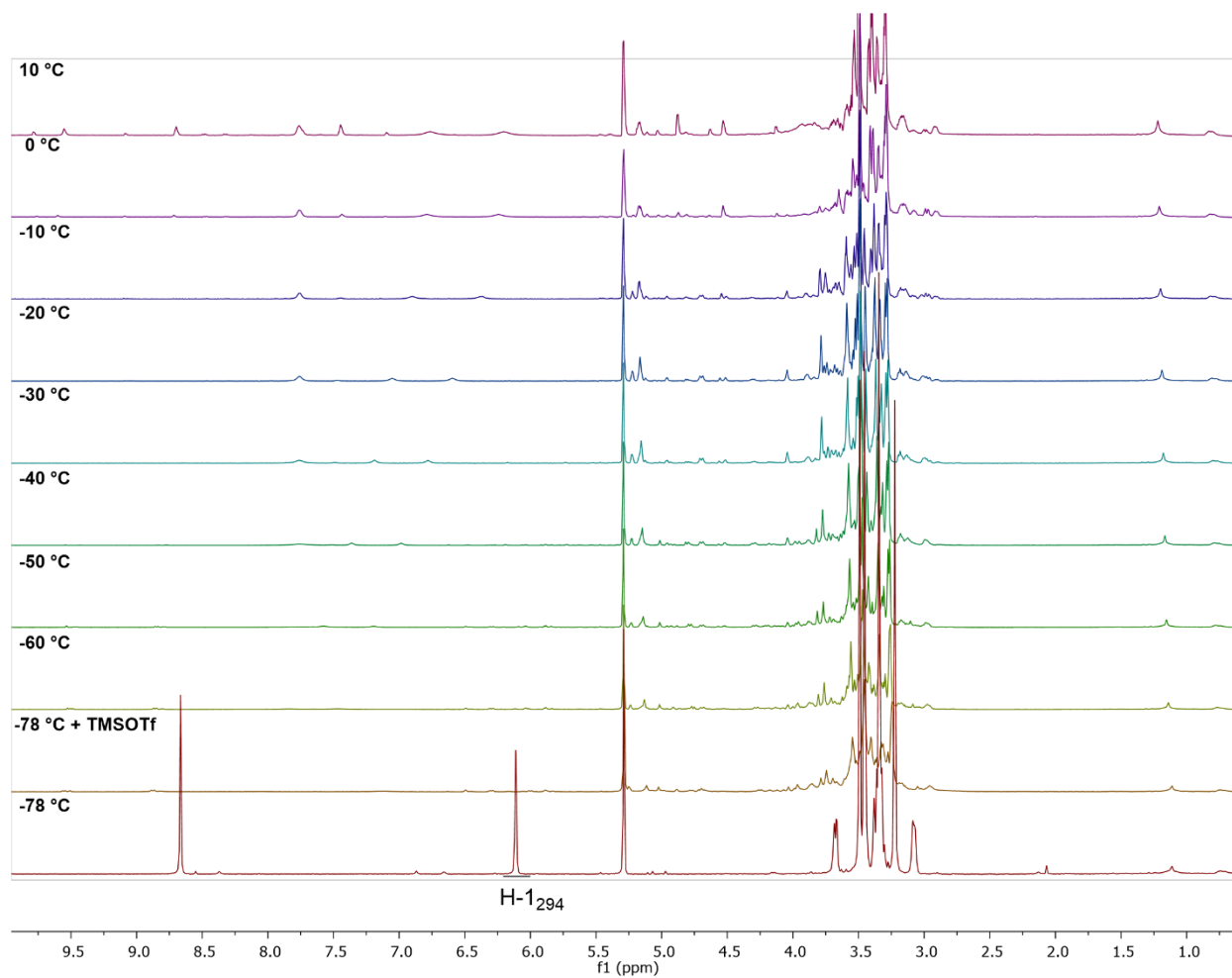
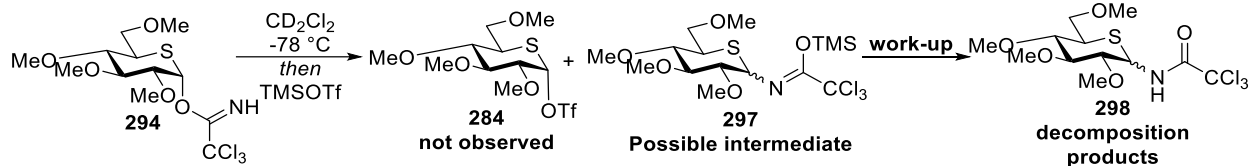


Figure 4.25. Stacked ^1H NMR spectra from a VT NMR experiment with 5-thioglycosyl trichloroacetimidate **294**.



Scheme 63. Structures of reactive intermediates and byproducts formed during a VT NMR experiment with trichloroacetimidate **294**.

Similarly to the disarmed glycosyl donor series, during the VT NMR experiments with both armed 5-thioglucoyl sulfoxides **269** and **272** and armed trichloroacetimidate **294** we did not detect any signals in ^1H or ^{13}C NMR spectra at any temperature that could correspond to the anomeric thienium cation.

4.6. Summary of the VT NMR experiments with glucosyl and thioglucoyl donors

The above ensemble of VT NMR experiments reveals clear differences in reactivity between glucopyranosyl donors and 5-thioglucoyl donors on activation at low temperature. A first difference is apparent in the decomposition of the disarmed peracetylated “activated sulfoxides” generated by reaction of peracetylated glucosyl and thioglucoyl ethyl sulfoxides with triflic anhydride. In the case of the thioglucoyl system the “activated sulfoxide” persists in the reaction mixture to a higher temperature than in the case of the analogous glucosyl system. When the “activated sulfoxide” is transformed to the dioxalenium ion and the corresponding glycosyl triflate, the relative proportions of these two intermediates vary between the glucosyl and thioglucoyl systems, with both being formed in approximately equal ratios in the glucosyl system but with the covalent triflate predominating for the thioglucoyl system. A directly analogous pattern was seen when attention was shifted to peracetylated glucosyl and thioglucoyl trichloroacetimidates, with the glucosyl system undergoing complete activation at a lower temperature than the corresponding 5-thioglucoyl system (**Figure 4.26**). Moreover, in full agreement with the peracetylated sulfoxides, the glucopyranosyl trichloroacetimidate yielded mixture of the dioxalenium ion and of the glycosyl triflate whose proportions changed with temperature, consistent with the observations of Huang, Whitfield and coworkers,²¹⁹ but which contained significant amounts of both intermediates. On the other hand, the activated peracetyl 5-thioglucoyl trichloroacetimidate was transformed to mixtures containing

significantly greater proportions of the covalent triflate compared to the dioxalenium ion arising from participation by the neighboring acetoxo group (**Figure 4.26**). In other words, neighboring group participation is apparently less favorable in the 5-thioglucofuranosyl series than in the glucofuranosyl series with respect to the corresponding glycosyl triflates. This observation might be interpreted in terms of greater stability of the fused dioxalenium ion in the glucosyl series or in terms of the reduced 1,3-diaxial interactions in the case of the thioglucofuranosyl system, as reflected in the greater anomeric effect seen in the 5-thioglucofuranosides^{49, 52} and the consequent greater stability of the axial triflate.

For the armed permethylated donors, very distinct differences were seen between the glucosyl and thioglucofuranosyl series (**Figure 4.27**). For the sulfoxides, activation of the simple glucofuranosyl donor gave rise to the formation of the anticipated glycosyl triflate being at -78 °C, whereas the corresponding 5-thioglucofuranosyl system did not provide an observable glycosyl triflate at any temperature with the “activated sulfoxide” seemingly undergoing direct decomposition at higher temperatures. A similar pattern was seen with the armed trichloroacetimidates, with the glucosyl system readily yielding the glycosyl triflate on activation and gradual warming while no such triflate was seen on activation of the thioglucofuranosyl trichloroacetimidate at any temperature, with the activated imidate seemingly converted directly to the rearranged thioglucofuranosyl trichloroacetamide in the reaction mixture (**Figure 4.27**). Overall, it is apparent that, following activation with either triflic anhydride for the sulfoxides or TMSOTf for the trichloroacetimidates, the 5-thioglucofuranosyl donors are less reactive than the corresponding glucofuranosyl donors whether armed or disarmed. One interesting question concerns the formation of a glycosyl triflate from the disarmed 5-thioglycosyl donors, **232**, **234**, and **52**, whereas none is seen on activation of the corresponding armed 5-thioglycosyl donors **269**, **272**, and **294**, which at first blush is an apparent contradiction of Fraser-Reid’s armed/disarmed concept. At this stage we can only speculate that the initial positively charged activated donors, triflated sulfoxides or silylated trichloroacetimidates, are destabilized in the disarmed peracetyl series and so more reactive with respect toward triflate formation than in the armed permethylated series.

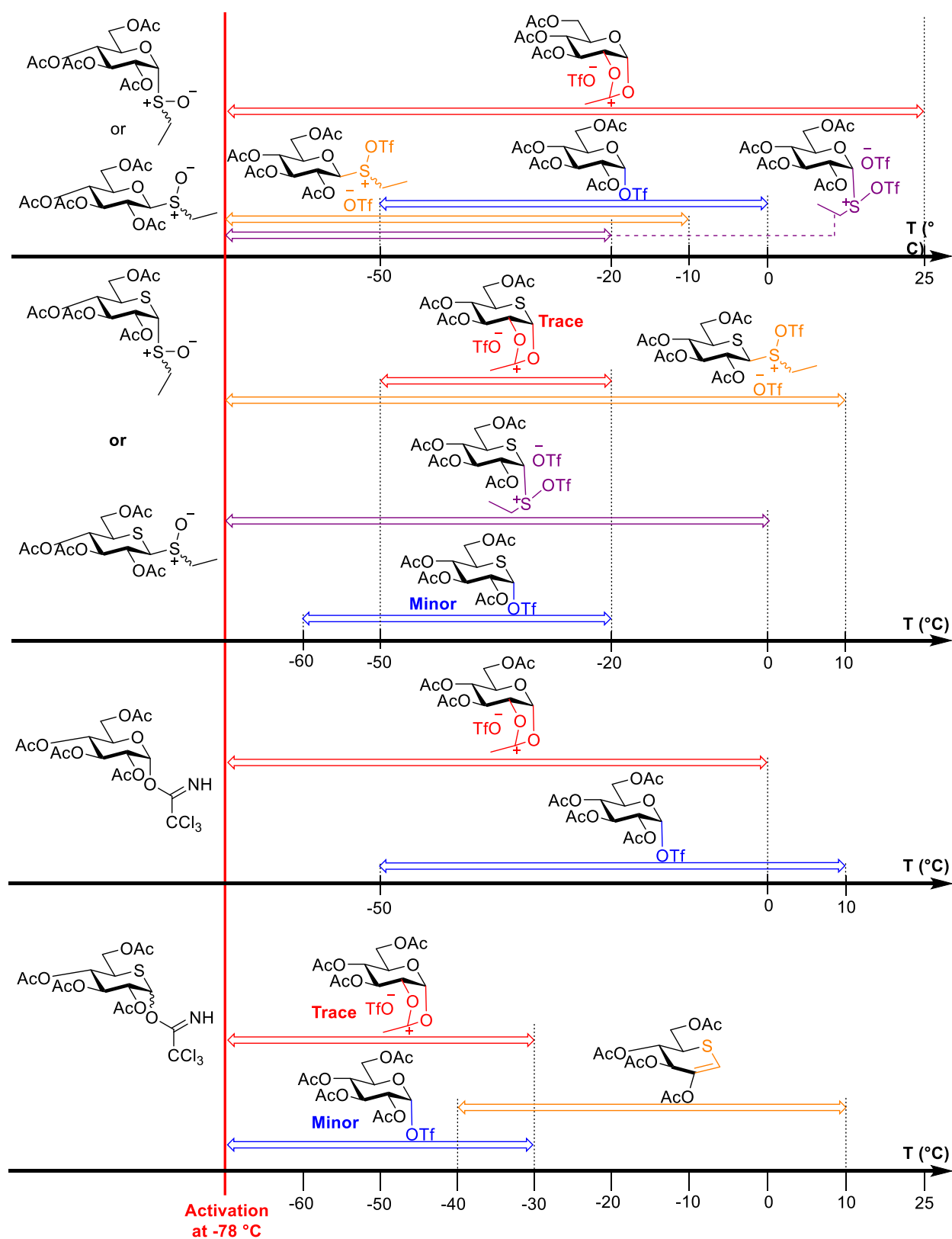


Figure 4.26. Summarized results of VT NMR experiments with peracetylated glycosyl donors.

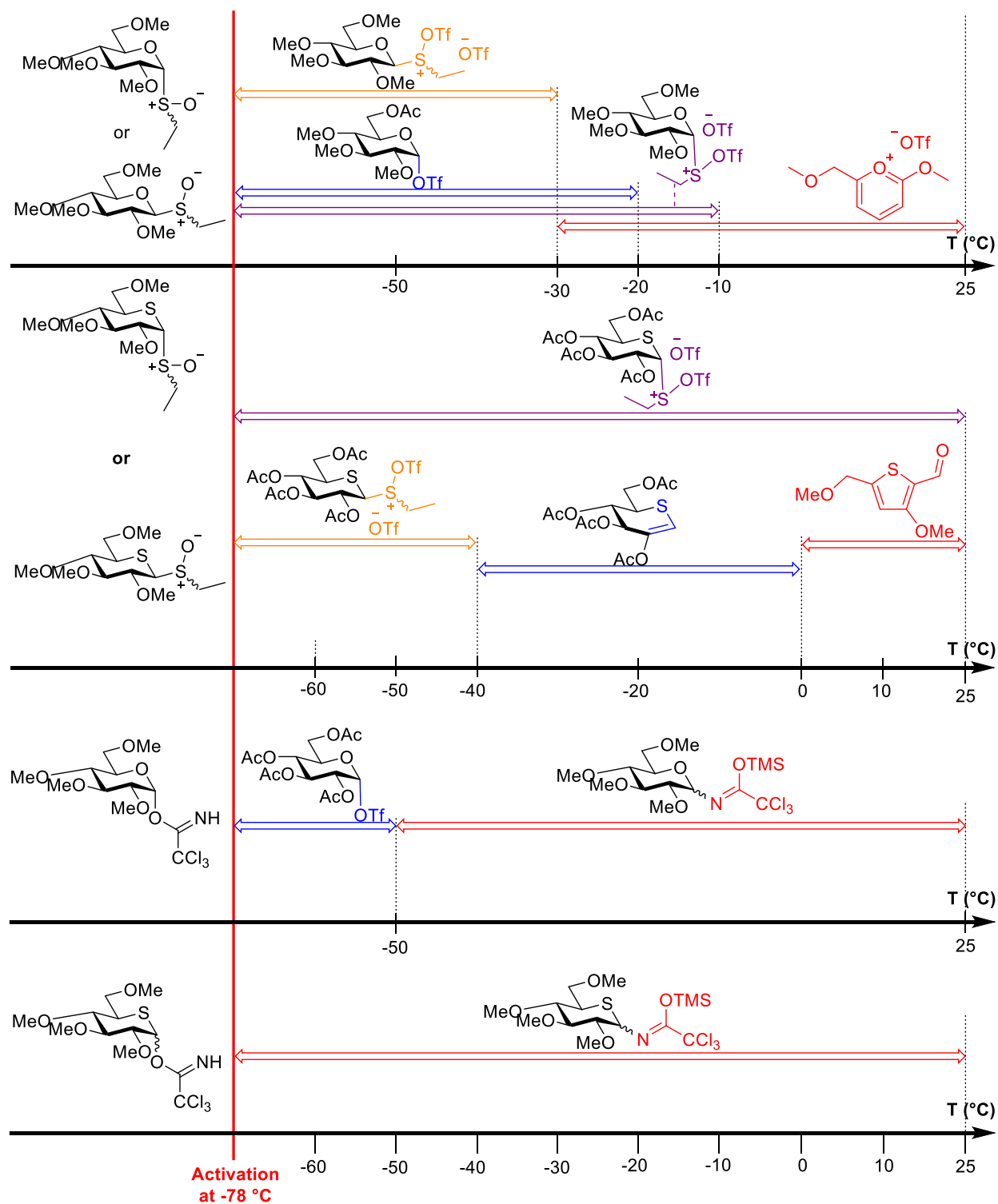


Figure 4.27. Summarized results of VT NMR experiments with permethylated glycosyl donors.

4.7. Conclusions

The generation of simple thiocarbenium cations was explored leading to the successful formation of the tetrahydrothiopyrilium cation, which was characterized spectroscopically. This simple thiocarbenium cation was found to be slightly more stable than the corresponding oxocarbenium cation. An extensive VT NMR study on generation and stability of reactive intermediates formed after activation of various glycosyl donors was performed. No signs of generation of thienium cation were observed during VT NMR experiments, suggesting that like glycosyl oxocarbenium ions, the glycosyl thiocarbenium ions are destabilized by the presence of the multiple electron-withdrawing C-O bonds. As such they are not sufficiently long-lived to be observed by VT NMR spectroscopy. Portions of this chapter are currently used in preparation of the manuscript for submission to the Journal of the American Chemical Society.

CHAPTER 5

OVERALL CONCLUSIONS

In this dissertation we explored the application of thioglycosides and thiosugars in medicinal and bioorganic chemistry. Evaluation of the novel tetraamide glycoclusters **142**, **146**, **150**, and **154** for their inhibitory activity against CR3 revealed the comparable inhibitory activity of 5-thioglucose mimetics of laminaribiose and -triose, thus demonstrating that in some cases 5-thioglycosyl mimetics can be used as inhibitors. However, the same glycoclusters showed little to no inhibitory activity against Dectin-1, presumably due to a poor fit of the aglycon with the Dectin-1 binding site. In addition, no clear pattern emerged regarding the number of carbohydrate units in the epitope nor the usefulness of the multivalent construct. The best compound of the series was tetravalent disaccharide **150**, which showed moderate inhibition of CR3 and some modest activity against Dectin-1.

Calorimetric analysis of the binding of thio-mimetic **187** to Jacalin in comparison to the parent compounds revealed that S- π interactions between ring sulfur atoms and appropriately disposed aromatic amino acid residues could positively contribute to the enthalpy of binding. However, the ring sulfur-for-oxygen exchange led to a decreased entropy of binding, which presumably, was caused by the puckering of the 5-thiosugar ring. Nevertheless, thio-mimetic **187** demonstrated moderate inhibitory activity against Jacalin, suggesting that the possibility of the S- π interactions between ring sulfur atoms and aromatic residues should be considered when selecting the thiosugar mimetics as potential inhibitors. Investigation of the 4-thiolactose-Galecin-1 interaction is still ongoing, such that no conclusions can be drawn at this time.

Variable temperature NMR studies revealed that a simple thiocarbenium cation was only slightly more stable than the corresponding oxocarbenium cation, which was evident from our ability to detect and characterize tetrahydrothiopyrilium cation **210** during VT NMR experiments, unlike the corresponding

oxocarbenium cation **221**. Introduction of the multiple functional groups with their electron-withdrawing C-O bonds led to destabilization of the corresponding glycosyl thiocarbenium cation, similarly to the parent glycosyl oxocarbenium cation, which was evident from our inability to observe any signs of generation of the cation at any temperatures during VT NMR experiments. Both armed and disarmed 5-thioglycosyl donors **232**, **234**, **52**, **269**, **272**, and **294** were found to be less reactive than the parent glycosyl donors **236**, **237**, **12**, **275**, **277**, and **291**. Trace amounts of the dioxalenium **251** and small amounts of covalent triflate **252** were generated at lower temperatures after activation of 5-thioglycosyl donors, while at higher temperatures rapid decomposition took place. This might be one of the reasons for contrasting differences in reactivity and stereoselectivity of 5-thioglycosyl donors as compared to the parent glycosyl donors.

CHAPTER 6

EXPERIMENTAL SECTION

6.1. General experimental

All reactions were conducted in flame/oven dried glassware capped with rubber septa under an atmosphere of argon or nitrogen unless otherwise stated. Commercially available starting materials were used without purification, unless otherwise stated. All organic solutions were concentrated under reduced pressure on a rotary evaporator and water bath. Flash-column chromatography was performed using a COMBIFLASH® NextGen system, unless otherwise stated. Thin-layer chromatography (TLC) was carried out with 250 μ m glass backed silica (XHL) plates with fluorescent indicator (254 nm) or 250 μ m glass backed C18 silica plates with fluorescent indicator (254 nm). TLC plates were visualized by submersion in ceric ammonium molybdate solution (CAM), or aqueous potassium permanganate solution (KMnO₄), or 10% sulfuric acid in ethanol followed by heating on a hot plate (120 °C). Nuclear Magnetic Resonance (NMR) spectra of all compounds were obtained in CDCl₃ (δ 7.27 and 77.0 ppm, respectively), CD₂Cl₂ (δ 5.32 and 53.5 ppm, respectively), CD₃CN (δ 1.94 and 1.32 ppm, respectively), DMSO-d₆ (δ 2.5 and 39.5 ppm, respectively), CD₃OD (δ 3.31 and 49.0 ppm, respectively), and D₂O (δ 4.67 ppm) using a 900 MHz Varian or 500 MHz EZC500 JEOL instrument. Various temperature NMR spectra were recorded using a 500 MHz EZC500 JEOL instrument. The chemical shifts (δ) are calculated with respect to residual solvent peaks and are given in ppm. Multiplicities are abbreviated as follows: s (singlet), m (multiplet), br (broad), d (doublet), t (triplet), q (quartet), p (quintet), and comp (complex). Assignments were made with the help of COSY, HMBC, HMQC or HSQC, DEPT-135, and DEPT-90 spectra. Specific rotations were recorded in CHCl₃ and DMSO, at 589 nm and 20-22 °C on a digital polarimeter with a path length of 10 cm. High resolution mass spectra were obtained on a ThermoFisher Orbitrap Q-Exactive using electrospray ionization (ESI). FTIR spectra were recorded with a JASCO FT/IR-4600 instrument. Reactions under

microwave irradiation were performed using a BIOTAGE Initiator microwave instrument. Photochemical reactions were performed in a Rayonet photochemical reactor.

Cell lines:

U937 cells, a human monocytic cell line (ATCC CRL-1593.2) and P388D1(IL-1), a murine monocytic cell line (ATCC, TIB-63), were obtained from the ATCC and maintained in RPMI 1640 medium supplemented with 10% heat-inactivated fetal bovine serum (FBS), penicillin (100 IU/mL), streptomycin (100 mg/mL) and l-glutamine (2 mM) in an incubator at 37 °C and a humidified atmosphere containing 5% CO₂.

Antibodies:

Mouse anti-human Dectin-1 (MCA4661F), rat anti-mouse Dectin-1 (MCA2289F) and a rat anti-mouse CD11b antibody (also detects human CD11b (MCA74F)), all fluorescein labeled (FITC), were obtained from Bio-Rad and used in the staining inhibition experiments at 1:200 dilution.

Lectins and biosensors:

Fluorescein-labeled Jacalin (FL-1151-5) was obtained from Vector Laboratories and used in the MST assay. His-tagged Galectin-1 (10290-H07E) was obtained from SinoBiological and used in the BLI assay. Ni-NTA biosensors (18-5101) were obtained from Sartorius and used in the BLI assay to immobilize the His-tagged Galectin-1.

6.2. Experimental procedures for the synthesis of compounds described in Chapter 2

Synthesis of tetraazide core (Scheme 17):

Tri-*O*-allylpentaerythritol (100a) and tetra-*O*-allylpentaerythritol (100b):

Pentaerythritol (3 g, 22.0 mmol) was dissolved in DMSO (40 mL) and NaOH (40% aq solution) (1.5 mL) was added followed by addition of allyl bromide (14.3 mL, 165 mmol, 7.5 equiv). The reaction mixture then was stirred for 16 h at 20 °C before it was diluted with H₂O (40 mL) and extracted with Et₂O (3×50 mL). The combined organic layers were washed with brine (100 mL), dried over MgSO₄, and concentrated

to dryness. The crude reaction mixture was purified by flash column chromatography on silica gel eluting with hexanes:EtOAc (0 → 30% EtOAc (v/v)) to give **100a** (3.74 g, 66%) and **100b** (1.6 g, 25%) ethers as a colorless liquids. The triallylated derivative **100a** (3.7g, 14.43 mmol) was then dissolved in anhydrous THF (48 mL) and the reaction mixture was cooled down to 0 °C before NaH (66% dispersion in mineral oil, 630 mg, 17.32 mmol, 1.2 equiv) was added. The reaction mixture was then stirred for 0.25 h at 0 °C before addition of allyl bromide (1.5 mL, 17.3 mmol, 1.2 equiv). The reaction mixture then heated to reflux with stirring for 12 h before further allyl bromide (1.5 mL, 17.3 mmol, 1.2 equiv) was added. After 1 h the reaction mixture was cooled to room temperature, quenched with MeOH (10 mL), concentrated under *vacuo*, redissolved in EtOAc (70 mL), washed with H₂O (40 mL), brine (40 mL), dried over MgSO₄ and concentrated to dryness. The crude product was purified by flash column chromatography on silica gel eluting with hexanes:EtOAc (0 → 20% EtOAc (v/v)) to afford the tetraallylated derivative **100b** as a colorless liquid (4.0 g, 93%).

100a:

Colorless liquid with spectral data identical to that in the literature.¹²⁹ *R_f* 0.47 (hexanes:EtOAc 4:1, (KMnO₄)); ¹H NMR (500 MHz, CDCl₃) δ 5.87 (ddt, *J* = 17.2, 10.7, 5.4 Hz, 3H, OCH₂CH=CH₂), 5.31– 5.07 (m, 6H, OCH₂CH=CH₂), 3.95 (dt, *J* = 5.4, 1.4 Hz, 6H, OCH₂CH=CH₂), 3.72 (s, 2H, CCH₂OH), 3.49 (s, 6H, C(CH₂OCH₂CH=CH₂)₃), 2.82 (br, 1H, OH); ¹³C NMR (126 MHz, CDCl₃) δ 134.7 (OCH₂CH=CH₂), 116.5 (OCH₂CH=CH₂), 72.4 (OCH₂CH=CH₂), 70.8 (C(CH₂OCH₂CH=CH₂)₃), 66.0 (CCH₂OH), 44.8 (C(CH₂O)₄); ESI-HRMS [M+K]⁺ calcd. for C₁₄H₂₄O₄K⁺ 295.1306, found 295.1297.

100b:

Colorless liquid. *R_f* 0.88 (hexanes:EtOAc 4:1, (KMnO₄)); ¹H NMR (500 MHz, CDCl₃) δ 5.89 (ddt, *J* = 17.3, 10.6, 5.4 Hz, 4H, OCH₂CH=CH₂), 5.26 (dq, *J* = 17.2, 1.8 Hz, 4H, OCH₂CH=CH₂), 5.14 (dq, *J* = 10.5, 1.6 Hz, 4H, OCH₂CH=CH₂), 3.96 (dt, *J* = 5.3, 1.6 Hz, 8H, OCH₂CH=CH₂), 3.47 (s, 8H, CCH₂O); ¹³C NMR (126 MHz, CDCl₃) δ 135.1 (OCH₂CH=CH₂), 115.9 (OCH₂CH=CH₂), 72.1 (OCH₂CH=CH₂), 69.2

(C(CH₂OCH₂CH=CH₂)₄), 45.3 (C(CH₂O)₄); ESI-HRMS [M+K]⁺ calcd. for C₁₇H₂₈O₄K⁺ 335.1619, found 335.1610.

Tetracarbamate (101):

Tetra-O-allyl-pentaerythritol **100b** (1.5 g, 5.06 mmol) was dissolved in anhydrous DMF (25.3 mL) and 2,2-dimethoxy-2-phenylacetophenone (DMPAP) (129 mg, 0.506 mmol, 0.1 equiv) was added followed by Boc-Cysteamine (7.18 g, 40.48 mmol, 8 equiv). The reaction vessel then was flushed with Ar, sealed, and irradiated with UV light ($\lambda = 254$ nm) for 2.5 h. After such time the reaction mixture was allowed to cool down to the room temperature (20 °C), quenched with H₂O (40 mL), and extracted with Et₂O (3 × 50 mL). The combined organic layers were washed with brine (30 mL), dried over Na₂SO₄, concentrated to dryness and co-evaporated with toluene (3 × 15 mL). The crude material was purified by flash column chromatography on a silica gel eluting with hexanes:EtOAc (0 → 40% EtOAc (v/v)) to give the product as a colorless syrup (3.4 g, 67%) containing ~6% of anti-Markovnikoff isomer based on NMR analysis. *R_f* 0.48 (hexanes:EtOAc 3:2, (CAM)); ¹H NMR (500 MHz, CDCl₃): δ 5.00 (br, 4H, NH), 3.40 (t, *J* = 6.0 Hz, 8H, OCH₂CH₂CH₂S), 3.36 – 3.19 (m, 16H, C(CH₂O)₄, SCH₂CH₂NHBoc), 2.59 (t, *J* = 6.6 Hz, 8H, SCH₂CH₂NHBoc), 2.53 (t, *J* = 7.3 Hz, 8H, OCH₂CH₂CH₂S), 1.76 (p, *J* = 6.4 Hz, 8H, OCH₂CH₂CH₂S), 1.40 (s, 36H, C(CH₃)₃); ¹³C NMR (126 MHz, CDCl₃): δ 155.8 (CO), 69.7 (C(CH₂O)₄, OCH₂CH₂CH₂S), 60.4 (C(CH₃)₃), 45.5 (C(CH₂O)₄), 39.8 (SCH₂CH₂NHBoc), 32.3 (SCH₂CH₂NHBoc), 29.8 (OCH₂CH₂CH₂S), 28.55 (OCH₂CH₂CH₂S), 28.5 (C(CH₃)₃). The minor isomer was identified in the mixture by the characteristic signal: 1.21 (d, *J* = 6.9, 3H, OCH₂CH(CH₃)S). ESI-HRMS [M+Na]⁺ calcd. for C₄₅H₈₈N₄NaO₁₂S₄⁺ 1027.5179, found 1027.5159.

Tetravalent ammonium salt (105):

Tetracarbamate **101** (3.4 g, 3.38 mmol) was dissolved in CH₂Cl₂ (40 mL) and 90% aq TFA (30 mL) added. The reaction mixture then was stirred at 20 °C for 1h. After such time the reaction mixture was concentrated to dryness and co-evaporated with toluene (3×15 mL) to produce tetraammonium salt **105** (3.41 g, quant.) containing ~6% of anti-Markovnikoff isomer based on NMR analysis. ¹H NMR (500 MHz, CD₃OD): δ

3.47 (qd, $J = 6.8, 3.8$ Hz, 8H, $\text{OCH}_2\text{CH}_2\text{CH}_2\text{S}$), 3.36 (s, 8H, $\text{C}(\text{CH}_2\text{O})_4$), 3.11 (t, $J = 7.0$ Hz, 8H, $\text{SCH}_2\text{CH}_2\text{NH}_3^+$), 2.77 (t, $J = 6.9$ Hz, 8H, $\text{SCH}_2\text{CH}_2\text{NH}_3^+$), 2.62 (t, $J = 7.2$ Hz, 8H, $\text{OCH}_2\text{CH}_2\text{CH}_2\text{S}$), 1.81 (t, $J = 6.7$ Hz, 8H, $\text{OCH}_2\text{CH}_2\text{CH}_2\text{S}$); ^{13}C NMR (126 MHz, CD_3OD) δ 69.3 ($\text{C}(\text{CH}_2\text{O})_4$, $\text{OCH}_2\text{CH}_2\text{CH}_2\text{S}$), 45.4 ($\text{C}(\text{CH}_2\text{O})_4$), 38.5 ($\text{SCH}_2\text{CH}_2\text{NH}_3^+$), 29.2 ($\text{OCH}_2\text{CH}_2\text{CH}_2\text{S}$), 28.4 ($\text{SCH}_2\text{CH}_2\text{NH}_3^+$), 27.8 ($\text{OCH}_2\text{CH}_2\text{CH}_2\text{S}$); ^{19}F NMR (470 MHz, CDCl_3) δ -75.50. The minor isomer was identified in the mixture by the characteristic signal: 1.26 (d, $J = 6.9$, 3H, $\text{OCH}_2\text{CH}(\text{CH}_3)\text{S}$). ESI-HRMS $[\text{M}+\text{Na}]^+$ calcd. for $\text{C}_{25}\text{H}_{57}\text{N}_4\text{O}_4\text{S}_4^+$ 605.3257, found 605.3257.

Tetraazide core (102):

Compound **105** (3.4 g, 3.36 mmol) was dissolved in MeCN : H_2O (4:1, (v/v)) (56 mL) and NEt_3 (7.48 mL, 53.70 mmol, 16 equiv) was added followed by $\text{CuSO}_4 \cdot 5\text{H}_2\text{O}$ (251 mg, 1.01 mmol, 0.3 equiv). The reaction mixture then was cooled down to 0 °C and Stick's reagent (5.23 g, 24.95 mmol, 8.9 equiv) was added. The reaction mixture then was stirred at 20 °C until complete consumption of the starting material was observed by LCMS. After completion of the reaction acetonitrile was removed under reduced pressure, and the reaction mixture was diluted with EtOAc (100 mL). The organic layer was separated and washed with 1M EDTA disodium salt (3×50 mL), brine (2×50 mL), dried over Na_2SO_4 and concentrated to dryness. The crude was purified by flash column chromatography on silica gel eluting with hexanes:EtOAc (0 → 20% EtOAc (v/v)) to give the product as a colorless syrup (1.38 g, 58%) containing ~5% of anti-Markovnikoff isomer based on NMR analysis. R_f 0.37 (hexanes:EtOAc 4:1, (CAM)); ^1H NMR (500 MHz, CDCl_3): δ 3.50 – 3.41 (m, 16H, $\text{OCH}_2\text{CH}_2\text{CH}_2\text{S}$, $\text{SCH}_2\text{CH}_2\text{N}_3$), 3.34 (s, 8H, $\text{C}(\text{CH}_2\text{O})_4$), 2.70 (t, $J = 7.0$ Hz, 8H, $\text{SCH}_2\text{CH}_2\text{N}_3$), 2.62 (t, $J = 7.3$ Hz, 8H, $\text{OCH}_2\text{CH}_2\text{CH}_2\text{S}$), 1.81 (p, $J = 6.4$ Hz, 8H, $\text{OCH}_2\text{CH}_2\text{CH}_2\text{S}$); ^{13}C NMR (126 MHz, CDCl_3): δ 69.8 ($\text{OCH}_2\text{CH}_2\text{CH}_2\text{S}$, $\text{C}(\text{CH}_2\text{O})_4$), 51.6 ($\text{SCH}_2\text{CH}_2\text{N}_3$), 45.6 ($\text{C}(\text{CH}_2\text{O})_4$), 31.4 ($\text{SCH}_2\text{CH}_2\text{N}_3$), 29.9 ($\text{OCH}_2\text{CH}_2\text{CH}_2\text{S}$), 29.2 ($\text{OCH}_2\text{CH}_2\text{CH}_2\text{S}$). The minor isomer was identified in the mixture by the characteristic signal: 1.25 (d, $J = 7.0$ Hz, 3H, $\text{OCH}_2\text{CH}(\text{CH}_3)\text{S}$). ESI-HRMS $[\text{M}+\text{Na}]^+$ calcd. for $\text{C}_{25}\text{H}_{48}\text{N}_{12}\text{NaO}_4\text{S}_4^+$ 731.2697, found 731.2681.

Synthesis of 5-thioglucose pentaacetate (Scheme 18):

1,2;5,6-Di-*O*-isopropylidene-3-*O*-acetyl- α -D-glucofuranose (107)

Diacetonide glucose **106** (110 g, 422.61 mmol) was dissolved in CH₂Cl₂ (300 mL) and Py (200 mL) followed by addition of Ac₂O (80.6 mL) at 0 °C, and the reaction mixture then was stirred with warming from 0 → 20 °C for 4h. After such time the reaction mixture was quenched with brine (100 mL), washed with H₂O (3×500 mL), 1M HCl (4×250 mL), dried over Na₂SO₄ and concentrated to dryness and dried on a high vacuum to give the product as white solid (127 g, 94%) with spectral data identical to that reported in the literature.²⁴⁷ *R*_f 0.36 (hexanes:EtOAc 4:1, (H₂SO₄/EtOH)); ¹H NMR (500 MHz, CDCl₃): δ 5.85 (d, *J* = 3.7 Hz, 1H), 5.23 (d, *J* = 2.4 Hz, 1H), 4.48 (d, *J* = 3.7 Hz, 1H), 4.23 – 4.15 (m, 2H), 4.05 (dd, *J* = 8.6, 5.6 Hz, 1H), 4.02 – 3.93 (m, 1H), 2.08 (s, 3H), 1.50 (s, 3H), 1.39 (s, 3H), 1.30 (s, 3H), 1.28 (s, 3H); ¹³C NMR (126 MHz, CDCl₃): δ 169.6, 112.3, 109.4, 105.1, 83.4, 79.8, 76.2, 72.5, 67.2, 26.9, 26.8, 26.3, 25.3, 20.9; ESI-HRMS [M+Na]⁺ calcd. for C₁₄H₂₂NaO₇⁺ 325.1263, found 325.1252

1,2-*O*-Isopropylidene-3-*O*-acetyl- α -D-glucofuranose (108)

The acetate **107** (120 g, 396.8 mmol) was suspended in 50% aq AcOH (600 mL) and the reaction mixture was stirred for 16h at 20 °C. After such time the reaction mixture was concentrated to dryness and co-evaporated with toluene (3×30 mL) to give the product as a white solid (98.5 g, 95%) with spectral data identical to that reported in the literature.²⁴⁷ *R*_f 0.14 (hexanes:EtOAc 7:3, (H₂SO₄/EtOH)); ¹H NMR (500 MHz, CDCl₃): δ 5.91 (d, *J* = 3.7 Hz, 1H), 5.28 (d, *J* = 2.6 Hz, 1H), 4.57 (d, *J* = 3.7 Hz, 1H), 4.18 (dd, *J* = 9.0, 2.6 Hz, 1H), 3.86 (dd, *J* = 11.4, 3.4 Hz, 1H), 3.73 (dd, *J* = 11.4, 5.8 Hz, 1H), 3.66 (ddd, *J* = 9.2, 5.8, 3.3 Hz, 1H), 2.16 (s, 3H), 1.52 (s, 3H), 1.32 (s, 3H); ¹³C NMR (126 MHz, CDCl₃): δ 171.3, 112.4, 104.8, 83.0, 79.5, 68.1, 64.2, 26.6, 26.2, 20.8; ESI-HRMS [M+Na]⁺ calcd. for C₁₁H₁₈NaO₇⁺ 285.0945, found 285.0945.

1,2-*O*-Isopropylidene-3-*O*-acetyl-5-*O*-methylsulfonyl-6-*O*-benzoyl- α -D-glucofuranose (109)

Diol **108** (98.4 g, 375.6 mmol) was dissolved in Py (300 mL) and CH₂Cl₂ (150 mL) and the reaction mixture was cooled down to -30 °C before BzCl (43.6 mL, 375.6 mmol) was added dropwise. The reaction mixture was stirred at -30 °C until complete conversion of the starting material into the monobenzoate (observed

by LCMS and TLC). After that MsCl (30 mL, 375.6 mmol) was added dropwise and the reaction mixture was stirred for 16h with gradual warming to 20 °C. After such time the reaction mixture was quenched with ice-water, diluted with CH₂Cl₂ (400 mL), washed with H₂O (3×600 mL), brine (3×600 mL), dried over Na₂SO₄, concentrated to dryness, and co-evaporated with toluene (3×50 mL) to give the product as a white solid (150.2 g, 90%) with spectral data identical to that reported in the literature.⁹² *R*_f 0.46 (hexanes:EtOAc 7:3, (H₂SO₄/EtOH)); ¹H NMR (500 MHz, CDCl₃): δ 8.15 – 7.97 (m, 2H), 7.61 – 7.51 (m, 1H), 7.49 – 7.37 (m, 2H), 5.92 (d, *J* = 3.6 Hz, 1H), 5.32 (d, *J* = 3.0 Hz, 1H), 5.25 (ddd, *J* = 8.6, 6.0, 2.1 Hz, 1H), 4.92 (dd, *J* = 12.7, 2.1 Hz, 1H), 4.58 – 4.35 (m, 3H), 3.00 (s, 3H), 2.14 (s, 3H), 1.50 (s, 3H), 1.30 (s, 3H); ¹³C NMR (126 MHz, CDCl₃): δ 170.0, 166.0, 133.4, 129.8, 129.6, 129.1, 128.6, 128.3, 112.8, 105.3, 83.1, 76.5, 75.0, 74.1, 64.0, 39.1, 26.8, 26.3, 21.0; ESI-HRMS [M+Na]⁺ calcd. for C₁₉H₂₄NaO₁₀S⁺ 467.0982, found 467.0982.

5,6-Anhydro-5,6-epithio-1,2-*O*-isopropylidene- α -D-glucofuranose (111):

Compound **109** (130 g, 292.5 mmol) was suspended in anhydrous MeOH (500 mL) and NaOMe (2M solution in MeOH, 146.2 mL, 2.92 mmol, 1 equiv) was added. The reaction mixture then was stirred at 20 °C until complete conversion of the starting material into epoxide was observed by LCMS. After that the reaction mixture was quenched with Amberlyst 15 (H⁺) ion-exchange resin until pH 5, and the resulting mixture was filtered. The filtrate was concentrated to dryness and the crude was taken into MeOH (1000 mL) and thiourea (33.4 g, 438 mmol, 1.5 equiv) was added, and the reaction mixture was refluxed at 80 °C for 4h. After such time the reaction mixture was concentrated to dryness, and CH₂Cl₂ (1500 mL) was added. The resulting suspension was filtered through Celite ®, and the filtrate was collected, washed with H₂O (3×500 mL), brine (3×500 mL), dried over Na₂SO₄ and concentrated to dryness. The desired product then was crystallized from EtOAc : hexanes = 1 : 4 (v/v) to give the product as white solid (36.5 g, 58% over 2 steps) with spectral data matching that reported in the literature.²⁴⁸ *R*_f 0.15 (hexanes:EtOAc 1:1, (H₂SO₄/EtOH)); ¹H NMR (500 MHz, CDCl₃): δ 5.98 (d, *J* = 3.7 Hz, 1H), 4.54 (d, *J* = 3.6 Hz, 1H), 4.23 (d, *J* = 2.7 Hz, 1H), 3.61 (dd, *J* = 8.6, 2.7 Hz, 1H), 3.13 (dt, *J* = 8.6, 5.8 Hz, 1H), 2.67 (dd, *J* = 6.21, 1.5 Hz,

1H), 2.45 (dd, $J = 5.4, 1.5$ Hz, 1H), 1.46 (s, 3H), 1.31 (s, 3H); ^{13}C NMR (126 MHz, CDCl_3): δ 112.0, 105.5, 86.2, 85.0, 76.3, 29.7, 26.8, 26.2, 25; ESI-HRMS $[\text{M}+\text{Na}]^+$ calcd. for $\text{C}_9\text{H}_{14}\text{NaO}_4\text{S}^+$ 241.0510, found 241.0495.

1,2-*O*-Isopropylidene-3,6-di-*O*-acetyl-5-*S*-acetyl-5-thio- α -D-glucofuranose (75):

Thiirane **111** (35 g, 160.35 mmol) was dissolved in Ac_2O (151 mL) and AcOH (200 mL) followed by addition of KOAc (23.61 g, 240.53 mmol) and the reaction mixture was refluxed at 140 °C for 12h. After such time the reaction mixture was allowed to cool down to 20 °C and was poured into ice water. The resulting mixture was extracted with CH_2Cl_2 (3×200 mL), and the combined organic layers were washed with NaHCO_3 (3×200 mL), brine (500 mL), dried over MgSO_4 , and concentrated to dryness. The crude residue was decolorized with activated charcoal in EtOH (200 mL), and the resulting mixture was filtered through Celite ®. The filtrate was concentrated to dryness to give product as a white solid (39.48 g, 68%) with spectral data identical to that reported in the literature.⁹² R_f 0.48 (hexanes: EtOAc 4:1, ($\text{H}_2\text{SO}_4/\text{EtOH}$)); ^1H NMR (500 MHz, CDCl_3): δ 5.90 (d, $J = 3.6$ Hz, 1H), 5.28 (d, $J = 2.8$ Hz, 1H), 4.46 – 4.37 (m, 3H), 4.33 (dd, $J = 11.5, 4.9$, 1H), 4.16 – 4.03 (m, 1H), 2.30 (s, 3H), 2.05 (s, 3H), 2.04 (s, 3H), 1.50 (s, 3H), 1.29 (s, 3H); ^{13}C NMR (126 MHz, CDCl_3): δ 192.8, 170.4, 169.7, 112.3, 105.0, 83.0, 77.5, 75.4, 64.5, 40.2, 30.5, 26.7, 26.2, 20.7, 20.6; ESI-HRMS $[\text{M}+\text{K}]^+$ calcd. for $\text{C}_{15}\text{H}_{22}\text{O}_8\text{KS}^+$ 401.0667, found 401.0649.

1,2,3,4,6-Penta-*O*-acetyl-5-thio- α,β -D-glucopyranose (33):

Thioacetate **75** (24 g, 66.23 mmol) was dissolved in 50% aq TFA (250 mL) and the reaction mixture was stirred for 16h at 20 °C. After such time the reaction mixture was concentrated to dryness and co-evaporated with toluene (3×40 mL). The crude was suspended in anhydrous MeOH (100 mL) and Na (550 mg, 23.93 mmol, 0.36 equiv) was added at 0 °C. The reaction mixture then was stirred until complete deprotection of the starting material was observed by LCMS. After that the reaction mixture was quenched with Amberlite IR-120 (H^+) ion-exchange resin until pH 4-5, and filtered. The filtrate was concentrated to dryness, redissolved in Py (50 mL), and Ac_2O (94.8 mL, 993.40 mmol, 15 equiv) was added at 0 °C. The reaction mixture then was stirred for 16h with gradual warming to 20 °C. After such the reaction mixture was

carefully quenched with MeOH (30 mL) at 0 °C, diluted with CH₂Cl₂ (150 mL), washed with H₂O (3×150 mL), 1M H₂SO₄ (3×100 mL), NaHCO₃ (150 mL), brine (150 mL), dried over MgSO₄, and concentrated to dryness. The crude product was purified by a column chromatography on silica gel eluting with hexanes : EtOAc (10 → 60% EtOAc (v/v)) to give mixture of anomeric acetates (α : β = 12.5 : 1) as a white solid (16.15 g, 60% over 3 steps). *R*_f 0.28 (hexanes:EtOAc 7:3, (H₂SO₄/EtOH)); ¹H NMR (500 MHz, CH₃CO₂CH₃): δ 6.12 (d, *J* = 3.2 Hz, 1H), 5.40 (t, *J* = 9.9 Hz, 1H), 5.29 (dd, *J* = 10.9, 9.6 Hz, 1H), 5.20 (dd, *J* = 10.2, 3.2 Hz, 1H), 4.34 (dd, *J* = 12.1, 4.9 Hz, 1H), 4.03 (dd, *J* = 12.1, 3.1 Hz, 1H), 3.56 (ddd, *J* = 10.9, 4.9, 3.1 Hz, 1H), 2.14 (s, 3H), 2.04 (s, 3H), 2.01 (s, 3H), 1.98 (s, 3H), 1.95 (s, 3H); ¹³C NMR (126 MHz, CDCl₃): δ 170.4, 169.7, 169.5, 169.3, 168.9, 73.0, 71.7, 70.6, 70.5, 60.9, 39.8, 20.8, 20.5, 20.5, 20.4, 20.4. The minor β -isomer was identified in the mixture by the characteristic signals: 5.86 (d, *J* = 8.6 Hz, 1H), 5.08 (t, *J* = 9.1 Hz, 1H), 4.29 – 4.22 (m, 1H), 3.29 (ddd, *J* = 9.8, 5.6, 3.8 Hz, 1H).

ESI-HRMS [M+Na]⁺ calcd. for C₁₆H₂₂NaO₁₀S⁺ 429.0826, found 429.0815.

Synthesis of 5-thiooligosaccharides (Scheme 19 and Scheme 20):

1,2-*O*;5-*S*,6-*O*-Di-isopropylidene-5-thio- α -D-glucofuranose (112):

5-Thioglucose pentaacetate **33** (2.2 g, 5.41 mmol) was suspended in anhydrous MeOH (20 mL) and NaOMe (2M solution in MeOH, 1 mL, 2 mmol, 0.4 equiv) was added, and the reaction mixture was stirred for 1h at 20 °C. After such time the reaction mixture was quenched with Amberlite IR-120 (H⁺) ion-exchange resin until pH 4-5, and the resulting mixture was filtered. The filtrate was concentrated to dryness, and the crude was suspended in acetone (80 mL) followed by addition of PTSA (1.86 g, 10.83 mmol, 2 equiv). The reaction mixture then was stirred for 12h at 20 °C. After such time the reaction mixture was quenched with NaHCO₃ (30 mL) and extracted with Et₂O (3×100 mL). The combined organic layers were washed with brine (200 mL), dried over MgSO₄, and concentrated to dryness. The crude product was purified by a column chromatography on silica gel eluting with hexanes : EtOAc (0 → 25% EtOAc (v/v)) to give product as a colorless oil (990 mg, 67% over 2 steps) with spectral data identical to that reported in the literature.⁹⁰ *R*_f 0.25 (hexanes:EtOAc 3:1, (H₂SO₄/EtOH)); ¹H NMR (500 MHz, CDCl₃): δ 5.91 (d, *J* = 3.7 Hz, 1H), 4.48

(d, $J = 3.7$ Hz, 1H), 4.34 (dd, $J = 9.9, 3.0$ Hz, 1H), 4.21 – 4.13 (m, 3H), 3.73 (ddd, $J = 10.1, 5.1, 3.0$ Hz, 1H), 2.38 (br, 1H), 1.66 (s, 3H), 1.60 (s, 3H), 1.50 (s, 3H), 1.30 (s, 3H); ^{13}C NMR (126 MHz, CDCl_3): δ 111.8, 105.3, 92.7, 85.2, 82.5, 75.4, 72.5, 48.1, 31.6, 30.8, 26.8, 26.2; ESI-HRMS $[\text{M}+\text{Na}]^+$ calcd. for $\text{C}_{12}\text{H}_{20}\text{NaO}_5\text{S}^+$ 299.0924, found 299.0925.

1,2-*O*;5-*S*,6-*O*-Di-isopropylidene-5-thio- α -D-allofuranose (113):

Compound **112** (773 mg, 2.8 mmol) was dissolved in anhydrous CH_2Cl_2 : DMSO = 2 : 1 (v/v) (20 mL) and DIPEA (2.4 mL, 14 mmol, 5 equiv). The reaction mixture was cooled down to 0 °C, and $\text{Py}\cdot\text{SO}_3$ (1.79 g, 11.2 mmol, 4 equiv) was added. The reaction mixture was stirred for 15 minutes at 0 °C, then gradually warmed up to 20 °C, and was stirred for an additional 30 minutes. After such time the reaction mixture was quenched with NaHCO_3 (20 mL) and extracted with Et_2O (4×50 mL). The combined organic layers were dried over Na_2SO_4 and concentrated to dryness. The crude ketosugar was dissolved in EtOH (20 mL) and NaBH_4 (158 mg, 4.2 mmol, 1.5 equiv) was added at 0 °C. The reaction mixture was then stirred for 30 minutes at 0 °C before acetone (5 mL) was added to quench the reaction. After that the reaction mixture was concentrated to dryness, and the crude product was purified by a flash column chromatography on silica gel eluting with hexanes : EtOAc (0 \rightarrow 35% EtOAc (v/v)) to give product as a white solid (620 mg, 80% over 2 steps) with spectral data identical to that reported in the literature.⁹⁰ R_f 0.13 (hexanes:EtOAc 3:1, ($\text{H}_2\text{SO}_4/\text{EtOH}$)); ^1H NMR (500 MHz, CDCl_3): δ 5.72 (d, $J = 3.8$ Hz, 1H), 4.60 (t, $J = 4.2$ Hz, 1H), 4.26 (dd, $J = 10.0, 3.6$ Hz, 1H), 4.16 (dd, $J = 10.0, 5.6$ Hz, 1H), 3.95 – 3.85 (m, 2H), 3.76 (td, $J = 5.8, 3.5$ Hz, 1H), 2.73 (d, $J = 6.7$ Hz, 1H), 1.68 (s, 3H), 1.62 (s, 3H), 1.57 (s, 3H), 1.34 (s, 3H); ^{13}C NMR (126 MHz, CDCl_3): δ 112.9, 103.4, 92.9, 80.4, 79.3, 73.8, 71.7, 52.4, 30.9, 30.8, 26.6, 26.4; ESI-HRMS $[\text{M}+\text{Na}]^+$ calcd. for $\text{C}_{12}\text{H}_{20}\text{NaO}_5\text{S}^+$ 299.0924, found 299.0920.

1,2-*O*;5-*S*,6-*O*-Di-isopropylidene-3-*O*-trifluoromethanesulfonyl-5-thio- α -D-allofuranose (63):

Alcohol **113** (650 mg, 2.35 mmol) was dissolved in Py (3 mL) and the reaction mixture was cooled down to 0 °C before Tf_2O (1.18 mL, 7.06 mmol, 3 equiv) was added dropwise. The reaction mixture then was stirred for 40 minutes at 0 °C before ice-cold NaHCO_3 (15 mL) was added to quench the reaction. After

that the reaction mixture was extracted with CH₂Cl₂ (3×30 mL), and the combined organic layers were washed with H₂O (100 mL), brine (100 mL), dried over Na₂SO₄, and concentrated to dryness. The crude product was purified by a flash column chromatography on silica gel eluting with hexanes : EtOAc (0 → 9% EtOAc (v/v)) to give product as a white solid (824 mg, 86%) with spectral data identical to that reported in the literature.⁸⁰ *R*_f 0.35 (hexanes:EtOAc 91:9, (H₂SO₄/EtOH)); ¹H NMR (500 MHz, CDCl₃): δ 5.78 (d, *J* = 3.8 Hz, 1H), 4.87 (dd, *J* = 7.6, 5.3 Hz, 1H), 4.73 (dd, *J* = 5.3, 3.8 Hz, 1H), 4.33 (dd, *J* = 7.6, 6.7 Hz, 1H), 4.25 (dd, *J* = 10.3, 2.6 Hz, 1H), 4.14 (dd, *J* = 10.3, 5.8 Hz, 1H), 3.79 (td, *J* = 6.2, 2.6 Hz, 1H), 1.69 (s, 3H), 1.61 (s, 3H), 1.57 (s, 3H), 1.36 (s, 3H); ¹³C NMR (126 MHz, CDCl₃): δ 119, 114.4, 103.9, 93.3, 83.4, 79.1, 77.8, 70.7, 51.9, 30.8, 30.6, 27.0, 26.6; ¹⁹F NMR (470 MHz, CDCl₃): δ -74.7; ESI-HRMS [M+Na]⁺ calcd. for C₁₃H₁₉NaO₇S₂⁺ 431.0417, found 431.0412.

1-*S*-Acetyl-2,3,4,6-tetra-*O*-acetyl-1,5-dithio-β-D-glucopyranose (61):

5-Thioglucose pentaacetate **33** (950 mg, 2.34 mmol) was dissolved in anhydrous CH₂Cl₂ (20 mL) and BiBr₃ (53 mg, 0.116 mmol, 0.05 equiv) was added, followed by TMSBr (1.23 mL, 9.35 mmol, 4 equiv) and the reaction mixture was stirred for 45 minutes at 20 °C. After such time the reaction mixture was quenched with aq sat NaHCO₃ (10 mL) and diluted with CH₂Cl₂ (40 mL). The organic layer was separated, washed with ice-cold H₂O (20 mL) and brine (20 mL), dried over Na₂SO₄, and concentrated to dryness. The crude was taken into anhydrous DMF (2.3 mL) and cooled down to 0 °C before KSac (390 mg, 3.412 mmol, 1.5 equiv) was added. The reaction mixture was stirred for 12h with gradual warming to 20 °C. After such time the reaction mixture was diluted with EtOAc (70 mL), washed with H₂O (50 mL), brine (50 mL), dried over Na₂SO₄, and concentrated to dryness. The crude product was purified by a flash column chromatography on silica gel eluting with hexanes : EtOAc (0 → 60% EtOAc (v/v)) to give product as a white solid (819 mg, 83% over 2 steps) with spectral data identical to that reported in the literature.⁸⁰ *R*_f 0.48 (hexanes:EtOAc 1:1, (H₂SO₄/EtOH)); ¹H NMR (500 MHz, CDCl₃): δ 5.31 – 5.19 (m, 2H), 5.10 (t, *J* = 9.5 Hz, 1H), 4.68 (d, *J* = 10.9 Hz, 1H), 4.27 (dd, *J* = 12.0, 5.4 Hz, 1H), 4.11 (dd, *J* = 12.1, 3.2 Hz, 1H), 3.40 (ddd, *J* = 10.7, 5.5, 3.2 Hz, 1H), 2.37 (s, 3H), 2.06 (s, 3H), 2.03 (s, 3H), 2.00 (s, 3H), 1.99 (s, 3H); ¹³C

NMR (126 MHz, CDCl₃): δ 191.4, 170.4, 169.5, 169.3, 169.3, 74.4, 72.4, 71.5, 61.0, 44.9, 44.0, 30.4, 20.6, 20.6, 20.4, 20.4, 20.4; ESI-HRMS [M+Na]⁺ calcd. for C₁₆H₂₂NaO₉S₂⁺ 445.0597, found 445.0591.

2,3,4,6-Tetra-*O*-acetyl-5-thio- β -D-glucopyranosyl-(1 \rightarrow 3)-1,2-*O*;5-*S*,6-*O*-di-isopropylidene-3-deoxy-3,5-dithio- α -D-glucofuranose (64):

Thioacetate **61** (205 mg, 0.485 mmol) and triflate **63** (218 mg, 0.533 mmol, 1.1 equiv) were dissolved in anhydrous DMF (0.5 mL), and the reaction mixture was cooled down to 0 °C before Et₂NH (126 μ L, 1.212 mmol, 2.5 equiv) was added. After that the reaction mixture was stirred for 2h with gradual warming to 20 °C. After such time the reaction mixture was diluted with EtOAc (60 mL), washed with H₂O (40 mL), brine (40 mL), dried over Na₂SO₄, and concentrated to dryness. The crude product was purified by a flash column chromatography on silica gel eluting with hexanes : EtOAc (10 \rightarrow 60% EtOAc (v/v)) to give product as a yellow foam (305 mg, 98%) with spectral data identical to that reported in the literature.⁸⁰ *R*_f 0.53 (hexanes:EtOAc 1:1, (H₂SO₄/EtOH)); ¹H NMR (500 MHz, CDCl₃): δ 5.86 (d, *J* = 3.5 Hz, 1H), 5.30 (t, *J* = 10.0 Hz, 1H), 5.14 (t, *J* = 10.1 Hz, 1H), 5.06 (t, *J* = 9.4 Hz, 1H), 4.70 (d, *J* = 3.5 Hz, 1H), 4.40 (dd, *J* = 10.5, 4.0 Hz, 1H), 4.36 – 4.25 (m, 2H), 4.17 – 4.06 (m, 2H), 3.99 (d, *J* = 10.6 Hz, 1H), 3.64 (ddd, *J* = 10.4, 5.0, 2.3 Hz, 1H), 3.58 (d, *J* = 4.0 Hz, 1H), 3.22 (ddd, *J* = 10.6, 5.2, 3.1 Hz, 1H), 2.08 (s, 3H), 2.07 (s, 3H), 2.02 (s, 3H), 2.00 (s, 3H), 1.67 (s, 3H), 1.60 (s, 3H), 1.54 (s, 3H), 1.35 (s, 3H); ¹³C NMR (126 MHz, CDCl₃): δ 170.5, 169.7, 169.2, 169.1, 112.3, 105.3, 92.7, 86.0, 81.4, 74.5, 73.7, 72.0, 71.7, 61.0, 53.4, 50.6, 47.9, 44.7, 31.6, 30.7, 26.6, 26.4, 20.6, 20.6, 20.5, 20.4; ESI-HRMS [M+Na]⁺ calcd. for C₂₆H₃₈NaO₁₂S₃⁺ 661.1418, found 661.1405.

2,3,4,6-Tetra-*O*-acetyl-5-thio- β -D-glucopyranosyl-(1 \rightarrow 3)-1,2,4,6-tetra-*O*-acetyl-3-deoxy-3,5-dithio- α,β -D-glucofuranose (114):

Disaccharide **64** (305 mg, 0.493 mmol) was suspended in MeOH (5 mL) and NaOMe (2M solution in MeOH, 73 μ L, 0.147 mmol, 0.3 equiv) was added, and the reaction mixture then was stirred for 1h at 20 °C. After such time the reaction mixture was quenched with Amberlyst 15 (H⁺) ion-exchange resin until pH 4-5, filtered, and the filtrate was concentrated to dryness. The crude was dissolved in 50% aq TFA (12 mL) and the resulting solution was stirred for 12h at 20 °C. After such time the reaction mixture was concentrated

to dryness and co-evaporated with toluene (3×2 mL). The crude was taken into Py (1 mL) and Ac₂O (0.7 mL) and the resulting solution was stirred for 5h at 20 °C. After such time the reaction mixture quenched with MeOH (4 mL) and concentrated to dryness. The crude was purified by a flash column chromatography on silica gel eluting with hexanes : EtOAc (0 → 30% EtOAc (v/v)) to give mixture of anomeric acetates (α : β = 33 : 1) as a white solid (229 mg, 64% over 3 steps) with spectral data identical to that reported in the literature.⁸⁰ R_f 0.55 (hexanes:EtOAc 2:3, (H₂SO₄/EtOH)); ¹H NMR (500 MHz, CDCl₃): δ 6.02 (d, J = 3.1 Hz, 1H), 5.34 – 5.19 (m, 2H), 5.12 – 4.95 (m, 3H), 4.32 – 4.20 (m, 2H), 4.15 (dd, J = 12.0, 3.5 Hz, 1H), 4.09 – 3.97 (m, 2H), 3.58 – 3.43 (m, 1H), 3.35 – 3.17 (m, 2H), 2.20 (s, 3H), 2.15 (s, 3H), 2.11 (s, 3H), 2.07 (s, 3H), 2.04 (s, 3H), 2.00 (s, 3H), 1.97 (s, 3H), 1.97 (s, 3H); ¹³C NMR (126 MHz, CDCl₃): δ 170.5, 168.9, 75.8, 74.3, 73.2, 71.8, 70.5, 61.5, 61.1, 50.3, 49.9, 44.5, 40.6, 21.1, 20.8, 20.6, 20.5, 20.4, 20.3. The minor β -isomer was identified in the mixture by the characteristic signals: 5.84 (d, J = 8.4 Hz, 1H), 5.40 – 5.34 (m, 1H).

ESI-HRMS [M+Na]⁺ calcd. for C₂₈H₃₈NaO₁₆S₃⁺ 749.1214, found 749.1208.

2,3,4,6-Tetra-*O*-acetyl-5-thio- β -D-glucopyranosyl-(1→3)-1-*S*-acetyl-2,4,6-tri-*O*-acetyl-3-deoxy-1,3,5-trithio- β -D-glucofuranose (115):

Disaccharide **114** (150 mg, 0.206 mmol) was dissolved in anhydrous CH₂Cl₂ (2.5 mL) and BiBr₃ (5 mg, 0.0103 mmol, 0.05 equiv) was added, followed by TMSBr (100 μ L, 0.825 mmol, 4 equiv) and the reaction mixture was stirred for 1.5h at 20 °C. After such time the reaction mixture was quenched with aq sat NaHCO₃ (10 mL) and diluted with CH₂Cl₂ (20 mL). The organic layer was separated, washed with ice-cold H₂O (20 mL) and brine (20 mL), dried over Na₂SO₄, and concentrated to dryness. The crude was taken into anhydrous DMF (0.2 mL) and cooled down to 0 °C before KSAc (33 mg, 0.29 mmol, 1.5 equiv) was added. The reaction mixture was stirred for 12h with gradual warming to 20 °C. After such time the reaction mixture was diluted with EtOAc (30 mL), washed with H₂O (20 mL), brine (20 mL), dried over Na₂SO₄, and concentrated to dryness. The crude product was purified by a flash column chromatography on silica gel eluting with hexanes : EtOAc (0 → 60% EtOAc (v/v)) to give product as a white solid (104 mg, 68% over 2 steps) with spectral data identical to that reported in the literature.⁸⁰ R_f 0.46 (hexanes:EtOAc 2:3,

(H₂SO₄/EtOH)); ¹H NMR (500 MHz, CDCl₃): δ 5.32 – 5.17 (m, 2H), 5.14 – 5.03 (m, 1H), 5.01 – 4.89 (m, 2H), 4.59 (d, *J* = 10.7 Hz, 1H), 4.25 (dd, *J* = 12.0, 5.2 Hz, 1H), 4.22 – 4.08 (m, 3H), 4.01 (d, *J* = 11.0 Hz, 1H), 3.36 (ddd, *J* = 9.4, 5.6, 3.3 Hz, 1H), 3.18 (ddd, *J* = 10.9, 5.2, 3.3 Hz, 1H), 3.03 (t, *J* = 10.8 Hz, 1H), 2.37 (s, 3H), 2.14 (s, 3H), 2.12 (s, 3H), 2.08 (s, 3H), 2.04 (s, 3H), 2.01 (s, 3H), 2.00 (s, 3H), 1.97 (s, 3H); ¹³C NMR (126 MHz, CDCl₃): δ 192.0 (SCoCH₃), 170.5, 170.2, 169.5, 169.3, 169.2, 169.1, 168.9, 75.0, 74.2, 72.5, 71.3, 70.5, 61.4, 61.2, 54.6, 50.2, 46.8, 45.4, 44.6, 30.2, 20.8, 20.8, 20.6, 20.6, 20.4, 20.4, 20.2; ESI-HRMS [M+Na]⁺ calcd. for C₂₈H₃₈NaO₁₅S₄⁺ 765.0986, found 765.0980.

2,3,4,6-Tetra-*O*-acetyl-5-thio-β-D-glucopyranosyl-(1→3)-2,4,6-tri-*O*-acetyl-3-deoxy-3,5-dithio-β-D-glucopyranosyl-(1→3)-1,2-*O*;5-*S*,6-*O*-di-isopropylidene-3-deoxy-3,5-dithio-α-D-glucofuranose (116):

Thioacetate **115** (100 mg, 0.134 mmol) and triflate **63** (82 mg, 0.201 mmol, 1.5 equiv) were dissolved in anhydrous DMF (0.14 mL), and the reaction mixture was cooled down to 0 °C before Et₂NH (35 μL, 0.335 mmol, 2.5 equiv) was added. After that the reaction mixture was stirred for 2h with gradual warming to 20 °C. After such time the reaction mixture was diluted with EtOAc (30 mL), washed with H₂O (20 mL), brine (20 mL), dried over Na₂SO₄, and concentrated to dryness. The crude product was purified by a flash column chromatography on silica gel eluting with hexanes : EtOAc (10 → 60% EtOAc (v/v)) to give product as a yellow foam (95 mg, 74%) with spectral data identical to that reported in the literature.⁸⁰ *R*_f 0.48 (hexanes:EtOAc 2:3, (H₂SO₄/EtOH)); ¹H NMR (500 MHz, CDCl₃) δ 5.85 (d, *J* = 3.6 Hz, 1H), 5.24 (dd, *J* = 10.7, 9.6 Hz, 1H), 5.13 (t, *J* = 10.6 Hz, 1H), 5.08 (dd, *J* = 11.0, 9.5 Hz, 1H), 5.02–4.94 (m, 2H), 4.70 (d, *J* = 3.6 Hz, 1H), 4.35 (dd, *J* = 10.5, 4.0 Hz, 1H), 4.31 (dd, *J* = 10.0, 2.5 Hz, 1H), 4.22 (dd, *J* = 12.0, 5.1 Hz, 1H), 4.22 (dd, *J* = 12.0, 5.4 Hz, 1H), 4.15–4.11 (m, 2H), 4.07 (dd, *J* = 12.0, 3.3 Hz, 1H), 4.00 (d, *J* = 11.0 Hz, 1H), 3.83 (d, *J* = 10.6 Hz, 1H), 3.64 (m, 1H), 3.52 (d, *J* = 4.0 Hz, 1H), 3.25–3.14 (m, 2H), 2.91 (t, *J* = 10.8 Hz, 1H), 2.26 (s, 3H), 2.12 (s, 3H), 2.10 (s, 3H), 2.07 (s, 3H), 2.04 (s, 3H), 2.00 (s, 3H), 1.95 (s, 3H), 1.66 (s, 3H), 1.60 (s, 3H), 1.53 (s, 3H), 1.35 (s, 3H); ¹³C NMR (126 MHz, CDCl₃): δ 170.5, 170.5, 169.5, 169.5, 169.2, 169.2, 168.8, 112.1, 105.1, 92.1, 86.4, 81.2, 76.0, 74.3, 72.4, 72.0, 71.7, 70.2, 61.7, 61.2, 55.3,

53.6, 50.9, 50.6, 50.1, 47.0, 44.2, 31.3, 30.5, 26.7, 26.2, 21.0, 20.7, 20.5, 20.5, 20.4, 20.2; ESI-HRMS $[M+Na]^+$ calcd. for $C_{38}H_{54}NaO_{16}S_5^+$ 981.1806, found 981.1797.

2,3,4,6-Tetra-*O*-acetyl-5-thio- β -D-glucopyranosyl-(1 \rightarrow 3)-2,4,6-tri-*O*-acetyl-3-deoxy-3,5-dithio- β -D-glucopyranosyl-(1 \rightarrow 3)-1,2,4,6-tetra-*O*-acetyl-3-deoxy-3,5-dithio- α,β -D-glucofuranose (117):

Disaccharide **116** (95 mg, 0.099 mmol) was suspended in MeOH (5 mL) and NaOMe (2M solution in MeOH, 15 μ L, 0.0297 mmol, 0.3 equiv) was added, and the reaction mixture then was stirred for 2.5h at 20 °C. After such time the reaction mixture was quenched with Amberlyst 15 (H^+) ion-exchange resin until pH 4-5, filtered, and the filtrate was concentrated to dryness. The crude was dissolved in 50% aq TFA (8 mL) and the resulting solution was stirred for 12h at 20 °C. After such time the reaction mixture was concentrated to dryness and co-evaporated with toluene (3 \times 2 mL). The crude was taken into Py (0.95 mL) and Ac_2O (0.1 mL) and the resulting solution was stirred for 4h at 20 °C. After such time the reaction mixture quenched with MeOH (4 mL) and concentrated to dryness. The crude was purified by a flash column chromatography on silica gel eluting with hexanes : EtOAc (10 \rightarrow 80% EtOAc (v/v)) to give mixture of anomeric acetates (α : β = 11 : 1) as a white solid (63 mg, 63% over 3 steps) with spectral data identical to that reported in the literature.⁸⁰ R_f 0.54 and 0.59 (hexanes:EtOAc 1:4, (H_2SO_4 /EtOH)); 1H NMR (500 MHz, $CDCl_3$): δ 6.04 (d, J = 3.1 Hz, 1H), 5.34 – 5.20 (m, 2H), 5.19 – 5.01 (m, 4H), 5.01 – 4.88 (m, 2H), 4.31 – 3.88 (m, 10H), 3.58 – 3.44 (m, 1H), 3.34 – 3.21 (m, 2H), 3.13 – 3.04 (m, 1H), 2.98 – 2.83 (m, 1H), 2.19 (s, 3H), 2.15 (s, 3H), 2.14 (s, 3H), 2.12 (s, 6H), 2.06 (s, 3H), 2.06 (s, 3H), 2.04 (s, 3H), 2.00 (s, 3H), 1.99 (s, 3H), 1.97 (s, 3H); ^{13}C NMR (126 MHz, $CDCl_3$) δ 170.6, 170.5, 170.4, 169.7, 169.2, 169.2, 169.1, 169.1, 169.1, 168.9, 168.7, 76.2, 75.6, 74.4, 72.7, 72.0, 70.8, 70.6, 61.9, 61.7, 61.2, 51.7, 50.9, 50.0, 46.8, 44.6, 40.8, 21.2, 21.0, 20.9, 20.8, 20.7, 20.7, 20.6, 20.6, 20.5, 20.4, 20.3. The minor β -isomer was identified in the mixture by the characteristic signals: 5.87 (d, J = 7.1 Hz, 1H), 5.40 – 5.34 (m, 1H).

HRMS $[M+Na]^+$ calcd. for $C_{40}H_{54}NaO_{22}S_5^+$ 1069.1603, found 1069.1584.

Synthesis of the alkyne linker (Scheme 21):

2-(Prop-2-ynyloxy)ethanol (118):

Ethylene glycol (14 mL, 250 mmol, 5 equiv) was dissolved in H₂O (8.8 mL) and the reaction mixture was cooled down to 0 °C and KOH (5.61 g, 100 mmol, 2 equiv) was added, followed by dropwise addition of propargyl bromide (80% wt solution in toluene, 5.57 mL, 50 mmol). The reaction mixture then was stirred for 15h with gradual warming to 20 °C. After such time the reaction mixture was diluted with H₂O (5 mL), the organic layer was separated, and the aqueous layer was extracted with CH₂Cl₂ (3×20 mL). The combined organic layers were dried over MgSO₄ and concentrated to dryness. The crude product was purified by a flash column chromatography on silica gel eluting with hexanes : EtOAc (0 → 50% EtOAc (v/v)) to give the product as a colorless liquid (3.7 g, 74%) with spectral data identical to that reported in the literature.²⁴⁹ *R*_f 0.21 (hexanes:EtOAc 2:1, (KMnO₄)); ¹H NMR (500 MHz, CDCl₃): δ 4.15 (d, *J* = 2.6 Hz, 2H), 3.70 (dd, *J* = 5.4, 3.9 Hz, 2H), 3.59 (dd, *J* = 5.4, 3.9 Hz, 2H), 2.83 (br, 1H), 2.44 (t, *J* = 2.4 Hz, 1H); ¹³C NMR (126 MHz, CDCl₃): δ 79.3, 74.6, 71.1, 61.3, 58.2; HRMS [M+Na]⁺ calcd. for C₅H₈NaO₂⁺ 123.0417, found 123.0414.

3-(2-(Acetylthio)ethoxy)prop-1-yne (119):

DIAD (4.12 mL, 20.98 mmol, 1.4 equiv) was added dropwise to a well stirred solution of Ph₃P (5.11 g, 19.48 mmol, 1.3 equiv) in anhydrous THF (40 mL) at 0 °C. The reaction mixture was stirred for 30 minutes at 0 °C, and a solution of AcSH (1.4 mL, 19.48 mmol, 1.3 equiv) and alcohol **118** (1.5 g, 14.98 mmol) in anhydrous THF (7 mL) was added. The reaction mixture then was stirred for 3h with gradual warming to 20 °C. After such time the reaction mixture was concentrated to dryness, and the crude was suspended in hexanes (30 mL). The resulting suspension was filtered, and the filtrate was concentrated to dryness. The crude product was purified by a flash column chromatography on silica gel eluting with hexanes : EtOAc (0 → 4% EtOAc (v/v)) to give the product as a yellow liquid (1.707 g, 72%). *R*_f 0.34 (hexanes:EtOAc 95:5, (KMnO₄)); FTIR (CHCl₃) cm⁻¹: 3304.4, 1687.9, 1098.3, 752.6; ¹H NMR (500 MHz, CDCl₃): δ 4.09 (d, *J* = 2.5 Hz, 2H, OCH₂CH₂S), 3.57 (t, *J* = 6.4 Hz, 2H, OCH₂CH₂S), 3.03 (t, *J* = 6.4 Hz, 2H, OCH₂CH₂S), 2.40 (t, *J* = 2.4 Hz, 1H, OCH₂CCH), 2.26 (s, 3H, CH₃COS); ¹³C NMR (126 MHz, CDCl₃): δ 195.1 (CO), 79.2

(OCH₂CCH), 74.6 (OCH₂CCH), 68.2 (OCH₂CH₂S), 57.9 (OCH₂CCH), 30.3 (CH₃COS), 28.5 (OCH₂CH₂S); HRMS [M+Na]⁺ calcd. for C₇H₁₀NaO₂S⁺ 181.0294, found 181.0290.

Attempted synthesis of 3-(2-(mercapto)ethoxy)prop-1-yne (120):

Thioacetate **119** (117 mg, 1.12 mmol) was dissolved in anhydrous MeOH (5 mL), and the solution was degassed for 30 minutes under the atmosphere of Ar. After such time NaOMe (2M solution in MeOH, 0.56 mL, 1.12 mmol) was added dropwise, and the reaction mixture was stirred for 1h at 20 °C. Only trace amounts of product were observed by LCMS and TLC analysis, and the major byproduct was identified by LCMS as a disulfide. HRMS [M+Na]⁺ calcd. for C₁₀H₁₄NaO₂S₂⁺ 253.0327, found 253.0327.

3-(2-Iodoethoxy)prop-1-yne (121):

Iodine (6.59 g, 25.97 mmol, 1.3 equiv) was added to a well stirred solution of Ph₃P (6.81 g, 25.97 mmol, 1.3 equiv) and imidazole (1.77 g, 25.97 mmol) in anhydrous CH₂Cl₂ (60 mL) at 0 °C. The reaction mixture was stirred for 5 minutes 0 °C, and alcohol **118** (2 g, 19.98 mmol) solution in anhydrous CH₂Cl₂ (7 mL) was added. The reaction mixture then was stirred for 2h with gradual warming to 20 °C. After such time the reaction mixture was filtered through Celite ® pad, and the filter cake was additionally washed with CH₂Cl₂ (3×30 mL). The filtrate was collected and concentrated to dryness, and the crude product was purified by a flash column chromatography on silica gel eluting with hexanes : Et₂O (0 → 1% Et₂O (v/v)) to give the product as a colorless liquid (2.77 g, 66%) with spectral data identical to that reported in the literature.²⁵⁰ *R*_f 0.65 (hexanes:Et₂O 9:1, (KMnO₄)); ¹H NMR (500 MHz, CDCl₃): δ 4.18 (t, *J* = 2.4 Hz, 2H), 3.77 (td, *J* = 6.8, 2.1 Hz, 2H), 3.25 (td, *J* = 6.8, 2.1 Hz, 2H), 2.46 – 2.41 (m, 1H); ¹³C NMR (126 MHz, CDCl₃): δ 79.1, 74.9, 70.3, 57.9, 2.1; HRMS [M+Na]⁺ calcd. for C₅H₇NaOI⁺ 232.9434, found 232.9427.

Synthesis of the alkyne partners (Scheme 22):

((2-(Prop-2-ynyloxy)ethyl) 2,3,4,6-tetra-*O*-acetyl-β-D-glucopyranoside (123):

Thioacetate **124** (200 mg, 0.49 mmol) and alkyl iodide **121** (514 mg, 2.45 mmol, 5 equiv) were dissolved in anhydrous DMF (10 mL) and 4Å AWMS (500 mg) were added, followed by NEt₃H (0.177 mL, 1.75 mmol, 3.5 equiv), and the reaction mixture then was stirred for 2.5h at 20 °C. After such time the reaction

mixture was diluted with EtOAc (30 mL), washed with H₂O (50 mL), brine (50 mL), dried over Na₂SO₄, and concentrated to dryness. The crude was purified by a flash column chromatography on silica gel eluting with hexanes : EtOAc (0 → 40% EtOAc (v/v)) to give the product as a colorless syrup (179 mg, 82%). *R_f* 0.47 (hexanes:EtOAc 3:2, (KMnO₄)); ¹H NMR (500 MHz, CDCl₃): δ 5.22 (t, *J* = 9.4 Hz, 1H, H-3), 5.08 (t, *J* = 9.8 Hz, 1H, H-4), 5.02 (t, *J* = 9.8 Hz, 1H, H-2), 4.60 (d, *J* = 10.1 Hz, 1H, H-1), 4.24 (dd, *J* = 12.4, 4.9 Hz, 1H, H-6a), 4.18 (d, *J* = 2.4 Hz, 2H, OCH₂CCH), 4.15 (dd, *J* = 12.4, 2.4 Hz, 1H, H-6b), 3.81 – 3.66 (m, 3H, H-5, SCH₂CH₂O), 2.97 (dt, *J* = 13.6, 6.8 Hz, 1H, SCH₂CH₂O), 2.80 (dt, *J* = 13.5, 6.4 Hz, 1H, SCH₂CH₂O), 2.46 (t, *J* = 2.3 Hz, 1H, OCH₂CCH), 2.09 (s, 3H), 2.06 (s, 3H), 2.02 (s, 3H), 2.01 (s, 3H, 4×CH₃CO); ¹³C NMR (126 MHz, CDCl₃): δ 170.7, 170.2, 169.5, 169.5 (4×CO), 83.7 (C-1), 79.5 (OCH₂CCH), 76.0 (C-5), 74.9 (OCH₂CCH), 73.9 (C-3), 70.0 (C-2), 69.7 (OCH₂CCH), 68.4 (C-4), 62.2 (C-6), 58.2 (OCH₂CCH), 29.4 (SCH₂CH₂O), 20.8, 20.8, 20.7, 20.6 (4×CH₃CO); HRMS [M+Na]⁺ calcd. for C₁₉H₂₆NaO₁₀S⁺ 469.1139, found 469.1129.

((2-(Prop-2-ynyloxy)ethyl) 2,3,4,6-tetra-*O*-acetyl-5-thio-β-D-glucopyranoside (125):

Thioacetate **124** (91 mg, 0.215 mmol) and alkyl iodide **121** (226 mg, 1.07 mmol, 5 equiv) were dissolved in anhydrous DMF (1.5 mL) and 4Å AWMS (600 mg) were added, followed by NEt₃H (78 μL, 0.754 mmol, 3.5 equiv), and the reaction mixture then was stirred for 2.5h at 20 °C. After such time the reaction mixture was diluted with EtOAc (20 mL), washed with H₂O (20 mL), brine (20 mL), dried over Na₂SO₄, and concentrated to dryness. The crude was purified by a flash column chromatography on silica gel eluting with hexanes : EtOAc (0 → 40% EtOAc (v/v)) to give the product as a colorless syrup (92 mg, 93%). *R_f* 0.32 (hexanes:EtOAc 3:2, (KMnO₄)); ¹H NMR (500 MHz, CDCl₃): δ 5.23 (dd, *J* = 10.7, 9.6 Hz, 1H, H-4), 5.12 (dd, *J* = 10.7, 9.5 Hz, 1H, H-2), 5.02 (t, *J* = 9.5 Hz, 1H, H-3), 4.22 (dd, *J* = 12.0, 5.6 Hz, 1H, H-6a), 4.15 (d, *J* = 2.3 Hz, 2H, OCH₂CCH), 4.10 (dd, *J* = 11.9, 3.3 Hz, 1H, H-6b), 3.93 (d, *J* = 10.7 Hz, 1H, H-1), 3.76 – 3.64 (m, 2H, SCH₂CH₂O), 3.25 (ddd, *J* = 10.7, 5.5, 3.3 Hz, 1H, SCH₂CH₂O), 2.94 (dt, *J* = 13.1, 6.4 Hz, 1H, SCH₂CH₂O), 2.82 (dt, *J* = 13.2, 6.3 Hz, 1H, H-5), 2.44 (t, *J* = 2.4 Hz, 1H, OCH₂CCH), 2.05 (s, 3H), 2.04 (s, 3H), 2.00 (s, 3H), 1.97 (s, 3H, 4×CH₃CO); ¹³C NMR (126 MHz, CDCl₃): δ 170.6, 169.8,

169.5, 169.4 (4×CO), 79.4 (OCH₂CCH), 74.9 (OCH₂CCH), 74.6 (C-3), 73.3 (C-2), 71.9 (C-4), 69.5 (SCH₂CH₂O), 61.3 (C-6), 58.3 (OCH₂CCH), 48.2 (C-1), 44.5 (C-5), 30.4 (SCH₂CH₂O), 20.7, 20.6, 20.6, 20.5 (4×CH₃CO); HRMS [M+Na]⁺ calcd. for C₁₉H₂₆NaO₉S₂⁺ 485.0916, found 485.0900.

2,3,4,6-Tetra-*O*-acetyl-5-thio-β-D-glucopyranosyl-(1→3)-2,4,6-tri-*O*-acetyl-3-deoxy-3,5-trithio-β-D-glucopyranosyl-(1→3)-1-*S*-acetyl-2,4,6-tetra-*O*-acetyl-3-deoxy-1,3,5-trithio-β-D-glucofuranose (126):

Disaccharide **114** (24 mg, 0.0229 mmol) was dissolved in anhydrous CH₂Cl₂ (0.5 mL) and BiBr₃ (1 mg, 0.0022 mmol, 0.096 equiv) was added, followed by TMSBr (12 μL, 0.0916 mmol, 4 equiv) and the reaction mixture was stirred for 5.5h at 20 °C. After such time the reaction mixture was quenched with aq sat NaHCO₃ (2 mL) and diluted with CH₂Cl₂ (10 mL). The organic layer was separated, washed with ice-cold H₂O (10 mL) and brine (10 mL), dried over Na₂SO₄, and concentrated to dryness. The crude was taken into anhydrous DMF (30 μL) and cooled down to 0 °C before KSAc (4 mg, 0.0337 mmol, 1.5 equiv) was added. The reaction mixture was stirred for 2.5h with gradual warming to 20 °C. After such time the reaction mixture was diluted with EtOAc (20 mL), washed with H₂O (10 mL), brine (10 mL), dried over Na₂SO₄, and concentrated to dryness. The crude product was purified by a flash column chromatography on silica gel eluting with CH₂Cl₂: Et₂O (0 → 30% Et₂O (v/v)) to give product as a colorless syrup (13 mg, 56% over 2 steps) with spectral data identical to that reported in the literature.⁸⁰ *R*_f 0.55 (CH₂Cl₂:Et₂O 3:7, (H₂SO₄/EtOH)); ¹H NMR (500 MHz, CDCl₃): δ 5.33 – 5.19 (m, 2H), 5.17 – 4.92 (m, 5H), 4.60 (d, *J* = 10.6 Hz, 1H), 4.31 – 4.07 (m, 6H), 3.99 – 3.87 (m, 2H), 3.37 (ddd, *J* = 9.6, 5.6, 3.4 Hz, 1H), 3.15 (dt, *J* = 9.3, 4.3 Hz, 1H), 3.10 (dt, *J* = 10.6, 4.2 Hz, 1H), 3.04 (t, *J* = 10.7 Hz, 1H), 2.85 (t, *J* = 10.8 Hz, 1H, OCH), 2.38 (s, 3H), 2.14 (s, 3H), 2.13 (s, 3H), 2.13 (s, 6H), 2.07 (s, 3H), 2.07 (s, 3H), 2.04 (s, 3H), 2.00 (s, 3H), 1.99 (s, 3H), 1.97 (s, 3H); ¹³C NMR (126 MHz, CDCl₃): 192.0, 170.5, 170.4, 169.7, 169.6, 169.5, 169.3, 169.1, 168.5, 168.5, 166.4, 76.3, 75.1, 74.0, 72.2, 71.5, 70.2, 70.3, 61.6, 61.3, 60.7, 55.1, 54.7, 52.1, 50.6, 47.1, 46.6, 45.5, 44.1, 30.3, 20.8, 20.7, 20.6, 20.6, 20.5, 20.5, 20.4, 20.4, 20.2, 20.1; HRMS [M+Na]⁺ calcd. for C₄₀H₅₄NaO₂₁S₆⁺ 1085.1374, found 1085.1355.

((2-(Prop-2-ynyloxy)ethyl) 2,3,4,6-tetra-*O*-acetyl-5-thio- β -D-glucopyranosyl-(1 \rightarrow 3)-2,4,6-tri-*O*-acetyl-3-deoxy-3,5-dithio- β -D-glucopyranosyl-(1 \rightarrow 3)-1-*S*-acetyl-2,4,6-tetra-*O*-acetyl-1,3-dideoxy-1,3,5-trithio- β -D-glucofuranoside (127):

To a solution of thioacetate **126** (15 mg, 0.0141 mmol), alkyl iodide **121** (15 mg, 0.070 mmol, 5 equiv) and 4Å AWMS (100 mg) in anhydrous DMF (0.1 mL) was added NEt₃H (5 μ L, 0.049 mmol, 3.5 equiv) at 0 °C, and the reaction mixture then was stirred for 6h with gradual warming to 20 °C. After such time the reaction mixture was concentrated to dryness and the crude product was purified by a flash column chromatography on silica gel eluting with CH₂Cl₂: Et₂O (0 \rightarrow 30% Et₂O (v/v)) to give product as a colorless syrup (11 mg, 71%). *R_f* 0.61 (CH₂Cl₂:Et₂O 3:7, (H₂SO₄/EtOH)); ¹H NMR (900 MHz, CD₃CN): δ 5.24 – 5.19 (m, 2H, H-3a, H-4a), 5.10 – 5.06 (m, 1H, H-2c), 4.99 – 4.92 (m, 4H, H-2a, H-4b, H-2b, H-4c), 4.25 – 4.09 (m, 10H, H-1a, H-1b, 2 \times H-6a, 2 \times H-6b, 2 \times H-6c, OCH₂CCH), 4.05 (d, *J* = 10.5 Hz, 1H, H-1c), 3.74 – 3.67 (m, 2H, SCH₂CH₂O), 3.46 (dt, *J* = 9.2, 4.4 Hz, 1H, H-5b), 3.44 – 3.39 (m, 2H, H-5a, H-5c), 3.12 (t, *J* = 10.7 Hz, 1H, H-3b), 3.07 (t, *J* = 10.8 Hz, 1H, H-3c), 2.94 (dt, *J* = 13.7, 6.9 Hz, 1H, SCH₂CH₂O), 2.85 (dt, *J* = 13.1, 6.3 Hz, 1H, SCH₂CH₂O), 2.77 (t, *J* = 2.4 Hz, 1H, OCH₂CCH), 2.29 (s, 3H), 2.19 (s, 3H), 2.15 (s, 3H), 2.13 (s, 3H), 2.11 (s, 3H), 2.03 (s, 3H), 2.02 (s, 3H), 2.01 (s, 6H), 1.99 (s, 3H, 11 \times CH₃CO); ¹³C NMR (226 MHz, CD₃CN): δ 170.3, 170.2, 169.8, 169.7, 169.7, 169.6, 169.6 (7 \times CO), 79.7 (OCH₂CCH), 76.0 (C-2a), 75.6 (C-2c), 75.0 (OCH₂CCH), 73.5 (C-2b), 73.0 (C-3a), 71.9 (C-4a), 70.9 (C-4b), 70.8 (C-4c), 69.0 (SCH₂CH₂O), 61.9 (C-6c), 61.6 (C-6b), 61.0 (C-6a), 57.6 (OCH₂CCH), 54.7 (C-3c), 54.6 (C-3b), 51.2 (C-1a), 49.7 (C-1b), 49.1 (C-1c), 46.0 (C-5b), 45.7 (C-5a), 43.8 (C-5c), 30.4 (SCH₂CH₂O), 20.6, 20.6, 20.4, 20.4, 20.2, 20.2, 19.9, 19.8, 19.7, 19.7 (10 \times CH₃CO); HRMS [M+Na]⁺ calcd. for C₄₃H₅₈NaO₂₁S₆⁺ 1125.1687, found 1125.1707.

Synthesis of the tetravalent triazole clusters (Scheme 23):

Triazole cluster 128:

Tetraazide core **102** (2 mg, 2.8 μ mol) and alkyne **123** (6.25 mg, 14 μ mol, 5.5 equiv) were dissolved in THF (1 mL) and a solution of CuSO₄•5H₂O (1.7 mg, 7 μ mol, 2.5 equiv) and Na-ascorbate (1.7 mg, 8.4 μ mol, 3

equiv) in H₂O (1 mL) was added. The reaction mixture then was transferred into a 5 mL microwave vial and irradiated for 1h at 60 °C. After such time the reaction mixture was diluted with EtOAc (20 mL), washed with 0.1M EDTA disodium salt (3×20 mL), brine (3×20 mL), dried over Na₂SO₄, and concentrated to dryness. The crude was purified by a flash column chromatography eluting with hexanes : EtOAc (0 → 100% EtOAc (v/v)) and EtOAc : MeOH (0 → 50% MeOH (v/v)) to give product as a yellowish syrup (5 mg, 72%). *R_f* 0.32 (EtOAc, (H₂SO₄/EtOH)); ¹H NMR (500 MHz, CDCl₃): δ 7.67 (s, 4H, Ar), 5.20 (t, *J* = 9.4 Hz, 4H, H-3), 5.06 (t, *J* = 9.7 Hz, 4H, H-4), 5.00 (t, *J* = 9.7 Hz, 4H, H-2), 4.64 (s, 8H, OCH₂Aryl), 4.58 (d, *J* = 10.0 Hz, 4H, H-1), 4.58 – 4.49 (m, 8H, SCH₂CH₂Aryl), 4.22 (dd, *J* = 12.4, 4.8 Hz, 4H, H-6a), 4.15 – 4.08 (m, 4H, H-6b), 3.79 – 3.66 (m, 12H, H-5, GlcpSCH₂CH₂O), 3.42 (t, *J* = 6.0 Hz, 8H, OCH₂CH₂CH₂S), 3.31 (s, 8H, C(CH₂O)₄), 2.99 (t, *J* = 7.1 Hz, 8H, SCH₂CH₂OAr), 2.94 (dt, *J* = 13.5, 6.7 Hz, 4H, GlcpSCH₂CH₂O), 2.79 (dt, *J* = 13.4, 6.5 Hz, 4H, GlcpSCH₂CH₂O), 2.56 (t, *J* = 7.1 Hz, 8H, OCH₂CH₂CH₂S), 2.06 (s, 12H), 2.04 (s, 12H), 2.01 (s, 12H), 1.99 (s, 12H, 4×CH₃CO), 1.79 (p, *J* = 6.8 Hz, 8H, OCH₂CH₂CH₂S); ¹³C NMR (126 MHz, CDCl₃): δ 170.7, 170.3, 169.5, 169.5 (4×CO), 144.9 (Aryl), 123.2 (Aryl), 83.7 (C-1), 76.0 (C-5), 73.9 (C-3), 70.3 (GlcpSCH₂CH₂O), 70.1 (C-2), 69.5 (OCH₂CH₂CH₂S), 68.4 (C-4), 64.4 (OCH₂Aryl), 62.2 (C-6), 60.5 (C(CH₂O)₄), 50.2 (SCH₂CH₂Aryl), 46.2 (C(CH₂O)₄), 32.1 (SCH₂CH₂Aryl), 30.7 (OCH₂CH₂CH₂S), 29.6 (GlcpSCH₂CH₂O), 29.1 (OCH₂CH₂CH₂S), 20.9, 20.8, 20.7, 20.7 (4×CH₃CO). The minor isomer was identified in mixture by the following diagnostic signals: 1.26 (s). HRMS [M+3Na]³⁺/3 calcd. for C₁₀₁H₁₅₂Na₃N₁₂O₄₄S₈⁺ 853.9156, found 853.9175.

Triazole cluster 129:

Tetraazide core **102** (3 mg, 4.2 μmol) and alkyne **125** (8.8 mg, 19 μmol, 4.5 equiv) were dissolved in THF (1 mL) and a solution of CuSO₄•5H₂O (4.37 mg, 17.5 μmol, 4 equiv) and Na-ascorbate (4.16 mg, 21.0 μmol, 5 equiv) in H₂O (1 mL) was added. The reaction mixture then was transferred into a 5 mL microwave vial and irradiated for 1h at 60 °C. After such time the reaction mixture was diluted with EtOAc (40 mL), washed with 0.1M EDTA disodium salt (3×40 mL), brine (3×40 mL), dried over Na₂SO₄, and concentrated to dryness. The crude was purified by a flash column chromatography eluting with hexanes : Acetone (0 →

100% EtOAc (v/v)) to give product as a yellowish syrup (8 mg, 75%). R_f 0.24 (Acetone, (H₂SO₄/EtOH)); ¹H NMR (500 MHz, CDCl₃): δ 7.68 (s, 4H, Aryl), 5.23 (dd, J = 10.8, 9.6 Hz, 4H, H-4), 5.12 (dd, J = 10.8, 9.5 Hz, 4H, H-2), 5.01 (t, J = 9.5 Hz, 4H, H-3), 4.64 (d, J = 2.0 Hz, 8H, OCH₂Aryl), 4.53 (dd, J = 8.1, 6.1 Hz, 8H, SCH₂CH₂Aryl), 4.23 (dd, J = 12.0, 5.5 Hz, 4H, H-6a), 4.13 – 4.06 (m, 4H, H-6b), 3.95 (d, J = 10.6 Hz, 4H, H-1), 3.78 – 3.64 (m, 8H, GlcpSCH₂CH₂O), 3.45 – 3.39 (m, 8H, OCH₂CH₂CH₂S), 3.31 (s, 8H, C(CH₂O)₄), 3.25 (ddd, J = 10.7, 5.4, 3.3 Hz, 4H, H-5), 2.99 (t, J = 6.6 Hz, 2H, SCH₂CH₂OAryl), 2.97 – 2.90 (m, 4H, GlcpSCH₂CH₂O), 2.89 – 2.78 (m, 4H, GlcpSCH₂CH₂O), 2.55 (t, J = 7.2 Hz, 8H, OCH₂CH₂CH₂S), 2.06 (s, 12H), 2.04 (s, 12H), 2.00 (s, 12H), 1.98 (s, 12H, 4×CH₃CO), 1.78 (p, J = 6.7 Hz, 8H, OCH₂CH₂CH₂S); ¹³C NMR (126 MHz, CDCl₃): δ 170.6, 169.8, 169.5, 169.4 (4×CO), 144.9 (Aryl), 123.2 (Aryl), 74.6 (C-3), 73.4 (C-2), 71.9 (C-4), 70.2 (GlcpSCH₂CH₂O), 69.5 (OCH₂CH₂CH₂S, C(CH₂O)₄), 64.6 (OCH₂Aryl), 61.3 (C-6), 50.1 (SCH₂CH₂Aryl), 48.2 (C-1), 44.5 (C-5), 32.1 (SCH₂CH₂Aryl), 30.7 (OCH₂CH₂CH₂S), 29.7 (GlcpSCH₂CH₂O), 29.1 (OCH₂CH₂CH₂S), 20.7, 20.7, 20.6, 20.6 (4×CH₃CO). The minor isomer was identified in mixture by the following diagnostic signals: 1.27 – 1.19 (m, 1H).

HRMS [$M+3Na$]³⁺/3 calcd. for C₁₀₁H₁₅₂Na₃N₁₂O₄₀S₁₂⁺ 875.8904, found 875.8882.

Attempted synthesis of the triazole cluster **130**:

Stock solutions of alkyne **127** in THF (C = 10 mg/mL, 0.4 mL), azide **102** in THF (C = 1 mg/mL, 8 mL), CuSO₄•5H₂O in H₂O (C = 8 mg/mL, 0.5 mL), and Na-ascorbate in H₂O (C = 8 mg/mL, 0.5 mL) were prepared, and were used in the reaction. Accordingly, a microwave vial was charged with stock solutions of alkyne **127** (116 μ L, 1.05 μ mol, 5 equiv), azide **102** (150 μ L, 0.2 μ mol), CuSO₄•5H₂O (20 μ L, 0.64 μ mol, 3.2 equiv), and Na-ascorbate (20 μ L, 0.81 μ mol, 4.03 equiv). After that the microwave vial was capped under Ar, and the reaction mixture was irradiated for 1h at 60 °C. After such time the LCMS analysis showed formation of mixture consisting of monomer, dimer, trimer and trace amount of tetramer, therefore the reaction mixture was irradiated for an additional 1h at 60 °C. No progress was observed after additional irradiation of the reaction mixture, and mixture consisting of monomer, dimer, trimer, and tetramer was observed by LCMS analysis.

Synthesis of the tetracarboxylic acid (Scheme 25):

Tetraester Core (131):

Tetra-*O*-allyl-pentaerythritol **100b** (2.1 g, 7.08 mmol) was dissolved in anhydrous DMF (30 mL) and 2,2-dimethoxy-2-phenylacetophenone (DMPAP) (0.544 g, 2.13 mmol, 0.3 equiv) was added followed by methyl thioglycolate (6.3 mL, 70.8 mmol, 10 equiv). The reaction vessel then was flushed with Ar, sealed, and irradiated with UV light ($\lambda = 260$ nm) for 2.5 h. After such time the reaction mixture was allowed to cool down to the room temperature (20 °C), quenched with H₂O (40 mL), and extracted with Et₂O (3×50 mL). The combined organic layers were dried over Na₂SO₄, concentrated to dryness and co-evaporated with toluene (3×15 mL). The crude material was purified by flash column chromatography on a silica gel eluting with hexanes:EtOAc (0 → 30% EtOAc (v/v)) to give product **131** as a colorless viscous liquid (3.55 g, 69%) containing ~5% of anti-Markovnikoff regioisomers. *R*_f 0.2 (hexanes:EtOAc 7:3 (CAM)); ¹H NMR (500 MHz, CDCl₃): δ 3.72 (s, 12H, CO₂Me), 3.43 (t, *J* = 6.0 Hz, 8H, OCH₂CH₂CH₂S), 3.33 (s, 8H, CCH₂O), 3.21 (s, 8H, SCH₂CO₂Me), 2.68 (t, *J* = 7.3 Hz, 8H, OCH₂CH₂CH₂S), 1.88 – 1.74 (m, 8H, OCH₂CH₂CH₂S); ¹³C NMR (126 MHz, CDCl₃): δ 171.1 (CO), 69.6 (CCH₂O/OCH₂CH₂CH₂S), 52.4 (CO₂Me), 45.5 (C(CH₂O)₄), 33.5 (SCH₂CO₂Me), 29.6 (OCH₂CH₂CH₂S), 29.2 (OCH₂CH₂CH₂S). The minor isomer was identified in the mixture by the characteristic signal: 1.24 (t, *J* = 6.9 Hz).

ESI-HRMS [M+Na]⁺ calcd. for C₂₉H₅₂NaO₁₂S₄⁺ 743.2234, found 743.2209.

Tetracarboxylic acid core (134):

Tetraester **131** (3.5 g, 4.85 mmol) was dissolved in THF:H₂O (1:1) (140 mL) and KOH (1.36 g, 24.3 mmol, 5 equiv) was added, and the reaction mixture was stirred for 3 h. After such time the reaction mixture was acidified with 1M aq H₂SO₄ (30 mL), and extracted with EtOAc (3×40 mL). The combined organic layers were washed with brine (100 mL), dried over Na₂SO₄, and concentrated to dryness to give tetracarboxylic acid **17** as a syrup (3.2 g, quant.) containing ~4% of the anti-Markovnikoff regioisomers, which were retained throughout the synthesis of glucoclusters: ¹H NMR (500 MHz, DMSO-*d*₆): δ 3.38 (t, *J* = 6.0 Hz, 8H, OCH₂CH₂CH₂S), 3.26 (s, 8H, C(CH₂O)₄), 3.19 (s, 8H, SCH₂CO₂H), 2.60 (t, *J* = 7.3 Hz, 8H,

OCH₂CH₂CH₂S), 1.73 (p, J = 6.5 Hz, 8H, OCH₂CH₂CH₂S); ¹³C NMR (126 MHz, DMSO-d₆): δ 171.7 (C=O), 69.2 (CCH₂O), 69.0 (OCH₂CH₂CH₂S), 45.2 (C(CH₂O)₄), 33.4 (SCH₂CO₂H), 28.8 (OCH₂CH₂CH₂S), 28.7 (OCH₂CH₂CH₂S). The minor isomer was identified in the mixture by the characteristic signal: 1.18 (d, J = 6.9 Hz).

ESI-HRMS: [M-2H]²⁻/2 calcd. for C₂₅H₄₂O₁₂S₄²⁻ 331.0785, found 331.0792.

Synthesis of the carbamate linker (Scheme 26):

***tert*-Butyl 2-(2-Hydroxyethoxy)ethylcarbamate (**138**):**

2-(2-Aminoethoxy)ethanol **137** (6.7 mL, 66.58 mmol) was dissolved in anhydrous CH₂Cl₂ (24 mL) and Boc₂O (14.53 g, 66.58 mmol) was added. The reaction mixture then was stirred for 1h at 20 °C. After such time the reaction mixture was concentrated to dryness and the crude product was purified by flash column chromatography on silica gel eluting with hexanes:EtOAc (0 → 80% EtOAc (v/v)) to give product as a colorless syrup (12 g, 87%) with spectral data identical to that reported in the literature.²⁵¹ R_f 0.49 (hexanes:EtOAc 9:1 (CAM)); ¹H NMR (500 MHz, CDCl₃): δ 4.96 (br, 1H), 3.71 (dd, J =5.1, 4.1 Hz, 2H), 3.57 – 3.50 (m, 4H), 3.30 (t, J =5.1 Hz, 2H), 1.42 (s, 9H); ¹³C NMR (126 MHz, CDCl₃) δ 156.3, 79.6, 72.4, 70.2, 61.7, 40.8, 28.3; ESI-HRMS [M+Na]⁺ calcd. for C₉H₁₉NNaO₄⁺ 743.2234, found 743.2209.

***tert*-Butyl 2-(2-iodoethoxy)ethylcarbamate (**132**):**

Imidazole (3.48 g, 51.16 mmol, 1.5 equiv) and PPh₃ (13.42 g, 51.16 mmol, 1.5 equiv) were dissolved in anhydrous THF (54 mL) and the reaction mixture was cooled down to 0 °C and I₂ (12.98 g, 51.16 mmol, 1.5 equiv) was added. The reaction mixture was vigorously stirred for 15 min at 0 °C before a solution of carbamate **138** (7 g, 34.10 mmol) in anhydrous THF (10 mL) was added. The reaction mixture then was stirred for 12h at 20 °C. After such time the reaction mixture was concentrated to dryness, diluted with EtOAc (100 mL) and filtered. The filter cake was washed with EtOAc (100 mL), and the filtrate was collected and concentrated to dryness. The crude was purified by flash column chromatography on silica gel eluting with hexanes:EtOAc (0 → 30% EtOAc (v/v)) to give product as a colorless liquid (7.97 g, 74%)

with spectral data identical to that reported in the literature.²⁵¹ R_f 0.75 (hexanes:EtOAc 7:3 (CAM)); ^1H NMR (500 MHz, CDCl_3): δ 4.91 (br, 1H), 3.70 (t, J = 6.6 Hz, 2H), 3.53 (t, J = 5.2 Hz, 2H), 3.31 (q, J = 5.3 Hz, 2H), 3.24 (t, J = 6.6 Hz, 2H), 1.43 (s, 9H); ^{13}C NMR (126 MHz, CDCl_3): δ 155.4, 79.5, 71.5, 69.9, 40.4, 28.5, 3.0; ESI-HRMS $[\text{M}+\text{Na}]^+$ calcd. for $\text{C}_9\text{H}_{19}\text{NNaO}_4^+$ 743.2234, found 743.2209.

Synthesis of tetravalent constructs and monovalent comparator (Scheme 27, Scheme 28, Scheme 29, Scheme 30):

((2-(*tert*-Butylcarbamoyl)ethoxy)ethyl) 2,3,4,6-Tetra-*O*-acetyl-1-thio- β -D-glucopyranoside (139):

1-*S*-Acetyl-2,3,4,6-tetra-*O*-acetyl-1-thio- β -D-glucopyranose **124** (250 mg, 0.615 mmol) and *tert*-butyl (2-(2-iodoethoxy)ethyl)carbamate (932.5 mg, 2.96 mmol, 4.8 equiv) were dissolved in anhydrous DMF (12 mL), treated with HNEt_2 (153 μL , 1.48 mmol, 2.4 equiv) and stirred for 4h at 20 °C. After such time the reaction mixture was diluted with EtOAc (60 mL), washed with H_2O (50 mL), brine (50 mL), dried over Na_2SO_4 , concentrated to dryness and co-evaporated with toluene (3 \times 15 mL). The crude product was purified by flash column chromatography on silica gel eluting with hexanes:EtOAc (0 \rightarrow 50% EtOAc (v/v)) to give compound **139** as a colorless syrup (247 mg, 73%). R_f 0.14 (hexanes:EtOAc 1:1 ($\text{H}_2\text{SO}_4/\text{EtOH}$)); $[\alpha]_D^{20-22} + 14.7$ (c 0.01, CHCl_3); ^1H NMR (500 MHz, CDCl_3): δ 5.23 (t, J = 9.4 Hz, 1H, H-3), 5.08 (t, J = 9.7 Hz, 1H, H-4), 5.03 (t, J = 9.7 Hz, 1H, H-2), 4.93 (br, 1H, NH), 4.57 (d, J = 10.0 Hz, 1H, H-1), 4.25 (dd, J = 12.4, 4.9 Hz, 1H, H-6a), 4.20 – 4.07 (m, 1H, H-6b), 3.72 (ddd, J = 10.0, 5.0, 2.4 Hz, 1H, H-5), 3.65 (qt, J = 10.0, 6.5 Hz, 2H, $\text{SCH}_2\text{CH}_2\text{O}$), 3.51 (t, J = 5.2 Hz, 2H, $\text{OCH}_2\text{CH}_2\text{NHBoc}$), 3.31 (q, J = 5.5 Hz, 2H, $\text{OCH}_2\text{CH}_2\text{NHBoc}$), 2.93 (dt, J = 13.4, 6.7 Hz, 1H, $\text{SCH}_2\text{CH}_2\text{O}$), 2.78 (dt, J = 13.2, 6.4 Hz, 1H, $\text{SCH}_2\text{CH}_2\text{O}$), 2.09 (s, 3H, CH_3CO), 2.07 (s, 3H, CH_3CO), 2.03 (s, 3H, CH_3CO), 2.01 (s, 3H, CH_3CO), 1.61 (s, 2H, $\text{C}(\text{CH}_3)_3^1$), 1.45 (s, 9H, $\text{C}(\text{CH}_3)_3$); ^{13}C NMR (126 MHz, CDCl_3): δ 170.6, 170.2, 169.4, 169.4 (4 \times CO), 83.5 (C-1), 76.0 (C-5), 73.8 (C-3), 70.6 ($\text{SCH}_2\text{CH}_2\text{O}$), 70.0 ($\text{OCH}_2\text{CH}_2\text{NHBoc}$), 70.0 (C-2), 68.3 (C-4), 62.1 (C-

¹ Peak corresponding to the rotamer signal of methyl group of the *tert*-butyl carbamate

6), 60.4 ($\underline{\text{C}}(\text{CH}_3)_3$), 40.4 ($\text{OCH}_2\underline{\text{C}}\text{H}_2\text{NHBoc}$), 29.4 ($\text{SCH}_2\underline{\text{C}}\text{H}_2\text{O}$), 28.4 ($\text{C}(\underline{\text{C}}\text{H}_3)_3$), 20.8, 20.7, 20.6, 20.6 ($4\times\underline{\text{C}}\text{H}_3\text{CO}$); ESI-HRMS $[\text{M}+\text{Na}]^+$ calcd. for $\text{C}_{23}\text{H}_{37}\text{NNaO}_{12}\text{S}^+$ 574.1929, found 574.1919.

(2-(2-Aminoethoxy)ethyl) 2,3,4,6-Tetra-*O*-acetyl-1-thio- β -D-glucopyranoside trifluoroacetate salt (140**):**

Carbamate **139** (219 mg, 0.40 mmol) was dissolved in CH_2Cl_2 (20 mL), and 90% aq TFA (4 mL) was added, and the reaction mixture was stirred for 40 minutes at 20 °C. After such time the reaction mixture was concentrated to dryness, co-evaporated with toluene (3×10 mL) and dried under high vacuum for 12h to give compound **140** as a colorless syrup (223 mg, quant). $[\alpha]_{\text{D}}^{20-22} + 5.2$ (c 0.021, CHCl_3); ^1H NMR (500 MHz, CDCl_3): δ 7.77 (br, 3H, NH_3), 5.23 (t, $J = 9.3$ Hz, 1H, H-3), 5.07 (t, $J = 9.8$ Hz, 1H, H-4), 5.00 (t, $J = 9.6$ Hz, 1H, H-2), 4.55 (d, $J = 10.0$ Hz, 1H, H-1), 4.26 – 4.14 (m, 2H, H-6a, H-6b), 3.81 – 3.66 (m, 5H, H-5/ $\text{SCH}_2\underline{\text{C}}\text{H}_2\text{O}$ / $\text{OCH}_2\underline{\text{C}}\text{H}_2\text{NH}_3$), 3.25 (s, 2H, $\text{OCH}_2\underline{\text{C}}\text{H}_2\text{NH}_3$), 2.93 (dt, $J = 12.7, 6.2$ Hz, 1H, $\text{SCH}_2\underline{\text{C}}\text{H}_2\text{O}$), 2.80 (dt, $J = 13.5, 6.1$ Hz, 1H, $\text{SCH}_2\underline{\text{C}}\text{H}_2\text{O}$), 2.08 (s, 3H, $\underline{\text{C}}\text{H}_3\text{CO}$), 2.05 (s, 3H, $\underline{\text{C}}\text{H}_3\text{CO}$), 2.03 (s, 3H, $\underline{\text{C}}\text{H}_3\text{CO}$), 2.01 (s, 3H, $\underline{\text{C}}\text{H}_3\text{CO}$); ^{13}C NMR (126 MHz, CDCl_3): δ 171.0, 170.2, 169.8, 169.5 ($4\times\text{CO}$), 83.3 (C-1), 76.0 (C-5), 73.6 (C-3), 70.1 ($\text{OCH}_2\underline{\text{C}}\text{H}_2\text{NH}_3$), 70.0 (C-2), 68.2 (C-4), 66.0 ($\text{SCH}_2\underline{\text{C}}\text{H}_2\text{O}$), 61.9 (C-6), 39.8 ($\text{OCH}_2\underline{\text{C}}\text{H}_2\text{NH}_3$), 29.4 ($\text{SCH}_2\underline{\text{C}}\text{H}_2\text{O}$), 20.6, 20.6, 20.5, 20.4 ($4\times\underline{\text{C}}\text{H}_3\text{CO}$); ^{19}F NMR (470 MHz, CDCl_3): δ -75.70; ESI-HRMS $[\text{M}+\text{H}]^+$ calcd. for $\text{C}_{18}\text{H}_{30}\text{NO}_{10}\text{S}^+$ 452.1585, found 452.1572.

Peracetylated tetraamide (141**):**

Tetracarboxylic acid **134** (10 mg, 15.0 μmol) and trifluoroacetate **140** (42.5 mg, 75.2 μmol , 5 equiv) were dissolved in anhydrous DMF (6 mL), DIPEA (34 μL , 195.5 μmol , 13 equiv) was added followed by PyBOP (47 mg, 90.24 μmol , 6 equiv), and the reaction mixture was stirred for 16 h at 20 °C. After such time H_2O (10 mL) was added and the reaction mixture was extracted with EtOAc (4×10 mL). The combined organic layers were washed with H_2O (30 mL), brine (30 mL), dried over Na_2SO_4 , concentrated to dryness and co-evaporated with toluene (3×10 mL). The crude product was purified by flash column chromatography on silica gel eluting with hexanes:acetone (10 \rightarrow 100% acetone (v/v)) to give compound **141** as a colorless

syrup (29 mg, 80%) containing ~4% of the anti-Markovnikoff regioisomers. R_f 0.21 (Acetone (H₂SO₄/EtOH)); ¹H NMR (500 MHz, CDCl₃) δ 7.17 (br, 4H, NH), 5.23 (t, J = 9.4 Hz, 4H, H-3), 5.08 (t, J = 9.8 Hz, 4H, H-4), 5.03 (t, J = 9.7 Hz, 4H, H-2), 4.57 (d, J = 10.0 Hz, 4H, H-1), 4.25 (dd, J = 12.4, 4.9 Hz, 4H, H-6a), 4.15 (dd, J = 12.4, 2.5 Hz, 4H, H-6b), 3.74 (ddd, J = 10.2, 4.9, 2.4 Hz, 4H, H-5), 3.69 (d, J = 7.1 Hz, 8H, SCH₂CH₂O), 3.55 (t, J = 5.3 Hz, 8H, OCH₂CH₂NH), 3.50 – 3.40 (m, 16H, OCH₂CH₂CH₂S/OCH₂CH₂NH), 3.33 (s, 8H, SCH₂CONH), 3.23 (s, 8H, C(CH₂O)₄), 2.93 (dt, J = 13.4, 6.6 Hz, 4H, SCH₂CH₂O), 2.80 (dt, J = 13.3, 6.5 Hz, 4H, SCH₂CH₂O), 2.62 (t, J = 7.4 Hz, 8H, OCH₂CH₂CH₂S), 2.09 (s, 12H, CH₃CO), 2.06 (s, 12H, CH₃CO), 2.03 (s, 12H, CH₃CO), 2.01 (s, 12H, CH₃CO), 1.82 (p, J = 6.4 Hz, 8H, OCH₂CH₂CH₂S); ¹³C NMR (126 MHz, CDCl₃) δ 170.6, 170.2, 169.5, 169.5, 169.2 (CO), 83.5 (C-1), 76.0 (C-5), 73.9 (C-3), 70.5 (SCH₂CH₂O), 69.9 (C-2), 69.7 (C(CH₂O)₄), 69.6 (OCH₂CH₂CH₂S), 69.5 (OCH₂CH₂NH), 68.4 (C-4), 62.2 (C-6), 39.5 (OCH₂CH₂NH), 36.1 (SCH₂CONH), 29.9 (OCH₂CH₂CH₂S), 29.5 (SCH₂CH₂O), 29.3 (OCH₂CH₂CH₂S), 20.8, 20.8, 20.7, 20.7 (CH₃CO). The minor isomer was identified in mixture by the following diagnostic signals: 1.26 (s).

ESI-HRMS [M+2Na]²⁺/2 calcd. for C₉₇H₁₅₂N₄Na₂O₄₈S₈²⁺ 1221.3563, found 1221.3525.

Tetraamide (142):

Peracetylated tetraamide **141** (33 mg, 13.7 μ mol) was suspended in anhydrous MeOH (1 mL) and NaOMe (freshly prepared 1M solution in MeOH) (5.5 μ L, 5.5 μ mol, 0.4 equiv) was added. The reaction mixture then was stirred until full consumption of the starting material was detected by LCMS. The reaction mixture was quenched with Amberlite IR-120 (H⁺) ion-exchange resin (washed with MeOH, CH₂Cl₂) until pH 6. The reaction mixture was filtered, and the filtrate was concentrated to dryness and the crude product was purified by flash column chromatography on a C18 silica gel eluting with H₂O:MeOH (20 \rightarrow 50% MeOH (v/v)) to give the product as a colorless foam (13.4 mg, 57%): R_f 0.54 (C18 plate, H₂O:MeOH 1:1 (v/v) (H₂SO₄/EtOH)); ¹H NMR (900 MHz, CD₃OD): δ 4.43 (d, J = 9.8 Hz, 4H, H-1), 3.87 (dd, J = 12.0, 1.6 Hz, 4H, H-6), 3.73 (dt, J = 10.0, 6.4 Hz, 4H, SCH₂CH₂O), 3.69 (dt, J = 10.0, 6.6 Hz, 4H, SCH₂CH₂O), 3.67 – 3.64 (m, 4H, H-6), 3.58 (tt, J = 5.6, 3.1 Hz, 8H, OCH₂CH₂NH), 3.49 (t, J = 5.9 Hz, 8H, OCH₂CH₂CH₂S),

3.41 (t, $J = 5.4$ Hz, 8H, OCH₂CH₂NH), 3.39 – 3.34 (m, 12H, H-3, C(CH₂O)₄), 3.31 – 3.28 (m, 8H, H-4, H-5)², 3.23 (s, 8H, SCH₂CONH), 3.21 (dd, $J = 8.8$ Hz, 4H, H-2), 2.96 (dt, $J = 13.4, 6.6$ Hz, 4H, SCH₂CH₂O), 2.84 (dt, $J = 13.4, 6.5$ Hz, 4H, SCH₂CH₂O), 2.68 (t, $J = 7.2$ Hz, 8H, OCH₂CH₂CH₂S), 1.85 (p, $J = 6.4$ Hz, 8H, OCH₂CH₂CH₂S); ¹³C NMR (226 MHz, CD₃OD): δ 172.7 (CONH), 87.3 (C-1), 82.1 (C-4), 79.6 (C-3), 74.5 (C-2), 71.9 (SCH₂CH₂O), 71.6 (C-5), 70.8 (OCH₂CH₂CH₂S), 70.7 (C(CH₂O)₄), 70.2 (OCH₂CH₂NH), 63.0 (C-6), 46.8 (q-C), 40.7 (OCH₂CH₂NH), 36.4 (SCH₂CONH), 30.5 (SCH₂CH₂O), 30.5 (OCH₂CH₂CH₂S), 30.5 (OCH₂CH₂CH₂S). The minor isomer was identified in mixture by the following diagnostic signals: 1.28 (d, $J = 6.8$ Hz).

ESI-HRMS [M+2Na]²⁺/2 calcd. for C₆₅H₁₂₀N₄Na₂O₃₂S₈²⁺ 885.2718, found 885.2710.

((2-(*tert*-Butylcarbamoyl)ethoxy)ethyl) 2,3,4,6-Tetra-*O*-acetyl-1,5-dithio- β -D-glucopyranoside (143):

1-*S*-Acetyl-2,3,4,6-tetra-*O*-acetyl-1,5-dithio- β -D-glucopyranose **61** (100 mg, 0.236 mmol) and *tert*-butyl (2-(2-iodoethoxy)ethyl)carbamate (387 mg, 1.2 mmol, 5.2 equiv) were dissolved in anhydrous DMF (12 mL) treated with HNEt₂ (65 μ L, 0.619 mmol, 2.6 equiv) and stirred for 4 h at 20 °C. After such time the reaction mixture was diluted with EtOAc (50 mL), washed with H₂O (30 mL), brine (30 mL), dried over Na₂SO₄, concentrated to dryness and co-evaporated with toluene (3 \times 15 mL). The crude product was purified by flash column chromatography on a silica gel eluting with hexanes:EtOAc (10 \rightarrow 60% EtOAc (v/v)) to give compound **143** as a colorless syrup (122 mg, 91%). R_f 0.43 (hexanes:EtOAc 1:1 (H₂SO₄/EtOH)); $[\alpha]_D^{22-23} - 3.06$ (c 0.047, CHCl₃); ¹H NMR (500 MHz, CDCl₃): δ 5.26 (dd, $J = 10.7, 9.6$ Hz, 1H, H-4), 5.15 (dd, $J = 10.7, 9.4$ Hz, 1H, H-2), 5.06 (t, $J = 9.5$ Hz, 1H, H-3), 4.97 (br, 1H, NH), 4.26 (dd, $J = 12.0, 5.7$ Hz, 1H, H-6a), 4.15 – 4.09 (m, 1H, H-6b), 3.96 (d, $J = 10.7$ Hz, 1H, H-1), 3.69 – 3.58 (m, 2H, SCH₂CH₂O), 3.51 (t, $J = 5.2$ Hz, 2H, OCH₂CH₂NHBoc), 3.35 – 3.26 (m, 3H, H-5/OCH₂CH₂NHBoc),

² Signal overlapping with residual solvent peak

2.92 (dt, $J = 12.8, 6.3$ Hz, 1H, SCH₂CH₂O), 2.83 (dt, $J = 13.2, 6.3$ Hz, 1H, SCH₂CH₂O), 2.08 (s, 3H, CH₃CO), 2.07 (s, 3H, CH₃CO), 2.02 (s, 3H, CH₃CO), 2.00 (s, 3H, CH₃CO), 1.45 (s, 9H, C(CH₃)₃); ¹³C NMR (126 MHz, CDCl₃): δ 170.4, 169.6, 169.4, 169.2 (4 \times CO), 155.9 (CONH), 79.2 (C(CH₃)₃), 74.4 (C-3), 73.2 (C-2), 71.7 (C-4), 70.4 (SCH₂CH₂O), 70.0 (OCH₂CH₂NHBoc), 61.2 (C-6), 47.9 (C-1), 44.3 (C-5), 40.3 (OCH₂CH₂NHBoc), 30.3 (SCH₂CH₂O), 28.3 (C(CH₃)₃), 20.5, 20.5, 20.40, 20.35 (4 \times CH₃CO); ESI-HRMS [M+Na]⁺ calcd. for C₂₃H₃₇NNaO₁₁S₂⁺ 590.1700, found 590.1690.

2-(2-Aminoethoxy)ethyl 2,3,4,6,-Tetra-*O*-acetyl-1,5-dithio- β -D-glucopyranoside trifluoroacetate salt (144):

Carbamate **143** (122 mg, 0.215 mmol) was dissolved in CH₂Cl₂ (40 mL) and 90% aq TFA (10 mL) was added, the reaction mixture then was stirred for 40 min at 20 °C. After such time the reaction mixture was concentrated to dryness, co-evaporated with toluene (3 \times 10 mL) and dried on a high vacuum for 12 h to give product **144** as a syrup (120 mg, 96%). [α]_D²⁰⁻²² – 1.75 (c 0.048, CHCl₃); ¹H NMR (500 MHz, CDCl₃): δ 7.79 (br, 3H, NH₃), 5.25 (t, $J = 10.0$ Hz, 1H, H-4), 5.16 – 5.03 (m, 2H, H-2/H-3), 4.31 – 4.21 (m, 1H, H-6a), 4.13 (dd, $J = 12.1, 3.2$ Hz, 1H, H-6b), 3.95 (d, $J = 10.2$ Hz, 1H, H-1), 3.74 – 3.65 (m, 4H, OCH₂CH₂NH₃/SCH₂CH₂O), 3.33 (dt, $J = 9.5, 4.3$ Hz, 1H, H-5), 3.25 (s, 2H, OCH₂CH₂NH₃), 2.97 – 2.90 (m, 1H, SCH₂CH₂O), 2.88 – 2.82 (m, 1H, SCH₂CH₂O), 2.07 (s, 3H, CH₃CO), 2.06 (s, 3H, CH₃CO), 2.03 (s, 3H, CH₃CO), 2.00 (s, 3H, CH₃CO); ¹³C NMR (126 MHz, CDCl₃): δ 170.9, 170.1, 169.9, 169.5 (4 \times CO), 74.3 (C-3), 73.4 (C-2), 71.8 (C-4), 70.3 (SCH₂CH₂O), 66.1 (OCH₂CH₂NH₃), 61.3 (C-6), 47.8 (C-1), 44.4 (C-5), 40.0 (OCH₂CH₂NH₃), 30.2, 20.6, 20.5, 20.4 (4 \times CH₃CO); ¹⁹F NMR (470 MHz, CDCl₃): δ –75.72; ESI-HRMS [M+H]⁺ calcd. for C₁₈H₃₀NO₉S₂⁺ 468.1357, found 468.1346.

Peracetylated tetraamide (145):

Tetracarboxylic acid **134** (10 mg, 15.04 μ mol) and trifluoroacetate **144** (43.7 mg, 75.2 μ mol, 5 equiv) were dissolved in anhydrous DMF (7 mL) followed by addition of DIPEA (34 μ L, 195.5 μ mol, 13 equiv) and PyBOP (47 mg, 90.24 μ mol, 6 equiv). The reaction mixture then was stirred for 16 h at 20 °C. After such time H₂O (10 mL) was added and the reaction mixture was extracted with EtOAc (4 \times 10 mL). The combined

organic layers were washed with H₂O (30 mL), brine (30 mL), dried over Na₂SO₄, concentrated to dryness and co-evaporated with toluene (3×10 mL). The crude product was purified by flash column chromatography on silica gel eluting with hexanes:acetone (10 → 100% acetone (v/v)) to give compound **145** as a white solid (29 mg, 78%). *R*_f 0.08 (Acetone (H₂SO₄/EtOH)); ¹H NMR (500 MHz, CDCl₃): δ 7.17 (t, *J* = 5.6 Hz, 4H, NH), 5.25 (t, *J* = 10.2 Hz, 4H, H-4), 5.14 (t, *J* = 10.0 Hz, 4H, H-2), 5.06 (t, *J* = 9.5 Hz, 4H, H-3), 4.26 (dd, *J* = 12.0, 5.7 Hz, 4H, H-6a), 4.11 (dd, *J* = 12.0, 3.4 Hz, 4H, H-6b), 3.94 (d, *J* = 10.6 Hz, 4H, H-1), 3.70 – 3.59 (m, 8H, SCH₂CH₂O), 3.54 (t, *J* = 5.1 Hz, 8H, OCH₂CH₂NH), 3.51 – 3.40 (m, 16H, OCH₂CH₂CH₂S/OCH₂CH₂NH), 3.32 (s, 12H, H-5/SCH₂CONH), 3.23 (s, 8H, (C(CH₂O)₄)), 2.93 (dt, *J* = 12.9, 6.3 Hz, 4H, SCH₂CH₂O), 2.83 (dt, *J* = 12.9, 6.3 Hz, 4H, SCH₂CH₂O), 2.61 (t, *J* = 7.3 Hz, 8H, OCH₂CH₂CH₂S), 2.07 (s, 12H, CH₃CO), 2.06 (s, 12H, CH₃CO), 2.02 (s, 12H, CH₃CO), 1.99 (s, 12H, CH₃CO), 1.83 (p, *J* = 6.2 Hz, 8H, OCH₂CH₂CH₂S); ¹³C NMR (126 MHz, CDCl₃): δ 170.5, 169.7, 169.5, 169.4, 169.2 (5×CO), 74.4 (C-3), 73.2 (C-2), 71.8 (C-4), 70.3 (SCH₂CH₂O), 69.6 ((C(CH₂O)₄)), 69.5 (OCH₂CH₂CH₂S/OCH₂CH₂NH), 61.3 (C-6), 47.9 (C-1), 44.4 (C-5), 39.5 (OCH₂CH₂NH), 36.1 (SCH₂CONH), 30.3 (OCH₂CH₂CH₂S), 29.8 (SCH₂CH₂O), 29.3 (OCH₂CH₂CH₂S), 20.7, 20.6, 20.5, 20.5 (4×CH₃CO). The minor isomer was identified in mixture by the following diagnostic signals: 1.25 (d, *J* = 3.8 Hz).

ESI-HRMS [M+2Na]²⁺/2 calcd. for C₉₇H₁₅₂N₄Na₂O₄₄S₁₂²⁺ 1253.3106, found 1253.3070.

Tetraamide (146):

Peracetylated tetraamide **145** (8 mg, 3.3 μmol) was suspended in anhydrous MeOH (1 mL) and NaOMe (freshly prepared 1M solution in MeOH) (6.6 μL, 6.6 μmol, 2 eq) was added. The reaction mixture then was stirred until full consumption of the starting material was detected by LCMS. After that the reaction mixture was quenched with Amberlite IR-120 (H⁺) ion-exchange resin (washed with MeOH, CH₂Cl₂) until pH 6. The reaction mixture then was filtered, and the filtrate was concentrated to dryness. The crude product was purified by column chromatography on a C18 silica gel eluting with H₂O:MeCN (H₂O:MeCN 1:1 (v/v)) to give product as a white foam (4.1 mg, 70%): *R*_f 0.68 (H₂O:MeCN 1:1, (H₂SO₄/EtOH)); ¹H NMR

(900 MHz, D₂O): δ 3.88 – 3.80 (m, 8H, H-1, H-6a), 3.71 (dd, J = 11.9, 6.2 Hz, 4H, H-6b), 3.67 (t, J = 6.2 Hz, 8H, SCH₂CH₂O), 3.56 (t, J = 5.4 Hz, 8H, OCH₂CH₂NH), 3.52 – 3.45 (m, 12H, OCH₂CH₂CH₂S, H-4), 3.38 (t, J = 9.6 Hz, 4H, H-2), 3.36 – 3.30 (m, 16H, C(CH₂O)₄, OCH₂CH₂NH), 3.23 – 3.17 (m, 12H, H-3, SCH₂CONH), 2.94 (ddd, J = 9.8, 6.1, 3.2 Hz, 4H, H-5), 2.90 (dt, J = 12.6, 6.1 Hz, 4H, SCH₂CH₂O), 2.85 (dt, J = 13.2, 6.1 Hz, 4H, SCH₂CH₂O), 2.57 (t, J = 7.1 Hz, 8H, OCH₂CH₂CH₂S), 1.83 – 1.72 (m, 8H, OCH₂CH₂CH₂S); ¹³C NMR (226 MHz, D₂O): δ 172.7 (CO), 78.1 (C-3), 75.5 (C-2), 73.1 (C-4), 69.9 (SCH₂CH₂O), 69.6 (OCH₂CH₂CH₂S), 69.2 (C(CH₂O)₄), 68.6 (OCH₂CH₂NH), 60.2 (C-6), 49.1 (C-1), 48.7 (C-5), 45.1 (q-C), 39.3 (OCH₂CH₂NH), 35.2 (SCH₂CONH), 30.4 (SCH₂CH₂O), 29.0 (OCH₂CH₂CH₂S), 28.4 (OCH₂CH₂CH₂S); ESI-HRMS [M+2Na]²⁺/2 calcd. for C₆₅H₁₂₀N₄Na₂O₂₈S₁₂²⁺ 917.2261, found 917.2259.

((2-(*tert*-Butylcarbamoyl)ethoxy)ethyl) 2,3,4,6-Tetra-*O*-acetyl-5-thio- β -D-glucopyranosyl-(1 \rightarrow 3)-2,4,6-tri-*O*-acetyl-1,3,5-trideoxy-1,3,5-trithio- β -D-glucopyranoside (147**):**

Thioacetate **115** (100 mg, 0.135 mmol) and *tert*-butyl (2-(2-iodoethoxy)ethyl)carbamate (212 mg, 0.67 mmol, 5 equiv) were dissolved in anhydrous DMF (1 mL) followed by addition of HNet₂ (35 μ L, 0.336 mmol, 2.5 equiv) and the reaction mixture then was stirred for 50 min at 20 °C. After such time the reaction mixture was diluted with EtOAc (50 mL), washed with H₂O (2 \times 10 mL), brine (2 \times 10 mL), dried over Na₂SO₄, concentrated to dryness and co-evaporated with toluene (3 \times 15 mL). The crude product was purified by flash column chromatography on a silica gel eluting with hexanes:EtOAc (10 \rightarrow 60% EtOAc (v/v)) to give compound **147** as a colorless syrup (108 mg, 90%). R_f 0.44 (hexanes:EtOAc 2:3 (H₂SO₄/EtOH)); $[\alpha]_D^{22-23}$ – 0.94 (c 0.0053, CHCl₃); ¹H NMR (900 MHz, CDCl₃): δ 5.29 (t, J = 9.9 Hz, 1H, H-4a), 5.19 (t, J = 10.5 Hz, 1H, H-2b), 5.10 (t, J = 10.4 Hz, 1H, H-2a), 5.03 – 4.95 (m, 2H, H-4b, H-3a), 4.93 (br, 1H, NH), 4.27 (dt, J = 12.1, 3.2 Hz, 1H, H-6a), 4.20 (dd, J = 12.1, 5.7 Hz, 1H, H-6b), 4.17 – 4.11 (m, 2H, H-6b, H-6a), 4.05 (d, J = 11.1 Hz, 1H, H-1a), 3.79 (d, J = 10.4 Hz, 1H, H-1b), 3.70 – 3.57 (m, 2H, SCH₂CH₂O), 3.51 (s, 2H, OCH₂CH₂NHBoc), 3.32 (s, 2H, OCH₂CH₂NHBoc), 3.28 (s, 1H, H-5b), 3.21 (d, J = 10.9 Hz, 1H, H-5a), 3.00 – 2.89 (m, 2H, H-3b, SCH₂CH₂O), 2.83 (dd, J = 13.9, 7.5 Hz, 1H, SCH₂CH₂O),

2.22 (s, 3H, CH₃CO), 2.15 (s, 3H, CH₃CO), 2.09 (s, 3H, CH₃CO), 2.07 (s, 3H, CH₃CO), 2.03 (s, 6H, 2×CH₃CO), 1.99 (s, 3H, CH₃CO), 1.60 (s, 4H, C(CH₃)₃), 1.46 (s, 9H, C(CH₃)₃); ¹³C NMR (226 MHz, CDCl₃): δ 170.6, 170.5, 169.7, 169.4, 169.2, 169.2, 169.1 (7×CH₃CO), 155.9 (CONH), 79.4 (C(CH₃)₃), 75.8 (C-2b), 74.4 (C-3a), 72.8 (C-2a), 71.8 (C-4a), 70.4 (SCH₂CH₂O), 70.3 (OCH₂CH₂NHBoc), 70.0 (C-4b), 61.9 (C-6a), 61.1 (C-6b), 55.2 (C-3b), 50.6 (C-1a), 49.7 (C-1b), 46.8 (C-5b), 44.5 (C-5a), 40.3 (OCH₂CH₂NHBoc), 30.0 (SCH₂CH₂O), 28.4 (C(CH₃)₃), 21.0, 20.9, 20.7, 20.6, 20.5, 20.4, 20.2 (7×CH₃CO); ESI-HRMS [M+Na]⁺ calcd. for C₃₅H₅₃NNaO₁₇S₄⁺ 910.2089, found 910.2050.

(2-(2-Aminoethoxy)ethyl) 2,3,4,6-Tetra-O-acetyl-5-thio-β-D-glucopyranosyl-(1→3)-2,4,6-tri-O-acetyl-1,3,5-trideoxy-1,3,5-trithio-β-D-glucopyranoside trifluoroacetate salt (148):

Carbamate **147** (99 mg, 0.11 mmol) was dissolved in CH₂Cl₂ (16 mL) and 90% aq TFA (4 mL) was added. The reaction mixture then was stirred for 40 min at 20 °C. After such time the reaction mixture was concentrated to dryness, co-evaporated with toluene (3×10 mL) and dried on a high vacuum for 12 h to give compound **148** as a colorless syrup (98 mg, 98%). [α]_D²⁰⁻²² – 6.5 (c 0.0023, CHCl₃); ¹H NMR (500 MHz, CDCl₃): δ 8.08 (br, 2H, NH), 5.29 (t, *J* = 10.0 Hz, 1H, H-4a), 5.17 (t, *J* = 10.1 Hz, 1H, H-2b), 5.10 (t, *J* = 10.2 Hz, 1H, H-2a), 5.05 – 4.93 (m, 2H, H-3a, H-4b), 4.27 (dd, *J* = 12.0, 4.7 Hz, 1H, H-6a), 4.23 – 4.11 (m, 3H, 2×H-6b, H-6a), 4.05 (d, *J* = 10.9 Hz, 1H, H-1a), 3.80 (d, *J* = 10.3 Hz, 1H, H-1b), 3.77 – 3.63 (m, 4H, SCH₂CH₂O, OCH₂CH₂NH₃), 3.34 – 3.17 (m, 4H, H-5b, H-5a, OCH₂CH₂NH₃), 3.02 – 2.91 (m, 2H, H-3b, SCH₂CH₂O), 2.89 – 2.80 (m, 1H, SCH₂CH₂O), 2.22 (s, 3H, CH₃CO), 2.15 (s, 3H, CH₃CO), 2.09 (s, 3H, CH₃CO), 2.07 (s, 3H, CH₃CO), 2.02 (s, 6H, 2×CH₃CO), 2.00 (s, 3H, CH₃CO); ¹³C NMR (126 MHz, CDCl₃): δ 170.8, 170.6, 170.4, 169.8, 169.6, 169.4, 169.2, 169.2 (7×CH₃CO), 75.8 (C-2b), 74.4 (C-3a), 72.8 (C-2a), 71.8 (C-4a), 70.4 (C-4b), 70.0 (SCH₂CH₂O), 66.1 (OCH₂CH₂NH₃), 61.9 (C-6a), 61.1 (C-6b), 55.1 (C-3b), 50.6 (C-1a), 49.4 (C-1b), 46.8 (C-5b), 44.4 (C-5a), 39.8 (OCH₂CH₂NH₃), 30.0 (SCH₂CH₂O),

³ Peak corresponding to the rotamer signal of methyl group of the *tert*-butyl carbamate

20.9, 20.9, 20.6, 20.5, 20.4, 20.4, 20.2 (7×CH₃CO); ¹⁹F NMR (470 MHz, CDCl₃): δ -75.44; ESI-HRMS [M+H]⁺ calcd. for C₃₀H₄₆NO₁₅S₄⁺ 788.1745, found 788.1726.

Peracetylated tetraamide (**149**):

Tetracarboxylic acid **134** (11 mg, 16.5 μmol) and trifluoroacetate **148** (75 mg, 82.5 μmol, 5 equiv) were dissolved in anhydrous DMF (7 mL) followed by addition of DIPEA (37 μL, 214.5 μmol, 13 equiv) and PyBOP (52 mg, 99 μmol, 6 equiv). The reaction mixture then was stirred for 16 h at 20 °C. After such time H₂O (10 mL) was added and the reaction mixture was extracted with EtOAc (4×20 mL). The combined organic layers were washed with H₂O (2×20 mL), brine (2×20 mL), dried over Na₂SO₄, concentrated to dryness and co-evaporated with toluene (3×10 mL). The crude product was purified by flash column chromatography on silica gel eluting with CH₂Cl₂:MeOH (0 → 5% MeOH (v/v)) to give compound **149** as yellowish syrup (41 mg, 66%). *R*_f 0.52 (CH₂Cl₂:MeOH (95:5) (v/v) (H₂SO₄/EtOH)); ¹H NMR (500 MHz, CDCl₃) δ 7.15 (t, *J* = 5.7 Hz, 4H, NH), 5.28 (dd, *J* = 10.7, 9.5 Hz, 4H, H-4a), 5.17 (t, *J* = 10.4 Hz, 4H, H-2b), 5.08 (dd, *J* = 11.0, 9.5 Hz, 4H, H-2a), 5.04 – 4.89 (m, 8H, H-3a, H-4b), 4.26 (dd, *J* = 12.0, 5.0 Hz, 4H, H-6a), 4.20 (dd, *J* = 12.0, 5.7 Hz, 4H, H-6a), 4.16 – 4.09 (m, 8H, H-6b), 4.05 (d, *J* = 11.0 Hz, 4H, H-1a), 3.77 (d, *J* = 10.5 Hz, 4H, H-1b), 3.63 (qt, *J* = 10.1, 6.3 Hz, 8H, SCH₂CH₂O), 3.54 (t, *J* = 5.2 Hz, 8H, OCH₂CH₂NH), 3.47 (t, *J* = 5.3 Hz, 8H, OCH₂CH₂NH), 3.44 (q, *J* = 6.0, 5.2 Hz, 8H, OCH₂CH₂CH₂S), 3.32 (s, 8H, (C(CH₂O)₄), 3.28 (td, *J* = 6.0, 2.9 Hz, 4H, H-5b), 3.22 (s, 8H, SCH₂CONH), 3.20 (dd, *J* = 5.0, 3.7 Hz, 4H, H-5a), 2.96 – 2.89 (m, 8H, SCH₂CH₂O, H-3a), 2.82 (dt, *J* = 12.8, 6.3 Hz, 4H, SCH₂CH₂O), 2.61 (t, *J* = 7.3 Hz, 8H, OCH₂CH₂CH₂S), 2.21 (s, 12H, CH₃CO), 2.14 (s, 12H, CH₃CO), 2.08 (s, 12H, CH₃CO), 2.06 (s, 12H, CH₃CO), 2.02 (s, 24H, CH₃CO), 1.98 (s, 12H, CH₃CO), 1.85 – 1.79 (m, 8H, OCH₂CH₂CH₂S); ¹³C NMR (126 MHz, CDCl₃) δ 170.5, 170.5, 169.7, 169.4, 169.2, 169.1, 169.1, 169.1 (CO), 75.6 (C-2b), 74.4 (C-3a), 72.8 (C-2a), 71.8 (C-4a), 70.4 (C-4b), 70.2 (SCH₂CH₂O), 69.6 ((C(CH₂O))₄), 69.5 (OCH₂CH₂CH₂S), 69.3 (OCH₂CH₂NH), 61.9 (C-6a), 61.1 (C-6b), 55.2 (C-3b), 50.6 (C-1a), 49.6 (C-1b), 46.8 (C-5b), 45.4 (q-C), 44.4 (C-5a), 39.4 (OCH₂CH₂NH), 36.0 (SCH₂CONH), 29.9 (SCH₂CH₂O), 29.8

(OCH₂CH₂CHCH₂S), 29.2 (OCH₂CHCH₂CH₂S), 21.0, 20.9, 20.6, 20.6, 20.4, 20.4, 20.2 (7×CHCH₃CO). The minor isomer was identified in mixture by the following diagnostic signal: 1.25 (d, *J* = 3.9 Hz).

ESI-HRMS [M+2Na]²⁺/2 calcd. for C₁₄₅H₂₁₆N₄Na₂O₆₈S₂₀²⁺ 1893.8900, found 1893.8904.

Tetraamide (150):

Peracetylated tetraamide **149** (5 mg, 1.33 μmol) was suspended in anhydrous MeOH (0.3 mL) and NaOMe (1.0 mg, 19.95 μmol, 15 equiv) was added, and the reaction mixture was stirred for 24 h at 20 °C. After such time the reaction mixture was quenched with Amberlite IR-120 (H⁺) ion-exchange resin (washed with MeOH, CH₂Cl₂) until pH 6, filtered and the filter cake was additionally washed with MeOH (10 mL). The filtrate was concentrated to dryness, redissolved in H₂O (10 mL) and washed with EtOAc (2×10 mL). The aqueous layer was concentrated to dryness and co-evaporated with EtOH. The crude product was purified by column chromatography on a C18 silica gel eluting with MeCN:H₂O (1:1) to give tetraamide **150** as a colorless syrup (2.6 mg, 76%). *R*_f 0.68 (C18, MeCN:H₂O (1:1), (H₂SO₄/EtOH)); ¹H NMR (900 MHz, D₂O): δ 4.14 (d, *J* = 10.4 Hz, 4H, H-1a), 4.02 – 3.90 (m, 12H, H-6a, H-6b, H-1b), 3.90 – 3.81 (m, 8H, H-6a, H-6b), 3.80 – 3.76 (m, 8H, SCH₂CHCH₂O), 3.70 – 3.55 (m, 28H, OCH₂CHCH₂NH, OCH₂CHCH₂CH₂S, H-4a, H-4b, H-2b), 3.51 (t, *J* = 9.8 Hz, 8H, H-2a), 3.48 – 3.41 (m, 16H, C(CHCH₂O)₄, OCH₂CHCH₂NH), 3.34 (d, *J* = 9.6 Hz, 8H, SCH₂CONH), 3.15 – 3.08 (m, 4H, H-5a), 3.06 – 2.95 (m, 12H, SCH₂CH₂O, H-5b), 2.89 (t, *J* = 10.3 Hz, 4H, H-3b), 2.69 (t, *J* = 7.3 Hz, 8H, OCH₂CH₂CHCH₂S), 1.94 – 1.82 (m, 8H, OCH₂CHCH₂CH₂S); ¹³C NMR (226 MHz, D₂O): δ 172.6 (C=O), 78.0 (C-3a), 76.3 (C-2a), 75.6 (C-4a), 72.9 (C-2b), 71.1 (C-4b), 69.9 (SCH₂CHCH₂O), 69.6 (OCH₂CH₂CH₂S), 69.2 (C(CHCH₂O)), 68.7 (OCH₂CH₂NH), 62.5 (q-C), 60.7 (C-6a), 60.1 (C-6b), 59.6 (C-3b), 50.8 (C-1b, C-5a), 49.2 (C-1a, C-5b), 48.8 (OCH₂CHCH₂NH), 39.4 (OCH₂CHCH₂NH₂), 35.3 (SCH₂CONH), 30.6 (SCH₂CH₂O), 29.0 (OCH₂CH₂CHCH₂S), 28.5 (OCH₂CHCH₂CH₂S). The minor isomer was identified in mixture by the following diagnostic signals: 1.94 – 1.82 (m, 1H) in ¹H NMR spectrum and 23.2 in ¹³C NMR spectrum.

ESI-HRMS [M+2Na]²⁺/2 calcd. for C₈₉H₁₆₀N₄Na₂O₄₀S₂₀²⁺ 1305.2404, found 1305.2424.

((2-(*tert*-Butylcarbamoyl)ethoxy)ethyl) 2,3,4,6-tetra-O-acetyl-5-thio- β -D-glucopyranosyl-(1 \rightarrow 3)-2,4,6-tri-O-acetyl-1,3,5-trideoxy-1,3,5-trithio- β -D-(1 \rightarrow 3)-2,4,6-tri-O-acetyl-1,3,5-trideoxy-1,3,5-trithio- β -D-glucopyranoside (151):

Thioacetate **126** (128 mg, 0.12 mmol) and *tert*-butyl (2-(2-iodoethoxy)ethyl)carbamate (190 mg, 0.6 mmol, 5 equiv) were dissolved in anhydrous DMF (0.9 mL) followed by addition of HNEt₂ (31 μ L, 0.300 mmol, 2.5 equiv) and the reaction mixture then was stirred for 1.5 h at 20 °C. After such time the reaction mixture was diluted with EtOAc (60 mL), washed with H₂O (2 \times 10 mL), brine (2 \times 10 mL), dried over Na₂SO₄, concentrated to dryness and co-evaporated with toluene (3 \times mL). The crude product was purified by flash column chromatography on a silica gel eluting with CH₂Cl₂:Et₂O (0 \rightarrow 40% Et₂O (v/v)) to give compound **151** as a colorless syrup (83 mg, 57%). *R*_f 0.46 (CH₂Cl₂:Et₂O 7:3 (H₂SO₄/EtOH)); [α]_D²²⁻²³ -2.7 (*c* 0.00073, CHCl₃); ¹H NMR (500 MHz, CDCl₃): δ 5.31 (dd, *J* = 10.3, 5.4 Hz, 1H, H-4a), 5.18 (t, *J* = 10.5 Hz, 1H, H-2c), 5.18 (t, *J* = 10.5 Hz, 1H, H-3a), 5.15 – 5.01 (m, 2H, H-2a, H-2b), 4.96 (t, *J* = 10.6 Hz, 2H, H-4b, H-4c), 4.74 (t, *J* = 10.2 Hz, 1H, H-6a), 4.27 – 4.09 (m, 6H, H-6a, H-6b, H-6c, H-1a), 4.00 (d, *J* = 9.7 Hz, 1H, H-1b), 3.80 (d, *J* = 9.7 Hz, 1H, H-1c), 3.63 (d, *J* = 6.3 Hz, 2H, SCH₂CH₂O), 3.52 (t, *J* = 5.0 Hz, 2H, OCH₂CH₂NHBoc), 3.35 – 3.18 (m, 4H, OCH₂CH₂NHBoc, H-5a, H-5b), 3.10 (s, 1H, H-5c), 3.03 – 2.88 (m, 3H, H-3b, H-3c, SCH₂CH₂O), 2.87 – 2.77 (m, 1H, SCH₂CH₂O), 2.25 (s, 3H, CH₃CO), 2.18 (s, 3H, CH₃CO), 2.17 (s, 3H, CH₃CO), 2.13 (s, 6H, 2 \times CH₃CO), 2.07 (s, 2H, CH₃CO), 2.06 (s, 3H, CH₃CO), 2.05 (s, 2H, CH₃CO), 2.02 (s, 3H, CH₃CO), 2.00 (s, 2H, CH₃CO), 1.64 (s, 1H, C(CH₃)₃⁴), 1.46 (s, 9H, C(CH₃)₃); ¹³C NMR (126 MHz, CDCl₃): δ 170.6, 169.5, 169.3, 169.3, 169.3, 169.3, 169.3, 169.2, 169.2, 169.1 (10 \times CH₃CO), 155.9 (CONH), 79.3 (C(CH₃)₃), 75.8 (C-2c), 75.5 (C-2b), 72.6 (C-2a), 72.6 (C-4a), 70.6 (C-3a), 70.5 (C-4b, C-4c), 70.3 (SCH₂CH₂O), 70.0 (OCH₂CH₂NHBoc), 62.0 (C-6b), 61.9 (C-6c), 59.5 (C-6a), 54.9 (C-3b), 54.7 (C-3c), 52.3 (C-1b), 49.6 (C-1c), 47.8 (C-1a), 46.9 (C-5a), 43.3 (C-5b), 40.3 (C-5c), 30.3

⁴ Peak corresponding to the rotamer signal of methyl group of the *tert*-butyl carbamate

(OCH₂CH₂NHBoc), 29.9 (SCH₂CH₂O), 28.4 (C(CH₃)), 21.1, 20.9, 20.9, 20.8, 20.7, 20.6, 20.6, 20.4, 20.2 (10×CH₃CO); ESI-HRMS [M+Na]⁺ calcd. for C₄₇H₆₉NNaO₂₃S₆⁺ 1230.2477, found 1230.2463.

(2-(2-Aminoethoxy)ethyl) 2,3,4,6-tetra-O-acetyl-5-thio-β-D-glucopyranosyl-(1→3)-2,4,6-tri-O-acetyl-1,3,5-trideoxy-1,3,5-trithio-β-D-(1→3)-2,4,6-tri-O-acetyl-1,3,5-trideoxy-1,3,5-trithio-β-D-glucopyranoside trifluoroacetate salt (152):

Carbamate **151** (60 mg, 49.65 μmol) was dissolved in CH₂Cl₂ (16 mL) and 90% aq TFA (4 mL) and the reaction mixture was stirred for 40 min at 20 °C. After such time the reaction mixture was concentrated to dryness, co-evaporated with toluene (3×10 mL) and dried on a high vacuum for 12 h to give compound **152** as a colorless syrup (60.5 mg, quant). [α]_D²⁰⁻²² -6.0 (*c* 0.002, CHCl₃); ¹H NMR (500 MHz, CD₃CN): δ 7.08 (br, 3H, OCH₂CH₂NH₃⁺), 5.34 – 5.21 (m, 2H, H-3a, H-4a), 5.06 (t, *J* = 10.5 Hz, 1H, H-2c), 5.01 – 4.87 (m, 4H, H-2a, H-4b, H-2b, H-4c), 4.59 (dd, *J* = 11.9, 8.1 Hz, 1H, H-6a), 4.29 – 4.20 (m, 2H, H-1a, H-6c), 4.19 – 4.10 (m, 5H, H-6a, H-6c, H-1b, H-6b), 4.01 (d, *J* = 10.5 Hz, 1H, H-1c), 3.68 – 3.61 (m, 4H, SCH₂CH₂O, OCH₂CH₂NH₃), 3.46 – 3.38 (m, 1H, H-5b), 3.35 – 3.25 (m, 2H, H-5a, H-5c), 3.17 – 3.03 (m, 4H, H-3b, H-3c, OCH₂CH₂NH₃), 2.91 (dt, *J* = 13.0, 6.3 Hz, 1H, SCH₂CH₂O), 2.83 (dt, *J* = 13.3, 6.5 Hz, 1H, SCH₂CH₂O), 2.23 (s, 3H, CH₃CO), 2.17 (s, 3H, CH₃CO), 2.12 (s, 3H, CH₃CO), 2.11 (s, 3H, CH₃CO), 2.09 (s, 3H, CH₃CO), 2.00 (s, 3H, CH₃CO), 1.98 (s, 6H, 2×CH₃CO), 1.98 (s, 3H, CH₃CO), 1.97 (s, 3H, CH₃CO)⁵; ¹³C NMR (126 MHz, CD₃CN): δ 171.6, 171.3, 170.9, 170.6, 170.5 (CO), 77.1 (C-2a), 76.5 (C-2c), 74.0 (C-2b), 73.4 (C-3a), 72.0 (C-4c), 71.6 (C-4b), 71.3 (C-4a), 71.1 (OCH₂CH₂NH₃), 66.8 (SCH₂CH₂O), 62.9 (C-6c), 62.6 (C-6b), 62.2 (C-6a), 55.5 (C-3b, C-3c), 52.3 (C-1a), 50.1 (C-1c), 48.9 (C-1b), 47.0 (C-5a), 46.9 (C-5b), 43.4 (C-5c), 40.7 (OCH₂CH₂NH₃), 31.3 (SCH₂CH₂O), 21.5, 21.4, 21.4, 20.9, 20.8, 20.8, 20.7 (CH₃CO); ¹⁹F NMR (470 MHz, CD₃CN): δ -76.2; ESI-HRMS [M+H]⁺ calcd. for C₄₂H₆₂NO₂₁S₆⁺ 1108.2133, found 1108.2136.

Peracetylated tetraamide (153):

⁵Two singlets overlapping, each with integral of 3

Tetracarboxylic acid **134** (7 mg, 10.5 μ mol) and trifluoroacetate **152** (64 mg, 52.5 μ mol, 5 equiv) were dissolved in anhydrous DMF (4 mL) followed by addition of DIPEA (24 μ L, 136.5 μ mol, 13 equiv) and PyBOP (33 mg, 63 μ mol, 6 equiv). The reaction mixture then was stirred for 16 h at 20 °C. After such time H₂O (10 mL) was added and the reaction mixture was extracted with EtOAc (4×20 mL). The combined organic layers were washed with H₂O (2×20 mL), brine (2×20 mL), dried over Na₂SO₄, concentrated to dryness and co-evaporated with toluene (3×10 mL). The crude product was purified by flash column chromatography on silica gel eluting with CH₂Cl₂:MeOH (0 → 5% MeOH (v/v)) to give compound **153** as colorless syrup (30 mg, 57%). *R_f* 0.4 (CH₂Cl₂:MeOH (95:5) (v/v) (H₂SO₄/EtOH)); ¹H NMR (500 MHz, CDCl₃): δ 7.15 (t, *J* = 5.7 Hz, 4H, CONH), 5.31 (dd, *J* = 10.3, 5.5 Hz, 4H, H-4a), 5.23 – 5.13 (m, 8H, H-2c, H-3a), 5.12 – 5.03 (m, 8H, H-2a, H-2b), 4.95 (t, *J* = 10.6 Hz, 8H, H-4b, H-4c), 4.75 (dd, *J* = 11.7, 9.8 Hz, 4H, H-6a), 4.26 – 4.11 (m, 20H, H-6b, H-6c, H-1a), 4.06 (dd, *J* = 11.6, 4.4 Hz, 4H, H-6a), 3.99 (d, *J* = 10.6 Hz, 4H, H-1b), 3.78 (d, *J* = 10.3 Hz, 4H, H-1c), 3.67 – 3.60 (m, 8H, SCH₂CH₂O), 3.55 (t, *J* = 5.2 Hz, 8H, OCH₂CH₂NH), 3.46 (dt, *J* = 23.0, 5.6 Hz, 16H, OCH₂CH₂NH, OCH₂CH₂CH₂S), 3.32 (s, 8H, C(CH₂O)), 3.28 (ddd, *J* = 9.7, 5.6, 3.6 Hz, 4H, H-5c), 3.25 – 3.20 (m, 12H, SCH₂CONH, H-5a), 3.09 (dd, *J* = 10.6, 4.9 Hz, 4H, H-5b), 3.01 – 2.89 (m, 12H, H-3b, H-3c, SCH₂CH₂O), 2.83 (dt, *J* = 12.9, 6.3 Hz, 4H, SCH₂CH₂O), 2.62 (t, *J* = 7.3 Hz, 8H, OCH₂CH₂CH₂S), 2.24 (s, 12H, CH₃CO), 2.18 (s, 12H, CH₃CO), 2.17 (s, 12H, CH₃CO), 2.13 (s, 24H, 2×CH₃CO), 2.06 (s, 12H, CH₃CO), 2.06 (s, 12H, CH₃CO), 2.04 (s, 12H, CH₃CO), 2.02 (s, 12H, CH₃CO), 2.00 (s, 12H, CH₃CO), 1.83 (p, *J* = 6.5 Hz, 8H, OCH₂CH₂CH₂S); ¹³C NMR (126 MHz, CDCl₃): δ 170.6, 170.5, 170.5, 169.5, 169.3, 169.2, 169.2, 169.1, 169.1 (C=O), 75.8 (C-2c), 75.4 (C-2b), 72.6 (C-2a), 72.5 (C-4a), 70.6 (C-3a), 70.5 (C-4b, C-4c), 70.2 (SCH₂CH₂O), 69.6 ((C(CH₂O))₄), 69.5 (OCH₂CH₂CH₂S), 69.3 (OCH₂CH₂NH), 62.0 (C-6b), 61.9 (C-6c), 59.5 (C-6a), 54.9 (C-3b), 54.7 (C-3c), 52.3 (C-1b), 49.5 (C-1c), 47.6 (C-1a), 46.9 (C-5a), 46.6 (C-5b), 45.4 (q-C), 43.2 (C-5c), 39.4 (OCH₂CH₂NH), 36.0 (SCH₂CONH), 29.8 (SCH₂CH₂O), 29.3 (OCH₂CH₂CH₂S / OCH₂CH₂CH₂S), 21.1, 20.9, 20.9, 20.7, 20.7, 20.6, 20.6, 20.4, 20.2 (11×CH₃CO); ESI-HRMS [M+3Na]³⁺/3 calcd. For C₁₉₃H₂₈₀N₄Na₃O₉₂S₂₈³⁺ 1697.9745, found 1697.9778.

Tetraamide (154):

A 200-500 μL microwave vial was charged with peracetylated tetraamide **153** (4 mg, 0.79 μmol) followed by addition of $\text{H}_2\text{O}:\text{MeOH}:\text{NEt}_3$ (5:4:1) mixture (200 μL). The reaction vessel then was sealed and subjected to microwave irradiation for 4 h at 71 $^\circ\text{C}$. After such time the reaction mixture was diluted with H_2O (5 mL) and washed with EtOAc (2×5 mL). The aqueous layer was concentrated to dryness and co-evaporated with EtOH (2×5 mL). The crude product was purified by column chromatography on a C18 silica gel eluting with $\text{MeCN}:\text{H}_2\text{O}$ (1:1) to give tetraamide **154** as a white foam (1.3 mg, 50%). R_f 0.57 (C18, $\text{H}_2\text{O}:\text{MeCN}$ (3:2)); ^1H NMR (900 MHz, D_2O): δ 4.15 (d, $J = 8.6$ Hz, 4H, H-1a), 4.07 (d, $J = 10.1$ Hz, 4H, H-1b), 3.96 – 3.81 (m, 16H, H-6c, H-6c, H-1c, H-3a), 3.79 – 3.73 (m, 12H, H-4a, H-6a), 3.68 (s, 8H, $\text{SCH}_2\text{CH}_2\text{O}$), 3.61 – 3.47 (m, 28H, H-6b, H-6b, H-2c, H-4b, H-2b, $\text{OCH}_2\text{CH}_2\text{NH}$), 3.44 – 3.39 (m, 8H, H-2a, H-4c), 3.39 – 3.29 (m, 16H, $\text{C}(\text{CH}_2\text{O})_4$, $\text{OCH}_2\text{CH}_2\text{NH}$), 3.24 (s, 8H, SCH_2CONH), 3.04 – 2.96 (m, 8H, H-5c, H-5b), 2.96 – 2.86 (m, 12H, $\text{SCH}_2\text{CH}_2\text{O}$, H-3b, H-5a), 2.81 (dt, $J = 21.4, 10.3$ Hz, 8H, $\text{SCH}_2\text{CH}_2\text{O}$), 2.59 (d, $J = 7.4$ Hz, 8H, $\text{OCH}_2\text{CH}_2\text{CH}_2\text{S}$), 1.84 – 1.73 (m, 8H, $\text{OCH}_2\text{CH}_2\text{CH}_2\text{S}$); ^{13}C NMR (226 MHz, D_2O): δ 76.8 (C-4b), 76.2 (C-4c), 76.0 (C-3a), 73.8 (C-2a), 73.3 (C-4a), 71.1 (C-2b), 71.0 (C-2c), 69.9 ($\text{SCH}_2\text{CH}_2\text{O}$), 69.6 ($\text{OCH}_2\text{CH}_2\text{CH}_2\text{S}$), 69.2 ($\text{C}(\text{CH}_2\text{O})$), 68.6 ($\text{OCH}_2\text{CH}_2\text{NH}$), 60.6 (C-6c), 60.5 (C-6b), 59.8 (C-6a), 59.6 (C-3c), 59.5 (C-3b), 58.4, 58.3 (C-6a), 51.0 (C-1b), 50.7 (C-1c), 48.0 (C-5a), 46.8 (C-5c), 46.7 (C-1a), 39.4 ($\text{OCH}_2\text{CH}_2\text{NH}$), 35.3 (SCH_2CONH), 30.5 ($\text{SCH}_2\text{CH}_2\text{O}$), 29.0 ($\text{OCH}_2\text{CH}_2\text{CH}_2\text{S}$), 28.5 ($\text{OCH}_2\text{CH}_2\text{CH}_2\text{S}$); ESI-HRMS $[\text{M}+3\text{Na}]^{3+}/3$ calcd. For $\text{C}_{113}\text{H}_{200}\text{N}_4\text{Na}_3\text{O}_{52}\text{S}_{28}^+$ 1137.4992, found 1137.4990.

Peracetylated propionylamide (155):

Trifluoroacetate **152** (21 mg, 17.3 μmol) and propionic acid (3 μL , 34.6 μmol , 2 equiv) were dissolved in anhydrous DMF (4 mL) followed by addition of DIPEA (12 μL , 69.2 μmol , 4 equiv) and PyBOP (18 mg, 34.6 μmol , 2 equiv). The reaction mixture then was stirred for 1 h at 20 $^\circ\text{C}$. After such time H_2O (10 mL) was added and the reaction mixture was extracted with EtOAc (4×10 mL). The combined organic layers were washed with H_2O (30 mL), brine (30 mL), dried over Na_2SO_4 , concentrated to dryness and co-evaporated with toluene (3×10 mL). The crude product was purified by flash column chromatography on

silica gel eluting with CH₂Cl₂:MeOH (0 → 10% MeOH (v/v)) to give compound **155** as a colorless syrup (18 mg, 90%). *R_f* 0.38 (MeOH:CH₂Cl₂ 5:95 (H₂SO₄/EtOH)); [α]_D²⁰⁻²² +9.5 (*c* 0.004, CHCl₃); ¹H NMR (500 MHz, CDCl₃): δ 5.95 (br, 1H, CONH), 5.32 (dd, *J* = 10.3, 5.5 Hz, 1H, H-4a), 5.23 – 5.14 (m, 2H, H-2c, H-3a), 5.13 – 5.02 (m, 2H, H-2b, H-2a), 4.96 (t, *J* = 10.6 Hz, 2H, H-4c, H-4b), 4.75 (t, *J* = 10.8 Hz, 1H, H-6a), 4.28 – 4.10 (m, 5H, H-6b, H-6c, H-1a), 4.05 (dd, *J* = 11.7, 4.5 Hz, 1H, H-6a), 4.00 (d, *J* = 10.7 Hz, 1H, H-1b), 3.78 (d, *J* = 10.4 Hz, 1H, H-1c), 3.70 – 3.58 (m, 1H, SCH₂CH₂O), 3.53 (t, *J* = 5.4 Hz, 2H, OCH₂CH₂NH), 3.46 (p, *J* = 5.2, 4.7 Hz, 2H, OCH₂CH₂NH), 3.29 (dt, *J* = 10.4, 4.8 Hz, 1H, H-5b), 3.23 (dt, *J* = 9.9, 5.0 Hz, 1H, H-5a), 3.09 (s, 1H, H-5c), 3.01 – 2.91 (m, 3H, SCH₂CH₂O, H-3c, H-3b), 2.86 (dt, *J* = 12.8, 6.2 Hz, 1H, SCH₂CH₂O), 2.27 – 2.22 (m, 7H, CH₃CH₂CO, CH₃CO), 2.18 (s, 3H, CH₃CO), 2.17 (s, 3H, CH₃CO), 2.13 (s, 6H, CH₃CO), 2.07 (s, 3H, CH₃CO), 2.07 (s, 3H, CH₃CO), 2.05 (s, 3H, CH₃CO), 2.02 (s, 3H, CH₃CO), 2.01 (s, 1H, CH₃CO), 1.18 (t, *J* = 7.6 Hz, 3H, CH₃CH₂CO); ¹³C NMR (126 MHz, CDCl₃): δ 173.8, 170.6, 170.6, 170.6, 169.6, 169.4, 169.3, 169.3, 169.3 (12×CO), 75.7 (C-2b), 75.4 (C-2c), 72.6 (C-2a), 72.5 (C-4a), 70.5 (C-3a), 70.4 (C-4b, C-4c), 69.9 (SCH₂CH₂O), 69.5 (OCH₂CH₂NH), 61.9 (C-6b), 61.9 (C-6c), 59.4 (C-6a), 54.9 (C-3b), 54.7 (C-3c), 52.3 (C-1b), 49.4 (C-1c), 47.8 (C-1a), 46.9 (C-5a), 46.5 (C-5b), 43.3 (C-5c), 39.0 (OCH₂CH₂NH₂), 29.9 (SCH₂CH₂O), 29.7 (CH₃CH₂CO), 21.1, 20.9, 20.9, 20.8, 20.7, 20.7, 20.7, 20.6, 20.4, 20.2 (11×CH₃CO), 9.9 (CH₃CH₂CO); ESI-HRMS [M+Na]⁺ calcd. For C₄₅H₆₅NNaO₂₂S₆⁺ 1186.2215, found 1186.2207.

Propionylamide (**156**):

Peracetylated propionylamide **155** (9 mg, 7.7 μ mol) was suspended in anhydrous MeOH (0.5 mL) and NaOMe (freshly prepared 1M solution in MeOH) (25 μ L, 25 μ mol, 3.25 equiv) was added. The reaction mixture then was stirred until full consumption of the starting material was detected by LCMS. The reaction mixture then was quenched with Amberlite IR-120 (H⁺) ion-exchange resin (washed with MeOH, CH₂Cl₂) until pH 6, filtered, and the filtrate was concentrated to dryness. The crude product was purified by column chromatography on a C18 silica gel eluting with MeOH:H₂O (1:1) to give product as a colorless syrup (4.9 mg, 86%). *R_f* 0.59 (CH₂Cl₂:MeOH 4:1 (H₂SO₄/EtOH)); [α]_D²⁰⁻²² –11.1 (*c* 0.00027, DMSO); ¹H NMR (500

MHz, D₂O): δ 4.16 (d, J = 10.1 Hz, 1H, H-1a), 4.08 (d, J = 10.2 Hz, 1H, H-1b), 3.98 – 3.90 (m, 2H, H-3a, H-6a), 3.89 – 3.81 (m, 4H, H-1c, H-6c), 3.80 – 3.72 (m, 3H, H-4a, H-6a, H-6b), 3.68 (t, J = 6.1 Hz, 2H, SCH₂CH₂O), 3.61 – 3.48 (m, 6H, H-2b, H-2c, H-4c, H-6b, OCH₂CH₂NH), 3.45 – 3.40 (m, 2H, H-2a, H-4b), 3.30 (t, J = 5.3 Hz, 3H, OCH₂CH₂NH), 2.96 (d, J = 25.6 Hz, 2H, H-5c, H-5b), 2.92 – 2.86 (m, 3H, H-3b, H-5a, SCH₂CH₂O), 2.80 (td, J = 10.2, 7.2 Hz, 2H, H-3c, SCH₂CH₂O), 2.18 (q, J = 7.7 Hz, 2H, CH₃CH₂CO), 1.02 (t, J = 7.7 Hz, 3H, CH₃CH₂O); ¹³C NMR (126 MHz, D₂O): δ 178.3 (CO), 76.9 (C-4b), 76.3 (C-4c), 75.6 (C-3a), 73.9 (C-2a), 73.4 (C-4a), 70.9 (C-2b), 70.8 (C-2c), 69.6 (SCH₂CH₂O), 68.7 (OCH₂CH₂NH), 60.6 (C-6c), 60.6 (C-6b), 59.6 (C-3c), 59.5 (C-3b), 58.5 (C-6a), 50.8 (C-1c, C-5c), 50.6 (C-1b, C-5b), 48.1 (C-5a), 46.8 (C-1a), 39.0 (OCH₂CH₂NH), 30.3 (SCH₂CH₂O), 29.3 (CH₃CH₂CO), 9.7 (CH₃CH₂CO); ESI-HRMS [M+Na]⁺ calcd. For C₂₅H₄₅NNaO₁₂S₆⁺ 766.1159, found 766.1158.

Evaluation of inhibitory activity of glucoclusters 142, 146, 150, 154 and 156 (Figure 2.5, Table 2, and Table 3):

Inhibition of anti-CR3-FITC antibody staining of human neutrophils and of anti-Dectin 1-FITC antibody staining of mouse macrophages:

After harvesting and counting, cells (5×10⁵/tube) were pre-incubated for 30 min on ice with medium alone or with medium containing the glucoclusters **142**, **146**, **150**, **154** and **156** (1–10 μ M) in a final volume of 250 μ L. Then, 250 μ L of the antibodies diluted in staining buffer (PBS containing 1% heat-inactivated FBS and 1% sodium azide) were added and the tubes further incubated for 60 minutes on ice. The cells were then washed three times with ice-cold staining buffer, resuspended and fixed by incubation with 2% paraformaldehyde for at least 60 minutes. Before analysis, the cells were centrifuged and resuspended in 0.5 mL of staining buffer before analysis in a BD-FACSCanto instrument (Becton Dickinson).

Phagocytosis assay:

U937 cells were used in this experiment. Phagocytosis was measured using a Phagocytosis Assay kit (Green *E. coli*) (Abcam, ab235900) following the instructions provided by the manufacturer. Briefly, cells were

plated on 24-well plates at 1×10^6 cells per well. After an overnight incubation at 37 °C, the cells were incubated with several concentrations of the glucoclusters **142**, **146**, **150**, **154** and **156** (0.5–5 μ M) for 2h at 37 °C. A suspension of FITC-labeled *E. coli* was added to the wells and further incubated for 3h at 37 °C. After washing by centrifugation and aspiration, a quenching solution of Trypan blue was added and incubated for 5 minutes at room temperature. Cells were then washed and resuspended in ice-cold phagocytosis buffer (provided by the kit) and fluorescence read using a plate reader at excitation/emission 490/520 nm respectively.

We thank Dr. Rafael Fernandez-Botran from Department of Pathology and Laboratory Medicine, University of Louisville for conducting the inhibition assays on our behalf.

6.3. Experimental procedures for the PDB database search and synthesis of compounds described in Chapter 3

PDB database search (Scheme 31):

Glyvicinity search protocol:

The Glyvicinity tool¹⁷⁰ was used for initial search of the PDB database. Tryptophan (Trp), Tyrosine (Tyr), Histidine (His), and Phenylalanine (Phe) were selected as target amino acids. The search was performed separately for the following carbohydrate configurations: α,β -D-Manp, α,β -D-Glcp, α,β -D-Galp, α,β -D-GlcNAc, α,β -D-GalNAc, α,β -D-Xylp, α,β -D-Neu5Ac, and α,β -L-Fucp. The following data was collected from the search output: PDB ID, X-ray crystal structure resolution (Å), structure of the ligand, interacting amino acid.

Privateer analysis protocol:

Atomic model file and observed structure factors or intensities file were imported using PDB ID, and used as input data in CCP4 Privateer tool.¹⁷² After conformation analysis job was completed, the configuration and conformation of the carbohydrate epitope was verified (4C_1 for D-sugars, and 1C_4 for L-sugars), and the RSCC coefficient value was collected.

PyMOL analysis protocol:

The X-ray crystal structures were imported and visualized using PyMOL Molecular Graphics System, Schrodinger software.¹⁷³ The relative distances between *O*-1 or *O*-5 atoms of the carbohydrate epitope and closest carbon atoms of the aromatic ring (for oxygen to edge of the ring arrangement), and to the center of the ring (for stacking arrangement) were measured using Wizard/Measurement tool in the PyMOL. The final search output is summarized in **Table 8** in the Appendix.

Synthesis of 4-thiolactose (Scheme 33):

Methyl 2,3,6-tri-*O*-acetyl- α,β -D-galactopyranoside (168):

Following a reported protocol,¹⁸⁸ galactose (5 g, 0.028 mol) was added to an HCl solution in MeOH (prepared by dropwise addition of AcCl (2 mL, 0.028 mol) to MeOH (40 mL) at 0 °C) and refluxed until complete dissolution of galactose was observed. After that the reaction mixture was concentrated to dryness to give a mixture of methyl glycosides as a white foam, which was used in the next step without further purification. Thus, the methyl galactosides (5.16 g, 0.0266 mol) were dissolved in Py (30 mL) and CH₂Cl₂ (20 mL) and the reaction mixture was cooled down to –30 °C before AcCl (6.0 mL, 0.084 mol, 3.15 equiv) was added dropwise. The reaction mixture then was stirred for 6h with warming from –30 → 0 °C. After such time the reaction mixture was quenched with brine (10 mL) and diluted with EtOAc (100 mL). The organic layer was washed with 1M H₂SO₄ (2×100 mL), brine (100 mL), dried over Na₂SO₄ and concentrated to dryness. The crude residue was purified by flash column chromatography on silica gel eluting with hexanes : EtOAc (10→ 80%, EtOAc (v/v)) to give the product as a mixture of anomers (α : β = 8 : 1) as a colorless syrup (5.29 g, 59% over 2 steps) with spectral data matching that reported in literature.^{252, 253} *R*_f 0.35 (hexanes : EtOAc 1:1 (H₂SO₄/EtOH)); ¹H NMR (500 MHz, CDCl₃): δ 5.29 – 5.18 (m, 2H, H-2, H-3), 4.96 (d, *J* = 3.1 Hz, 1H, H-1), 4.40 – 4.29 (m, 1H, H-6a), 4.24 (dd, *J* = 11.5, 6.8 Hz, 1H, H-6b), 4.15 – 4.07 (m, 1H, H-4), 4.03 (t, *J* = 6.3 Hz, 1H, H-5), 3.39 (s, 3H, OCH₃), 2.62 (d, *J* = 4.4 Hz, 1H, OH), 2.09 (s, 3H, CH₃CO), 2.07 (s, 6H, 2×CH₃CO). ¹³C NMR (126 MHz, CDCl₃): δ 170.9, 170.4, 170.0 (3×CO), 97.1 (C-1), 70.0 (C-2), 68.1 (C-3), 67.7 (C-5), 67.3 (C-4), 62.8 (C-6), 55.3 (OCH₃), 20.8, 20.76, 20.74 (3×CH₃CO).

The minor β -isomer was identified in the mixture by the following diagnostic signals: 4.92 (dt, $J = 10.9$, 3.2 Hz, 1H, H-3), 4.37 (d, $J = 7.9$ Hz, 1H, H-1), 3.49 (s, 3H, OCH₃), 2.67 (d, $J = 5.8$ Hz, 1H, OH).

HRMS-ESI (m/z): [M+Na]⁺ calcd. for C₁₃H₂₀O₉Na⁺ 343.1000, found 343.0982.

Methyl 2,3,4,6-tetra-*O*-acetyl- β -D-galactopyranosyl-(1 \rightarrow 4)-2,3,6-tri-*O*-acetyl-4-thio-4-deoxy- α,β -D-glucopyranoside (169**):**

Methyl 2,3,6-tri-*O*-acetyl-D-galactopyranoside **168** (696 mg, 2 mmol) was dissolved in anhydrous CH₂Cl₂ (15 mL) and Py (5 mL). The reaction mixture then was cooled down to 0 °C and Tf₂O (845 μ L, 5 mmol, 2.5 equiv) was added dropwise. The reaction mixture then was stirred for 2h with warming from 0 \rightarrow 20 °C. After such time the reaction mixture was quenched with brine (10 mL) and diluted with CH₂Cl₂ (30 mL). The organic layer was washed with brine (2 \times 30 mL), dried over Na₂SO₄ and concentrated to dryness. The crude triflate **165** (600 mg, 1.33 mmol, 1.2 equiv) then was mixed with 2,3,4,6-tetra-*O*-acetyl-1-*S*-acetyl-1-thio- β -D-galactopyranoside¹⁸⁹ **166** (450 mg, 1.108 mmol) in anhydrous DMF (2 mL, 0.554 M) and NEt₂H (280 μ L, 0.7 mmol, 2.5 equiv) was added at 0 °C. The reaction mixture then was stirred until complete consumption of pentaacetate **166** was observed (monitored by TLC and LCMS). After the completion, the reaction mixture was quenched with brine (5 mL) and subsequently diluted with EtOAc (70 mL). The organic layer was separated, and the aqueous layer was additionally extracted with EtOAc (10 mL). The combined organic layers were washed with brine (70 mL), dried over Na₂SO₄ and concentrated to dryness. The crude product was purified by flash column chromatography on silica gel eluting with hexanes : EtOAc (10 \rightarrow 50%, EtOAc (v/v)) to give the product as a mixture of anomers (α : β = 20 : 1) as a foam (600 mg, 81%) with spectral data in agreement with that reported in the literature.²⁵⁴ R_f 0.22 (hexanes : EtOAc 1:1 (H₂SO₄/EtOH); ¹H NMR (500 MHz, CDCl₃): δ 5.53 – 5.29 (m, 2H, H-4Galp, H-3Glc), 5.06 (t, $J = 9.9$ Hz, 1H, H-2Galp), 4.99 (td, $J = 9.1$, 2.6 Hz, 1H, H-3Galp), 4.87 (d, $J = 3.7$ Hz, 1H, H-1Glc), 4.82 (dd, $J = 9.6$, 3.6 Hz, 1H, H-2Glc), 4.71 (d, $J = 9.8$ Hz, 1H, H-1Galp), 4.45 (d, $J = 3.1$ Hz, 2H, H-6aGlc, H-6bGlc), 4.07 (dt, $J = 10.6$, 2.9 Hz, 1H, H-5Glc), 4.02 (d, $J = 6.5$ Hz, 2H, H-6aGalp, H-6bGalp), 3.88 (t, $J = 6.5$ Hz, 1H, H-5Galp), 3.37 (s, 3H, OCH₃), 2.89 (t, $J = 11.1$ Hz, 1H, H-4Glc), 2.11

(s, 3H, CH₃CO), 2.06 (s, 4H, CH₃CO), 2.02 (s, 3H, CH₃CO), 2.01 (s, 3H, CH₃CO), 2.00 (s, 4H, CH₃CO), 1.98 (s, 3H, CH₃CO), 1.91 (s, 3H, CH₃CO); ¹³C NMR (126 MHz, CDCl₃): δ 170.6, 170.3, 170.3, 170.2, 169.9, 169.7, 169.5 (7×CO), 97.1 (C-1Glc), 82.5 (C-1Gal), 74.2 (C-5Gal), 72.3 (C-2Glc), 71.8 (C-3Gal), 69.0 (C-5Glc), 67.5 (C-2Gal), 67.1 (C-3Glc), 67.1 (C-4Gal), 63.5 (C-6Glc), 61.5 (C-6Gal), 55.6 (OCH₃), 46.4 (C-4Glc), 20.9, 20.8, 20.8, 20.7, 20.7, 20.6, 20.5 (7×CH₃CO). The minor β-isomer was identified in the mixture by the following diagnostic signal: 3.37 (s, 3H, OCH₃).

HRMS-ESI (*m/z*): [M+Na]⁺ calcd. for C₂₇H₃₈O₁₇NaS⁺ 689.1722, found 689.1705.

2,3,4,6-Tetra-*O*-acetyl-β-D-galactopyranosyl-(1→4)-1,2,3,6-tetra-*O*-acetyl-4-thio-4-deoxy-α,β-D-glucopyranoside (167):

Disaccharide **169** (356 mg, 0.534 mmol) was dissolved in Ac₂O (5 mL) and H₂SO₄ (98%wt, 3 drops) was added at 0 °C. The reaction mixture immediately turned yellow after the addition and was stirred at 0 °C until completion (detected by TLC and LCMS analysis). After completion, the reaction mixture was carefully quenched with NaHCO₃ (20 mL), diluted with CH₂Cl₂ (50 mL). The organic layer was separated, and the aqueous layer was additionally extracted with CH₂Cl₂ (2×30 mL). The combined organic layers were washed with brine (50 mL), dried over MgSO₄ and concentrated to dryness. The crude product was purified by flash column chromatography on silica gel eluting with hexanes : EtOAc (10→ 60%, EtOAc (v/v)) to give a mixture of anomeric acetates (α : β = 3.3 : 1) as a white foam (192 mg, 52%) with spectral data in agreement with that reported in the literature.²⁵⁴ *R*_f 0.19 and 0.17 (hexanes : EtOAc 1:1 (H₂SO₄/EtOH)).

167α:

¹H NMR (500 MHz, CDCl₃)⁶: δ 6.29 (d, *J* = 3.6 Hz, 1H, H-1Glc), 5.45 – 5.34 (m, 2H, H-3Glc, H-3Gal), 5.14 – 4.95 (m, 3H, H-2Glc, H-2Gal, H-4Gal), 4.70 (d, *J* = 9.8 Hz, 1H, H-1Gal), 4.50 – 4.37 (m, 2H, H-6aGlc, H-6bGlc), 4.25 (dt, *J* = 11.4, 2.8 Hz, 1H, H-5Glc), 4.14 – 3.83 (m, 3H, H-6aGal, H-6bGal, H-5Gal), 2.99 (t, *J* = 11.4 Hz, 1H, H-4Glc), 2.15 (s, 3H), 2.13 (s, 3H), 2.06 (s, 3H), 2.03 (s, 3H), 2.00 (s,

⁶ “Glc” and “Gal” refer to the glucose and galactose unit of disaccharide

6H), 1.98 (s, 3H), 1.93 (s, 3H, each CH_3CO); ^{13}C NMR (126 MHz, CDCl_3): δ 170.4, 170.3, 170.2, 107.2, 169.9, 169.8, 169.5, 168.8 ($8\times\text{CO}$), 89.6 (C-1Glc), 82.8 (C-1Galp), 74.4 (C-5Galp), 71.8 (C-5Glc), 71.7 (C-2Galp, C-2Glc), 70.7 (C-2Glc), 67.1 (C-3Glc), 67.0 (C-4Galp, C-3Galp), 63.2 (C-6Glc), 61.9 (C-6Galp), 46.2 (C-4Glc), 20.9, 20.9, 20.7, 20.7, 20.6, 20.6, 20.6, 20.5 ($8\times\text{CH}_3\text{CO}$).

167 β :

^1H NMR (500 MHz, CDCl_3): δ 5.62 (d, $J = 8.4$ Hz, 1H, H-1Glc), 5.45 – 5.34 (m, 1H, H-3Galp), 5.28 – 5.19 (m, 1H, H-3Glc), 5.14 – 4.95 (m, 3H, H-2Glc, H-2Galp, H-4Galp), 4.74 (d, $J = 9.8$ Hz, 1H, H-1Galp), 4.50 – 4.37 (m, 2H, H-6aGlc, H-6bGlc), 4.14 – 3.83 (m, 4H, H-6aGalp, H-6bGalp, H-5Galp, H-5Glc), 2.99 (t, $J = 11.4$ Hz, 1H, H-4Glc), 2.13 (s, 3H), 2.08 (s, 3H), 2.04 (s, 3H), 2.03 (s, 3H), 2.00 (s, 6H), 1.98 (s, 3H), 1.92 (s, 3H, each CH_3CO); ^{13}C NMR (126 MHz, CDCl_3): δ 170.4, 170.3, 170.2, 170.2, 169.9, 169.8, 169.5, 168.8 ($8\times\text{CO}$), 91.7 (C-1Glc), 81.6 (C-1Galp), 74.7 (C-5Galp, C-5Glc), 71.7 (C-2Galp, C-2Glc), 69.8 (C-3Glc), 67.3 (C-3Galp), 63.4 (C-6Glc), 62.6 (C-6Galp), 45.9 (C-4Glc), 20.9, 20.9, 20.7, 20.7, 20.6, 20.6, 20.6, 20.5 ($8\times\text{CH}_3\text{CO}$).

HRMS-ESI (m/z): $[\text{M}+\text{Na}]^+$ calcd. for $\text{C}_{28}\text{H}_{38}\text{O}_{18}\text{NaS}^+$ 717.1671, found 717.1675.

β -D-Galactopyranosyl-(1 \rightarrow 4)-4-thio-4-deoxy-D-glucopyranose (170):

Octaacetate **167** (172 mg, 0.248 mmol) was dissolved in anhydrous MeOH (5 mL) and NaOMe (4 mg, 0.0744 mmol, 0.3 equiv) and the reaction mixture was stirred until completion (detected by LCMS). After the completion, the reaction mixture was quenched with Amberlite IR120 ion-exchanger (H^+) until pH 4-5. The reaction mixture then was filtered, and the filtrate was concentrated to dryness to give product as mixture of anomeric hemiacetals ($\alpha : \beta = 1.26 : 1$) as a white foam (76 mg, 85%) with spectral data in agreement with that reported in the literature.²⁵⁴

170 α :

^1H NMR (500 MHz, D_2O)⁷: δ 5.17 (d, $J = 3.7$ Hz, 1H, H-1Glc), 4.57 – 4.42 (m, 1H, H-1Galp), 4.06 – 3.94 (m, 2H, H-6aGalp, H-6bGalp), 3.93 – 3.79 (m, 2H, H-6aGlc, H-6bGlc), 3.74 – 3.53 (m, 5H, H-3Glc,

⁷ “Glc” and “Galp” refer to the glucose and galactose unit of disaccharide.

H-3Galp, H-4Galp, H-5Galp, H-5Glc), 3.52 – 3.38 (m, 2H, H-2Galp, H-2Glc), 2.78 (t, $J = 10.8$ Hz, 1H, H-4Glc); ^{13}C NMR (126 MHz, D_2O): δ 92.2 (C-1Glc), 84.4 (C-1Galp), 79.1 (C-5Glc), 76.5 (C-5Galp, C-4Galp), 72.7 (C-3Galp), 71.8 (C-3Glc), 69.9 (C-2Galp), 69.7 (C-2Glc), 61.6 (C-6 Galp), 61.3 (C-6Glc), 47.4 (C-4Glc).

170 β :

^1H NMR (500 MHz, D_2O): δ 4.57 – 4.42 (m, 2H, H-1Galp, H-1Glc), 3.93 – 3.79 (m, 2H, H-6aGalp, H-6bGalp), 3.74 – 3.53 (m, 6H, H-5Glc, H-5Galp, H-4Galp, H-3Galp, H-6bGlc, H-6aGlc), 3.52 – 3.38 (m, 2H, H-3Glc, H-2Galp), 3.18 (t, $J = 8.5$ Hz, 1H, H-2Glc), 2.78 (t, $J = 10.8$ Hz, 1H, H-4Glc); ^{13}C NMR (126 MHz, D_2O): δ 95.7 (C-1Glc), 84.4 (C-1Galp), 79.1 (C-5Glc), 76.5 (C-5Galp), 75.4 (C-2Glc), 73.9 (C-3Galp), 73.1 (C-2Galp), 69.9 (C-3Glc), 68.8 (C-4Galp), 61.6 (C-6Glc), 61.3 (C-6Galp), 47.4 (C-4Glc).

HRMS-ESI (m/z): $[\text{M}+\text{Na}]^+$ calcd. for $\text{C}_{12}\text{H}_{22}\text{O}_{10}\text{NaS}^+$ 381.0826, found 381.0824.

Synthesis of 5-thiogalactose (Scheme 35):

Methyl 4,6-*O*-benzylidene-5-thio- α,β -D-glucopyranoside (176):

Thioacetate **75** (8 g, 0.022 mol) was dissolved in 50% aq TFA (60 mL) and the reaction mixture was stirred for 16h at 20 °C. After such time the reaction mixture was concentrated to dryness and co-evaporated with toluene (3×30 mL). The crude was dissolved in MeOH (30 mL) and NaOMe (1.19 g, 0.022 mol) was added portion-wise until pH 10, and the reaction mixture then was stirred for 1h at 20 °C. After such time the reaction mixture was quenched with Amberlyst 15 (H^+) until pH 3-4. The resulting suspension was filtered, and the filtration cake was additionally washed with MeOH (30 mL). The filtrate was then collected, HCl (2M solution in Et_2O , 11 mL, 0.022 mol) was added, and the resulting solution was heated until reflux for 36h. After such time the reaction mixture was allowed to cool down, and, subsequently, concentrated to dryness. The crude was taken into anhydrous DMF (20 mL) and MeCN (20 mL) followed by addition of benzaldehyde dimethyl acetal (10 mL, 0.066 mol, 3 equiv) and PTSA (5.2 g, 0.0275 mol, 1.25 equiv). The reaction mixture then was stirred for 12h at 20 °C. After such time the reaction mixture was diluted with

EtOAc (100 mL), washed with H₂O (100 mL), sat aq NaHCO₃ (100 mL), brine (100 mL), dried over MgSO₄, and concentrated to dryness. The crude product was purified by flash column chromatography on silica gel eluting with hexanes : EtOAc (10→ 60%, EtOAc (v/v)) to give the product as a mixture of anomers (α : β = 4 : 1) as a colorless syrup (2.03 g, 30% over 4 steps). R_f 0.12 (hexanes : EtOAc 1:1 (H₂SO₄/EtOH));

176 α :

¹H NMR (500 MHz, CDCl₃): δ 7.52 – 7.45 (m, 3H, Ar), 7.39 – 7.29 (m, 2H, Ar), 5.55 (s, 1H, PhCH), 4.46 (d, J = 2.7 Hz, 1H, H-1), 4.18 (dd, J = 10.9, 4.7 Hz, 1H, H-6a), 3.88 – 3.64 (m, 4H, H-3, H-4, H-2, H-6b), 3.41 (s, 3H, OCH₃), 3.23 (ddd, J = 11.3, 10.0, 4.7 Hz, 1H, H-5); ¹³C NMR (126 MHz, CDCl₃): δ 137.3, 129.2, 128.3, 128.2, 126.3, 126.2 (6 \times Ar), 101.8 (PhCH), 85.3 (C-1), 83.9 (C-4), 83.6 (C-3), 75.5 (C-2), 72.0 (C-6), 68.4 (C-6), 56.6 (OCH₃), 34.7 (C-5).

176 β :

¹H NMR (500 MHz, CDCl₃): δ 7.52 – 7.45 (m, 3H, Ar), 7.39 – 7.29 (m, 2H, Ar), 5.55 (s, 1H, PhCH), 4.38 (d, J = 9.0 Hz, 1H, H-1), 4.24 – 4.20 (m, 1H, H-6a), 3.88 – 3.64 (m, 4H, H-2, H-3, H-4), 3.51 (s, 3H, OCH₃), 2.94 – 2.86 (m, 1H, H-5); ¹³C NMR (126 MHz, CDCl₃): δ 137.3, 129.2, 128.3, 128.2, 126.3, 126.2 (6 \times Ar), 101.8 (PhCH), 83.9 (C-1), 83.0 (C-4), 77.2 (C-3), 76.97 (C-2), 74.7 (C-6), 58.7 (OCH₃), 34.9 (C-5).

HRMS-ESI (m/z): [M+Na]⁺ calcd. for C₁₄H₁₈O₅NaS⁺ 321.0767, found 321.0749.

Methyl 2,3-di-*O*-benzyl-4,6-*O*-benzylidene-5-thio- α,β -D-glucopyranoside (172):

Methyl 4,6-*O*-benzylidene-5-thio-D-glucopyranoside **176** (1.7 g, 5.7 mmol) was dissolved in anhydrous DMF (30 mL) and NaH (60% dispersion in the mineral oil, 910 mg, 22.8 mmol, 4 equiv) was added at 0 °C portion-wise followed by BnBr (4.1 mL, 34.47 mmol, 6.05 equiv). The reaction mixture then was stirred for 5h at 0 → 20 °C. After such time the reaction mixture was quenched with MeOH (10 mL), diluted with EtOAc (100 mL), washed with H₂O (100 mL), dried over MgSO₄, and concentrated to dryness. The crude was purified by flash column chromatography on silica gel eluting with hexanes : EtOAc (0 → 20%, EtOAc

(v/v)) to give product as a mixture of anomers ($\alpha : \beta = 17 : 1$) as a yellowish syrup (1.59 g, 59%). R_f 0.44 and 0.48 (hexanes : EtOAc 9:1 (UV and H₂SO₄/EtOH)); ¹H NMR (500 MHz, CDCl₃): δ 7.56 – 7.46 (m, 2H, Ar), 7.42 – 7.23 (m, 13H, Ar), 5.66 (s, 1H, PhCH), 4.92 – 4.80 (m, 3H, PhCH₂), 4.70 (d, $J = 12.1$ Hz, 1H, PhCH₂), 4.45 (d, $J = 2.9$ Hz, 1H, H-1), 4.24 (dd, $J = 10.9, 4.6$ Hz, 1H, H-6a), 4.01 (t, $J = 9.1$ Hz, 1H, H-3), 3.94 (t, $J = 9.5$ Hz, 1H, H-4), 3.82 (dd, $J = 9.2, 2.9$ Hz, 1H, H-2), 3.74 (t, $J = 11.2$ Hz, 1H, H-6b), 3.45 (s, 3H, OCH₃), 3.33 (ddd, $J = 11.3, 9.8, 4.6$ Hz, 1H, H-5); ¹³C NMR (126 MHz, CDCl₃): δ 138.9, 138.4, 137.9, 129.0, 128.6, 128.4, 128.4, 128.3, 128.2, 128.0, 127.7, 126.1 (12×Ar), 101.4 (PhCH), 85.0 (C-4), 83.5 (C-2), 83.1 (C-1), 80.4 (C-3), 76.6, 73.7 (2×PhCH₂), 68.7 (C-6), 56.8 (OCH₃), 35.3 (C-5). The minor β -isomer was identified in mixture by the following diagnostic signals: 4.77 (d, $J = 10.8$ Hz, 2H, PhCH₂), 4.58 (d, $J = 8.5$ Hz, 1H, H-1), 4.30 (dd, $J = 11.1, 4.7$ Hz, 1H, H-6a), 3.57 (s, 3H, OCH₃). HRMS-ESI (m/z): [M+Na]⁺ calcd. for C₂₈H₃₀O₅NaS⁺ 501.1706, found 501.1690.

Methyl 2,3-di-*O*-benzyl-5-thio- α,β -D-glucopyranoside (177):

Methyl 2,3-di-*O*-benzyl-4,6-*O*-benzylidene-5-thio-D-glucopyranoside **172** (1.7 g, 3.55 mmol) was dissolved in MeOH (30 mL) and PTSA (1.35 g, 7.1 mmol, 2 equiv) was added, and the reaction mixture then was stirred until completion (detected by TLC and LCMS). After complete consumption of the starting material the reaction mixture was quenched with NaHCO₃ (30 mL) and methanol was removed under reduced pressure. The remaining solution was diluted with EtOAc (80 mL), washed with brine (80 mL), dried over MgSO₄, and concentrated to dryness. The crude was purified by flash column chromatography on silica gel eluting with hexanes : EtOAc (0 → 50%, EtOAc (v/v)) to give the product as a mixture of anomers ($\alpha : \beta = 17 : 1$) as a colorless syrup (870 mg, 63%). R_f 0.31 (hexanes : EtOAc 1:1 (H₂SO₄/EtOH)); ¹H NMR (500 MHz, CDCl₃): δ 7.43 – 7.26 (m, 10H), 5.06 (d, $J = 11.3$ Hz, 1H, PhCH₂), 4.73 (d, $J = 11.9$ Hz, 1H, PhCH₂), 4.65 (d, $J = 11.7$ Hz, 2H, PhCH₂), 4.41 (d, $J = 2.6$ Hz, 1H, H-1), 3.83 – 3.71 (m, 5H, H-6a, H-6b, H-3, H-4, H-2), 3.43 (s, 3H, OCH₃), 3.17 – 3.07 (m, 1H, H-5), 2.68 (br, 2H, OH); ¹³C NMR (126 MHz, CDCl₃): δ 138.5, 138.0, 128.8, 128.6, 128.2, 128.1, 128.1, 128.1 (8×Ar), 83.9 (C-2), 82.4 (C-3), 82.1 (C-1), 76.8 (C-4), 76.1, 72.9 (2×PhCH₂), 63.8 (C-6), 56.7 (OCH₃), 41.8 (C-5). The minor β -isomer was

identified in mixture by the following diagnostic signals: 4.50 (d, $J = 7.5$ Hz, 1H, H-1), 3.52 (s, 3H, OCH₃).

HRMS-ESI (m/z): [M+Na]⁺ calcd. for C₂₁H₂₆O₅NaS⁺ 413.1392 found 413.1379.

Methyl 2,3-di-*O*-benzyl-6-*O*-triisopropylsilyl-5-thio- α,β -D-glucopyranoside (178):

Methyl 2,3-di-*O*-benzyl-5-thio-D-glucopyranoside **177** (868 mg, 2.22 mmol) was dissolved in anhydrous DMF (15 mL) and imidazole (302 mg, 4.44 mmol, 2 equiv) was added followed by TIPSCl (710 μ L, 3.33 mmol, 1.5 equiv) and the reaction mixture was stirred for 1.5h at 20 °C. After such time an additional amount of imidazole (150 mg, 2.22 mmol) and TIPSCl (710 μ L, 3.33 mmol, 1.5 equiv) was added and the reaction mixture was stirred for 2h. After such time the reaction mixture was quenched with MeOH (10 mL), diluted with EtOAc (80 mL), washed with H₂O (80 mL), brine (80 mL), dried over MgSO₄, and concentrated to dryness. The crude product was purified by flash column chromatography on silica gel eluting with hexanes : EtOAc (0 \rightarrow 50%, EtOAc (v/v)) to give the product as a mixture of anomers ($\alpha : \beta = 33 : 1$) as a colorless syrup (930 mg, 76%). R_f 0.59 (hexanes : EtOAc 4:1 (H₂SO₄/EtOH)); ¹H NMR (500 MHz, CDCl₃): δ 7.66 – 6.91 (m, 10H, Ar), 5.02 (d, $J = 11.1$ Hz, 1H, PhCH₂), 4.80 – 4.62 (m, 3H, PhCH₂), 4.42 (d, $J = 2.8$ Hz, 1H, H-1), 4.07 (dd, $J = 10.3, 4.8$ Hz, 1H, H-6A), 3.89 (dd, $J = 10.3, 4.4$ Hz, 1H, H-6b), 3.87 – 3.67 (m, 3H, H-2, H-3, H-4), 3.43 (s, 3H, OCH₃), 3.07 (dt, $J = 9.7, 4.6$ Hz, 1H, H-5), 2.98 (d, $J = 1.7$ Hz, 1H, OH), 1.27 – 0.90 (m, 21H, 3 \times CH(CH₃)₂); ¹³C NMR (126 MHz, CDCl₃): δ 138.7, 138.2, 128.5, 128.4, 128.1, 128.0, 127.8, 127.8 (8 \times Ar), 84.0 (C-2), 83.0 (C-3), 81.9 (C-1), 76.2 (PhCH₂), 74.5 (C-4), 72.8 (PhCH₂), 62.7 (C-6), 56.3 (OCH₃), 43.2 (C-5), 17.9 (CH(CH₃)₂), 11.9 (CH(CH₃)₂). The minor β -isomer was identified in mixture by the following diagnostic signals: 4.47 (d, $J = 7.5$ Hz, 1H, H-1), 3.53 (s, 3H, OCH₃). HRMS-ESI (m/z): [M+Na]⁺ calcd. for C₃₀H₄₆O₅NaSSi⁺ 569.2727, found 569.2726.

Methyl 2,3-di-*O*-benzyl-6-*O*-triisopropylsilyl-5-thio- α,β -D-galactopyranoside (179):

Methyl 2,3-di-*O*-benzyl-6-*O*-triisopropylsilyl-5-thio-D-glucopyranoside **178** (1.1 g, 2.01 mmol) was dissolved in anhydrous CH₂Cl₂ : DMSO = 2 : 1 (v/v) (22.5 mL) and DIPEA (1.75 mL, 10.05 mmol, 5 equiv) was added. The reaction mixture was then cooled down to 0 °C and Py•SO₃ (800 mg, 5.025 mmol, 2.5

equiv) was added at 0 °C. The reaction mixture then was stirred for 1h with warming from 0 → 20 °C. After such time the reaction mixture was quenched with H₂O (5 mL), diluted with CH₂Cl₂ (50 mL), washed with NaHCO₃ (60 mL), brine (60 mL), dried over MgSO₄, and concentrated to dryness. The crude ketosugar was redissolved in anhydrous THF (20 mL) and the reaction mixture was cooled down to -78 °C before L-selectride (1M solution in THF, 4 mL, 4 mmol, 2 equiv) was added. The reaction mixture then was stirred for 1h at -78 °C, before acetone (5 mL) was added to quench the reaction. After that the reaction mixture was allowed to warm up to the room temperature (20 °C), diluted with EtOAc (70 mL), washed with H₂O (60 mL), brine (60 mL), dried over MgSO₄, and concentrated to dryness. The crude product was purified by flash column chromatography on silica gel eluting with hexanes : EtOAc (0 → 20%, EtOAc (v/v)) to give product as a mixture of anomers (α : β = 24 : 1) as a colorless syrup (683 mg, 62% over 2 steps). *R_f* 0.18 (hexanes : EtOAc 9:1 (H₂SO₄/EtOH)); ¹H NMR (500 MHz, CDCl₃): δ 7.44 – 7.21 (m, 10H, Ar), 4.91 – 4.76 (m, 2H, PhCH₂), 4.76 – 4.60 (m, 2H, PhCH₂), 4.41 (d, *J* = 3.0 Hz, 1H, H-1), 4.37 (d, *J* = 2.3 Hz, 1H, H-4), 4.07 (dd, *J* = 9.8, 3.0 Hz, 1H, H-2), 3.91 (dd, *J* = 9.9, 7.7 Hz, 1H, H-6a), 3.82 – 3.72 (m, 2H, H-6b, H-3), 3.42 (s, 3H, OCH₃), 3.23 (ddd, *J* = 7.3, 5.3, 1.5 Hz, 1H, H-5), 2.79 (d, *J* = 3.0 Hz, 1H, OH), 1.11 – 0.96 (m, 21H, 3×CH(CH₃)₂); ¹³C NMR (126 MHz, CDCl₃): δ 138.6, 138.4, 128.3, 128.3, 128.0, 127.8, 127.7, 127.6 (8×Ar), 82.7 (C-1), 79.6 (C-2), 78.8 (C-3), 73.5, 73.4 (2×PhCH₂), 69.1 (C-4), 62.7 (C-6), 56.5 (OMe), 43.3 (C-5), 17.9, 17.9 (CH(CH₃)₂), 11.8 (CH(CH₃)₂). The minor β -isomer was identified in mixture by the following diagnostic signals: 4.46 (d, *J* = 7.9 Hz, 1H, H-1), 3.52 (s, 3H, OCH₃).

HRMS-ESI (*m/z*): [M+Na]⁺ calcd. for C₃₀H₄₆O₅NaSSi⁺ 569.2727, found 569.2723.

Methyl 2,3,4,6-tetra-*O*-acetyl-5-thio- α,β -D-galactopyranoside (180):

Methyl 2,3-di-*O*-benzyl-6-*O*-triisopropylsilyl-5-thio-D-galactopyranoside **179** (617 mg, 1.13 mmol) was dissolved in anhydrous CH₂Cl₂ (20 mL) and the reaction mixture was cooled down to 0 °C and BCl₃ (1M solution in THF (5.7 mL, 5.7 mmol, 5.04 equiv) was added. The reaction mixture then was stirred for 16h at 0 °C. After such time the reaction mixture was quenched with MeOH (20 mL) and concentrated to dryness. The crude was taken into Py (15 mL) and CH₂Cl₂ (10 mL) followed by addition of Ac₂O (2 mL,

22.6 mmol, 20 equiv). The reaction mixture then was stirred for 16h at 20 °C. After such time the reaction mixture was quenched with MeOH (20 mL) at 0 °C, diluted with CH₂Cl₂ (60 mL), washed with H₂O (70 mL), 1M H₂SO₄ (70 mL), NaHCO₃ (70 mL), brine (60 mL), dried over MgSO₄, and concentrated to dryness. The crude was purified by flash column chromatography on silica gel eluting with hexanes : EtOAc (0 → 50%, EtOAc (v/v)) to give the product as a mixture of anomers (α : β = 8 : 1) as a colorless syrup (112 mg, 26% over 2 steps). *R_f* 0.44 (hexanes : EtOAc 3:2 (H₂SO₄/EtOH)); ¹H NMR (500 MHz, CDCl₃): δ 5.62 (d, *J* = 3.0, 1H, H-4), 5.43 – 5.22 (m, 2H, H-3, H-2), 4.65 (d, *J* = 2.7 Hz, 1H, H-1), 4.05 (dd, *J* = 11.2, 9.3 Hz, 1H, H-6a), 3.95 (dd, *J* = 11.2, 5.8 Hz, 1H, H-6b), 3.63 – 3.55 (m, 1H, H-5), 3.40 (s, 3H, OCH₃), 2.11 (s, 3H), 2.04 (s, 3H), 2.01 (s, 3H), 1.93 (s, 3H, 4×CH₃CO); ¹³C NMR (126 MHz, CDCl₃): δ 170.2, 170.18, 170.18, 169.6 (4×CO), 81.6 (C-1), 71.2 (C-2), 68.33 (C-4), 68.26 (C-3), 60.9 (C-6), 56.6 (OCH₃), 38.1 (C-5), 20.7, 20.6, 20.5, 20.4 (4×CH₃CO). The minor β -isomer was identified in mixture by the following diagnostic signals: 5.54 (t, *J* = 2.9 Hz, 1H, H-3), 4.48 (d, *J* = 7.9 Hz, 1H, H-1), 3.42 (s, 3H, OCH₃).

HRMS-ESI (*m/z*): [M+Na]⁺ calcd. for C₁₅H₂₂O₉NaS⁺ 401.0877, found 401.0865.

1,2,3,4,6-Penta-*O*-acetyl-5-thio- α,β -D-galactopyranoside (181):

Methyl 2,3,4,6-tetra-*O*-acetyl-5-thio-D-galactopyranoside **180** (112 mg, 0.296 mmol) was dissolved in Ac₂O (10 mL) and AcOH (5 mL) and the reaction mixture was cooled down to 0 °C before conc H₂SO₄ (3 drops) was added, and the reaction mixture was stirred for 12h at 0 °C. After such time the reaction mixture was quenched with MeOH (25 mL), diluted with CH₂Cl₂ (60 mL), washed with sat aq NaHCO₃ (60 mL), brine (60 mL), dried over MgSO₄, and concentrated to dryness. The crude was purified by flash column chromatography on silica gel eluting with hexanes : EtOAc (0 → 50%, EtOAc (v/v)) to give a mixture of anomeric acetates (α : β = 30 : 1) as a colorless syrup (84 mg, 73% over 2 steps) with spectral data matching the one reported in the literature.²⁵⁵ *R_f* 0.49 (hexanes : EtOAc 1:1 (H₂SO₄/EtOH)); ¹H NMR (500 MHz, CDCl₃): δ 6.19 (d, *J* = 3.2 Hz, 1H, H-1), 5.72 (dd, *J* = 3.0, 1.7 Hz, 1H, H-4), 5.46 (dd, *J* = 10.8, 3.2 Hz, 1H, H-2), 5.31 (dd, *J* = 10.8, 3.0 Hz, 1H, H-3), 4.12 (dd, *J* = 11.2, 8.8 Hz, 1H, H-6a), 3.98 (dd, *J* = 11.2, 6.1 Hz, 1H, H-6b), 3.82 (ddd, *J* = 8.2, 6.0, 1.7 Hz, 1H, H-5), 2.17 (s, 6H, 2×CH₃CO), 2.06 (s, 3H), 2.01 (s, 3H),

2.00 (s, 3H, 3×CH₃CO); ¹³C NMR (126 MHz, CDCl₃): δ 170.25, 170.24, 170.0, 169.8, 169.1 (5×CO), 71.2 (C-1), 69.4 (C-2), 68.6 (C-3), 68.0 (C-4), 61.0 (C-6), 39.5 (C-5), 20.9, 20.7, 20.7, 20.6, 20.6 (5×CH₃CO).

The minor β-isomer was identified in the mixture by the following diagnostic signal: 5.86 (d, *J* = 7.0 Hz, 1H, H-1).

HRMS-ESI (*m/z*): [M+Na]⁺ calcd. for C₁₆H₂₂O₁₀NaS⁺ 429.0826, found 429.0817.

Attempted synthesis of 5-thio-α,β-D-galactopyranose (182):

Peracetylated 5-thiogalactose **181** (43 mg, 0.106 mmol) was dissolved in anhydrous MeOH (10 mL) and NaOMe (2.29 mg, 0.0424 mmol, 0.4 equiv) was added and the reaction mixture was stirred at 20 °C until complete deprotection of the starting material was observed by TLC and LCMS. After that the reaction mixture was quenched with Amberlyst 15 (H⁺) and the reaction mixture was filtered. The filtrate was concentrated to dryness to give crude product as a yellowish syrup. The crude was purified by a flash column chromatography on a C18 silica gel eluting with H₂O : MeOH (0 → 50 %) to give a mixture of products that underwent caramelization upon removal of the solvent under *vacuo*.

Synthesis of methyl 5-thiogalactoside (Scheme 36):

Methyl 2,3,6-tetra-O-acetyl-5-thio-α,β-D-glucopyranoside (183):

1,2,3,4,6-Penta-O-benzoyl-5-thio-5-deoxy-D-glucopyranoside¹⁸⁹ **182** (1.9 g, 2.65 mmol) was suspended in anhydrous MeOH (30 mL) and NaOMe (1M solution in MeOH, 1 mL, 1 mmol, 0.4 equiv) was added and the reaction mixture was stirred at 20 °C until completion (monitored by TLC and LCMS analysis). After 2h the reaction was quenched with Amberlite IRC120 (H⁺) ion-exchange resin (washed with H₂O, MeOH) until pH 6. After that the reaction mixture was filtered and the filtrate was concentrated under reduced pressure. The crude product was dissolved in H₂O (40 mL) and washed with Et₂O (3×40 mL) and concentrated to dryness. The residue then was redissolved in anhydrous MeOH (30 mL) and HCl (2M solution in Et₂O, 1.33 mL, 2.66 mmol, 1 equiv) was added and the reaction mixture stirred under reflux conditions until completion (monitored by LCMS). After 24 h, the reaction mixture was concentrated to dryness and the crude was taken up in pyridine (10 mL) and CH₂Cl₂ (5 mL), followed by addition of Ac₂O

(3 mL) at 0 °C. The reaction mixture then was stirred for 12h at 0→20 °C. After such time the reaction was quenched with MeOH (10 mL) at 0 °C, diluted with EtOAc (100 mL), washed with H₂O (3×70 mL), dried over MgSO₄ and concentrated to dryness. The crude was purified by flash column chromatography on silica gel eluting with hexanes : EtOAc (0→ 30%, EtOAc (v/v)) to give a mixture of anomers (α : β = 7.14 : 1) as colorless syrup (453 mg, 45% over 3 steps) with spectral data identical to that reported in the literature.⁹⁰,²⁵⁶ ¹H NMR (500 MHz, CDCl₃): δ 5.48 (t, J = 9.8 Hz, 1H, H-4), 5.35 – 5.22 (m, 1H, H-3), 5.18 (dd, J = 10.2, 2.0 Hz, 1H, H-2), 4.67 (d, J = 2.9 Hz, 1H, H-1), 4.38 (dd, J = 12.0, 4.7 Hz, 1H, H-6a), 4.05 (dd, J = 12.0, 3.2 Hz, 1H, H-6b), 3.44 (s, 3H, OCH₃), 3.42 – 3.33 (m, 1H, H-5), 2.07 (s, 3H, CH₃CO), 2.06 (s, 3H, CH₃CO), 2.02 (s, 3H, CH₃CO), 2.0 (s, 3H, CH₃CO); ¹³C NMR (126 MHz, CDCl₃): δ 170.7, 170.2, 169.8, 169.6 (4×CO), 81.2 (C-1), 74.9 (C-2), 72.2 (C-3), 70.9 (C-4), 61.4 (C-6), 56.7 (OCH₃), 38.3 (C-5), 20.9, 20.7, 20.6, 20.6 (4×CH₃CO). The minor β -isomer was identified in mixture by the following diagnostic signals: 4.52 (d, J = 8.3 Hz, 1H, H-1), 4.29 (dd, J = 11.7, 5.6 Hz, 1H, H-6a), 4.15 (dd, J = 11.8, 4.0 Hz, 1H, H-6b), 3.49 (s, 3H, OCH₃).

HRMS-ESI (m/z): [M+Na]⁺ calcd. for C₁₅H₂₂O₉NaS⁺ 401.0877, found 401.0866.

Methyl 2,3,6-tri-*O*-benzoyl-5-thio-5-deoxy- α,β -D-glucopyranoside (184):

Methyl 2,3,4,6-tri-*O*-acetyl-5-thio-D-glucopyranoside **183** (453 mg, 1.197 mmol) was dissolved in anhydrous MeOH (10 mL) and NaOMe (1M solution in MeOH, 0.48 mL, 0.48 mmol, 0.4 equiv) was added and the reaction mixture was stirred until completion (detected by TLC and LCMS analysis). After 1h the reaction mixture was quenched with Dowex 50X8 (H⁺) ion-exchange resin (washed with H₂O, MeOH) until pH 6 and the resulting mixture was filtered. The filtrate was concentrated to dryness, and the crude product was taken up in Py (4 mL) and CH₂Cl₂ (3 mL). The reaction mixture was cooled down to 0 °C and BzCl (280 μ L, 2.41 mmol, 2 equiv) was added dropwise, and the reaction mixture was stirred with warming 0→20 °C for 1h. After such time further BzCl (170 μ L, 1.46 mmol, 1.2 equiv) was added and the reaction mixture was stirred for 1h. After such time the reaction was quenched with MeOH (10 mL), diluted with CH₂Cl₂ (40 mL), washed with H₂O (2×30 mL), brine (30 mL), dried over MgSO₄ and concentrated to

dryness. The crude product was purified by flash column chromatography on silica gel eluting with hexanes : EtOAc (0 → 30%, EtOAc (v/v)) to give a mixture of anomers (α : β = 9 : 1) as a white foam (252 mg, 40% over 2 steps). R_f 0.49 (hexanes : EtOAc 3:2 (UV, H₂SO₄/EtOH); ¹H NMR (500 MHz, CDCl₃): δ 8.13 – 7.99 (m, 3H, Ar), 7.98 – 7.91 (m, 4H, Ar), 7.66 – 7.40 (m, 4H, Ar), 7.39 – 7.29 (m, 4H, Ar), 5.84 (t, J = 9.7 Hz, 1H, H-4), 5.55 (dd, J = 10.2, 2.8 Hz, 1H, H-2), 5.07 (dd, J = 11.9, 4.0 Hz, 1H, H-6a), 4.87 (d, J = 2.9 Hz, 1H, H-1), 4.53 (dd, J = 11.8, 3.1 Hz, 1H, H-6b), 4.09 (dd, J = 9.8, 5.3 Hz, 1H, H-3), 3.54 – 3.46 (m, 4H, H-5, OCH₃), 3.28 (d, J = 5.4 Hz, 1H, OH); ¹³C NMR (126 MHz, CDCl₃): δ 167.0, 166.9, 166.1 (3×CO), 133.5, 133.4, 133.3, 130.0, 129.9, 129.9, 129.9, 129.6, 129.5, 129.3, 128.6, 128.5, 128.5, 128.4, 128.4 (15×Aryl), 81.6 (C-1), 75.4 (C-2), 74.1 (C-4), 73.3 (C-3), 62.7 (C-6), 56.9 (OCH₃), 41.6 (C-5). The minor β -isomer was identified in mixture by the following diagnostic signals: 5.68 (t, J = 10.0 Hz, 1H, H-4), 3.49 (s, 3H, OCH₃). HRMS-ESI (m/z): [M+Na]⁺ calcd. for C₂₈H₂₆O₈NaS⁺ 545.1241, found 545.1204

Methyl 2,3,4,6-tetra-*O*-benzoyl-5-thio-5-deoxy- α,β -D-galactopyranoside (186):

Methyl glycoside **184** (219 mg, 0.419 mmol) was dissolved in anhydrous CH₂Cl₂ (10 mL) and Dess-Martin periodinane (319 mg, 0.754 mmol, 1.8 equiv) was added. The reaction mixture was stirred for 1.5h at 20 °C. After such time 1M aq Na₂S₂O₃ (10 mL) was added followed by sat aq NaHCO₃ (10 mL) and the resulting mixture was stirred for 10 minutes. After that CH₂Cl₂ (40 mL) was added, and the organic layer was separated. The aqueous layer was extracted with CH₂Cl₂ (20 mL). The combined organic layers were washed with brine (40 mL), dried over MgSO₄, and concentrated to dryness. The crude was redissolved in anhydrous THF (10 mL) and the reaction mixture was cooled down to -78 °C, and L-selectride (1M solution in THF, 0.84 mL, 0.84 mmol, 2 equiv) was added dropwise, and the reaction mixture then was stirred for 1.5h. After such time acetone (10 mL) was added to quench the reaction, and the reaction mixture was allowed to warm up to 20 °C. After that the reaction mixture was diluted with CH₂Cl₂ (50 mL), washed with brine (40 mL), dried over MgSO₄ and concentrated to dryness. The residue was taken into CH₂Cl₂ (10 mL) and pyridine (2 mL). The reaction mixture then was cooled down to 0 °C and BzCl (0.12 mL, 1.048 mmol, 2.5 equiv) was added dropwise. The reaction mixture then was stirred at 0 → 20 °C until completion

(monitored by TLC and LCMS). After completion the reaction was quenched with H₂O (10 mL), diluted with CH₂Cl₂ (50 mL). The organic layer was separated, washed with H₂O (3×50 mL), brine (50 mL), dried over MgSO₄, co-evaporated with toluene (3×10 mL) and concentrated to dryness. The crude was purified by flash column chromatography on silica gel eluting with hexanes : EtOAc (0→ 30%, EtOAc (v/v)) to give compound as a mixture of anomers (α : β = 12 : 1) as a white foam (94 mg, 36% over 3 steps). *R*_f 0.34 (hexanes : EtOAc 7:3 (UV, H₂SO₄/EtOH); ¹H NMR (500 MHz, CDCl₃): δ 8.20 – 8.09 (m, 2H), 8.08 – 7.98 (m, 2H), 7.98 – 7.91 (m, 2H), 7.83 – 7.74 (m, 2H), 7.66 – 7.58 (m, 2H), 7.57 – 7.45 (m, 4H), 7.44 – 7.37 (m, 2H), 7.37 – 7.29 (m, 2H), 7.28 – 7.16 (m, 2H), 6.24 (s, 1H, H-4), 6.02 (dd, *J* = 10.6, 3.1 Hz, 1H, H-2), 5.94 (dd, *J* = 10.6, 2.6 Hz, 1H, H-3), 5.00 (d, *J* = 2.8 Hz, 1H, H-1), 4.54 (dd, *J* = 11.3, 5.9 Hz, 1H, H-6a), 4.34 (dd, *J* = 11.3, 8.5 Hz, 1H, H-6b), 4.02 (t, *J* = 7.3 Hz, 1H, H-5), 3.52 (s, 3H, OCH₃); ¹³C NMR (126 MHz, CDCl₃): δ 166.1, 165.9, 165.5, 165.4 (4×CO), 133.5, 133.3, 133.2, 133.0 (4×qC), 130.2, 130.0, 129.8, 129.8, 129.6, 129.4, 129.2, 129.2, 128.6, 128.4, 128.4, 128.3, 128.2 (15×Aryl), 82.1 (C-1), 72.7 (C-2), 69.8 (C-4), 69.3 (C-3), 62.1 (C-6), 56.9 (OCH₃), 39.2 (C-5). The trace β -isomer was identified in the mixture by the following diagnostic signals: 6.25 – 6.15 (m, 1H, H-4), 3.56 (s, 3H, OCH₃).

HRMS-ESI (*m/z*): [M+Na]⁺ calcd. for C₃₅H₃₀O₉NaS⁺ 649.1503, found 649.1489.

Methyl 5-thio-5-deoxy- α,β -D-galactopyranoside (187):

Per-benzoylated methyl galactoside **186** (70 mg, 0.112 mmol) was suspended in anhydrous MeOH (10 mL) and NaOMe (1M solution in MeOH, 22 μ L, 0.022 mmol, 0.2 equiv) was added and the reaction mixture was stirred until completion (monitored by TLC and LCMS analysis). After completion the reaction mixture was quenched with Dowex 50WX8 (H⁺) ion-exchange resin (washed with CH₂Cl₂, Water, Methanol) until pH 5. After that the reaction mixture was filtered and the filtrate was concentrated under reduced pressure. The residue was dissolved in H₂O (20 mL), washed with Et₂O (3×30 mL), concentrated to dryness, and dried under vacuum overnight to give a mixture of anomers (α : β = 11 : 1) as a yellowish syrup (18 mg, 77%). ¹H NMR (500 MHz, CD₃OD): δ 4.46 (d, *J* = 3.2 Hz, 1H, H-1), 4.20 (dd, *J* = 3.1, 1.6 Hz, 1H, H-4), 3.98 (dd, *J* = 10.0, 3.2 Hz, 1H, H-2), 3.77 – 3.64 (m, 2H, H-3, H-6a), 3.61 – 3.54 (m, 1H, H-6b), 3.44 (s,

3H, OCH₃), 3.23 (ddd, $J = 7.7, 6.1, 1.6$ Hz, 1H, H-5); ¹³C NMR (126 MHz, CD₃OD): δ 86.0 (C-1), 73.1 (C-2), 72.4 (C-3), 71.7 (C-4), 62.4 (C-6), 56.9 (OCH₃), 45.1 (C-5). The trace β -isomer was identified in mixture by the following diagnostic signals: 4.36 (d, $J = 8.8$ Hz, 1H, H-1), 3.51 (s, 3H, OCH₃). HRMS-ESI (m/z): [M+Na]⁺ calcd. for C₇H₁₄O₅NaS⁺ 233.0454, found 233.0447.

Evaluation of the binding affinity of thio-mimetics 170 and 187:

MST assay protocol:

The binding of methyl 5-thio- α -D-galactoside **187** and methyl α -D-galactoside (1.5 μ M-50 mM solution in PBS) to Fluorescein-labeled Jacalin (320 nM solution in PBS) were determined using a Monolith Pico instrument, associated premium capillaries (MO-K022), and a blue laser with 30% excitation and medium power. The assay was performed in triplicate at 20 °C, 22 °C, 24 °C, and 26 °C. The raw data was processed by internal MST software (MO.Control) and fitted to the dose response curve using a non-linear fit model to determine K_d values.

We thank Dr. Rich Helm, Dr. Ryan Porell, and Caylyn McNaul from GlycoMIP, a National Science Foundation Materials Innovation Platform funded through Cooperative Agreement DMR-1933525, at Virginia Tech for conducting the MST assays on our behalf, and Prof. Rob Woods and Dr. Sawsan Mahmoud from GlycoMIP, a National Science Foundation Materials Innovation Platform funded through Cooperative Agreement DMR-1933525, at the University of Georgia CCRC for conducting the BLI assays on our behalf.

6.3. Experimental procedures for the synthesis of compounds described in Chapter 4

Synthesis of thiopyran derivatives (Scheme 40):

Methyl 5-hydroxyvalerate (212):

Adopting a reported protocol,²⁵⁷ δ -valerolactone (3 mL, 32.3 mmol) was dissolved in anhydrous MeOH (20 mL) and NaOMe (262 mg, 4.85 mmol, 0.15 equiv) was added and the reaction mixture was stirred for 1h at 20 °C. After such time the reaction mixture quenched with Amberlite IR-120 (H⁺) ion-exchanger and filtered. The filtrate was collected and concentrated to dryness to give the product as an opaque orangish

liquid (4.01 g, 94%) with spectral data matching that reported in the literature.²⁵⁸ ¹H NMR (500 MHz, CD₃OD): δ 3.63 (s, 3H, OCH₃), 3.53 (t, J = 6.5 Hz, 2H), 2.33 (t, J = 7.4 Hz, 2H), 1.70 – 1.59 (m, 2H), 1.57 – 1.47 (m, 2H); ¹³C NMR (126 MHz, CD₃OD): δ 174.4, 61.1, 50.7, 33.2, 31.6, 21.1; HRMS-ESI (m/z): [M+Na]⁺ calcd. for C₆H₁₂O₃Na⁺ 155.0679, found 155.0671.

Methyl 5-(acetylthio)valerate (213):

Compound **212** (1 g, 7.57 mmol) was dissolved in anhydrous THF (15 mL) and CBr₄ (3.8 g, 11.355 mmol, 1.5 equiv) was added at 0 °C followed by Ph₃P (6 g, 22.71 mmol, 3 equiv). The reaction mixture then was stirred at 0 → 20 °C until complete consumption of the starting material was observed by LCMS. After such time the reaction mixture was diluted with Et₂O (100 ml) and filtered, and the filtrate was collected and concentrated to dryness. The crude product was taken into anhydrous DMF (10 mL) and KSAc (1.73 g, 15.14 mmol, 2 equiv) was added. The reaction mixture then was stirred for 16h at 20 °C. After such time the reaction mixture was quenched with H₂O (10 mL) and diluted with EtOAc (60 mL). The organic layer was separated and washed with brine (50 mL), dried over MgSO₄, and concentrated to dryness. The crude was purified by flash column chromatography on silica gel eluting with hexanes : EtOAc (5% EtOAc) to give the product as an orangish liquid (930 mg, 64% yield over 2 steps) with spectral data identical to that reported in the literature.²⁵⁹ R_f 0.48 (hexanes : EtOAc 4:1 (CAM)); ¹H NMR (500 MHz, CDCl₃): δ 3.64 (s, 3H, OCH₃), 2.85 (t, J = 7.1 Hz, 2H), 2.33 – 2.21 (m, 5H), 1.67 (ddd, J = 12.8, 11.1, 7.8 Hz, 2H), 1.58 (ddd, J = 9.7, 6.9, 5.1 Hz, 2H); ¹³C NMR (126 MHz, CDCl₃): δ 195.8, 173.8, 51.6, 33.5, 30.7, 29.1, 28.7, 24.0; HRMS-ESI (m/z): [M+Na]⁺ calcd. for C₈H₁₄NaO₃S⁺ 213.0556, found 213.0548.

Tetrahydro-thiopyran-2-one (215):

Methyl 5-(acetylthio)valerate **213** (500 mg, 2.63 mmol) was dissolved in 10% aq MeOH (26.3 mL) and NaOH (523 mg, 13.1 mmol, 5 equiv) was added. The reaction mixture then was stirred for 45 minutes at 90 °C. After such time the reaction mixture was allowed to cool down to rt and 1M NaOH (20 mL) was added. The aqueous layer was washed with CH₂Cl₂ (4×40 mL), acidified with 1M H₂SO₄ until pH 2, and extracted with CH₂Cl₂ (5×40 mL). The combined organic layers were dried over Na₂SO₄ and concentrated

to dryness. The crude was dissolved in anhydrous CH_2Cl_2 (30 mL) and PyBOP (1.64 g, 3.145 mmol, 1.2 equiv) was added, followed by DIPEA (916 μL , 5.26 mmol, 2 equiv). The reaction mixture then was stirred for 2h at 20 °C. After such time the reaction mixture was washed with H_2O (30 mL), brine (30 mL), dried over MgSO_4 , and concentrated to dryness, and the residue was purified by flash column chromatography on silica gel eluting with hexanes:EtOAc (0→10%, EtOAc) to give the product as a yellowish syrup (140 mg, 49%) with spectral data identical to that reported in the literature.²²³ R_f 0.26 (hexanes:EtOAc 3:2 (KMnO_4)); ^1H NMR (500 MHz, CDCl_3): δ 3.31 – 2.98 (m, 2H), 2.60 (dd, J = 6.9, 5.6 Hz, 2H), 2.05 – 1.92 (m, 4H); ^{13}C NMR (126 MHz, CDCl_3): δ 201.4, 41.3, 30.6, 23.1, 22.9; HRMS-ESI (m/z): $[\text{M}+\text{H}]^+$ calcd. for $\text{C}_5\text{H}_9\text{OS}^+$ 117.0369, found 117.0367.

2-Acetoxythiane (216)

Thiolactone **215** (720 mg, 6.2 mmol) was dissolved in anhydrous CH_2Cl_2 (36 mL) and the reaction mixture was cooled down to -78 °C and DIBAL-H (1M solution in hexanes, 12.4 mL, 12.4 mmol, 2 equiv) was added. The reaction mixture was stirred for 50 minutes at -78 °C before Py (1.5 mL, 18.6 mmol, 3 equiv) was added followed by DMAP (1.5 g, 12.4 mmol, 2 equiv) solution in CH_2Cl_2 (8 mL) and Ac_2O (3.6 mL, 37.2 mmol, 6 equiv). The reaction mixture then was stirred for 12h at -78 °C. After such time the reaction mixture was allowed to warm up to 0 °C, and brine (10 mL) was added, and the reaction mixture then was stirred at 0 °C for 40 minutes. After such time the reaction mixture was CH_2Cl_2 (70 mL), washed with 1M H_2SO_4 (60 mL), NaHCO_3 (100 mL), brine (100 mL), dried over MgSO_4 , and concentrated to dryness. The crude was purified by flash column chromatography on silica gel eluting with hexanes:EtOAc (0→35%, EtOAc) to give 2-acetoxythiane **216** as a colorless liquid (639 mg, 64%) with spectral data in agreement with that reported in the literature.²⁶⁰ R_f 0.47 (hexanes:EtOAc 9:1 ($\text{H}_2\text{SO}_4/\text{EtOH}$)); FTIR (CHCl_3) cm^{-1} : 1736.1, 1373.6, 1223.1; ^1H NMR (500 MHz, CDCl_3): δ 5.90 – 5.77 (m, 1H, H-2), 2.97 (ddd, J = 13.4, 11.6, 2.9 Hz, 1H, H-6a), 2.47 – 2.39 (m, 1H, H-6b), 2.09 (s, 3H, CH_3CO), 2.07 – 1.90 (m, 3H, H-3a, H-3b, H-4b), 1.86 – 1.62 (m, 3H, H-5a, H-5b, H-4a); ^{13}C NMR (126 MHz, CDCl_3): δ 169.7 (CO), 71.6 (C-2), 32.0

(C-3), 26.2 (C-5), 25.2 (C-6), 21.2 (CH₃CO), 20.4 (C-4); ESI-HRMS (m/z): [M+Na]⁺ calcd. for C₇H₁₂O₂NaS⁺ 183.0450, found 183.0448.

Thiane 1-oxide (218):

Thiane (5 g, 48.92 mmol) was dissolved in MeOH (60 mL) and the reaction mixture was cooled down to 0 °C before H₂O₂ (50% aq solution, 30 mL, 53.82 mmol, 1.1 equiv) was added. The reaction mixture then was stirred for 2h at 0 → 20 °C. After such time the reaction mixture was quenched with 1M NaHSO₃ (10 mL), and methanol was removed under reduced pressure. The remains were distributed between CHCl₃ (60 mL) and brine (30 mL). The organic layer was collected, dried over MgSO₄ and concentrated to dryness to give desired sulfoxide **218** as a colorless viscous liquid (5.21 g, 96%) with spectral data identical to that reported in the literature.²⁶¹ *R*_f 0.21 and 0.34 (EtOAc (KMnO₄)); ¹H NMR (500 MHz, CDCl₃) δ 2.93 – 2.79 (m, 1H), 2.79 – 2.61 (m, 1H), 2.27 – 2.14 (m, 1H), 1.70 – 1.43 (m, 2H); ¹³C NMR (126 MHz, CDCl₃) δ 49.0, 24.7, 19.2; ESI-HRMS (m/z): [M+H]⁺ calcd. for C₅H₁₁OS⁺ 119.0525, found 119.0521.

2,3-Dihydrothiopyran (208):

Sulfoxide **218** (5.2 g, 44 mmol) was dissolved in Ac₂O (21 mL) and the reaction mixture was stirred at 100 °C for 1h. After such time the reaction mixture was allowed to cool down to room temperature (20 °C), and was poured into sat aq NaHCO₃ solution with ice (100 mL) and stirred for 1h. After such time the reaction mixture was extracted with Et₂O (3×30 mL). The combined organic layers were washed with sat aq NaHCO₃ (3×100 mL), brine (100 mL), dried over MgSO₄, and concentrated under reduced pressure (no lower than 200 mbar). The residue then was purified by flash column chromatography on silica gel eluting with hexanes:EtOAc (0→5%, EtOAc) to give the product as a colorless liquid (1.76 g, 40%) with spectral data identical to that reported in the literature.²⁶² *R*_f 0.32 (hexanes (KMnO₄)); ¹H NMR (500 MHz, CDCl₃): δ 5.99 (d, *J* = 10.2, 1H), 5.70 (dt, *J* = 10.1, 4.2 Hz, 1H), 2.88 – 2.82 (m, 2H), 2.24 – 2.07 (m, 2H), 2.07 – 1.88 (m, 2H); ¹³C NMR (126 MHz, CDCl₃): δ 121.2, 119.2, 26.2, 23.7, 22.4; ESI-HRMS (m/z): [M+H]⁺ calcd. for C₅H₉S⁺ 101.0420, found 101.0417.

Synthesis of disarmed sulfoxides (Scheme 43 and Scheme 44):

Ethyl 2,3,4,6-tetra-*O*-acetyl-1,5-di-thio-D-glucopyranosides (50a, 50b):

Pentaacetate **33** (3.46 g) was dissolved in anhydrous CH₂Cl₂ (50 mL) and HSEt (1.89 mL, 25.56 mmol, 3 equiv) was added followed by BF₃•Et₂O (4.2 mL, 34.08 mmol, 4 equiv) at 0 °C and the reaction mixture was then stirred with warming from 0→20 °C for 12h. After such time the reaction mixture was quenched with H₂O (10 mL), diluted with CH₂Cl₂ (40 mL). The organic layer was washed with sat aq NaHCO₃ (2×50 mL), brine (50 mL) and dried over MgSO₄. The crude mixture of anomers (α : β = 1.2 : 1) was purified by flash column chromatography on silica gel eluting with hexanes:EtOAc (0→50%, EtOAc) to give α -thioglycoside **50a** (1.32 g, 38%) as a yellowish syrup and β -thioglycoside **50b** (1.1 g, 32%) as a yellowish syrup with spectral data identical to that reported in the literature.⁸⁶

α -thioglycoside 50a:

R_f 0.37 (hexanes:EtOAc 3:2 (H₂SO₄/EtOH)); ¹H NMR (500 MHz, CDCl₃) δ 5.38 (dd, *J* = 10.2, 9.3 Hz, 1H), 5.31 – 5.18 (m, 2H), 4.51 (d, *J* = 4.6 Hz, 1H), 4.42 (dd, *J* = 12.1, 4.8 Hz, 1H), 4.09 (dd, *J* = 12.1, 3.2 Hz, 1H), 3.70 (ddd, *J* = 10.8, 4.8, 3.2 Hz, 1H), 2.67 (qd, *J* = 7.4, 4.3 Hz, 2H), 2.07 (s, 3H), 2.06 (s, 3H), 2.03 (s, 3H), 2.00 (s, 3H), 1.25 (t, *J* = 7.4 Hz, 3H); ¹³C NMR (126 MHz, CDCl₃) δ 170.5, 169.9, 169.5, 169.5, 77.3, 77.0, 76.7, 74.6, 72.3, 71.3, 61.2, 49.0, 39.4, 25.7, 20.7, 20.6, 20.5, 14.0; ESI-HRMS (*m/z*): [M+Na]⁺ calcd. for C₁₆H₂₄O₈NaS₂⁺ 431.0804, found 431.0797.

β -thioglycoside 50b:

R_f 0.32 (hexanes:EtOAc 3:2 (H₂SO₄/EtOH)); ¹H NMR (500 MHz, CDCl₃) δ 5.27 (dd, *J* = 10.7, 9.6 Hz, 1H), 5.18 (dd, *J* = 10.7, 9.5 Hz, 1H), 5.05 (t, *J* = 9.6 Hz, 1H), 4.25 (dd, *J* = 12.0, 5.7 Hz, 1H), 4.13 (dd, *J* = 12.0, 3.4 Hz, 1H), 3.83 (d, *J* = 10.7 Hz, 1H), 3.28 (ddd, *J* = 10.7, 5.7, 3.4 Hz, 1H), 2.80 – 2.63 (m, 2H), 2.08 (s, 3H), 2.07 (s, 3H), 2.03 (s, 3H), 2.00 (s, 3H), 1.26 (t, *J* = 7.4 Hz, 3H); ¹³C NMR (126 MHz, CDCl₃): δ 169.8, 169.7, 169.6, 169.3, 74.5, 73.1, 71.9, 61.3, 47.7, 44.4, 24.9, 20.6, 20.5, 20.5, 20.4, 14.5; ESI-HRMS (*m/z*): [M+Na]⁺ calcd. for C₁₆H₂₄O₈NaS₂⁺ 431.0804, found 431.0795.

Ethyl 2,3,4,6-tetra-*O*-acetyl-1,5-di-thio- β -D-glucopyranoside-*S*-Oxides (232, 233):

Thioglycoside **50b** (377 mg, 0.923 mmol) was dissolved in anhydrous CH₂Cl₂ (15 mL) and the reaction mixture was cooled down to –50 °C before *m*CPBA (77% wt, 227 mg, 1.015 mmol, 1.1 equiv.) solution in anhydrous CH₂Cl₂ (5 mL) was added and the reaction mixture was stirred for 1h at –50 °C. After such time the reaction mixture was quenched with aq. sat. NaHCO₃ (5 mL) at –30 °C and gradually warmed up to 20 °C. After that the reaction mixture was diluted with Et₂O CH₂Cl₂ (40 mL), washed with aq. sat. NaHCO₃ (40 mL), 1M NaHSO₃ (60 mL), brine (60 mL), dried over MgSO₄ and concentrated to dryness. The crude product was purified by flash column chromatography on silica gel eluting with hexanes:EtOAc (20→100%, EtOAc) to give a mixture of (*R*_s),(*S*_s)-1-*S*-sulfoxides **232** as a white solid (251 mg, 64%) and (*R*_s),(*S*_s)-5-*S*-sulfoxides **233** (40 mg, 10%) as a white solid.

(*R*_s),(*S*_s)-1-*S*-oxides 232:

d.r. = 1.6:1; *R*_f 0.61 (100% EtOAc, (H₂SO₄/EtOH)); ¹H NMR (500 MHz, CDCl₃): **Major diastereomer:** δ 5.58 (dd, *J* = 10.8, 9.4 Hz, 1H, H-2), 5.42 – 5.23 (m, 1H, H-4), 5.16 (t, *J* = 9.1, 1H, H-3), 4.34 (dt, *J* = 11.2, 5.5 Hz, 1H, H-6a), 4.23 – 4.15 (m, 2H, H-6b, H-1), 3.30 (ddd, *J* = 9.7, 5.8, 3.8 Hz, 1H, H-5), 3.15 (dq, *J* = 13.0, 7.5 Hz, 1H, SCH₂CH₃), 2.86 – 2.73 (m, 1H, SCH₂CH₃), 2.08 (s, 3H), 2.06 (s, 3H), 2.04 (s, 3H), 2.02 (s, 3H, each CH₃CO), 1.43 – 1.34 (m, 3H, SCH₂CH₃); **Minor diastereomer:** δ 5.42 – 5.23 (m, 2H, H-2, H-4), 5.16 (t, *J* = 9.1, 1H, H-3), 4.34 (dd, *J* = 11.2, 5.5 Hz, 1H, H-6a), 4.23 – 4.15 (m, 1H, H-6b), 3.90 (d, *J* = 10.8 Hz, 1H, H-1), 3.37 (ddd, *J* = 10.5, 5.4, 3.3 Hz, 1H, H-5), 3.03 – 2.87 (m, 1H, SCH₂CH₃), 2.86 – 2.73 (m, 1H, SCH₂CH₃), 2.09 (s, 3H, CH₃CO), 2.07 (s, 3H, CH₃CO), 2.05 (s, 3H, CH₃CO), 2.04 (s, 3H, CH₃CO), 1.43 – 1.34 (m, 3H, OSCH₂CH₃); ¹³C NMR (126 MHz, CDCl₃): **Major diastereomer:** δ 170.6, 170.0, 169.4, 169.0 (4×CO), 73.5 (C-3), 71.2 (C-2), 70.7 (C-4), 61.8 (C-1), 61.5 (C-6), 45.1 (CH₃CH₂SO), 42.7 (C-5), 20.7, 20.6, 20.6, 20.5 (4×CH₃CO), 7.7 (CH₃CH₂SO); **Minor diastereomer:** δ 170.6, 170.0, 169.7, 169.5 (4×CO), 74.6 (C-3), 71.5 (C-2), 70.8 (C-4), 62.4 (C-1), 61.7 (C-6), 43.3 (CH₃CH₂SO), 43.2 (C-5), 20.7, 20.7, 20.6, 20.6 (4×CH₃CO), 7.32 (CH₃CH₂SO); ESI-HRMS (*m/z*): [M+Na]⁺ calcd. for C₁₆H₂₄O₁₀NaS⁺ 447.0754, found 447.0744.

(*R*_s),(*S*_s)-5-*S*-oxides 233:

d.r. = 2:1; R_f 0.74 (100% EtOAc, (H₂SO₄/EtOH)); ¹H NMR (500 MHz, CDCl₃): (peaks assigned for the major diastereomer) δ 5.37 – 5.24 (m, 2H, H-3, H-4), 5.10 (dd, J = 11.9, 9.1 Hz, 1H, H-2), 4.70 (dd, J = 12.5, 2.5 Hz, 1H, H-6a), 4.44 – 4.37 (m, 1H, H-6b), 3.81 (d, J = 11.8 Hz, 1H, H-1), 3.18 (dt, J = 11.3, 2.4 Hz, 1H, H-5), 2.96 – 2.81 (m, 2H, SCH₂CH₃), 2.10 (s, 3H), 2.07 (s, 3H), 2.03 (s, 3H), 1.99 (s, 3H, each CH₃CO), 1.31 – 1.24 (m, 3H, SCH₂CH₃); ¹³C NMR (126 MHz, CDCl₃): δ 170.4, 169.6, 169.2, 169.0 (4×CO), 74.1 (C-4), 69.7 (C-1), 66.0 (C-2), 64.2 (C-5), 63.8 (C-3), 56.0 (C-6), 26.4 (CH₃CH₂SO), 25.6 (CH₃CH₂SO), 20.8, 20.6, 20.5, 20.5 (4×CH₃CO), 14.4 (CH₃CH₂SO); ESI-HRMS (m/z): [M+Na]⁺ calcd. for C₁₆H₂₄O₁₀NaS⁺ 447.0754, found 447.0744.

Ethyl 2,3,4,6-tetra-*O*-acetyl-1,5-di-thio- α -D-glucopyranoside-1-*S*-Oxide (234):

Thioglycoside **50a** (500 mg, 1.22 mmol) was dissolved in anhydrous CH₂Cl₂ (20 mL) and the reaction mixture was cooled down to –50 °C before *m*CPBA (77% wt, 300 mg, 1.342 mmol, 1.1 equiv.) solution in anhydrous CH₂Cl₂ (6 mL) was added and the reaction mixture was stirred for 1h at –50 °C. After such time the reaction mixture was quenched with aq. sat. NaHCO₃ (10 mL) at –50 °C, and gradually warmed up to 20 °C. After that the reaction mixture was diluted with CH₂Cl₂ (60 mL), washed with aq. sat. NaHCO₃ (40 mL), 1M NaHSO₃ (40 mL), brine (40 mL), dried over MgSO₄ and concentrated to dryness. The crude product was purified by flash column chromatography on silica gel eluting with hexanes:EtOAc (0→100%, EtOAc) to give single diastereomer of exo-sulfoxide **234** as a white solid (494 mg, 96%). R_f 0.33 (hexanes:EtOAc 1:9 (H₂SO₄/EtOH)); $[\alpha]_D^{22}$ +146.4 (CHCl₃, 0.0033); ¹H NMR (500 MHz, CDCl₃) δ 5.71 (d, J = 9.6 Hz, 1H, H-3), 5.45 (dd, J = 9.9, 4.7 Hz, 1H, H-2), 5.28 (dd, J = 10.8, 9.0 Hz, 1H, H-4), 4.26 (dd, J = 12.2, 5.3 Hz, 1H, H-6), 4.15 (d, J = 4.6 Hz, 1H, H-1), 4.09 (dd, J = 12.2, 3.3 Hz, 1H, H-6), 3.57 (ddd, J = 10.7, 5.3, 3.3 Hz, 1H, H-5), 3.17 (dq, J = 13.2, 7.6 Hz, 1H, CH₃CH₂SO), 2.93 (dq, J = 13.2, 7.4 Hz, 1H, CH₃CH₂SO), 2.09 (s, 6H, 2×CH₃CO), 2.05 (s, 6H, 2×CH₃CO), 1.39 (t, J = 7.5 Hz, 3H, CH₃CH₂SO); ¹³C NMR (126 MHz, CDCl₃) δ 170.5, 169.5, 169.3, 169.3 (4×CO), 73.6 (C-2), 71.7 (C-4), 70.8 (C-3), 61.1 (C-6), 57.5 (C-1), 45.7 (CH₃CH₂SO), 41.0 (C-5), 20.9, 20.7, 20.6, 20.6 (4×CH₃CO), 6.2 (CH₃CH₂SO); ESI-HRMS (m/z): [M+Na]⁺ calcd. for C₁₆H₂₄O₉NaS₂⁺ 447.0754, found 447.0742.

(*R_S*)-Ethyl 2,3,4,6-tetra-*O*-acetyl-1-thio- α -D-glucopyranoside-*S*-Oxide (236):

Thioglycoside **51a** (360 mg, 0.917 mmol) was dissolved in anhydrous CH₂Cl₂ (20 mL) and the reaction mixture was cooled down to –40 °C before *m*CPBA (77% wt, 226 mg, 1.0087 mmol, 1.1 equiv.) solution in anhydrous CH₂Cl₂ (3 mL) was added and the reaction mixture was stirred for 2h at –40 °C. After such time the reaction mixture was quenched with aq. sat. NaHCO₃ (10 mL) at –40 °C, and gradually warmed up to 20 °C. After that the reaction mixture was diluted with CH₂Cl₂ (40 mL), washed with aq. sat. NaHCO₃ (30 mL), 1M NaHSO₃ (30 mL), brine (30 mL), dried over MgSO₄ and concentrated to dryness. The crude product was purified by flash column chromatography on silica gel eluting with hexanes:EtOAc (0→100%, EtOAc) to give single diastereomer of sulfoxide **236** as a white solid (230 mg, 55%) with spectral data identical to that reported in the literature.²⁶³ *R_f* 0.44 (EtOAc (H₂SO₄/EtOH)); ¹H NMR (500 MHz, CDCl₃): δ 5.58 (t, *J* = 7.8 Hz, 1H, H-3), 5.34 (dd, *J* = 8.2, 5.2 Hz, 1H, H-2), 5.01 (dd, *J* = 9.4, 7.4 Hz, 1H, H-4), 4.80 (d, *J* = 5.1 Hz, 1H, H-1), 4.19 (dd, *J* = 12.4, 5.9 Hz, 1H, H-6a), 4.09 (dd, *J* = 12.4, 2.6 Hz, 1H, H-6b), 3.91 (ddd, *J* = 8.9, 5.9, 2.6 Hz, 1H, H-5), 2.94 (dq, *J* = 13.3, 7.5 Hz, 1H, SCH₂CH₃), 2.77 (dq, *J* = 13.2, 7.4 Hz, 1H, SCH₂CH₃), 2.11 (s, 3H, CH₃CO), 2.08 (s, 6H, 2×CH₃CO), 2.05 (s, 3H, CH₃CO), 1.39 (t, *J* = 7.5 Hz, 3H, SCH₂CH₃); ¹³C NMR (126 MHz, CDCl₃): δ 170.2, 169.9, 169.3, 169.3 (4×CO), 87.1 (C-1), 73.6 (C-5), 69.8 (C-3), 68.7 (C-2), 68.0 (C-4), 61.9 (C-6), 42.4 (SCH₂CH₃), 20.6, 20.6, 20.5, 20.5 (4×CH₃CO), 5.6 (SCH₂CH₃); ESI-HRMS (*m/z*): [M+Na]⁺ calcd. for C₁₆H₂₄O₁₀NaS⁺ 431.0982, found 431.0960.

(*R_S*),(*S_S*)-Ethyl 2,3,4,6-tetra-*O*-acetyl-1-thio- β -D-glucopyranoside-*S*-Oxides (237):

Thioglycoside **51b** (1 g, 2.55 mmol) was dissolved in anhydrous CH₂Cl₂ (10 mL) and the reaction mixture was cooled down to –40 °C before *m*CPBA (77% wt, 440 mg, 2.55 mmol, 1.1 equiv.) solution in anhydrous CH₂Cl₂ (10 mL) was added and the reaction mixture was stirred for 1h at –40 °C. After such time the reaction mixture was quenched with aq. sat. NaHCO₃ (10 mL) at –40 °C, and gradually warmed up to 20 °C. After that the reaction mixture was diluted with CH₂Cl₂ (60 mL), washed with aq. sat. NaHCO₃ (30 mL), 1M NaHSO₃ (30 mL), brine (50 mL), dried over MgSO₄ and concentrated to dryness. The crude product was purified by flash column chromatography on silica gel eluting with hexanes:EtOAc

(50→100%, EtOAc) to give a mixture of (*R*_s),(*S*_s)-sulfoxides **237** as a white solid (674 mg, 65%) with spectral data identical to that reported in the literature.²⁶⁴ d.r. (**237S** : **237R**) = 2.4:1; *R*_f 0.11 (hexanes:acetone 1:1 (H₂SO₄/EtOH));

237S:

¹H NMR (500 MHz, CDCl₃): δ 5.31 – 5.20 (m, 2H, H-3, H-2), 5.15 – 5.02 (m, 1H, H-4), 4.31 (d, *J* = 9.7 Hz, 1H, H-1), 4.26 (dd, *J* = 12.6, 4.7 Hz, 1H, H-6a), 4.23 – 4.13 (m, 1H, H-6b), 3.85 – 3.70 (m, 1H, H-5), 2.98 – 2.83 (m, 2H, SCH₂CH₃), 2.06 (s, 3H), 2.05 (s, 3H), 2.02 (s, 3H), 2.01 (s, 3H, 4×CH₃CO), 1.36 (t, *J* = 7.5 Hz, 3H, SCH₂CH₃); ¹³C NMR (126 MHz, CDCl₃): δ 170.4, 170.0, 169.7, 169.3 (4×CO), 89.9 (C-1), 76.9 (C-5), 73.2 (C-3), 68.4 (C-2), 67.7 (C-4), 61.4 (C-6), 41.3 (SCH₂CH₃), 20.6, 20.5, 20.5, 20.5 (4×CH₃CO), 6.5 (SCH₂CH₃).

237R:

¹H NMR (500 MHz, CDCl₃): δ 5.43 (dd, *J* = 10.0, 9.3 Hz, 1H, H-2), 5.34 (t, *J* = 9.3 Hz, 1H, H-3), 5.15 – 5.02 (m, 1H, H-4), 4.26 (dd, *J* = 12.6, 4.7 Hz, 1H, H-6a), 4.23 – 4.13 (m, 2H, H-6b, H-1), 3.85 – 3.70 (m, 1H, H-5), 3.11 (dq, *J* = 12.8, 7.6 Hz, 1H, SCH₂CH₃), 2.83 – 2.71 (m, 1H, SCH₂CH₃), 2.06 (s, 3H), 2.05 (s, 3H), 2.02 (s, 3H), 2.01 (s, 3H, 4×CH₃CO), 1.32 (t, *J* = 7.6 Hz, 3H, SCH₂CH₃); ¹³C NMR (126 MHz, CDCl₃): δ 170.5, 170.4, 169.7, 169.3 (4×CO), 86.6 (C-1), 76.9 (C-5), 73.8 (C-3), 67.8 (C-4), 66.9 (C-2), 61.9 (C-6), 41.2 (SCH₂CH₃), 20.7, 20.6, 20.5, 20.5 (4×CH₃CO), 7.3 (SCH₂CH₃).

ESI-HRMS (*m/z*): [M+Na]⁺ calcd. for C₁₆H₂₄O₁₀NaS⁺ 431.0982, found 431.0965.

Synthesis of disarmed trichloroacetimidates (Scheme 50):

2,3,4,6-Tetra-*O*-acetyl- α -D-glucopyranosyl trichloroacetimidate (12**):**

2,3,4,6-Tetra-*O*-acetyl-D-glucopyranose **254** (105 mg, 0.301 mmol) was dissolved in anhydrous CH₂Cl₂ (5 mL) and CCl₃CN (150 μ L, 1.505 mmol, 5 equiv) was added followed by DBU (5 μ L, 0.0334 mmol, 0.11 equiv) and the reaction mixture was stirred for 1h at 20 °C. After such time the reaction mixture

was diluted with CH₂Cl₂ (30 mL), washed with 1M HCl (20 mL), saturated aqueous NaHCO₃ (50 mL), brine (50 mL), dried over MgSO₄ and concentrated to dryness. The crude product was purified by a column chromatography eluting with hexanes:EtOAc (10→50%, EtOAc) to give the product as a colorless syrup (112 mg, 76%) with spectra data identical to that reported in the literature.²⁶⁵ *R*_f 0.60 (hexanes:EtOAc 1:1 (H₂SO₄/EtOH)); ¹H NMR (500 MHz, CDCl₃): δ 8.68 (s, 1H), 6.55 (d, *J* = 3.7 Hz, 1H), 5.56 (t, *J* = 9.9 Hz, 1H), 5.17 (t, *J* = 9.9 Hz, 1H), 5.12 (dd, *J* = 10.2, 3.6 Hz, 1H), 4.32 – 4.17 (m, 2H), 4.15 – 4.07 (m, 1H), 2.07 (s, 3H), 2.04 (s, 3H), 2.02 (s, 3H), 2.01 (s, 3H); ¹³C NMR (126 MHz, CDCl₃): δ 170.7, 170.1, 169.9, 169.6, 160.9, 93.0, 70.1, 70.0, 69.8, 67.9, 61.5, 20.7, 20.5; ESI-HRMS (*m/z*): [M+Na]⁺ calcd. for C₁₆H₂₀O₁₀NCl₃Na⁺ 514.0045, found 514.0020.

2,3,4,6-Tetra-*O*-acetyl-5-thio- α -D-glucopyranosyl trichloroacetimidate (52):

2,3,4,6-Tetra-*O*-acetyl-5-thio-5-deoxy-D-glucopyranose **255** (99 mg, 0.271 mmol) was dissolved in anhydrous CH₂Cl₂ (10 mL) and the reaction mixture was cooled down to 0 °C and CCl₃CN (270 μ L, 2.69 mmol, 10 equiv) was added followed by DBU (4 μ L, 0.0271 mmol, 0.11 equiv) and the reaction mixture was stirred for 2h at 20 °C. After such time the reaction mixture was diluted with CH₂Cl₂ (20 mL), washed with 1M HCl (10 mL), saturated aqueous NaHCO₃ (20 mL), dried over MgSO₄ and concentrated to dryness. The crude product was purified by a column chromatography eluting with hexanes:EtOAc (0→40%, EtOAc) to give a mixture of anomeric imidates (α : β = 17 : 1) as a colorless syrup (89 mg, 65%) with spectral data identical to that reported in the literature.¹⁹¹ *R*_f 0.52 (hexanes:EtOAc 1:1 (H₂SO₄/EtOH)); ¹H NMR (500 MHz, CDCl₃): δ 8.71 (s, 1H), 6.36 (d, *J* = 3.2 Hz, 1H), 5.57 (t, *J* = 9.9 Hz, 1H), 5.38 (dd, *J* = 10.9, 9.6 Hz, 1H), 5.31 (dd, *J* = 10.2, 3.1 Hz, 1H), 4.39 (dd, *J* = 12.2, 4.9 Hz, 1H), 4.08 (dd, *J* = 12.1, 3.0 Hz, 1H), 3.64 (ddd, *J* = 10.8, 4.9, 3.1 Hz, 1H), 2.07 (s, 3H), 2.06 (s, 3H), 2.03 (s, 3H), 2.00 (s, 3H); ¹³C NMR (126 MHz, CDCl₃): δ 170.5, 169.8, 169.6, 169.6, 160.8, 75.9, 73.6, 71.7, 70.7, 60.9, 40.1, 20.7, 20.6, 20.6; ESI-HRMS (*m/z*): [M+Na]⁺ calcd. for C₁₆H₂₀O₉NCl₃NaS⁺ 529.9817, found 529.9804.

Synthesis of perbenzylated sulfoxide (Scheme 54):

Ethyl 2,3,4,6-tetra-*O*-benzyl-1,5-dithio- β -D-glucopyranoside (263):

Thioglycoside **50b** (0.9 g, 2.21 mmol) was dissolved in anhydrous MeOH (30 mL) and NaOMe (34 mg, 0.636 mmol, 0.3 equiv) was added. The reaction mixture then was stirred for 1 h at 20 °C. After such time the reaction mixture was quenched with Amberlite IR-120 (H⁺) ion-exchange resin until pH 3-4. The reaction mixture was then filtered, and the filtrate was collected and concentrated to dryness. The crude residue was redissolved in anhydrous DMF (20 mL) and NaH (60% dispersion in the mineral oil, 508 mg, 12.72 mmol, 6 equiv) was added portion-wise at 0 °C followed by addition of BnBr (2.3 mL, 19.08 mmol, 9 equiv). The reaction mixture then was stirred for 8 h at 0 → 20 °C. After such time the reaction mixture was quenched with MeOH (10 mL) and diluted with EtOAc (60 mL), washed with H₂O (50 mL), brine (50 mL), dried over Na₂SO₄ and concentrated to dryness. The crude was purified by flash column chromatography on silica gel eluting with hexanes:EtOAc (0→30%, EtOAc) to give product as a yellowish syrup (787 mg, 62%). *R_f* 0.40 (hexanes:EtOAc 9:1 (H₂SO₄/EtOH)); [α]_D²² +38.4 (CHCl₃, *C* = 0.0153); ¹H NMR (500 MHz, CDCl₃): δ 7.43 – 7.17 (m, 18H, Aryl), 7.11 (dd, *J* = 6.7, 2.9 Hz, 2H, Aryl), 4.95 – 4.77 (m, 5H, PhCH₂), 4.57 – 4.44 (m, 3H, PhCH₂), 3.85 – 3.66 (m, 4H, H-1, H-6a, H-6b, H-4), 3.61 (dd, *J* = 10.4, 8.9 Hz, 1H, H-2), 3.44 (t, *J* = 9.0 Hz, 1H, H-3), 2.99 (ddd, *J* = 10.4, 5.4, 2.9 Hz, 1H, H-5), 2.88 – 2.71 (m, 2H, SCH₂CH₃), 1.30 (t, *J* = 7.4 Hz, 3H, SCH₂CH₃); ¹³C NMR (126 MHz, CDCl₃): δ 138.6, 138.1, 138.1, 137.7, 128.4, 128.4, 128.4, 128.3, 128.2, 128.0, 127.8, 127.8, 127.7, 127.5, 127.5 (20×Aryl), 88.2 (C-3), 85.4 (C-2), 82.0 (C-4), 76.4 (PhCH₂), 76.1 (PhCH₂), 75.6 (PhCH₂), 73.4 (PhCH₂), 68.0 (C-6), 49.6 (C-1), 47.4 (C-5), 26.4 (SCH₂CH₃), 14.8 (SCH₂CH₃); ESI-HRMS (*m/z*): [M+Na]⁺ calcd. for C₃₆H₄₀O₄NaS₂⁺ 623.2260, found 623.2256.

Ethyl 2,3,4,6-tetra-*O*-benzyl-1,5-dithio- β -D-glucopyranoside-*S*-Oxides (264, 265):

Thioglycoside **263** (320 mg, 0.53 mmol) was dissolved in anhydrous CH₂Cl₂ (20 mL) and the reaction mixture was cooled down to -70 °C before *m*CPBA (77% wt, 144 mg, 0.586 mmol, 1.1 equiv) solution in anhydrous CH₂Cl₂ (5 mL) was added. The reaction mixture then was stirred for 2 h at -70 °C. After such time the reaction mixture was quenched with sat aq NaHCO₃ (5 mL) and allowed to warm up to room temperature (20 °C). After that the reaction mixture was diluted with EtOAc (60 mL), washed with brine

(60 mL), 1M NaHSO₃ (60 mL), dried over MgSO₄, and concentrated to dryness. The resulting exo- and endo-sulfoxides **264** and **265**, respectively, were inseparable by chromatographic methods on both normal phase silica gel and C18 silica gel.

Synthesis of the armed sulfoxides (Scheme 55 and Scheme 56):

Ethyl 2,3,4,6-tetra-*O*-methyl-1,5-dithio- β -D-glucopyranoside (268**):**

Thioglycoside **50b** (1.1 g, 2.69 mmol) was dissolved in anhydrous MeOH (40 mL) and NaOMe (58 mg, 1.077 mmol, 0.4 equiv) was added (pH 10) and the reaction mixture was stirred for 1 h at 20 °C. After such time the reaction was quenched by addition of the Amberlyst 15 (H⁺) ion-exchange resin until pH 3-4. The reaction mixture was filtered, and the filtrate was concentrated to dryness. The crude product was redissolved in anhydrous DMF (40 mL) and NaH (60% dispersion in the mineral oil, 540 mg, 13.47 mmol, 5 equiv) was added at 0 °C followed by addition of MeI (1.0 mL, 16.5 mmol, 6 equiv) and the reaction mixture was stirred at 0→20 °C until completion (detected by TLC and LCMS). After completion the reaction mixture was quenched with MeOH (15 mL) at 0 °C, diluted with EtOAc (70 mL), washed with H₂O (70 mL), brine (70 mL), dried over MgSO₄ and concentrated to dryness. The crude product was purified by flash column chromatography on silica gel eluting with hexanes:EtOAc (0→40%, EtOAc) to give the product as a colorless syrup (604 mg, 76%). *R*_f 0.58 (hexanes:EtOAc 7:3 (H₂SO₄/EtOH)); [α]_D²² +12.3 (CHCl₃, 0.0047); ¹H NMR (500 MHz, CDCl₃): δ 3.71 – 3.61 (m, 9H, 2×OMe, H-1, H-6a, H-6b), 3.57 (s, 3H, OMe), 3.37 (s, 3H, OMe), 3.30 (dd, *J* = 10.5, 9.0 Hz, 1H, H-4), 3.15 (dd, *J* = 10.4, 8.8 Hz, 1H, H-2), 2.96 (t, *J* = 9.0 Hz, 1H, H-3), 2.85 – 2.67 (m, 3H, H-5, SCH₂CH₃), 1.29 (td, *J* = 7.4, 0.9 Hz, 3H, SCH₂CH₃); ¹³C NMR (126 MHz, CDCl₃): δ 90.3 (C-3), 87.2 (C-2), 83.9 (C-4), 70.7 (C-6), 61.8, 61.6, 61.1, 59.3 (4×OMe), 49.3 (C-1), 47.0 (C-5), 26.1 (SCH₂CH₃), 14.8 (SCH₂CH₃); ESI-HRMS (*m/z*): [M+Na]⁺ calcd. for C₁₂H₂₄O₄NaS₂⁺ 319.1008, found 319.0995.

Ethyl 2,3,4,6-tetra-*O*-methyl-1,5-dithio- β -D-glucopyranoside-*S*-Oxides (269**, **270**):**

Thioglycoside **268** (450 mg, 1.52 mmol) was dissolved in anhydrous CH₂Cl₂ (40 mL) and the reaction mixture was cooled down to -60 °C before *m*CPBA (77% wt, 412 mg, 1.84 mmol, 1.2 equiv) solution in CH₂Cl₂ (10 mL) was added. The reaction mixture then was stirred at -60 °C for 3h. After such time the reaction mixture was quenched with saturated aq NaHCO₃ and allowed to warm up to 20 °C, and then diluted with CH₂Cl₂. The organic layer was separated and washed with 1M NaHSO₃ (50 mL), brine (50 mL), dried over MgSO₄ and concentrated to dryness. The crude was purified by flash column chromatography on silica gel eluting with hexanes:acetone (0→60%, acetone) to give mixture of (*R*_s),(*S*_s)-1-*S*-sulfoxides **269** (200 mg, 42%) as a colorless syrup, and a mixture of (*R*_s),(*S*_s)-5-*S*-sulfoxides **270** (46 mg, 10%) as a colorless syrup.

(*R*_s),(*S*_s)-1-*S*-sulfoxides **269:**

d.r. = 2.6 : 1; *R*_f 0.58 and 0.63 (hexanes : acetone 1 : 1 (H₂SO₄/EtOH)); ¹H NMR (500 MHz, CD₂Cl₂):

Major diastereomer: δ 3.88 – 3.77 (m, 2H, H-1, H-2), 3.70 – 3.60 (m, 1H, H-6a), 3.59 – 3.46 (m, 10H, H-6b, 3xOMe), 3.37 – 3.19 (m, 5H, H-3, H-4, OMe), 3.09 – 3.03 (m, 1H, H-3), 3.03 – 2.73 (m, 3H, H-5, SCH₂CH₃), 1.37 – 1.25 (m, 3H, SCH₂CH₃); **Minor diastereomer:** δ 3.70 – 3.60 (m, 7H, H-6a', 2xOMe), 3.59 – 3.46 (m, 5H, H-1, H-6b, OMe), 3.37 – 3.19 (m, 4H, H-4, OMe), 3.09 – 3.03 (m, 1H, H-3), 3.03 – 2.73 (m, 3H, H-5, SCH₂CH₃), 1.37 – 1.25 (m, 3H, SCH₂CH₃); ¹³C NMR (126 MHz, CD₂Cl₂): **Major diastereomer:** δ 88.0 (C-3), 82.6 (C-4), 79.7 (C-2), 72.0 (C-6), 61.4 (C-1), 60.4 (OMe), 60.2 (OMe), 59.2 (2xOMe), 44.8 (SCH₂CH₃), 44.4 (C-5), 7.4 (SCH₂CH₃); **Minor diastereomer:** 90.6 (C-3), 83.9 (C-4), 82.9 (C-2), 71.4 (C-6), 64.1 (C-1), 61.7 (OMe), 61.6 (OMe), 61.2 (OMe), 59.3 (OMe), 45.6 (C-5), 45.2 (SCH₂CH₃), 7.9 (SCH₂CH₃); ESI-HRMS (m/z): calcd. for C₁₂H₂₄O₅NaS₂⁺ [M+Na]⁺ 335.0957, found 335.0933.

(*R*_s),(*S*_s)-5-*S*-sulfoxides **270:**

d.r. = 1.1 : 1; *R*_f 0.40 (hexanes : acetone 3 : 2 (H₂SO₄/EtOH)); ¹H NMR (500 MHz, CDCl₃): **Major**

diastereomer: δ 3.94 – 3.84 (m, 1H, H-6a), 3.79 (t, *J* = 10.1 Hz, 1H, H-6b), 3.66 – 3.61 (m, 6H, 2xOMe), 3.57 (s, 3H, OMe), 3.54 – 3.49 (m, 4H, OMe, H-1), 3.37 – 3.26 (m, 1H, H-4), 3.20 (t, *J* = 9.1 Hz, 1H, H-

3), 2.99 (dd, $J = 11.2, 8.7$ Hz, 1H, H-2), 2.92 (q, $J = 7.4$ Hz, 2H, SCH₂CH₃), 2.68 – 2.56 (m, 1H, H-5), 1.29 (t, $J = 7.4$ Hz, 3H, SCH₂CH₃); **Minor diastereomer:** δ 3.94 – 3.84 (m, 2H, H-6b, H-6a), 3.66 – 3.61 (m, 8H, 2xOMe, H-1, H-2), 3.43 – 3.36 (m, 6H, 2xOMe), 3.37 – 3.26 (m, 1H, H-4), 3.20 (t, $J = 9.1$ Hz, 1H, H-3), 2.84 – 2.75 (m, 2H, SCH₂CH₃), 2.68 – 2.56 (m, 1H, H-5'), 1.29 (t, $J = 7.4$ Hz, 3H, 2xSCH₂CH₃); ¹³C NMR (126 MHz, CDCl₃): **Major diastereomer:** δ 89.2 (C-3), 78.9 (C-2), 75.1 (C-4), 70.7 (C-1), 67.7 (C-6), 62.0, 61.9, 61.6, 61.3 (4xOCH₃), 61.0 (C-5), 27.3 (SCH₂CH₃), 14.6 (SCH₂CH₃); **Minor diastereomer:** δ 89.6 (C-3), 79.5 (C-2), 67.0 (C-5), 70.7 (C-1), 64.9 (C-6), 64.6 (C-4), 61.4, 61.4 (2xOCH₃), 61.0 (C-5), 59.4, 59.2 (2xOCH₃), 26.5 (SCH₂CH₃), 14.5 (SCH₂CH₃); ESI-HRMS (m/z): [M+Na]⁺ calcd. for C₁₂H₂₄O₅NaS₂⁺ 335.0957, found 335.0931.

Ethyl 2,3,4,6-tetra-*O*-methyl-1,5-dithio- α -D-glucopyranoside (271):

Thioglycoside **50a** (1.3 g, 3.18 mmol) was dissolved in anhydrous MeOH (30 mL) and NaOMe (68 mg, 1.272 mmol, 0.4 equiv) was added and the reaction mixture was stirred at 20 °C for 1 h. After such time the reaction mixture was quenched with Amberlyst 15 (H⁺) ion-exchange resin until pH 5. The reaction mixture was then filtered, and the filtrate was concentrated to dryness. The crude residue was taken up in anhydrous DMF (20 mL) and the resulting solution was cooled down to 0 °C before NaH (60% dispersion in the mineral oil, 636 mg, 15.9 mmol, 5 equiv) was added followed by addition of MeI (1.2 mL, 19.08 mmol, 6 equiv). The reaction mixture was then stirred for 12h with warming from 0→20 °C. After such time the reaction mixture was quenched with MeOH (910 mL), diluted with EtOAc (80 mL), washed with H₂O (80 mL), brine (80 mL), dried over MgSO₄ and concentrated to dryness. The crude product was purified by a flash column chromatography eluting with hexanes:EtOAc (0→60%, EtOAc) to give the product as a yellowish syrup (425 mg, 45%). R_f 0.28 (hexanes:EtOAc 3:2 (H₂SO₄/EtOH)); $[\alpha]_D^{22}$ +202.6 (CHCl₃, 0.0127); ¹H NMR (500 MHz, CDCl₃): δ 4.27 (d, $J = 4.5$ Hz, 1H, H-1), 3.80 (dd, $J = 10.2, 3.5$ Hz, 1H, H-6a), 3.62 (dd, $J = 8.8, 4.3$ Hz, 1H, H-2), 3.59 – 3.50 (m, 7H, 2xOCH₃, H-6b), 3.47 (s, 3H, OCH₃), 3.36 (s, 3H, OCH₃), 3.33 – 3.24 (m, 3H, H-3, H-4, H-5), 2.67 (qd, $J = 10.3, 6.3$ Hz, 2H, SCH₂CH₃), 1.25 (t, $J = 7.3$ Hz, 3H, SCH₂CH₃); ¹³C NMR (126 MHz, CDCl₃): δ 85.8 (C-2), 85.5 (C-3), 83.9 (C-4), 70.6 (C-6), 61.5,

61.0, 59.1, 57.8 (4×OCH₃), 49.6 (C-1), 41.9 (C-5), 25.6 (SCH₂CH₃), 14.2 (SCH₂CH₃); ESI-HRMS (m/z): [M+Na]⁺ calcd. for C₁₂H₂₄O₄NaS₂⁺ 319.1008, found 319.0997.

Ethyl 2,3,4,6-tetra-*O*-methyl-1,5-dithio- α -D-glucopyranoside-*S*-Oxides (272):

Thioglycoside **271** (246 mg, 0.830 mmol) was dissolved in anhydrous CH₂Cl₂ (10 mL) and the reaction mixture was cooled down to -60 °C before *m*CPBA (77% wt, 205 mg, 0.913 mmol, 1.1 equiv) solution in anhydrous CH₂Cl₂ (5 mL) was added. The reaction mixture then was stirred at -60 °C for 2h. After such time the reaction mixture was quenched with saturated aq NaHCO₃ (5 mL), allowed to warm up to 20 °C. The resulting emulsion was diluted with CH₂Cl₂ (50 mL) and the organic layer was separated, washed with saturated aq NaHCO₃ (50 mL), 1M NaHSO₃ (50 mL), brine (50 mL), dried over MgSO₄ and concentrated to dryness. The crude was purified by flash column chromatography on silica gel eluting with hexanes:acetone (0→80%, acetone) to give a complex mixture of (*R*_s),(*S*_s)-5-*S*-sulfoxides **273** (82 mg, 32%) as a colorless syrup and (*R*_s),(*S*_s)-1-*S*-sulfoxides **272** (81 mg, 31%) as a colorless syrup.

(*R*_s),(*S*_s)-1-*S*-sulfoxides 272:

d.r. = 4.2 : 1; *R*_f 0.48 (hexanes : acetone 1 : 1 (H₂SO₄/EtOH)); ¹H NMR (500 MHz, CD₂Cl₂): **Major diastereomer:** δ 3.99 (dd, *J* = 6.0, 4.2 Hz, 1H, H-2), 3.84 (d, *J* = 4.1 Hz, 1H, H-1), 3.61 – 3.22 (m, 17H, H-5, H-4, H-3, H-6a, H-6b, 4×OCH₃), 2.98 – 2.83 (m, 1H, SCH₂CH₃), 2.75 – 2.64 (m, 1H, SCH₂CH₃), 1.28 (t, *J* = 7.5 Hz, 3H, SCH₂CH₃); **Minor diastereomer:** δ 3.87 (dd, *J* = 10.0, 4.7 Hz, 1H, H-2), 3.61 – 3.22 (m, 18H, H-1, H-3, H-4, H-5, H-6a, H-6b, 4×OCH₃), 2.98 – 2.83 (m, 1H, SCH₂CH₃), 2.75 – 2.64 (m, 1H, SCH₂CH₃), 1.35 (t, *J* = 7.4 Hz, 3H, SCH₂CH₃); ¹³C NMR (126 MHz, CD₂Cl₂): **Major diastereomer:** δ 83.1 (C-4), 82.6 (C-3), 80.3 (C-2), 71.5 (C-6), 59.5, 59.4, 59.1, 58.9 (4×OMe), 58.8 (C-1), 44.5 (SCH₂CH₃), 42.5 (C-5), 6.7 (SCH₂CH₃); **Minor diastereomer:** δ 83.0 (C-4), 76.8 (C-3), 72.5 (C-2), 66.4 (C-6), 60.2, 59.3, 58.5, 58.1 (4×OMe), 57.2 (C-1), 46.3 (SCH₂CH₃), 42.5 (C-5), 6.69 (SCH₂CH₃); ESI-HRMS (m/z): [M+Na]⁺ calcd. for C₁₂H₂₄O₅NaS₂⁺ 335.0957, found 335.0932.

Ethyl 2,3,4,6-tetra-*O*-methyl-1-thio- β -D-glucopyranoside (274):

Thioglycoside **51b** (1.08 g, 2.75 mmol) was dissolved in anhydrous MeOH (60 mL) and NaOMe (59 mg, 1.1 mmol, 0.4 equiv) was added (pH 10) and the reaction mixture was stirred for 1 h at 20 °C. After such time the reaction mixture was quenched with Amberlyst 15 (H⁺) ion-exchange resin until pH 3. The resulting mixture was filtered, and the filtrate was concentrated to dryness. The crude intermediate was redissolved in anhydrous DMF (40 mL) and the resulting solution was cooled down to 0 °C before NaH (60% dispersion in mineral oil, 550 mg, 13.75 mmol, 5 equiv) was added followed by MeI (1.0 mL, 16.5 mmol, 6 equiv) and the reaction mixture was stirred with warming from 0 → 20 °C until completion (detected by LCMS and TLC analysis). After completion the reaction mixture was quenched with MeOH (until gas formation was no longer observed) at 0 °C, diluted with EtOAc (100 mL), washed with H₂O (80 mL), brine (80 mL), dried over MgSO₄ and concentrated to dryness. The crude product was purified by flash column chromatography on silica gel eluting with hexanes:EtOAc (0→50%, EtOAc) to give the product as a colorless oil (544 mg, 70%) with spectral data identical to that reported in the literature.³³ *R_f* 0.48 (hexanes:EtOAc 7:3 (H₂SO₄/EtOH)); ¹H NMR (500 MHz, CDCl₃): δ 4.26 (dd, *J* = 9.8, 1.0 Hz, 1H), 3.66 – 3.55 (m, 7H), 3.56 – 3.49 (m, 4H), 3.36 (d, *J* = 1.0 Hz, 3H), 3.27 – 3.21 (m, 1H), 3.17 (t, *J* = 8.8 Hz, 1H), 3.10 (t, *J* = 9.3 Hz, 1H), 2.95 (dd, *J* = 9.7, 8.5 Hz, 1H), 2.76 – 2.65 (m, 2H), 1.27 (t, *J* = 7.4 Hz, 3H); ¹³C NMR (126 MHz, CDCl₃): δ 88.5, 84.8, 83.4, 79.5, 78.8, 71.5, 60.9, 60.8, 60.4, 59.3, 24.9, 14.9; ESI-HRMS (*m/z*): [*M*+Na]⁺ calcd. for C₁₂H₂₄O₅NaS⁺ 303.1237, found 303.1223.

(*R_S*),(*S_S*)-Ethyl 2,3,4,6-tetra-*O*-methyl-1-thio-β-D-glucopyranoside-1-*S*-Oxides (275):

Thioglycoside **274** (190 mg, 0.678 mmol) was dissolved in anhydrous CH₂Cl₂ (10 mL) and the reaction mixture was cooled down to –60 °C before *m*CPBA (77% wt, 167 mg, 0.7458 mmol, 1.1. equiv) solution in anhydrous CH₂Cl₂ (5 mL) was added. The reaction mixture then was stirred at –60 °C for 1.5 h. After such time the reaction mixture was quenched with sat aq NaHCO₃ (5 mL) and allowed to warm up to 20 °C. The reaction mixture was then diluted with CH₂Cl₂ (40 mL), washed with sat aq NaHCO₃ (50 mL), 1M NaHSO₃ (30 mL), brine (50 mL), dried over MgSO₄ and concentrated to dryness. The crude product was purified by flash column chromatography on silica gel eluting with hexanes:EtOAc (0→100%, EtOAc) and

EtOAc:MeOH (0→50%, MeOH) to give the product as a white solid (124 mg, 62%). d.r. = 1.9 : 1; R_f 0.37, 0.51 (EtOAc (H₂SO₄/EtOH)); ¹H NMR (500 MHz, CD₂Cl₂): **Major isomer:** δ 4.03 (d, J = 9.1 Hz, 1H, H-1), 3.64 – 3.42 (m, 11H, 3×OCH₃, H-2, H-6a), 3.37 – 3.24 (m, 6H, OCH₃, H-3, H-4, H-6b), 3.18 – 3.03 (m, 1H, H-5), 3.03 – 2.91 (m, 1H, SCH₂CH₃), 2.80 – 2.61 (m, 1H, SCH₂CH₃), 1.32 – 1.17 (m, 3H, SCH₂CH₃); **Minor isomer:** δ 3.67 (d, J = 10.2 Hz, 1H, H-1), 3.64 – 3.42 (m, 11H, 3×OCH₃, H-2, H-6a), 3.37 – 3.24 (m, 6H, OCH₃, H-3, H-4, H-6b), 3.18 – 3.03 (m, 1H, H-5), 3.03 – 2.91 (m, 1H, SCH₂CH₃), 2.80 – 2.61 (m, 1H, SCH₂CH₃), 1.32 – 1.17 (m, 3H, SCH₂CH₃); ¹³C NMR (126 MHz, CD₂Cl₂): **Major isomer:** δ 91.8 (C-1), 88.5 (C-3), 79.3 (C-4), 79.0 (C-5), 77.5 (C-2), 71.3 (C-6), 60.6, 60.2, 59.9, 59.0 (4×OCH₃), 42.5 (SCH₂CH₃), 7.4 (SCH₂CH₃); **Minor isomer:** δ 88.9 (C-1), 88.5 (C-3), 79.8 (C-4), 79.0 (C-5), 77.3 (C-2), 71.1 (C-6), 60.7, 60.6, 60.4, 59.0 (4×OCH₃), 40.9 (SCH₂CH₃), 7.2 (SCH₂CH₃); ESI-HRMS (m/z): [M+Na]⁺ calcd. for C₁₂H₂₄O₅NaS⁺ 319.1186, found 319.1174.

Ethyl 2,3,4,6-tetra-*O*-methyl-1-thio- α -D-glucopyranoside (276):

Thioglycoside **51a** (1.5 g, 3.82 mmol) was dissolved in anhydrous MeOH (30 mL) and NaOMe (83 mg, 1.53 mmol, 0.4 equiv) was added (pH 10) and the reaction mixture was stirred for 1h at 20 °C. After such time the reaction mixture was quenched with Amberlyst 15 (H⁺) ion-exchange resin until pH 3. The resulting mixture was filtered, and the filtrate was concentrated to dryness. The crude intermediate was redissolved in anhydrous DMF (30 mL) and the resulting solution was cooled down to 0 °C before NaH (60% dispersion in mineral oil, 765 mg, 19.1 mmol, 5 equiv) was added followed by MeI (1.43 mL, 22.92 mmol, 6 equiv) and the reaction mixture was stirred at 0 → 20 °C until completion (detected by LCMS and TLC analysis). After completion the reaction mixture was quenched with MeOH (until gas formation was no longer observed) at 0 °C, diluted with EtOAc (100 mL), washed with H₂O (80 mL), brine (80 mL), dried over MgSO₄ and concentrated to dryness. The crude product was purified by flash column chromatography on silica gel eluting with hexanes:EtOAc (0→50%, EtOAc) to give the product as a yellowish syrup (732 mg, 68%) with spectral data identical to that reported in the literature.²⁶⁶ R_f 0.51 (hexanes:EtOAc 7:3 (H₂SO₄/EtOH)); ¹H NMR (500 MHz, CDCl₃): δ 5.47 (d, J = 5.4 Hz, 1H), 4.01 (ddd, J = 10.0, 3.7, 2.1 Hz,

1H), 3.70 – 3.30 (m, 18H), 3.20 (dd, $J = 10.1, 8.8$ Hz, 1H), 2.64 – 2.47 (m, 2H), 1.27 (t, $J = 7.4$ Hz, 3H); ^{13}C NMR (126 MHz, CDCl_3): δ 84.0, 82.8, 81.6, 79.3, 71.1, 70.3, 61.0, 60.5, 59.3, 58.2, 23.9, 14.8; ESI-HRMS (m/z): $[\text{M}+\text{Na}]^+$ calcd. for $\text{C}_{12}\text{H}_{24}\text{O}_5\text{NaS}^+$ 303.1237, found 303.1225.

Ethyl 2,3,4,6-tetra-*O*-methyl-1-thio- α -D-glucopyranoside-1-*S*-oxide (277):

Thioglycoside **276** (548 mg, 1.95 mmol) was dissolved in anhydrous CH_2Cl_2 (20 mL) and the reaction mixture was cooled down to -50°C and *m*CPBA (77% wt, 480 mg, 2.145 mmol, 1.1 equiv) solution in anhydrous CH_2Cl_2 (10 mL) was added and the reaction mixture was stirred for 1.5h at -50°C . After such time sat aq NaHCO_3 (10 mL) was added to quench the reaction, and the reaction mixture was allowed to warm up to 20°C . After that the reaction mixture was diluted with CH_2Cl_2 (30 mL), washed with NaHCO_3 (60 mL), 1M NaHSO_3 (60 mL), brine (60 mL), dried over MgSO_4 and concentrated to dryness. The crude product was purified by flash column chromatography on silica gel eluting with hexanes:EtOAc (0 \rightarrow 100%, EtOAc) to give the product as a colorless syrup (316 mg, 55%). R_f 0.57 (EtOAc ($\text{H}_2\text{SO}_4/\text{EtOH}$)); $[\alpha]_{\text{D}}^{20} +101.7$ (CHCl_3 , $C = 0.0047$); ^1H NMR (500 MHz, CDCl_3): δ 4.92 (d, $J = 6.1$ Hz, 1H, H-1), 4.16 (ddd, $J = 10.0, 4.4, 2.1$ Hz, 1H, H-5), 3.96 (t, $J = 8.1$ Hz, 1H, H-3), 3.78 – 3.71 (m, 1H, H-2), 3.68 – 3.48 (m, 11H, H-6a, H-6b, $3\times\text{OCH}_3$), 3.38 (s, 3H, OCH_3), 3.23 – 3.08 (m, 2H, H-4, SCH_2CH_3), 3.08 – 2.94 (m, 1H, SCH_2CH_3), 1.50 – 1.32 (t, $J = 7.5$ Hz, 3H, SCH_2CH_3); ^{13}C NMR (126 MHz, CDCl_3): δ 86.5 (C-1), 81.6 (C-3), 80.4 (C-2), 78.2 (C-4), 74.9 (C-5), 70.9 (C-6), 60.4, 59.9, 59.7, 59.2 ($4\times\text{OCH}_3$), 46.6 (SCH_2CH_3), 5.9 (SCH_2CH_3); ESI-HRMS (m/z): $[\text{M}+\text{Na}]^+$ calcd. for $\text{C}_{12}\text{H}_{24}\text{O}_5\text{NaS}^+$ 319.1186, found 319.1175.

Synthesis of the armed trichloroacetimidates (Scheme 61):

2,3,4,6-Tetra-*O*-methyl- α -D-glucopyranose (290):

2,3,4,6-Tetra-*O*-acetyl-D-glucopyranose **254** (2.06 g, 5.91 mmol) was dissolved in anhydrous THF (20 mL) and 2,3-dihydropyran (1.6 mL, 17.73 mmol, 3 equiv) was added followed by PTSA (112 mg, 0.591 mmol, 0.1 equiv) and the reaction mixture was stirred until completion (detected by LCMS and TLC). After completion, the reaction mixture was quenched with saturated aqueous NaHCO_3 (10 mL), and diluted with

EtOAc (60 mL). The organic layer was separated, washed with brine (60 mL), dried over MgSO₄ and concentrated to dryness. The crude was used in the next step without further purification. Thus, 2-tetrahydropyranyl 2,3,4,6-tetra-*O*-acetyl-D-glucopyranoside **289** (2.28 g, 5.25 mmol) was suspended in anhydrous MeOH (40 mL) and NaOMe (1M solution in MeOH, 1.58 mL, 1.58 mmol, 0.3 equiv) and the reaction mixture was stirred for 1h at 20 °C. After such time the reaction mixture was quenched with Amberlite IR-120 (H⁺) until pH 6. The resulting mixture was filtered, and the filtrate was concentrated to dryness. The crude was taken up in DMF (30 mL) and NaH (60% dispersion in mineral oil, 1.15 g, 31.5 mmol, 6 equiv) was added at 0 °C and the reaction mixture was stirred for 10 minutes before MeI (2 mL, 32.1 mmol, 6.1 equiv) was added. The reaction mixture then was stirred at 0→20 °C for 16h. After such time the reaction mixture was quenched with MeOH (10 mL) at 0 °C and the resulting solution was distributed between EtOAc (100 mL) and H₂O (100 mL). The organic layer was collected, and the aqueous layer was extracted with EtOAc (50 mL). The combined organic layers were washed with brine (60 mL), dried over MgSO₄ and concentrated to dryness and co-evaporated with toluene (3×10 mL). The crude was taken into MeOH (20 mL) and cat HCl (37% aq. solution) was added, and the reaction mixture was stirred for 1h at 20 °C. After such time the reaction mixture was concentrated to dryness. The crude product was purified by column chromatography eluting with hexanes:EtOAc (10→60%, EtOAc) to give a mixture of anomeric hemiacetals ($\alpha : \beta = 2.3 : 1$) as a white solid (1.01 g, 72% over 4 steps) with spectral data identical to those reported in the literature.²⁶⁷ *R*_f 0.22 (hexanes:EtOAc 1:1 (H₂SO₄/EtOH)); ¹H NMR (500 MHz, CDCl₃): δ 5.28 (d, *J* = 3.6 Hz, 1H), 4.54 (d, *J* = 7.7 Hz, 1H), 3.86 (dt, *J* = 10.2, 3.4 Hz, 1H), 3.70 – 3.41 (m, 18H), 3.39 – 3.35 (m, 5H), 3.32 (ddd, *J* = 9.8, 5.7, 1.9 Hz, 1H), 3.20 – 3.03 (m, 3H), 2.93 (dd, *J* = 9.0, 7.7 Hz, 1H); ¹³C NMR (126 MHz, CDCl₃): δ 97.2, 90.7, 86.5, 84.9, 83.2, 82.0, 79.8, 79.7, 74.4, 71.7, 71.4, 69.9, 60.9, 60.8, 60.6, 60.5, 60.5, 59.2, 59.2, 58.9; ESI-HRMS (*m/z*): [M+Na]⁺ calcd. for C₁₆H₂₄O₁₀NaS⁺ 259.1152, found 259.1140.

2,3,4,6-Tetra-*O*-methyl- α,β -D-glucopyranosyl trichloroacetimidate (291):

Hemiacetal **290** (85 mg, 0.36 mmol) was dissolved in anhydrous CH₂Cl₂ (6 mL) and the reaction mixture was cooled down to 0 °C before CCl₃CN (360 μL, 3.6 mmol, 10 equiv) was added followed by DBU (5 μL, 0.037 mmol, 0.1 equiv). The reaction mixture then was stirred for 1h at 20 °C. After such time the reaction mixture was concentrated to dryness and the crude product was purified by flash column chromatography on silica gel eluting with hexanes:EtOAc (0→40%, EtOAc) to give a mixture of anomeric imidates ($\alpha : \beta = 2 : 1$) as a colorless syrup (80 mg, 59%) with spectral data matching that reported in the literature.²⁶⁸ R_f 0.57, 0.51 (hexanes:EtOAc 1:1 (H₂SO₄/EtOH)).

291 α :

¹H NMR (500 MHz, CDCl₃): δ 8.58 (s, 1H, NH), 6.47 (d, $J = 3.5$ Hz, 1H, H-1 α), 3.80 (dt, $J = 10.4, 2.7$ Hz, 1H, H-5 α), 3.67 – 3.50 (m, 9H, H-6a, H-6b, H-4 α , 2×OCH₃), 3.47 (s, 3H, OCH₃), 3.38 (s, 3H, OCH₃), 3.37 – 3.22 (m, 5H); ¹³C NMR (126 MHz, CDCl₃): δ 161.3 (C=NH), 94.0 (C-1), 91.3 (CCl₃), 83.0 (C-4), 81.1 (C-2), 78.6 (C-3), 72.8 (C-5), 70.6 (C-6), 61.0, 60.6, 59.2, 58.8 (4×OCH₃).

291 β :

¹H NMR (500 MHz, CDCl₃): δ 8.63 (s, 1H, NH), 5.59 (d, $J = 7.3$ Hz, 1H, H-1), 3.67 – 3.50 (m, 12H, H-6a, H-6b, H-4, 3×OCH₃), 3.46 – 3.39 (m, 1H, H-5), 3.38 (s, 3H, OCH₃), 3.37 – 3.22 (m, 2H, H-3, H-2); ¹³C NMR (126 MHz, CDCl₃): 161.4 (C=NH), 98.3 (C-1), 91.0 (CCl₃), 86.4 (C-4), 82.9 (C-2), 78.8 (C-3), 75.6 (C-5), 70.8 (C-6), 61.0, 60.8, 59.4 (4×OCH₃).

ESI-HRMS (m/z): [M+Na]⁺ calcd. for C₁₂H₂₀O₆NCl₃Na⁺ 402.0248, found 402.0229.

2,3,4,6-Tetra-*O*-methyl-5-thio- α,β -D-glucopyranoside (293):

Hemiacetal **255** (1.2 g, 3.29 mmol) was dissolved in anhydrous THF (20 mL) and 2,3-dihydropyran (0.9 mL, 9.87 mmol, 3 equiv) was added followed by PTSA (63 mg, 0.329 mmol, 0.1 equiv) and the reaction mixture was stirred for 1h at 20 °C. After 1h additional PTSA (63 mg, 0.329 mmol, 0.1 equiv) was added followed by 2,3-dihydropyran (0.5 mL, 3.29 mmol, 1 equiv) and the reaction mixture was stirred for 1h. After such time the reaction mixture was quenched with saturated aqueous NaHCO₃ (10 mL), and diluted

with EtOAc (60 mL). The organic layer was separated, washed with brine (60 mL), dried over MgSO₄ and concentrated to dryness. The crude was used in the next step without further purification. Accordingly, tetrahydropyranyl glycoside **292** (820 mg, 1.828 mmol) was suspended in anhydrous MeOH (15 mL) and NaOMe (29 mg, 0.548 mmol, 0.3 equiv) was added and the reaction mixture was stirred for 1h at 20 °C. After such time the reaction mixture was quenched with Amberlite IRC120 (H⁺) (portion-wise addition until pH 5-6). After that the reaction mixture was filtered and the filtrate was concentrated to dryness. The crude product was taken up in anhydrous DMF (15 mL) and the reaction mixture was cooled down to 0 °C before NaH (60% dispersion in mineral oil, 474 mg, 11.85 mmol, 6.5 equiv) was added and the reaction mixture was stirred for 10 minutes at 0 °C. After such time MeI (682 µL, 10.97 mmol, 6 equiv) was added and the reaction mixture was stirred until completion (monitored by TLC and LCMS). After 3h the reaction mixture was quenched with MeOH (10 mL) at 0 °C, and the resulting mixture was distributed between EtOAc (100 mL) and H₂O (50 mL). The organic layer was collected, and the aqueous layer was additionally extracted with EtOAc (50 mL). The combined organic layers were washed with brine (50 mL), dried over MgSO₄ and concentrated to dryness and co-evaporated with toluene (3×10 mL). The crude residue was taken into MeOH (20 mL) followed by addition of PTSA (35 mg, 0.1828 mmol, 0.1 equiv) and the reaction mixture was stirred for 1h at 45 °C. After such time the reaction mixture was allowed to cool down to 20 °C, and subsequently quenched with saturated aq NaHCO₃ (5 mL). After that the reaction mixture was concentrated to dryness, redissolved in EtOAc (40 mL), washed with saturated aqueous NaHCO₃ (20 mL), brine (20 mL), dried over MgSO₄ and concentrated to dryness. The crude was purified by column chromatography on a silica gel eluting with hexanes:EtOAc (0→40%, EtOAc) to give a mixture of anomeric hemiacetals ($\alpha : \beta = 16:1$) as a colorless syrup (395 mg, 48% over 4 steps); *R*_f 0.21 (hexanes:EtOAc 1:1 (H₂SO₄/EtOH)); ¹H NMR (500 MHz, CD₂Cl₂): δ 4.97 (d, *J* = 3.4 Hz, 1H, H-1), 3.72 (dd, *J* = 9.9, 5.0 Hz, 1H, H-6a), 3.56 (s, 3H, OCH₃), 3.54 – 3.51 (m, 4H, H-6b, OCH₃), 3.47 (s, 3H, OCH₃), 3.38 – 3.27 (m, 7H, OCH₃, H-2, H-3, H-4), 3.23 – 3.17 (m, 1H, H-5), 2.75 (br, 1H, OH); ¹³C NMR (126 MHz, CD₂Cl₂): δ 86.7 (C-2), 84.9 (C-3), 84.0 (C-4), 71.1 (C-1), 70.9 (C-6), 61.4, 61.0, 59.1, 58.3 (4×OCH₃), 41.4 (C-5); The

minor β -isomer was identified in mixture by the following diagnostic signal: 4.61 (dd, $J = 7.3, 5.0$ Hz, 1H, H-1).

ESI-HRMS (m/z): $[M+Na]^+$ calcd. for $C_{10}H_{20}O_5NaS^+$ 275.0924, found 275.0918.

2,3,4,6-Tetra-*O*-methyl-5-thio- α -D-glucopyranosyl trichloroacetimidate (294):

Hemiacetal **293** (87 mg, 0.345 mmol) was dissolved in anhydrous CH_2Cl_2 (6 mL) and the reaction mixture was cooled down to 0 °C before CCl_3CN (350 μ L, 3.45 mmol, 10 equiv) was added followed by DBU (5 μ L, 0.0345 mmol, 0.1 equiv). The reaction mixture then was stirred at 20 °C for 1h. After such time the reaction mixture was concentrated to dryness, and the crude product was purified by flash column chromatography eluting with hexanes:EtOAc (0 \rightarrow 40%, EtOAc) to give the product as a colorless syrup (82 mg, 60%). R_f 0.53 (hexanes:EtOAc 3:2 (H_2SO_4 /EtOH)); $[\alpha]_D^{20} +141.5$ ($CHCl_3$, $C = 0.031$); 1H NMR (500 MHz, $CDCl_3$): δ 8.61 (s, 1H, NH), 6.26 (d, $J = 3.0$ Hz, 1H, H-1), 3.81 (dd, $J = 10.0, 4.5$ Hz, 1H, H-6a), 3.63 (s, 3H, OCH_3), 3.61 (s, 3H, OCH_3), 3.57 – 3.40 (m, 7H, H-6b, H-2, H-4, H-3, OCH_3), 3.36 (s, 3H, OCH_3), 3.24 (ddd, $J = 10.2, 4.6, 2.7$ Hz, 1H, H-5); ^{13}C NMR (126 MHz, $CDCl_3$): δ 161.1 (C=NH), 91.3 (CCl_3), 85.3 (C-2), 84.8 (C-3), 83.3 (C-4), 75.9 (C-5), 70.1 (C-6), 61.6, 61.2, 59.1, 58.3 (4 \times OCH_3), 42.6 (C-5); ESI-HRMS (m/z): $[M+Na]^+$ calcd. for $C_{12}H_{20}O_5NCl_3NaS^+$ 418.0020, found 418.0003.

6.4. Experimental procedures for the VT NMR experiments described in Chapter 4

VT NMR experiments with tetrahydrothiopyran derivatives and simple vinyl sulfides (Scheme 41, Scheme 42):

Protonation of 2,3-dihydrothiopyran 208 with TfOH at -78 °C:

2,3-Dihydrothiopyran **208** (43 mg, 0.429 mmol) was dissolved in CD_2Cl_2 (0.75 mL), and the reaction mixture was transferred into a vacuum dried NMR tube and sealed with a septum cap under an Ar atmosphere. The NMR tube containing glycosyl donor solution then was placed into the NMR probe and cooled down to -78 °C. The first 1H , ^{13}C spectra were collected, then the sample was quickly removed from the probe and precooled TfOH (41 μ L, 0.089 mmol, 1.1 equiv) was quickly added and the tube quickly

shaken. The sample then was returned to the cold NMR probe, and ^1H , ^{19}F spectra were recorded as soon as possible. The temperature then was increased to $-60\text{ }^\circ\text{C}$ and ^1H , ^{19}F spectra were recorded after 5 minutes. After that the temperature was increased by $10\text{ }^\circ\text{C}$ increments and ^1H , ^{19}F spectra were recorded at each temperature after 5 minutes. After termination of the VT NMR experiment the sample was collected and diluted with EtOAc (30 mL), washed with NaHCO_3 (10 mL), brine (20 mL), dried over MgSO_4 and concentrated to dryness to give complex mixture (20 mg) of self-condensation products containing dimer **219**, which was identified by the following diagnostic signals:²²⁹ ^1H NMR (500 MHz, CDCl_3): δ 5.99 (s, 1H), 3.27 – 3.21 (m, 1H); ^{13}C NMR (126 MHz, CDCl_3): δ 132.4, 115.4; HRMS (m/z): $[\text{M}+\text{H}]^+$ calcd. for $\text{C}_{10}\text{H}_{17}\text{S}_2^+$ 201.0766, found 201.0760.

Protonation of 2,3-dihydrothiopyran with TfOH at $-78\text{ }^\circ\text{C}$ in the presence of quaternary ammonium salt:

2,3-Dihydrothiopyran **208** (40 mg, 0.399 mmol) and Bu_4NPF_6 (87 mg, 0.225 mmol, 1.77 equiv) were dissolved in CD_2Cl_2 (0.75 mL), and the reaction mixture was transferred into a vacuum dried NMR tube and sealed with a septum cap under an Ar atmosphere. The NMR tube containing glycosyl donor solution then was placed into the NMR probe and cooled down to $-78\text{ }^\circ\text{C}$. The first ^1H , ^{13}C spectra were collected, then the sample was quickly removed from the probe and precooled TfOH (39 μL , 0.089 mmol, 1.1 equiv) was quickly added and the tube quickly shaken. The sample then was returned to the cold NMR probe, and ^1H , ^{13}C , DEPT, HMQC, and ^{19}F spectra were recorded as soon as possible. The temperature then was increased to $-60\text{ }^\circ\text{C}$ and ^1H , ^{19}F spectra were recorded after 5 minutes. After that the temperature was increased by $10\text{ }^\circ\text{C}$ increments and ^1H , ^{19}F spectra were recorded at each temperature after 5 minutes. After termination of the VT NMR experiment the sample was collected and diluted with EtOAc (30 mL), washed with NaHCO_3 (10 mL), brine (20 mL), dried over MgSO_4 and concentrated to dryness to give complex mixture (25 mg) of self-condensation products containing dimer²²⁹ **219** and quaternary ammonium salt identified by the following diagnostic signals. ^1H NMR (500 MHz, CDCl_3): δ 5.99 (s, 1H), 3.34 – 2.95 (m, 2H), 3.27 – 3.21 (m, 1H), 1.62 – 1.52 (m, 2H), 1.37 (h, $J = 7.4\text{ Hz}$, 2H), 0.95 (t, $J = 7.4\text{ Hz}$, 3H); ^{13}C NMR

(126 MHz, CDCl₃): δ 132.4, 115.4, 58.5, 23.8, 19.6, 13.5; HRMS (m/z): [M+H]⁺ calcd. for C₁₀H₁₇S₂⁺ 201.0766, found 201.0760.

Protonation of 2,3-dihydrothiopyran 208 with TfOH at -88 °C:

2,3-Dihydrothiopyran **208** (30 mg, 0.3 mmol) was dissolved in CD₂Cl₂ (0.75 mL), and the reaction mixture was transferred into a vacuum dried NMR tube and sealed with a septum cap under an Ar atmosphere. The NMR tube containing glycosyl donor solution then was placed into the NMR probe and cooled down to -88 °C. The first ¹H, ¹³C spectra were collected, then the sample was quickly removed from the probe and precooled TfOH (58 μ L, 0.66 mmol, 2.2 equiv) was quickly added and the tube quickly shaken. The sample then was returned to the cold NMR probe, and ¹H, DEPT, ¹³C, HMQC, HMBC, and ¹⁹F spectra were recorded as soon as possible at -88 °C. The temperature then was increased to -78 °C and ¹H, ¹⁹F spectra were recorded after 5 minutes. After that the temperature was increased -60 °C and ¹H, ¹⁹F spectra were recorded after 5 minutes. After that the temperature was increased by 10 °C increments and ¹H, ¹⁹F spectra were recorded at each temperature after 5 minutes. After termination of the VT NMR experiment the sample was collected and diluted with EtOAc (30 mL), washed with NaHCO₃ (10 mL), brine (20 mL), dried over MgSO₄ and concentrated to dryness to give a complex mixture (18 mg) of self-condensation products containing dimer **219** identified by diagnostic signals identical to those described above.²²⁹

Generation of thienium cation 210 at -88 °C in presence of quaternary ammonium salt:

2,3-Dihydrothiopyran **208** (25mg, 0.25 mmol) and Bu₄NPF₆ (87 mg, 0.225 mmol, 0.9 equiv) were dissolved in CD₂Cl₂ (0.75 mL), and the reaction mixture was transferred into a vacuum dried NMR tube and sealed with a septum cap under an Ar atmosphere. The NMR tube containing glycosyl donor solution then was placed into the NMR probe and cooled down to -88 °C. The first ¹H, ¹³C spectra were collected, then the sample was quickly removed from the probe and precooled TfOH (49 μ L, 0.55 mmol, 2.2 equiv) was quickly added and the tube quickly shaken. The sample then was returned to the cold NMR probe, and ¹H, DEPT, ¹³C, HMQC, HMBC, and ¹⁹F spectra were recorded as soon as possible at -88 °C. The temperature then was increased to -78 °C and ¹H, ¹⁹F spectra were recorded after 5 minutes. After termination of the VT

NMR experiment the sample was collected and diluted with EtOAc (30 mL), washed with NaHCO₃ (10 mL), brine (20 mL), dried over MgSO₄ and concentrated to dryness to give complex mixture (18 mg) of self-condensation products containing dimer **219** identified by diagnostic signals identical to those described above.²²⁹

Diagnostic signals of thiocarbenium cation (210):

¹H NMR (500 MHz, CD₂Cl₂): δ 11.23 (s, 1H, H-1), 3.72 – 3.60 (m, 1H, H-5), 2.44 – 1.57 (m, 1H, H-2); ¹³C NMR (126 MHz, CD₂Cl₂) δ 238.3 (C=S⁺), 40.1 (C-5), 20.8 (C-2); ¹⁹F NMR (470 MHz CD₂Cl₂) δ -76.54.

Protonation of 2,3-dihydropyran **220 with TfOH at -88 °C:**

2,3-Dihydropyran **220** (44 mg, 0.523 mmol) was dissolved in CD₂Cl₂ (0.75 mL), and the reaction mixture was transferred into a vacuum dried NMR tube and sealed with a septum cap under an Ar atmosphere. The NMR tube containing glycosyl donor solution then was placed into the NMR probe and cooled down to -88 °C. The first ¹H, ¹³C spectra were collected, then the sample was quickly removed from the probe and precooled TfOH (102 μL, 1.15 mmol, 2.2 equiv) was quickly added and the tube quickly shaken. The sample then was returned to the cold NMR probe, and ¹H, ¹³C and ¹⁹F spectra were recorded as soon as possible at -88 °C. The temperature then was increased to -78 °C and ¹H, ¹⁹F spectra were recorded after 5 minutes. After that the temperature was increased to -60 °C and ¹H, ¹³C, and ¹⁹F spectra were recorded after 5 minutes. After that the temperature was increased by 10 °C increments and ¹H, ¹³C, and ¹⁹F spectra were recorded at each temperature after 5 minutes. After termination of the VT NMR experiment the sample was collected and diluted with EtOAc (40 mL), washed with NaHCO₃ (30 mL), brine (30 mL), dried over MgSO₄ and concentrated to dryness to give mixture (21 mg) of self-condensation products containing dimer **222**. HRMS (m/z): [M+H]⁺ calcd. for C₁₀H₁₇O₂⁺ 169.1223, found 169.1215.

Protonation of ethyl vinyl sulfide **223 with TfOH at -88 °C:**

Ethyl vinyl sulfide **223** (30 mg, 0.316 mmol) was dissolved in CD₂Cl₂ (0.75 mL), and the reaction mixture was transferred into a vacuum dried NMR tube and sealed with a septum cap under an Ar atmosphere. The

NMR tube containing glycosyl donor solution then was placed into the NMR probe and cooled down to -88 °C. The first ^1H , ^{13}C spectra were collected, then the sample was quickly removed from the probe and precooled TfOH (61 μL , 0.695 mmol, 2.2 equiv) was quickly added and the tube quickly shaken. The sample then was returned to the cold NMR probe, and ^1H , ^{13}C and ^{19}F spectra were recorded as soon as possible at -88 °C. The temperature then was increased to -78 °C and ^1H , ^{19}F spectra were recorded after 5 minutes. After that the temperature was increased to -60 °C and ^1H , ^{13}C , and ^{19}F spectra were recorded after 5 minutes. After that the temperature was increased by 10 °C increments and ^1H , ^{13}C , and ^{19}F spectra were recorded at each temperature after 5 minutes. After termination of the VT NMR experiment the sample was collected and diluted with EtOAc (30 mL), washed with NaHCO_3 (20 mL), brine (20 mL), dried over MgSO_4 and concentrated to dryness to give mixture (26 mg) of self-condensation products containing dimer **225**. HRMS (m/z): $[\text{M}+\text{H}]^+$ calcd. for $\text{C}_8\text{H}_{17}\text{S}_2^+$ 177.0766, found 177.0757.

Protonation of phenyl vinyl sulfide 226 with TfOH at -88 °C:

Phenyl vinyl sulfide **226** (40 mg, 0.293 mmol) was dissolved in CD_2Cl_2 (0.75 mL), and the reaction mixture was transferred into a vacuum dried NMR tube and sealed with a septum cap under an Ar atmosphere. The NMR tube containing glycosyl donor solution then was placed into the NMR probe and cooled down to -88 °C. The first ^1H , ^{13}C spectra were collected, then the sample was quickly removed from the probe and precooled TfOH (57 μL , 0.645 mmol, 2.2 equiv) was quickly added and the tube quickly shaken. The sample then was returned to the cold NMR probe, and ^1H , ^{13}C and ^{19}F spectra were recorded as soon as possible at -88 °C. The temperature then was increased to -78 °C and ^1H , ^{19}F spectra were recorded after 5 minutes. After that the temperature was increased to -60 °C and ^1H , ^{13}C , and ^{19}F spectra were recorded after 5 minutes. After that the temperature was increased by 10 °C increments and ^1H , ^{13}C , and ^{19}F spectra were recorded at each temperature after 5 minutes. After termination of the VT NMR experiment the sample was collected and diluted with EtOAc (30 mL), washed with NaHCO_3 (20 mL), brine (20 mL), dried over MgSO_4 and concentrated to dryness to give mixture (26 mg) of self-condensation products containing dimer **228**. HRMS (m/z): $[\text{M}+\text{H}]^+$ calcd. for $\text{C}_{24}\text{H}_{25}\text{S}_3^+$ 409.1113, found 409.1090.

Activation of 2-acetoxythiane **216** with TMSOTf:

2-Acetoxythiane **216** (37 mg, 0.231 mmol) was dissolved in CD₂Cl₂ (0.75 mL), and the reaction mixture was transferred into a vacuum dried NMR tube and sealed with a septum cap under an Ar atmosphere. The NMR tube containing glycosyl donor solution then was placed into the NMR probe and cooled down to -78 °C. The first ¹H, ¹³C spectra were collected, then the sample was quickly removed from the probe and pre-cooled TMSOTf (46 µL, 0.254 mmol, 1.1 equiv) was quickly added and the tube quickly shaken. The sample then was returned to the cold NMR probe, and ¹H, ¹³C and ¹⁹F spectra were recorded as soon as possible at -78 °C. The temperature was increased to -60 °C and ¹H, DEPT, and ¹⁹F spectra were recorded after 5 minutes. After that the temperature was increased by 10 °C increments and ¹H, ¹³C, and ¹⁹F spectra were recorded at each temperature after 5 minutes. After termination of the VT NMR experiment the sample was collected and diluted with CH₂Cl₂ (20 mL), washed with NaHCO₃ (20 mL), brine (20 mL), dried over MgSO₄ and concentrated to dryness to give mixture (15 mg) of self-condensation products containing alkene **208**. ESI-HRMS (m/z): [M+H]⁺ calcd. for C₅H₉S⁺ 101.0420, found 101.0414.

Activation of 2-acetoxythiane **229** with TMSOTf:

2-Acetoxythiane **229** (45 mg, 0.312 mmol) was dissolved in CD₂Cl₂ (0.75 mL), and the reaction mixture was transferred into a vacuum dried NMR tube and sealed with a septum cap under an Ar atmosphere. The NMR tube containing glycosyl donor solution then was placed into the NMR probe and cooled down to -78 °C. The first ¹H, ¹³C spectra were collected, then the sample was quickly removed from the probe and pre-cooled TMSOTf (62 µL, 0.343 mmol, 1.1 equiv) was quickly added and the tube quickly shaken. The sample then was returned to the cold NMR probe, and ¹H, ¹³C and ¹⁹F spectra were recorded shortly after at -78 °C. The temperature was increased to -60 °C and ¹H and ¹⁹F spectra were recorded after 5 minutes. After that the temperature was increased by 10 °C increments and ¹H and ¹⁹F spectra were recorded at each temperature after 5 minutes. After termination of the VT NMR experiment the sample was collected and diluted with CH₂Cl₂ (30 mL), washed with NaHCO₃ (30 mL), brine (30 mL), dried over MgSO₄ and

concentrated to dryness to give mixture (19 mg) of self-condensation products containing alkene **220**. ESI-HRMS (m/z): [M+H]⁺ calcd. for C₅H₉O⁺ 85.0648, found 85.0642.

VT NMR experiments with disarmed glycosyl donors (Scheme 45, Scheme 46, Scheme 48, Scheme 49, Scheme 51, and Scheme 53):

Activation of (*R*_s),(*S*_s)-Ethyl 2,3,4,6-tetra-*O*-acetyl-1-thio- β -D-glucopyranoside-*S*-Oxides (237**) with Tf₂O:**

Glycosyl sulfoxide **236** (32 mg, 0.079 mmol) was dissolved in CD₂Cl₂ (0.75 mL), and the reaction mixture was transferred into a vacuum dried NMR tube and sealed with a septum cap under an Ar atmosphere. The NMR tube containing glycosyl donor solution then was placed into the NMR probe and cooled down to -78 °C. The first ¹H, ¹⁹F spectra were collected, then the sample was quickly removed from the probe and precooled Tf₂O (15 μ L, 0.089 mmol, 1.13 equiv) was quickly added and the tube quickly shaken. The sample then was returned to the cold NMR probe, and ¹H, ¹³C spectra were recorded shortly after. The temperature then was increased to -60 °C and ¹H, ¹⁹F spectra were recorded after 5 minutes. After that the temperature was increased by 10 °C increments and ¹H, ¹⁹F spectra were recorded at each temperature after 5 minutes. Additionally, at -30 °C ¹³C, DEPT, COSY, HMQC, and HMBC spectra were recorded. After termination of the VT NMR experiment the sample was collected and diluted with EtOAc (30 mL). The resulting solution was washed with sat aq NaHCO₃ (20 mL), brine (20 mL), dried over MgSO₄ and concentrated to dryness. The crude product was purified by flash column chromatography eluting with hexanes:EtOAc (0 \rightarrow 50%, EtOAc) to give a mixture containing anomeric acetates **7** (α : β = 9 : 1, 10.1 mg, 33%) and enone **241** (1 mg, 5.5%) with molar ratio **7** : **241** = 6.86 : 1⁸ as yellowish syrup (10 mg) with spectral data identical to that reported in the literature:^{244, 245}

1,2,3,4,6-penta-*O*-acetyl- α,β -D-glucopyranoside (7**):**

⁸ Determined spectroscopically

^1H NMR (500 MHz, CDCl_3): δ 6.31 (d, $J = 3.7$ Hz, 1H), 5.50 – 5.40 (m, 1H), 5.16 – 5.05 (m, 2H), 4.37 (dd, $J = 11.7, 5.2$ Hz, 1H), 4.30 – 4.17 (m, 1H), 4.14 – 4.02 (m, 1H), 2.16 (s, 3H), 2.07 (s, 3H), 2.02 (s, 3H), 2.01 (s, 3H), 2.00 (s, 3H); ^{13}C NMR (126 MHz, CDCl_3): δ 170.7, 170.3, 169.7, 169.5, 168.8, 89.2, 69.9, 69.3, 68.0, 64.4, 20.9, 20.8, 20.7, 20.6, 20.5. The minor β -isomer was identified by characteristic signals: δ 5.70 (d, $J = 8.3$ Hz, 1H), 5.23 (t, $J = 9.4$ Hz, 1H).

ESI-HRMS (m/z): $[\text{M}+\text{Na}]^+$ calcd. for $\text{C}_{16}\text{H}_{32}\text{O}_{11}\text{Na}^+$ 413.1054, found 413.1045.

1,6-di-*O*-acetyl-3,4-dideoxy- β -D-glycero-hex-3-enopyranos-2-ulose (241):

^1H NMR (500 MHz, CDCl_3): δ 7.03 (dd, $J = 10.7, 1.7$ Hz, 1H), 6.27 (dd, $J = 10.8, 2.6$ Hz, 1H), 6.18 – 6.13 (m, 1H), 4.84 – 4.77 (m, 1H), 4.30 – 4.17 (m, 1H), 4.14 – 4.02 (m, 1H), 2.11 (s, 3H), 2.08 (s, 3H); ^{13}C NMR (126 MHz, CDCl_3): δ 188.5, 170.7, 168.8, 147.3, 126.6, 89.5, 68.2, 61.5, 20.9, 20.8; ESI-HRMS (m/z): $[\text{M}+\text{Na}]^+$ calcd. for $\text{C}_{10}\text{H}_{12}\text{O}_6\text{Na}^+$ 251.0526, found 251.0520.

Activation of (*R*_S)-Ethyl 2,3,4,6-tetra-*O*-acetyl-1-thio- α -D-glucopyranoside-*S*-Oxide (236) with Tf_2O :

Glycosyl sulfoxide **236** (37 mg, 0.081 mmol) was dissolved in CD_2Cl_2 (0.75 mL), and the reaction mixture was transferred into a vacuum dried NMR tube and sealed with a septum cap under an Ar atmosphere. The NMR tube containing glycosyl donor solution then was placed into the NMR probe and cooled down to -78 °C. The first ^1H , ^{13}C spectra were collected, then the sample was quickly removed from the probe and precooled Tf_2O (15 μL , 0.089 mmol, 1.1 equiv) was quickly added and the tube quickly shaken. The sample then was returned to the cold NMR probe, and ^1H , ^{19}F spectra were recorded shortly after. The temperature then was increased to -60 °C and ^1H , ^{19}F spectra were recorded after 5 minutes. After that the temperature was increased by 10 °C increments and ^1H , ^{19}F spectra were recorded at each temperature after 5 minutes. Additionally, at -60° C ^{13}C , DEPT, COSY, HMQC, and HMBC spectra were recorded. After termination of the VT NMR experiment the sample was collected and diluted with EtOAc (20 mL). The resulting solution was washed with sat aq NaHCO_3 (15 mL), brine (15 mL), dried over MgSO_4 and concentrated to dryness. The crude product was purified by flash column chromatography eluting with hexanes:EtOAc (0→50%,

EtOAc) to give a mixture containing anomeric acetates **7** ($\alpha : \beta = 9 : 1$, 8 mg, 26%) and enone **241** (2 mg, 11%) with molar ratio **7** : **241** = 2.36 : 1⁹ as yellowish syrup (10 mg) with spectral data identical to that presented above.^{244, 245}

Diagnostic signals of 3,4,6-tri-O-acetyl- α -D-glucopyranose-1,2-O-acetoxonium trifluoromethanesulfonate intermediate (239):

¹H NMR (500 MHz, CD₂Cl₂): δ 7.24 (d, $J = 7.5$ Hz, 1H, H-1), 5.70 – 5.60 (m, 1H, H-2), 5.00 (d, $J = 9.9$ Hz, 1H, H-3), 5.34 – 5.25 (m, 1H, H-4), 2.85 (s, 3H, CH₃C⁺); ¹³C NMR (126 MHz, CD₂Cl₂): δ 191.6 (CH₃C⁺), 112.0 (C-1), 81.4 (C-2), 68.0 (C-3), 66.8 (C-4), 16.3 (C⁺CH₃).

Diagnostic signals of 1-O-trifluoromethanesulfonyl-2,3,4,6-tetra-O-acetyl- α -D-glucopyranose intermediate (240):

¹H NMR (500 MHz, CD₂Cl₂): δ 6.16 (d, $J = 3.4$ Hz, 1H, H-1), 5.16 – 5.11 (m, 2H, H-2, H-3); ¹³C NMR (126 MHz, CD₂Cl₂): 103.5 (C-1), 68.4 (C-2); ¹⁹F NMR (470 MHz, CD₂Cl₂): δ -75.51.

Activation of (*R*_S), (*S*_S)-Ethyl 2,3,4,6-tetra-O-acetyl-1,5-di-thio- β -D-glucopyranoside-1-*S*-Oxides (232) with Tf₂O:

Glycosyl sulfoxide **232** (30 mg, 0.071 mmol) was dissolved in CD₂Cl₂ (0.75 mL), and the reaction mixture was transferred into a vacuum dried NMR tube and sealed with a septum cap under an Ar atmosphere. The NMR tube containing glycosyl donor solution then was placed into the NMR probe and cooled down to -78 °C. The first ¹H, ¹³C spectra were collected, then the sample was quickly removed from the probe and precooled Tf₂O (13 μ L, 0.078 mmol, 1.1 equiv) was quickly added and the tube quickly shaken. The sample then was returned to the cold NMR probe, and ¹H, ¹⁹F spectra were recorded shortly after. The temperature then was increased to -60 °C and ¹H, ¹⁹F spectra were recorded after 5 minutes. After that the temperature was increased by 10 °C increments and ¹H, ¹⁹F spectra were recorded at each temperature after 5 minutes. Additionally, at -50 °C ¹³C, DEPT, COSY, HMQC, and HMBC spectra were recorded. After termination of

⁹ Determined spectroscopically

the VT NMR experiment the sample was collected and diluted with EtOAc (20 mL). The resulting solution was washed with sat aq NaHCO₃ (10 mL), brine (10 mL), dried over MgSO₄ and concentrated to dryness. The crude product was purified by a flash column chromatography eluting with hexanes:EtOAc (0→50%, EtOAc) to give a single anomeric α -acetate **33a** as a syrup (9 mg, 31%) with spectral data identical to that reported in the literature.^{70, 80} ¹H NMR (500 MHz, CDCl₃): δ 6.14 (d, J = 3.2 Hz, 1H), 5.42 (t, J = 9.9 Hz, 1H), 5.31 (dd, J = 10.8, 9.5 Hz, 1H), 5.23 (dd, J = 10.2, 3.2 Hz, 1H), 4.43 – 4.33 (m, 1H), 4.06 (dd, J = 12.1, 3.1 Hz, 1H), 3.58 (ddd, J = 10.8, 4.9, 3.1 Hz, 1H), 2.17 (s, 3H), 2.06 (s, 3H), 2.03 (s, 3H), 2.00 (s, 3H), 1.98 (s, 3H); ¹³C NMR (126 MHz, CDCl₃): δ 170.6, 169.9, 169.7, 169.5, 169.1, 73.2, 71.8, 70.7, 70.7, 61.0, 39.9, 21.0, 20.7, 20.6, 20.6, 20.6; ESI-HRMS [M+Na]⁺ calcd. for C₁₆H₂₂NaO₁₀S⁺ 429.0826, found 429.0820.

Activation of Ethyl 2,3,4,6-tetra-*O*-acetyl-1,5-di-thio- α -D-glucopyranoside-1-*S*-Oxide (234) with Tf₂O:

Glycosyl sulfoxide **234** (32 mg, 0.075 mmol) was dissolved in CD₂Cl₂ (0.75 mL), and the reaction mixture was transferred into a vacuum dried NMR tube and sealed with a septum cap under an Ar atmosphere. The NMR tube containing glycosyl donor solution then was placed into the NMR probe and cooled down to -78 °C. The first ¹H, ¹³C spectra were collected, then the sample was quickly removed from the probe and precooled Tf₂O (14 μ L, 0.0825 mmol, 1.1 equiv) was quickly added and the tube quickly shaken. The sample then was returned to the cold NMR probe, and ¹H, ¹⁹F spectra were recorded shortly after. The temperature then was increased to -60 °C and ¹H, ¹⁹F spectra were recorded after 5 minutes. After that the temperature was increased by 10 °C increments and ¹H, ¹⁹F spectra were recorded at each temperature after 5 minutes. Additionally, at -50 °C ¹³C, DEPT, COSY, HMQC, and HMBC spectra were recorded. After termination of the VT NMR experiment the sample was collected and diluted with EtOAc (20 mL). The resulting solution was washed with sat aq NaHCO₃ (20 mL), brine (20 mL), dried over MgSO₄ and concentrated to dryness. The crude product was purified by a flash column chromatography eluting with

hexanes:EtOAc (0→50%, EtOAc) to give α -acetate **33a** as a syrup (11 mg, 36%) with spectral data identical to that presented above.^{70, 80}

Activation of 2,3,4,6-tetra-*O*-acetyl- α -D-glucopyranosyl trichloroacetimidate (12**) with TMSOTf:**

Trichloroacetimidate **12** (57 mg, 0.116 mmol) was dissolved in CD₂Cl₂ (0.75 mL), and the reaction mixture was transferred into a vacuum dried NMR tube and sealed with a septum cap under an Ar atmosphere. The NMR tube containing glycosyl donor solution then was placed into the NMR probe and cooled down to -78 °C. The first ¹H, ¹³C, and DEPT spectra were collected, then the sample was quickly removed from the probe and precooled TMSOTf (23 μ L, 0.128 mmol, 1.1 equiv) was quickly added and the tube quickly shaken. The sample then was returned to the cold NMR probe, and ¹H, ¹⁹F, DEPT spectra were recorded shortly after. The temperature then was increased to -60 °C and ¹H, ¹⁹F, DEPT spectra were recorded after 5 minutes. After that the temperature was increased by 10 °C increments and ¹H, ¹⁹F, and DEPT spectra were recorded at each temperature after 5 minutes. Additionally, at -40° C COSY, HSQC, and HMBC spectra were recorded. After termination of the VT NMR experiment the sample was collected and diluted with CH₂Cl₂ (20 mL). The resulting solution was washed with sat aq NaHCO₃ (20 mL), brine (20 mL), dried over MgSO₄ and concentrated to dryness. The crude product was purified by a flash column chromatography eluting with hexanes:EtOAc (0→50%, EtOAc) to give mixture containing anomeric acetates **7** (α : β = 3 : 1, 12 mg, 27%) and enone **256** (4 mg, 10%) with molar ratio **7** : **256** = 2.56 : 1¹⁰ as yellowish syrup (16 mg) with spectral data identical to that reported in the literature:^{244, 245}

1-*N*-trichloroacetamidyl-6-di-*O*-acetyl-1,3,4-trideoxy- β -D-glycero-hex-3-enopyranos-2-ulose intermediate (256**):**

¹H NMR (500 MHz, CDCl₃): δ 7.47 (d, J = 7.5 Hz, 1H, CCl₃CONH), 7.06 (dd, J = 10.5, 3.0 Hz, 1H, H-4), 6.37 – 6.31 (m, 1H, H-3), 5.87 (d, J = 7.4 Hz, 1H, H-1), 4.83 (appear s, 1H, H-5), 4.58 (dd, J = 12.1, 5.3 Hz, 1H, H-6a), 4.39 (dd, J = 12.0, 4.1 Hz, 1H, H-6b), 2.17 (s, 3H), 2.06 (s, 3H); ¹³C NMR (126 MHz,

¹⁰ Determined spectroscopically

CDCl₃): δ 188.5 (C-2), 170.7, 168.8 (2 \times CH₃C=O), 162.3 (CCl₃C=NH), 147.7 (C-4), 127.1 (C-3), 77.6 (C-1), 71.5 (C-5), 63.8 (C-6), 20.5, 20.4 (2 \times CH₃CO); ESI-HRMS [M+Na]⁺ calcd. for C₁₀H₁₀O₅NC₃Na⁺ 351.9517, found 351.9496.

Activation of 2,3,4,6-tetra-*O*-acetyl- α -D-glucopyranosyl trichloroacetimidate (52) with TMSOTf:

Trichloroacetimidate **52** (63 mg, 0.124 mmol) was dissolved in CD₂Cl₂ (0.75 mL), and the reaction mixture was transferred into a vacuum dried NMR tube and sealed with a septum cap under an Ar atmosphere. The NMR tube containing glycosyl donor solution then was placed into the NMR probe and cooled down to -78 °C. The first ¹H, ¹³C, and DEPT spectra were collected, then the sample was quickly removed from the probe and precooled TMSOTf (25 μ L, 0.138 mmol, 1.11 equiv) was quickly added and the tube quickly shaken. The sample then was returned to the cold NMR probe, and ¹H, ¹⁹F, and DEPT spectra were recorded shortly after. The temperature then was increased to -60 °C and ¹H, ¹⁹F, and DEPT spectra were recorded after 5 minutes. After that the temperature was increased by 10 °C increments and ¹H, ¹⁹F, and DEPT spectra were recorded at each temperature after 5 minutes. Additionally, at -40° C COSY, HSQC, and HMBC spectra were recorded. After termination of the VT NMR experiment the sample was collected and diluted with CH₂Cl₂ (20 mL). The resulting solution was washed with sat aq NaHCO₃ (20 mL), brine (20 mL), dried over MgSO₄ and concentrated to dryness. The crude product was purified by a flash column chromatography eluting with hexanes:EtOAc (0 \rightarrow 60%, EtOAc) to give α -acetate **33a** as a syrup (8 mg, 16%) with spectral data identical to that reported in the literature.^{70, 80}

Diagnostic signals of 3,4,6-tri-*O*-acetyl-5-thio- α -D-glucopyranose-1,2-*O*-acetoxonium trifluoromethanesulfonate intermediate (251):

¹H NMR (500 MHz, CD₂Cl₂): δ 7.22 (d, *J* = 9.5 Hz, 1H, H-1), 2.89 (s, 3H, CH₃C⁺); ¹³C NMR (126 MHz, CD₂Cl₂): δ 191.4 (CH₃C⁺), 16.4 (C⁺CH₃).

Diagnostic signals of 1-trifluoromethanesulfonyl-2,3,4,6-tetra-*O*-acetyl-5-thio- α -D-glucopyranoside intermediate (252):

^1H NMR (500 MHz, CD_2Cl_2): δ 6.05 (d, $J = 3.0$ Hz, 1H, H-1), 5.24 – 5.15 (m, 1H, H-2); ^{13}C NMR (126 MHz, CD_2Cl_2): δ 87.9 (C-1), 73.3 (C-2); ^{19}F NMR (470 MHz, CD_2Cl_2): δ -75.35.

VT NMR experiments with armed glycosyl donors (Scheme 57, Scheme 58, Scheme 59, Scheme 60, Scheme 62, and Scheme 63):

Activation of (*R_S*),(*S_S*)-Ethyl 2,3,4,6-tetra-*O*-methyl-1-thio- β -D-glucopyranoside-1-*S*-Oxides (275) with Tf_2O :

Glycosyl sulfoxide **275** (27 mg, 0.093 mmol) was dissolved in CD_2Cl_2 (0.75 mL), and the reaction mixture was transferred into a vacuum dried NMR tube and sealed with a septum cap under an Ar atmosphere. The NMR tube containing glycosyl donor solution then was placed into the NMR probe and cooled down to -78 °C. The first ^1H , ^{13}C spectra were collected, then the sample was quickly removed from the probe and precooled Tf_2O (17 μL , 0.1021 mmol, 1.1 equiv) was quickly added and the tube quickly shaken. The sample then was returned to the cold NMR probe, and ^1H , ^{19}F spectra were recorded shortly after. The temperature then was increased to -60 °C and ^1H , ^{19}F spectra were recorded after 5 minutes. After that the temperature was increased by 10 °C increments and ^1H , and ^{19}F spectra were recorded at each temperature after 5 minutes. Additionally, at -50 °C ^{13}C , DEPT, COSY, HMQC, and HMBC spectra were recorded. After termination of the VT NMR experiment the sample was collected and diluted with EtOAc (30 mL). The resulting solution was washed with sat aq NaHCO_3 (30 mL), brine (30 mL), dried over MgSO_4 and concentrated to dryness. The crude product was purified by flash column chromatography eluting with hexanes:EtOAc (0→60%, EtOAc) to give single anomer of pentamethyl glucose **281** as a syrup (7 mg, 30%) with spectral data identical to that reported in the literature.²⁶⁷ ^1H NMR (500 MHz, CDCl_3): δ 4.81 (d, $J = 3.6$ Hz, 1H), 3.61 (s, 3H), 3.60 – 3.55 (m, 3H), 3.53 (s, 3H), 3.51 – 3.45 (m, 5H), 3.40 (s, 3H), 3.40 (s, 3H), 3.23 – 3.12 (m, 2H); ^{13}C NMR (126 MHz, CDCl_3): δ 97.7, 83.6, 81.8, 79.5, 71.2, 69.9, 61.0, 60.5, 59.3, 59.1, 55.2; ESI-HRMS $[\text{M}+\text{Na}]^+$ calcd. for $\text{C}_{11}\text{H}_{22}\text{O}_6\text{Na}^+$ 273.1309, found 273.1300.

Activation of Ethyl 2,3,4,6-tetra-*O*-methyl-1-thio- α -D-glucopyranoside-1-*S*-oxide (277) with Tf_2O :

Glycosyl sulfoxide **277** (30 mg, 0.101 mmol) was dissolved in CD₂Cl₂ (0.75 mL), and the reaction mixture was transferred into a vacuum dried NMR tube and sealed with a septum cap under an Ar atmosphere. The NMR tube containing glycosyl donor solution then was placed into the NMR probe and cooled down to -78 °C. The first ¹H, ¹³C spectra were collected, then the sample was quickly removed from the probe and precooled Tf₂O (19 μL, 0.113 mmol, 1.11 equiv) was quickly added and the tube quickly shaken. The sample then was returned to the cold NMR probe, and ¹H, ¹⁹F spectra were recorded shortly after. The temperature then was increased to -60 °C and ¹H, ¹⁹F spectra were recorded after 5 minutes. After that the temperature was increased by 10 °C increments and ¹H, and ¹⁹F spectra were recorded at each temperature after 5 minutes. Additionally, at -50 °C and -30 °C ¹³C, DEPT, COSY, HMQC, and HMBC spectra were recorded. After termination of the VT NMR experiment the sample was collected and diluted with EtOAc (20 mL). The resulting solution was washed with sat aq NaHCO₃ (20 mL), brine (20 mL), dried over MgSO₄ and concentrated to dryness. The crude product was purified by a flash column chromatography eluting with hexanes:EtOAc (0→60%, EtOAc) to give single anomer of pentamethyl glucose **281** as a syrup (8 mg, 32%) with spectral data identical to presented above.²⁶⁷

Diagnostic signals of 1-trifluoromethanesulfonyl-2,3,4,6-tetra-*O*-methyl- α -D-glucopyranoside intermediate (279):

¹H NMR (500 MHz, CD₂Cl₂): δ 6.11 (s, 1H, H-1), 3.87 – 2.83 (m, 1H, H-2); ¹³C NMR (126 MHz, CD₂Cl₂): δ 106.8 (C-1); ¹⁹F NMR (470 MHz, CD₂Cl₂): δ -76.13.

Diagnostic signals of 2-methoxy-6-(methoxymethyl)pyrilium trifluoromethanesulfonate (279):

¹H NMR (500 MHz, CD₂Cl₂): δ 9.19 (d, J = 3.3 Hz, 1H), 8.62 (dd, J = 9.4, 3.3 Hz, 1H), 8.26 (d, J = 9.2 Hz, 1H); ¹³C NMR (126 MHz, CDCl₃): δ 175.3, 157.1, 152.9, 145.6, 124.0; ESI-HRMS [M]⁺ calcd. for C₈H₁₁O₃⁺ 155.0703, found 155.0697.

Activation of (*R*_S),(*S*_S)-Ethyl 2,3,4,6-tetra-*O*-methyl-1,5-dithio- β -D-glucopyranoside-1-*S*-Oxides (269) with Tf₂O:

Glycosyl sulfoxide **269** (30 mg, 0.096 mmol) was dissolved in CD₂Cl₂ (0.75 mL), and the reaction mixture was transferred into a vacuum dried NMR tube and sealed with a septum cap under an Ar atmosphere. The NMR tube containing glycosyl donor solution then was placed into the NMR probe and cooled down to -78 °C. The first ¹H, ¹³C spectra were collected, then the sample was quickly removed from the probe and precooled Tf₂O (18 μL, 0.107 mmol, 1.11 equiv) was quickly added and the tube quickly shaken. The sample then was returned to the cold NMR probe, and ¹H, ¹⁹F spectra were recorded shortly after. The temperature then was increased to -60 °C and ¹H, ¹⁹F spectra were recorded after 5 minutes. After that the temperature was increased by 10 °C increments and ¹H, and ¹⁹F spectra were recorded at each temperature after 5 minutes. Additionally, at -50 °C and -30 °C ¹³C, DEPT, COSY, HMQC, and HMBC spectra were recorded. After termination of the VT NMR experiment the sample was collected and diluted with EtOAc (20 mL). The resulting solution was washed with sat aq NaHCO₃ (20 mL), brine (20 mL), dried over MgSO₄ and concentrated to dryness. The crude product was purified by a flash column chromatography eluting with hexanes:EtOAc (0→60%, EtOAc) to give thiophene **287** as a syrup (6 mg, 34%). FTIR (CHCl₃) cm⁻¹: 2924.5, 1642.5, 1549.0, 1461.3, 1396.2; ¹H NMR (500 MHz, CDCl₃): δ 9.94 (s, 1H, CHO), 6.79 (s, 1H, Aryl CH), 4.54 (s, 2H, CH₂OCH₃), 3.95 (s, 3H, OCH₃), 3.42 (s, 3H, OCH₃); ¹³C NMR (126 MHz, CDCl₃): δ 181.0 (CHO), 164.5 (qC-OMe), 151.7 (qC-CH₂OCH₃), 120.6 (qC-CHO), 114.0 (Aryl CH), 69.9, 58.7 (2×OCH₃); ESI-HRMS [M+H]⁺ calcd. for C₈H₁₁O₃S⁺ 187.0423, found 187.0434.

Activation of Ethyl 2,3,4,6-tetra-*O*-methyl-1,5-dithio- α -D-glucopyranoside-1-*S*-Oxides (272) with Tf₂O:

Glycosyl sulfoxide **272** (30 mg, 0.096 mmol) was dissolved in CD₂Cl₂ (0.75 mL), and the reaction mixture was transferred into a vacuum dried NMR tube and sealed with a septum cap under an Ar atmosphere. The NMR tube containing glycosyl donor solution then was placed into the NMR probe and cooled down to -78 °C. The first ¹H, ¹³C spectra were collected, then the sample was quickly removed from the probe and precooled Tf₂O (18 μL, 0.107 mmol, 1.11 equiv) was quickly added and the tube quickly shaken. The sample then was returned to the cold NMR probe, and ¹H, ¹⁹F spectra were recorded shortly after. The temperature then was increased to -60 °C and ¹H, ¹⁹F spectra were recorded after 5 minutes. After that the

temperature was increased by 10 °C increments and ^1H , and ^{19}F spectra were recorded at each temperature after 5 minutes. Additionally, at -50 °C and -30 °C ^{13}C , DEPT, COSY, HMQC, and HMBC spectra were recorded. After termination of the VT NMR experiment the sample was collected and diluted with EtOAc (30 mL). The resulting solution was washed with sat aq NaHCO_3 (30 mL), brine (30 mL), dried over MgSO_4 and concentrated to dryness. The crude product was purified by flash column chromatography eluting with hexanes:EtOAc (0→60%, EtOAc) to give thiophene **287** as a syrup (5 mg, 28%) with spectral data identical to that presented above.

Activation of 2,3,4,6-tetra-*O*-methyl- α,β -D-glucopyranosyl trichloroacetimidate (291) with TMSOTf:

Trichloroacetimidate **291** (20 mg, 0.053 mmol) was dissolved in CD_2Cl_2 (0.75 mL), and the reaction mixture was transferred into a vacuum dried NMR tube and sealed with a septum cap under an Ar atmosphere. The NMR tube containing glycosyl donor solution then was placed into the NMR probe and cooled down to -78 °C. The first ^1H , ^{13}C , and DEPT spectra were collected, then the sample was quickly removed from the probe and precooled TMSOTf (10 μL , 0.0583 mmol, 1.1 equiv) was quickly added and the tube quickly shaken. The sample then was returned to the cold NMR probe, and ^1H , ^{19}F , DEPT spectra were recorded shortly after. The temperature then was increased to -60 °C and ^1H , ^{19}F , DEPT spectra were recorded after 5 minutes. After that the temperature was increased by 10 °C increments and ^1H , ^{19}F , and DEPT spectra were recorded at each temperature after 5 minutes. Additionally, at -40° C COSY, HSQC, and HMBC spectra were recorded. After termination of the VT NMR experiment the sample was collected and diluted with EtOAc (20 mL). The resulting solution was washed with sat aq NaHCO_3 (20 mL), brine (20 mL), dried over MgSO_4 and concentrated to dryness. The crude product was purified by a flash column chromatography eluting with hexanes:EtOAc (0→50%, EtOAc) to give a mixture of anomeric amides **295** ($\alpha : \beta = 4.8 : 1$) as a syrup (5 mg, 25%). R_f 0.42 (hexanes:EtOAc 1:1 ($\text{H}_2\text{SO}_4/\text{EtOH}$)); ^1H NMR (500 MHz, CDCl_3): δ 7.19 (d, $J = 5.9$ Hz, 1H, NH), 5.65 (t, $J = 5.7$ Hz, 1H, H-1), 3.62 (s, 3H, OCH_3), 3.60 – 3.54 (m, 2H, H-6a, H-6b), 3.53 (s, 3H, OCH_3), 3.52 – 3.45 (m, 2H, H-2, H-5), 3.43 (s, 3H, OCH_3), 3.38 (s, 3H,

OCH₃), 3.33 (t, $J = 9.0$ Hz, 1H, H-4), 3.20 (t, $J = 8.7$ Hz, 1H, H-3); ¹³C NMR (126 MHz, CDCl₃): δ 162.2 (CO), 92.4 (CCl₃), 83.2 (C-3), 79.1 (C-2), 78.1 (C-4), 76.4 (C-1), 71.6 (C-5), 70.4 (C-6), 60.8, 60.4, 59.2, 58.3 (4×OCH₃). The minor β -isomer was identified by characteristic signals: ¹H NMR (500 MHz, CDCl₃): δ 7.06 (d, $J = 9.3$ Hz, 1H, NH), 4.97 (t, $J = 9.1$ Hz, 1H, H-1), 3.64 (s, 3H, OCH₃), 3.53 (s, 3H, OCH₃), 3.39 (s, 3H, OCH₃), 3.30 – 3.26 (m, 1H, H-4), 3.04 (t, $J = 8.6$ Hz, 1H, H-3); ¹³C NMR (126 MHz, CDCl₃): δ 162.2 (CO), 92.4 (CCl₃), 86.9 (C-3), 83.3 (C-2), 80.9 (C-1), 78.6 (C-4), 60.6 (OCH₃), 60.4 (OCH₃). ESI-HRMS (m/z): [M+Na]⁺ calcd. for C₁₂H₂₀O₆NC₃Na⁺ 402.0248, found 402.0237.

Activation of 2,3,4,6-tetra-*O*-methyl- α,β -D-glucopyranosyl trichloroacetimidate (294**) with TMSOTf:**

Trichloroacetimidate **294** (25 mg, 0.063 mmol) was dissolved in CD₂Cl₂ (0.75 mL), and the reaction mixture was transferred into a vacuum dried NMR tube and sealed with a septum cap under an Ar atmosphere. The NMR tube containing glycosyl donor solution then was placed into the NMR probe and cooled down to -78 °C. The first ¹H, ¹³C, and DEPT spectra were collected, then the sample was quickly removed from the probe and precooled TMSOTf (13 μ L, 0.0718 mmol, 1.14 equiv) was quickly added and the tube quickly shaken. The sample then was returned to the cold NMR probe, and ¹H, ¹⁹F, DEPT spectra were recorded shortly after. The temperature then was increased to -60 °C and ¹H, ¹⁹F, DEPT spectra were recorded after 5 minutes. After that the temperature was increased by 10 °C increments and ¹H, ¹⁹F, and DEPT spectra were recorded at each temperature after 5 minutes. Additionally, at -30° C COSY, HSQC, and HMBC spectra were recorded. After termination of the VT NMR experiment the sample was collected and diluted with EtOAc (20 mL). The resulting solution was washed with sat aq NaHCO₃ (20 mL), brine (20 mL), dried over MgSO₄ and concentrated to dryness. The crude product was purified by flash column chromatography eluting with hexanes:EtOAc (0→50%, EtOAc) to give a mixture of anomeric amides **298** ($\alpha : \beta = 3.3 : 1$) as a syrup (10 mg, 41%). R_f 0.37 and 0.29 (hexanes:EtOAc 3:2 (H₂SO₄/EtOH)); ¹H NMR (500 MHz, CDCl₃): δ 7.70 (d, $J = 9.1$ Hz, 1H, NH), 5.45 (dd, $J = 9.2, 4.8$ Hz, 1H, H-1), 3.98 – 3.94 (m, 1H, H-2), 3.94 – 3.87 (m, 1H, H-3), 3.55 (s, 3H, OCH₃), 3.51 (dd, $J = 5.0, 3.7$ Hz, 2H, H-6a, H-6b), 3.48 – 3.26

(m, 11H, H-4, H-5, 3×OCH₃); ¹³C NMR (126 MHz, CDCl₃): δ 161.2 (CO), 92.6 (CCl₃), 89.6 (C-2), 82.9 (C-3), 81.4 (C-4), 72.2 (C-6), 59.6, 59.4, 58.5, 57.9 (4×OCH₃), 56.3 (C-1), 48.8 (C-5). The minor *β*-isomer was identified by characteristic signals: ¹H NMR (500 MHz, CDCl₃): δ 7.82 (d, *J* = 9.5 Hz, 1H, NH), 5.55 (d, *J* = 9.5 Hz, 1H, H-1), 4.20 (appear s, 1H, H-4), 3.98 – 3.94 (m, 1H, H-2), 3.94 – 3.87 (m, 1H, H-3), 3.79 (d, *J* = 10.8 Hz, 1H, H-5), 3.65 – 3.58 (m, 2H, H-6a, H-6b), 3.55 (s, 4H); ¹³C NMR (126 MHz, CDCl₃): δ 161.2 (CO), 92.6 (CCl₃), 87.3 (C-3), 70.7 (C-6), 62.6 (C-1), 59.4, 57.8, 57.8, 57.5 (4×OCH₃), 53.0 (C-5). ESI-HRMS (*m/z*): [M+Na]⁺ calcd. for C₁₂H₂₀O₅NCl₃NaS⁺ 418.0020, found 418.0015.

REFERENCES

- (1) Stick, R. V.; Williams, S. J. Chapter 6 - Monosaccharide Metabolism. In *Carbohydrates: The Essential Molecules of Life (Second Edition)*, Stick, R. V., Williams, S. J. Eds.; Elsevier, 2009; pp 225-251.
- (2) Stick, R. V.; Williams, S. J. Chapter 11 - Glycoproteins and Proteoglycans. In *Carbohydrates: The Essential Molecules of Life (Second Edition)*, Stick, R. V., Williams, S. J. Eds.; Elsevier, 2009; pp 369-412.
- (3) Takahashi, M.; Kizuka, Y.; Ohtsubo, K.; Gu, J.; Taniguchi, N. Disease-Associated Glycans on Cell Surface Proteins. *Molecular Aspects of Medicine* **2016**, *51*, 56-70. DOI: 10.1016/j.mam.2016.04.008.
- (4) Gerwig, G. J. The World of Carbohydrates. In *The Art of Carbohydrate Analysis*, Springer International Publishing, 2021; pp 1-10.
- (5) Krasavina, M. S.; Burmistrova, N. A.; Raldugina, G. N. Chapter 11 - the Role of Carbohydrates in Plant Resistance to Abiotic Stresses. In *Emerging Technologies and Management of Crop Stress Tolerance*, Ahmad, P., Rasool, S. Eds.; Academic Press, 2014; pp 229-270.
- (6) Maughan, R. Carbohydrate Metabolism. *Surgery (Oxford)* **2009**, *27* (1), 6-10. DOI: 10.1016/j.mpsur.2008.12.002.
- (7) Hooper, L. V.; Manzella, S. M.; Baenziger, J. U. From Legumes to Leukocytes: Biological Roles for Sulfated Carbohydrates. *The FASEB Journal* **1996**, *10* (10), 1137-1146. DOI: 10.1096/fasebj.10.10.8751716.
- (8) Bessesen, D. H. The Role of Carbohydrates in Insulin Resistance. *J. Nutr.* **2001**, *131* (10), 2782S-2786S. DOI: 10.1093/jn/131.10.2782S.
- (9) Wang, J.; Zhang, Y.; Lu, Q.; Xing, D.; Zhang, R. Exploring Carbohydrates for Therapeutics: A Review on Future Directions. *Front Pharmacol* **2021**, *12*, 756724. DOI: 10.3389/fphar.2021.756724.
- (10) Xavier, N. M.; Andreana, P. R.; Carvalho, I.; von Itzstein, M. Editorial: Carbohydrate-Based Molecules in Medicinal Chemistry. *Front Chem* **2021**, *9*, 655200. DOI: 10.3389/fchem.2021.655200.
- (11) Mahara, G.; Tian, C.; Xu, X.; Zhu, J. Breakthrough of Glycobiology in the 21st Century. *Front Immunol* **2022**, *13*, 1071360. DOI: 10.3389/fimmu.2022.1071360.
- (12) Berman, H. M.; Westbrook, J.; Feng, Z.; Gilliland, G.; Bhat, T. N.; Weissig, H.; Shindyalov, I. N.; Bourne, P. E. The Protein Data Bank. *Nucleic Acids Res.* **2000**, *28* (1), 235-242.
- (13) Cao, X.; Du, X.; Jiao, H.; An, Q.; Chen, R.; Fang, P.; Wang, J.; Yu, B. Carbohydrate-Based Drugs Launched During 2000–2021. *Acta Pharm. Sin. B* **2022**, *12* (10), 3783-3821. DOI: 10.1016/j.apsb.2022.05.020.
- (14) Nicotra, F.; Airoldi, C.; Cardona, F. 1.16 - Synthesis of C- and S-Glycosides. In *Comprehensive Glycoscience*, Kamerling, H. Ed.; Elsevier, 2007; pp 647-683.
- (15) Sangwan, R.; Khanam, A.; Mandal, P. K. An Overview on the Chemical N-Functionalization of Sugars and Formation of N-Glycosides. *Eur. J. Org. Chem.* **2020**, *2020* (37), 5949-5977. DOI: 10.1002/ejoc.202000813.
- (16) Pritchard, H. O.; Skinner, H. A. The Concept of Electronegativity. *Chem. Rev.* **1955**, *55* (4), 745-786. DOI: 10.1021/cr50004a005.
- (17) Cotton, F. A.; Wilkinson, G.; Murillo, C. A.; Bochmann, M. *Advanced Inorganic Chemistry*; John Wiley and Sons, Inc., 1999.
- (18) Nikolaienko, T. Y.; Chuiko, V. S.; Bulavin, L. A. The Dataset of Covalent Bond Lengths Resulting from the First-Principle Calculations. *Comput. Theor. Chem.* **2019**, *1163*, 112508. DOI: 10.1016/j.comptc.2019.112508.
- (19) Johns, T.; Kitts, W. D.; Newsome, F.; Towers, G. H. N. Anti-Reproductive and Other Medicinal Effects of *Tropaeolum Tuberosum* Um. *J. Ethnopharmacol.* **1982**, *5* (2), 149-161. DOI: 10.1016/0378-8741(82)90040-X.

- (20) Hashem, F. A.; Saleh, M. M. Antimicrobial Components of Some Cruciferae Plants (*Diplotaxis Harra* Forsk. And *Erucaria Microcarpa* Boiss.). *Phytother. Res.* **1999**, *13* (4), 329-332. DOI: 10.1002/(SICI)1099-1573(199906)13:4<329::AID-PTR458>3.0.CO;2-U.
- (21) Drobnica, L.; Zemanova, M.; Nemec, P.; Antos, K.; Kristian, P.; Stullerova, A.; Knoppova, V.; Nemec, P. Antifungal Activity of Isothiocyanates and Related Compounds. *Appl. Microbiol.* **1967**, *15* (4), 701-709. DOI: 10.1128/am.15.4.701-709.1967.
- (22) Manici, L. M.; Lazzeri, L.; Palmieri, S. In Vitro Fungitoxic Activity of Some Glucosinolates and Their Enzyme-Derived Products Toward Plant Pathogenic Fungi. *J. Agric. Food. Chem.* **1997**, *45* (7), 2768-2773. DOI: 10.1021/jf9608635.
- (23) Mari, M.; Iori, R.; Leoni, O.; Marchi, A. In Vitro Activity of Glucosinolate-Derived Isothiocyanates Against Postharvest Fruit Pathogens*. *Ann. Appl. Biol.* **1993**, *123* (1), 155-164. DOI: 10.1111/j.1744-7348.1993.tb04082.x.
- (24) Brown, P. D.; Morra, M. J. Control of Soil-Borne Plant Pests Using Glucosinolate-Containing Plants. In *Advances in Agronomy*, Sparks, D. L. Ed.; Vol. 61; Academic Press, 1997; pp 167-231.
- (25) Macleod, A. J.; Ross, H. B.; Ozere, R. L.; Digout, G.; Van, R. Lincomycin: A New Antibiotic Active against Staphylococci and Other Gram-Positive Cocci: Clinical and Laboratory Studies. *Can Med Assoc J* **1964**, *91* (20), 1056-1060.
- (26) Codee, J. D. C.; Litjens, R. E. J. N.; van den Bos, L. J.; Overkleeft, H. S.; van der Marel, G. A. Thioglycosides in Sequential Glycosylation Strategies. *Chem. Soc. Rev.* **2005**, *34* (9), 769-782. DOI: 10.1039/B417138C.
- (27) Escopy, S.; Demchenko, A. V. Transition-Metal-Mediated Glycosylation with Thioglycosides. *Chemistry* **2022**, *28* (14), e202103747. DOI: 10.1002/chem.202103747.
- (28) Garegg, P. J.; Henrichson, C.; Norberg, T. A Reinvestigation of Glycosidation Reactions Using 1-Thioglycosides as Glycosyl Donors and Thiophilic Cations as Promoters. *Carbohydr. Res.* **1983**, *116* (1), 162-165. DOI: 10.1016/S0008-6215(00)90965-0.
- (29) Veeneman, G. H.; van Leeuwen, S. H.; van Boom, J. H. Iodonium Ion Promoted Reactions at the Anomeric Centre. II an Efficient Thioglycoside Mediated Approach toward the Formation of 1,2-Trans Linked Glycosides and Glycosidic Esters. *Tetrahedron Lett.* **1990**, *31* (9), 1331-1334. DOI: 10.1016/S0040-4039(00)88799-7.
- (30) Crawford, C. J.; Seeberger, P. H. Advances in Glycoside and Oligosaccharide Synthesis. *Chem. Soc. Rev.* **2023**, *52* (22), 7773-7801. DOI: 10.1039/D3CS00321C.
- (31) Driguez, H. Thioligosaccharides in Glycobiology. In *Glycoscience Synthesis of Substrate Analogs and Mimetics*, Driguez, H., Thiem, J. Eds.; Springer Berlin Heidelberg, 1998; pp 85-116.
- (32) Pachamuthu, K.; Schmidt, R. R. Synthetic Routes to Thioligosaccharides and Thioglycopeptides. *Chem. Rev.* **2006**, *106* (1), 160-187. DOI: 10.1021/cr040660c.
- (33) Deore, B.; Ocando, J. E.; Pham, L. D.; Sanhueza, C. A. Anodic Reactivity of Alkyl S-Glucosides. *J. Org. Chem.* **2022**, *87* (9), 5952-5960. DOI: 10.1021/acs.joc.2c00222.
- (34) Andrews, J. S.; Mario Pinto, B. Synthesis of a Thio Analogue of N-Propyl Kojibioside, a Potential Glucosidase Inhibitor. *Carbohydr. Res.* **1995**, *270* (1), 51-62. DOI: 10.1016/0008-6215(95)00014-K.
- (35) Blanc-Muesser, M.; Defaye, J.; Driguez, H. Stereoselective Thioglycoside Syntheses. Part 4. A New Approach to 1,4-Linked 1-Thio-Disaccharides and a Synthesis of Thiomaltose. *J. Chem. Soc., Perkin Trans. I* **1982**, 15-18. DOI: 10.1039/P19820000015.
- (36) Cottaz, S.; Driguez, H. A Convenient Synthesis of *S*-(α -D- and *S*-(β -D)-Glucopyranosyl-6-thiomaltodextrins. *Synthesis* **1989**, *1989* (10), 755-758. DOI: 10.1055/s-1989-27384.
- (37) Mehta, S.; Jordan, K. L.; Weimar, T.; Kreis, U. C.; Batchelor, R. J.; Einstein, F. W. B.; Pinto, B. M. Synthesis of Sulfur Analogues of Methyl and Allyl Kojibiosides and Methyl Isomaltoside and Conformational Analysis of the Kojibiosides. *Tetrahedron: Asymmetry* **1994**, *5* (12), 2367-2396. DOI: 10.1016/S0957-4166(00)80386-9.
- (38) Alonso, E. R.; Peña, I.; Cabezas, C.; Alonso, J. L. Structural Expression of Exo-Anomeric Effect. *J. Phys. Chem. Lett.* **2016**, *7* (5), 845-850. DOI: 10.1021/acs.jpcclett.6b00028.

- (39) Garcia-Herrero, A.; Montero, E.; Muñoz, J. L.; Espinosa, J. F.; Vian, A.; Garcia, J. L.; Asensio, J. L.; Cañada, F. J.; Jimenez-Barbero, J. Conformational Selection of Glycomimetics at Enzyme Catalytic Sites: Experimental Demonstration of the Binding of Distinct High-Energy Distorted Conformations of C-, S-, and O-Glycosides by E. Coli B-Galactosidases. *J. Am. Chem. Soc.* **2002**, *124* (17), 4804-4810. DOI: 10.1021/ja0122445.
- (40) Rye, C. S.; Withers, S. G. The Synthesis of a Novel Thio-Linked Disaccharide of Chondroitin as a Potential Inhibitor of Polysaccharide Lyases. *Carbohydr. Res.* **2004**, *339* (3), 699-703. DOI: 10.1016/j.carres.2003.12.011.
- (41) Zanini, D.; Roy, R. Synthesis of New Alpha-thiosialodendrimers and Their Binding Properties to the Sialic Acid Specific Lectin from Limax Flavus. *J. Am. Chem. Soc.* **1997**, *119* (9), 2088-2095, Article. DOI: 10.1021/ja963874n.
- (42) Rodrigue, J.; Ganne, G.; Blanchard, B.; Saucier, C.; Giguere, D.; Shiao, T. C.; Varrot, A.; Imbert, A.; Roy, R. Aromatic Thioglycoside Inhibitors against the Virulence Factor LecA from Pseudomonas Aeruginosa. *Org. Biomol. Chem.* **2013**, *11* (40), 6906-6918. DOI: 10.1039/C3OB41422A.
- (43) Castaneda, F.; Burse, A.; Boland, W.; Kinne, R. K. H. Thioglycosides as Inhibitors of HSGLT1 and HSGLT2: Potential Therapeutic Agents for the Control of Hyperglycemia in Diabetes. *Int. J. Med. Sci.* **2007**, *4* (3), 131-139. DOI: 10.7150/ijms.4.131.
- (44) Sylla, B.; Legentil, L.; Saraswat-Ohri, S.; Vashishta, A.; Daniellou, R.; Wang, H. W.; Vetvicka, V.; Ferrieres, V. Oligo-Beta-(1 -> 3)-Glucans: Impact of Thio-Bridges on Immunostimulating Activities and the Development of Cancer Stem Cells. *J. Med. Chem.* **2014**, *57* (20), 8280-8292, Article. DOI: 10.1021/jm500506b.
- (45) Yang, Y.; Liu, H. P.; Yu, Q.; Yang, M. B.; Wang, D. M.; Jia, T. W.; He, H. J.; He, Y.; Xiao, H. X.; Iyer, S. S.; et al. Multivalent S-Sialoside Protein Conjugates Block Influenza Hemagglutinin and Neuraminidase. *Carbohydr. Res.* **2016**, *435*, 68-75, Article. DOI: 10.1016/j.carres.2016.09.017.
- (46) Wang, S.-S.; Gao, X.; Solar, V. d.; Yu, X.; Antonopoulos, A.; Friedman, A. E.; Matich, E. K.; Atilla-Gokcumen, G. E.; Nasirikenari, M.; Lau, J. T.; et al. Thioglycosides Are Efficient Metabolic Decoys of Glycosylation That Reduce Selectin Dependent Leukocyte Adhesion. *Cell Chem. Biol.* **2018**, *25* (12), 1519-1532.e1515. DOI: 10.1016/j.chembiol.2018.09.012.
- (47) Quintana, I. d. l. L.; Paul, A.; Chowdhury, A.; Moulton, K. D.; Kulkarni, S. S.; Dube, D. H. Thioglycosides Act as Metabolic Inhibitors of Bacterial Glycan Biosynthesis. *ACS Infect. Dis.* **2023**, *9* (10), 2025-2035. DOI: 10.1021/acsinfecdis.3c00324.
- (48) Zetterberg, F. R.; Diehl, C.; Håkansson, M.; Kahl-Knutson, B.; Leffler, H.; Nilsson, U. J.; Peterson, K.; Roper, J. A.; Slack, R. J. Discovery of Selective and Orally Available Galectin-1 Inhibitors. *J. Med. Chem.* **2023**, *66* (24), 16980-16990. DOI: 10.1021/acs.jmedchem.3c01787.
- (49) Lambert, J. B.; Wharry, S. M. Distortion Analysis of Thio Sugars. *Carbohydr. Res.* **1983**, *115*, 33-40. DOI: 10.1016/0008-6215(83)88132-4.
- (50) Adlercreutz, D.; Yoshimura, Y.; Mannerstedt, K.; Wakarchuk, W. W.; Bennett, E. P.; Dovichi, N. J.; Hindsgaul, O.; Palcic, M. M. Thiogalactopyranosides are Resistant to Hydrolysis by A-Galactosidases. *ChemBioChem* **2012**, *13* (11), 1673-1679. DOI: 10.1002/cbic.201200155.
- (51) Elzagheid, M. I.; Oivanen, M.; Walker, R. T.; Secrist, J. A. Kinetics for the Acid-Catalyzed Hydrolysis of Purine and Cytosine 2'-Deoxy-4'-thionucleosides. *Nucleosides and Nucleotides* **1999**, *18* (2), 181-186. DOI: 10.1080/15257779908043065.
- (52) Lambert, J. B.; Wharry, S. M. Conformational Analysis of 5-Thio-D-glucose. *J. Org. Chem.* **1981**, *46* (16), 3193-3196. DOI: 10.1021/jo00329a009.
- (53) Bennet, A. J.; Kitos, T. E. Mechanisms of Glycopyranosyl and 5-Thioglycopyranosyl Transfer Reactions in Solution. *J. Chem. Soc., Perkin Trans. 2* **2002**, (7), 1207-1222. DOI: 10.1039/B108446C.
- (54) Hughes, N. A.; Munkombwe, N. M. Synthesis of 5-Thio-D-arabinose and 5-Thio-D-Lyxose and Their Methyl Glycopyranosides. *Carbohydr. Res.* **1985**, *136*, 397-409. DOI: 10.1016/0008-6215(85)85213-7.
- (55) Capon, R. J.; MacLeod, J. K. 5-Thio-D-mannose from the Marine Sponge Clathria Pyramida(Lendenfeld). The First Example of a Naturally Occurring 5-Thiosugar. *J. Chem. Soc., Chem. Commun.* **1987**, (15), 1200-1201. DOI: 10.1039/C39870001200.

- (56) Matsuda, H.; Morikawa, T.; Yoshikawa, M. Antidiabetogenic Constituents from Several Natural Medicines. *Pure Appl. Chem.* **2002**, *74* (7), 1301-1308. DOI: 10.1351/pac200274071301.
- (57) Yoshikawa, M.; Murakami, T.; Shimada, H.; Matsuda, H.; Yamahara, J.; Tanabe, G.; Muraoka, O. Salacinol, Potent Antidiabetic Principle with Unique Thiosugar Sulfonium Sulfate Structure from the Ayurvedic Traditional Medicine Salacia Reticulata in Sri Lanka and India. *Tetrahedron Lett.* **1997**, *38* (48), 8367-8370. DOI: 10.1016/S0040-4039(97)10270-2.
- (58) Yoshikawa, M.; Murakami, T.; Yashiro, K.; Matsuda, H. Kotalanol, a Potent α -Glucosidase Inhibitor with Thiosugar Sulfonium Sulfate Structure, from Antidiabetic Ayurvedic Medicine Salacia Reticulata. *Chem. Pharm. Bull.* **1998**, *46* (8), 1339-1340. DOI: 10.1248/cpb.46.1339.
- (59) Witeczak, Z. J.; Culhane, J. M. Thiosugars: New Perspectives Regarding Availability and Potential Biochemical and Medicinal Applications. *Appl. Microbiol. Biotechnol.* **2005**, *69* (3), 237-244. DOI: 10.1007/s00253-005-0156-x.
- (60) Whistler, R. L.; Feather, M. S.; Ingles, D. L. Introduction of a New Hetero Atom into a Sugar Ring. *J. Am. Chem. Soc.* **1962**, *84* (1), 122-122. DOI: 10.1021/ja00860a037.
- (61) Feather, M. S.; Whistler, R. L. Derivatives of 5-Deoxy-5-mercapto-D-glucose. *Tetrahedron Lett.* **1962**, *3* (15), 667-668. DOI: 10.1016/S0040-4039(00)70929-4.
- (62) Al Bujuq, N. Strategies for Introducing Sulfur Atom in a Sugar Ring: Synthesis of 5-Thioaldopyranoses and their NMR Data. *J. Sulphur Chem.* **2019**, *40* (6), 664-702. DOI: 10.1080/17415993.2019.1616734.
- (63) Yuasa, H.; Izumi, M.; Hashimoto, H. Thiasugars: Potential Glycosidase Inhibitors. *Curr. Top. Med. Chem.* **2009**, *9* (1), 76-86. DOI: 10.2174/156802609787354270.
- (64) Malone, A.; Scanlan, E. M. Applications of Thiyl Radical Cyclizations for the Synthesis of Thiosugars. *Org. Lett.* **2013**, *15* (3), 504-507. DOI: 10.1021/ol303310u.
- (65) Madern, J. M.; Hansen, T.; van Rijssel, E. R.; Kistemaker, H. A. V.; van der Vorm, S.; Overkleef, H. S.; van der Marel, G. A.; Filippov, D. V.; Codée, J. D. C. Synthesis, Reactivity, and Stereoselectivity of 4-Thiofuranosides. *J. Org. Chem.* **2019**, *84* (3), 1218-1227. DOI: 10.1021/acs.joc.8b02536.
- (66) Tsuruta, O.; Yuasa, H.; Hashimoto, H.; Sujino, K.; Otter, A.; Li, H.; Palcic, M. M. Synthesis of GDP-5-Thiosugars and their Use as Glycosyl Donor Substrates for Glycosyltransferases. *J. Org. Chem.* **2003**, *68* (16), 6400-6406. DOI: 10.1021/jo0300035.
- (67) Whistler, R. L.; Dick, W.; Ingle, T.; Rowell, R.; Urbas, B. Methyl 4-Deoxy-4-mercapto-D-ribofuranoside. *J. Org. Chem.* **1964**, *29* (12), 3723-3725.
- (68) Whistler, R. L.; Rowell, R. Preparation of Methyl L-Arabinothiopyranoside and Disulfide Derivatives of 5-Mercapto-L-arabinose. *J. Org. Chem.* **1964**, *29* (5), 1259-1261.
- (69) Yuasa, H.; Jouyabu, M.; Mitsuhashi, N.; Hashimoto, H. Syntheses of 5-Thio-D-mannose from Petrochemicals and a Disaccharide Analog Containing It. *Lett. Org. Chem.* **2008**, *2008*, 784173. DOI: 10.1155/2008/784173.
- (70) Nayak, U. G.; Whistler, R. L. Synthesis of 5-Thio-D-glucose. *J. Org. Chem.* **1969**, *34* (1), 97-100. DOI: 10.1021/jo00838a023.
- (71) Hashimoto, H.; Kawanishi, M.; Yuasa, H. Novel Conversion of Aldopyranosides into 5-Thioaldopyranosides via Acyclic Monothioacetals with Inversion and Retention of Configuration at C-5. *Carbohydr. Res.* **1996**, *282* (2), 207-221. DOI: 10.1016/0008-6215(95)00386-X.
- (72) Guinan, M.; Huang, N.; Hawes, C. S.; Lima, M. A.; Smith, M.; Miller, G. J. Chemical Synthesis of 4'-Thio and 4'-Sulfinyl Pyrimidine Nucleoside Analogues. *Org. Biomol. Chem.* **2022**, *20* (7), 1401-1406. DOI: 10.1039/D1OB02097H.
- (73) Dyson, M. R.; Coe, P. L.; Walker, R. T. The Synthesis and Antiviral Properties of E-5-(2-Bromovinyl)-4'-thio-2'-deoxyuridine. *J. Chem. Soc., Chem. Commun.* **1991**, (10), 741-742. DOI: 10.1039/C39910000741.
- (74) Bobek, M.; Whistler, R. L.; Bloch, A. Synthesis and Biological Activity of 4'-Thio Analogs of the Antibiotic Toyocamycin. *J. Med. Chem.* **1972**, *15* (2), 168-171. DOI: 10.1021/jm00272a011.
- (75) Secrist, J. A.; Tiwari, K. N.; Riordan, J. M.; Montgomery, J. A. Synthesis and Biological Activity of 2'-Deoxy-4'-thio Pyrimidine Nucleosides. *J. Med. Chem.* **1991**, *34* (8), 2361-2366. DOI: 10.1021/jm00112a007.

- (76) Ototani, N.; Whistler, R. L. Preparation and Antitumor Activity of 4'-Thio Analogs of 2,2'-Anhydro-1-beta-D-arabinofuranosylcytosine. *J. Med. Chem.* **1974**, *17* (5), 535-537. DOI: 10.1021/jm00251a015.
- (77) Tannock, I. F.; Guttman, P.; Rauth, A. M. Failure of 2-Deoxy-D-Glucose and 5-Thio-D-glucose to Kill Hypoxic Cells of Two Murine Tumors. *Cancer Res.* **1983**, *43* (3), 980.
- (78) Seidensticker, M.; Ulrich, G.; Muehlberg, F. L.; Pethe, A.; Grosser, O. S.; Steffen, I. G.; Stiebler, M.; Goldschmidt, J.; Smalla, K. H.; Seidensticker, R.; et al. Tumor Cell Uptake of 99MTC-Labeled 1-Thio-b-D-glucose and 5-Thio-D-glucose in Comparison with 2-Deoxy-2-[18 F]fluoro-D-glucose in Vitro: Kinetics, Dependencies, Blockage and Cell Compartment of Accumulation. *Mol. Imaging Biol.* **2014**, *16* (2), 189-198. DOI: 10.1007/s11307-013-0690-3.
- (79) Liu, T.-W.; Zandberg, W. F.; Gloster, T. M.; Deng, L.; Murray, K. D.; Shan, X.; Vocadlo, D. J. Metabolic Inhibitors of O-GlcNAc Transferase That Act in Vivo Implicate Decreased O-GlcNAc Levels in Leptin-Mediated Nutrient Sensing. *Angew. Chem. Int. Ed.* **2018**, *57* (26), 7644-7648. DOI: 10.1002/anie.201803254.
- (80) Liao, X. X.; Vetvicka, V.; Crich, D. Synthesis and Evaluation of 1,5-Dithia-D-Iaminaribiose, Triose, and Tetraose as Truncated Beta-(1 -> 3)-glucan Mimetics. *J. Org. Chem.* **2018**, *83* (24), 14894-14904, Article. DOI: 10.1021/acs.joc.8b01645.
- (81) Wang, Z.; Dohle, C.; Friemann, J.; Green, B. S.; Gleichmann, H. Prevention of High- and Low-Dose STZ-Induced Diabetes with D-Glucose and 5-Thio-D-glucose. *Diabetes* **1993**, *42* (3), 420-428. DOI: 10.2337/diab.42.3.420.
- (82) Palma, A. S.; Feizi, T.; Zhang, Y. B.; Stoll, M. S.; Lawson, A. M.; Diaz-Rodriguez, E.; Campanero-Rhodes, M. A.; Costa, J.; Gordon, S.; Brown, G. D.; et al. Ligands for the Beta-glucan Receptor, Dectin-1, Assigned Using "Designer" Microarrays of Oligosaccharide Probes (Neoglycolipids) Generated from Glucan Polysaccharides. *J. Biol. Chem.* **2006**, *281* (9), 5771-5779, Article. DOI: 10.1074/jbc.M511461200.
- (83) Bushway, A. A.; Keenan, T. W. 5-Thio-D-glucose is an Acceptor for UDP-Galactose: D-Glucose 1-Galactosyltransferase. *Biochem. Biophys. Res. Commun.* **1978**, *81* (2), 305-309. DOI: 10.1016/0006-291X(78)91533-4.
- (84) Critchley, D. R.; Eichholz, A.; Crane, R. K. Transport of 5-Thio-D-glucose in Hamster Small Intestine. *Biochim. Biophys. Acta* **1970**, *211*, 244-254.
- (85) Kelley, M. J.; Chen, T. S. Action of 5-Thio-D-glucose on D-Glucose Metabolism: Possible Mechanism for Diabetogenic Effect. *J. Pharmacol. Exp. Ther.* **1985**, *232* (3), 760-763.
- (86) Svensson, L.; Johnston, B. D.; Gu, J.-H.; Patrick, B.; Pinto, B. M. Synthesis and Conformational Analysis of a Sulfonium-Ion Analogue of the Glycosidase Inhibitor Castanospermine. *J. Am. Chem. Soc.* **2000**, *122* (44), 10769-10775. DOI: 10.1021/ja002038h.
- (87) Bachmann, T.; Rychlik, M. Chemical Glucosylation of Pyridoxine. *Carbohydr. Res.* **2020**, *489*, 107929. DOI: 10.1016/j.carres.2020.107929.
- (88) Mehta, S.; Andrews, J. S.; Svensson, B.; Pinto, B. M. Synthesis and Enzymic Activity of Novel Glycosidase Inhibitors Containing Sulfur and Selenium. *J. Am. Chem. Soc.* **1995**, *117* (39), 9783-9790. DOI: 10.1021/ja00144a001.
- (89) Hummel, G.; Hindsgaul, O. Solid-Phase Synthesis of Thio-Oligosaccharides. *Angew. Chem. Int. Ed.* **1999**, *38* (12), 1782-1784. DOI: 10.1002/(SICI)1521-3773(19990614)38:12<1782::AID-ANIE1782>3.0.CO;2-1.
- (90) Al-Mosoudi, N. A. L.; Hughes, N. A. Synthesis of 5-Thio-D-allose and the Methyl 5-Thio-a- and -b-D-allopyranosides. *Carbohydr. Res.* **1986**, *148* (1), 25-37. DOI: 10.1016/0008-6215(86)80033-7.
- (91) Grimshaw, C. E.; Whistler, R. L.; Cleland, W. W. Ring Opening and Closing Rates for Thiosugars. *J. Am. Chem. Soc.* **1979**, *101* (6), 1521-1532. DOI: 10.1021/ja00500a026.
- (92) Yuasa, H.; Tamura, J.-i.; Hashimoto, H. Synthesis of Per-O-alkylated 5-Thio-D-glucono-1,5-lactones and Transannular Participation of the Ring Sulphur Atom of 5-Thio-D-glucose Derivatives on Solvolysis under Acidic Conditions. *J. Chem. Soc., Perkin Trans. 1* **1990**, (10), 2763-2769. DOI: 10.1039/P19900002763.
- (93) Hashimoto, H.; Yuasa, H. Sulfur Participation in Methanolysis and Acetolysis of 5-Deoxy-5-thio-D-glucose Derivatives. *Tetrahedron Lett.* **1988**, *29* (16), 1939-1942. DOI: 10.1016/S0040-4039(00)82084-5.

- (94) Sze, D. M. Y.; Chan, G. C. F. Effects of Beta-glucans on Different Immune Cell Populations and Cancers. In *Recent Trends in Medicinal Plants Research*, Shyur, L. F., Lau, A. S. Y. Eds.; Advances in Botanical Research, Vol. 62; Academic Press Ltd-Elsevier Science Ltd, 2012; pp 179-196.
- (95) Tsoni, S. V.; Brown, G. D. Beta-glucans and Dectin-1. In *Year in Immunology 2008*, Rose, N. R. Ed.; Annals of the New York Academy of Sciences, Vol. 1143; Wiley-Blackwell, 2008; pp 45-60.
- (96) Barsanti, L.; Passarelli, V.; Evangelista, V.; Frassanito, A. M.; Gualtieri, P. Chemistry, Physico-Chemistry and Applications Linked to Biological Activities of Beta-Glucans. *Nat. Prod. Rep.* **2011**, 28 (3), 457-466, Review. DOI: 10.1039/c0np00018c.
- (97) Chlubnova, I.; Sylla, B.; Nugier-Chauvin, C.; Daniellou, R.; Legentil, L.; Kralova, B.; Ferrieres, V. Natural Glycans and Glycoconjugates as Immunomodulating Agents. *Nat. Prod. Rep.* **2011**, 28 (5), 937-952, Review. DOI: 10.1039/c1np00005e.
- (98) Xiang, D.; Sharma, V. R.; Freter, C. E.; Yan, J. Anti-Tumor Monoclonal Antibodies in Conjunction with Beta-Glucans: A Novel Anti-cancer Immunotherapy. *Curr. Med. Chem.* **2012**, 19 (25), 4298-4305, Review. DOI: 10.2174/092986712802884303.
- (99) Descroix, K.; Ferrieres, V.; Jamois, F.; Yvin, J. C.; Plusquellec, D. Recent Progress in the Field of Beta-(1,3)-glucans and New Applications. *Mini-Rev. Med. Chem.* **2006**, 6 (12), 1341-1349, Review. DOI: 10.2174/138955706778993058.
- (100) Krosi, G.; Korbelik, M. Potentiation of Photodynamic Therapy by Immunotherapy - the Effect of Schizophyllan (SPG). *Cancer Lett.* **1994**, 84 (1), 43-49, Article. DOI: 10.1016/0304-3835(94)90356-5.
- (101) Kirmaz, C.; Bayrak, P.; Yilmaz, O.; Yuksel, H. Effects of Glucan Treatment on the TH1/TH2 Balance in Patients with Allergic Rhinitis: A Double-Blind Placebo-Controlled Study. *Eur. Cytokine. Netw.* **2005**, 16 (2), 128-134.
- (102) Legentil, L.; Paris, F.; Ballet, C.; Trouvelot, S.; Daire, X.; Vetvicka, V.; Ferrieres, V. Molecular Interactions of Beta-(1 → 3)-glucans with Their Receptors. *Molecules* **2015**, 20 (6), 9745-9766, Review. DOI: 10.3390/molecules20069745.
- (103) Horvathova, E.; Eckl, P. M.; Bresgen, N.; Slamenova, D. Evaluation of Genotoxic and Cytotoxic Effects of H₂O₂ and Dmnq on Freshly Isolated Rat Hepatocytes; Protective Effects of Carboxymethyl Chitin-Glucan. *Neuro Endocrinol. Lett.* **2008**, 29 (5), 644-648.
- (104) Liao, G. C.; Zhou, Z. F.; Liao, J.; Zu, L. N.; Wu, Q. Y.; Guo, Z. W. 6-O-Branched Oligo-beta-glucan-Based Antifungal Glycoconjugate Vaccines. *ACS Infect. Dis.* **2016**, 2 (2), 123-131, Article. DOI: 10.1021/acsinfecdis.5b00104.
- (105) Liao, G. C.; Zhou, Z. F.; Burgula, S.; Liao, J.; Yuan, C.; Wu, Q. Y.; Guo, Z. W. Synthesis and Immunological Studies of Linear Oligosaccharides of Beta-glucan as Antigens for Antifungal Vaccine Development. *Bioconjugate Chem.* **2015**, 26 (3), 466-476, Article. DOI: 10.1021/bc500575a.
- (106) Weishaupt, M. W.; Matthies, S.; Seeberger, P. H. Automated Solid-Phase Synthesis of a Beta-(1,3)-glucan Dodecasaccharide. *Chem. Eur. J.* **2013**, 19 (37), 12497-12503, Article. DOI: 10.1002/chem.201204518.
- (107) Tanaka, H.; Kawai, T.; Adachi, Y.; Ohno, N.; Takahashi, T. Beta(1,3) Branched Heptadeca- and Linear Hexadeca-Saccharides Possessing an Aminoalkyl Group as a Strong Ligand to Dectin-1. *Chem. Commun.* **2010**, 46 (43), 8249-8251, Article. DOI: 10.1039/c0cc03153d.
- (108) Ross, G. D.; Vetvicka, V.; Yan, J.; Xia, Y.; Vetvickova, J. Therapeutic Intervention with Complement and Beta-glucan in Cancer. *Immunopharmacology* **1999**, 42 (1-3), 61-74, Article; Proceedings Paper. DOI: 10.1016/s0162-3109(99)00013-2.
- (109) Bohn, J. A.; BeMiller, J. N. (1->3)-Beta-D-glucans as Biological Response Modifiers: A Review of Structure-Functional Activity Relationships. *Carbohydr. Polym.* **1995**, 28 (1), 3-14, Article; Proceedings Paper. DOI: 10.1016/0144-8617(95)00076-3.
- (110) Goodridge, H. S.; Reyes, C. N.; Becker, C. A.; Katsumoto, T. R.; Ma, J.; Wolf, A. J.; Bose, N.; Chan, A. S. H.; Magee, A. S.; Danielson, M. E.; et al. Activation of the Innate Immune Receptor Dectin-1 Upon Formation of a 'Phagocytic Synapse'. *Nature* **2011**, 472 (7344), 471-U541, Article. DOI: 10.1038/nature10071.

- (111) Brown, G. D.; Gordon, S. Immune Recognition - a New Receptor for Beta-glucans. *Nature* **2001**, *413* (6851), 36-37, Article. DOI: 10.1038/35092620.
- (112) Ariizumi, K.; Shen, G. L.; Shikano, S.; Xu, S.; Ritter, R.; Kumamoto, T.; Edelbaum, D.; Morita, A.; Bergstresser, P. R.; Takashima, A. Identification of a Novel, Dendritic Cell-Associated Molecule, Dectin-1, by Subtractive cDNA Cloning. *J. Biol. Chem.* **2000**, *275* (26), 20157-20167, Article. DOI: 10.1074/jbc.M909512199.
- (113) Descroix, K.; Vetvicka, V.; Laurent, I.; Jamois, F.; Yvin, J.-C.; Ferrieres, V. New Oligo-B-(1,3)-Glucan Derivatives as Immunostimulating Agents. *Bioorg. Med. Chem* **2010**, *18* (1), 348-357. DOI: 10.1016/j.bmc.2009.10.053.
- (114) Vetvicka, V.; Saraswat-Ohri, S.; Vashishta, A.; Descroix, K.; Jamois, F.; Yvin, J. C.; Ferrieres, V. New 4-Deoxy-(1 → 3)-Beta-D-Glucan-Based Oligosaccharides and Their Immunostimulating Potential. *Carbohydr. Res.* **2011**, *346* (14), 2213-2221, Article. DOI: 10.1016/j.carres.2011.06.020.
- (115) Brown, J.; O'Callaghan, C. A.; Marshall, A. S. J.; Gilbert, R. J. C.; Siebold, C.; Gordon, S.; Brown, G. D.; Jones, E. Y. Structure of the Fungal B-Glucan-Binding Immune Receptor Dectin-1: Implications for Function. *Protein Sci.* **2007**, *16* (6), 1042-1052. DOI: 10.1110/ps.072791207.
- (116) Sylla, B.; Guean, J.-P.; Wieruszeski, J.-M.; Nugier-Chauvin, C.; Legentil, L.; Daniellou, R.; Ferrières, V. Probing B-(1→3)-D-Glucans Interactions with Recombinant Human Receptors Using High-Resolution NMR Studies. *Carbohydr. Res.* **2011**, *346* (12), 1490-1494. DOI: 10.1016/j.carres.2011.03.038.
- (117) Hanashima, S.; Ikeda, A.; Tanaka, H.; Adachi, Y.; Ohno, N.; Takahashi, T.; Yamaguchi, Y. Nmr Study of Short B(1-3)-Glucans Provides Insights into the Structure and Interaction with Dectin-1. *Glycoconj. J.* **2014**, *31* (3), 199-207. DOI: 10.1007/s10719-013-9510-x.
- (118) Pieters, R. J. Maximising Multivalency Effects in Protein–Carbohydrate Interactions. *Org. Biomol. Chem.* **2009**, *7* (10), 2013-2025. DOI: 10.1039/B901828J.
- (119) Chabre, Y. M.; Roy, R. Chapter 6 - Design and Creativity in Synthesis of Multivalent Neoglycoconjugates. In *Adv. Carbohydr. Chem. Biochem.*, Horton, D. Ed.; Vol. 63; Academic Press, 2010; pp 165-393.
- (120) Reynolds, M.; Perez, S. Thermodynamics and Chemical Characterization of Protein–Carbohydrate Interactions: The Multivalency Issue. *CR. Chim.* **2011**, *14* (1), 74-95. DOI: 10.1016/j.crci.2010.05.020.
- (121) Adams, E. L.; Rice, P. J.; Graves, B.; Ensley, H. E.; Yu, H.; Brown, G. D.; Gordon, S.; Monteiro, M. A.; Papp-Szabo, E.; Lowman, D. W.; et al. Differential High-Affinity Interaction of Dectin-1 with Natural or Synthetic Glucans Is Dependent Upon Primary Structure and Is Influenced by Polymer Chain Length and Side-Chain Branching. *J. Pharmacol. Exp. Ther.* **2008**, *325* (1), 115-123. DOI: 10.1124/jpet.107.133124.
- (122) Sylla, B.; Legentil, L.; Saraswat-Ohri, S.; Vashishta, A.; Daniellou, R.; Wang, H.-W.; Vetvicka, V.; Ferrieres, V. Oligo-B-(1 → 3)-Glucans: Impact of Thio-Bridges on Immunostimulating Activities and the Development of Cancer Stem Cells. *J. Med. Chem.* **2014**, *57* (20), 8280-8292. DOI: 10.1021/jm500506b.
- (123) Ferry, A.; Malik, G.; Guinchard, X.; Vetvicka, V.; Crich, D. Synthesis and Evaluation of Di- and Trimeric Hydroxylamine-Based B-(1→3)-Glucan Mimetics. *J. Am. Chem. Soc.* **2014**, *136* (42), 14852-14857. DOI: 10.1021/ja507084t.
- (124) Wen, P.; Vetvicka, V.; Crich, D. Synthesis and Evaluation of Oligomeric Thioether-Linked Carbacyclic B-(1→3)-Glucan Mimetics. *J. Org. Chem.* **2019**, *84* (9), 5554-5563. DOI: 10.1021/acs.joc.9b00504.
- (125) Roy, R. A Decade of Glycodendrimer Chemistry. *Trends Glycosci. Glycotechnol.* **2003**, *15* (85), 291-310, Review. DOI: 10.4052/tigg.15.291.
- (126) Chen, A.; Wang, D.; Bietsch, J.; Wang, G. Synthesis and Characterization of Pentaerythritol Derived Glycoconjugates as Supramolecular Gelators. *Org. Biomol. Chem.* **2019**, *17* (24), 6043-6056. DOI: 10.1039/C9OB00475K.
- (127) Wang, G.; Wang, D.; Bietsch, J.; Chen, A.; Sharma, P. Synthesis of Dendritic Glycoclusters and Their Applications for Supramolecular Gelation and Catalysis. *J. Org. Chem.* **2020**, *85* (24), 16136-16156. DOI: 10.1021/acs.joc.0c01978.

- (128) Lundquist, J. J.; Toone, E. J. The Cluster Glycoside Effect. *Chem. Rev.* **2002**, *102* (2), 555-578, Review. DOI: 10.1021/cr000418f.
- (129) Turgis, R.; Billault, I.; Acherar, S.; Auge, J.; Scherrmann, M. C. Total Synthesis of High Loading Capacity Peg-Based Supports: Evaluation and Improvement of the Process by Use of Ultrafiltration and Peg as a Solvent. *Green Chem.* **2013**, *15* (4), 1016-1029, Article. DOI: 10.1039/c3gc37097f.
- (130) Meng, Q. Q.; Wang, Z. T.; Cui, J. H.; Cui, Q.; Dong, J. Y.; Zhang, Q. J.; Li, S. S. Design, Synthesis, and Biological Evaluation of Cytochrome P450 1B1 Targeted Molecular Imaging Probes for Colorectal Tumor Detection. *J. Med. Chem.* **2018**, *61* (23), 10901-10909, Article. DOI: 10.1021/acs.jmedchem.8b01633.
- (131) Gening, M. L.; Titov, D. V.; Cecioni, S.; Audfray, A.; Gerbst, A. G.; Tsvetkov, Y. E.; Krylov, V. B.; Imberty, A.; Nifantiev, N. E.; Vidal, S. Synthesis of Multivalent Carbohydrate-Centered Glycoclusters as Nanomolar Ligands of the Bacterial Lectin Leca from *Pseudomonas Aeruginosa*. *Chem. Eur. J.* **2013**, *19* (28), 9272-9285. DOI: 10.1002/chem.201300135.
- (132) Cecioni, S.; Imberty, A.; Vidal, S. Glycomimetics Versus Multivalent Glycoconjugates for the Design of High Affinity Lectin Ligands. *Chem. Rev.* **2015**, *115* (1), 525-561, Review. DOI: 10.1021/cr500303t.
- (133) Fakhrutdinov, A. N.; Karlinskii, B. Y.; Minyaev, M. E.; Ananikov, V. P. Unusual Effect of Impurities on the Spectral Characterization of 1,2,3-Triazoles Synthesized by the Cu-Catalyzed Azide-Alkyne Click Reaction. *J. Org. Chem.* **2021**, *86* (17), 11456-11463. DOI: 10.1021/acs.joc.1c00943.
- (134) Han, S.-Y.; Kim, Y.-A. Recent Development of Peptide Coupling Reagents in Organic Synthesis. *Tetrahedron* **2004**, *60* (11), 2447-2467. DOI: 10.1016/j.tet.2004.01.020.
- (135) Cheng, J.; Gu, Z.; He, C.; Jin, J.; Wang, L.; Li, G.; Sun, B.; Wang, H.; Bai, J. An Efficient Synthesis of Novel Bis-Triazole Glycoconjugates via a Three-Component Condensation as a Key Reaction. *Carbohydr. Res.* **2015**, *414*, 72-77. DOI: 10.1016/j.carres.2015.07.004.
- (136) Thornton, B. P.; Vetvicka, V.; Pitman, M.; Goldman, R. C.; Ross, G. D. Analysis of the Sugar Specificity and Molecular Location of the Beta-glucan-Binding Lectin Site of Complement Receptor Type 3 (Cd11b/Cd18). *J. Immun. J.* **1996**, *156* (3), 1235-1246.
- (137) Vetvicka, V.; Yvin, J.-C. Effects of Marine B-1,3 Glucan on Immune Reactions. *Int. Immunopharmacol.* **2004**, *4* (6), 721-730. DOI: 10.1016/j.intimp.2004.02.007.
- (138) Weis, W. I.; Drickamer, K. Structural Basis of Lectin-Carbohydrate Recognition. *Annu. Rev. Biochem.* **1996**, *65* (Volume 65, 1996), 441-473. DOI: 10.1146/annurev.bi.65.070196.002301.
- (139) Gabius, H.-J.; André, S.; Jimenez-Barbero, J.; Romero, A.; Solís, D. From Lectin Structure to Functional Glycomics: Principles of the Sugar Code. *Trends Biochem. Sci.* **2011**, *36* (6), 298-313. DOI: 10.1016/j.tibs.2011.01.005.
- (140) Adhav, V. A.; Saikrishnan, K. The Realm of Unconventional Noncovalent Interactions in Proteins: Their Significance in Structure and Function. *ACS Omega* **2023**, *8* (25), 22268-22284. DOI: 10.1021/acsomega.3c00205.
- (141) Xiao, Y.; Woods, R. J. Protein-Ligand CH- π Interactions: Structural Informatics, Energy Function Development, and Docking Implementation. *J. Chem. Theory Comput.* **2023**, *19* (16), 5503-5515. DOI: 10.1021/acs.jctc.3c00300.
- (142) Laughrey, Z. R.; Kiehna, S. E.; Riemen, A. J.; Waters, M. L. Carbohydrate- π Interactions: What Are They Worth? *J. Am. Chem. Soc.* **2008**, *130* (44), 14625-14633. DOI: 10.1021/ja803960x.
- (143) Asensio, J. L.; Arda, A.; Canada, F. J.; Jimenez-Barbero, J. Carbohydrate-Aromatic Interactions. *Acc. Chem. Res.* **2013**, *46* (4), 946-954, Review. DOI: 10.1021/ar300024d.
- (144) Kiessling, L. L.; Diehl, R. C. CH- π Interactions in Glycan Recognition. *ACS Chem. Biol.* **2021**, *16* (10), 1884-1893. DOI: 10.1021/acscchembio.1c00413.
- (145) Fernández-Alonso, M. d. C.; Cañada, F. J.; Jimenez-Barbero, J.; Cuevas, G. Molecular Recognition of Saccharides by Proteins. Insights on the Origin of the Carbohydrate-Aromatic Interactions. *J. Am. Chem. Soc.* **2005**, *127* (20), 7379-7386. DOI: 10.1021/ja051020+.
- (146) Kozmon, S.; Matuška, R.; Spiwok, V.; Koča, J. Three-Dimensional Potential Energy Surface of Selected Carbohydrates' Ch/ π Dispersion Interactions Calculated by High-Level Quantum Mechanical Methods. *Chem. Eur. J.* **2011**, *17* (20), 5680-5690. DOI: 10.1002/chem.201002876.

- (147) Jimenez-Moreno, E.; Jimenez-Oses, G.; Gomez, A. M.; Santana, A. G.; Corzana, F.; Bastida, A.; Jimenez-Barberodef, J.; Asensio, J. L. A Thorough Experimental Study of CH/ π Interactions in Water: Quantitative Structure-Stability Relationships for Carbohydrate/Aromatic Complexes. *Chem. Sci.* **2015**, *6* (11), 6076-6085, Article. DOI: 10.1039/c5sc02108a.
- (148) Motherwell, W. B.; Moreno, R. B.; Pavlakos, I.; Arendorf, J. R. T.; Arif, T.; Tizzard, G. J.; Coles, S. J.; Aliev, A. E. Noncovalent Interactions of π Systems with Sulfur: The Atomic Chameleon of Molecular Recognition. *Angew. Chem. Int. Ed.* **2018**, *57* (5), 1193-1198, Article. DOI: 10.1002/anie.201708485.
- (149) Beno, B. R.; Yeung, K.-S.; Bartberger, M. D.; Pennington, L. D.; Meanwell, N. A. A Survey of the Role of Noncovalent Sulfur Interactions in Drug Design. *J. Med. Chem.* **2015**, *58* (11), 4383-4438. DOI: 10.1021/jm501853m.
- (150) Reid, K.; Lindley, P.; Thornton, J. Sulphur-Aromatic Interactions in Proteins. *FEBS Lett.* **1985**, *190* (2), 209-213.
- (151) Valley, C. C.; Cembran, A.; Perlmutter, J. D.; Lewis, A. K.; Labello, N. P.; Gao, J.; Sachs, J. N. The Methionine-Aromatic Motif Plays a Unique Role in Stabilizing Protein Structure. *J. Biol. Chem.* **2012**, *287* (42), 34979-34991.
- (152) Meyer, E. A.; Castellano, R. K.; Diederich, F. Interactions with Aromatic Rings in Chemical and Biological Recognition. *Angew. Chem. Int. Ed.* **2003**, *42* (11), 1210-1250. DOI: 10.1002/anie.200390319.
- (153) Newberry, R. W.; Raines, R. T. Secondary Forces in Protein Folding. *ACS Chem. Biol.* **2019**, *14* (8), 1677-1686. DOI: 10.1021/acscchembio.9b00339.
- (154) Zauhar, R.; Colbert, C.; Morgan, R.; Welsh, W. Evidence for a Strong Sulfur-Aromatic Interaction Derived from Crystallographic Data. *Biopolymers* **2000**, *53* (3), 233-248.
- (155) Viguera, A. R.; Serrano, L. Side-Chain Interactions between Sulfur-Containing Amino Acids and Phenylalanine In. α -Helices. *Biochemistry* **1995**, *34* (27), 8771-8779.
- (156) Tatko, C. D.; Waters, M. L. Investigation of the Nature of the Methionine- π Interaction in B-Hairpin Peptide Model Systems. *Protein Sci.* **2004**, *13* (9), 2515-2522.
- (157) Duan, G.; Smith, V. H.; Weaver, D. F. Characterization of Aromatic-Thiol π -Type Hydrogen Bonding and Phenylalanine-Cysteine Side Chain Interactions through ab initio Calculations and Protein Database Analyses. *Mol. Phys.* **2001**, *99* (19), 1689-1699. DOI: 10.1080/00268970110063917.
- (158) Petersen, M. T. N.; Jonson, P. H.; Petersen, S. B. Amino Acid Neighbours and Detailed Conformational Analysis of Cysteines in Proteins. *Protein Eng.* **1999**, *12* (7), 535-548.
- (159) Pranata, J. Sulfur-Aromatic Interactions: A Computational Study of the Dimethyl Sulfide-Benzene Complex☆. *Bioorg. Chem.* **1997**, *25*, 213-219.
- (160) Morgado, C. A.; McNamara, J. P.; Hillier, I. H.; Burton, N. A.; Vincent, M. A. Density Functional and Semiempirical Molecular Orbital Methods Including Dispersion Corrections for the Accurate Description of Noncovalent Interactions Involving Sulfur-Containing Molecules. *J. Chem. Theory Comput.* **2007**, *3* (5), 1656-1664. DOI: 10.1021/ct700072a.
- (161) Valley, C. C.; Cembran, A.; Perlmutter, J. D.; Lewis, A. K.; Labello, N. P.; Gao, J.; Sachs, J. N. The Methionine-Aromatic Motif Plays a Unique Role in Stabilizing Protein Structure*. *J. Biol. Chem.* **2012**, *287* (42), 34979-34991. DOI: 10.1074/jbc.M112.374504.
- (162) Hwang, J.; Li, P.; Smith, M. D.; Warden, C. E.; Sirianni, D. A.; Vik, E. C.; Maier, J. M.; Yehl, C. J.; Sherrill, C. D.; Shimizu, K. D. Tipping the Balance between S- π and O- π Interactions. *J. Am. Chem. Soc.* **2018**, *140* (41), 13301-13307. DOI: 10.1021/jacs.8b07617.
- (163) Ilardi, E. A.; Vitaku, E.; Njardarson, J. T. Data-Mining for Sulfur and Fluorine: An Evaluation of Pharmaceuticals to Reveal Opportunities for Drug Design and Discovery. *J. Med. Chem.* **2014**, *57* (7), 2832-2842. DOI: 10.1021/jm401375q.
- (164) Hudson, K. L.; Bartlett, G. J.; Diehl, R. C.; Agirre, J.; Gallagher, T.; Kiessling, L. L.; Woolfson, D. N. Carbohydrate-Aromatic Interactions in Proteins. *J. Am. Chem. Soc.* **2015**, *137* (48), 15152-15160. DOI: 10.1021/jacs.5b08424.
- (165) Zetterberg, F. R.; Peterson, K.; Johnsson, R. E.; Brimert, T.; Håkansson, M.; Logan, D. T.; Leffler, H.; Nilsson, U. J. Monosaccharide Derivatives with Low-Nanomolar Lectin Affinity and High Selectivity

Based on Combined Fluorine–Amide, Phenyl–Arginine, Sulfur– π , and Halogen Bond Interactions. *ChemMedChem* **2018**, *13* (2), 133–137. DOI: 10.1002/cmdc.201700744.

(166) McMahon, C. M.; Isabella, C. R.; Windsor, I. W.; Kosma, P.; Raines, R. T.; Kiessling, L. L. Stereoelectronic Effects Impact Glycan Recognition. *J. Am. Chem. Soc.* **2020**, *142* (5), 2386–2395. DOI: 10.1021/jacs.9b11699.

(167) Quirke, J. C. K.; Crich, D. Glycoside Hydrolases Restrict the Side Chain Conformation of Their Substrates to Gain Additional Transition State Stabilization. *J. Am. Chem. Soc.* **2020**, *142* (40), 16965–16973. DOI: 10.1021/jacs.0c05592.

(168) Quirke, J. C. K.; Crich, D. Gh47 and Other Glycoside Hydrolases Catalyze Glycosidic Bond Cleavage with the Assistance of Substrate Super-Arming at the Transition State. *ACS Catal.* **2021**, *11* (16), 10308–10315. DOI: 10.1021/acscatal.1c02750.

(169) Quirke, J. C. K.; Crich, D. Side Chain Conformation Restriction in the Catalysis of Glycosidic Bond Formation by Leloir Glycosyltransferases, Glycoside Phosphorylases, and Transglycosidases. *ACS Catal.* **2021**, *11* (9), 5069–5078. DOI: 10.1021/acscatal.1c00896.

(170) Rojas-Macias, M. A.; Lütke, T. Statistical Analysis of Amino Acids in the Vicinity of Carbohydrate Residues Performed by Glyvicinity. *Methods Mol Biol* **2015**, *1273*, 215–226. DOI: 10.1007/978-1-4939-2343-4_16.

(171) Agirre, J.; Davies, G.; Wilson, K.; Cowtan, K. Carbohydrate Anomalies in the PDB. *Nat. Chem. Biol* **2015**, *11* (5), 303–303. DOI: 10.1038/nchembio.1798.

(172) Agirre, J.; Iglesias-Fernández, J.; Rovira, C.; Davies, G. J.; Wilson, K. S.; Cowtan, K. D. Privateer: Software for the Conformational Validation of Carbohydrate Structures. *Nat. Struct. Mol. Biol.* **2015**, *22* (11), 833–834. DOI: 10.1038/nsmb.3115.

(173) The Pymol Molecular Graphics System, Version 2.5.2 Schrödinger LLC.

(174) Doyle, M. L. Characterization of Binding Interactions by Isothermal Titration Calorimetry. *Curr. Opin. Biotechnol.* **1997**, *8* (1), 31–35. DOI: 10.1016/s0958-1669(97)80154-1.

(175) Hirabayashi, J.; Arata, Y.; Kasai, K. Reinforcement of Frontal Affinity Chromatography for Effective Analysis of Lectin-Oligosaccharide Interactions. *J. Chromatogr. A* **2000**, *890* (2), 261–271. DOI: 10.1016/s0021-9673(00)00545-8.

(176) Magnez, R.; Bailly, C.; Thuru, X. Microscale Thermophoresis as a Tool to Study Protein Interactions and Their Implication in Human Diseases. *Int. J. Mol. Sci.* **2022**, *23* (14), 7672.

(177) Mann, D. A.; Kanai, M.; Maly, D. J.; Kiessling, L. L. Probing Low Affinity and Multivalent Interactions with Surface Plasmon Resonance: Ligands for Concanavalin A. *J. Am. Chem. Soc.* **1998**, *120* (41), 10575–10582. DOI: 10.1021/ja9818506.

(178) López-Lucendo, M. F.; Solís, D.; André, S.; Hirabayashi, J.; Kasai, K.-i.; Kaltner, H.; Gabius, H.-J.; Romero, A. Growth-Regulatory Human Galectin-1: Crystallographic Characterisation of the Structural Changes Induced by Single-Site Mutations and Their Impact on the Thermodynamics of Ligand Binding. *J. Mol. Biol.* **2004**, *343* (4), 957–970. DOI: 10.1016/j.jmb.2004.08.078.

(179) Barondes, S. H.; Castronovo, V.; Cooper, D. N. W.; Cummings, R. D.; Drickamer, K.; Felzi, T.; Gitt, M. A.; Hirabayashi, J.; Hughes, C.; Kasai, K.-i.; et al. Galectins: A Family of Animal B-Galactoside-Binding Lectins. *Cell* **1994**, *76* (4), 597–598. DOI: 10.1016/0092-8674(94)90498-7.

(180) Nesmelova, I. V.; Ermakova, E.; Daragan, V. A.; Pang, M.; Menendez, M.; Lagartera, L.; Solís, D.; Baum, L. G.; Mayo, K. H. Lactose Binding to Galectin-1 Modulates Structural Dynamics, Increases Conformational Entropy, and Occurs with Apparent Negative Cooperativity. *J. Mol. Biol.* **2010**, *397* (5), 1209–1230. DOI: 10.1016/j.jmb.2010.02.033.

(181) Chien, C.-T. H.; Ho, M.-R.; Lin, C.-H.; Hsu, S.-T. D. Lactose Binding Induces Opposing Dynamics Changes in Human Galectins Revealed by NMR-Based Hydrogen–Deuterium Exchange. *Molecules* **2017**, *22* (8), 1357.

(182) Stowell, S. R.; Dias-Baruffi, M.; Penttilä, L.; Renkonen, O.; Nyame, A. K.; Cummings, R. D. Human Galectin-1 Recognition of Poly-N-Acetylglucosamine and Chimeric Polysaccharides. *Glycobiology* **2004**, *14* (2), 157–167. DOI: 10.1093/glycob/cwh018 (accessed 3/12/2024).

- (183) Rao, K. N.; Suresh, C. G.; Katre, U. V.; Gaikwad, S. M.; Khan, M. I. Two Orthorhombic Crystal Structures of a Galactose-Specific Lectin from *Artocarpus Hirsuta* in Complex with Methyl [α]-D-galactose. *Acta Cryst. D* **2004**, *60* (8), 1404-1412. DOI: 10.1107/S090744490401354X.
- (184) Arockia Jeyaprakash, A.; Jayashree, G.; Mahanta, S. K.; Swaminathan, C. P.; Sekar, K.; Surolia, A.; Vijayan, M. Structural Basis for the Energetics of Jacalin–Sugar Interactions: Promiscuity Versus Specificity. *J. Mol. Biol.* **2005**, *347* (1), 181-188. DOI: 10.1016/j.jmb.2005.01.015.
- (185) Sahasrabuddhe, A. A.; Gaikwad, S. M.; Krishnasastri, M. V.; Khan, M. I. Studies on Recombinant Single Chain Jacalin Lectin Reveal Reduced Affinity for Saccharides Despite Normal Folding Like Native Jacalin. *Protein Sci.* **2004**, *13* (12), 3264-3273. DOI: 10.1110/ps.04968804.
- (186) Bourne, Y.; Astoul, C. H.; Zamboni, V.; Peumans, W. J.; Menu-Bouaouiche, L.; Van Damme, E. J. M.; Barre, A.; Rouge, P. Structural Basis for the Unusual Carbohydrate-Binding Specificity of Jacalin Towards Galactose and Mannose. *Biochem. J* **2002**, *364* (1), 173-180. DOI: 10.1042/bj3640173.
- (187) Astoul, C. H.; Pemans, W. J.; Damme, E. J. M. v.; Barre, A.; Bourne, Y.; Rouge, P. The Size, Shape and Specificity of the Sugar-Binding Site of the Jacalin-Related Lectins Is Profoundly Affected by the Proteolytic Cleavage of the Subunits. *Biochem. J* **2002**, *367* (3), 817-824. DOI: 10.1042/bj20020856.
- (188) Sasaki, G. L.; Gorin, P. A. J.; Souza, L. M.; Czelusniak, P. A.; Iacomini, M. Rapid Synthesis of Partially O-Methylated Alditol Acetate Standards for GC–MS: Some Relative Activities of Hydroxyl Groups of Methyl Glycopyranosides on Purdie Methylation. *Carbohydr. Res.* **2005**, *340* (4), 731-739. DOI: 10.1016/j.carres.2005.01.020.
- (189) Hribernik, N.; Tamburrini, A.; Falletta, E.; Bernardi, A. One Pot Synthesis of Thio-glycosides via Aziridine Opening Reactions. *Org. Biomol. Chem.* **2021**, *19* (1), 233-247, Article. DOI: 10.1039/d0ob01956a.
- (190) Abhinav, K. V.; Sharma, K.; Surolia, A.; Vijayan, M. Effect of Linkage on the Location of Reducing and Nonreducing Sugars Bound to Jacalin. *IUBMB Life* **2016**, *68* (12), 971-979. DOI: 10.1002/iub.1572.
- (191) Morii, Y.; Matsuda, H.; Ohara, K.; Hashimoto, M.; Miyairi, K.; Okuno, T. Synthetic Studies on Oligosaccharides Composed of 5-Thioglucopyranose Units. *Biorg. Med. Chem.* **2005**, *13* (17), 5113-5144. DOI: 10.1016/j.bmc.2005.05.028.
- (192) Tso, S.-C.; Brautigam, C. A. Measuring the K_d of Protein–Ligand Interactions Using Microscale Thermophoresismicroscale Thermophoresis (Mst). In *Protein-Ligand Interactions: Methods and Applications*, Daviter, T., Johnson, C. M., McLaughlin, S. H., Williams, M. A. Eds.; Springer US, 2021; pp 161-181.
- (193) Metha, S.; Pinto, B. M. Phenyl Selenoglycosides as Versatile Glycosylating Agents in Oligosaccharide Synthesis and the Chemical Synthesis of Disaccharides Containing Sulfur and Selenium. In *Modern Methods in Carbohydrate Synthesis*, Khan, S. H., O'Neill, R. A. Eds.; Harwood Academic, 1996; pp 107-129.
- (194) Andrews, J. S.; Johnston, B. D.; Pinto, B. M. Synthesis of a Dithio Analogue of N-Propyl Kojibioside as a Potential Glucosidase I Inhibitor. *Carbohydr. Res.* **1998**, *310* (1), 27-33. DOI: 10.1016/S0008-6215(98)00165-7.
- (195) Indurugalla, D.; Bennet, A. J. A Kinetic Isotope Effect Study on the Hydrolysis Reactions of Methyl Xylopyranosides and Methyl 5-Thioxylopyranosides: Oxygen Versus Sulfur Stabilization of Carbenium Ions. *J. Am. Chem. Soc.* **2001**, *123* (44), 10889-10898. DOI: 10.1021/ja011232g.
- (196) Johnston, B. D.; Indurugalla, D.; Pinto, B. M.; Bennet, A. J. The 5-Thioglucopyranosyl Carbenium Ion is a Solvent-Equilibrated Cation. *J. Am. Chem. Soc.* **2001**, *123* (50), 12698-12699. DOI: 10.1021/ja017118f.
- (197) Richard, J. P.; Amyes, T. L.; Toteva, M. M. Formation and Stability of Carbocations and Carbanions in Water and Intrinsic Barriers to Their Reactions. *Acc. Chem. Res.* **2001**, *34* (12), 981-988. DOI: 10.1021/ar0000556.
- (198) Horenstein, N. A. Mechanisms for Nucleophilic Aliphatic Substitution at Glycosides. In *Advances in Physical Organic Chemistry*, Richard, J. P. Ed.; Vol. 41; Academic Press, 2006; pp 275-314.

- (199) Adero, P. O.; Amarasekara, H.; Wen, P.; Bohé, L.; Crich, D. The Experimental Evidence in Support of Glycosylation Mechanisms at the SN1–SN2 Interface. *Chem. Rev.* **2018**, *118* (17), 8242–8284. DOI: 10.1021/acs.chemrev.8b00083.
- (200) Jensen, J. L.; Jencks, W. P. Hydrolysis of Benzaldehyde O,S-Acetals. *J. Am. Chem. Soc.* **1979**, *101* (6), 1476–1488. DOI: 10.1021/ja00500a019.
- (201) Satchell, D. P. N.; Satchell, R. S. Mechanisms of Hydrolysis of Thioacetals. *Chem. Soc. Rev.* **1990**, *19* (1), 55–81. DOI: 10.1039/CS9901900055.
- (202) Jagannadham, V.; Amyes, T. L.; Richard, J. P. Kinetic and Thermodynamic Stabilities Of Alpha-oxygen- And Alpha-sulfur-Stabilized Carbocations in Solution. *J. Am. Chem. Soc.* **1993**, *115* (18), 8465–8466. DOI: 10.1021/ja00071a073.
- (203) Apeloig, Y.; Karni, M. The Stabilities of A-Oxy and A-Thio Carbenium Ions: The Importance of the Ground-State Energies of the Neutral Precursors. *J. Chem. Soc., Perkin Trans. 2* **1988**, (5), 625–636. DOI: 10.1039/P29880000625.
- (204) Laali, K. K.; Borosky, G. L. A-Sulfur or A-Fluorine—Which Is More Stabilizing for a Carbocation? A Computational Study of Electrophilic Addition to Hfch(Sme) and Fc(R1)Cr2(Sme) and Related Model Systems. *J. Fluorine Chem.* **2013**, *151*, 26–31. DOI: 10.1016/j.jfluchem.2013.04.003.
- (205) Chapter 4 - Sulfur-Containing Carbocations. In *Organic Chemistry: A Series of Monographs*, Block, E. Ed.; Vol. 37; Academic Press, 1978; pp 128–175.
- (206) Bohé, L.; Crich, D. A Propos of Glycosyl Cations and the Mechanism of Chemical Glycosylation. *CR. Chim.* **2011**, *14* (1), 3–16. DOI: 10.1016/j.crci.2010.03.016.
- (207) Lambert, J. B.; Majchrzak, M. W.; Stec, D., III. Protonic and Conformational Equilibriums of 1,3-Dithiaalkanes and Their Congeners in Highly Acidic Media. *J. Org. Chem.* **1979**, *44* (25), 4689–4695. DOI: 10.1021/jo00393a046.
- (208) Dhakal, B.; Bohé, L.; Crich, D. Trifluoromethanesulfonate Anion as Nucleophile in Organic Chemistry. *J. Org. Chem.* **2017**, *82* (18), 9263–9269. DOI: 10.1021/acs.joc.7b01850.
- (209) Zefirov, N. S.; Koz'min, A. S. Competitive Binding of Nucleofugal Anions in Carbocationic-Like Processes. *Acc. Chem. Res.* **1985**, *18* (5), 154–158. DOI: 10.1021/ar00113a005.
- (210) Zefirov, N. S.; Koz'min, A. S.; Sorokin, V. D.; Zhdankin, V. V.; Studnev, Y. N.; Fokin, A. V. Competitive Binding of Fluorosulfate Anion in Reactions of Halogens and Nitronium Borofluoride with Olefins. *Bull. Acad. Sci. USSR, Div. Chem. Sci.* **1985**, *34* (2), 356–358. DOI: 10.1007/BF00951286.
- (211) Crich, D. En Route to the Transformation of Glycoscience: A Chemist's Perspective on Internal and External Crossroads in Glycochemistry. *J. Am. Chem. Soc.* **2021**, *143* (1), 17–34. DOI: 10.1021/jacs.0c11106.
- (212) Franconetti, A.; Arda, A.; Asensio, J. L.; Blériot, Y.; Thibaudeau, S.; Jimenez-Barbero, J. Glycosyl Oxocarbenium Ions: Structure, Conformation, Reactivity, and Interactions. *Acc. Chem. Res.* **2021**, *54* (11), 2552–2564. DOI: 10.1021/acs.accounts.1c00021.
- (213) Hartke, K.; Akgün, E. Zur Reaktion A-Halogenierter Sulfide Mit Antimonpentachlorid. *Chem. Ber.* **1979**, *112* (7), 2436–2443. DOI: 10.1002/cber.19791120711.
- (214) Hartke, K.; Akgün, E. Stabilisierung Von Thioniumcarbenium-Salzen Durch + M-Substituenten. *Liebigs Ann. Chem.* **1981**, *1981* (1), 47–51. DOI: 10.1002/jlac.198119810109.
- (215) Shimizu, A.; Takeda, K.; Mishima, S.; Saito, K.; Kim, S.; Nokami, T.; Yoshida, J.-i. Generation, Characterization, and Reactions of Thionium Ions Based on the Indirect Cation Pool Method. *Bull. Chem. Soc. Jpn.* **2015**, *89* (1), 61–66. DOI: 10.1246/bcsj.20150323 (accessed 4/1/2024).
- (216) Brenninger, C.; Bach, T. A-Thio Carbocations (Thionium Ions) as Intermediates in Brønsted Acid-Catalyzed Reactions of Enone-Derived 1,3-Dithianes and 1,3-Dithiolanes. *Top. Catal.* **2018**, *61* (7), 623–629. DOI: 10.1007/s11244-018-0905-6.
- (217) Crich, D.; Sun, S. Are Glycosyl Triflates Intermediates in the Sulfoxide Glycosylation Method? A Chemical and 1h, 13c, and 19f Nmr Spectroscopic Investigation. *J. Am. Chem. Soc.* **1997**, *119* (46), 11217–11223. DOI: 10.1021/ja971239r.
- (218) Upadhyaya, K.; Subedi, Y. P.; Crich, D. Direct Experimental Characterization of a Bridged Bicyclic Glycosyl Dioxacarbenium Ion by 1H and 13C NMR Spectroscopy: Importance of Conformation on

- Participation by Distal Esters. *Angew. Chem. Int. Ed.* **2021**, *60* (48), 25397-25403. DOI: 10.1002/anie.202110212.
- (219) Zeng, Y.; Wang, Z.; Whitfield, D.; Huang, X. Installation of Electron-Donating Protective Groups, a Strategy for Glycosylating Unreactive Thioglycosyl Acceptors Using the Preactivation-Based Glycosylation Method. *J. Org. Chem.* **2008**, *73* (20), 7952-7962. DOI: 10.1021/jo801462r.
- (220) Blériot, Y. Contributing to the Study of Enzymatic and Chemical Glycosyl Transfer through the Observation and Mimicry of Glycosyl Cations. *Synthesis* **2020**, *53* (05), 904-924. DOI: 10.1055/s-0040-1706073.
- (221) Martin, A.; Arda, A.; Désiré, J.; Martin-Mingot, A.; Probst, N.; Sinaÿ, P.; Jimenez-Barbero, J.; Thibaudeau, S.; Bleriot, Y. Catching Elusive Glycosyl Cations in a Condensed Phase with HF/SbF₅ Superacid. *Nat. Chem* **2016**, *8* (2), 186-191. DOI: 10.1038/nchem.2399.
- (222) Marples, B. A.; Saint, C. G.; Traynor, J. R. Regiochemistry of Nucleophilic Opening of *b*-Substituted Styrene Oxides with Thiolate Anions: Model Experiments in the Synthesis of Leukotriene Analogues. *J. Chem. Soc., Perkin Trans. 1* **1986**, (4), 567-574. DOI: 10.1039/P19860000567.
- (223) McCourt, R. O.; Scanlan, E. M. A Sequential Acyl Thiol–Ene and Thiolactonization Approach for the Synthesis of Δ -Thiolactones. *Org. Lett.* **2019**, *21* (9), 3460-3464. DOI: 10.1021/acs.orglett.9b01271.
- (224) Kopecky, D. J.; Rychnovsky, S. D. Improved Procedure for the Reductive Acetylation of Acyclic Esters and a New Synthesis of Ethers. *J. Org. Chem.* **2000**, *65* (1), 191-198. DOI: 10.1021/jo9914521.
- (225) Dahanukar, V. H.; Rychnovsky, S. D. General Synthesis of *a*-Acetoxy Ethers from Esters by Dibalh Reduction and Acetylation. *J. Org. Chem.* **1996**, *61* (23), 8317-8320. DOI: 10.1021/jo961205m.
- (226) Tamres, M.; Searles, S., Jr. Hydrogen Bonding Abilities of Cyclic Sulfoxides and Cyclic Ketones I. *J. Am. Chem. Soc.* **1959**, *81* (9), 2100-2104. DOI: 10.1021/ja01518a019.
- (227) Crumbie, R.; Ridley, D.; Steel, P. Stereoselectivity in the Reactions between the Anion of 4-Phenyl-5,6-dihydro-2H-thiopyran 1-Oxide and Electrophiles. *Aust. J. Chem.* **1985**, *38* (1), 119-132. DOI: 10.1071/CH9850119.
- (228) *Chemspider*. <http://www.chemspider.com/Chemical-Structure.141111.html> (accessed 2024 05-16).
- (229) Tokmakov, G. P.; Grandberg, I. I. Reaction of 3,4-Dihydro-2H-thiopyran with Phenylhydrazines. Synthesis of Homothiotryptophols. *Chem. Heterocycl. Compd.* **1989**, *25* (10), 1134-1139. DOI: 10.1007/BF00470691.
- (230) Matsumoto, K.; Ueoka, K.; Suzuki, S.; Suga, S.; Yoshida, J.-i. Direct and Indirect Electrochemical Generation of Alkoxy-carbenium Ion Pools from Thioacetals. *Tetrahedron* **2009**, *65* (52), 10901-10907. DOI: 10.1016/j.tet.2009.09.020.
- (231) Andreana, P. R.; Crich, D. Guidelines for O-Glycoside Formation from First Principles. *ACS Cent. Sci.* **2021**, *7* (9), 1454-1462. DOI: 10.1021/acscentsci.1c00594.
- (232) Whitfield, D. M. Chapter 4 Computational Studies of the Role of Glycopyranosyl Oxacarbenium Ions in Glycobiology and Glycochemistry. In *Advances in Carbohydrate Chemistry and Biochemistry*, Vol. 62; Academic Press, 2009; pp 83-159.
- (233) Satoh, H.; Hansen, H. S.; Manabe, S.; van Gunsteren, W. F.; Hünenberger, P. H. Theoretical Investigation of Solvent Effects on Glycosylation Reactions: Stereoselectivity Controlled by Preferential Conformations of the Intermediate Oxacarbenium-Counterion Complex. *J. Chem. Theory Comput.* **2010**, *6* (6), 1783-1797. DOI: 10.1021/ct1001347.
- (234) Hosoya, T.; Takano, T.; Kosma, P.; Rosenau, T. Theoretical Foundation for the Presence of Oxacarbenium Ions in Chemical Glycoside Synthesis. *J. Org. Chem.* **2014**, *79* (17), 7889-7894. DOI: 10.1021/jo501012s.
- (235) Hosoya, T.; Kosma, P.; Rosenau, T. Contact Ion Pairs and Solvent-Separated Ion Pairs from D-Mannopyranosyl and D-Glucopyranosyl Triflates. *Carbohydr. Res.* **2015**, *401*, 127-131. DOI: 10.1016/j.carres.2014.10.013.
- (236) Hosoya, T.; Kosma, P.; Rosenau, T. Theoretical Study on the Effects of a 4,6-O-Diacetal Protecting Group on the Stability of Ion Pairs from D-Mannopyranosyl and D-Glucopyranosyl Triflates. *Carbohydr. Res.* **2015**, *411*, 64-69. DOI: 10.1016/j.carres.2015.03.010.

- (237) Mootoo, D. R.; Konradsson, P.; Udodong, U.; Fraser-Reid, B. Armed and Disarmed N-Pentenyl Glycosides in Saccharide Couplings Leading to Oligosaccharides. *J. Am. Chem. Soc.* **1988**, *110* (16), 5583-5584. DOI: 10.1021/ja00224a060.
- (238) Fraser-Reid, B.; Lopez, J. C. Armed–Disarmed Effects in Carbohydrate Chemistry: History, Synthetic and Mechanistic Studies. In *Reactivity Tuning in Oligosaccharide Assembly*, Fraser-Reid, B., Cristobal Lopez, J. Eds.; Springer Berlin Heidelberg, 2011; pp 1-29.
- (239) Fascione, M. A.; Brabham, R.; Turnbull, W. B. Mechanistic Investigations into the Application of Sulfoxides in Carbohydrate Synthesis. *Chem. Eur. J.* **2016**, *22* (12), 3916-3928. DOI: 10.1002/chem.201503504.
- (240) Frihed, T. G.; Bols, M.; Pedersen, C. M. Mechanisms of Glycosylation Reactions Studied by Low-Temperature Nuclear Magnetic Resonance. *Chem. Rev.* **2015**, *115* (11), 4963-5013. DOI: 10.1021/cr500434x.
- (241) Kahne, D.; Walker, S.; Cheng, Y.; Van Engen, D. Glycosylation of Unreactive Substrates. *J. Am. Chem. Soc.* **1989**, *111* (17), 6881-6882. DOI: 10.1021/ja00199a081.
- (242) Yuasa, H.; Kamata, Y.; Hashimoto, H. Relative Nucleophilicity of the Two Sulfur Atoms in 1,5-Dithioglucopyranoside. *Angew. Chem. Int. Ed.* **1997**, *36* (8), 868-870. DOI: 10.1002/anie.199708681.
- (243) Crich, D.; Mataka, J.; Zakharov, L. N.; Rheingold, A. L.; Wink, D. J. Stereoselective Formation of Glycosyl Sulfoxides and Their Subsequent Equilibration: Ring Inversion of an A-Xylopyranosyl Sulfoxide Dependent on the Configuration at Sulfur. *J. Am. Chem. Soc.* **2002**, *124* (21), 6028-6036. DOI: 10.1021/ja0122694.
- (244) Shafizadeh, F.; Furneaux, R. H.; Stevenson, T. T. Some Reactions of Levoglucosenone. *Carbohydr. Res.* **1979**, *71* (1), 169-191. DOI: 10.1016/S0008-6215(00)86069-3.
- (245) Koll, P.; Steinweg, E.; Meyer, B.; Metzger, J. Darstellung Ungesättigter Kohlenhydrate Durch Esterpyrolyse, II. Thermische Cis-Eliminierungen Aus Vollständig Acetylierten Aldopyranosen. *Liebigs Ann. Chem.* **1982**, *1982* (6), 1039-1051. DOI: 10.1002/jlac.198219820605.
- (246) Polakova, M.; Sestak, S.; Lattova, E.; Petrus, L.; Mucha, J.; Tvaroska, I.; Konaa, J. A-D-Mannose Derivatives as Models Designed for Selective Inhibition of Golgi A-Mannosidase II. *Eur. J. Med. Chem.* **2011**, *46* (3), 944-952. DOI: 10.1016/j.ejmech.2011.01.012.
- (247) Tsui, H. C.; Paquette, L. A. Reversible Charge-Accelerated Oxy-Cope Rearrangements. *J. Org. Chem.* **1998**, *63* (26), 9968-9977, Article. DOI: 10.1021/jo982002w.
- (248) Liao, X.; Yuan, K.; Crich, D. Intramolecular Displacement Reactions Involving Sulfur Leading to the Formation of 3,6-Thiahydro Sugar Derivatives during the Synthesis of 3,5-Dithio-Glucofuranose. *Eur. J. Org. Chem.* **2022**, *2022* (9), e202101496. DOI: 10.1002/ejoc.202101496.
- (249) Bucher, J.; Wurm, T.; Nalivela, K. S.; Rudolph, M.; Rominger, F.; Hashmi, A. S. K. Cyclization of Gold Acetylides: Synthesis of Vinyl Sulfonates via Gold Vinylidene Complexes. *Angew. Chem. Int. Ed.* **2014**, *53* (15), 3854-3858. DOI: 10.1002/anie.201310280.
- (250) Longin, O.; Hezwani, M.; van de Langemheen, H.; Liskamp, R. M. J. Synthetic Antibody Protein Mimics of Infliximab by Molecular Scaffolding on Novel Cyclotrimeratrilene (CTV) Derivatives. *Org. Biomol. Chem.* **2018**, *16* (29), 5254-5274. DOI: 10.1039/C8OB01104D.
- (251) Heller, K.; Ochtrop, P.; Albers, M. F.; Zauner, F. B.; Itzen, A.; Hedberg, C. Covalent Protein Labeling by Enzymatic Phosphocholination. *Angew. Chem. Int. Ed.* **2015**, *54* (35), 10327-10330. DOI: 10.1002/anie.201502618.
- (252) Horrobin, T.; Hao Tran, C.; Crout, D. Esterase-Catalysed Regioselective 6-Deacylation of Hexopyranose Per-Acetates, Acid-Catalysed Rearrangement to the 4-Deprotected Products and Conversions of These into Hexose 4- and 6-Sulfates. *J. Chem. Soc., Perkin Trans. 1* **1998**, (6), 1069-1080. DOI: 10.1039/A708596F.
- (253) Kiefel, M. J.; Beisner, B.; Bennett, S.; Holmes, I. D.; von Itzstein, M. Synthesis and Biological Evaluation of N-Acetylneuraminic Acid-Based Rotavirus Inhibitors. *J. Med. Chem.* **1996**, *39* (6), 1314-1320. DOI: 10.1021/jm950611f.
- (254) Reed, L. A.; Goodman, L. Synthesis of Thiolactose (4-S-b-D-Galactopyranosyl-4-thio-D-glucopyranose). *Carbohydr. Res.* **1981**, *94* (1), 91-100. DOI: 10.1016/S0008-6215(00)85599-8.

- (255) Wang, Y. C.; Du, Y. G. Synthesis of 5-Thio-D-galactopyranose. *J. Carbohydr. Chem.* **2013**, *32* (4), 240-248, Article. DOI: 10.1080/07328303.2013.800086.
- (256) Yuasa, H.; Takenaka, A.; Hashimoto, H. Stereoselectivity in the Oxidation of 5-Thiogluucose Derivatives with 3-Chloroperoxybenzoic Acid. *Bull. Chem. Soc. Jpn.* **2006**, *63* (12), 3473-3479. DOI: 10.1246/bcsj.63.3473 (accessed 3/14/2024).
- (257) Ohta, A.; Sawamoto, D.; Jayasundera, K. P.; Kinoshita, H.; Inomata, K. Efficient Synthesis of b- and C-Rings Components of Phycobilin Derivatives for Structure/Function Analysis of Phytochrome. *Chem. Lett.* **2003**, *29* (5), 492-493. DOI: 10.1246/cl.2000.492 (accessed 5/22/2024).
- (258) Yimthachote, S.; Phomphrai, K. Rapid Alcoholysis of Cyclic Esters Using Metal Alkoxides: Access to Linear Lactyllactate-Grafted Polyglycidol. *New J. Chem.* **2023**, *47* (6), 2701-2705. DOI: 10.1039/D2NJ05564C.
- (259) Barrell, M. J.; Campaña, A. G.; von Delius, M.; Geertsema, E. M.; Leigh, D. A. Light-Driven Transport of a Molecular Walker in Either Direction Along a Molecular Track. *Angew. Chem. Int. Ed.* **2011**, *50* (1), 285-290. DOI: 10.1002/anie.201004779.
- (260) Cox, J. M.; Owen, L. N. Cyclic Hemithioacetals: Analogues of Thiosugars with Sulphur in the Ring. *J. Chem. Soc. C* **1967**, (0), 1130-1134. DOI: 10.1039/J39670001130.
- (261) Gu, X.; Li, X.; Chai, Y.; Yang, Q.; Li, P.; Yao, Y. A Simple Metal-Free Catalytic Sulfoxidation under Visible Light and Air. *Green Chem.* **2013**, *15* (2), 357-361. DOI: 10.1039/C2GC36683E.
- (262) Dupuy, C.; Crozet, M.-P.; Surzur, J.-M. Heterocyclisation Radicalaire De Thiols Acetyleniques. *Bull. Soc. Chim. Fr.* **1980**, *2* (7), 361-373.
- (263) Sanhueza, C. A.; Arias, A. C.; Dorta, R. L.; Vazquez, J. T. Absolute Configuration of Glycosyl Sulfoxides. *Tetrahedron: Asymmetry* **2010**, *21* (15), 1830-1832. DOI: 10.1016/j.tetasy.2010.06.019.
- (264) Sanhueza, C. A.; Dorta, R. L.; Vázquez, J. T. Stereochemical Properties of Glucosyl Sulfoxides in Solution. *J. Org. Chem.* **2011**, *76* (19), 7769-7780. DOI: 10.1021/jo201130x.
- (265) Neumaier, J. M.; Madani, A.; Klein, T.; Ziegler, T. Low-Budget 3D-Printed Equipment for Continuous Flow Reactions. *Beilstein J. Org. Chem.* **2019**, *15*, 558-566. DOI: 10.3762/bjoc.15.50.
- (266) Bowden, T.; Garegg, P. J.; Maloisel, J.-L.; Konradsson, P. A Mechanistic Study: Nucleophile Dependence in Glucosylations with Glucosyl Bromides. *Isr. J. Chem.* **2000**, *40* (3-4), 271-277. DOI: 10.1560/P2J6-2MN2-0WHQ-R3BF.
- (267) Xu, G.; Moeller, K. D. Anodic Coupling Reactions and the Synthesis of C-Glycosides. *Org. Lett.* **2010**, *12* (11), 2590-2593. DOI: 10.1021/ol100800u.
- (268) Addanki, R. B.; Moktan, S.; Halder, S.; Sharma, M.; Sarmah, B. K.; Bhattacharyya, K.; Kancharla, P. K. Exploiting the Strained Ion-Pair Interactions of Sterically Hindered Pyridinium Salts toward SN2 Glycosylation of Glycosyl Trichloroacetimidates. *J. Org. Chem.* **2024**, *89* (6), 3713-3725. DOI: 10.1021/acs.joc.3c02207.

APPENDIX

Table 8. Search output data after Privateer and PyMOL analyses. Highlighted targeted examples

Protein ID	Type Of Protein	Name of ligand	PDB #	Amino Acid	Interacting O atom/distance	
					Glycosidic	Endocyclic
Lectin EW29Ch	Lectin	N-acetyl- α -neuraminic acid-(2-6)- β -D-galactopyranose-(1-4)- β -D-glucopyranose	2DS0	Trp	3.9	n/a
Fucoatlectin-Related Protein	Hydrolase	α -L-fucopyranose-(1-2)-[2-acetamido-2-deoxy- α -D-galactopyranose-(1-3)] β -D-galactopyranose	2WMI	Trp, His	n/a	3.4 (Trp), 3.4 (His)
Lacto- <i>N</i> -Biose Phosphorylase	Transferase	2-acetamido-2-deoxy- α -D-galactopyranose	2ZUT	Phe	n/a	4.1
Jacalin-Me- α -T-Antigen	Lectin	β -D-galactopyranose-(1-3)-methyl 2-acetamido-2-deoxy- α -D-galactopyranoside	1UGX	Tyr	n/a	4.4 and 4.3
Galacto- <i>N</i> -Biose/Lacto- <i>N</i> -Biose I Phosphorylase	Transferase	2-acetamido-2-deoxy- α -D-glucopyranose	2ZUV	Phe	n/a	3.5
Hglcat-P	Transferase	β -D-galactopyranose-(1-4)-2-acetamido-2-deoxy- α -D-glucopyranose	1V84	Phe	n/a	4.03
Humanized Fab Fragment (Hu3s193)	Immune System	α -L-fucopyranose-(1-2)- β -D-galactopyranose-(1-4)-[α -L-fucopyranose-(1-3)]2-acetamido-2-deoxy- α -D-glucopyranose	1S3K	Phe, Tyr	n/a	3.8 (Phe), 3.7 (Tyr)
Ralstonia Solanacearum	Lectin	methyl α -L-fucopyranoside	2BT9	Trp	4.6	n/a

Norovirus Funabashi258 P Domain	Viral Protein	α -L-fucopyranose-(1-2)- β -D-galactopyranose-(1-3)-2-acetamido-2-deoxy- β -D-glucopyranose	3ASQ	Trp	n/a	3.5
Norovirus Funabashi258 P Domain	Viral Protein	α -L-fucopyranose-(1-2)- β -D-galactopyranose-(1-3)-[α -L-fucopyranose-(1-4)]2-acetamido-2-deoxy- β -D-glucopyranose	3ASS	Trp	n/a	3.5
Erythrina Cristagalli Lectin	Lectin	α -L-fucopyranose-(1-2)- β -D-galactopyranose-(1-4)- β -D-glucopyranose	1GZ9	Tyr	n/a	4.1
Gtb C80s/C196s/C209s	Transferase	α -L-fucopyranose-(1-2)-hexyl β -D-galactopyranoside	3I0J	His	n/a	3.9
Marasmius Oreades Mushroom Lectin	Lectin	α -L-fucopyranose-(1-2)-[α -D-galactopyranose-(1-3)] β -D-galactopyranose	3EF2	His	n/a	3.4
Pectin Methylesterase	Hydrolase	methyl α -D-galactopyranuronate-(1-4)-methyl α -D-galactopyranuronate-(1-4)- α -D-galactopyranuronic acid-(1-4)- α -D-galactopyranuronic acid-(1-4)- α -D-galactopyranuronic acid-(1-4)- α -D-galactopyranuronic acid	2NTQ	Trp	n/a	3.3
Pectin Methylesterase	Hydrolase	methyl α -D-galactopyranuronate-(1-4)- α -D-galactopyranuronic acid-(1-4)- α -D-galactopyranuronic acid-(1-4)- α -D-galactopyranuronic acid-(1-4)- α -D-galactopyranuronic acid-	2NTP	Trp	n/a	3.3

		(1-4)- α -D-galactopyranuronic acid				
Pectin Methylesterase	Hydrolase	α -D-galactopyranuronic acid-(1-4)- α -D-galactopyranuronic acid-(1-4)- α -D-galactopyranuronic acid-(1-4)- α -D-galactopyranuronic acid-(1-4)- α -D-galactopyranuronic acid-(1-4)- α -D-galactopyranuronic acid	2NTB	Trp	n/a	3.3
Pectin Methylesterase	Hydrolase	α -D-galactopyranuronic acid-(1-4)- α -D-galactopyranuronic acid-(1-4)- α -D-galactopyranuronic acid-(1-4)- α -D-galactopyranuronic acid-(1-4)- α -D-galactopyranuronic acid-(1-4)- α -D-galactopyranuronic acid	2NT6	Trp	n/a	3.3
Pectin Methylesterase	Hydrolase	α -D-galactopyranuronic acid-(1-4)- α -D-galactopyranuronic acid-(1-4)- α -D-galactopyranuronic acid-(1-4)- α -D-galactopyranuronic acid-(1-4)- α -D-galactopyranuronic acid-(1-4)- α -D-galactopyranuronic acid	2NSP	Trp	n/a	3.2
Periplasmic Oligogalacturonide Binding Protein From Yersinia Enterocolitica	Lectin	α -D-galactopyranuronic acid-(1-4)- α -D-galactopyranuronic acid-	2UVJ	Trp	n/a	3.5

		(1-4)- α -D-galactopyranuronic acid				
Enterotoxin B-Pentamer	Toxin	α -D-galactopyranose	1DJR	Trp	4.2	4.6
Enterotoxin B-Pentamer	Toxin	4-aminophenyl α -D-galactopyranoside	1EFI	Trp	5	n/a
β -Fructosidase From <i>Thermotoga Maritima</i>	Hydrolase	β -D-fructofuranose-(2-1)-[α -D-galactopyranose-(1-6)] α -D-glucopyranose	1W2T	Trp	4.3	n/a
Enterotoxin B-Pentamer	Toxin	4-aminophenyl α -D-galactopyranoside	1EEI	Trp	4.3	n/a
<i>Pyrococcus Horikoshii</i>	Transferase	α -D-galactopyranose	2DEI	Tyr	n/a	3.8
<i>Pyrococcus Horikoshii</i>	Transferase	α -D-galactopyranose	2DEJ	Tyr	n/a	3.7
<i>Pseudomonas Aeruginosa</i> Lectin 1	Lectin	α -D-galactopyranose	1OKO	Tyr, His	n/a	3.7 (Tyr), 3.7 (His)
β -Phosphoglucomutase	Isomerase	1-O-phosphono- α -D-galactopyranose	1Z4O	His	4.1	n/a
Glycoside Hydrolase From <i>Streptococcus Pneumoniae</i> SP3-BS71	Hydrolase	α -L-fucopyranose-(1-2)-[α -D-galactopyranose-(1-3)] β -D-galactopyranose	2WMJ	His	n/a	3.9
β -Phosphoglucomutase	Isomerase	1-O-phosphono- α -D-galactopyranose	1Z4N	His	4	n/a
<i>Clostridium Thermocellum</i> Xyloglucanase	Hydrolase	α -D-xylopyranose-(1-6)- β -D-glucopyranose-(1-4)-[α -D-xylopyranose-(1-6)] β -D-glucopyranose-(1-4)-[β -D-galactopyranose-(1-2)- α -D-xylopyranose-(1-6)] β -D-glucopyranose-(1-4)- α -D-glucopyranose	2CN3	Trp, Tyr	n/a	3.7 (Trp), 3.7 (Tyr)
Xylanase Xyn10B Mutant (E262S) From <i>Cellvibrio Mixtus</i>	Hydrolase	β -D-xylopyranose-(1-4)- β -D-xylopyranose-(1-4)- α -D-xylopyranose	1UQY	Trp, Phe	n/a	4.9 (Trp), 4.9 (Phe)
Xylanase Xyn10B Mutant (E262S) From <i>Cellvibrio Mixtus</i>	Hydrolase	4-O-methyl- α -D-glucopyranuronic acid-(1-2)- β -D-xylopyranose-(1-4)- β -D-xylopyranose-(1-4)- β -D-xylopyranose	1UQZ	Trp, Phe	n/a	4.9 (Trp), 4.9 (Phe)

Xylanase A1 Of Paenibacillus Sp. JDR-2	Hydrolase	4-O-methyl- α -D-glucopyranuronic acid-(1-2)- β -D-xylopyranose-(1-4)- β -D-xylopyranose-(1-4)- α -D-xylopyranose	3RDK	Trp	n/a	4
Galactose Mutarotase From Lactococcus Lactis	Isomerase	α -D-xylopyranose	1MN0	Phe	n/a	3.5
Xeg-Xyloglucan	Hydrolase	β -D-glucopyranose-(1-4)-[α -D-xylopyranose-(1-6)] β -D-glucopyranose-(1-4)-[α -D-xylopyranose-(1-6)] β -D-glucopyranose-(1-4)- β -D-glucopyranose	3VL9	Trp, Tyr	n/a	4.3 (Tyr), 4.3 (Trp)
Paenibacillus Polymyxa Xyloglucanase From GH Family 44	Hydrolase	β -D-glucopyranose-(1-4)-[α -D-xylopyranose-(1-6)] β -D-glucopyranose-(1-4)- β -D-glucopyranose-(1-4)- β -D-glucopyranose	2YIH	His	n/a	4
Calreticulin	Chaperone	α -D-glucopyranose-(1-3)- α -D-mannopyranose-(1-2)- α -D-mannopyranose-(1-2)- α -D-mannopyranose	3O0X	Trp, Phe	n/a	3.5 (Trp), 4.0 (Phe)
Calreticulin	Chaperone	α -D-glucopyranose-(1-3)- α -D-mannopyranose-(1-2)- α -D-mannopyranose-(1-2)- α -D-mannopyranose	3O0W	Trp	n/a	3.6

β -N-Acetylhexosaminidase	Hydrolase	α -D-mannopyranose-(1-2)- α -D-mannopyranose-(1-2)- α -D-mannopyranose-(1-3)- [α -D-mannopyranose-(1-2)- α -D-mannopyranose-(1-6)] α -D-mannopyranose-(1-3)] α -D-mannopyranose-(1-6)] α -D-mannopyranose-(1-4)-2-acetamido-2-deoxy- β -D-glucopyranose-(1-4)-2-acetamido-2-deoxy- β -D-glucopyranose	2YL8	Trp, Tyr	n/a	4 (Trp), 3.9 (Trp)
α -Bungarotoxin	Protein binding	α -D-mannopyranose-(1-2)- α -D-mannopyranose-(1-2)- α -D-mannopyranose-(1-3)- [α -D-mannopyranose-(1-2)- α -D-mannopyranose-(1-6)] α -D-mannopyranose-(1-3)] α -D-mannopyranose-(1-6)] α -D-mannopyranose-(1-4)-2-acetamido-2-deoxy- β -D-glucopyranose-(1-4)-2-acetamido-2-deoxy- β -D-glucopyranose	2QC1	Trp	n/a	4.0
Mannose-Binding Lectin From Morus Nigra	Lectin	α -D-mannopyranose	1XXR	Phe	n/a	4
DC-SIGN Carbohydrate Recognition Domain	Lectin	α -D-mannopyranose-(1-3)- [α -D-mannopyranose-(1-6)] α -D-mannopyranose-(1-6)- α -D-mannopyranose	1SL4	Phe	n/a	3.4
Pterocarpus Angolensis Lectin	Lectin	2-acetamido-2-deoxy- β -D-glucopyranose-(1-2)- α -D-mannopyranose-(1-3)-[2-acetamido-2-deoxy- β -D-glucopyranose-(1-2)- α -D-mannopyranose-(1-6)] α -D-mannopyranose	2AR6	Phe	3.5	n/a

Pterocarpus Angolensis Lectin	Lectin	α -D-mannopyranose-(1-3)- α -D-mannopyranose	2PHX	Phe	3.5	n/a
Pterocarpus Angolensis Seed Lectin	Lectin	β -D-galactopyranose-(1-4)-2-acetamido-2-deoxy- β - D-glucopyranose-(1-2)- α - D-mannopyranose-(1-3)- [2-acetamido-2-deoxy- β - D-glucopyranose-(1-2)- α - D-mannopyranose-(1-6)] β - D-mannopyranose-(1-4)-2- acetamido-2-deoxy- α -D- glucopyranose	2ARX	Phe	3.6	n/a
Human M340h- β -1,4- Galactosyltransferase-I	Transferase	2-acetamido-2-deoxy- β -D- glucopyranose-(1-2)- α -D- mannopyranose-(1-6)- β -D- mannopyranose	2AEC	Tyr	4	n/a
Jacalin	Lectin	methyl α -D- mannopyranoside	1WS5	Tyr	n/a	3.8
Jacalin	Lectin	methyl α -D- mannopyranoside	1KUJ	Tyr	n/a	3.8
Cellvibrio Japonicus Man26A E121A And E320G Double Mutant	Hydrolase	β -D-mannopyranose-(1-4)- α -D-mannopyranose	2WHM	Tyr, Trp	n/a	3.6 (Tyr), 3.6 (Trp)
P. Aeruginosa Pmm/Pgm	Isomerase	1-O-phosphono- α -D- mannopyranose	1PCJ	Tyr	3.5	n/a
Mannan Endo-1,4- β -Mannosidase	Hydrolase	β -D-mannopyranose-(1-4)- α -D-mannopyranose	1ODZ	Tyr, Trp	n/a	3.5 (Tyr), 3.5 (Trp)
Endoglucanase	Hydrolase	β -D-mannopyranose-(1-4)- β -D-mannopyranose-(1-4)- α -D-mannopyranose	3AZS	Tyr	n/a	3.7
Rat Mannose-Binding Protein A	Immune System, Lectin	methyl α -D- mannopyranoside	1KWU	His	3.9	n/a
Bcla Lectin From Burkholderia Cenocepacia	Lectin	methyl α -D- mannopyranoside	2VNV	His	3.6	n/a
α -Amylase	Hydrolase	a-D-Glcp(1-4)-a-D-Glcp (oligosaccharides)	1WO2	Trp	n/a	3.6
G6-Amylase	Hydrolase	a-D-Glcp(1-4)-a-D-Glcp (oligosaccharides)	2D3N	Tyr, Trp	4.2 (Tyr)	4 (Tyr), 3.5 (Trp)

α -Amylase I	Hydrolase	α -D-glucopyranose-(1-4)- α -D-glucopyranose-(1-4)- α -D-glucopyranose-(1-4)- α -D-glucopyranose-(1-4)- α -D-glucopyranose	1UH2	Tyr, Trp	n/a	3.8 (Tyr), 4.3(Trp)
Cyclodextrin Glycosyltransferase	Transferase	α -D-glucopyranose-(1-4)- α -D-glucopyranose	1D3C	Phe	n/a	4.1
Amylomaltase	Transferase	4,6-dideoxy-4- ([(1S,4R,5S,6S)-4,5,6- trihydroxy-3- (hydroxymethyl)cyclohex- 2-en-1-yl]amino)- α -D- glucopyranose-(1-4)- α -D- glucopyranose-(1-4)- α -D- glucopyranose	1ESW	Tyr, Trp	n/a	4 (Tyr), 4 (Trp)
Maltose ABC Transporter, Periplasmic Maltose-Binding Protein	Lectin	α -D-glucopyranose-(1-4)- α -D-glucopyranose-(1-4)- α -D-glucopyranose	2FNC	Tyr, Trp	n/a	4.0 (Trp), 4.2 (Tyr)
Ullulanase	Hydrolase	α -D-glucopyranose-(1-4)- α -D-glucopyranose-(1-4)- α -D-glucopyranose	2FHC	Tyr, Trp	n/a	4.5 (Tyr), 4.5 (Trp)
Trehalose/Maltose Binding Protein	Lectin	α -D-glucopyranose-(1-1)- α -D-glucopyranose	1EU8	Trp	n/a	3.5
β -Amylase	Hydrolase	α -D-glucopyranose-(1-4)- α -D-glucopyranose/ α -D- glucopyranose-(1-4)- β -D- glucopyranose	1Q6E	Trp	n/a	3.9
β -Amylase	Hydrolase	α -D-glucopyranose-(1-4)- α -D-glucopyranose/ α -D- glucopyranose-(1-4)- β -D- glucopyranose	1Q6G	Trp	n/a	3.9
Maltodextrin-Binding Protein	Transport Protein	α -D-glucopyranose-(1-4)- α -D-glucopyranose	1JYV	Trp	n/a	3.9
Maltose-Maltodextrin Binding Protein	Lectin	α -D-glucopyranose-(1-4)- α -D-glucopyranose-(1-4)- α -D-glucopyranose	1URD	Trp, Tyr	n/a	4.5 (Tyr), 4.2 (Trp)

Maltose-Maltodextrin Binding Protein	Lectin	α -D-glucopyranose-(1-4)- α -D-glucopyranose-(1-4)- α -D-glucopyranose	1URS	Trp, Tyr	n/a	4.3 (Trp), 4.3 (Tyr)
Maltose Abc Transporter, Periplasmic Maltose-Binding Protein	Lectin	α -D-glucopyranose-(1-4)- α -D-glucopyranose-(1-4)- α -D-glucopyranose	2GHA	Tyr	n/a	4.1
Pullulanase	Hydrolase	α -D-glucopyranose-(1-6)- α -D-glucopyranose-(1-4)- α -D-glucopyranose-(1-4)- α -D-glucopyranose	2J73	Trp	n/a	3.5
Cyclomaltodextrin Glucanotransferase	Transferase	α -D-glucopyranose-(1-4)- α -D-glucopyranose	3BMW	Trp	n/a	3.5
Fusion Protein Of Maltose-Binding Periplasmic Protein And Parathyroid Hormone/Parathyroid Hormone- Related Peptide Receptor	Membrane Protein	α -D-glucopyranose-(1-4)- α -D-glucopyranose	3C4M	Tyr, Trp	n/a	4.3 (Tyr), 4.3 (Trp)
Maltose-Binding Periplasmic Protein, Islet Amyloid Polypeptide Fusion Protein	Lectin	α -D-glucopyranose-(1-4)- α -D-glucopyranose	3G7V	Trp	n/a	3.9
Fusion Protein Of Maltose-Binding Periplasmic Protein And Pituitary Adenylate Cyclase 1 Receptor-Short	Membrane Receptor	α -D-glucopyranose-(1-4)- α -D-glucopyranose	3N94	Trp	n/a	4.2
Maltose-Binding Periplasmic Protein, Advanced Glycosylation End Product- Specific Receptor	Transport Protein/ Signaling Protein	α -D-glucopyranose-(1-4)- α -D-glucopyranose-(1-4)- α -D-glucopyranose	3O3U	Trp	n/a	4
Maltose-Binding Periplasmic Protein,Green Fluorescent Protein	Fluorescent Protein/ Transport Protein	α -D-glucopyranose-(1-4)- α -D-glucopyranose	3OSR	Tyr, Trp	n/a	4.1 (Tyr), 4.1 (Trp)
Maltose-Binding Periplasmic Protein	Lectin	α -D-glucopyranose-(1-4)- α -D-glucopyranose	3SEW	Trp	n/a	4
Maltose-Binding Periplasmic Protein	Lectin	α -D-glucopyranose-(1-4)- α -D-glucopyranose	3SEX	Trp	n/a	4.1
Maltose-Binding Periplasmic Protein	Lectin	α -D-glucopyranose-(1-4)- α -D-glucopyranose	3SEY	Trp	n/a	4.2
Fusion Protein Of Crfr1 Extracellular Domain And Mbp	Membrane Protein	α -D-glucopyranose-(1-4)- α -D-glucopyranose	3EHU	Trp	4.3	n/a
Glycosyl Hydrolase Family 71	Hydrolase	α -D-glucopyranose	4AD5	Trp	4.1	n/a

β -Amylase	Hydrolase	α -D-glucopyranose-(1-4)- α -D-glucopyranose	1V3I	Trp	n/a	3.6
β -Amylase	Hydrolase	α -D-glucopyranose-(1-4)- α -D-glucopyranose	1V3H	Trp	n/a	3.9
Glucosamine-6-Phosphate Isomerase	Hydrolase	α -D-glucopyranose-(1-1)- α -D-glucopyranose	1NE7	Phe	n/a	3.2
Galactose Mutarotase	Isomerase	α -D-glucopyranose	1NSZ	Trp	n/a	4.2
Maltose/Maltodextrin-Binding Protein	Lectin	α -D-glucopyranose-(1-4)- α -D-glucopyranose-(1-4)- α -D-glucopyranose	2GH9	Phe	4	n/a
α -Glucosidase	Hydrolase	α -D-glucopyranose-(1-4)- α -D-glucopyranose	1OBB	Phe	n/a	5
Cyclomaltodextrin Glucanotransferase	Transferase	α -D-glucopyranose-(1-4)- α -D-glucopyranose-(1-4)- α -D-glucopyranose-(1-4)- β -D-glucopyranose	1OT1	Tyr	3.9	n/a
Maltose Binding Protein Fused With Designed Helical Protein	De Novo Protein	α -D-glucopyranose-(1-4)- α -D-glucopyranose	1Y4C	Tyr	n/a	4
Maltodextrin Phosphorylase	Transferase	α -D-glucopyranose-(1-4)- α -D-glucopyranose-(1-4)- α -D-glucopyranose-(1-4)- α -D-glucopyranose	1L5W	Tyr	n/a	3.9
Maltodextrin Phosphorylase	Transferase	α -D-glucopyranose-(1-4)- α -D-glucopyranose-(1-4)- α -D-glucopyranose-(1-4)- α -D-glucopyranose-(1-4)- β -D-glucopyranose	2AV6	Tyr	n/a	3.6
Maltose-Binding Periplasmic Protein, Dna Mismatch Repair Protein Muts Fusion Protein	Lectin	α -D-glucopyranose-(1-4)- α -D-glucopyranose	2OK2	Tyr	n/a	4.1
Maltose-Binding Periplasmic Protein	Lectin	α -D-glucopyranose-(1-4)- α -D-glucopyranose	3SES	Tyr	n/a	4.1
Maltose-Binding Periplasmic Protein	Lectin	α -D-glucopyranose-(1-4)- α -D-glucopyranose	3SET	Tyr	n/a	4.3
Cyclomaltodextrin Glucanotransferase	Transferase	α -D-glucopyranose-(1-4)- α -D-glucopyranose	1PJ9	Tyr	n/a	3.9

Maltose-Binding Periplasmic Protein, LINKER, SAGA-Associated Factor 29	Histone Binding Protein	α -D-glucopyranose-(1-4)- α -D-glucopyranose	3MP8	Tyr	n/a	4.2
Cyclodextrin Glycosyltransferase	Transferase	α -D-glucopyranose-(1-4)- α -D-glucopyranose-(1-4)- β -D-glucopyranose	1KCL	Tyr	n/a	3.8
Putative Cellulase Cel6	Hydrolase	β -D-glucopyranose-(1-4)- β -D-glucopyranose-(1-4)-4-thio- β -D-glucopyranose-(1-4)-methyl β -D-glucopyranoside	1UP3	Trp	n/a	4.3
Endoglucanase F	Hydrolase	4-thio- β -D-glucopyranose-(1-4)- β -D-glucopyranose-(1-4)-4-thio- β -D-glucopyranose-(1-4)- β -D-glucopyranose-(1-4)-4-thio- β -D-glucopyranose-(1-4)- β -D-glucopyranose-(1-4)-4-thio- β -D-glucopyranose-(1-4)- β -D-glucopyranose-(1-4)-4-thio- β -D-glucopyranose	2QNO	Trp	4.4	n/a
β -Galactosidase	Hydrolase	1-methylethyl 1-thio- β -D-galactopyranoside	1JYX	Trp	see Table 9	4.5
Galacto- <i>N</i> -Biose/Lacto- <i>N</i> -Biose I Transporter Substrate-Binding Protein	Lectin	β -D-galactopyranose-(1-3)-2-acetamido-2-deoxy- β -D-galactopyranose	2Z8E	Trp	n/a	4.4
Cellvibrio Japonicus Mannanase Cjman26c	Hydrolase	β -D-mannopyranose-(1-4)- β -D-mannopyranose	2VX7	Trp, Tyr	n/a	4.2 (Trp), 5.0 (Tyr)
S-Layer Associated Multidomain Endoglucanase	Hydrolase	β -D-mannopyranose-(1-4)- β -D-mannopyranose-(1-4)- β -D-mannopyranose-(1-4)- β -D-mannopyranose-(1-4)- α -D-mannopyranose	3OEB	Trp	n/a	4.2
Cellvibrio Japonicus Mannanase Cjman26c	Hydrolase	β -D-mannopyranose	2VX5	Trp	n/a	4.1
Cellvibrio Japonicus Mannanase Cjman26c	Hydrolase	β -D-mannopyranose-(1-4)-[α -D-galactopyranose-(1-	2VX6	Trp	5	n/a

		6)] β -D-mannopyranose-(1-4)- β -D-mannopyranose-(1-4)- β -D-mannopyranose				
Non-Catalytic Protein 1	Lectin	β -D-mannopyranose-(1-4)- β -D-mannopyranose-(1-4)- β -D-mannopyranose-(1-4)- β -D-mannopyranose-(1-4)- β -D-mannopyranose	1GWL	Trp, Tyr	4.1 (Trp), 4.1 (Tyr)	n/a
Non Catalytic Protein 1	Lectin	β -D-mannopyranose-(1-4)- β -D-mannopyranose-(1-4)- β -D-mannopyranose-(1-4)- β -D-mannopyranose-(1-4)- β -D-mannopyranose	1W8U	Trp, Tyr	4.2 (Trp), 4.2 (Tyr)	n/a
Putative Isomerase	Isomerase	β -D-mannopyranose	2ZBL	His	n/a	3.5
Agglutinin Isolectin Vi	Plant Protein	2-acetamido-2-deoxy- β -D-glucopyranose-(1-4)-2-acetamido-2-deoxy- β -D-glucopyranose-(1-4)-2-acetamido-2-deoxy- β -D-glucopyranose	1EHH	Trp	n/a	3.9
Chitinase B	Hydrolase	2-acetamido-2-deoxy- β -D-glucopyranose-(1-4)-2-acetamido-2-deoxy- β -D-glucopyranose	1E6Z	Trp	4.5	n/a
Hevamine A	Hydrolase	2-acetamido-2-deoxy- β -D-glucopyranose-(1-4)-2-acetamido-2-deoxy- β -D-glucopyranose-(1-4)-2-acetamido-2-deoxy- β -D-glucopyranose-(1-4)-2-acetamido-2-deoxy- β -D-glucopyranose-(1-4)-2-acetamido-2-deoxy- β -D-glucopyranose	1KQY	Trp	3.9	3.7
Hevamine A	Hydrolase	2-acetamido-2-deoxy- β -D-glucopyranose-(1-4)-2-acetamido-2-deoxy- β -D-	1KQZ	Trp	3.9	3.7

		glucopyranose-(1-4)-2-acetamido-2-deoxy- β -D-glucopyranose-(1-4)-2-acetamido-2-deoxy- β -D-glucopyranose				
Chitinase A	Hydrolase	2-acetamido-2-deoxy- β -D-glucopyranose-(1-4)-2-acetamido-2-deoxy- β -D-glucopyranose	3N13	Trp	3.7	4.7
Chitinase A	Hydrolase	2-acetamido-2-deoxy- β -D-glucopyranose-(1-4)-2-acetamido-2-deoxy- β -D-glucopyranose	3N15	Trp	3.7	4.7
Chitinase A	Hydrolase	2-acetamido-2-deoxy- β -D-glucopyranose-(1-4)-2-acetamido-2-deoxy- β -D-glucopyranose-(1-4)-2-acetamido-2-deoxy- β -D-glucopyranose	3B9D	Trp	4.5	n/a
Lysozyme	Hydrolase	2-acetamido-2-deoxy- β -D-glucopyranose-(1-4)-2-acetamido-2-deoxy- β -D-glucopyranose-(1-4)-2-acetamido-2-deoxy- β -D-glucopyranose	1JEF	Trp	4.2	n/a
Hevamine A	Hydrolase	2-acetamido-2-deoxy- β -D-glucopyranose-(1-4)-2-acetamido-2-deoxy- β -D-glucopyranose-(1-4)-2-acetamido-2-deoxy- β -D-glucopyranose	1KR0	Trp	4	n/a
Hevamine A	Hydrolase	2-acetamido-2-deoxy- β -D-glucopyranose-(1-4)-2-acetamido-2-deoxy- β -D-glucopyranose-(1-4)-2-	1KR1	Trp	4.1	n/a

		acetamido-2-deoxy- β -D-glucopyranose-(1-4)-2-acetamido-2-deoxy- β -D-glucopyranose				
β -1,4-Galactosyltransferase 1	Transferase	2-acetamido-2-deoxy- β -D-glucopyranose-(1-3)-[2-acetamido-2-deoxy- β -D-glucopyranose-(1-6)] β -D-galactopyranose-(1-4)- β -D-glucopyranose	4EE4	Trp	n/a	3.9
β -N-Acetylhexosaminidase	Hydrolase	2-acetamido-2-deoxy- β -D-glucopyranose	1M04	Trp	n/a	3.6
Mannan-Binding Lectin	Lectin	α -D-mannopyranose-(1-3)-[α -D-mannopyranose-(1-6)] β -D-mannopyranose-(1-4)-2-acetamido-2-deoxy- β -D-glucopyranose-(1-4)-2-acetamido-2-deoxy- β -D-glucopyranose	1ZHS	Trp	n/a	3.5
F17g Adhesin Subunit	Cell Adhesion	2-acetamido-2-deoxy- β -D-glucopyranose	1ZK5	Trp	n/a	4
F17a-G Adhesin	Lectin	2-acetamido-2-deoxy- β -D-glucopyranose	2BSC	Trp	n/a	3.9
α -Lactalbumin/ β -1,4-Galactosyltransferase	Transferase	2-acetamido-2-deoxy- β -D-glucopyranose	1NQI	Phe	n/a	3.7
Chitobiose Phosphorylase	Transferase	2-acetamido-2-deoxy- β -D-glucopyranose	1V7W	Phe	n/a	3.6
Tailspike Protein Hk620	Viral Protein	α -L-rhamnopyranose-(1-6)- α -D-glucopyranose-(1-4)-[2-acetamido-2-deoxy- β -D-glucopyranose-(1-3)] α -D-galactopyranose-(1-3)-[α -D-glucopyranose-(1-6)]2-acetamido-2-deoxy- β -D-glucopyranose	2X85	Tyr	n/a	3.8
Tail Spike Protein	Viral Protein	α -L-rhamnopyranose-(1-6)- α -D-glucopyranose-(1-4)-[2-acetamido-2-deoxy-	2X6Y	Tyr	n/a	3.9

		β -D-glucopyranose-(1-3)] α -D-galactopyranose-(1-3)-[α -D-glucopyranose-(1-6)]2-acetamido-2-deoxy- β -D-glucopyranose				
Galectin-9	Lectin	β -D-galactopyranose-(1-4)-2-acetamido-2-deoxy- β -D-glucopyranose-(1-3)- β -D-galactopyranose-(1-4)-2-acetamido-2-deoxy- β -D-glucopyranose	2ZHL	His	n/a	3.8
Galectin-9	Lectin	β -D-galactopyranose-(1-4)-2-acetamido-2-deoxy- β -D-glucopyranose-(1-3)- β -D-galactopyranose-(1-4)-2-acetamido-2-deoxy- β -D-glucopyranose	2ZHK	His	n/a	3.8
Galectin-8	Lectin	α -L-fucopyranose-(1-3)-[β -D-galactopyranose-(1-4)]2-acetamido-2-deoxy- β -D-glucopyranose-(1-3)- β -D-galactopyranose-(1-4)- β -D-glucopyranose	3AP9	His	n/a	3.6
Galactosylgalactosylxylosylprotein 3- β -Glucuronosyltransferase 3	Transferase	β -D-galactopyranose-(1-3)- β -D-galactopyranose	3CU0	Trp	n/a	4.5
Uncharacterized Protein Ygjk	Hydrolase	α -D-galactopyranose	3W7U	Trp	n/a	3.7
Histo-Blood Group Abo System Transferase	Transferase	α -L-fucopyranose-(1-2)-hexyl β -D-galactopyranoside	1WT1	Phe	n/a	3.2
Agglutinin α Chain	Lectin	β -D-galactopyranose	1UGW	Tyr	n/a	3.7 and 4.7
Boletus Edulis Lectin	Lectin	β -D-galactopyranose-(1-3)-2-acetamido-2-deoxy- α -D-galactopyranose	3QDT	Tyr	n/a	3.7
Agglutinin α Chain	Lectin	β -D-galactopyranose-(1-3)-2-acetamido-2-deoxy- β -D-galactopyranose	3LLZ	Tyr	n/a	3.5

Glycosyltransferase A	Transferase	α -L-fucopyranose-(1-2)-hexyl β -D-galactopyranoside	1LZI	Phe	n/a	3.2
Glycosyltransferase A	Transferase	α -L-fucopyranose-(1-2)-hexyl β -D-galactopyranoside	1LZJ	Phe	n/a	3.2
Abo Blood Group (Transferase A, A 1- 3- <i>N</i> -Acetylgalactosaminyltransferase; Transferase B, α -1-3- Galactosyltransferase)	Transferase	β -D-galactopyranose	1ZIZ	His	n/a	3.4
Abo Blood Group (Transferase A, A 1- 3- <i>N</i> -Acetylgalactosaminyltransferase; Transferase B, α -1-3- Galactosyltransferase)	Transferase	β -D-galactopyranose-(1-4)-2-acetamido-2-deoxy- α -D-glucopyranose	1ZJ1	His	n/a	3.9
Botulinum Neurotoxin A Heavy Chain	Hydrolase	N-acetyl- α -neuraminic acid-(2-3)- β -D-galactopyranose-(1-3)-2-acetamido-2-deoxy- β -D-galactopyranose-(1-4)-[N-acetyl- α -neuraminic acid-(2-3)] β -D-galactopyranose-(1-4)- β -D-glucopyranose	2VU9	His, Trp	n/a	3.4 (His), 5 (Trp)
Abo Glycosyltransferase	Transferase	α -L-fucopyranose-(1-2)-hexyl β -D-galactopyranoside	3I0E	His, Phe	n/a	3.2 (His), 3.8 (Phe)
Bont/F	Toxin	N-acetyl- α -neuraminic acid-(2-3)- β -D-galactopyranose-(1-3)-2-acetamido-2-deoxy- β -D-galactopyranose-(1-4)-[N-acetyl- α -neuraminic acid-(2-3)] β -D-galactopyranose	3RSJ	His, Trp	3.5 (His)	4.7 (Trp)
Histo-Blood Group Abo System Transferase	Transferase	β -D-galactopyranose	3SX3	His, Trp	n/a	3.6 (His), 4.4 (Trp)

Histo-Blood Group Abo System Transferase	Transferase	β -D-galactopyranose	3SX5	His, Trp	n/a	3.7 (His), 4.4 (Trp)
Histo-Blood Group Abo System Transferase	Transferase	β -D-galactopyranose	3SX7	His, Trp	n/a	3.6 (His), 4.4 (Trp)
Histo-Blood Group Abo System Transferase	Transferase	β -D-galactopyranose	3SX8	His, Trp	n/a	3.7 (His), 4.1 (Trp)
Histo-Blood Group Abo System Transferase	Transferase	β -D-galactopyranose	3SXA	His, Trp	n/a	3.5 (His), 4.2 (Trp)
Histo-Blood Group Abo System Transferase	Transferase	β -D-galactopyranose	3SXC	His, Trp	n/a	3.7 (His), 4.4 (Trp)
Histo-Blood Group Abo System Transferase	Transferase	β -D-galactopyranose	3SXD	His, Trp	n/a	3.6 (His), 4.3 (Trp)
Histo-Blood Group Abo System Transferase	Transferase	β -D-galactopyranose	3SXE	His, Trp	n/a	3.7 (His), 4.5 (Trp)
Histo-Blood Group Abo System Transferase	Transferase	β -D-galactopyranose	3SXG	His, Trp	n/a	3.7 (His), 4.4 (Trp)
Pa-I Galactophilic Lectin	Lectin	4-nitrophenyl β -D-galactopyranoside	3ZYF	His, Tyr	n/a	3.7 (His), 3.7 (Tyr)
Galectin-1	Lectin	β -D-galactopyranose-(1-4)- β -D-glucopyranose	1GZW	His	3.8	n/a
β -Galactosidase	Hydrolase	4-nitrophenyl β -D-galactopyranoside	1JYW	His, Trp	3.8 (His)	4.5 (Trp)
Galectin-1	Lectin	β -D-galactopyranose-(1-4)- β -D-glucopyranose	1W6O	His	3.9	n/a
β -1,4-Xylanase	Hydrolase	β -D-xylopyranose	1FH8	Trp	4.6	n/a
Xylanase	Hydrolase	4-O-methyl- α -D-glucopyranuronic acid-(1-2)-[β -D-xylopyranose-(1-4)] β -D-xylopyranose-(1-4)- β -D-xylopyranose	2Y24	Trp, Tyr	4.3 (Trp)	4.4 (Tyr)
Endo-1,4- β -Xylanase A	Hydrolase	β -D-xylopyranose-(1-4)-2-deoxy-2-fluoro- α -D-xylopyranose	1E0X	Trp	4.6	n/a
β -1,4-Xylanase	Hydrolase	β -D-xylopyranose	1FH7	Trp	4.6	n/a
β -1,4-Xylanase	Hydrolase	β -D-xylopyranose	1FH9	Trp	4.5	n/a
β -1,4-Xylanase	Hydrolase	β -D-xylopyranose	1FHD	Trp	4.6	n/a
Endo-1,4- β -Xylanase A	Hydrolase	β -D-xylopyranose	1V0K	Trp	4.5	n/a

Endo-1,4- β -Xylanase A	Hydrolase	β -D-xylopyranose	1V0M	Trp	4.5	n/a
Endo-1,4- β -Xylanase A	Hydrolase	β -D-xylopyranose	1V0N	Trp	4.6	n/a
β -1,4-Glycanase	Hydrolase	β -D-xylopyranose-(1-4)-2-deoxy-2-fluoro- α -D-xylopyranose	2XYL	Trp	4.4	n/a
Xylanase U	Lectin	β -D-xylopyranose-(1-4)- β -D-xylopyranose-(1-4)- β -D-xylopyranose-(1-4)- β -D-xylopyranose-(1-4)- β -D-xylopyranose	1UXX	Trp, Tyr	n/a	4.8 (Tyr), 4.8 (Trp)
Endo-1,4- β -Xylanase	Hydrolase	β -D-xylopyranose-(1-4)-1,5-anhydro-2-deoxy-2-fluoro-D-xylitol	1C5I	Trp	3.5	4.4
Endo-1,4- β -Xylanase A	Hydrolase	β -D-xylopyranose	1V0L	Trp	3.8	n/a
Xylanase	Hydrolase	β -D-xylopyranose-(1-4)- β -D-xylopyranose-(1-4)- β -D-xylopyranose-(1-4)- β -D-xylopyranose-(1-4)- β -D-xylopyranose	2Y64	Phe	n/a	4.7
Endo-1,4- β -Xylanase	Hydrolase	β -D-xylopyranose-(1-4)- β -D-xylopyranose-(1-4)- β -D-xylopyranose-(1-4)- β -D-xylopyranose	3C7G	Trp, Phe	4.2 (Phe)	4.5 (Trp)
Endo-1,4- β -Xylanase	Hydrolase	β -D-xylopyranose-(1-4)- β -D-xylopyranose-(1-4)- β -D-xylopyranose-(1-4)- β -D-xylopyranose	3C7F	Trp, Phe	3.8 (Phe)	4.5 (Trp)
Enxyn11a	Hydrolase	β -D-xylopyranose-(1-4)- β -D-xylopyranose-(1-4)- β -D-xylopyranose	2VGD	Trp, Tyr	n/a	4.3 (Trp), 3.9 (Tyr)
Endo- β -1,4-Xylanase	Hydrolase	β -D-xylopyranose-(1-4)- β -D-xylopyranose-(1-4)- β -D-xylopyranose-(1-4)- β -D-xylopyranose	1US2	Trp	4.7	n/a
Endo-1,4- β -Xylanase	Hydrolase	β -D-xylopyranose-(1-4)- β -D-xylopyranose-(1-4)- β -D-xylopyranose-(1-4)- β -D-xylopyranose	2B4F	Trp, Phe, Tyr	n/a	4.4 (Phe), 4.5 (Tyr), 4.3 (Trp)

		xylopyranose-(1-4)- β -D-xylopyranose				
Endo-1,4- β -Glucanase F	Hydrolase	β -D-glucopyranose-(1-4)- β -D-glucopyranose-(1-4)- β -D-glucopyranose-(1-4)- β -D-glucopyranose-(1-4)- β -D-glucopyranose	1FBW	Trp, Tyr	3.5 (Trp), 4.1 (Tyr)	4.1 (Trp)
Cellobiohydrolase II	Hydrolase	β -D-glucopyranose	1OCN	Trp	4.3	n/a
Non-Catalytic Protein 1	Lectin	β -D-glucopyranose-(1-4)- β -D-glucopyranose-(1-4)- β -D-glucopyranose-(1-4)- β -D-glucopyranose-(1-4)- β -D-glucopyranose-(1-4)- α -D-glucopyranose	1OH3	Trp	n/a	3.9
Cela1 Protein	Hydrolase	β -D-glucopyranose	1UP2	Trp	n/a	4.1
Endoglucanase E-2	Hydrolase	β -D-glucopyranose-(1-4)- β -D-glucopyranose-(1-4)- β -D-glucopyranose-(1-4)- β -D-glucopyranose	2BOF	Trp	3.6	4.8
Oligopeptide ABC Transporter, Periplasmic Oligopeptide-Binding Protein	Lectin	β -D-glucopyranose-(1-4)- β -D-glucopyranose	2O7I	Trp	n/a	4.8
T. Fusca Endo/Exo-Cellulase E4 Catalytic Domain and Cellulose- Binding Domain	Hydrolase	β -D-glucopyranose-(1-4)- β -D-glucopyranose-(1-4)- β -D-glucopyranose-(1-4)- α -D-glucopyranose	4TF4	Trp, Tyr, His	4.5 (His), 4.3 (Tyr), 4.4 (Trp)	4.4 (Trp)
1,4- β -D-Glucan Cellobiohydrolase I	Hydrolase	β -D-glucopyranose-(1-4)- β -D-glucopyranose-(1-4)- β -D-glucopyranose-(1-4)- β -D-glucopyranose	5CEL	Trp	4.1	4.4
1,4- β -D-Glucan Cellobiohydrolase I	Hydrolase	β -D-glucopyranose-(1-4)- β -D-glucopyranose-(1-4)- β -D-glucopyranose-(1-4)- β -D-glucopyranose	6CEL	Trp, Tyr	3.9 (Tyr)	4.4 (Trp)
1,4- β -D-Glucan Cellobiohydrolase I	Hydrolase	β -D-glucopyranose-(1-4)- β -D-glucopyranose-(1-4)-	7CEL	Trp	4.4	4.1

		β -D-glucopyranose-(1-4)- β -D-glucopyranose				
S-Layer Associated Multidomain Endoglucanase	Hydrolase	β -D-glucopyranose-(1-4)- β -D-glucopyranose-(1-4)- β -D-glucopyranose-(1-4)- β -D-glucopyranose-(1-4)- β -D-glucopyranose	2ZEX	Trp	3.8	4.1
Cellobiohydrolase II	Hydrolase	β -D-glucopyranose-(1-4)- β -D-glucopyranose-(1-4)- 4-thio- β -D-glucopyranose- (1-4)-methyl β -D- glucopyranoside	1OC5	Trp	4.0	5
Endoglucanase 5a	Hydrolase	β -D-glucopyranose	1OCQ	Trp	4.1	n/a
Putative Cellulase Cel6	Hydrolase	β -D-glucopyranose-(1-4)- β -D-glucopyranose	1UP0	Trp	n/a	4.2
Endoglucanase	Hydrolase	β -D-glucopyranose-(1-4)- β -D-glucopyranose-(1-4)- α -D-glucopyranose	3A3H	His	3.8	n/a
Xyloglucanase	Hydrolase	β -D-glucopyranose	3ZQ9	Trp	4	n/a
Non Catalytic Protein 1	Lectin	β -D-glucopyranose-(1-4)- β -D-glucopyranose-(1-4)- β -D-glucopyranose-(1-4)- β -D-glucopyranose-(1-4)- β -D-glucopyranose-(1-4)- α -D-glucopyranose	1W8T	Trp, Tyr	4.5 (Trp)	4.2 (Trp), 4.4 (Tyr)
Endoglucanase E	Hydrolase	β -D-glucopyranose-(1-4)- β -D-glucopyranose-(1-4)- β -D-glucopyranose-(1-4)- β -D-glucopyranose-(1-4)- β -D-glucopyranose	2WAB	Trp, Tyr, His	n/a	3.9 (His), 4.6 (Tyr), 3.8 (Trp)
Endoglucanase H	Hydrolase	β -D-glucopyranose-(1-4)- β -D-glucopyranose	2VI0	Trp	4.1	n/a
β -1,4-Endoglucanase	Hydrolase	β -D-glucopyranose-(1-4)- β -D-glucopyranose	3ACG	Trp	4.2	n/a
β -1,4-Endoglucanase	Hydrolase	β -D-glucopyranose-(1-4)- β -D-glucopyranose-(1-4)-	3ACH	Trp	4.2	n/a

		β -D-glucopyranose-(1-4)- β -D-glucopyranose				
β -1,4-Endoglucanase	Hydrolase	β -D-glucopyranose-(1-4)- β -D-glucopyranose-(1-4)- β -D-glucopyranose-(1-4)- β -D-glucopyranose-(1-4)- β -D-glucopyranose	3ACI	Trp	4.3	n/a
Endoglucanase E	Hydrolase	β -D-glucopyranose-(1-4)- β -D-glucopyranose-(1-4)- β -D-glucopyranose-(1-4)- β -D-glucopyranose-(1-4)- β -D-glucopyranose	2WAO	Trp, Tyr	4.2 (Trp)	4.5 (Tyr)
β -Galactosidase	Hydrolase	β -D-galactopyranose-(1-4)- β -D-glucopyranose	1JYN	Trp	n/a	4
Cellulase B	Lectin	β -D-glucopyranose-(1-3)- β -D-glucopyranose-(1-4)- β -D-glucopyranose-(1-3)- β -D-glucopyranose	1UY0	Trp	n/a	4.2
Cellulase B	Lectin	β -D-glucopyranose-(1-3)- β -D-glucopyranose-(1-4)- β -D-glucopyranose-(1-3)- β -D-glucopyranose	1UYY	Trp	n/a	4.1
Carbohydrate Binding Module Vcbm60	Lectin	β -D-glucopyranose-(1-4)- β -D-glucopyranose	2XFD	Trp	n/a	4.2
β -Glucosidase 7	Hydrolase	β -D-glucopyranose-(1-4)- β -D-glucopyranose-(1-4)- β -D-glucopyranose-(1-4)- β -D-glucopyranose	3SCW	Trp, Tyr	n/a	4.1 (Trp), 4.5 (Tyr)
Endoglucanase	Hydrolase	β -D-glucopyranose-(1-4)- α -D-glucopyranose	3AZR	Trp	n/a	4.5
Cellulase Cel48f	Hydrolase	β -D-glucopyranose-(1-4)- 4-thio- β -D-glucopyranose- (1-4)- β -D-glucopyranose- (1-4)-4-thio- β -D- glucopyranose-(1-4)- β -D- glucopyranose-(1-4)-4- thio- β -D-glucopyranose-	1G9J	Trp, Tyr	n/a	4.3 (Trp), 4.1 (Tyr)

		(1-4)- β -D-glucopyranose-(1-4)-4-thio- β -D-glucopyranose				
458aa Long Hypothetical Endo-1,4- β -Glucanase	Hydrolase	β -D-glucopyranose-(1-4)- β -D-glucopyranose-(1-4)- β -D-glucopyranose-(1-4)- β -D-glucopyranose	3QHM	Trp, Tyr	n/a	4.9 (Tyr), 4.3 (Trp)
β -Glucosidase	Hydrolase	β -D-glucopyranose-(1-4)- β -D-glucopyranose	3VIK	Trp	n/a	3.7
Putative Laminarinase	Hydrolase	β -D-glucopyranose-(1-3)- β -D-glucopyranose-(1-3)- β -D-glucopyranose	2W52	Trp, Tyr	n/a	4.4 (Tyr), 3.3 (Trp)
Putative Laminarinase	Hydrolase	β -D-glucopyranose-(1-3)- β -D-glucopyranose-(1-3)- β -D-glucopyranose-(1-3)- β -D-glucopyranose-(1-3)- β -D-glucopyranose-(1-3)- β -D-glucopyranose	2WLQ	Trp	n/a	4.4
Endo-1,4- β -Glucanase	Hydrolase	β -D-glucopyranose-(1-4)- β -D-glucopyranose-(1-4)- β -D-glucopyranose-(1-4)- β -D-glucopyranose	3AMN	Trp	3.8	4.5
Endo-1,4- β -Glucanase	Hydrolase	β -D-glucopyranose-(1-4)- β -D-glucopyranose-(1-4)- β -D-glucopyranose-(1-4)- β -D-glucopyranose	3AMP	Trp	n/a	4.5
Endo-1,4- β -Glucanase	Hydrolase	β -D-glucopyranose-(1-4)- β -D-glucopyranose-(1-4)- β -D-glucopyranose-(1-4)- β -D-glucopyranose	3AMQ	Trp	n/a	4.3
Cellobiohydrolase 1 Catalytic Domain	Hydrolase	β -D-glucopyranose-(1-4)- β -D-glucopyranose-(1-4)- β -D-glucopyranose-(1-4)- β -D-glucopyranose	3PFZ	Trp	n/a	4.2
Endoglucanase H	Hydrolase	β -D-glucopyranose-(1-4)- β -D-glucopyranose-(1-3)-	2CIT	Phe	4.3	4.6

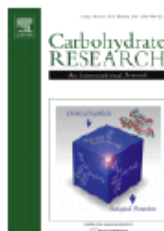
		2-deoxy-2-fluoro- α -D-glucopyranose				
Cellulase	Hydrolase	β -D-glucopyranose-(1-4)- β -D-glucopyranose	3RX5	Tyr, Phe	4.3 (Phe)	4.6 (Tyr)
Endoglucanase H	Hydrolase	β -D-glucopyranose	2V3G	Phe	n/a	4.3
Galactose Mutarotase	Isomerase	β -D-glucopyranose	1NSV	Phe	n/a	4
Glucan 1,3- β -Glucosidase	Hydrolase	β -D-glucopyranose-(1-3)- β -D-glucopyranose	3N9K	Phe	n/a	4.2
Endoglucanase I	Hydrolase	β -D-glucopyranose-(1-4)- α -D-glucopyranose	1OJK	Trp	4.5	n/a
Sugar ABC Transporter, Periplasmic Sugar-Binding Protein	Lectin	β -D-glucopyranose	2H3H	Tyr	n/a	4.4
β -Glucosidase	Hydrolase	β -D-glucopyranose	3VIJ	Tyr	n/a	4.3
Glycolipid-Anchored Surface Protein 2	Transferase	β -D-glucopyranose-(1-3)- β -D-glucopyranose-(1-3)- β -D-glucopyranose-(1-3)- β -D-glucopyranose-(1-3)- β -D-glucopyranose	2W62	Tyr	n/a	4.5
Glycolipid-Anchored Surface Protein 2	Transferase	β -D-glucopyranose-(1-3)- β -D-glucopyranose-(1-3)- β -D-glucopyranose-(1-3)- β -D-glucopyranose-(1-3)- β -D-glucopyranose	2W63	Tyr	n/a	4.7
Glucose 1-Dehydrogenase 4	Oxidoreductase	β -D-glucopyranose	3AUU	His	n/a	3.3
Phenazine Biosynthesis Protein Phzd	Hydrolase	octyl β -D-glucopyranoside	1NF8	His	n/a	3.6
Endoglucanase	Endoglucanase	β -D-glucopyranose-(1-4)- β -D-glucopyranose	2A3H	His	n/a	3.9
N-Acyl Gln Pseudo-Teicoplanin Deacetylase	Hydrolase	octyl β -D-glucopyranoside	2X9L	His	n/a	3.2
Jacalin	lectin	Methyl α -D-galactopyranoside	5JM1	Tyr	n/a	4.8 and 4.1

Table 9. Examples of glycosidic S atom being in close proximity to aromatic residues.

Protein ID	Type Of Protein	Name of ligand	PDB #	Amino Acid	Distance to glycosidic S atom
Galectin-3	lectin	2,3-Dichlorophenyl 1-thio,3- <i>N</i> -(4-(3,4,5-trifluorophenyl)-1,2,3-triazol-1-yl)-1,3-dideoxy- α -D-galactopyranoside	6EOL	Trp	4.3
Galectin-1	lectin	2,3-Dichloro-4-fluorophenyl 1-thio,3- <i>N</i> -(4-(1,3-thiazol-2-yl)-1,2,3-triazol-1-yl)-1,3-dideoxy- α -D-galactopyranoside	8OJP	Trp	4.5
β -Galactosidase	Hydrolase	1-methylethyl 1-thio- β -D-galactopyranoside	1PX4	His	3.9
β -Galactosidase	Hydrolase	1-methylethyl 1-thio- β -D-galactopyranoside	3T08	His	4
β -Galactosidase	Hydrolase	1-methylethyl 1-thio- β -D-galactopyranoside	3VD4	His	3.9
β -Galactosidase	Hydrolase	1-methylethyl 1-thio- β -D-galactopyranoside	3VD9	His	3.8
Cellobiohydrolase II	Hydrolase	β -D-glucopyranose-(1-4)-4-thio- β -D-glucopyranose-(1-4)-4-thio- β -D-glucopyranose-(1-4)-4-thio- β -D-glucopyranose-(1-4)-methyl 4-thio- α -D-glucopyranoside	1OC7	Trp	3.5
β -Galactosidase	Hydrolase	1-methylethyl 1-thio- β -D-galactopyranoside	1JYX	His	4.1



RightsLink

[Sign in/Register](#)

Synthesis and evaluation of 1,5-dithialaminaribiose and -triose tetravalent constructs

Author: Daniil Ahiadorme, Chennaiah Ande, Rafael Fernandez-Botran, David Crich

Publication: Carbohydrate Research

Publisher: Elsevier

Date: March 2023

© 2023 Elsevier Ltd. All rights reserved.

Journal Author Rights

Please note that, as the author of this Elsevier article, you retain the right to include it in a thesis or dissertation, provided it is not published commercially. Permission is not required, but please ensure that you reference the journal as the original source. For more information on this and on your other retained rights, please visit: <https://www.elsevier.com/about/our-business/policies/copyright#Author-rights>

[BACK](#)[CLOSE WINDOW](#)

Re: Dissertation writing copyright permission

Daniil Abramovich Ahiadorme <Daniil.Ahiadorme@uga.edu>

Fri 5/3/2024 10:25 AM

To: Jin Xie <jinxie@uga.edu>; Amanda L Cross <amandalc@uga.edu>

Thank you.

Best regards,

From: Jin Xie <jinxie@uga.edu>

Sent: Friday, May 3, 2024 10:24 AM

To: Amanda L Cross <amandalc@uga.edu>; Daniil Abramovich Ahiadorme <Daniil.Ahiadorme@uga.edu>

Subject: RE: Dissertation writing copyright permission

Permission is granted.

Jin

From: Amanda L Cross <amandalc@uga.edu>

Sent: Friday, May 3, 2024 10:21 AM

To: Daniil Abramovich Ahiadorme <Daniil.Ahiadorme@uga.edu>; Jin Xie <jinxie@uga.edu>

Subject: Re: Dissertation writing copyright permission

Daniil,

I have cc'd Dr. Xie so he can answer this for you.

Thanks
Amanda

Amanda Cross
Graduate Program Administrator
University of Georgia
Department of Chemistry
ISTEM-2, Suite 1299B, Room 1204
Athens, GA
Phone: 706-542-1936

From: Daniil Abramovich Ahiadorme <Daniil.Ahiadorme@uga.edu>

Sent: Thursday, May 2, 2024 3:07 PM

To: Amanda L Cross <amandalc@uga.edu>

Subject: Dissertation writing copyright permission

Hello, Amanda,

I hope you are doing well.

I am currently writing my dissertation thesis, and I am emailing you to ask for a permission to use and incorporate figures and schemes from the article for which I have an authorship right, with proper footnotes referencing my article.

AUTOBIOGRAPHICAL STATEMENT

DANIIL ABRAMOVICH AHIADORME

Education

- 2019-Present** Ph.D. in Organic Chemistry under the supervision of Prof. David Crich
Department of Chemistry, University of Georgia, Athens, GA, USA
- 2013-2019** Diploma degree in Chemistry
Department of Chemistry, Lomonosov Moscow State University, Moscow, Russia

Professional Experience

- 2020-Present** Graduate Research Assistant under the supervision of Prof. David Crich
Department of Chemistry, University of Georgia, Athens, GA, USA
- 2019-2020** Graduate Teaching Assistant under the supervision of Dr. Richard Hubbard
Science Learning Center, University of Georgia, Athens, GA, USA
- 2014-2019** Undergraduate Researcher under the supervision of Dr. Sc. Leonid Kononov
Zelinsky Institute of Organic Chemistry Russian Academy of Sciences, Moscow,
Russia
- 2017** Visiting Undergraduate Researcher under the supervision of Prof. Timor Baasov
Department of Chemistry, Technion, Haifa, Israel
- 2016** Visiting Undergraduate Researcher under the supervision of Prof. Pol Besenius
and David Strassburger
Department of Chemistry, Johannes Gutenberg-Universität Mainz,
Mainz-Frankfurt, Germany

2015	Visiting Undergraduate Researcher under the supervision of Prof. Alexei Demchenko University of Missouri St Louis, St Louis, MO, USA
2013-2014	Undergraduate Researcher under the supervision of Igor Chizhevsky A. N. Nesmeyanov Institute of Organoelement Compounds Russian Academy of Sciences, Moscow, Russia

Publications

- **Ahiadorme, D.**; Ande, C.; Fernandez-Botran, R.; Crich, D. Synthesis and Evaluation of 1,5-Dithialaminaribiose and -Triose Tetravalent Constructs. *Carbohydr. Res.* **2023**, 525, 108781.
- Freitas, B. T.; **Ahiadorme, D. A.**; Bagul, R. S.; Durie, I. A.; Ghosh, S.; Hill, J.; Kramer, N. E.; Murray, J.; O'Boyle, B. M.; Onobun, E.; et al. Exploring Noncovalent Protease Inhibitors for the Treatment of Severe Acute Respiratory Syndrome and Severe Acute Respiratory Syndrome-Like Coronaviruses. *ACS Infect. Dis.* **2022**, 8 (3), 596-611.
- Orlova, A. V.; **Ahiadorme, D. A.**; Laptinskaya, T. V.; Kononov, L. O. Supramer Analysis of 2,3,5-Tri-O-benzoyl- α -D-arabinofuranosyl Bromide Solutions in Different Solvents: Supramolecular Aggregation of Solute Molecules in 1,2-Dichloroethane Mediated by Halogen Bonds. *Russ. Chem. Bull.* **2021**, 70 (11).
- **Ahiadorme, D. A.**; Podvalnyy, N. M.; Orlova, A. V.; Chizhov, A. O.; Kononov, L. O. Glycosylation of Dibutyl Phosphate Anion with Arabinofuranosyl Bromide: Unusual Influence of Concentration of the Reagents on the Ratio of Anomeric Glycosyl Phosphates Formed. *Russ. Chem. Bull.* **2016**, 65 (11), 2776-2778.

Patent Applications

Compositions and Methods of Treatment for SARS-COV-2 through Papain Protease Inhibition B.T. Freitas,
D.A. Ahiadorme, R.S. Bagul, I.A. Durie, J. Hill, E. Onobun, M.G. Pirrone, Y.P. Subedi, K. Upadhyaya,
R.A. Tripp, B.S. Cummings, D. Crich, and S.D. Pegan. U.S. Patent Application US2021071439W